

Document made available under the Patent Cooperation Treaty (PCT)

International application number: PCT/US05/000073

International filing date: 05 January 2005 (05.01.2005)

Document type: Certified copy of priority document

Document details: Country/Office: US
Number: 60/640,213
Filing date: 03 January 2005 (03.01.2005)

Date of receipt at the International Bureau: 13 June 2005 (13.06.2005)

Remark: Priority document submitted or transmitted to the International Bureau in compliance with Rule 17.1(a) or (b)



World Intellectual Property Organization (WIPO) - Geneva, Switzerland
Organisation Mondiale de la Propriété Intellectuelle (OMPI) - Genève, Suisse

1307573

THE UNITED STATES OF AMERICA

TO ALL TO WHOM THESE PRESENTS SHALL COME:

UNITED STATES DEPARTMENT OF COMMERCE

United States Patent and Trademark Office

June 03, 2005

THIS IS TO CERTIFY THAT ANNEXED HERETO IS A TRUE COPY FROM THE RECORDS OF THE UNITED STATES PATENT AND TRADEMARK OFFICE OF THOSE PAPERS OF THE BELOW IDENTIFIED PATENT APPLICATION THAT MET THE REQUIREMENTS TO BE GRANTED A FILING DATE.

APPLICATION NUMBER: 60/640,213

FILING DATE: *January 03, 2005*

RELATED PCT APPLICATION NUMBER: *PCT/US05/00073*



Certified by

Under Secretary of Commerce
for Intellectual Property
and Director of the United States
Patent and Trademark Office

010305

13281 U.S. PTO

PTO/SB/16 (12-04)

Approved for use through 07/31/2006. OMB 0651-0032
U.S. Patent and Trademark Office; U.S. DEPARTMENT OF COMMERCE

Under the Paperwork Reduction Act of 1995, no persons are required to respond to a collection of information unless it displays a valid OMB control number.

PROVISIONAL APPLICATION FOR PATENT COVER SHEET

This is a request for filing a PROVISIONAL APPLICATION FOR PATENT under 37 CFR 1.53(c).

Express Mail Label No. _____

INVENTOR(S)		
Given Name (first and middle [if any])	Family Name or Surname	Residence (City and either State or Foreign Country)
Randell L.	Mills	Cranbury, New Jersey

Additional inventors are being named on the _____ separately numbered sheets attached hereto

TITLE OF THE INVENTION (500 characters max):

The Grand Unified Theory of Classical Quantum Mechanics

112896 U.S. PTO
60/640213

010305

Direct all correspondence to:

CORRESPONDENCE ADDRESS

☒ The address corresponding to Customer Number:

20736

OR

☐ Firm or
Individual Name

Address

City

State

Zip

Country

Telephone

Fax

ENCLOSED APPLICATION PARTS (check all that apply)

☐ Application Data Sheet. See 37 CFR 1.76

☐ CD(s), Number of CDs _____

☒ Specification Number of Pages 345

☐ Other (specify) _____

☐ Drawing(s) Number of Sheets _____

Application Size Fee: If the specification and drawings exceed 100 sheets of paper, the application size fee due is \$250 (\$125 for small entity) for each additional 50 sheets or fraction thereof. See 35 U.S.C. 41(a)(1)(G) and 37 CFR 1.16(s).

METHOD OF PAYMENT OF FILING FEES AND APPLICATION SIZE FEE FOR THIS PROVISIONAL APPLICATION FOR PATENT

☒ Applicant claims small entity status. See 37 CFR 1.27.

TOTAL FEE AMOUNT (\$)

☒ A check or money order is enclosed to cover the filing fee and application size fee (if applicable).

725

☐ Payment by credit card. Form PTO-2038 is attached

☒ The Director is hereby authorized to charge the filing fee and application size fee (if applicable) or credit any overpayment to Deposit

Account Number: 50-0687

A duplicative copy of this form is enclosed for fee processing.

The invention was made by an agency of the United States Government or under a contract with an agency of the United States Government.

☐ No.

☐ Yes, the name of the U.S. Government agency and the Government contract number are: _____

SIGNATURE _____

Date January 3, 2005

TYPED or PRINTED NAME Jeffrey S. Melcher

REGISTRATION NO. 35,950

(If appropriate)

TELEPHONE 202.261.1000

Docket Number: 62226-BOOK1

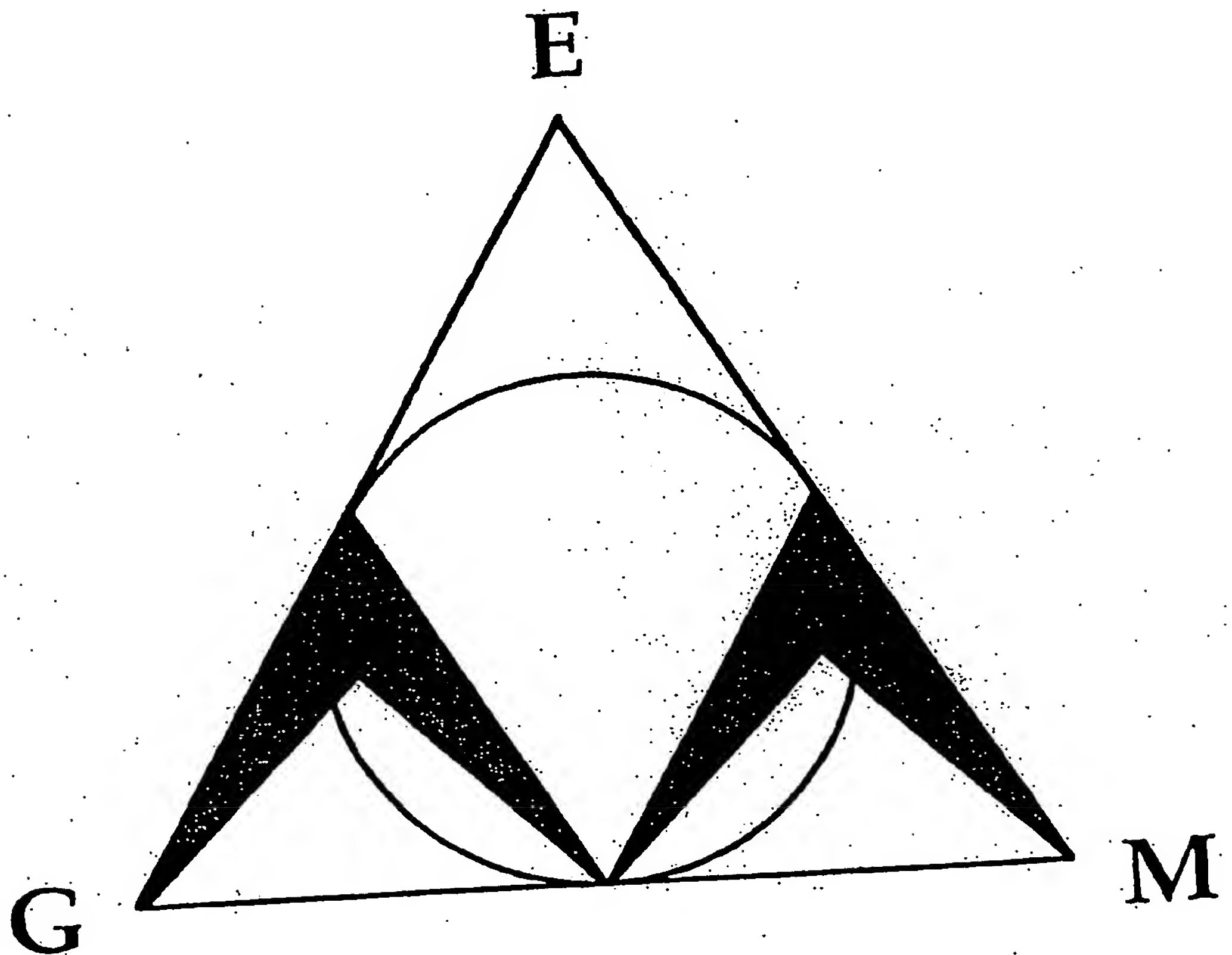
USE ONLY FOR FILING A PROVISIONAL APPLICATION FOR PATENT

This collection of information is required by 37 CFR 1.51. The information is required to obtain or retain a benefit by the public which is to file (and by the USPTO to process) an application. Confidentiality is governed by 35 U.S.C. 122 and 37 CFR 1.11 and 1.14. This collection is estimated to take 8 hours to complete, including gathering, preparing, and submitting the completed application form to the USPTO. Time will vary depending upon the individual case. Any comments on the amount of time you require to complete this form and/or suggestions for reducing this burden, should be sent to the Chief Information Officer, U.S. Patent and Trademark Office, U.S. Department of Commerce, P.O. Box 1450, Alexandria, VA 22313-1450. DO NOT SEND FEES OR COMPLETED FORMS TO THIS ADDRESS. SEND TO: Commissioner for Patents, P.O. Box 1450, Alexandria, VA 22313-1450.

If you need assistance in completing the form, call 1-800-PTO-9199 and select option 2.

THE GRAND UNIFIED THEORY OF CLASSICAL QUANTUM MECHANICS

Dr. Randell L. Mills



**THE GRAND UNIFIED THEORY
OF CLASSICAL
QUANTUM MECHANICS**

BY

Dr. Randell L. Mills

**BLACKLIGHT^{SM, TM}
P O W E R inc.**

493 Old Trenton Road
Cranbury, NJ 08512

January 2005 EDITION

SECTION I

Atoms and Molecules

1. The One-Electron Atom	48
1.1 The Boundary Condition of Nonradiation and the Radial Function—the Concept of the "Orbitsphere"	48
1.1.1 The Boundary Condition	48
1.1.2 Derivation of the Condition of Nonradiation	48
1.1.3 Derivation of the Boundary Condition	49
1.2 Spacetime Fourier Transform of the Electron Function	50
1.3 The Angular Function	58
1.4 The Orbitsphere Equation of Motion for $\ell = 0$	65
1.4.1 Stern-Gerlach-Experiment Boundary Condition	65
1.5 Generation of the Orbitsphere-cvf in Two Steps	74
1.6 Spin Angular Momentum of the Orbitsphere with $\ell = 0$	74
1.7 Exact Generation of $Y_0^0(\phi, \theta)$ from the Orbitsphere-cvf	74
1.7.1 Convolution Operator	84
1.8 Resonant Precession of the Spin-1/2-Current-Density Function Gives Rise to the Bohr Magneton	65
1.9 Rotational Parameters of the Electron (Angular Momentum, Rotational Energy, Moment of Inertia)	83
1.9.1 Derivation of the Rotational Parameters of the Electron	84
1.10 Magnetic Parameters of the Electron (Bohr Magneton)	90
1.10.1 The Magnetic Field of an Orbitsphere from Spin	90
1.10.2 Derivation of the Magnetic Field	92
1.10.3 Derivation of the Energy	94
1.11 Electron g Factor	102
1.11.1 Stored Magnetic Energy	104
1.11.2 Stored Electric Energy	104
1.11.3 Dissipated Energy	109
1.11.4 Total Energy of Spin-Flip Transition	111
1.12 Determination of Orbitsphere Radii	114
1.13 Energy Calculations	121
1.14 Special Relativistic Correction to the Ionization Energies	125
Appendix I: Nonradiation Based on the Electromagnetic Fields and the Poynting Power Vector	135
Appendix II: Quantum Electrodynamics (QED) is Purely Mathematical and Has No Basis in Reality	142
Appendix III: Analytical Equations to Generate the Orbitsphere Current Vector Field and the Uniform Current (Charge)-Density	

	Function $Y_0^0(\phi, \theta)$	147
Ap. III.1	STEP ONE by the Rotation of a Great Circle about the $(\mathbf{i}_x, \mathbf{i}_y, 0\mathbf{i}_z)$ -Axis by 2π	147
Ap. III.1.1	Great Circle in the yz-Plane about the $(\mathbf{i}_x, \mathbf{i}_y, 0\mathbf{i}_z)$ -Axis	147
Ap. III.1.2	Great Circle in the xz-Plane about the $(\mathbf{i}_x, \mathbf{i}_y, 0\mathbf{i}_z)$ -Axis	147
Ap. III.2	STEP TWO by the Rotation of a Great Circle about the $(-\mathbf{i}_x, 0\mathbf{i}_y, \mathbf{i}_z)$ -Axis by 2π Followed by a Rotation about the z-Axis by $\frac{\pi}{4}$	147
Ap. III.2.1	Great Circle in the xy-Plane about the $(-\mathbf{i}_x, 0\mathbf{i}_y, \mathbf{i}_z)$ -Axis by 2π Followed by a Rotation about the z-Axis by $\frac{\pi}{4}$	147
Ap. III.2.2	Great Circle in the yz-Plane about the $(-\mathbf{i}_x, 0\mathbf{i}_y, \mathbf{i}_z)$ -Axis by 2π Followed by a Rotation about the z-Axis by $\frac{\pi}{4}$	147
Ap. III.3	STEP TWO by Rotation of a Great Circle About the $(-\mathbf{i}_x, \mathbf{i}_y, \mathbf{i}_z)$ -Axis by 2π	147
Ap. III.4	Characteristics of the Orbitsphere-cvf	147
Ap. III.5	The Uniform Current (Charge)-Density Function $Y_0^0(\phi, \theta)$	147
Ap. III.5.1	Boundary Constraints	147
Ap. III.5.2	Properties of the Orbitsphere-cvf Permissive to Generate $Y_0^0(\phi, \theta)$	147
Ap. III.5.3	Component Orbitsphere-cvf Orthogonal to that of STEP ONE by the Rotation of a Great Circle about the $(\mathbf{i}_x, -\mathbf{i}_y, 0\mathbf{i}_z)$ -Axis by 2π	147
Ap. III.5.3.1	Great Circle in the yz-Plane about the $(\mathbf{i}_x, -\mathbf{i}_y, 0\mathbf{i}_z)$ -Axis	147
Ap. III.5.4	Matching Phase, Angular Momentum, and Orientation	147
Ap. III.6	Convolution Operator	147
Ap. III.7	Component Orbitsphere-cvf Squared for STEP ONE Using the Rotation of a Great Circle about the $(\mathbf{i}_x, \mathbf{i}_y, 0\mathbf{i}_z)$ -Axis by 2π	147
Ap. III.8	Component Orbitsphere-cvf Squared for STEP TWO Using the Rotation of a Great Circle about the $(-\mathbf{i}_x, 0\mathbf{i}_y, \mathbf{i}_z)$ -Axis by 2π Followed by a Rotation about the z-Axis by $\frac{\pi}{4}$	147
Ap. III.9	Component Orbitsphere-cvf Squared for STEP TWO by the Rotation of a Great Circle About the $(-\mathbf{i}_x, \mathbf{i}_y, \mathbf{i}_z)$ -Axis by 2π	147
Ap. III.10	Orbitsphere-cvf Squared	147
Ap. III.11	Matrices to Demonstrate the Convolution to Generate the Uniform Current (Charge)-Density Function $Y_0^0(\phi, \theta)$	147

Ap. III.11.1	STEP-ONE Matrices to Visualize the Currents of $Y_0^0(\phi, \theta)$	147
Ap. III.11.2	STEP-Two Matrices to Visualize the Currents of $Y_0^0(\phi, \theta)$	147
Ap. III.11.2.1	Discrete Convolution with a Secondary Component Orbitsphere-cvf in a Plane Along the $(\mathbf{i}_x, \mathbf{i}_y, 0\mathbf{i}_z)$ - and z-Axes (xyz-Plane)	147
Ap. III.11.2.2	Discrete Convolution with a Secondary Component Orbitsphere-cvf in the xy-Plane	147
Ap. III.12	Simple Approximation Method for Visualizing the Current Pattern of $Y_0^0(\phi, \theta)$ by a Discrete Convolution about L_R	147
Appendix IV: Muon g Factor		156
References		160
2.	Excited States of the One-Electron Atom (Quantization)	160
2.1	Equation of the Electric Field inside the Orbitsphere	164
2.2	Photon Absorption	166
2.3	Selection Rules	168
2.4	Orbital and Spin Splitting	168
2.5	Stark Effect	170
2.6	Resonant Line Shape	170
2.7	Lamb Shift	177
2.8	Spin-Orbital Coupling (Fine Structure)	180
2.9	Knight Shift	181
2.10	Spin-Nuclear Coupling (Hyperfine Structure)	182
2.11	Energy Calculations	183
2.12	Muonium Hyperfine Structure Interval	183
2.13	Energy Calculations	190
References		192
3.	Electron in Free Space	192
3.1	Charge-Density Function	196
3.2	Current-Density Function	201
3.3	Stern-Gerlach Experiment	210
3.4	Electric Field of a Free Electron	210
References		212
4.	Equation of the Photon	212
4.1	Right and Left Hand Circular and Elliptically Polarized Photons	220
4.2	Linear Polarized Photons	225
4.3	Spherical Wave	227
4.4	Photon Torpedoes	227
4.5	Photoelectric Effect	230
4.6	Compton Effect	233
References		235
5.	Hydrino Theory—BlackLight Process	235
5.1	BlackLight Process	237
5.2	Energy Hole Concept	244
5.3	Catalysts	248
5.4	Disproportionation of Energy States	254
5.5	Interstellar Disproportionation Rate	255
5.6	Hydrino Catalyzed Fusion (HCF)	256
5.7	New "Ground" State	256
5.8	Spin-Nuclear and Orbital-Nuclear Coupling of Hydrinos	256
5.8.1	Energy Calculations	256
5.9	Einstein A Coefficient	256

5.10	Intensity of Spin-Nuclear and Orbital-Nuclear Coupling	256
	Transitions of Hydrinos	258
	References	260
6.	Stability of Atoms and Hydrinos	261
6.1	Instability of Excited States	264
6.2	Stability of "Ground" and Hydrino States	264
6.3	Energy Transfer Mechanism	268
6.4	Energy Hole as a Multipole Expansion	269
6.5	Power Density of a Gas Energy Cell	272
	References	274
7.	The Two-Electron Atom	274
7.1	Determination of Orbitsphere Radii	277
7.2	Energy Calculations	278
7.2.1	Conservation of Energy	278
7.2.2	Ionization Energies	281
7.2.3	Dissipated Energy	284
7.3	Hydride Ion	284
7.3.1	Determination of the Orbitsphere Radius, r_n	285
7.3.2	Ionization Energy	287
7.4	Hydrino Hydride Ion	289
7.5	Hydrino Hydride Ion Nuclear Magnetic Resonance Shift	294
7.6	Hydrino Hydride Ion Hyperfine Lines	299
	References	301
8.	Classical Photon and Electron Scattering	301
8.1	Classical Scattering of Electromagnetic Radiation	302
8.1.1	The Array Theorem	303
8.1.2	Applications of the Array Theorem	303
8.1.2.1	Two-Slit Interference (Wave-Particle Duality)	304
8.2	Classical Wave Theory of Electron Scattering	310
8.2.1	Classical Wave Theory Applied to Scattering from Atoms and Molecules	310
8.3	Electron Scattering Equation for the Helium Atom Based on the Orbitsphere Model	313
8.3.1	Results	315
8.4	Discussion	321
	References	322
9.	Excited States of Helium	160
9.1	Singlet Excited States with $\ell = 0$ ($1s^2 \rightarrow 1s^1(ns)^1$)	331
9.2	Triplet Excited States with $\ell = 0$ ($1s^2 \rightarrow 1s^1(ns)^1$)	331
9.3	Singlet Excited States with $\ell \neq 0$	331
9.4	Triplet Excited States with $\ell \neq 0$	170
9.5	All Excited He I States	331
9.6	Spin-Orbital Coupling of Excited States with $\ell \neq 0$	331
	References	331
10.	Three, Four, Five, Six, Seven, Eight, Nine, Ten, Eleven, Twelve, Thirteen, Fourteen, Fifteen, Sixteen, Seventeen, Eighteen, Nineteen, and Twenty-Electron Atoms	333
10.1	Three-Electron Atoms	333
10.1.1	The Lithium Atom	335
10.1.2	The Radius of the Outer Electron of the Lithium Atom	335
10.1.3	The Ionization Energy of Lithium	335
10.1.4	Three Electron Atoms with a Nuclear Charge $Z > 3$	337
10.1.5	The Radius of the Outer Electron of Three-Electron	

	Atoms with a Nuclear Charge $Z > 3$	339
10.1.6	The Ionization Energies of Three-Electron Atoms with a Nuclear Charge $Z > 3$	345
10.2	Four Electron Atoms	345
10.2.1	Radii of the Outer Electrons of Four Electron Atoms	347
10.2.2	Energies of the Beryllium Atom	348
10.2.3	The Ionization Energies of Four Electron Atoms with a Nuclear Charge $Z > 4$	345
10.3	P-Orbital Electrons Based on an Energy Minimum	345
10.4	Five-Electron Atoms	345
10.4.1	Radius and Ionization Energy of the Outer Electron of the Boron Atom	345
10.4.2	The Ionization Energies of Five-Electron Atoms with a Nuclear Charge $Z > 5$	345
10.5	Six-Electron Atoms	345
10.5.1	Radius and Ionization Energy of the Outer Electron of the Carbon Atom	345
10.5.2	The Ionization Energies of Six-Electron Atoms with a Nuclear Charge $Z > 6$	345
10.6	Seven-Electron Atoms	345
10.6.1	Radius and Ionization Energy of the Outer Electron of the Nitrogen Atom	345
10.6.2	The Ionization Energies of Seven-Electron Atoms with a Nuclear Charge $Z > 7$	345
10.7	Eight-Electron Atoms	345
10.7.1	Radius and Ionization Energy of the Outer Electron of the Oxygen Atom	345
10.7.2	The Ionization Energies of Eight-Electron Atoms with a Nuclear Charge $Z > 8$	345
10.8	Nine-Electron Atoms	345
10.8.1	Radius and Ionization Energy of the Outer Electron of the Fluorine Atom	345
10.8.2	The Ionization Energies of Nine-Electron Atoms with a Nuclear Charge $Z > 9$	345
10.9	Ten-Electron Atoms	345
10.9.1	Radius and Ionization Energy of the Outer Electron of the Neon Atom	345
10.9.2	The Ionization Energies of Ten-Electron Atoms with a Nuclear Charge $Z > 10$	345
10.10	General Equation for the Ionization Energies of Five Through Ten-Electron Atoms	345
10.11	Eleven-Electron Atoms	345
10.11.1	Radius and Ionization Energy of the Outer Electron of the Sodium Atom	345
10.11.2	The Ionization Energies of Eleven-Electron Atoms with a Nuclear Charge $Z > 11$	345
10.12	Twelve-Electron Atoms	345
10.12.1	Radius and Ionization Energy of the Outer Electron of the Magnesium Atom	345
10.12.2	The Ionization Energies of Twelve-Electron Atoms with a Nuclear Charge $Z > 12$	345
10.13	3P-Orbital Electrons Based on an Energy Minimum	345
10.14	Thirteen-Electron Atoms	345
10.14.1	Radius and Ionization Energy of the Outer Electron	345

10.14.2	of the Aluminum Atom	345
10.15	The Ionization Energies of Thirteen-Electron Atoms with a Nuclear Charge $Z > 13$	345
10.15.1	Fourteen-Electron Atoms	345
10.15.2	Radius and Ionization Energy of the Outer Electron of the Silicon Atom	345
10.16	The Ionization Energies of Fourteen-Electron Atoms with a Nuclear Charge $Z > 14$	345
10.16.1	Fifteen-Electron Atoms	345
10.16.2	Radius and Ionization Energy of the Outer Electron of the Phosphorous Atom	345
10.17	The Ionization Energies of Fifteen-Electron Atoms with a Nuclear Charge $Z > 15$	345
10.17.1	Sixteen-Electron Atoms	345
10.17.2	Radius and Ionization Energy of the Outer Electron of the Sulfur Atom	345
10.18	The Ionization Energies of Sixteen-Electron Atoms with a Nuclear Charge $Z > 16$	345
10.18.1	Seventeen-Electron Atoms	345
10.18.2	Radius and Ionization Energy of the Outer Electron of the Chlorine Atom	345
10.19	The Ionization Energies of Seventeen-Electron Atoms with a Nuclear Charge $Z > 17$	345
10.19.1	Eighteen-Electron Atoms	345
10.19.2	Radius and Ionization Energy of the Outer Electron of the Argon Atom	345
10.20	The Ionization Energies of Eighteen-Electron Atoms with a Nuclear Charge $Z > 18$	345
10.21	General Equation for the Ionization Energies of Thirteen Through Eighteen-Electron Atoms	345
10.21.1	Nineteen-Electron Atoms	345
10.21.2	Radius and Ionization Energy of the Outer Electron of the Potassium Atom	345
10.22	The Ionization Energies of Nineteen-Electron Atoms with a Nuclear Charge $Z > 19$	345
10.22.1	Twenty-Electron Atoms	345
10.22.2	Radius and Ionization Energy of the Outer Electron of the Calcium Atom	345
10.23	The Ionization Energies of Twenty-Electron Atoms with a Nuclear Charge $Z > 20$	345
11.	General Equation for the Ionization Energies of Atoms Having an Outer S-Shell	350
12.	References	346
12.1	The Electron Configuration of Atoms	347
12.1.1	The Nature of the Chemical Bond of Hydrogen-Type Molecules	347
12.1.2	Hydrogen-Type Molecular Ions	355
12.1.3	Force Balance of Hydrogen-Type Molecular Ions	356
12.1.4	Energies of Hydrogen-Type Molecular Ions	357
12.1.5	Vibration of Hydrogen-Type Molecular Ions	364
12.2	The Doppler Energy Term of Hydrogen-type Molecular Ions	367
	Total (Ionization) and Bond Energies of Hydrogen and Deuterium Molecular Ions	368

12.2.1	Force Balance of Hydrogen-Type Molecules.....	368
12.2.2	Energies of Hydrogen-Type Molecules.....	369
12.2.3	Vibration of Hydrogen-Type Molecules.....	370
12.2.4	The Doppler Energy Term of Hydrogen-type Molecules.....	372
12.2.5	Total, Ionization, and Bond Energies of Hydrogen and Deuterium Molecules.....	374
12.3	The Hydrogen Molecular Ion.....	376
12.3.1	Force Balance of the Hydrogen Molecular Ion.....	376
12.3.2	Energies of the Hydrogen Molecular Ion.....	378
12.3.3	Vibration of the Hydrogen Molecular Ion.....	379
12.4	The Hydrogen Molecule.....	379
12.4.1	Force Balance of the Hydrogen Molecule.....	379
12.4.2	Energies of the Hydrogen Molecule.....	381
12.4.3	Vibration of the Hydrogen Molecule.....	384
12.5	The Dihydrino Molecular Ion.....	384
12.5.1	Force Balance of the Dihydrino Molecular Ion.....	384
12.5.2	Energies of the Dihydrino Molecular Ion.....	385
12.5.3	Vibration of the Dihydrino Molecular Ion.....	386
12.6	The Dihydrino Molecule.....	386
12.6.1	Force Balance of the Dihydrino Molecule.....	387
12.6.2	Energies of the Dihydrino Molecule.....	387
12.6.3	Vibration of the Dihydrino Molecule.....	388
12.7	Geometry.....	388
12.8	Dihydrino Ionization Energies.....	389
12.9	Sizes of Representative Atoms and Molecules.....	392
12.10	Ortho-Para Transition of Hydrogen-Type Molecules.....	393
12.11	Nuclear Magnetic Resonance Shift.....	405
12.12	Data Supporting $H(1/p)$, $H^-(1/p)$, $H_2^+(1/p)$, and $H_2(1/p)$	405
	References.....	409
13.	Molecular BlackLight Process.....	409
13.1	Below "Ground" State Transitions of Hydrogen-Type Molecules and Molecular Ions.....	409
13.2	Energy Holes.....	413
13.3	Catalytic Energy Holes for Hydrogen-Type Molecules.....	416
14.	Diatomic Molecular Energy States.....	416
14.1	Excited Electronic States of Ellipsoidal Molecular Orbitals.....	416
14.2	Magnetic Moment of an Ellipsoidal Molecular Orbital.....	416
14.3	Magnetic Field of an Ellipsoidal Molecular Orbital.....	417
14.4	Diatomic Molecular Vibration.....	417
14.4.1	Vibration of Hydrogen-Type Molecular Ions.....	420
14.4.2	Vibration of Hydrogen-Type Molecules.....	424
14.5	Diatomic Molecular Rotation.....	425
14.6	Diatomic Molecular Rotation of Hydrogen-Type Molecules.....	425
14.7	Diatomic Molecular Rotation of Hydrogen-Type Molecular Ions.....	426
14.1	Centrifugal Distortion.....	426
	References.....	426

THE ONE-ELECTRON ATOM

One-electron atoms include the hydrogen atom, He(II), Li(III), Be(IV), and so on. The mass-energy and angular momentum of the electron are constant; this requires that the equation of motion of the electron be temporally and spatially harmonic. Thus, the classical wave equation (4-dimensional Laplace equation) applies and

$$\left[\nabla^2 - \frac{1}{v^2} \frac{\partial^2}{\partial t^2} \right] \rho(r, \theta, \phi, t) = 0 \quad (1.1)$$

where $\rho(r, \theta, \phi, t)$ is the function of the electron in time and space. In each case, the nucleus contains Z protons and the atom has a net positive charge of $(Z-1)e$. All forces are central and Special Relativity applies. Thus, the coordinates must be three dimensional spherically harmonic coordinates plus time. The time, radial, and angular solutions of Laplace's Equation are separable. The motion is time harmonic with frequency ω_n . To be a harmonic solution of Laplace's equation in spherical coordinates, the angular functions must be spherical harmonic functions.

THE BOUNDARY CONDITION OF NONRADIATION AND THE RADIAL FUNCTION—THE CONCEPT OF THE "ORBITSphere"

A zero of the spacetime Fourier transform of the product function of two spherical harmonic angular functions, a time harmonic function, and an unknown radial function is sought.

The Boundary Condition

The condition for radiation by a moving charge is derived from Maxwell's equations. To radiate, the spacetime Fourier transform of the current-density function must possess components synchronous with waves traveling at the speed of light [1]. Alternatively,

For non-radiative states, the current-density function must not possess spacetime Fourier components that are synchronous with waves traveling at the speed of light.

Derivation of the Condition for Nonradiation

The condition for radiation by a moving point charge given by Haus [1] is that its spacetime Fourier transform does possess components that are synchronous with waves traveling at the speed of light. Conversely, it is proposed that the condition for nonradiation by an ensemble of moving point charges that comprises a charge-density function is that its spacetime Fourier transform does NOT possess components that are

synchronous with waves traveling at the speed of light. The Haus derivation applies to a moving charge-density function as well because charge obeys superposition. The Haus derivation is summarized below.

The Fourier components of the current produced by the moving charge are derived. The electric field is found from the vector equation in Fourier space (\mathbf{k} , ω -space). The inverse Fourier transform is carried over the magnitude of \mathbf{k} . The resulting expression demonstrates that the radiation field is proportional to $\mathbf{J}_\perp\left(\frac{\omega}{c}\mathbf{n}, \omega\right)$, where $\mathbf{J}_\perp(\mathbf{k}, \omega)$ is the spacetime Fourier transform of the current perpendicular to \mathbf{k} and $\mathbf{n} \equiv \frac{\mathbf{k}}{|\mathbf{k}|}$. Specifically,

$$\mathbf{E}_\perp(\mathbf{r}, \omega) \frac{d\omega}{2\pi} = \frac{c}{2\pi} \int \rho(\omega, \Omega) d\omega d\Omega \sqrt{\frac{\mu_0}{\epsilon_0}} \mathbf{n} \times \left(\mathbf{n} \times \mathbf{J}_\perp\left(\frac{\omega}{c}\mathbf{n}, \omega\right) e^{i\left(\frac{\omega}{c}\right)\mathbf{n} \cdot \mathbf{r}} \right) \quad (1.2)$$

The field $\mathbf{E}_\perp(\mathbf{r}, \omega) \frac{d\omega}{2\pi}$ is proportional to $\mathbf{J}_\perp\left(\frac{\omega}{c}\mathbf{n}, \omega\right)$, namely, the Fourier component for which $\mathbf{k} = \frac{\omega}{c}\mathbf{n}$. Factors of ω that multiply the Fourier component of the current are due to the density of modes per unit volume and unit solid angle. An unaccelerated charge does not radiate in free space, not because it experiences no acceleration, but because it has no Fourier component $\mathbf{J}_\perp\left(\frac{\omega}{c}\mathbf{n}, \omega\right)$.

Derivation of the Boundary Condition

In general, radial solutions of the Helmholtz wave equation are spherical Bessel functions, Neumann functions, Hankel functions, associated Laguerre functions, and the radial Dirac delta function. The Dirac delta function eliminates the radial dependence and reduces the number of dimensions of the Helmholtz wave equation from four to three. The solution for the radial function which satisfies the boundary condition is a three dimensional delta function in spherical coordinates—a spherical shell [2]

$$f(r) = \frac{1}{r^2} \delta(r - r_n) \quad (1.3)$$

where r_n is an allowed radius. The Fourier transform of the radial Dirac delta function is a sinc function. For time harmonic motion, with angular velocity, ω , the relationship between the radius and the wavelength is

$$2\pi r = \lambda \quad (1.4)$$

Consider the radial wave vector of the sinc function, when the radial projection of the velocity is c , the relativistically corrected wavelength is

$$\lambda = r \quad (1.5)$$

Substitution of Eq. (1.5) into the sinc function results in the vanishing of the entire Fourier transform of the current-density function.

SPACETIME FOURIER TRANSFORM OF THE ELECTRON FUNCTION

The electron charge-density (mass-density) function is the product of a radial delta function ($f(r) = \frac{1}{r^2} \delta(r - r_n)$), two angular functions (spherical harmonic functions), and a time harmonic function. The spacetime Fourier transform in three dimensions in spherical coordinates plus time is given [3, 4] as follows:

$$M(s, \Theta, \Phi, \omega) = \int_0^\infty \int_0^\pi \int_0^{2\pi} \int_0^\infty \rho(r, \theta, \phi, t) \exp(-i2\pi sr[\cos \Theta \cos \theta + \sin \Theta \sin \theta \cos(\phi - \Phi)]) \exp(-i\omega t) r^2 \sin \theta dr d\theta d\phi dt \quad (1.6)$$

With circular symmetry [3]

$$M(s, \Theta, \omega) = 2\pi \int_0^\infty \int_0^\pi \rho(r, \theta, t) J_0(2\pi sr \sin \Theta \sin \theta) \exp(-i2\pi sr \cos \Theta \cos \theta) r^2 \sin \theta \exp(-i\omega t) dr d\theta dt \quad (1.7)$$

With spherical symmetry [3],

$$M(s, \omega) = 4\pi \int_0^\infty \rho(r, t) \text{sinc}(2sr) r^2 \exp(-i\omega t) dr dt \quad (1.8)$$

The solutions of the classical wave equation are separable.

$$\rho(r, \theta, \phi, t) = f(r)g(\theta)h(\phi)k(t) \quad (1.9)$$

The orbitsphere function is separable into a product of functions of independent variables, r, θ, ϕ , and t . The radial function which satisfies the boundary condition is a delta function. The time functions are of the form $e^{i\omega t}$, the angular functions are spherical harmonics, sine or cosine trigonometric functions or sums of these functions, each raised to various powers. The spacetime Fourier transform is derived of the separable variables for the angular space function of $\sin \phi$ and $\sin \theta$. It follows from the spacetime Fourier transform given below that other possible spherical harmonics angular functions give the same form of result as the transform of $\sin \theta$ and $\sin \phi$. Using Eq. (1.8), $F(s)$, the space Fourier transform of ($f(r) = \delta(r - r_n)$) is given as follows:

$$F(s) = 4\pi \int_0^\infty \frac{1}{r^2} \delta(r - r_n) \text{sinc}(2sr) r^2 dr \quad (1.10)$$

$$F(s) = 4\pi \text{sinc}(2sr_n) \quad (1.11)$$

The subscript n is used hereafter; however, the quantization condition appears in the Excited States of the One-Electron

Atom (Quantization) section. Quantization arises as "allowed" solutions of the wave equation corresponding to a resonance between the electron and a photon.

Using Eq. (1.7), $G(s, \Theta)$, the space Fourier transform of $g(\theta) = \sin \theta$ is given as follows where there is no dependence on ϕ :

$$G(s, \Theta) = 2\pi \int_0^\infty \int_0^\pi \sin \theta J_0(2\pi sr \sin \Theta \sin \theta) \exp(-i2\pi sr \cos \Theta \cos \theta) \sin \theta r^2 d\theta dr \quad (1.12)$$

$$G(s, \Theta) = 2\pi \int_0^\infty \int_0^\pi r^2 \sin^2 \theta J_0(2\pi sr \sin \Theta \sin \theta) \cos(2\pi sr \cos \Theta \cos \theta) d\theta dr \quad (1.13)$$

From Luke [5] and [6]:

$$J_\nu(z) = \left(\frac{1}{2}z\right)^\nu \sum_{n=0}^\infty \frac{(-1)^n \left(\frac{z}{2}\right)^{2n}}{n! \Gamma(\nu + n + 1)} = \left(\frac{1}{2}z\right)^\nu \sum_{n=0}^\infty \frac{(-1)^n \left(\frac{z}{2}\right)^{2n}}{n! (\nu + n)!} \quad (1.14)$$

Let

$$Z = 2\pi sr \sin \Theta \sin \theta \quad (1.15)$$

With substitution of Eqs. (1.15) and (1.14) into Eq. (1.13),

$$G(s, \Theta) = 2\pi \int_0^\infty \int_0^\pi r^2 \sin^2 \theta \left[\sum_{n=0}^\infty \frac{(-1)^n (\pi sr \sin \Theta \sin \theta)^{2n}}{n! n!} \right] \cos(2\pi sr \cos \Theta \cos \theta) d\theta dr \quad (1.16)$$

$$G(s, \Theta) = 2\pi \int_0^\infty r^2 \int_0^\pi \sum_{n=0}^\infty \frac{(-1)^n (\pi sr \sin \Theta)^{2n}}{n! n!} \sin^{2(n+1)} \theta \cos(2\pi sr \cos \Theta \cos \theta) d\theta dr \quad (1.17)$$

$$G(s, \Theta) = 2\pi \int_0^\infty r^2 \int_0^\pi \sum_{n=1}^\infty \frac{(-1)^{n-1} (\pi sr \sin \Theta)^{2(n-1)}}{(n-1)! (n-1)!} \sin^{2n} \theta \cos(2\pi sr \cos \Theta \cos \theta) d\theta dr \quad (1.18)$$

From Luke [7], with $\text{Re}(\nu) > -\frac{1}{2}$:

$$J_\nu(z) = \frac{\left(\frac{1}{2}z\right)^\nu}{\Gamma\left(\frac{1}{2}\right)\Gamma\left(\nu + \frac{1}{2}\right)} \int_0^\pi \cos(z \cos \theta) \sin^{2\nu} \theta d\theta \quad (1.19)$$

Let

$$z = 2\pi sr \cos \theta, \text{ and } n = \nu \quad (1.20)$$

Applying the relationship, the integral of a sum is equal to the sum of the integrals to Eq. (1.18), and transforming Eq. (1.18) into the form of Eq. (1.19) by multiplication by

$$1 = \frac{\Gamma\left(\frac{1}{2}\right)\Gamma\left(v + \frac{1}{2}\right)(\pi sr \cos \Theta)^v}{(\pi sr \cos \Theta)^v \Gamma\left(\frac{1}{2}\right)\Gamma\left(v + \frac{1}{2}\right)} \quad (1.21)$$

and by moving the constant outside of the integral gives:

$$G(s, \Theta) = 2\pi \int_0^\infty r^2 \sum_{v=1}^\infty \int_0^\pi \frac{(-1)^{v-1} (\pi r \sin \Theta)^{2(v-1)}}{(v-1)!(v-1)!} \frac{\Gamma\left(\frac{1}{2}\right)\Gamma\left(v + \frac{1}{2}\right)(\pi sr \cos \Theta)^v}{(\pi sr \cos \Theta)^v \Gamma\left(\frac{1}{2}\right)\Gamma\left(v + \frac{1}{2}\right)} \sin^{2v} \theta \cos(2\pi sr \cos \Theta \cos \theta) d\theta dr \quad (1.22)$$

$$G(s, \Theta) = 2\pi \int_0^\infty r^2 \sum_{v=1}^\infty \frac{(-1)^{v-1} (\pi r \sin \Theta)^{2(v-1)}}{(v-1)!(v-1)!} \frac{\Gamma\left(\frac{1}{2}\right)\Gamma\left(v + \frac{1}{2}\right)(\pi sr \cos \Theta)^v}{(\pi sr \cos \Theta)^v \Gamma\left(\frac{1}{2}\right)\Gamma\left(v + \frac{1}{2}\right)} \int_0^\pi \sin^{2v} \theta \cos(2\pi sr \cos \Theta \cos \theta) d\theta dr \quad (1.23)$$

Applying Eq. (1.19),

$$G(s, \Theta) = 2\pi \int_0^\infty r^2 \sum_{v=1}^\infty \frac{(-1)^{v-1} (\pi r \sin \Theta)^{2(v-1)}}{(v-1)!(v-1)!} \frac{\Gamma\left(\frac{1}{2}\right)\Gamma\left(v + \frac{1}{2}\right)}{(\pi sr \cos \Theta)^v} J_v(2\pi sr \cos \Theta) dr \quad (1.24)$$

Using the Hankel transform formula from Bateman [8]:

$$\int_0^\infty r^{-\left(\frac{1}{2}\right)} (rs)^{\left(\frac{1}{2}\right)} J_v(rs) dr = s^{\left(\frac{1}{2}\right)} \quad (1.25)$$

and the Hankel transform relationship from Bateman [9], the general Eq. (1.31) is derived as follows:

$$f(x) \Longleftrightarrow g(y; v) = \int_0^\infty f(x) (xy)^{\left(\frac{1}{2}\right)} J_v(xy) dx \quad (1.26)$$

$$x^m f(x), m = 0, 1, 2, \dots \Longleftrightarrow y^{\left(\frac{1}{2}-v\right)} \left(\frac{d}{y dy}\right)^m \left[y^{\left(m+v-\frac{1}{2}\right)} g(y; m+v) \right] \quad (1.27)$$

$$\int_0^\infty r^v r^{-\left(\frac{1}{2}\right)} (rs)^{\left(\frac{1}{2}\right)} J_v(rs) dr = s^{\left(\frac{1}{2}-v\right)} \left(\frac{d}{s ds}\right)^v \left[s^{\left(v+v-\frac{1}{2}\right)} s^{\left(\frac{1}{2}\right)} \right] \quad (1.28)$$

$$\int_0^\infty r^\nu s^{\left(\frac{1}{2}\right)} J_\nu(rs) dr = \frac{s^{\left(\frac{1}{2}-\nu\right)}}{s^\nu} \left(\frac{d}{ds}\right)^\nu [s^{(2\nu)}] \quad (1.29)$$

$$\int_0^\infty r^\nu s^{\left(\frac{1}{2}\right)} J_\nu(rs) dr = s^{\left(\frac{1}{2}-2\nu\right)} \frac{2\nu!}{(\nu-1)!} s^\nu = \frac{2\nu!}{(\nu-1)!} s^{\left(\frac{1}{2}-\nu\right)} \quad (1.30)$$

$$\int_0^\infty r^\nu s^{-\left(\frac{1}{2}\right)} s^{\left(\frac{1}{2}\right)} J_\nu(rs) dr = \frac{2\nu!}{(\nu-1)!} s^{-\nu} \quad (1.31)$$

Collecting the r raised to a power terms, Eq. (1.24) becomes,

$$G(s, \Theta) = 2\pi \sum_{\nu=1}^{\infty} \int_0^\infty \frac{(-1)^{\nu-1} (\pi \sin \Theta)^{2(\nu-1)}}{(\nu-1)!(\nu-1)!} \frac{\Gamma\left(\frac{1}{2}\right) \Gamma\left(\nu + \frac{1}{2}\right)}{(\pi s \cos \Theta)^\nu} r^\nu J_\nu(2\pi s r \cos \Theta) dr \quad (1.32)$$

Let $r = \frac{r'}{2\pi \cos \Theta}$; $dr = \frac{dr'}{2\pi \cos \Theta}$,

$$G(s, \Theta) = 2\pi \sum_{\nu=1}^{\infty} \int_0^\infty \frac{(-1)^{\nu-1} (\pi \sin \Theta)^{2(\nu-1)}}{(\nu-1)!(\nu-1)!} \frac{\Gamma\left(\frac{1}{2}\right) \Gamma\left(\nu + \frac{1}{2}\right)}{(\pi s \cos \Theta)^\nu} \frac{r^\nu}{(2\pi \cos \Theta)^{\nu+1}} J_\nu(sr') dr' \quad (1.33)$$

By applying Eq. (1.31), Eq. (1.33) becomes,

$$G(s, \Theta) = 2\pi \sum_{\nu=1}^{\infty} \frac{(-1)^{\nu-1} (\pi \sin \Theta)^{2(\nu-1)}}{(\nu-1)!(\nu-1)!} \frac{\Gamma\left(\frac{1}{2}\right) \Gamma\left(\nu + \frac{1}{2}\right)}{(\pi s \cos \Theta)^\nu (2\pi \cos \Theta)^{\nu+1}} \frac{2\nu!}{(\nu-1)!} s^{-\nu} \quad (1.34)$$

By collecting power terms of s , Eq. (1.34) becomes,

$$G(s, \Theta) = 2\pi \sum_{\nu=1}^{\infty} \frac{(-1)^{\nu-1} (\pi \sin \Theta)^{2(\nu-1)}}{(\nu-1)!(\nu-1)!} \frac{\Gamma\left(\frac{1}{2}\right) \Gamma\left(\nu + \frac{1}{2}\right)}{(\pi \cos \Theta)^{2\nu+1} 2^{\nu+1}} \frac{2\nu!}{(\nu-1)!} s^{-2\nu} \quad (1.35)$$

$H(s, \Phi)$, the space Fourier transform of $h(\phi) = \sin \phi$ is given as follows where there is no dependence on θ :

The spectrum of $\sin \phi$ and $\sin \theta$ are equivalent. Applying a change of variable to the Fourier transform of $g(\theta) = \sin \theta$.

$$\theta \implies \phi \quad \text{implies} \quad \Theta \implies \Phi$$

Therefore, Φ replaces Θ in Eq. (1.35),

$$H(s, \Phi) = 2\pi \sum_{\nu=1}^{\infty} \frac{(-1)^{\nu-1} (\pi \sin \Phi)^{2(\nu-1)}}{(\nu-1)!(\nu-1)!} \frac{\Gamma\left(\frac{1}{2}\right) \Gamma\left(\nu + \frac{1}{2}\right)}{(\pi \cos \Phi)^{2\nu+1} 2^{\nu+1}} \frac{2\nu!}{(\nu-1)!} s^{-2\nu} \quad (1.36)$$

The time Fourier transform of $K(t) = \text{Re}\{\exp(i\omega_n t)\}$ where ω_n is the

angular frequency is given [4] as follows:

$$\int_0^{\infty} \cos \omega_n t \exp(-i\omega t) dt = \frac{1}{2\pi} \frac{1}{2} [\delta(\omega - \omega_n) + \delta(\omega + \omega_n)] \quad (1.37)$$

A very important theorem of Fourier analysis states that the Fourier transform of a product is the convolution of the individual Fourier transforms [10]. By applying this theorem, the spacetime Fourier transform of an orbitsphere, $M(s, \Theta, \Phi, \omega)$ is of the following form:

$$M(s, \Theta, \Phi, \omega) = F(s) \otimes G(s, \Theta) \otimes H(s, \Phi) K(\omega) \quad (1.38)$$

Therefore, the spacetime Fourier transform, $M(s, \Theta, \Phi, \omega)$, is the convolution of Eqs. (1.11), (1.35), (1.36), and (1.37).

$$\begin{aligned} M(s, \Theta, \Phi, \omega) = & 4\pi \text{sinc}(2sr_n) \otimes 2\pi \sum_{v=1}^{\infty} \frac{(-1)^{v-1} (\pi \sin \Theta)^{2(v-1)}}{(v-1)!(v-1)!} \frac{\Gamma\left(\frac{1}{2}\right) \Gamma\left(v + \frac{1}{2}\right)}{(\pi \cos \Theta)^{2v+1} 2^{v+1}} \frac{2v!}{(v-1)!} s^{-2v} \\ & \otimes 2\pi \sum_{v=1}^{\infty} \frac{(-1)^{v-1} (\pi \sin \Phi)^{2(v-1)}}{(v-1)!(v-1)!} \frac{\Gamma\left(\frac{1}{2}\right) \Gamma\left(v + \frac{1}{2}\right)}{(\pi \cos \Phi)^{2v+1} 2^{v+1}} \frac{2v!}{(v-1)!} s^{-2v} \frac{1}{4\pi} [\delta(\omega - \omega_n) + \delta(\omega + \omega_n)] \end{aligned} \quad (1.39)$$

The condition for nonradiation of a moving charge-density function is that the spacetime Fourier transform of the current-density function must not have waves synchronous with waves traveling at the speed of light, that is synchronous with $\frac{\omega_n}{c}$ or synchronous with $\frac{\omega_n}{c} \sqrt{\frac{\epsilon}{\epsilon_0}}$ where ϵ is

the dielectric constant of the medium. The Fourier transform of the charge-density function of the orbitsphere (bubble of radius r) is given by Eq. (1.39). In the case of time harmonic motion, the current-density function is given by the time derivative of the charge-density function. Thus, the current-density function is given by the product of the constant angular velocity and the charge-density function. The Fourier transform of the current-density function of the orbitsphere is given by the product of the constant angular velocity and Eq. (1.39). Consider the radial and time parts of, K_{\perp} , the Fourier transform of the current-density function where the angular transforms are not zero:

$$\begin{aligned} K(s, \Theta, \Phi, \omega) = & 4\pi \omega_n \frac{\sin(2sr_n)}{2sr_n} \otimes 2\pi \sum_{v=1}^{\infty} \frac{(-1)^{v-1} (\pi \sin \Theta)^{2(v-1)}}{(v-1)!(v-1)!} \frac{\Gamma\left(\frac{1}{2}\right) \Gamma\left(v + \frac{1}{2}\right)}{(\pi \cos \Theta)^{2v+1} 2^{v+1}} \frac{2v!}{(v-1)!} s^{-2v} \\ & \otimes 2\pi \sum_{v=1}^{\infty} \frac{(-1)^{v-1} (\pi \sin \Phi)^{2(v-1)}}{(v-1)!(v-1)!} \frac{\Gamma\left(\frac{1}{2}\right) \Gamma\left(v + \frac{1}{2}\right)}{(\pi \cos \Phi)^{2v+1} 2^{v+1}} \frac{2v!}{(v-1)!} s^{-2v} \frac{1}{4\pi} [\delta(\omega - \omega_n) + \delta(\omega + \omega_n)] \end{aligned} \quad (1.40)$$

For the case that the current-density function is constant, the delta function of Eq. (1.40) is replaced by a constant. For time harmonic motion, with angular velocity, ω_n , Eq. (1.40) is nonzero only for $\omega = \omega_n$; thus, $-\infty < s < \infty$ becomes finite only for the corresponding wavenumber, s_n . The relationship between the radius and the wavelength is

$$v_n = \lambda_n f_n \quad (1.41)$$

$$v_n = 2\pi r_n f_n = \lambda_n f_n \quad (1.42)$$

$$2\pi r_n = \lambda_n \quad (1.43)$$

The motion on the orbitsphere is angular; however, a radial component exists due to Special Relativistic effects. Consider the radial wave vector of the sinc function. When the radial projection of the velocity is c

$$s_n \cdot v_n = s_n \cdot c = \omega_n \quad (1.44)$$

the relativistically corrected wavelength given by Eq. (1.249) is²

2. The special relativistic length contraction relationship observed for a laboratory frame relative to an inertial frame moving at constant rectilinear velocity v in the direction of velocity v is

$$l = l_o \sqrt{1 - \frac{v^2}{c^2}} \quad (1)$$

Consider the distance on a great circle given by

$$\int_0^{2\pi} r d\theta = r\theta \Big|_0^{2\pi} = 2\pi r \quad (2)$$

In a gedanken experiment at a fixed position, the distance undergoes length contraction only in the θ direction as $v \rightarrow c$. Thus, as $v \rightarrow c$ the distance on a great circle approaches its radius which is the relativistically contracted electron wavelength. In the case of the charge motion, the components must be checked relative to waves traveling at the speed of light. In this case a contracted wavelength arises.

The charge motion may be visualized. From the visualization, the nonradiation condition becomes apparent. At light speed, there can be no motion transverse to the radius. The radial projection of the time harmonic motion of a point charge of a great circle becomes equivalent to a time harmonic oscillator moving along an axis of distance $2r_n$ in the direction of r . In spherical coordinates, the lab frame is at rest at the origin. Relativistic invariance of charge requires that all of the charge of a current loop be projected onto a line in the radial direction. For $n=1$, $\ell=0$, the charge is uniformly distributed. Consider, the radial projection of a point charge on a great circle at $\phi=0$ and a point charge at $\phi=\pi$. Both points move from opposite ends of a line of length $2r_n$ ($-r_n \leq r \leq +r_n$) and are at the origin in a quarter of a period which is time $t = \frac{r_n}{2c}$. The points then cross. (The crossing is equivalent to elastic scattering at the origin which results in a momentum reversal for both points.) The points interchange roles and travel to the opposite starting points in a half of a period which is time $t = \frac{2r_n}{2c}$. So, with

$$\lambda_n = r_n \quad (1.45)$$

(i.e. the lab frame motion in the angular direction goes to zero as the velocity approaches the speed of light as given by Eq. (24.15)). The charge-density functions in spherical coordinates plus time are given by Eqs. (1.64-1.65). In the case of Eq. (1.64), the wavelength of Eq. (1.44) is independent of θ ; whereas, in the case of Eq. (1.65), the wavelength in Eq. (1.44) is a function of $\sin\theta$. Thus, in the latter case, Eq. (1.45) holds wherein the relationship of wavelength and the radius as a function of θ are given by $r_n \sin\theta = \lambda_n \sin\theta$.

The equipotential, uniform or constant charge-density function (Eq. (1.64)) further comprises a current pattern given in the ORBITSphere EQUATION OF MOTION FOR $\ell = 0$ section and corresponds to the spin function of the electron. It also corresponds to the nonradiative $n=1, \ell = 0$ state of atomic hydrogen. There is acceleration without radiation. In this case, centripetal acceleration. A static charge distribution exists even though each point on the surface is accelerating along a great circle. Haus' condition predicts no radiation for the entire ensemble.

In cases of orbitals of heavier elements and excited states of one electron-atoms and atoms or ions of heavier elements which are not constant as given by Eq. (1.65), the constant spin function is modulated by a time and spherical harmonic function. The modulation or traveling charge-density wave corresponds to an orbital angular momentum in addition to a spin angular momentum. These states are typically referred to as p, d, f, etc. orbitals and correspond to an ℓ quantum number not equal to zero. Haus' condition also predicts nonradiation for a constant spin function modulated by a time and spherically harmonic orbital function. However, in the case that such a state arises as an excited state by photon absorption, it is radiative due to a radial dipole term in its current-density function since it possesses spacetime Fourier transform

respect to each position, a point left and a point reappeared in $t = \frac{2r_n}{2c}$. Since

$T = \frac{2\pi}{\omega} = \frac{\lambda}{c}$, the wavelength is r_n . This situation applies for any ϕ . In the lab frame, the current is uniform and constant. In the frame synchronous with waves traveling at the speed of light, the motion is equivalent to no net current and no net charge motion. Thus, no radiation is possible.

When all positions of the orbitsphere are considered in the gedanken experiment, it is apparent that the lab-frame electron motion in on a sphere with a radius contracted by the factor 2π . The derivation is given in the Special Relativistic Correction to the Ionization Energies section. With the wavelength in the speed of light frame given by Eq. (1.45), the relativistic invariance of the angular momentum of the electron of \hbar (Eq. (1.57) gives the corresponding electron mass in the mass density as $2\pi m_e$.

components synchronous with waves traveling at the speed of light as given in the INSTABILITY OF EXCITED STATES section.

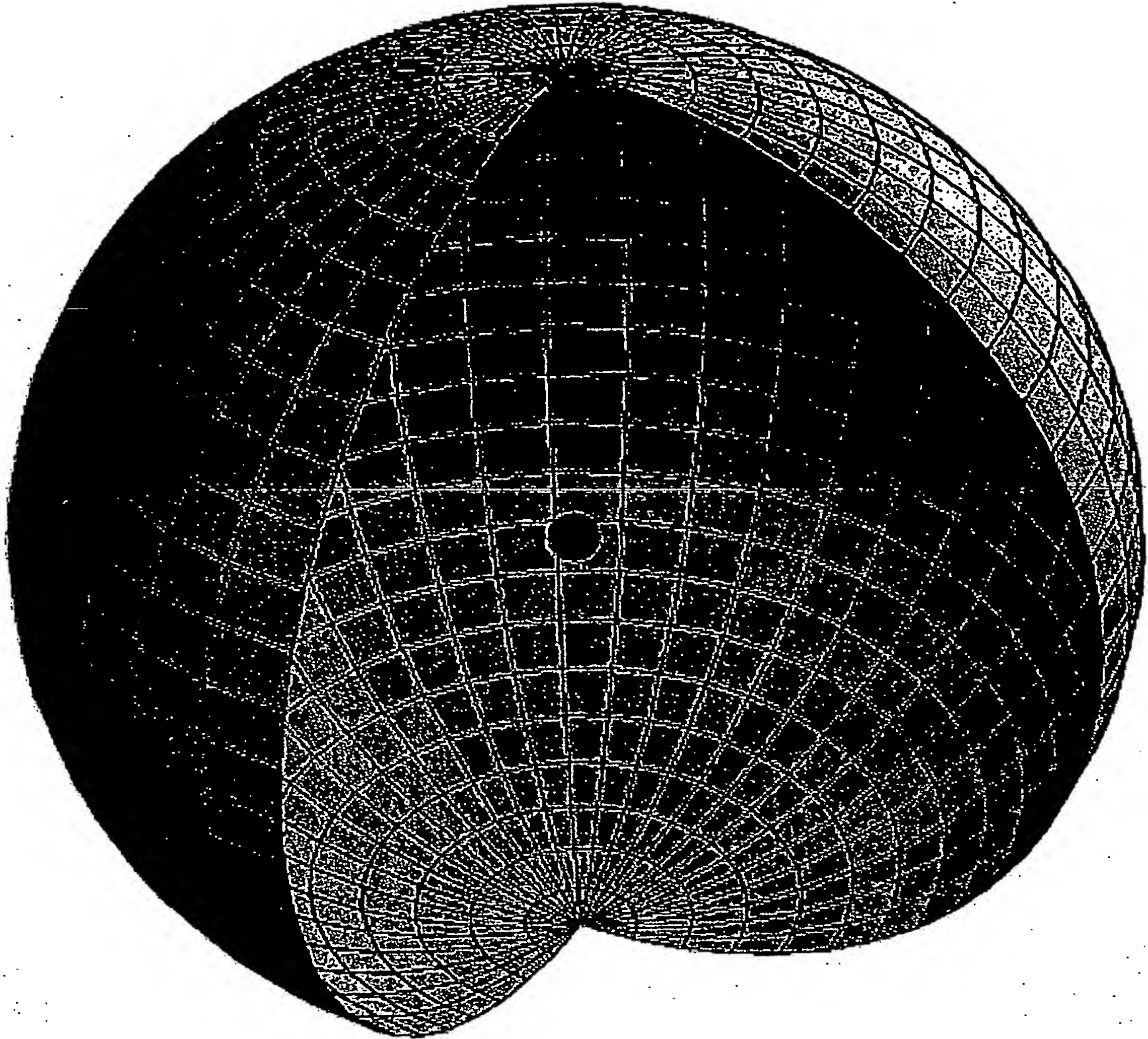
Substitution of Eq. (1.45) into the sinc function results in the vanishing of the entire Fourier transform of the current-density function.

Thus, spacetime harmonics of $\frac{\omega_n}{c} = k$ or $\frac{\omega_n}{c} \sqrt{\frac{\epsilon}{\epsilon_0}} = k$ do not exist for which

the Fourier transform of the current-density function is nonzero. Radiation due to charge motion does not occur in any medium when this boundary condition is met. Note that the boundary condition for the solution of the radial function of the hydrogen atom with the Schrödinger equation is that $\Psi \rightarrow 0$ as $r \rightarrow \infty$. Here, however, the boundary condition is derived from Maxwell's equations: For non-radiative states, the current-density function must not possess spacetime Fourier components that are synchronous with waves traveling at the speed of light. An alternative derivation which provides acceleration without radiation is given by Abbott [11]. Bound electrons are described by a charge-density (mass-density) function which is the product of a radial delta function, Eq. (1.3), two angular functions (spherical harmonic functions), and a time harmonic function. This is a solution of Laplace's Equation. Thus, this radial function implies that allowed states are two-dimensional spherical shells (zero thickness ³) of charge density (and mass density) at specific radii r_n . These shells are referred to as electron orbitspheres. See Figure 1.1 for a pictorial representation of an orbitsphere.

³ The orbitsphere has zero thickness, but in order that the speed of light is a constant maximum in any frame including that of the gravitational field that propagates out as a light-wave front at particle production, it gives rise to a spacetime dilation equal to 2π times the Newtonian gravitational or Schwarzschild radius $r_g = \frac{2Gm_e}{c^2} = 1.3525 \times 10^{-57} \text{ m}$ according to Eqs. (23.36) and (23.140b) and discussion at the footnote after Eq. (23.40). This corresponds to a spacetime dilation of $8.4980 \times 10^{-57} \text{ m}$ or $2.8346 \times 10^{-65} \text{ s}$. Although the orbitsphere does not occupy space in the third spatial dimension, its mass discontinuity effectively "displaces" spacetime wherein the spacetime dilation can be considered a "thickness" associated with its gravitational field.

Figure 1.1. The orbitsphere is a two dimensional spherical shell of zero thickness with the Bohr radius of the hydrogen atom, $r = a_H$.



Given time harmonic motion and a radial delta function, the relationship between an allowed radius and the electron wavelength is given by Eq. (1.43). Using the de Broglie relationship for the electron mass where the coordinates are spherical,

$$\lambda_n = \frac{h}{p_n} = \frac{h}{m_e v_n} \quad (1.46)$$

the magnitude of the velocity for every point on the orbitsphere is

$$v_n = \frac{\hbar}{m_e r_n} \quad (1.47)$$

THE ANGULAR FUNCTION

The radial function for the electron indicates that the electron is two-dimensional. Therefore, the angular mass-density function of the electron, $A(\theta, \phi, t)$, must be a solution of the Laplace equation in two dimensions (plus time),

$$\left[\nabla^2 - \frac{1}{v^2} \frac{\partial^2}{\partial t^2} \right] A(\theta, \phi, t) = 0 \quad (1.48)$$

where $\rho(r, \theta, \phi, t) = f(r)A(\theta, \phi, t) = \frac{1}{r^2} \delta(r - r_n)A(\theta, \phi, t)$ and $A(\theta, \phi, t) = Y(\theta, \phi)k(t)$

$$\left[\frac{1}{r^2 \sin \theta} \frac{\partial}{\partial \theta} \left(\sin \theta \frac{\partial}{\partial \theta} \right)_{r, \phi} + \frac{1}{r^2 \sin^2 \theta} \left(\frac{\partial^2}{\partial \phi^2} \right)_{r, \theta} - \frac{1}{v^2} \frac{\partial^2}{\partial t^2} \right] A(\theta, \phi, t) = 0 \quad (1.49)$$

where v is the linear velocity of the electron. Conservation of momentum and energy allows the angular functions and time functions to be separated.

$$A(\theta, \phi, t) = Y(\theta, \phi)k(t) \quad (1.50)$$

Charge is conserved as well, and the charge of an electron is superimposable with its mass. That is, the angular mass-density function, $A(\theta, \phi, t)$, is also the angular charge-density function.

The electron orbitsphere experiences a constant potential energy because it is fixed at $r = r_n$. In general, the kinetic energy for an inverse squared electric force is half the potential energy. It is the rotation of the orbitsphere that causes spin angular momentum. The rotational energy of a rotating body, E_{rot} , is

$$E_{rot} = \frac{1}{2} I \omega^2 \quad (1.51)$$

where I is the moment of inertia and ω is the angular velocity. The angular velocity must be constant (at a given n) because r is constant and the energy and angular momentum are constant. The allowed angular velocities are related to the allowed frequencies by

$$\omega_n = 2\pi \nu_n \quad (1.52)$$

The allowed frequencies are related to allowed velocities by

$$\nu_n = v_n \lambda_n \quad (1.53)$$

The allowed velocities and angular frequencies are related to r_n by

$$v_n = r_n \omega_n \quad (1.54)$$

$$\omega_n = \frac{\hbar}{m_e r_n^2} \quad (1.55)$$

$$v_n = \frac{\hbar}{m_e r_n} \quad (1.56)$$

The scalar sum of the magnitude of the angular momentum of each infinitesimal point of the orbitsphere L_i of mass m_i must be constant. The constant is \hbar .

$$\sum |L_i| = \sum |r \times m_i v| = m_e r_n \frac{\hbar}{m_e r_n} = \hbar \quad (1.57)$$

where the velocity is given by Eq. (1.47). In the limit, the sum is replaced by a continuous integral over the surface wherein the point element masses and angular momenta are replaced by the corresponding densities. The integral of the magnitude of the angular momentum of the electron is \hbar in any inertial frame and is **relativistically invariant**. The vector projections of the orbitsphere spin angular momentum relative to the Cartesian coordinates are given in the Spin Angular Momentum of the Orbitsphere with $\mathbf{l} = 0$ section.

In the case of an excited state, the charge-density function of the electron orbitsphere can be modulated by the corresponding "trapped" photon to give rise to orbital angular momentum about the z-axis. The "trapped photon" is a "standing electromagnetic wave" which actually is a circulating wave that propagates around the z-axis. Its source current superimposes with each great circle current loop of the orbitsphere. In order to satisfy the boundary (phase) condition at the orbitsphere surface, the angular and time functions of the photon must match those of its source current which modulates the orbitsphere charge-density function as given in the Equation of the Electric Field Inside the Orbitsphere section. The time-function factor, $k(t)$, for the photon "standing wave" is identical to the time-function factor of the orbitsphere. Thus, the angular frequency of the "trapped photon" has to be identical to the angular frequency of the electron orbitsphere, ω_n given by Eq. (1.55). However, the linear velocity of the modulation component is not given by Eq. (1.54)—the orbital angular frequency is with respect to the z-axis; thus, the distance from the z-axis must be substituted for the orbitsphere radius of Eq. (1.54). The vector projections of the orbital angular momentum and the spin angular momentum of the orbitsphere are given in the Rotational Parameters of the Electron (Angular Momentum, Rotational Energy, and Moment of Inertia) section. Eq. (1.49) becomes

$$-\frac{\hbar^2}{2I} \left[\frac{1}{\sin \theta} \frac{\partial}{\partial \theta} \left(\sin \theta \frac{\partial}{\partial \theta} \right)_{r,\phi} + \frac{1}{\sin^2 \theta} \left(\frac{\partial^2}{\partial \phi^2} \right)_{r,\theta} \right] A(\theta, \phi, t) = E_{rot} A(\theta, \phi, t) \quad (1.58)$$

The spacetime angular function, $A(\theta, \phi, t)$, is separated into an angular and a time function, $Y(\theta, \phi)k(t)$. The solution of the time harmonic function is $k(t) = e^{i\omega_n t}$. When the time harmonic function is eliminated,

$$-\frac{\hbar^2}{2I} \left[\frac{1}{\sin \theta} \frac{\partial}{\partial \theta} \left(\sin \theta \frac{\partial}{\partial \theta} \right)_{r,\phi} + \frac{1}{\sin^2 \theta} \left(\frac{\partial^2}{\partial \phi^2} \right)_{r,\theta} \right] Y(\theta, \phi) = E_{rot} Y(\theta, \phi) \quad (1.59)$$

Eq. (1.59) is the equation for the rigid rotor. The angular function can be separated into a function of θ and a function of ϕ and the solutions are well known [12]. The energies are given by

$$E_{rot} = \frac{\hbar^2 \ell(\ell+1)}{2I} \quad \ell = 0, 1, 2, 3, \dots, \quad (1.60)$$

where the moment of inertia, I , is derived in the Rotational Parameters of the Electron (Angular Momentum, Rotational Energy, and Moment of Inertia) section. The angular functions are the spherical harmonics, $Y_\ell^m(\theta, \phi) = P_\ell^m(\cos \theta) e^{im\phi}$. The spherical harmonic $Y_0^0(\theta, \phi) = 1$ is also a solution. The real parts of the spherical harmonics vary between -1 and 1 . But the mass of the electron cannot be negative; and the charge cannot be positive. Thus, to insure that the function is positive definite, the form of the angular solution must be a superposition:

$$Y_0^0(\theta, \phi) + Y_\ell^m(\theta, \phi) \quad (1.61)$$

(Note that $Y_\ell^m(\theta, \phi) = P_\ell^m(\cos \theta) e^{im\phi}$ are not normalized here as given by Eq. (3.53) of Jackson [13]; however, it is implicit that magnitude is made to satisfy the boundary condition that the function is positive definite and Eq. (1.63) is satisfied.) $Y_0^0(\theta, \phi)$ is called the angular spin function corresponding to the quantum numbers $s = \frac{1}{2}$; $m_s = \pm \frac{1}{2}$ as given in the Spin

Angular Momentum of the Orbitsphere with $\ell = 0$ section. $Y_\ell^m(\theta, \phi)$ is called the angular orbital function corresponding to the quantum numbers $\ell = 0, 1, 2, 3, 4, \dots$; $m_\ell = -\ell, -\ell + 1, \dots, 0, \dots, +\ell$. $Y_\ell^m(\theta, \phi)$ can be thought of as a modulation function. The charge density of the entire orbitsphere is the total charge divided by the total area, $\frac{-e}{4\pi r_n^2}$. The

fraction of the charge of an electron in any area element is given by

$$N[Y_0^0(\theta, \phi) + Y_\ell^m(\theta, \phi)] r_n^2 \sin \theta d\theta d\phi, \quad (1.62)$$

where N is the normalization constant. Therefore, the normalization constant is given by

$$-e = N r_n^2 \int_0^\pi \int_0^{2\pi} [Y_0^0(\theta, \phi) + Y_\ell^m(\theta, \phi)] \sin \theta d\theta d\phi \quad (1.63)$$

For $\ell = 0$, $N = \frac{-e}{8\pi r_n^2}$. For $\ell \neq 0$, $N = \frac{-e}{4\pi r_n^2}$. The charge-density functions including the time-function factor are

$$\ell = 0$$

$$\rho(r, \theta, \phi, t) = \frac{e}{8\pi r^2} [\delta(r - r_n)] [Y_0^0(\theta, \phi) + Y_\ell^m(\theta, \phi)] \quad (1.64)$$

$$\ell \neq 0$$

$$\rho(r, \theta, \phi, t) = \frac{e}{4\pi r^2} [\delta(r - r_n)] [Y_0^0(\theta, \phi) + \text{Re}\{Y_\ell^m(\theta, \phi)[1 + e^{i\omega_n t}]\}] \quad (1.65a)$$

$$\rho(r, \theta, \phi, t) = \frac{e}{4\pi r^2} [\delta(r - r_n)] [Y_0^0(\theta, \phi) + \text{Re}\{Y_\ell^m(\theta, \phi)e^{i\omega_n t}\}] \quad (1.65b)$$

where

$$\text{Re}\{Y_\ell^m(\theta, \phi)[1 + e^{i\omega_n t}]\} = \text{Re}\{Y_\ell^m(\theta, \phi) + Y_\ell^m(\theta, \phi)e^{i\omega_n t}\} = P_\ell^m(\cos\theta)\cos m\phi + P_\ell^m(\cos\theta)\cos(m\phi + \omega_n t)$$

or $\text{Re}\{Y_\ell^m(\theta, \phi)e^{i\omega_n t}\} = P_\ell^m(\cos\theta)\cos(m\phi + \omega_n t)$ and to keep the form of the spherical harmonic as a traveling wave about the z-axis, $\omega_n = m\omega_n^4$. In the cases that $m \neq 0$, Eq. (1.65) is a traveling charge-density wave that moves on the surface of the orbitsphere about the z-axis with frequency ω_n and modulates the orbitsphere corresponding to $\ell = 0$. The latter gives rise to spin angular momentum as given in the SPIN ANGULAR MOMENTUM OF THE ORBITSPHERE WITH $\ell = 0$ section. The spin and orbital angular momenta may couple as given in the ORBITAL AND SPIN SPLITTING section. In the cases that $\ell \neq 0$ and $m=0$ the charge is moving or rotating about the z-axis with frequency ω_n , but the charge density is not time dependent. The photon equations which correspond to the orbitsphere states, Eqs. (1.64) and (1.65), are given in the Excited States of the One-Electron Atom (Quantization) section. In addition to Haus' condition given by Eqs. (1.44-1.45), the orbitsphere states given by Eqs. (1.64-1.65) are shown to be nonradiative with the same condition as that of Eq. (1.45) applied to the vector potential as shown in Appendix I: Nonradiation Based on the Electromagnetic Fields and the Poynting Power

⁴ In Eq. (1.65a), $Y_0^0(\theta, \phi)$, a constant function, is added to a spherical harmonic function times $[1 + e^{i\omega_n t}]$. Consider the term $\text{Re}\{Y_\ell^m(\theta, \phi)[1 + e^{i\omega_n t}]\}$. The first term corresponds to $Y_\ell^m(\theta, \phi)$ times one and has $\omega_n = 0$; so, $m=0$ and $\ell=0$ is selected. This is equivalent to another constant function modulated by the spherical harmonic function (second term) which spins around the z-axis and comprises a traveling modulation wave. One rotation of the spherical harmonic function occurs in one period. Thus, Eq. (1.65a) can be rearranged to represent the electron as a superposition of a pure spin function plus a spin function that is modulated. Or, directly, Eq. (1.65a) represents the sum of a spin function and a modulation function times a time dependent function, $[1 + e^{i\omega_n t}]$. The latter can be considered a phasor corresponding to the modulation function spinning about the z-axis.

Vector.

For $n=1$, and $\ell = 0$, $m=0$, and $s=1/2$, the charge (and mass) distribution is spherically symmetric and $M_{1,0,0,1/2} = -4.552 \text{ Cm}^{-2}$ everywhere on the orbitsphere. Similarly, for $n=2$, $\ell = 0$, $m=0$, and $s=1/2$, the charge distribution everywhere on the sphere is $M_{2,0,0,1/2} = -1.138 \text{ Cm}^{-2}$. For $n=2$, $\ell = 1$, $m=0$, and $s=1/2$, the charge distribution varies with θ . $Y_1^0(\phi, \theta)$ is a maximum at $\theta=0^\circ$ and the charge density is also a maximum at this point, $M_{2,1,0,1/2}(\theta=0^\circ) = -2.276 \text{ Cm}^{-2}$. The charge density decreases as θ increases; a minimum in the charge density is reached at $\theta=180^\circ$, $M_{2,1,0,1/2}(\theta=180^\circ) = 0 \text{ Cm}^{-2}$.

For $\ell = 1$ and $m=\pm 1$, the spherical harmonics are complex, and the angular functions comprise linear combinations of

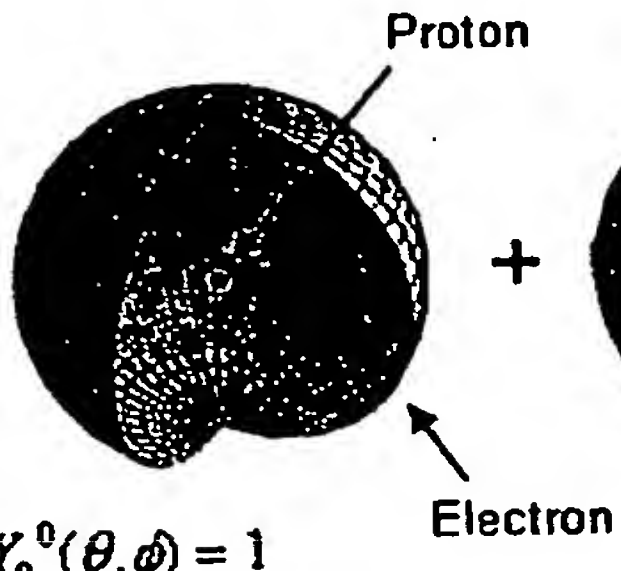
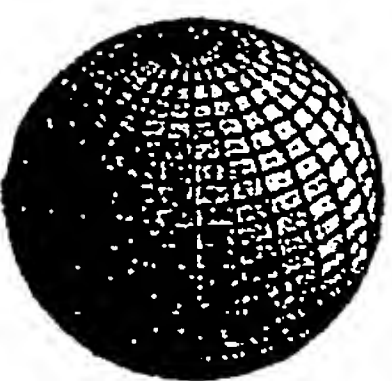
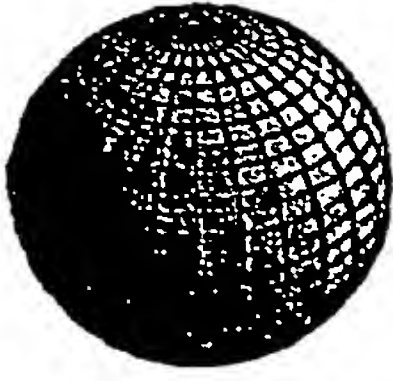
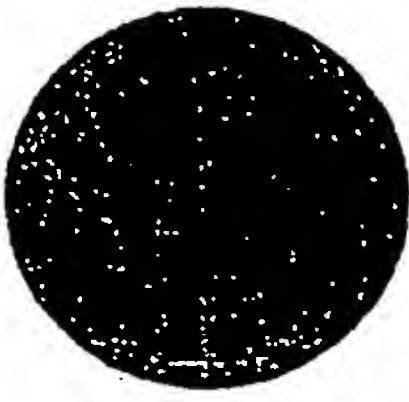
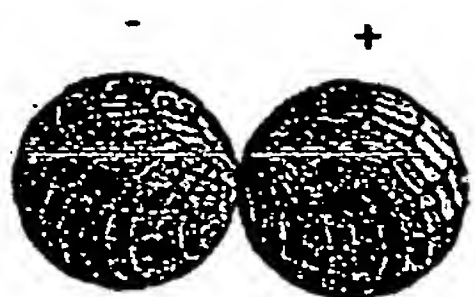
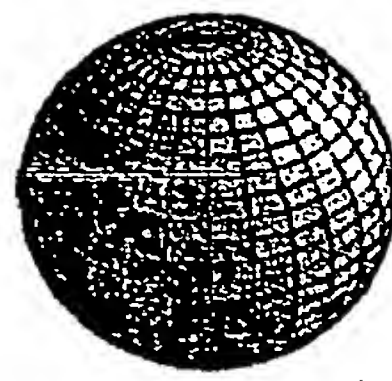
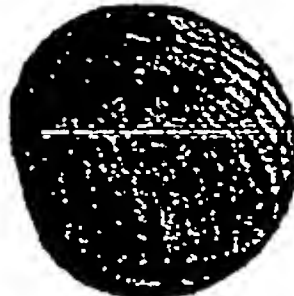
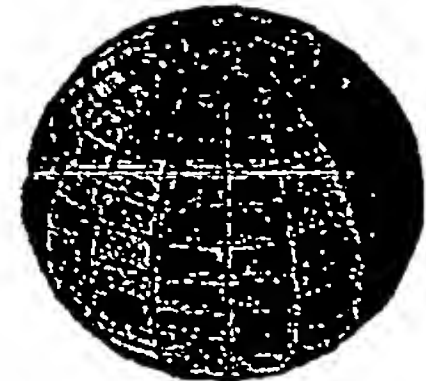
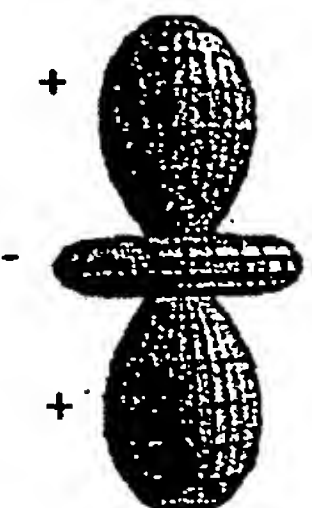
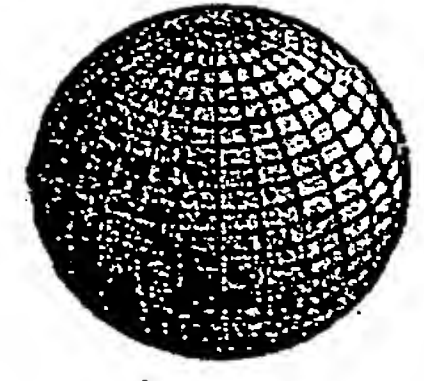
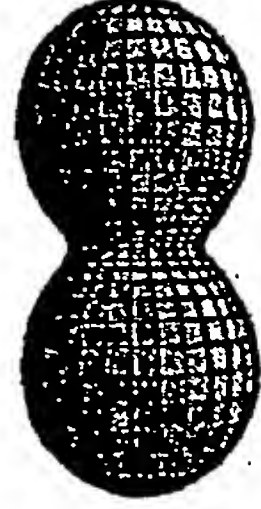
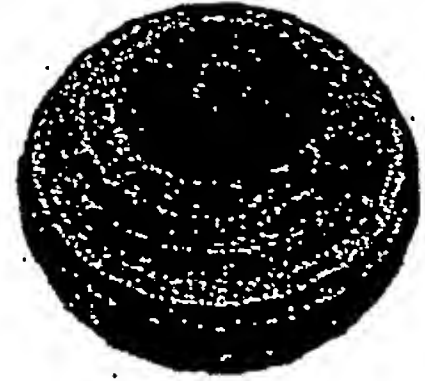
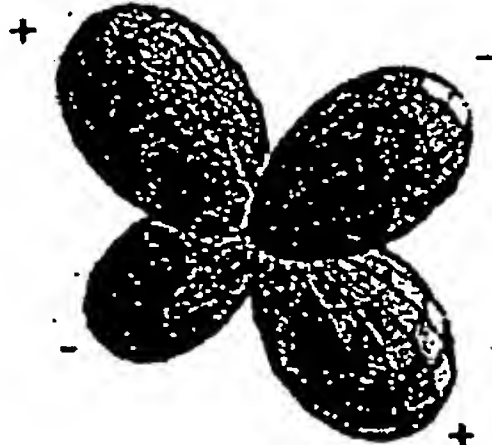
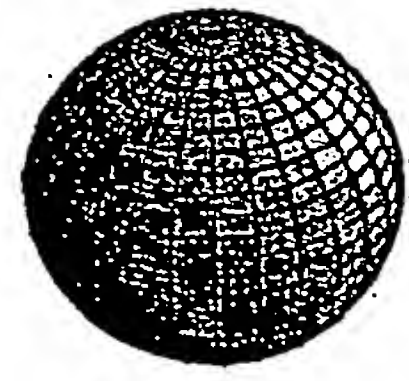

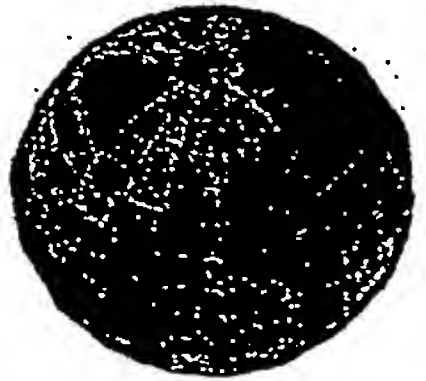
$$Y_{1,x} = \sin \theta \cos \phi \quad (1.66)$$

$$Y_{1,y} = \sin \theta \sin \phi \quad (1.67)$$

Each of $Y_{1,x}$ and $Y_{1,y}$ is the component factor-part of a phasor. They are not components of a vector; however, the x and y designation corresponds, respectively, to the historical p_x and p_y probability-density functions of quantum mechanics. $Y_{1,x}$ is a maximum at $\theta=90^\circ$ and $\phi=0^\circ$; $M_{2,1,x,1/2}(90^\circ, 0^\circ) = -1.138 \text{ Cm}^{-2}$. Figure 1.2 gives pictorial representation of how the modulation function changes the electron density on the orbitsphere for several ℓ values⁵. Figure 1.3 gives a pictorial representation of the charge-density wave of a p orbital that modulates the constant spin function and rotates around the z -axis. A single time point is shown for $\ell = 1$ and $m=\pm 1$ in Eq. (1.65).

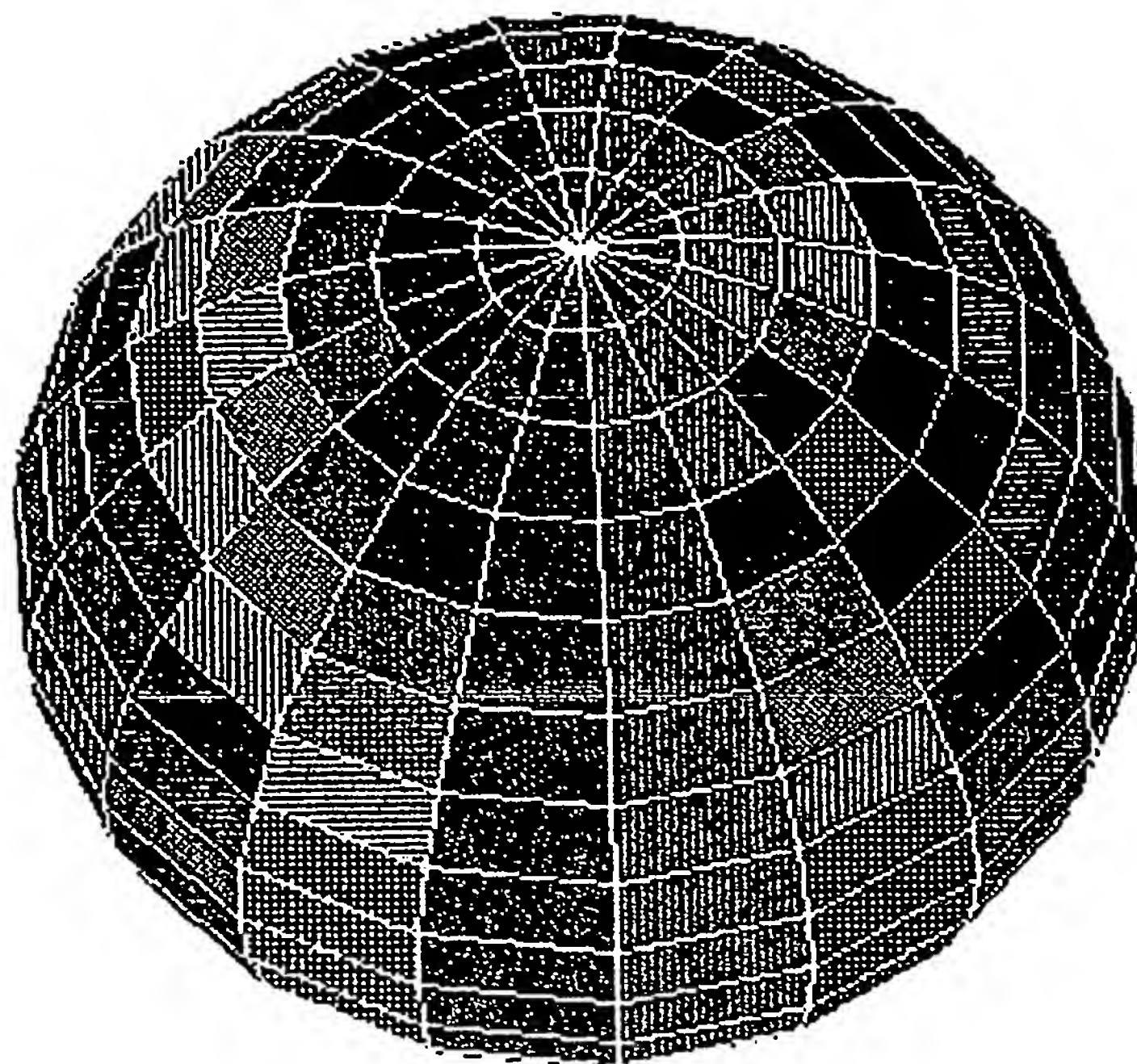
⁵ When the electron charge appears throughout this text in a function involving a linear combination of the spin and orbital functions, it is implicit that the charge is normalized. A constant times a solution to the wave equation such as a constant times a spherical harmonic function is a solution. The integral of the constant mass-density function corresponding to spin over the orbitsphere is the mass of the electron. The integral of any spherical harmonic modulation function corresponding to orbital angular momentum over the orbitsphere is zero. The modulated mass-density function has a lower limit of zero due to the trapped photon which is phase-locked to the modulation function. And, the mass density can not be negative. Thus, the maximum magnitude of the unnormalized spherical harmonic function over all angles must be one. The summation of the constant function and the orbital function is normalized.

Figure 1.2 The orbital function modulates the constant (spin) function.
(shown for $t = 0$; three-dimensional view)

l, m, t	Modulation Function (Orbital)	Constant Function (Spin)	Spatial Charge Density Function	Surface Charge Density Function (Orbitsphere)
0,0,0	 $Y_0^0(\theta, \phi) = 1$			
1,1,0	 $\text{Re} \{Y_1^1(\theta, \phi)e^{i\omega_1 t}\} = \sin \theta \cos(\phi + \omega_1 t)$			
2,0,0	 $\text{Re} \{Y_2^0(\theta, \phi)e^{i\omega_2 t}\} = \frac{3}{2}\cos^2 \theta - \frac{1}{2}$			
2,1,0	 $\text{Re} \{Y_2^1(\theta, \phi)e^{i\omega_2 t}\} = \sin \theta \cos \theta \cos(\phi + \omega_2 t)$			

Increasing Electron Density

Figure 1.3. A pictorial representation of the charge-density wave of a p orbital that modulates the constant spin function and travels on the surface of the orbitsphere around the z-axis. A single time point is shown for $\lambda = 1$ and $m = \pm 1$ in Eq. (1.65). The charge density increases from red to violet. The z-axis is the vertical axis.



THE ORBITSPIHERE EQUATION OF MOTION FOR $\ell = 0$

Stern-Gerlach-Experiment Boundary Conditions

It is known from the Stern-Gerlach experiment that a beam of silver atoms is split into two components when passed through an inhomogeneous magnetic field. This implies that the electron is a spin $1/2$ particle with an intrinsic angular momentum in the direction of the applied field (spin axis) of $\pm \frac{\hbar}{2}$, and the magnitude of the angular

momentum vector which precesses about the spin axis is $\sqrt{\frac{3}{4}}\hbar$.

Furthermore, the magnitude of the splitting implies a magnetic moment of μ_B , a full Bohr magneton, given by Eq. (1.99) corresponding to \hbar of total angular momentum on the axis of the applied field.

The algorithm to generate the $Y_0^0(\phi, \theta)$ orbitsphere equation of motion of the electron (Eqs. (1.64-1.65)) is developed in this section. It was shown in the Angular Function section that the integral of the magnitude of the angular momentum over the orbitsphere must be constant. The constant is \hbar as given by Eq. (1.57). It is shown in this section that the projection of the intrinsic orbitsphere angular momentum onto the spin axis is $\pm \frac{\hbar}{2}$, and the projection onto S , the axis which precesses about the spin axis, is \hbar with a precessing component in the perpendicular plane of $\sqrt{\frac{3}{4}}\hbar$ and a component on the spin axis of $\pm \frac{\hbar}{2}$.

Thus, the mystery of an intrinsic angular momentum of $\pm \frac{\hbar}{2}$ and a total angular momentum in a resonant RF experiment of $L_z = \hbar$ is resolved since the sum of the intrinsic and spin-axis projection of the precessing component is \hbar . The Stern-Gerlach experiment implies a magnetic moment of one Bohr magneton and an associated angular momentum quantum number of $1/2$. Historically, this quantum number is called the spin quantum number, s ($s = \frac{1}{2}$; $m_s = \pm \frac{1}{2}$), and that designation is maintained.

The electron has a measured magnetic field and corresponding magnetic moment of a Bohr magneton and behaves as a spin $1/2$ particle or fermion. For any magnetic field, the solution for the corresponding current from Maxwell's equations is unique. Thus, the electron field requires a unique current according to Maxwell's equations. Several boundary conditions must be satisfied, and the orbitsphere equation of

motion for $\mathbf{l} = 0$ is solved as a boundary value problem. The boundary conditions are:

- (1) each infinitesimal point (position) on the orbitsphere comprising a charge (mass)-density element must have the same angular and linear velocity given by Eqs. (1.55) and (1.56), respectively;
- (2) according to condition 1, every such infinitesimal point must move along a great circle and the current-density distribution must be uniform;
- (3) the electron magnetic moment must align completely parallel or antiparallel with an applied magnetic field in agreement with the Stern-Gerlach experiment;
- (4) according to condition 3, the projection of the intrinsic angular momentum of the orbitsphere onto the z-axis must be $\pm \frac{\hbar}{2}$, and the projection into the transverse plane must be $\pm \frac{\hbar}{4}$ to achieve the spin 1/2 aspect;
- (5) the Larmor excitation of the electron in the applied magnetic field must give rise to a component of electron spin angular momentum that precess about the applied magnetic field such that the contribution along the z-axis is $\pm \frac{\hbar}{2}$ and the projection onto the orthogonal axis which precesses about the z-axis must be $\pm \sqrt{\frac{3}{4}}\hbar$;
- (6) due to conditions 4 and 5, the angular momentum components corresponding to the current of the orbitsphere and that due to the Larmor precession must rise to a total angular momentum on the applied-field axis of $\pm \hbar$;
- (7) due to condition 6, the precessing electron has a magnetic moment of a Bohr magneton, and
- (8) the energy of the transition of the alignment of the magnetic moment with an applied magnetic field must be given by Eqs. (1.194-1.195) corresponding to the extended electron having a total angular momentum on the applied-field axis of $\pm \hbar$.

Consider the derivation of Eqs. (1.58) and (1.59). The moment of inertia of a point particle is mr^2 , and that of a globe spinning about some axis is $I = \frac{2}{3}mr^2$. For $\mathbf{l} = 0$, the electron mass and charge are uniformly distributed over the orbitsphere, a two-dimensional, spherical shell, but the orbitsphere is *not* analogous to a globe. The velocity of a point mass on a spinning globe is a function of θ , but the magnitude of the velocity at each point of the orbitsphere is not a function of θ . To picture the distinction, it is a useful concept to consider that the orbitsphere is comprised of an infinite number of point elements that move on the spherical surface. Then, each point on the sphere with mass m , has the

same angular velocity (ω_n), the same magnitude of linear velocity (v_n), and the same moment of inertia ($m_n r_n^2$). The motion of each point of the orbitsphere is along a great circle, and the motion along each great circle is correlated with the motion on all other great circles such that the sum of all the contributions of the corresponding angular momenta is different from that of a point or globe. The orbitsphere angular momentum is uniquely directed disproportionately along two orthogonal axes.

The current-density function of the orbitsphere is generated from a basis set current-vector field defined as the orbitsphere current-vector field ("orbitsphere-cvf"). This in turn is generated from orthogonal great circle current loops that serve as basis elements. As given in Appendix III, the *continuous* uniform electron current density function $Y_0^0(\phi, \theta)$ (Eqs. (1.64-1.65)) is then exactly generated from this orbitsphere-cvf as a basis element by a convolution operator comprising an autocorrelation-type function. The operator comprises the convolution of each great circle current loop of the orbitsphere-cvf designated as the primary orbitsphere-cvf with a second orbitsphere-cvf basis element designated as the secondary orbitsphere-cvf. Each secondary element is weighted according to the angular momentum of each great circle of a primary orbitsphere-cvf that it replaces by the convolution. The uniform, equipotential charge-density function of the orbitsphere having only a radial discontinuous field at the surface according to Eq. (1) of footnote 8 is constant in time due to the motion of the current along great circles. The current flowing into any given point of the orbitsphere equals the current flowing out to satisfy the current continuity condition, $\nabla \cdot J = 0$.

The current-vector field pattern of the orbitsphere-cvf is not spatially uniform. There is no coincidence or nonuniqueness of elements of the current-vector field. But, there are many crossings among elements at single points on the two dimensional surface of the electron, and the density of the crossings is nonuniform over the surface. *Thus, each element of the basis set to generate the current pattern, a great circle current loop, must be one dimensional so that the crossings are zero dimensional with no element interaction at their crossing.* (This is a logical and necessary geometric progression for the construction of a fundamental particle which is two-dimensional.) In the limit, the basis set generates a continuous two-dimensional current density with a constant charge (mass) density wherein the crossings have no effect on the vector fields. Each one-dimensional element is independent of the others, and its contribution to the angular momentum and magnetic field independently superimposes with that of the others.

This unique aspect of a fundamental particle has the same properties of the superposition properties of the electric and magnetic

fields of a photon. As shown in the Excited States of the One-Electron Atom (Quantization), the Creation of Matter from Energy, Pair Production, and the Leptons sections, the angular momentum in the electric and magnetic fields is conserved in excited states and in the creation of an electron from a photon in agreement with Maxwell's equations. It is useful to regard an electron as a photon frozen in time. The particle-production conditions are given in the latter sections.

GENERATION OF THE ORBITSPIHERE-CVF IN TWO STEPS

The equation of motion for each charge-density element (and correspondingly for each mass-density element) which gives the current pattern of the orbitsphere-cvf is generated in two steps, STEP ONE and STEP TWO, as follows:

Here a procedure is used to generate the current pattern of the orbitsphere-cvf from which the physical properties are derived in the Spin Angular Momentum of the Orbitsphere with $\lambda = 0$ section and are shown to match the boundary conditions.

The current-density of the orbitsphere-cvf is *continuous*, but it may be modeled as a current pattern comprising a superposition of an infinite series of correlated orthogonal great circle current loops. The *time-independent* current pattern is obtained by defining a basis set for generating the current distribution over the surface of a spherical shell of zero thickness. As such a basis set, consider that the electron current is first evenly distributed within two orthogonally linked great-circle current loops. These loops will be further divided into two sets of linked orthogonal pairs wherein each pair undergoes independent transformations over the surface wherein the electron current is correspondingly divided by the number of basis loops, four, and then by the angular span of the transformations to form a normalized current density in each case. In Appendix III, the *continuous* uniform electron current density function $Y_0^0(\phi, \theta)$ (Eqs. (1.64-1.65)) is then exactly generated from this orbitsphere-cvf as a basis element by a convolution operator comprising an autocorrelation-type function.

The stationary or laboratory Cartesian coordinate system for the first step, Step One, of the algorithm to generate the orbitsphere-cvf is shown in Figure 1.4A as the xyz-system. It is also designated the orbitsphere-cvf reference frame. The primed coordinate system is the stationary frame for the basis elements wherein a first current loop always lies in the y'z'-plane, and a second current loop always lies in the x'z'-plane. The primed coordinates are only coincident with the

corresponding xyz-coordinates for the initial positions as shown in Figure 1.4A since the current density pattern is generated by a series of transformations of the primed coordinates relative to the unprimed coordinates. Each successive transformation of the primed system defines an orientation of the basis set in the x'y'z'-frame relative to the xyz-frame that comprises a current element of the current density pattern.

Rotations and reflections are the transformations on the surface of a sphere that may be used to generate the orbitsphere-cvf. The orbitsphere-cvf is simply generated by two steps, each comprising an infinite series of nested rotations of the two orthogonal great circle current loops each by an infinitesimal angle $\pm\Delta\alpha_x$ and $\pm\Delta\alpha_y$ about the new i'-axis and new j'-axis, respectively, which results from the preceding such rotation. Each orientation following the conjugate i' and j' rotation of the two orthogonal great circle current loops wherein the first current loop lies in the j'k'-plane, and the second current loop lies in the i'k'-plane is an element of the infinite series wherein for Step One i'=x', j'=y', k'=z' and for Step Two i'=z', j'=x', k'=y'.

For Step One, the first such pair of orthogonal great circle current loops is shown in Figure 1.4A. The second element of the series is generated by rotation of the first element by an infinitesimal angle $\pm\Delta\alpha_x$ about the first x'-axis followed by a rotation by the infinitesimal angle $\pm\Delta\alpha_y$ about the new (second) y'-axis to form a second x'-axis. The third element of the series is generated by the rotation of the second element by the same infinitesimal angle $\pm\Delta\alpha_x$ about the second x'-axis followed by the rotation by the same infinitesimal angle $\pm\Delta\alpha_y$ about the new (third) y'-axis. In general, the (n+1)th element of the series is generated by the rotation of the nth basis coordinate system by the infinitesimal angle $\pm\Delta\alpha_x$ about the nth x'-axis followed by the rotation of the nth orbitsphere-cvf coordinate system by the infinitesimal angle $\pm\Delta\alpha_y$ about the (n+1)th new y'-axis.

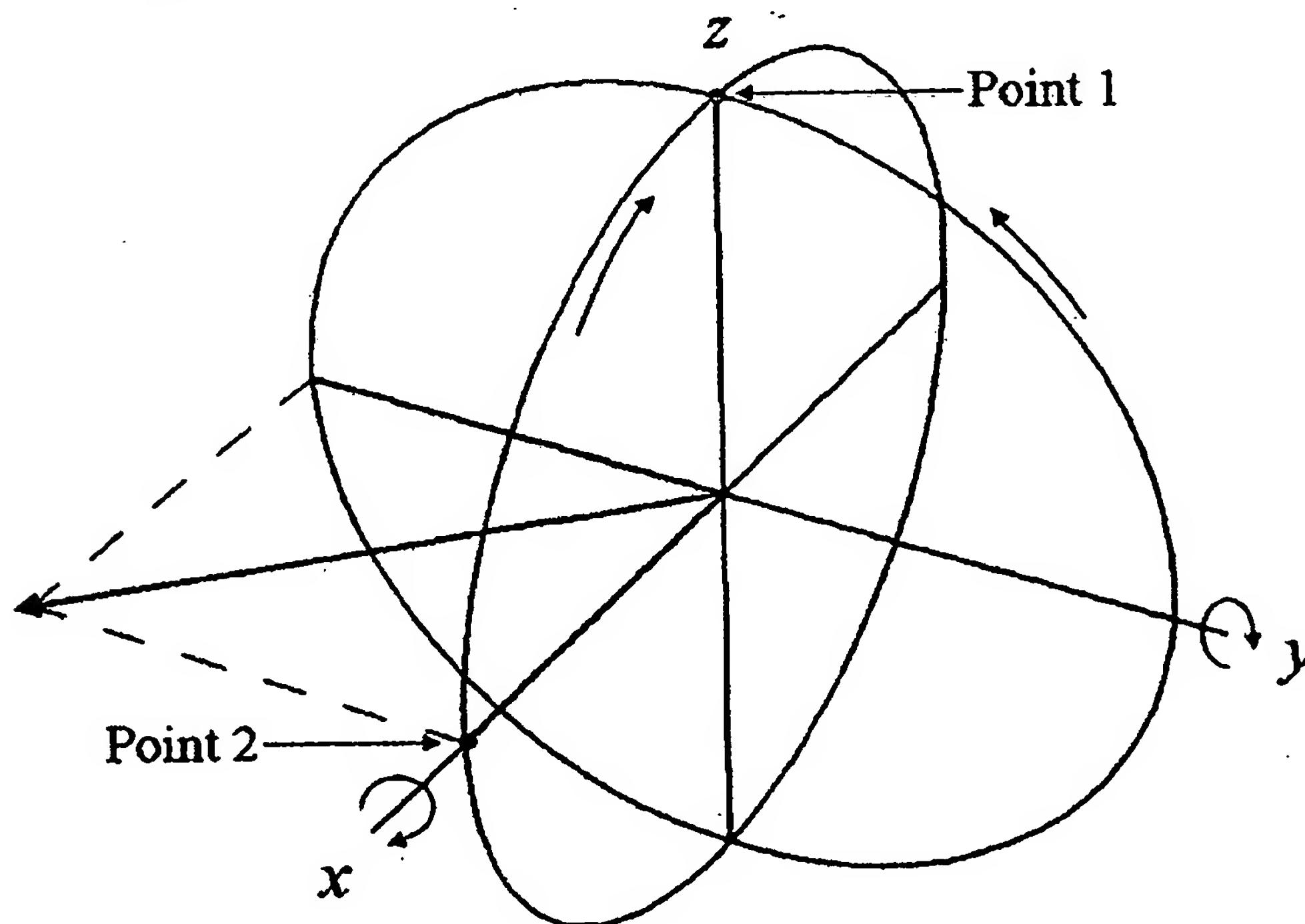
The sign of the corresponding angle is maintained throughout the rotations, and the summation of the reiterative rotations about each of

the i'-axis and the j'-axis is $\lim_{\Delta\alpha \rightarrow 0} \sum_{n=1}^{\frac{\sqrt{2}}{2}\pi} |\Delta\alpha_{i,j}| = \frac{\sqrt{2}}{2}\pi$ when the k'-axis rotates from the k-axis to the -k-axis. (The total angle, $\frac{\sqrt{2}}{2}\pi$, is the hypotenuse of the triangle having the sides of $\frac{\pi}{2}$ radians corresponding to i'-axis

rotations and $\frac{\pi}{2}$ radians corresponding to j'-axis rotations.) Step One and Step Two comprise the use of $\Delta\alpha_i$ and $\Delta\alpha_j$ as given in Table 1.1.

Next, consider two infinitesimal charge (mass)-density elements at two separate positions or points, one and two, of the two orthogonal great circle current loops that serve as the basis set as shown in Figures 1.4A and 1.4B. The vector projection of the corresponding angular momentum at each point of each current element is integrated over the entire orbitsphere-cvf surface to give the electron angular momentum. The correct current pattern is confirmed by achieving the condition that the magnitude of the velocity at any point on the surface is given by Eq. (1.56) and by obtaining the required angular momentum projections of $\frac{\hbar}{2}$ and $\frac{\hbar}{4}$ along the z-axis and along an axis in the xy-plane, respectively, as given in the Spin Angular Momentum of the Orbitsphere with $\ell=0$ section.

Figure 1.4A. Step One. Each point or coordinate position on the continuous two-dimensional electron orbitsphere-cvf defines an infinitesimal charge (mass)-density element which moves along a geodesic orbit comprising a great circle. Two such infinitesimal charges (masses) at points one (moving counter clockwise on the great circle in the $y'z'$ -plane) and two (moving clockwise on the great circle in the $x'z'$ -plane) of two orthogonal great circle current loops in the basis frame are considered as sub-basis elements to generate the current density corresponding to the spin quantum number, $s = \frac{1}{2}$; $m_s = \pm \frac{1}{2}$. The xyz -system is the laboratory frame, and the orthogonal-current-loop basis set is rigid with respect to the $x'y'z'$ -system that undergoes transformations to generate the elements of the electron current density function. The angular momentum of the orthogonal great circle current loops in the $x'y'$ -plane is $\frac{\hbar}{2\sqrt{2}}$.



Thus, the orbitsphere-cvf is generated from two orthogonal great circle current loops which are rotated about the n th i' -axis and then about the $(n+1)$ th j' -axis in Two Steps.

For Step One, consider two charge (mass)-density elements, point one and two, in the basis-set reference frame at time zero. Element one

is at $x'=0$, $y'=0$, and $z'=r_n$ and element two is at $x'=r_n$, $y'=0$, and $z'=0$. Let element one move on a great circle counter clockwise toward the $-y'$ -axis, as shown in Figure 1.4A, and let element two move clockwise on a great circle toward the z' -axis, as shown in Figure 1.4A. The equations of motion, in the sub-basis-set reference frame are given by

point one:

$$x'_1 = 0 \quad y'_1 = -r_n \sin(\omega_n t) \quad z'_1 = r_n \cos(\omega_n t) \quad (1.68a)$$

point two:

$$x'_2 = r_n \cos(\omega_n t) \quad y'_2 = 0 \quad z'_2 = r_n \sin(\omega_n t) \quad (1.68b)$$

For Step Two, consider two charge (mass)-density elements, point one and two, in the basis-set reference frame at time zero. Element one is at $x'=0$, $y'=r_n$, and $z'=0$ and element two is at $x'=r_n$, $y'=0$, and $z'=0$. Let element one move clockwise on a great circle toward the $-z'$ -axis as shown in Figure 1.4B, and let element two move counter clockwise on a great circle toward the y' -axis as shown in Figure 1.4B. The equations of motion, in the basis-set reference frame are given by

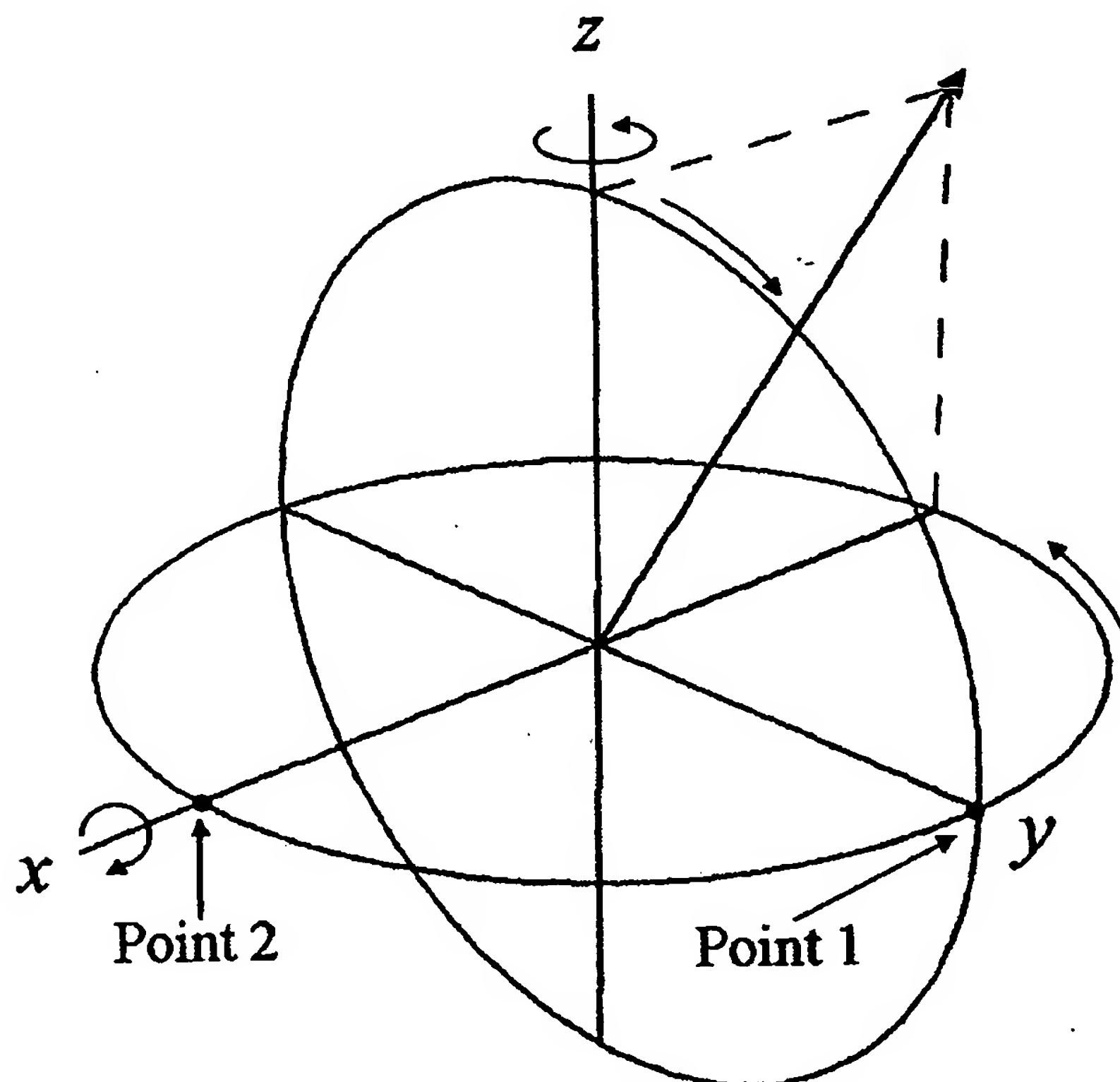
point one:

$$x'_1 = 0 \quad y'_1 = r_n \cos(\omega_n t) \quad z'_1 = -r_n \sin(\omega_n t) \quad (1.69a)$$

point two:

$$x'_2 = r_n \cos(\omega_n t) \quad y'_2 = r_n \sin(\omega_n t) \quad z'_2 = 0 \quad (1.69b)$$

Figure 1.4B. Step Two. The orthogonal great circle basis set is rotated $\Delta\alpha_x = \frac{\pi}{2}$ with respect to the basis set of Step One shown in Figure 1.4A and the direction of the current of the loop in the $y'z'$ -plane is reversed. Point one now moves clockwise on the great circle in the $y'z'$ -plane, and point two moves counter clockwise on the great circle in the $x'y'$ -plane. The angular momentum of the orthogonal great circle current loops in the $-xz$ -plane is $\frac{\hbar}{2\sqrt{2}}$ corresponding to each of the z and $-x$ -components of magnitude $\frac{\hbar}{4}$.



The great circles are rotated by an infinitesimal angle $\pm\Delta\alpha_x$ (a rotation around the x' -axis or z' -axis for Steps One and Two, respectively) and then by $\pm\Delta\alpha_y$ (a rotation around the new y' -axis or x' -axis for Steps One and Two, respectively) where the positive directions are shown in Figures 1.4A and 1.4B, respectively. The coordinates of each point on each rotated great circle (x',y',z') is expressed in terms of the first (x,y,z) coordinates by the following transforms where clockwise rotations are defined as positive:

Step One

$$\begin{bmatrix} x \\ y \\ z \end{bmatrix} = \begin{bmatrix} \cos(\Delta\alpha_y) & 0 & -\sin(\Delta\alpha_y) \\ 0 & 1 & 0 \\ \sin(\Delta\alpha_y) & 0 & \cos(\Delta\alpha_y) \end{bmatrix} \begin{bmatrix} 1 & 0 & 0 \\ 0 & \cos(\Delta\alpha_x) & \sin(\Delta\alpha_x) \\ 0 & -\sin(\Delta\alpha_x) & \cos(\Delta\alpha_x) \end{bmatrix} \begin{bmatrix} x' \\ y' \\ z' \end{bmatrix}$$

$$\begin{bmatrix} x \\ y \\ z \end{bmatrix} = \begin{bmatrix} \cos(\Delta\alpha_y) & \sin(\Delta\alpha_y)\sin(\Delta\alpha_x) & -\sin(\Delta\alpha_y)\cos(\Delta\alpha_x) \\ 0 & \cos(\Delta\alpha_x) & \sin(\Delta\alpha_x) \\ \sin(\Delta\alpha_y) & -\cos(\Delta\alpha_y)\sin(\Delta\alpha_x) & \cos(\Delta\alpha_y)\cos(\Delta\alpha_x) \end{bmatrix} \begin{bmatrix} x' \\ y' \\ z' \end{bmatrix} \quad (1.70a)$$

Step Two

$$\begin{bmatrix} x \\ y \\ z \end{bmatrix} = \begin{bmatrix} 1 & 0 & 0 \\ 0 & \cos(\Delta\alpha_x) & \sin(\Delta\alpha_x) \\ 0 & -\sin(\Delta\alpha_x) & \cos(\Delta\alpha_x) \end{bmatrix} \begin{bmatrix} \cos(\Delta\alpha_z) & \sin(\Delta\alpha_z) & 0 \\ -\sin(\Delta\alpha_z) & \cos(\Delta\alpha_z) & 0 \\ 0 & 0 & 1 \end{bmatrix} \begin{bmatrix} x' \\ y' \\ z' \end{bmatrix}$$

$$\begin{bmatrix} x \\ y \\ z \end{bmatrix} = \begin{bmatrix} \cos(\Delta\alpha_z) & \sin(\Delta\alpha_z) & 0 \\ -\cos(\Delta\alpha_x)\sin(\Delta\alpha_z) & \cos(\Delta\alpha_x)\cos(\Delta\alpha_z) & \sin(\Delta\alpha_x) \\ \sin(\Delta\alpha_x)\sin(\Delta\alpha_z) & -\sin(\Delta\alpha_x)\cos(\Delta\alpha_z) & \cos(\Delta\alpha_x) \end{bmatrix} \begin{bmatrix} x' \\ y' \\ z' \end{bmatrix} \quad (1.70b)$$

where the angular sum is $\lim_{\Delta\alpha \rightarrow 0} \sum_{n=1}^{\frac{\sqrt{2}}{2}\pi} |\Delta\alpha_{i,j}| = \frac{\sqrt{2}}{2}\pi$.

The orbitsphere-cvf is given by n reiterations of Eqs. (1.70a) and (1.70b) for each point on each of the two orthogonal great circles during each of Steps One and Two where the sign of $\pm\Delta\alpha_x$ and $\pm\Delta\alpha_y$ for each Step are given in Table 1.1. The output given by the non-primed coordinates

is the input of the next iteration corresponding to each successive nested rotation by the infinitesimal angle $\pm\Delta\alpha_i$ or $\pm\Delta\alpha_j$, where the magnitude of the angular sum of the n rotations about each of the i '-axis and the j '-axis is $\frac{\sqrt{2}}{2}\pi$. Half of the orbitsphere-cvf is generated during each of Steps One and Two.

Table 1.1. Summary of the results of the matrix transformations of the two sets of two orthogonal current loops to generate the orbitsphere-cvf.

Step	Initial Direction of Angular Momentum Components ($\hat{r} \times \hat{K}$) ^a	Final Direction of Angular Momentum Components ($\hat{r} \times \hat{K}$) ^a	Sign of $\Delta\alpha_i$	Sign of $\Delta\alpha_j$	Initial to Final Axis Transformation	L_{xy}	L_z
1	$\hat{x}, -\hat{y}$	$-\hat{x}, \hat{y}$	$+\Delta\alpha_x$	$+\Delta\alpha_y$	$+x' \rightarrow +y$ $+y' \rightarrow +x$ $+z' \rightarrow -z$	0	$\frac{\hbar}{4}$
2	$-\hat{x}, \hat{z}$	$-\hat{x}, \hat{z}$	$-\Delta\alpha_x$	$+\Delta\alpha_x$	$+z' \rightarrow -x$ $+x' \rightarrow -z$ $+y' \rightarrow -y$	$\frac{\hbar}{4}$	$\frac{\hbar}{4}$
Total						$\frac{\hbar}{4}$	$\frac{\hbar}{2}$

^a \mathbf{K} is the current density, \mathbf{r} is the polar vector of the great circle, and " $\hat{}$ " denotes the unit vectors $\hat{u} \equiv \frac{\mathbf{u}}{|\mathbf{u}|}$.

Thus, in the limit as the number of nested conjugate rotations n goes to infinity and the incremental rotation angles $\pm\Delta\alpha_i$ and $\pm\Delta\alpha_j$, each go to zero, the orbitsphere-cvf is generated from two orthogonal great circle current loops which are rotated about the n th i '-axis and then about the $(n+1)$ th j '-axis until the k '-axis coincides with the $-k$ -axis in two separate implementations of the algorithm comprising the Two Steps. Each Step involves a unique combination of the initial direction of the angular momentum vectors and orientation of the incremental rotation angles as summarized in Table 1.1. In the case of the n th element of Step One, the intersection of the two orthogonal great circle current loops occurs at the n th z '-axis which is along a great circle in a half-plane that is parallel with the z -axis and bisects the $-x+y$ -quadrant of Figure 1.4A. The nested rotations is also equivalent to rotating the orthogonal-great-

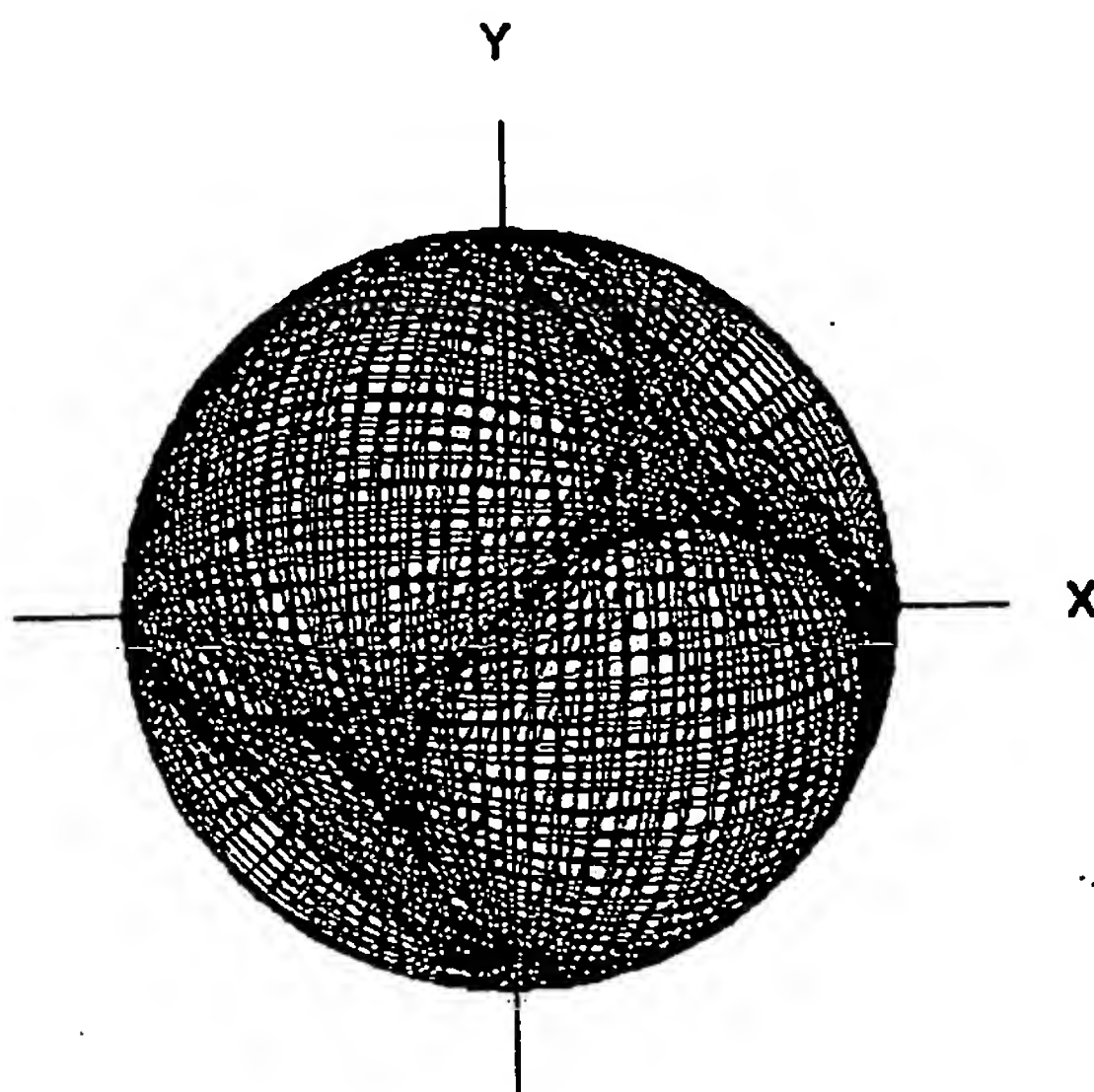
circle basis set about the axis $(i_x, i_y, 0i_z)$ by an angle π or one of the great-circles by 2π as given in Appendix III: Analytical Equations to Generate the Orbitsphere Current Vector Field and the Uniform Current (Charge)-Density Function $Y_0^0(\phi, \theta)$. In the case of the n th element of Step Two, the intersection of the two orthogonal great circle current loops occurs at the n th y' -axis which is along a great circle in a half-plane that is parallel with the y -axis and bisects the $-x$ - z -quadrant of Figure 1.4B. The nested rotations is also equivalent to rotating the orthogonal-great-circle basis set about the axis $(-i_x, 0i_y, i_z)$ by an angle $-\pi$ or one of the great-circles by 2π as given in Appendix III.

Following Step Two, in order to match the boundary condition that the magnitude of the velocity at any given point on the surface is given by Eq. (1.56), the output half of the orbitsphere-cvf is rotated clockwise by an angle of $\frac{\pi}{4}$ about the z -axis. Using Eq. (1.70b) with $\Delta\alpha_z = \frac{\pi}{4}$ and $\Delta\alpha_x = 0$ gives the rotation. Then, the one half of the orbitsphere-cvf generated from Step One is superimposed with the complementary half obtained from Step Two following its rotation about the z -axis of $\frac{\pi}{4}$ to give the orbitsphere-cvf. The nested rotations and $\frac{\pi}{4}$ - z -axis rotation of the output is also equivalent to forming a new basis set by rotating the orthogonal-great-circles shown in Figure 1.4B by $\frac{\pi}{4}$ about the z -axis then continuously rotating the set about the axis $(-i_x, i_y, i_z)$ by an angle $-\pi$ or rotating one of the reoriented great-circles by 2π as given in Appendix III.

The current pattern of the orbitsphere-cvf generated by the nested rotations of the orthogonal great circle current loops is a continuous and total coverage of the spherical surface, but it is shown as visual representations using 6 degree increments of the infinitesimal angular variable $\pm\Delta\alpha_x$ and $\pm\Delta\alpha_y$ of Eqs. (1.70a) and (1.70b) from seven perspectives in Figures 1.5A-G. In each case, the complete orbitsphere-cvf current pattern corresponds to all the correlated points, points one and two, of the orthogonal great circles shown in Figures 1.4A and 1.4B which are rotated according to Eqs. (1.70a) and (1.70b) where $\pm\Delta\alpha_x$ and $\pm\Delta\alpha_y$ approach zero and the summation of the infinitesimal angular rotations of $\pm\Delta\alpha_x$ and $\pm\Delta\alpha_y$ about the successive i' -axes and j' -axes is $\frac{\sqrt{2}}{2}\pi$ for each Step. The pattern also represents the momentum-vector field which is not equivalent to the mass (charge) density which for

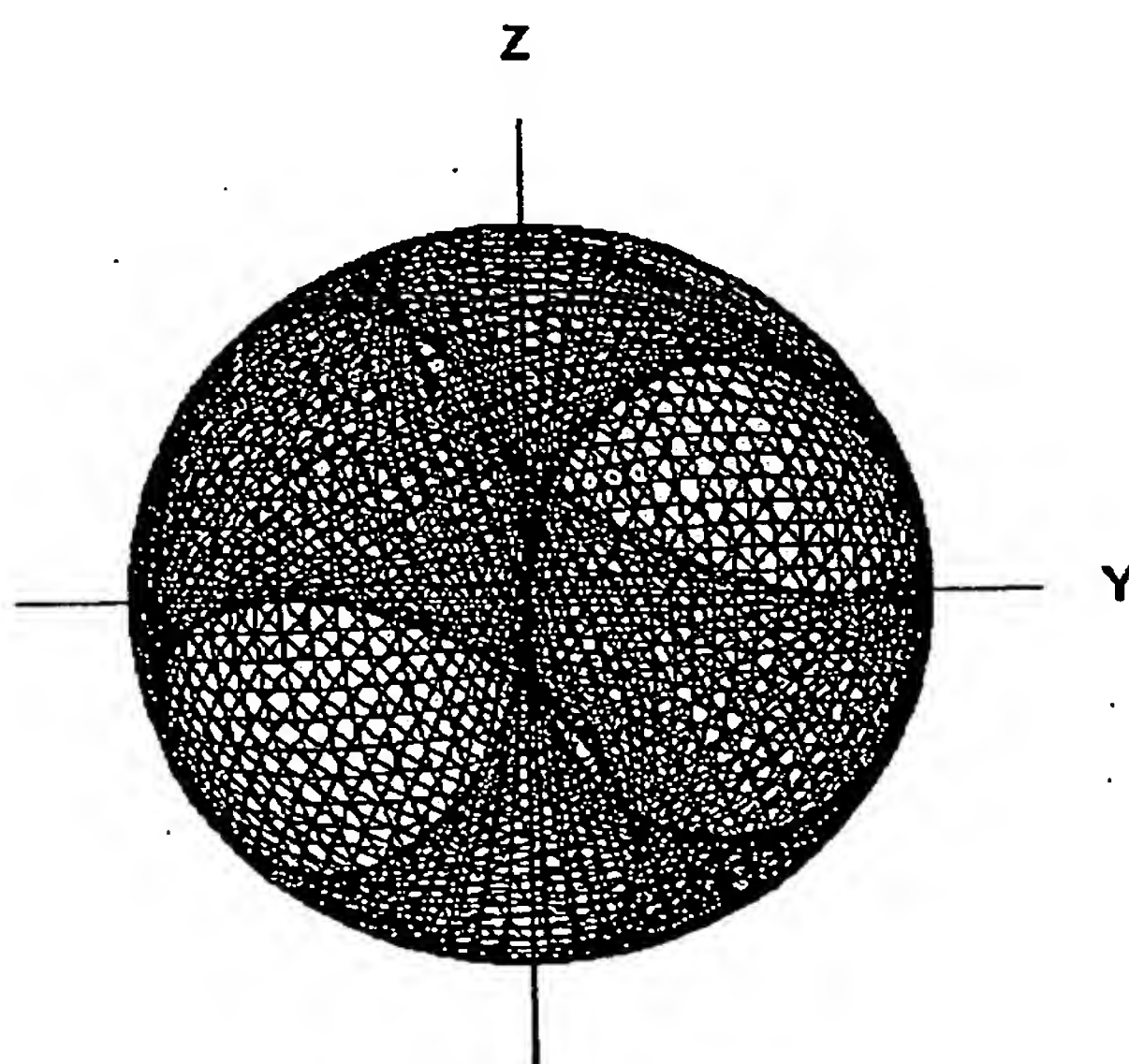
$Y_0^0(\phi, \theta)$ is uniform. Thus, the patterns represent the directions of the nonuniform flow of the uniform and constant mass and charge distribution of $Y_0^0(\phi, \theta)$. The resultant angular momentum vector of the L_x and L_z components of the orbitsphere-cvf, L_R , is aligned along the z-axis, and the orbitsphere-cvf serves as a basis element to generate $Y_0^0(\phi, \theta)$ as given in Appendix III.

Figure 1.5A. The current pattern of the orbitsphere-cvf shown with 6 degree increments of the infinitesimal angular variables $\pm\Delta\alpha_i$ and $\pm\Delta\alpha_j$ from the perspective of looking along the z-axis.



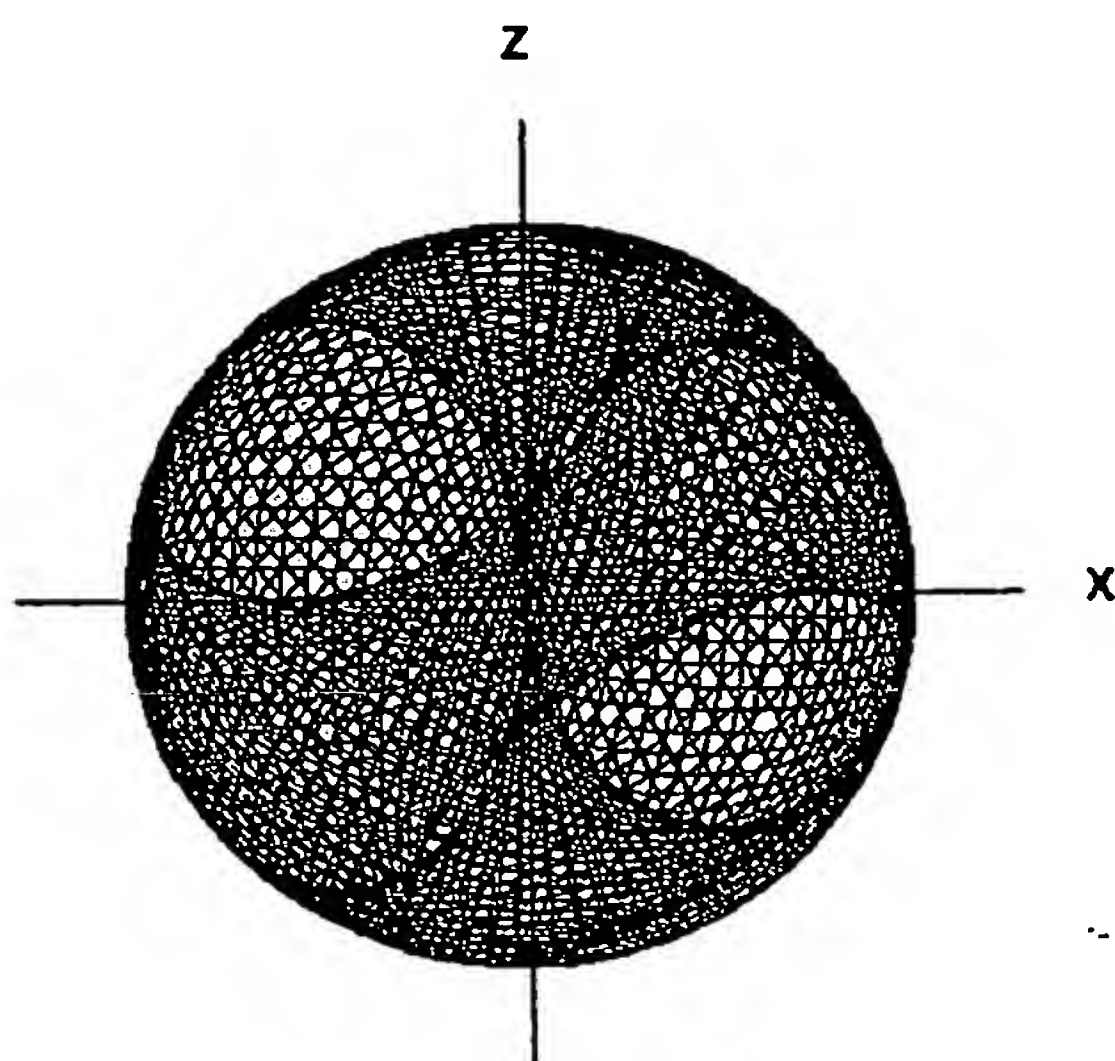
View Along the Positive Z Axis

Figure 1.5 B. The current pattern of the orbitsphere-cvf shown with 6 degree increments of the infinitesimal angular variables $\pm\Delta\alpha_i$ and $\pm\Delta\alpha_j$ from the perspective of looking along the x-axis.



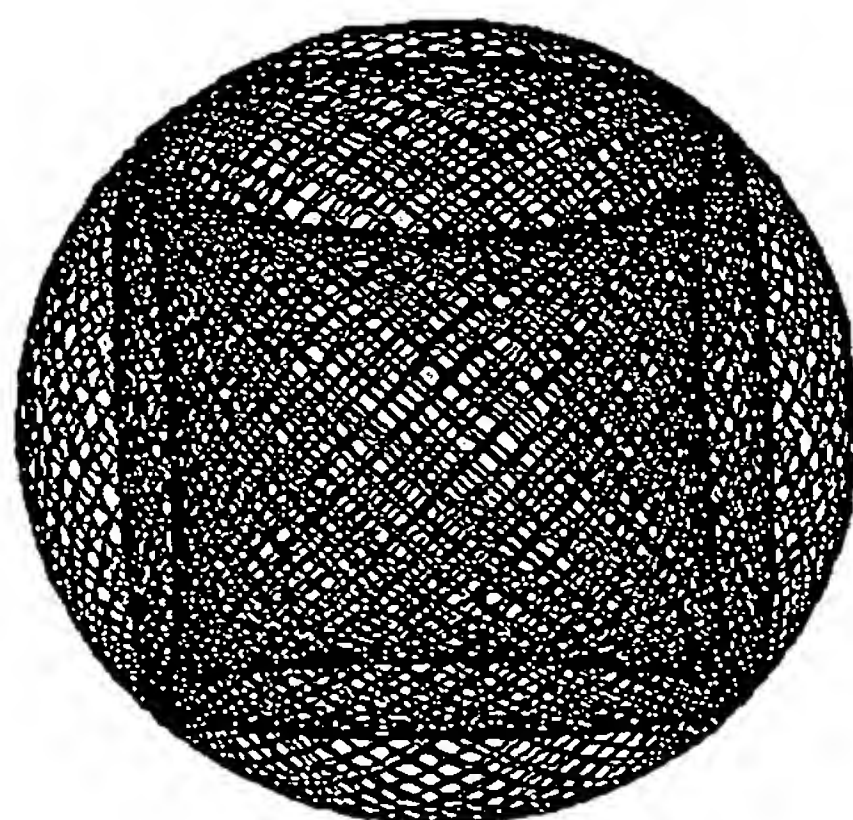
View Along the Positive X Axis

Figure 1.5C. The current pattern of the orbitsphere-cvf shown with 6 degree increments of the infinitesimal angular variables $\pm\Delta\alpha_i$ and $\pm\Delta\alpha_j$ from the perspective of looking along the y-axis.



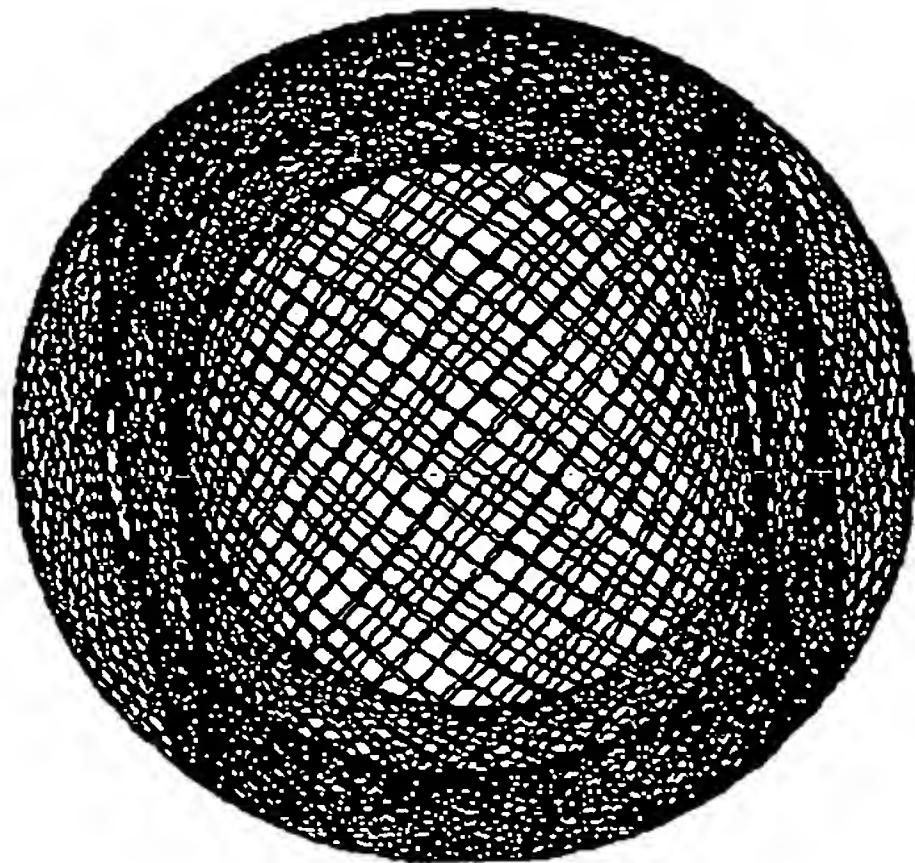
View Along the Positive Y Axis

Figure 1.5D. The current pattern of the orbitsphere-cvf shown with 6 degree increments of the infinitesimal angular variables $\pm\Delta\alpha_i$ and $\pm\Delta\alpha_j$ from the perspective of looking along the direction of the spherical-coordinate angles $\theta = 0.838 \text{ rad}$, $\phi = 0.660 \text{ rad}$ which shows the "box view".



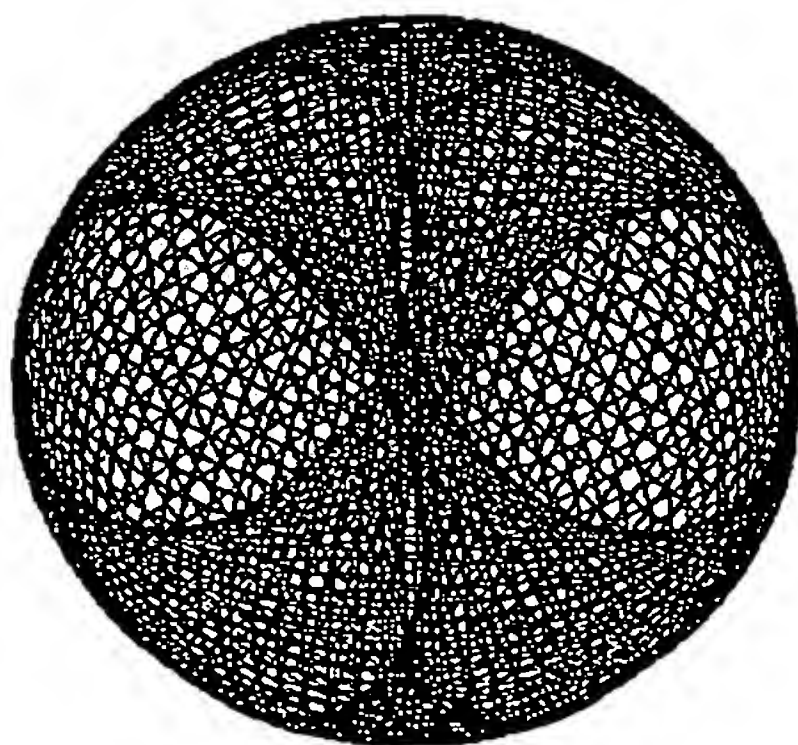
'Box' View

Figure 1.5E. The current pattern of the orbitsphere-cvf shown with 6 degree increments of the infinitesimal angular variables $\pm\Delta\alpha$, and $\pm\Delta\alpha$, from the perspective of looking along the direction of the spherical-coordinate angles $\theta = \frac{\pi}{2}$, $\phi = -0.0524 \text{ rad}$ which shows the "circle view".



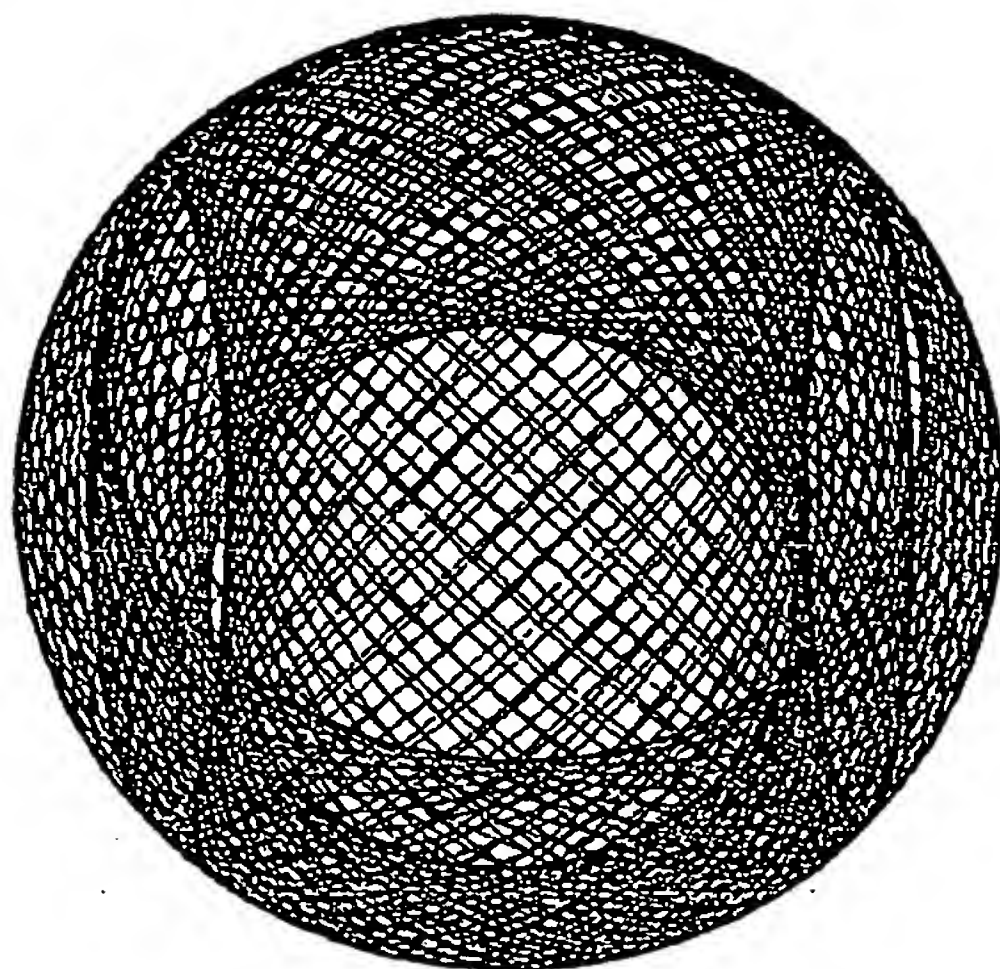
'Circle' View

Figure 1.5F. The current pattern of the orbitsphere-cvf shown with 6 degree increments of the infinitesimal angular variables $\pm\Delta\alpha$, and $\pm\Delta\alpha$, from the perspective of looking along the direction of the spherical-coordinate angles $\theta = 0.620 \text{ rad}$, $\phi = -0.175 \text{ rad}$ which shows the "diamond view".



'Diamond' View

Figure 1.5G. The current pattern of the orbitsphere-cvf shown with 6 degree increments of the infinitesimal angular variables $\pm\Delta\alpha_r$ and $\pm\Delta\alpha_z$, from the perspective of looking along the z-axis onto which L_R , the resultant angular momentum vector of the L_{xy} and L_z components, was aligned.



SPIN ANGULAR MOMENTUM OF THE ORBITSPHERE WITH $l = 0$

As demonstrated in Figures 1.4 and 1.5, the orbitsphere-cvf is generated from two orthogonal great circle current loops which are rotated about the n th i' -axis and then about the $(n+1)$ th j' -axis in Two Steps of the series of n nested conjugate rotations. Next, consider two infinitesimal charge (mass)-density elements at two separate positions or points, one and two, of the two orthogonal great circle current loops that serve as the sub-basis set as shown in each of Figures 1.4A and 1.4B. The vector projection of the corresponding angular momentum at each point of each current element is integrated over the entire orbitsphere-cvf surface to give the corresponding electron angular momentum. The correct current pattern is confirmed by achieving the condition that the magnitude of the velocity at any point on the surface is given by Eq. (1.56) and by obtaining the required angular momentum projections of $\frac{\hbar}{2}$

and $\frac{\hbar}{4}$ along and the z-axis and along an axis in the xy-plane, respectively, to satisfy the Stern-Gerlach-experimental boundary condition.

The mass density, $\frac{m_e}{4\pi r_1^2}$, of the orbitsphere of radius r_1 is uniform; however, the projections of the angular momenta of the great circle current loops of the orbitsphere onto the z-axis and onto the xy-plane are

not. The resultant vectors can be derived by considering the contributions of the momenta corresponding to the two orthogonal great circle current loops of Figures 1.4A-B as each basis set generates the current pattern of the orbitsphere-cvf in the Two Steps. The electron current, and thus, the momentum is first evenly distributed within the two orthogonally linked great-circle current loops each with a mass $\frac{m_e}{2}$. The total sum of the magnitude of the angular momentum from the contributions from all of the infinitesimal points on the orbitsphere is \hbar (Eq. (1.57)). Thus, the angular momentum of each great circle at this point is $\frac{\hbar}{2}$. The planes of the great circles are oriented at an angle of $\frac{\pi}{2}$ with respect to each other, and the resultant angular momentum is $\frac{\hbar}{\sqrt{2}}$ in the plane transverse to the axis on which they intersect. These loops are further divided into two sets of linked orthogonal pairs that undergo the independent transformations over the surface during Steps One and Two where the electron momentum and mass is correspondingly divided again by two. Thus, the angular momentum of each great circle of each algorithmic Step is $\frac{\hbar}{4}$ and the resultant angular momentum is $\frac{\hbar}{2\sqrt{2}}$ in the transverse plane. In cases where the angular momentum vectors are rotated relative to the xyz-coordinate system during the algorithm, the angular momenta are then divided by the angular span of the rotation to form normalized momentum densities corresponding to the normalized current densities. Half of the angular momentum is distributed over the orbitsphere-cvf in Step One and the other half is distributed in Step Two.

Consider the vector current directions shown in Figure 1.4A. During Step One, $\Delta\alpha_x$ and $\Delta\alpha_y$ are both positive, and the resultant angular momentum vector of magnitude $\frac{\hbar}{2\sqrt{2}}$ moves along a half a great circle in the plane that is parallel to the z-axis and bisects the +x-y-quadrant and the -x+y-quadrant. The trajectory of the resultant angular momentum vector from the xy-plane to the z-axis and back to the xy-plane is shown in Figure 1.6 where the angle θ of the resultant angular momentum vector from the initial xy-plane position varies from $\theta=0$ to $\theta=\pi$. Here it can be appreciated that the vector projections onto the z-axis all add positively and the vector projections into the xy-plane sum to zero. With the initial direction defined as positive, the projection in the xy-plane varies from a maximum of $\frac{\hbar}{2\sqrt{2}}$ to zero to $\frac{\hbar}{2\sqrt{2}}$. The projection onto the z-axis varies from zero to a maximum of $\frac{\hbar}{2\sqrt{2}}$ to zero again. In each case,

the projection of the angular momentum is periodic over the angular range of θ . The total of each projection, L_x and L_z , is the integral as a function of θ of the magnitude of the resultant vector of the two orthogonal angular momentum component vectors corresponding to the two orthogonal great circles. For Step One, the vector projection of the angular momentum onto the xy-plane is given by sum of the vector contributions from each great circle:

$$L_x = \sqrt{\frac{2}{\pi} \int_0^{\frac{\pi}{2}} \left[\frac{\hbar}{4} \cos \theta \right]^2 + \left[\frac{\hbar}{4} \cos \theta \right]^2 d\theta} - \sqrt{\frac{2}{\pi} \int_{\frac{\pi}{2}}^{\pi} \left[\frac{\hbar}{4} \cos \theta \right]^2 + \left[\frac{\hbar}{4} \cos \theta \right]^2 d\theta} \quad (1.71a)$$

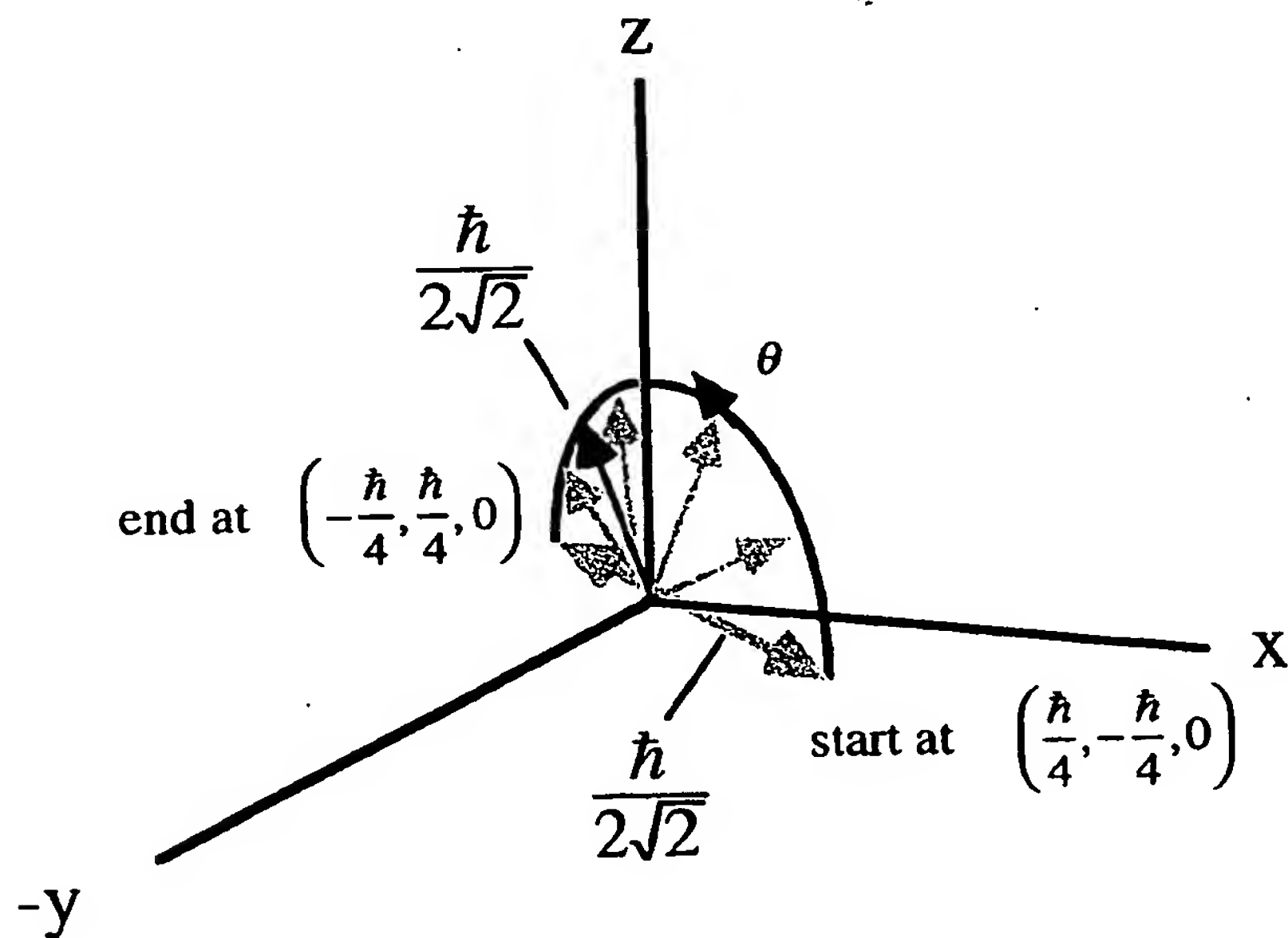
$$= \frac{\hbar}{2\sqrt{2}} \frac{1}{\sqrt{2}} - \frac{\hbar}{2\sqrt{2}} \frac{1}{\sqrt{2}} = 0$$

where each angular integral is normalized by, $\frac{\pi}{2}$, the angular range of θ . Similarly, the vector projection of the angular momentum onto the z-axis as shown in Figure 1.6 is

$$L_z = \sqrt{\frac{1}{\pi} \int_0^{\pi} \left[\frac{\hbar}{4} \sin \theta \right]^2 + \left[\frac{\hbar}{4} \sin \theta \right]^2 d\theta} = \frac{\hbar}{2\sqrt{2}} \frac{1}{\sqrt{2}} = \frac{\hbar}{4} \quad (1.71b)$$

where each angular integral is normalized by, π , the angular range of θ . Thus, from the initial $\frac{\hbar}{4}$ of angular momentum along each of the x and y-axes, $\frac{\hbar}{4}$ canceled in the xy-plane and $\frac{\hbar}{4}$ was projected onto the z-axis as the angular momentum was spread over one half of the surface of the sphere with Step One.

Figure 1.6. The trajectory of the resultant angular momentum vector of the orthogonal great circle current loops of magnitude $\frac{\hbar}{2\sqrt{2}}$ during Step One (yellow vectors) gives $L_z = \frac{\hbar}{4}$. The resultant angular momentum vector of the orthogonal great circle current loops of magnitude $\frac{\hbar}{2\sqrt{2}}$ of Step Two (black vector) is stationary. With the $\frac{\pi}{4}$ rotation about the z-axis the projections of the resultant vector for Step Two are $L_{xy} = \frac{\hbar}{4}$ and $L_z = \frac{\hbar}{4}$.



Consider the vector current directions shown in Figure 1.4B. During Step Two, $\Delta\alpha_z$ is negative, $\Delta\alpha_x$ is positive, and the nested rotations causes the orthogonal great-circle basis set to rotate about the vector $(-\frac{\hbar}{4}\mathbf{i}_x, 0\mathbf{i}_y, \frac{\hbar}{4}\mathbf{i}_z)$. Thus, the resultant angular momentum vector of magnitude $\frac{\hbar}{2\sqrt{2}}$ is stationary throughout the nested rotations that

transform the axes as given in Table 1.1. Then, the $\frac{\pi}{4}$ rotation of about the z-axis following Step Two only rotates L_x by the same angle in the xy-plane such that the component is oriented along the bisector of the -x+y-quadrant as shown in Figures 1.4B and 1.6. Thus, the resultant angular momentum component of Step Two that is transverse to the z-axis, L_{xy} , is in the direction of $(-i_x, i_y, 0i_z)$ which is also the direction of the trajectory of the angular momentum component vectors of Step One as shown in Figure 1.6. The resultant angular momentum projections are as given in Figure 1.4B:

$$L_{xy} = \frac{\hbar}{4} \quad (1.72a)$$

$$L_z = \frac{\hbar}{4} \quad (1.72b)$$

The total vector projection of the angular momentum onto the xy-plane given by the sum of Eqs. (1.71a) and (1.72a) is

$$L_{xy} = 0 + \frac{\hbar}{4} = \frac{\hbar}{4} \quad (1.73a)$$

The total vector projection of the angular momentum into the z-axis given by the sum of Eqs. (1.71b) and (1.72b) is

$$L_z = \frac{\hbar}{4} + \frac{\hbar}{4} = \frac{\hbar}{2} \quad (1.73b)$$

The trajectories of the angular momenta and the resultant projections, L_{xy} and L_z , given in Table 1.1 have been confirmed by computer simulations [14]. These results meet the boundary condition for the unique current having an angular velocity magnitude at each point on the surface given by Eq. (1.56) and give rise to the Stern Gerlach experiment as shown *infra.*, in the Magnetic Parameters of the Electron (Bohr Magneton) section, and in the Electron g Factor section. The further constraint that the current density is uniform such that the charge density is uniform, corresponding to an equipotential, minimum energy surface is satisfied by using the orbitsphere-cvf as a basis element to generate $Y_0^0(\phi, \theta)$ as given in Appendix III.

EXACT GENERATION OF $Y_0^0(\phi, \theta)$ FROM THE ORBITSPHERE-CVF

The further constraint that the current density is uniform such that the charge density is uniform, corresponding to an equipotential, minimum energy surface is exactly satisfied by the using orbitsphere-cvf as a basis element to generate $Y_0^0(\phi, \theta)$. Utilizing the symmetry properties of each component of the orbitsphere-cvf corresponding to either STEP ONE or STEP TWO and the orthonormality of the trigonometric functions that generate the orbitsphere-cvf, a convolution operator comprising an

autocorrelation-type function gives rise to the spherically-symmetric current density, $Y_0^0(\phi, \theta)$. The operator comprises the convolution of each great circle current loop of the orbitsphere-cvf designated as the primary orbitsphere-cvf with a second orbitsphere-cvf designated as the secondary orbitsphere-cvf. The angular momenta of the convolved elements are matched. The elements are also orientation matched by rotation of the secondary about the appropriate axis (axes), and the elements are phase matched using a rotation of each secondary orbitsphere-cvf element about its C_∞ -axis. The convolution is over the angular span $\theta=0$ to $\theta=2\pi$ corresponding to the rotation of the basis-current loop which generated the primary orbitsphere-cvf. The angular momenta of the secondary elements project onto the resultant angular momentum axis, L_R -axis, of the primary orbitsphere-cvf equivalently to those of its great circles. The resulting exact uniform current distribution obtained from the convolution has the same angular momentum distribution, resultant, L_R , and components of $L_x = \frac{\hbar}{4}$ and $L_z = \frac{\hbar}{2}$ as those of the orbitsphere-cvf used as a primary basis element.

Convolution Operator

The orbitsphere-cvf comprises two components corresponding to each of STEP ONE and STEP TWO. As shown for STEP TWO, the angular momentum vector is stationary on the $(-i_x, i_y, i_z)$ -axis as the component orbitsphere-cvf is generated by the series of nested rotations using Eq. (1.70b). It is shown in Appendix III that STEP TWO can also be generated by a 2π -rotation of a single basis-element current loop about the $(-i_x, i_y, i_z)$ -axis. In the general case that the resultant angular momentum of each pair of orthogonal great circle current loops of the component orbitsphere-cvf is along the 2π -rotational axis (defined as the rotational axis which generates the component orbitsphere-cvf from a basis-element great circle), a secondary nth component orbitsphere-cvf can serve as a basis element to match the angular momentum of any given nth great circle of a primary component orbitsphere-cvf. The replacement of each great circle of the primary orbitsphere-cvf with a secondary orbitsphere-cvf of matching angular momentum, orientation, and phase comprises an autocorrelation-type function that exactly gives rise to the spherically-symmetric current density, $Y_0^0(\phi, \theta)$.

The orbitsphere-cvf comprises the superposition or sum of the components corresponding to STEPS ONE and STEP TWO. Thus, the convolution is performed on each component. The convolution of a secondary component orbitsphere-cvf element with the each great circle

current loop of a primary orbitsphere-cvf comprising two components is designated as the convolution operator, $A(\phi, \theta)$, given by

$$A(\phi, \theta) = \frac{1}{r_n^2} \lim_{\theta_2 \rightarrow 0} \sum_{m'=1}^{\frac{2\pi}{|\Delta\theta_2|}} \lim_{\theta_1 \rightarrow 0} \sum_{m=1}^{\frac{2\pi}{|\Delta\theta_1|}} O(r_n, \phi, \theta) \otimes \begin{pmatrix} \delta(GC_{STEPONE}(\phi, \theta - \phi', \theta_1)) \\ + \delta(GC_{STEPTWO}(\phi, \theta - \phi', \theta_2)) \end{pmatrix} \quad (1.73c)$$

wherein the secondary component orbitsphere-cvf is defined by the symbol $O(r_n, \phi, \theta)$ -cvf and each rotated great circle of each component orbitsphere-cvf of STEP M is defined by the symbol $GC_{STEPM}(\phi', \theta_M)$. In Eq. (1.73c), the angular momentum of each secondary component orbitsphere-cvf is equal in magnitude and direction as that of the current loop with which it is convolved. Furthermore, the orientations and phases of the convolved elements are matched by rotating the secondary component orbitsphere-cvf about the appropriate principle axis (axes) and about the C_∞ -axis along its angular momentum vector, respectively. With the magnitude of the angular momentum of the secondary component orbitsphere-cvf matching that of the current loop which it replaces during the convolution and the loop then serving as a unit vector, the angular momentum resulting from the convolution operation is inherently normalized to that of the primary component orbitsphere-cvf.

The convolution of a sum is the sum of the convolutions. Thus, the convolution operation may be performed on each of STEP ONE and STEP TWO separately, and the result may be superposed in terms of the current densities and angular momenta.

$$A(\phi, \theta) = \frac{1}{r_n^2} \left(\lim_{\theta_1 \rightarrow 0} \sum_{m=1}^{\frac{2\pi}{|\Delta\theta_1|}} O(r_n, \phi, \theta) \otimes \delta(\phi, \theta - GC_{STEPONE}(\phi', \theta_1)) + \lim_{\theta_2 \rightarrow 0} \sum_{m'=1}^{\frac{2\pi}{|\Delta\theta_2|}} O(r_n, \phi, \theta) \otimes \delta(\phi, \theta - GC_{STEPTWO}(\phi', \theta_2)) \right) \quad (1.73d)$$

Factoring out the secondary component orbitsphere-cvf gives

$$A(\phi, \theta) = \frac{1}{r_n^2} O(r_n, \phi, \theta) - cvf \left(\lim_{\theta_1 \rightarrow 0} \sum_{m=1}^{\frac{2\pi}{|\Delta\theta_1|}} GC_{STEPONE}(\phi', \theta_1) + \lim_{\theta_2 \rightarrow 0} \sum_{m'=1}^{\frac{2\pi}{|\Delta\theta_2|}} GC_{STEPTWO}(\phi', \theta_2) \right) \quad (1.73e)$$

The summation is the operator that generates the component orbitsphere-cvf of STEP M, $O_M(r_n, \phi, \theta)$ -cvf. Thus, the current-density function is given by the primary orbitsphere-cvf squared comprised of two superimposed components.

$$A(\phi, \theta) = \frac{1}{r_n^2} (O_1^2 - cvf(r_n, \phi, \theta) + O_2^2 - cvf(r_n, \phi, \theta)) \quad (1.74f)$$

The orbitsphere-cvf squared given in Eq. (1.74f) is the equation of a uniform sphere. The superposition of the uniform distributions from STEP ONE and STEP TWO is the exact uniform current density function $Y_0^0(\phi, \theta)$ that is an equipotential, minimum energy surface shown in Figure 13. The angular momentum is identically that of the superposition of the component orbitsphere-cvfs of the primary orbitsphere-cvf, $L_x = \frac{\hbar}{4}$ and $L_z = \frac{\hbar}{2}$ given by Eqs. (1.73a-1.73b).

RESONANT PRECESSION OF THE SPIN-1/2-CURRENT-DENSITY FUNCTION GIVES RISE TO THE BOHR MAGNETON

The Stern Gerlach experiment described below demonstrates that the magnetic moment of the electron can only be parallel or antiparallel to an applied magnetic field. In spherical coordinates, this implies a spin quantum number of 1/2 corresponding to an angular momentum on the z-axis of $\frac{\hbar}{2}$. However, the Zeeman splitting energy corresponds to a magnetic moment of μ_B and implies an electron angular momentum on the z-axis of \hbar —twice that given by Eq. (1.68-1.71). Consider the case of a magnetic field applied to the orbitsphere. The magnetic moment corresponding to the angular momentum along the z-axis results in the alignment of the z-axis of the orbitsphere with the magnetic field while the $\frac{\hbar}{4}$ resultant vector in the xy-plane causes precession about the applied field. The precession frequency is the Larmor frequency given by the product of the gyromagnetic ratio of the electron, $\frac{e}{2m}$, and the magnetic flux B [15]. The precessing electron can interact with a resonant photon that gives rise to Zeeman splitting—energy levels corresponding to parallel or antiparallel alignment of the electron magnetic moment with the magnetic field. The energy of the transition between these states is that of the resonant photon. The angular momentum of the precessing orbitsphere comprises the initial $\frac{\hbar}{2}$ projection on the z-axis and the initial $\frac{\hbar}{4}$ vector component in the xy-plane that then precesses about the z-axis. As shown in the Excited States of the One-Electron Atom (Quantization) section, conservation of the angular momentum of the photon of \hbar gives rise to \hbar of electron angular momentum. The parameters of the photon standing wave for the

Zeeman effect are given in the Magnetic Parameters of the Electron (Bohr Magneton) section and Box 1.2.

The angular momentum of the orbitsphere in a magnetic field comprises the static $\frac{\hbar}{2}$ projection on the z-axis (Eq. (1.73b)) and the $\frac{\hbar}{4}$ vector component in the xy-plane (Eq. (1.73a)) that precesses about the z-axis at the Larmor frequency. A resonant excitation of the Larmor precession frequency gives rise to a trapped photon with \hbar of angular momentum along a precessing S-axis. In the coordinate system rotating at the Larmor frequency (denoted by the axes labeled X_R , Y_R , and Z_R in Figure 1.7), the X_R -component of magnitude $\frac{\hbar}{4}$ and S of magnitude \hbar are stationary. The $\frac{\hbar}{4}$ angular momentum along X_R with a corresponding magnetic moment of $\frac{\mu_B}{4}$ (Eq. (28) of Box 1.2) causes S to rotate in the $Y_R Z_R$ -plane to an angle of $\theta = \frac{\pi}{3}$ such that the torques due to the Z_R -component of $\frac{\hbar}{2}$ and the orthogonal X_R -component of $\frac{\hbar}{4}$ are balanced. Then the Z_R -component due to S is $\pm \hbar \cos \frac{\pi}{3} = \pm \frac{\hbar}{2}$. The reduction of the magnitude of S along Z_R from \hbar to $\frac{\hbar}{2}$ corresponds to the ratio of the X_R -component and the static Z_R -component of $\frac{\frac{\hbar}{4}}{\frac{\hbar}{2}} = \frac{1}{2}$ ⁶. Since the X_R -

⁶ The torque balance can be appreciated by considering that S is aligned with Z_R if the X_R -component is zero, and the three vectors are mutually orthogonal if the X_R -component is $\frac{\hbar}{2}$. The balance can be shown by considering the magnetic energies resulting from the corresponding torques when they are balanced. Using Eqs. (23) and (25) of Box 1.2, the potential energy E_V due to the projection of S's angular momentum of \hbar along Z_R having $\frac{\hbar}{2}$ of angular momentum is

$$E_V = \mu_B B \cos \theta = \mu_B \frac{1}{2} B_{\mu_B} \cos \theta = \frac{1}{2} \hbar \omega_{\mu_B} \cos \theta \quad (1)$$

where B_{μ_B} is the flux due to a magnetic moment of a Bohr magneton and ω_{μ_B} is the corresponding gyromagnetic frequency. The application of a magnetic moment along the X_R -axis causes S to precess about the Z_R and X_R -axes. In the $X_R Y_R Z_R$ -frame rotating at ω_{μ_B} , S precesses about the X_R -axis. The corresponding

component is $\frac{\hbar}{4}$, the Z_R -component of S is $\frac{\hbar}{2}$ which adds to the initial $\frac{\hbar}{2}$ component to give a total Z_R -component of \hbar .

precession energy E_{X_R} of S about the X_R -component of $\frac{\hbar}{4}$ is the corresponding Larmor energy

$$E_{X_R} = -\frac{1}{4}\hbar\omega_{\mu_B} \quad (2)$$

The energy E_{Z_R} of the magnetic moment corresponding to S rotating about Z_R having $\frac{\hbar}{2}$ of angular momentum is the corresponding Larmor energy:

$$E_{Z_R} = \frac{1}{2}\hbar\omega_{\mu_B} \quad (3)$$

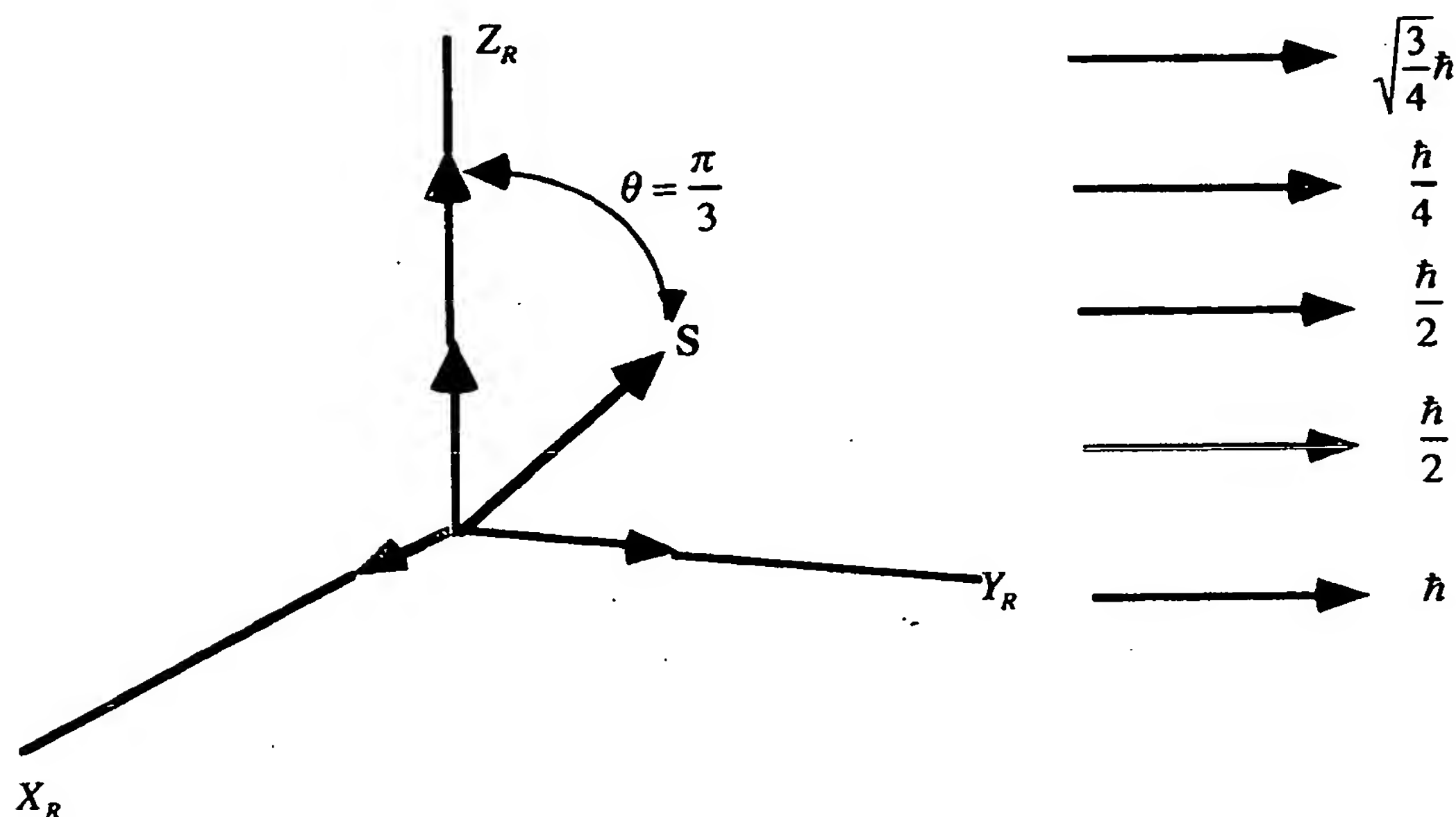
At torque balance, the potential energy is equal to the sum of the Larmor energies:

$$E_{Z_R} + E_{X_R} = \hbar\left(\frac{1}{2} - \frac{1}{4}\right)\omega_{\mu_B} = \frac{\hbar}{2}\left(1 - \frac{\frac{1}{4}}{\frac{1}{2}}\right)\omega_{\mu_B} = \frac{1}{2}\hbar\omega_{\mu_B}\cos\theta \quad (4)$$

Balance occurs when $\theta = \frac{\pi}{3}$. Thus, the intrinsic torques are balanced.

Furthermore, energy is conserved relative to the external field as well as the intrinsic, Z_R and X_R -components of the orbitsphere, and the Larmor relationships for both the gyromagnetic ratio and the potential energy of the resultant magnetic moment are satisfied as shown in Box 1.2.

Figure 1.7. The angular momentum components of the orbitsphere and S in the rotating coordinate system X_R , Y_R , and Z_R that precesses at the Larmor frequency about Z_R such that the vectors are stationary.



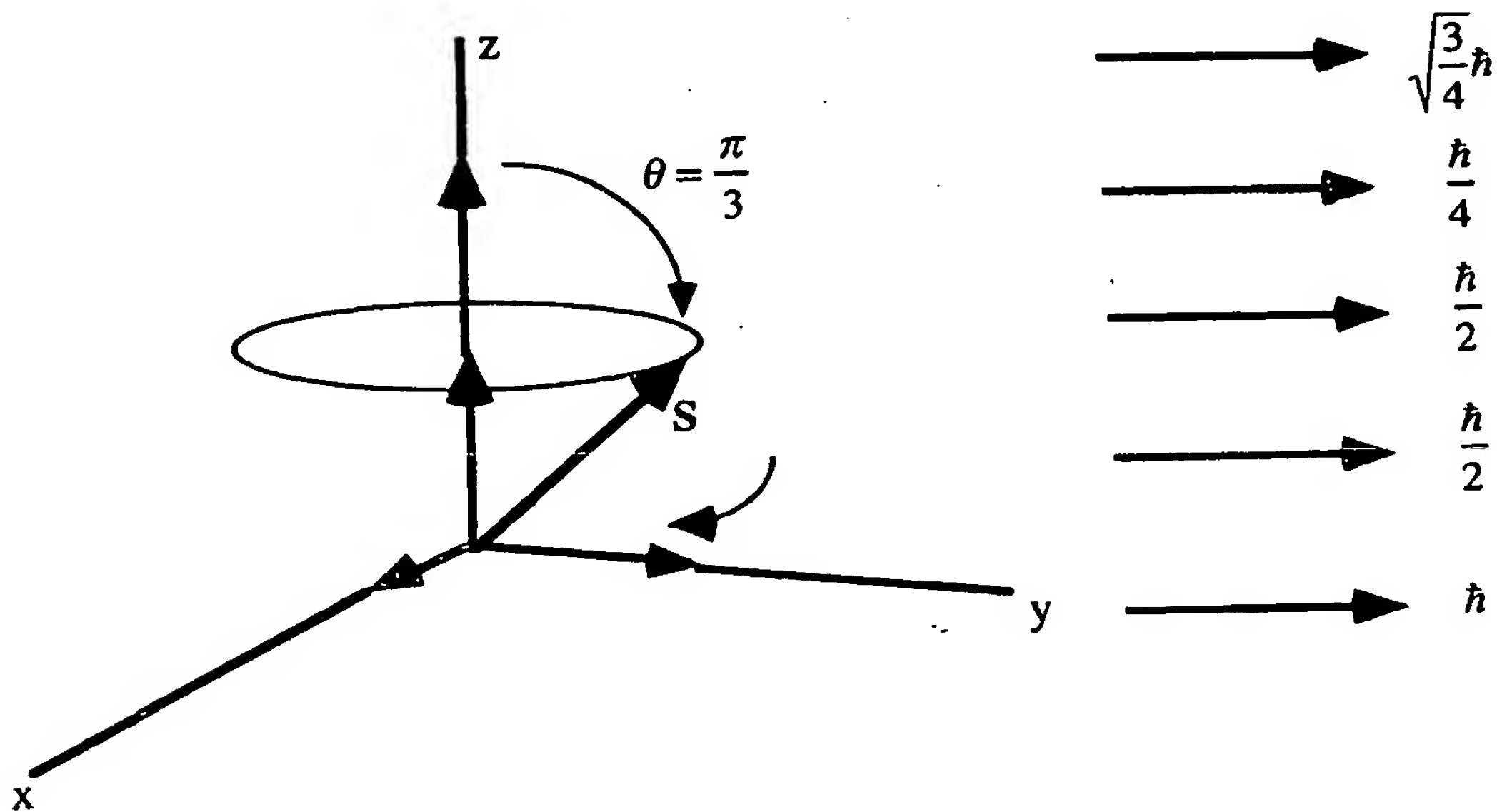
In summary, since the vector S that precesses about the z -axis at an angle of $\theta = \frac{\pi}{3}$ and an angle of $\phi = \frac{\pi}{2}$ with respect to L_{xy} given by Eq. (1.73a) and has a magnitude of \hbar , the S projections in the $X_R Y_R$ -plane and along the Z_R -axis are

$$S_{\perp} = \hbar \sin \frac{\pi}{3} = \pm \sqrt{\frac{3}{4}} \hbar \mathbf{i}_{Y_R} \quad (1.74a)$$

$$S_{\parallel} = \pm \hbar \cos \frac{\pi}{3} = \pm \frac{\hbar}{2} \mathbf{i}_{Z_R} \quad (1.74b)$$

The plus or minus sign of Eqs. (1.74a) and (1.74b) corresponds to the two possible vector orientations which are observed with the Stern-Gerlach experiment described below. The sum of the torques in the external magnetic field is balanced unless an RF field is applied to cause a Stern-Gerlach transition as discussed in Box 1.2.

Figure 1.8. The angular momentum components of the orbitsphere and S in the stationary coordinate system. S and the components in the xy-plane precess at the Larmor frequency about the z-axis.



As shown in Figure 1.8, S forms a cone in time in the nonrotating laboratory frame with an angular momentum of \hbar that is the source of the known magnetic moment of a Bohr magneton (Eq. (28) of Box 1.2) as shown in the Magnetic Parameters of the Electron (Bohr Magnetron) section. The projection of this angular momentum onto the z-axis of $\frac{\hbar}{2}$ adds to the z-axis component before the magnetic field was applied to give a total of \hbar . Thus, in the absence of a resonant precession, the z-component of the angular momentum is $\frac{\hbar}{2}$, but the excitation of the precessing S component gives \hbar —twice the angular momentum on the z-axis. In addition, rather than a continuum of orientations with corresponding energies, the orientation of the magnetic moment must be only parallel or antiparallel to the magnetic field. This arises from conservation of angular momentum between the "static" and "dynamic" z-axis projections of the angular momentum with the additional constraint that the angular momentum has a "kinetic" as well as a "potential" or vector potential component. To conserve angular momentum, flux linkage by the electron is quantized in units of the magnetic flux quantum, $\Phi_0 = \frac{h}{2e}$, as shown in Box 1.2 and in the Electron g Factor section.

Thus, the spin quantum number is $s = \frac{1}{2}$; $m_s = \pm \frac{1}{2}$, but the observed Zeeman splitting corresponds to a full Bohr magneton due to \hbar of angular momentum. This aspect was historically felt to be inexplicable in terms of classical physics and merely postulated in the past.

The demonstration that the boundary conditions of the electron in a magnetic field are met appears in Box 1.2. The observed electron parameters are explained physically. Classical laws give 1.) a gyromagnetic ratio of $\frac{e}{2m}$, 2.) a Larmor precession frequency of $\frac{eB}{2m}$, 3.) the Stern-Gerlach experimental result of quantization of the angular momentum that implies a spin quantum number of $1/2$ corresponding to an angular momentum of $\frac{\hbar}{2}$ on the z-axis, and 4.) the observed Zeeman

splitting due to a magnetic moment of a Bohr magneton $\mu_B = \frac{e\hbar}{2m_e}$ corresponding to an angular momentum of \hbar on the z-axis. Furthermore, the solution is relativistically invariant as shown in the Special Relativistic Correction to the Ionization Energies section. Dirac originally attempted to solve the bound electron physically with stability with respect to radiation according to Maxwell's equations with the further constraints that it was relativistically invariant and gave rise to electron spin [16]. He was unsuccessful and resorted to the current mathematical probability-wave model that has many problems as discussed in Appendix II: Quantum Electrodynamics (QED) is Purely Mathematical and Has No Basis in Reality.

ROTATIONAL PARAMETERS OF THE ELECTRON (ANGULAR MOMENTUM, ROTATIONAL ENERGY, AND MOMENT OF INERTIA)

One result of the correlated motion along great circles is that some of the kinetic energy is not counted in the rotational energy. That is, for any spin axis there will be an infinite number of great circles with planes passing through that axis with θ angles other than 90° . All points on any one of these great circles will be moving, but not all of that motion will be part of the rotational energy; only that motion perpendicular to the spin axis will be part of the rotational energy. Thus, the rotational kinetic energy will always be less than the total kinetic energy. Furthermore, the following relationships must hold.

$$E_{\text{rotational}} = \frac{1}{2} I \omega^2 \leq \frac{1}{2} m_e v^2 \quad (1.75)$$

$$I \omega \leq \hbar \quad (1.76)$$

$$I \leq m_e r^2 \quad (1.77)$$

Furthermore, it is known from the Stern-Gerlach experiment that a beam of silver atoms splits into two components when passed through an inhomogeneous magnetic field. This experiment implies a magnetic moment of one Bohr magneton and an associated angular momentum quantum number of 1/2. Historically, this quantum number is called the spin quantum number, and that designation will be retained. The angular momentum can be thought of arising from a spin component or equivalently an orbital component of the spin. The z-axis projection of the spin angular momentum was derived in the Spin Angular Momentum of the Orbitsphere with $l = 0$ section.

$$L_z = I\omega_z = \pm \frac{\hbar}{2} \quad (1.78)$$

where ω is given by Eq. (1.55); so,

$$l = 0$$

$$|L_z| = I \frac{\hbar}{m_e r^2} = \frac{\hbar}{2} \quad (1.79)$$

Thus,

$$I_z = I_{spin} = \frac{m_e r_n^2}{2} \quad (1.80)$$

From Eq. (1.51),

$$E_{rotational\ spin} = \frac{1}{2} [I_{spin} \omega^2] \quad (1.81)$$

From Eqs. (1.55) and (1.80),

$$E_{rotational} = E_{rotational\ spin} = \frac{1}{2} \left[I_{spin} \left(\frac{\hbar}{m_e r_n^2} \right)^2 \right] = \frac{1}{2} \left[\frac{m_e r_n^2}{2} \left(\frac{\hbar}{m_e r_n^2} \right)^2 \right] = \frac{1}{4} \left[\frac{\hbar^2}{2I_{spin}} \right] \quad (1.82)$$

When $l \neq 0$, the spherical harmonic is not a constant and the charge-density function is not uniform over the orbitsphere. Thus, the angular momentum can be thought of arising from a spin component and an orbital component.

Derivation of the Rotational Parameters of the Electron

In the derivation of Eq. (1.59) and its solution for $E_{rotational}$ (Eq. (1.60)), the moment of inertia, I , was assumed by McQuarrie [12] to be the moment of inertia of a point particle, mr_n^2 . However, the correct equation of the electron is a two dimensional shell with a constant or a constant plus a spherical harmonic angular dependence. In that case, the relationships given by Eqs. (1.75) to (1.77) must hold.

The substitution of $C_1 I$ for I in the rigid rotor problem [12] where C_1 is a positive constant does not change the form of the previous solution given by Eq. (1.60). However, the result that

$$C_1 = \left[\frac{\ell(\ell+1)}{\ell^2 + 2\ell + 1} \right]^{\frac{1}{2}} < 1 \quad (1.83)$$

derived below gives

$$E_{\text{rotational}} = \frac{\hbar^2 \ell(\ell+1)}{2I(\ell^2 + 2\ell + 1)} \quad (1.84)$$

and gives the moment of inertia of the orbitsphere, I_{orbital} , where $\ell \neq 0$ as

$$C_1 I = I_{\text{orbital}} = m_e r_n^2 \left[\frac{\ell(\ell+1)}{(\ell^2 + 2\ell + 1)} \right]^{\frac{1}{2}} \quad (1.85)$$

The solution of Eq. (1.59) for $|\mathbf{L}|$, the magnitude of the orbital angular momentum, is [12]

$$|\mathbf{L}| = \hbar \sqrt{\ell(\ell+1)} \quad (1.86)$$

where I of Eq. (1.59) is the moment of inertia of a point charge. It is demonstrated by Eq. (1.57) that the total sum of the magnitudes of the angular momenta of the infinitesimal points of the electron orbitsphere is \hbar ; therefore, the magnitude of the angular momentum of an electron orbitsphere about the z-axis must be less than \hbar , and the corresponding moment of inertia must be less than that given by $m_e r_n^2$. For example, the moment of inertia of the uniform spherical shell, I_{RS} , is [17]

$$I_{\text{RS}} = \frac{2}{3} m r_n^2 \quad (1.87)$$

Thus, Eq. (1.86) must be multiplied by a constant, $0 < C_2 < 1$, to give the correct angular momentum. Given that generally \mathbf{L} is

$$\mathbf{L} = I \boldsymbol{\omega}_z \quad (1.88)$$

then

$$I_{\text{orbital}} \boldsymbol{\omega}_z = \hbar C_2 \sqrt{\ell(\ell+1)}, \quad (1.89)$$

where ω is given by Eq. (1.55). The orbital moment of inertia, I_{orbital} , is

$$I_{\text{orbital}} = m_e r_n^2 C_2 \sqrt{\ell(\ell+1)} \quad (1.90)$$

The total kinetic energy, T , of the orbitsphere is

$$T = \frac{1}{2} m_e v_n^2 \quad (1.91)$$

Substitution of Eq. (1.56) gives

$$T = \frac{\hbar^2}{2m_e r_n^2} \quad (1.92)$$

$E_{\text{rotational}}$ of the rigid shell is given by Eq. (1.51) with I given by Eq. (1.87).

$E_{\text{rotational orbital}}$ of the orbitsphere is given by Eq. (1.60) multiplied by C_2^2 so that Eqs. (1.75) to (1.77) hold with $I = m_e r_n^2$.

$$E_{\text{rotational orbital}} = C_2^2 \frac{\hbar^2}{2I} \ell(\ell+1) \quad (1.93)$$

Eq. (1.59) can be expressed in terms of the variable x which is substituted for $\cos\theta$. The resulting function $P(x)$ is called Legendre's equation and is a well-known equation in classical physics. It occurs in a variety of problems that are formulated in spherical coordinates. When the power series method of solution is applied to $P(x)$, the series must be truncated in order that the solutions be finite at $x=\pm 1$. The solution to Legendre's equation given by Eq. (1.60) is the maximum term of a series of solutions corresponding to the m and ℓ values [12, 18]. The rotational energy must be normalized by the total number of states—each corresponding to a set of quantum numbers of the power series solution. As demonstrated in the Excited States of the One-Electron Atom (Quantization) section, the quantum numbers of the excited states are

$$n = 2, 3, 4, \dots$$

$$\ell = 1, 2, \dots, n-1$$

$$m = -\ell, -\ell+1, \dots, 0, \dots, +\ell$$

In the case of an orbitsphere excited state, each rotational state solution of Eq. (1.59) (Legendre's equation) corresponds to a multipole moment of the charge-density function (Eq. (1.65)). $E_{\text{rotational orbital}}$ is normalized by $N_{\ell,s}$, the total number of multipole moments. $N_{\ell,s}$, the total number of multipole moments where each corresponds to an ℓ and m_ℓ quantum number of an energy level corresponding to a principal quantum number of n is

$$N_{\ell,s} = \sum_{\ell=0}^{n-1} \sum_{m_\ell=-\ell}^{+\ell} 1 = \sum_{\ell=0}^{n-1} 2\ell+1 = n^2 = (\ell+1)^2 = \ell^2 + 2\ell + 1 \quad (1.94)$$

Thus, C_2^2 is equal to $N_{\ell,s}^{-1}$ given by Eq. (1.94). Substitution of Eq. (1.94) into Eqs. (1.90) and (1.93) gives

$$E_{\text{rotational orbital}} = \frac{\hbar^2}{2I} \left[\frac{\ell(\ell+1)}{\ell^2 + 2\ell + 1} \right] = \frac{\hbar^2}{2I} \left[\frac{\ell}{\ell+1} \right] = \frac{\hbar^2}{2m_e r_n^2} \left[\frac{\ell}{\ell+1} \right] \quad (1.95)$$

Substitution of Eq. (1.94) into Eq. (1.90) with Eqs. (1.55) and (1.90) gives the orbital moment of inertia and angular momentum:

$$I_{\text{orbital}} = m_e r_n^2 \left[\frac{\ell(\ell+1)}{\ell^2 + 2\ell + 1} \right]^{\frac{1}{2}} = m_e r_n^2 \sqrt{\frac{\ell}{\ell+1}} \quad (1.96a)$$

$$L = I\omega_z = I_{\text{orbital}}\omega_z = m_e r_n^2 \left[\frac{\ell(\ell+1)}{\ell^2 + 2\ell + 1} \right]^{\frac{1}{2}} \omega_z = m_e r_n^2 \frac{\hbar}{m_e r_n^2} \sqrt{\frac{\ell}{\ell+1}} = \hbar \sqrt{\frac{\ell}{\ell+1}} \quad (1.96b)$$

In the case of the excited states, the orbitsphere charge-density function for $\ell \neq 0$, Eq. (1.65), is the sum of two functions of equal magnitude. L_z , total is given by the sum of the spin and orbital angular momenta. The principal energy levels of the excited states are split when a magnetic field is applied. The energy shifts due to spin and orbital angular momenta are given in the Spin and Orbital Splitting section.

$$l \neq 0$$

$$L_{z \text{ total}} = L_{z \text{ spin}} + L_{z \text{ orbital}} \quad (1.97)$$

Similarly, the orbital rotational energy arises from a spin function (spin angular momentum) modulated by a spherical harmonic angular function (orbital angular momentum). The time-averaged mechanical angular momentum and rotational energy associated with the traveling charge-density wave on the orbitsphere is zero:

$$\langle L_{z \text{ orbital}} \rangle = 0 \quad (1.98a)$$

$$\langle E_{\text{rotational orbital}} \rangle = 0 \quad (1.98b)$$

And, in the case of an excited state, the angular momentum of \hbar is carried by the fields of the trapped photon. The amplitudes that couple to external magnetic and electromagnetic fields are given by Eq. (1.95) and (1.96), respectively. The rotational energy due to spin is given by Eq. (1.82), and the total kinetic energy is given by Eq. (1.92). The demonstration that the modulated orbitsphere solutions are solutions of the wave equation appears in Box 1.1.

BOX 1.1. DERIVATION OF THE ROTATIONAL PARAMETERS OF THE ELECTRON FROM A SPECIAL CASE OF THE WAVE EQUATION—THE RIGID ROTOR EQUATION

For a time harmonic charge-density function, Eq. (1.49) becomes

$$\left[\frac{1}{r^2 \sin \theta} \frac{\partial}{\partial \theta} \left(\sin \theta \frac{\partial}{\partial \theta} \right)_{r, \phi} + \frac{1}{r^2 \sin^2 \theta} \left(\frac{\partial^2}{\partial \phi^2} \right)_{r, \theta} + \frac{\omega^2}{v^2} \right] A(\theta, \phi) = 0 \quad (1)$$

Substitution of the velocity about a Cartesian coordinate axis, $v = \rho \omega$, into Eq. (1) gives

$$\left[\frac{1}{r^2 \sin \theta} \frac{\partial}{\partial \theta} \left(\sin \theta \frac{\partial}{\partial \theta} \right)_{r, \phi} + \frac{1}{r^2 \sin^2 \theta} \left(\frac{\partial^2}{\partial \phi^2} \right)_{r, \theta} + \frac{\omega^2}{(\rho \omega)^2} \right] A(\theta, \phi) = 0 \quad (2)$$

Substitution of Eq. (1.55) into Eq. (1.2) gives

$$\left[\frac{1}{r^2 \sin \theta} \frac{\delta}{\delta \theta} \left(\sin \theta \frac{\delta}{\delta \theta} \right)_{r, \phi} + \frac{1}{r^2 \sin^2 \theta} \left(\frac{\delta^2}{\delta \phi^2} \right)_{r, \theta} + \frac{\omega_n^2}{\left(\rho \frac{\hbar}{m_e r_n^2} \right)^2} \right] A(\theta, \phi) = 0 \quad (4)$$

Multiplication by the denominator of the second term in Eq. (3) gives

$$\left[\left(\rho \frac{\hbar}{m_e r_n^2} \right)^2 \left[\frac{1}{r^2 \sin \theta} \frac{\partial}{\partial \theta} \left(\sin \theta \frac{\partial}{\partial \theta} \right)_{r, \phi} + \frac{1}{r^2 \sin^2 \theta} \left(\frac{\partial^2}{\partial \phi^2} \right)_{r, \theta} \right] + \omega_n^2 \right] A(\theta, \phi) = 0 \quad (4)$$

Substitution of Eq. (1.51) gives

$$\left[\left(\rho \frac{\hbar}{m_e r_n^2} \right)^2 \left[\frac{1}{r^2 \sin \theta} \frac{\partial}{\partial \theta} \left(\sin \theta \frac{\partial}{\partial \theta} \right)_{r,\phi} + \frac{1}{r^2 \sin^2 \theta} \left(\frac{\partial^2}{\partial \phi^2} \right)_{r,\theta} \right] + \frac{2E_{rot}}{I} \right] A(\theta, \phi) = 0 \quad (5)$$

The total rotational energy is given by the superposition of ℓ quantum states corresponding to a multipole expansion of total rotational energy of the orbitsphere. The total number, N , of multipole moments where each corresponds to an ℓ and m_ℓ quantum number of an energy level corresponding to a principal quantum number of n is

$$N = \sum_{\ell=0}^{n-1} \sum_{m_\ell=-\ell}^{+\ell} 1 = \sum_{\ell=0}^{n-1} 2\ell + 1 = \ell^2 + 2\ell + 1 = (\ell + 1)^2 = n^2 \quad (6)$$

Summing over all quantum states gives

$$\left[\sum_{\ell=0}^{n-1} \sum_{m_\ell=-\ell}^{+\ell} \left(\rho \frac{\hbar}{m_e r_n^2} \right)^2 \left[\frac{1}{r^2 \sin \theta} \frac{\partial}{\partial \theta} \left(\sin \theta \frac{\partial}{\partial \theta} \right)_{r,\phi} + \frac{1}{r^2 \sin^2 \theta} \left(\frac{\partial^2}{\partial \phi^2} \right)_{r,\theta} \right] + \sum_{\ell=0}^{n-1} \sum_{m_\ell=-\ell}^{+\ell} \frac{2E_{rot}}{I} \right] A(\theta, \phi) = 0 \quad (7)$$

Each of the orbital energy, orbital moment of inertia, and orbital angular momentum is a modulation of the orbitsphere function. Thus, the sum of ρ^2 over all ℓ quantum numbers is r_n^2 . Substitution of $\rho_z = r_n \cos \theta$; $\rho_x = r_n \sin \theta \cos \phi$; $\rho_y = r_n \sin \theta \sin \phi$ into Eq. (7) gives

$$\left[\left(r_n \frac{\hbar}{m_e r_n^2} \right)^2 \left[\frac{1}{r_n^2 \sin \theta} \frac{\partial}{\partial \theta} \left(\sin \theta \frac{\partial}{\partial \theta} \right)_{r,\phi} + \frac{1}{r_n^2 \sin^2 \theta} \left(\frac{\partial^2}{\partial \phi^2} \right)_{r,\theta} \right] + (\ell^2 + 2\ell + 1) \frac{2E_{rot}}{I} \right] A(\theta, \phi) = 0 \quad (8)$$

where $\frac{2E_{rot}}{I}$ is the constant, ω_n given by Eq. (1.55), and $r = r_n$. Eq. (8) can be expressed in terms of the rotational energy of any given mode by dividing the denominator of the first term by, K^2 , the factor corresponding to the vector projection of the rotational energy onto the z-axis.

$$\left[\frac{I \hbar^2}{2m_e^2 r_n^4 (\ell^2 + 2\ell + 1)} \left[\frac{1}{\sin \theta} \frac{\partial}{\partial \theta} \left(\sin \theta \frac{\partial}{\partial \theta} \right)_{r,\phi} + \frac{1}{\sin^2 \theta} \left(\frac{\partial^2}{\partial \phi^2} \right)_{r,\theta} \right] + E_{rot} \right] A(\theta, \phi) = 0 \quad (9)$$

In the case that E_{rot} is the total rotational energy which is equal to the kinetic energy of the orbitsphere given by Eq. (1.92) and that the moment of inertia is given by

$$I = m_e r_n^2 \quad (10)$$

Eq. (9) becomes equivalent to Eq. (1.59).

$$\left[\frac{1}{N} \frac{\hbar^2}{2I} \left[\frac{1}{\sin \theta} \frac{\partial}{\partial \theta} \left(\sin \theta \frac{\partial}{\partial \theta} \right)_{r,\phi} + \frac{1}{\sin^2 \theta} \left(\frac{\partial^2}{\partial \phi^2} \right)_{r,\theta} \right] + E_{rot \text{ total}} \right] A(\theta, \phi) = 0$$

where N is one. Eq. (11) applies to all of the multipole modes of the rotational energy with the appropriate moment of inertia, I , and factor N ; thus, the rotational energy of each mode is given by Eq. (1.58) with these conditions. Eq. (9) can be expressed in terms of the rotational energy of any given mode by dividing the first term by, K^2 , the factor corresponding to the vector projection of the rotational energy and the moment of inertia onto the z-axis.

$$\frac{I\hbar^2}{2m_e^2 r_n^4 K^2 (\ell^2 + 2\ell + 1)} \left[\frac{1}{\sin \theta} \frac{\partial}{\partial \theta} \left(\sin \theta \frac{\partial}{\partial \theta} \right)_{r,\phi} + \frac{1}{\sin^2 \theta} \left(\frac{\partial^2}{\partial \phi^2} \right)_{r,\theta} + E_{rot} \right] A(\theta, \phi) = 0 \quad (12)$$

where in the case of the spherical harmonics, $N = \ell^2 + 2\ell + 1$. From Eq. (1.51) and Eq. (1.88), Eq. (12) can be expressed as

$$\left[\frac{\hbar^2}{m_e^2 r_n^4 K^2 (\ell^2 + 2\ell + 1)} \left[\frac{1}{\sin \theta} \frac{\partial}{\partial \theta} \left(\sin \theta \frac{\partial}{\partial \theta} \right)_{r,\phi} + \frac{1}{\sin^2 \theta} \left(\frac{\partial^2}{\partial \phi^2} \right)_{r,\theta} \right] + \frac{L^2}{I^2} \right] A(\theta, \phi) = 0 \quad (13)$$

In the case of the spherical harmonic functions with Eq. (1.88) and Eq. (1.55), Eq. (12) gives

$$\sqrt{\frac{\hbar^2 (\ell(\ell+1))}{m_e^2 r_n^4 K^2 (\ell^2 + 2\ell + 1)}} = \frac{L}{I} = \frac{\hbar}{m_e r_n^2} \quad (14)$$

Thus,

$$\sqrt{\frac{(\ell(\ell+1))}{(\ell^2 + 2\ell + 1)}} = K \quad (15)$$

Eq. (12) becomes Eq. (11) where the rotational energy is given by Eq. (1.95).

$$E_{\text{rotational orbital}} = \frac{\hbar^2}{2I} \left[\frac{\ell(\ell+1)}{\ell^2 + 2\ell + 1} \right] \quad (16)$$

and the orbital moment of inertia is given by Eq. (1.96).

$$I_{\text{orbital}} = m_e r_n^2 \left[\frac{\ell(\ell+1)}{\ell^2 + 2\ell + 1} \right]^{\frac{1}{2}} \quad (17)$$

The Substitution of Eqs. (1.65), (6), and (16) into Eq. (11) gives

$$-\frac{\hbar^2}{2I} \left[\frac{\ell(\ell+1)}{\ell^2 + 2\ell + 1} \right] + \frac{\hbar^2}{2m_e r_n^2} \sqrt{\frac{\ell(\ell+1)}{\ell^2 + 2\ell + 1}} = 0 \quad (18)$$

Substitution of Eq. (17) into Eq. (18) gives

$$-\frac{\hbar^2}{2m_e r_n^2 \sqrt{\frac{\ell(\ell+1)}{\ell^2 + 2\ell + 1}}} \left[\frac{\ell(\ell+1)}{\ell^2 + 2\ell + 1} \right] + \frac{\hbar^2}{2m_e r_n^2} \sqrt{\frac{\ell(\ell+1)}{\ell^2 + 2\ell + 1}} = 0 \quad (19)$$

$$0 = 0 \quad (20)$$

Thus, the modulated orbitsphere solutions are shown to be solutions of the wave equation by their substitution into the wave

equation (Eqs. (18-20). The present derivation of the rigid rotor equation given by the substitution of

$$\begin{aligned} E_{rot} &= \frac{1}{2} I \omega_n^2 \\ \omega_n &= \frac{\hbar}{m_e r_n^2} \\ v &= \rho \omega_n \end{aligned} \quad (21)$$

is consistent with the wave equation relationship:

$$v = \lambda \frac{\omega}{2\pi} \quad (22)$$

Whereas, Schrödinger derivation from the Helmholtz equation [1] with the substitution of

$$\lambda = \frac{h}{m_e v} \quad (23)$$

gives the rigid rotor equation with the paradox that

$$v^2 = \frac{h}{m_e} \frac{\omega}{2\pi} \quad (24)$$

which is not the wave relationship,

$$v = \lambda \frac{\omega}{2\pi} \quad (25)$$

References

1. McQuarrie, D. A., Quantum Chemistry, University Science Books, Mill Valley, CA, (1983), pp. 78-79.

MAGNETIC PARAMETERS OF THE ELECTRON (BOHR MAGNETON)

The Magnetic Field of an Orbitsphere from Spin

The orbitsphere with $\ell = 0$ is a shell of negative charge current comprising correlated charge motion along great circles. The superposition of the vector projection of the orbitsphere angular momentum on the z-axis is $\frac{\hbar}{2}$ with an orthogonal component of $\frac{\hbar}{4}$. As

shown in the Orbitsphere Equation of Motion for $\ell = 0$ section, the application of a magnetic field to the orbitsphere gives rise to a precessing angular momentum vector S directed from the origin of the orbitsphere at an angle of $\theta = \frac{\pi}{3}$ relative to the applied magnetic field.

The precession of S with an angular momentum of \hbar forms a cone in the nonrotating laboratory frame to give a perpendicular projection of

$S_1 = \pm \sqrt{\frac{3}{4}}\hbar$ (Eq. (1.74a)) and a projection onto the axis of the applied magnetic field of $S_0 = \pm \frac{\hbar}{2}$ (Eq. (1.74b)). The superposition of the $\frac{\hbar}{2}$ z-axis component of the orbitsphere angular momentum and the $\frac{\hbar}{2}$ z-axis component of S gives \hbar corresponding to the observed magnetostatic electron magnetic moment of a Bohr magneton. The \hbar of angular momentum along S has a corresponding precessing magnetic moment of 1 Bohr magneton [19]:

$$\mu_B = \frac{e\hbar}{2m_e} = 9.274 \times 10^{-24} \text{ JT}^{-1} \quad (1.99)$$

The rotating magnetic field of S is discussed in Box 1.2. The magnetostatic magnetic field corresponding to μ_B derived below is given by

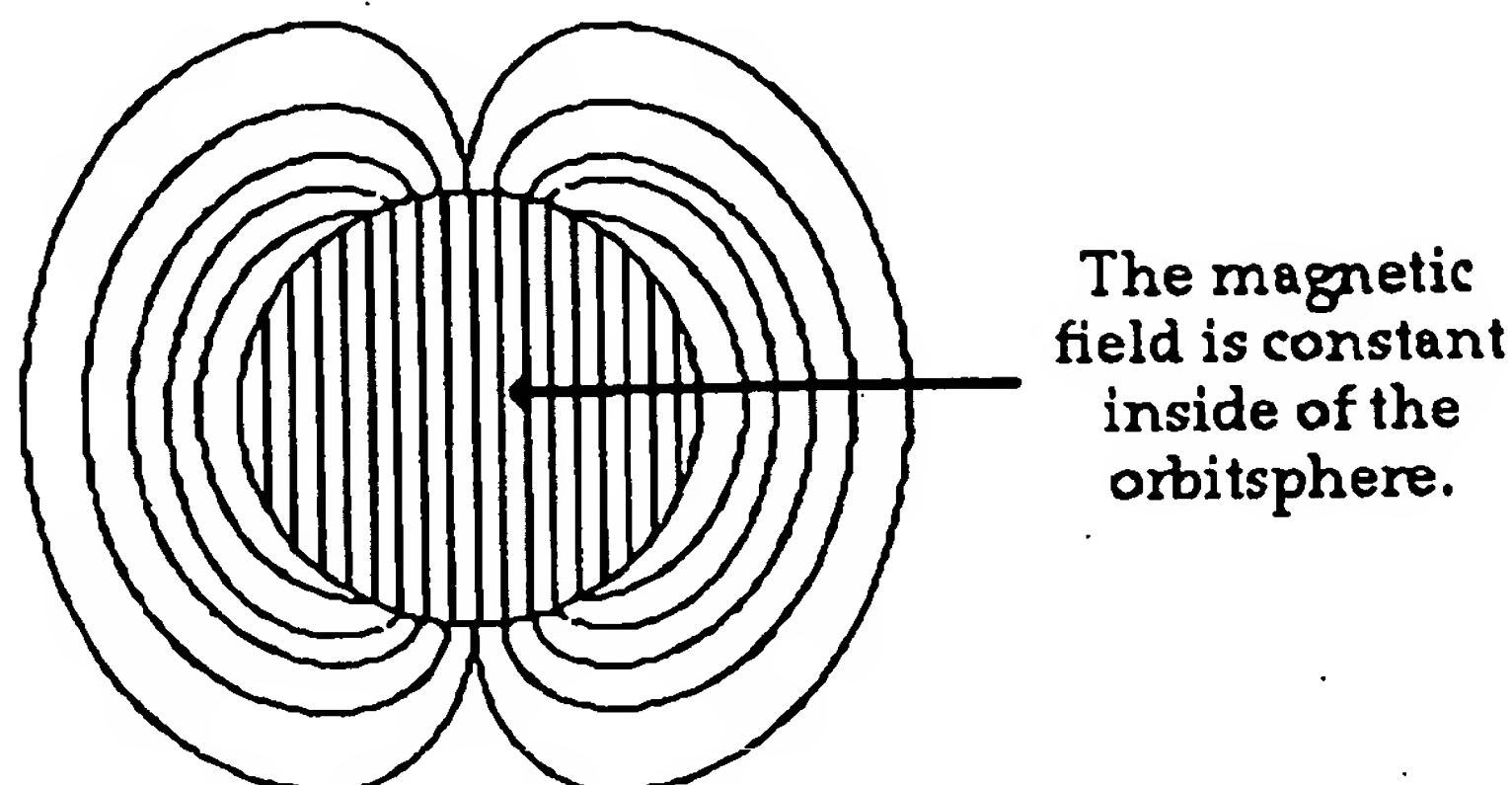
$$\mathbf{H} = \frac{e\hbar}{m_e r_n^3} (\mathbf{i}_r \cos \theta - \mathbf{i}_\theta \sin \theta) \quad \text{for } r < r_n \quad (1.100)$$

$$\mathbf{H} = \frac{e\hbar}{2m_e r^3} (\mathbf{i}_r 2 \cos \theta + \mathbf{i}_\theta \sin \theta) \quad \text{for } r > r_n \quad (1.101)$$

It follows from Eq. (1.99), the relationship for the Bohr magneton, and relationship between the magnetic dipole field and the magnetic moment \mathbf{m} [20] that Eqs. (1.100) and (1.101) are the equations for the magnetic field due to a magnetic moment of a Bohr magneton, $\mathbf{m} = \mu_B \mathbf{i}_z$, where $\mathbf{i}_z = \mathbf{i}_r \cos \theta - \mathbf{i}_\theta \sin \theta$. Note that the magnetic field is a constant for $r < r_n$. See Figure 1.9. It is shown in the Magnetic Parameters of the Electron (Bohr Magnetron) section that the energy stored in the magnetic field of the electron orbitsphere is

$$E_{\text{mag, total}} = \frac{\pi \mu_0 e^2 \hbar^2}{m_e^2 r_1^3} \quad (1.102)$$

Figure 1.9. The magnetic field of an electron orbitsphere (z-axis defined as the vertical axis).



Derivation of the Magnetic Field

For convenience the angular momentum vector with a magnitude in the stationary frame of \hbar will be defined as the z-axis as shown in Figure 1.9⁷. The magnetic field must satisfy the following relationships:

$$\nabla \cdot \mathbf{H} = 0 \text{ in free space} \quad (1.103)$$

$$\mathbf{n} \times (\mathbf{H}_a - \mathbf{H}_b) = \mathbf{K} \quad (1.104)$$

$$\mathbf{n} \cdot (\mathbf{H}_a - \mathbf{H}_b) = 0 \quad (1.105)$$

$$\mathbf{H} = -\nabla \psi \quad (1.106)$$

Since the field is magnetostatic, the current is equivalent to current loops along the z-axis. Then, the z-component of the current, $|i|$, for a current loop of total charge, e , oriented at an angle θ with respect to the z-axis is given by the product of the charge, the angular velocity given by Eq. (1.55), and $\sin\theta$ where the projection of the current of the orbitsphere perpendicular to the z-axis which carries the incremental current, ii_ϕ , is a function of $\sin\theta$.

⁷ As shown in Box 1.2, the angular momentum of \hbar on the S-axis is due to a photon standing wave that is phase-matched to a spherical harmonic source current, a spherical harmonic dipole $Y_l^m(\theta, \phi) = \sin\theta$ with respect to the S-axis. The dipole spins about the S-axis at the angular velocity given by Eq.(1.55). Since the field is magnetostatic in the RF rotating frame, the current is equivalent to current loops along the S-axis. Thus, the derivation of the corresponding magnetic field is the same as that of the stationary field given in this section.

$$|i| = \frac{e\hbar}{m_e r_n^2} \sin \theta \quad (1.107)$$

The angular function of the current density of the orbitsphere is normalized by the geometrical factor N [17] given by

$$N = \frac{4\pi r_n^3}{2\pi \int_{-r_n}^{r_n} (r_n^2 - z^2) dz} = \frac{3}{2} \quad (1.108)$$

corresponding to the angular momentum of \hbar . (Eq. (1.108) can also be expressed in spherical coordinates for the density of a uniform shell divided by the integral in θ and ϕ of that of a spherical dipole squared [12]. The integration gives $\frac{8\pi}{3}$ which normalized by the uniform mass-

density factor of 4π gives the geometrical factor of $\left(\frac{2}{3}\right)^{-1}$. The current density Ki_ϕ along the z -axis having a vector orientation perpendicular to the angular momentum vector is given by dividing the magnitude of ii_ϕ (Eq. (1.107)) by the length r_n . The current density of the orbitsphere in the incremental length dz is

$$K(\rho, \phi, z) = i_\phi N \frac{e\hbar}{m_e r_n^3} = i_\phi \frac{3}{2} \frac{e\hbar}{m_e r_n^3} \quad (1.109)$$

Because

$$z = r \cos \theta \quad (1.110)$$

the differential length is given by

$$dz = -\sin \theta r_n d\theta \quad (1.111)$$

and so the current density in the differential length $r_n d\theta$ as measured along the periphery of the orbitsphere is a function of $\sin \theta$ as given in Eq. (1.107). From Eq. (1.109), the surface current-density function of the orbitsphere about the z -axis (S -axis) is given by

$$K(r, \theta, \phi) = i_\phi \frac{3}{2} \frac{e\hbar}{m_e r_n^3} \sin \theta \quad (1.112)$$

Substitution of Eq. (1.112) into Eq. (1.104) gives

$$H_\theta^a - H_\theta^b = \frac{3}{2} \frac{e\hbar}{m_e r_n^3} \sin \theta \quad (1.113)$$

To obtain H_θ , the derivative of Ψ with respect to θ must be taken, and this suggests that the θ dependence of Ψ be taken as $\cos \theta$. The field is finite at the origin and is zero at infinity; so, solutions of Laplace's equation in spherical coordinates are selected because they are consistent with these conditions [21].

$$\Psi = C \left[\frac{r}{r_n} \right] \cos \theta ; \quad r < r_n \quad (1.114)$$

$$\Psi = A \left[\frac{r_n}{r} \right]^2 \cos \theta ; \quad r > r_n \quad (1.115)$$

The negative gradients of these potentials are

$$\mathbf{H} = \frac{-C}{r_n} (\mathbf{i}_r \cos \theta - \mathbf{i}_\theta \sin \theta) \quad \text{for } r < r_n \quad (1.116)$$

$$\mathbf{H} = \frac{A}{r_n} \left[\frac{r_n}{r} \right]^3 (\mathbf{i}_r 2 \cos \theta + \mathbf{i}_\theta \sin \theta) \quad \text{for } r > r_n \quad (1.117)$$

The continuity conditions of Eqs. (1.104), (1.105), (1.112), and (1.113) are applied to obtain the following relationships among the variables

$$\frac{-C}{r_n} = \frac{2A}{r_n} \quad (1.118)$$

$$\frac{A}{r_n} - \frac{C}{r_n} = \frac{3}{2} \frac{e\hbar}{m_e r_n^3} \quad (1.119)$$

Solving the variables algebraically gives the magnetic fields of an electron:

$$\mathbf{H} = \frac{e\hbar}{m_e r_n^3} (\mathbf{i}_r \cos \theta - \mathbf{i}_\theta \sin \theta) \quad \text{for } r < r_n \quad (1.120)$$

$$\mathbf{H} = \frac{e\hbar}{2m_e r^3} (\mathbf{i}_r 2 \cos \theta + \mathbf{i}_\theta \sin \theta) \quad \text{for } r > r_n \quad (1.121)$$

The field is that of a Bohr magneton which matches the observed boundary conditions given in the Orbitsphere Equation of Motion for $\ell=0$ section including the required spherical symmetry. The demonstration that the boundary conditions of the electron in a magnetic field are met appears in Box 1.2.

Derivation of the Energy

The energy stored in the magnetic field of the electron is

$$E_{mag} = \frac{1}{2} \mu_o \int_0^{2\pi} \int_0^\pi \int_0^\infty H^2 r^2 \sin \theta dr d\theta d\Phi \quad (1.122)$$

$$E_{mag \text{ total}} = E_{mag \text{ external}} + E_{mag \text{ internal}} \quad (1.123)$$

$$E_{mag \text{ internal}} = \frac{1}{2} \mu_o \int_0^{2\pi} \int_0^{\pi} \int_0^{r_1} \left[\frac{e\hbar}{m_e r_1^3} \right]^2 (\cos^2 \theta + \sin^2 \theta) r^2 \sin \theta dr d\theta d\Phi \quad (1.124)$$

$$E_{mag \text{ internal}} = \frac{2\pi\mu_o e^2 \hbar^2}{3m_e^2 r_1^3} \quad (1.125)$$

$$E_{mag \text{ external}} = \frac{1}{2} \mu_o \int_0^{2\pi} \int_0^{\pi} \int_{r_1}^{\infty} \left[\frac{e\hbar}{2m_e r_1^3} \right]^2 (4\cos^2 \theta + \sin^2 \theta) r^2 \sin \theta dr d\theta d\Phi \quad (1.126)$$

$$E_{mag \text{ external}} = \frac{\pi\mu_o e^2 \hbar^2}{3m_e^2 r_1^3} \quad (1.127)$$

$$E_{mag \text{ total}} = \frac{2\pi\mu_o e^2 \hbar^2}{3m_e^2 r_1^3} + \frac{\pi\mu_o e^2 \hbar^2}{3m_e^2 r_1^3} \quad (1.128)$$

$$E_{mag \text{ total}} = \frac{\pi\mu_o e^2 \hbar^2}{m_e^2 r_1^3} \quad (1.129)$$

$$E_{mag \text{ total}} = \frac{4\pi\mu_o \mu_B^2}{r_1^3} \quad (1.130)$$

BOX 1.2. BOUNDARY CONDITIONS OF THE ELECTRON IN A MAGNETIC FIELD ARE MET

As shown in the Electron g Factor section, when a magnetic field with flux B is applied to an electron in a central field which comprises current loops, the orbital radius of each does not change due to the Lorentzian force provided by B , but the velocity changes as follows [1]:

$$\Delta v = \frac{e r B}{2m_e} \quad (1)$$

corresponding to precession frequency of

$$\omega = \frac{\Delta v}{r} = \frac{eB}{2m_e} = \gamma_e B \quad (2)$$

where γ_e is the electron gyromagnetic ratio and ω is the Larmor frequency. Eq. (1) applies to the current perpendicular to the magnetic flux. In this case, the moment of inertia I of the orbitsphere which is a uniformly charged sphere [2] is

$$I = \frac{2}{3} m_e r_1^2 \quad (3)$$

From Eqs. (2) and (3), the corresponding angular momentum L and rotational energy E_{rot} are

$$L = I\omega = \frac{2}{3}m_e r_1^2 \gamma_e B \quad (4)$$

and

$$E_{rot} = \frac{1}{2}I\omega^2 = \frac{1}{3}m_e r_1^2 (\gamma_e B)^2 \quad (5)$$

respectively. The change in the magnetic moment corresponding to Eq. (1) is [1]:

$$\Delta m = -\frac{e^2 r_1^2}{4m_e} B \quad (6)$$

Using Eqs. (2-6), in the case of a very strong magnetic flux of 10 T applied to atomic hydrogen:

$$\omega = 8.794 \times 10^{11} \text{ rad} \cdot \text{sec}^{-1} \quad (7)$$

$$I = 1.701 \times 10^{-51} \text{ kg} \cdot \text{m}^2 \quad (8)$$

$$L = 1.496 \times 10^{-39} \text{ J} \cdot \text{s} \quad (9)$$

$$E_{rot} = 6.576 \times 10^{-28} \text{ J} = 4.104 \times 10^{-9} \text{ eV} \quad (10)$$

and

$$\Delta m = 1.315 \times 10^{-28} \text{ J} \cdot \text{T}^{-1} \quad (11)$$

where the radius is given by Eq. (1.229) and $2/3$, the geometrical factor of a uniformly charged sphere [2], was used in the case of Eq. (11). Thus, these effects of the magnetic field are very small when they are compared to the intrinsic angular momentum of the electron of

$$L = \hbar = 1.055 \times 10^{-34} \text{ J} \cdot \text{s} \quad (12)$$

The electronic angular frequency of hydrogen given by Eqs. (1.55) and (1.229)

$$\omega_1 = \frac{\hbar}{m_e r_1^2} = 4.134 \times 10^{16} \text{ rad} \cdot \text{sec}^{-1} \quad (13)$$

the total kinetic energy given by Eq. (1.231)

$$T = 13.606 \text{ eV} \quad (14)$$

and the magnetic moment of a Bohr magneton given by Eq. (1.99)

$$\mu_B = \frac{e\hbar}{2m_e} = 9.274 \times 10^{-24} \text{ JT}^{-1} \quad (15)$$

E_{rot} is the energy that arises due to the application of the external flux B . Thus, the external work required to apply the field is also given by Eq. (10). Since the orbitsphere is uniformly charged and is superconducting, this energy is conserved when the field is removed. It is also independent of the direction of the magnetic moment due to the intrinsic angular momentum of the orbitsphere of \hbar . The corresponding magnetic moment given by Eq. (6) does not change when the intrinsic magnetic moment of the electron changes orientation. Thus, it does not contribute

to the energy of a spin-flip transition observed by the Stern Gerlach experiment. It always opposes the applied field and gives rise to the phenomenon of the diamagnetic susceptibility of materials which Eq. (6) predicts with very good agreement with observations [1]. Eq. (6) also predicts the absolute chemical shifts of hydride ions that match experimental observations as shown in the Hydrino Hydride Ion Nuclear Magnetic Resonance Shift section.

As shown in the Spin Angular Momentum of the Orbitsphere with $\ell = 0$ section, the angular momentum of the orbitsphere in a magnetic field comprises the initial $\frac{\hbar}{2}$ projection on the z-axis and the initial $\frac{\hbar}{4}$ vector component in the xy-plane that precesses about the z-axis. A resonant excitation of the Larmor precession frequency gives rise to an additional component of angular momentum which is consistent with Maxwell's equations. As shown in the Excited States of the One-Electron Atom (Quantization) section, conservation of the \hbar of angular momentum of a trapped photon can give rise to \hbar of electron angular momentum along the S-axis. The photon standing waves of excited states are spherical harmonic functions which satisfy Laplace's equation in spherical coordinates and provide the force balance for the corresponding charge (mass)-density waves. Consider the photon in the case of the precessing electron with a Bohr magneton of magnetic moment along the S-axis. The radius of the orbitsphere is unchanged, and the photon gives rise to current on the surface that satisfies the condition

$$\nabla \cdot J = 0 \quad (16)$$

corresponding to a rotating spherical harmonic dipole [3] that phase-matches the current (mass) density of Eq. (1.112). Thus, the electrostatic energy is constant, and only the magnetic energy need be considered as given by Eqs. (23-25). The corresponding central field at the orbitsphere surface given by the superposition of the central field of the proton and that of the photon follows from Eqs. (2.10-2.17):

$$\mathbf{E} = \frac{e}{4\pi\epsilon_0 r^2} \left[Y_0^0(\theta, \phi) \mathbf{i}_r + \text{Re} \{ Y_1^m(\theta, \phi) e^{i\omega t} \} \mathbf{i}_y \delta(r - r_1) \right] \quad (17)$$

where the spherical harmonic dipole $Y_1^m(\theta, \phi) = \sin\theta$ is with respect to the S-axis. Force balance according to Eq. (1.222) is maintained by the equivalence of the harmonic modulation of the charge and the mass where e/m_e is invariant as given in the Special Relativistic Correction to the Ionization Energies section. The dipole spins about the S-axis at the angular velocity given by Eq. (1.55). In the frame rotating about the S axis, the electric field of the dipole is

$$\mathbf{E} = \frac{e}{4\pi\epsilon_0 r^2} \sin\theta \sin\phi \delta(r - r_1) \mathbf{i}_y \quad (18)$$

$$\mathbf{E} = \frac{e}{4\pi\epsilon_0 r^2} (\sin\theta \sin\phi \mathbf{i}_r + \cos\theta \sin\phi \mathbf{i}_\theta + \sin\theta \cos\phi \mathbf{i}_\phi) \delta(r - r_1) \quad (19)$$

The resulting current is nonradiative as shown by Eq. (1.39) and in Appendix I: Nonradiation Based on the Electromagnetic Fields and the Poynting Power Vector. Thus, the field in the RF rotating frame is magnetostatic as shown in Figure 1.9 but directed along the S-axis. The time-averaged angular momentum and rotational energy due to the charge density wave are zero as given by Eqs. (1.98a) and (1.98b). However, the corresponding time-dependent surface charge density $\langle\sigma\rangle$ that gives rise to the dipole current of Eq. (1.112) as shown by Haus [4] is equivalent to the current due to a uniformly charged sphere rotating about the S-axis at the constant angular velocity given by Eq. (1.55). The charge density is given by Gauss' law at the two-dimensional surface:

$$\sigma = -\epsilon_0 \mathbf{n} \cdot \nabla \Phi|_{r=r_1} = -\epsilon_0 \mathbf{n} \cdot \mathbf{E}|_{r=r_1} \quad (20)$$

From Eq. (19), $\langle\sigma\rangle$ is

$$\langle\sigma\rangle = \frac{e}{4\pi r_1^2} \frac{3}{2} \sin\theta \quad (21)$$

and the current (Eq. (1.112)) is given by the product of Eq. (21) and the constant angular frequency (Eq. (1.55)). The precession of the magnetostatic dipole results in magnetic dipole radiation or absorption during a Stern-Gerlach transition. The application of a magnetic field causes alignment of the intrinsic electron magnetic moment of atoms of a material such that the population of electrons parallel versus antiparallel is a Boltzmann distribution which depends on the temperature of the material. Following the removal of the field, the original random-orientation distribution is restored as is the original temperature. The distribution may be altered by the application of an RF pulse at the Larmor frequency.

The application of a magnetic field with a resonant Larmor excitation gives rise to a precessing angular momentum vector \mathbf{S} of magnitude \hbar directed from the origin of the orbitsphere at an angle of $\theta = \frac{\pi}{3}$ relative to the applied magnetic field. \mathbf{S} rotates about the axis of the applied field at the Larmor frequency. The magnitude of the components of \mathbf{S} that are parallel and orthogonal to the applied field (Eqs (1.74a-1.74b)) are $\frac{\hbar}{2}$ and $\sqrt{\frac{3}{4}}\hbar$, respectively. Since both the RF field and the orthogonal components shown in Figure 1.7 rotate at the Larmor frequency, the RF field that causes a Stern Gerlach transition produces a stationary magnetic field with respect to these components as described by Patz [5].

The component of Eq. (1.74b) adds to the initial $\frac{\hbar}{2}$ parallel component to give a total of \hbar in the stationary frame corresponding to a Bohr magneton, μ_B , of magnetic moment. Eqs. (2) and (6) also hold in the case of the Stern Gerlach experiment. Superposition holds for Maxwell's equations, and only the angular momentum given by Eqs. (1.68-1.71) and the source current corresponding to Eq. (17) need be considered. Since it does not change, the diamagnetic component given from Eq. (1) does not contribute to the spin-flip transition as discussed *supra*. The potential energy of a magnetic moment m in the presence of flux B [6] is

$$E = m \cdot B \quad (22)$$

The angular momentum of the electron gives rise to a magnetic moment of μ_B . Thus, the energy ΔE_{mag}^{spin} to switch from parallel to antiparallel to the field is given by Eq. (1.136)

$$\Delta E_{mag}^{spin} = 2\mu_B \mathbf{i}_z \cdot \mathbf{B} = 2\mu_B B \cos \theta = 2\mu_B B \quad (23)$$

In the case of an applied flux of 10 T, Eq. (23) gives

$$\Delta E_{mag}^{spin} = 1.855 \times 10^{-22} \text{ J} = 1.158 \times 10^{-3} \text{ eV} \quad (24)$$

ΔE_{mag}^{spin} is also given by Planck's equation. It can be shown from conservation of angular momentum considerations (Eqs. (26-32)) that the Zeeman splitting is given by Planck's equation and the Larmor frequency based on the gyromagnetic ratio (Eq. (2)). The electron's magnetic moment may only be parallel or antiparallel to the magnetic field rather than at a continuum of angles including perpendicular according to Eq. (22). No continuum of energies predicted by Eq. (22) for a pure magnetic dipole are possible. The energy difference for the magnetic moment to flip from parallel to antiparallel to the applied field is

$$\Delta E_{mag}^{spin} = 2\hbar\omega = 1.855 \times 10^{-22} \text{ J} = 1.158 \times 10^{-3} \text{ eV} \quad (25)$$

corresponding to magnetic dipole radiation.

As demonstrated in the Orbitsphere Equation of Motion for $\ell = 0$ section, $\frac{\hbar}{2}$ of the orbitsphere angular momentum designated the static component is initially parallel to the field. An additional $\frac{\hbar}{2}$ parallel component designated the dynamic component comes from the \hbar of angular momentum along S . The angular momentum in the presence of an applied magnetic field is [7]

$$\mathbf{L} = \mathbf{r} \times (m_e \mathbf{v} + e\mathbf{A}) \quad (26)$$

where \mathbf{A} is the vector potential evaluated at the location of the orbitsphere. The circular integral of \mathbf{A} is the flux linked by the electron. During a Stern-Gerlach transition a resonant RF photon is absorbed or emitted, and the \hbar component along S reverses direction. It is shown by

Eqs. (29-32) that the dynamic parallel component of angular momentum corresponding to the vector potential due to the lightlike transition is equal to the "kinetic angular momentum" ($\mathbf{r} \times m\mathbf{v}$) of $\frac{\hbar}{2}$. Conservation of angular momentum of the orbitsphere requires that the static angular momentum component concomitantly flips. The static component of angular momentum undergoes a spin flip, and concomitantly the "potential angular momentum" ($\mathbf{r} \times e\mathbf{A}$) of the dynamic component must change by $-\frac{\hbar}{2}$ due to the linkage of flux by the electron such that the total angular momentum is conserved.

In spherical coordinates, the relationship between the vector potential A and the flux B is

$$2\pi r A = \pi r^2 B \quad (27)$$

Eq. (27) can be substituted into Eq. (26) since the magnetic moment m is given [6] as

$$m = \frac{\text{charge} \cdot \text{angular momentum}}{2 \cdot \text{mass}} \quad (28)$$

and the corresponding energy is consistent with Eqs. (23) and (25) in this case as follows:

$$\Delta m = -\frac{e(\mathbf{r} \times e\mathbf{A})}{2m_e} = \frac{e\frac{\hbar}{2}}{2m_e} = \frac{\mu_B}{2} \quad (29)$$

The boundary condition that the angular momentum is conserved is shown by Eqs. (1.133-1.135). It can be shown that Eq. (29) is also consistent with the vector potential along the axis of the applied field [8] given by

$$A = \cos \frac{\pi}{3} \mu_0 \frac{e\hbar}{2m_e r^2} \sin \theta_i = \mu_0 \frac{1}{2} \frac{e\hbar}{2m_e r^2} \sin \theta_i \quad (30)$$

Substitution of Eq. (30) into Eq. (29) gives

$$\Delta m = -\frac{e(\mathbf{r} \times e\mu_0 \frac{1}{2} \frac{e\hbar}{2m_e r^2} \sin \theta_i)}{2m_e} = -\frac{1}{2} \left[\frac{\mu_0 e^2}{2m_e r} \right] \frac{e\hbar}{2m_e} \quad (31)$$

with the geometrical factor of $2/3$ [2] and the current given by Eq. (1.112). Since k is the lightlike k^0 , then $k = \omega_n / c$ corresponding to the RF photon field. The relativistic corrections of Eq. (31) are given by Eqs. (1.218) and (1.219) and the relativistic radius $r = \lambda_e$ given by Eq. (1.217).

The relativistically corrected Eq. (31) is

$$\Delta m = -\frac{1}{2} (2\pi\alpha)^{-1} \left[\frac{\mu_0 e^2}{2m_e \alpha a_0} \right] \frac{e\hbar}{2m_e} = \frac{\mu_B}{2} \quad (32)$$

The magnetic flux of the electron is given by

$$\nabla \times \mathbf{A} = \mathbf{B}$$

(33)

Substitution of Eq. (30) into Eq. (33) gives 1/2 the flux of Eq. (1.121).

From Eq. (28), the $\frac{\hbar}{2}$ of angular momentum before and after the field is applied corresponds to an initial magnetic moment on the applied-field-axis of $\frac{\mu_B}{2}$. After the field is applied, the contribution of $\frac{\mu_B}{2}$ from Eq. (29) with Eq. (27) gives a total magnetic moment along the applied-field-axis of μ_B , a Bohr magneton, wherein the additional contribution (Eq. (28)) arises from the angular momentum of \hbar on the S-axis. Thus, even though the magnitude of the vector projection of the angular momentum of the electron in the direction of the magnetic field is $\frac{\hbar}{2}$, the magnetic moment corresponds to \hbar due to the $\frac{\hbar}{2}$ contribution from the dynamic component, and the quantized transition is due to the requirement of angular momentum conservation as given by Eq. (28).

Eq. (22) implies a continuum of energies; whereas, Eq. (29) shows that the static-kinetic and dynamic vector potential components of the angular momentum are quantized at $\frac{\hbar}{2}$. Consequently, as shown in the Electron g Factor section, the flux linked during a spin transition is quantized as the magnetic flux quantum:

$$\Phi_0 = \frac{h}{2e} \quad (34)$$

Only the states corresponding to

$$m_s = \pm \frac{1}{2} \quad (35)$$

are possible due to conservation of angular momentum. It is further shown using the Poynting power vector with the requirement that flux is linked in units of the magnetic flux quantum, that the factor 2 of Eqs. (23) and (25) is replaced by the electron g factor.

Thus, in terms of flux linkage, the electron behaves as a superconductor with a weak link [9] as described in the Josephson Junction, Weak Link section and the Superconducting Quantum Interference Device (SQUID) section. Consider the case of a current loop with a weak link comprising a large number of superconducting electrons (e.g. 10^{10}). As the applied field increases, the Meissner current increases. In equilibrium, a dissipationless supercurrent can flow around the loop driven by the difference between the flux Φ that threads the loop and the external flux Φ_e applied to the loop. Based on the physics of the electrons carrying the supercurrent, when the current reaches the critical current, the kinetic angular momentum change of $\frac{\hbar}{2}$ equals the

magnitude of the potential angular momentum change corresponding to the vector potential according to Eqs. (26) and (31). As a consequence, the flux is linked in units of the magnetic flux quantum as shown in the Electron g Factor section.

References

1. E. M. Purcell, Electricity and Magnetism, McGraw-Hill, New York, (1965), pp. 370-379.
2. G. R. Fowles, Analytical Mechanics, Third Edition, Holt, Rinehart, and Winston, New York, (1977), p. 196.
3. J. D. Jackson, Classical Electrodynamics, Second Edition, John Wiley & Sons, New York, (1975), pp. 84-102; 752-763.
4. H. A. Haus, J. R. Melcher, "Electromagnetic Fields and Energy", Department of Electrical engineering and Computer Science, Massachusetts Institute of Technology, (1985), Sec. 8.6.
5. S. Patz, Cardiovasc Interven Radiol, (1986), 8:25, pp. 225-237.
6. D. A. McQuarrie, Quantum Chemistry, University Science Books, Mill Valley, CA, (1983), pp. 238-241.
7. E. M. Purcell, Electricity and Magnetism, McGraw-Hill, New York, (1965), p. 447.
8. E. M. Purcell, Electricity and Magnetism, McGraw-Hill, New York, (1965), pp. 361-367.
9. C. E. Gough, Colclough, M. S., Forgan, E. M., Jordan, R. G., Keene, M., Muirhead, C. M., Rae, A. I. M., Thomas, N., Abell, J. S., Sutton, S., Nature, Vol. 326, (1987), P. 855.

ELECTRON g FACTOR

As demonstrated by Purcell [15], when a magnetic field is applied to an electron in a central field which comprises a current loop, the orbital radius does not change, but the velocity changes as follows:

$$\Delta v = \frac{e r B}{2 m_e} \quad (1.131)$$

This corresponds to diamagnetism and gives rise to precession with a corresponding resonance as shown in Box 1.2. The angular momentum in the presence of an applied magnetic field is [15]

$$\mathbf{L} = \mathbf{r} \times (m_e \mathbf{v} + e \mathbf{A}) \quad (1.132)$$

where \mathbf{A} is the vector potential evaluated at the location of the orbitsphere. Conservation of angular momentum of the orbitsphere permits a discrete change of its "kinetic angular momentum" ($\mathbf{r} \times m \mathbf{v}$) with

respect to the field of $\frac{\hbar}{2}$, and concomitantly the "potential angular momentum" ($\mathbf{r} \times e\mathbf{A}$) must change by $-\frac{\hbar}{2}$. The flux change, ϕ , of the orbitsphere for $r < r_n$ is determined as follows [15]:

$$\Delta\mathbf{L} = \frac{\hbar}{2} - \mathbf{r} \times e\mathbf{A} \quad (1.133)$$

$$= \left[\frac{\hbar}{2} - \frac{e2\pi r A}{2\pi} \right] \hat{z} \quad (1.134)$$

$$= \left[\frac{\hbar}{2} - \frac{e\phi}{2\pi} \right] \hat{z} \quad (1.135)$$

In order that the change in angular momentum, $\Delta\mathbf{L}$, equals zero, ϕ must be $\Phi_0 = \frac{\hbar}{2e}$, the magnetic flux quantum. Thus, to conserve angular momentum in the presence of an applied magnetic field, the orbitsphere magnetic moment can be parallel or antiparallel to an applied field as observed with the Stern-Gerlach experiment, and the flip between orientations is accompanied by the "capture" of the magnetic flux quantum by the orbitsphere "coils" comprising infinitesimal loops of charge moving along geodesics (great circles). A superconducting loop with a weak link also demonstrates this effect [22].

The energy to flip the orientation of the orbitsphere due to its magnetic moment of a Bohr magneton, μ_B , is

$$\Delta E_{mag}^{spin} = 2\mu_B B \quad (1.136)$$

where

$$\mu_B = \frac{e\hbar}{2m_e} \quad (1.137)$$

During the spin-flip transition, power must be conserved. Power flow is governed by the Poynting power theorem,

$$\nabla \cdot (\mathbf{E} \times \mathbf{H}) = -\frac{\partial}{\partial t} \left[\frac{1}{2} \mu_0 \mathbf{H} \cdot \mathbf{H} \right] - \frac{\partial}{\partial t} \left[\frac{1}{2} \epsilon_0 \mathbf{E} \cdot \mathbf{E} \right] - \mathbf{J} \cdot \mathbf{E} \quad (1.138)$$

Stored Magnetic Energy

Energy superimposes; thus, the calculation of the spin-flip energy is determined as a sum of contributions. The energy change corresponding to the "capture" of the magnetic flux quantum is derived below. From Eq. (1.129) for one electron,

$$\frac{1}{2} \mu_0 \mathbf{H} \cdot \mathbf{H} = E_{mag}^{fluxon} = \frac{\pi \mu_0 e^2 \hbar^2}{(m_e)^2 r_n^3} \quad (1.139)$$

is the energy stored in the magnetic field of the electron. The orbitsphere is equivalent to a Josephson junction which can trap integer

numbers of fluxons where the quantum of magnetic flux is $\Phi_0 = \frac{h}{2e}$. Consider Eq. (1.139). During the flip transition a fluxon treads the orbitsphere at the speed of light; therefore, the radius of the orbitsphere in the lab frame is 2π times the relativistic radius in the fluxon frame as shown in the Special Relativistic Correction to the Ionization Energies section. Thus, the energy of the transition corresponding to the "capture" of a fluxon by the orbitsphere, E_{mag}^{fluxon} , is

$$E_{mag}^{fluxon} = \frac{\pi\mu_0 e^2 \hbar^2}{(m_e)^2 (2\pi r_n)^3} \quad (1.140)$$

$$= \frac{\mu_0 e^2}{4\pi^2 m_e r_n} \left(\frac{e\hbar}{2m_e} \right) \left(\frac{h}{2e\pi r_n^2} \right) \quad (1.141)$$

$$= \frac{\mu_0 e^2}{4\pi^2 m_e r_n} \mu_B \left(\frac{\Phi_0}{A} \right) \quad (1.142)$$

where A is the area and Φ_0 is the magnetic flux quantum.

$$E_{mag}^{fluxon} = 2 \left[\frac{e^2 \mu_0}{2m_e r_n} \right] \frac{1}{4\pi^2} \mu_B B \quad (1.143)$$

where the n th fluxon treading through the area of the orbitsphere is equivalent to the applied magnetic flux. Furthermore, the term in brackets can be expressed in terms of the fine structure constant, α , as follows:

$$\frac{e^2 \mu_0}{2m_e r_n} = \frac{e^2 \mu_0 c v}{2m_e v r_n c} \quad (1.144)$$

Substitution of Eq. (1.47) gives

$$\frac{e^2 \mu_0}{2m_e r_n} = \frac{e^2 \mu_0 c v}{2\hbar c} \quad (1.145)$$

Substitution of

$$c = \sqrt{\frac{1}{\epsilon_0 \mu_0}} \quad (1.146)$$

and

$$\alpha = \frac{\mu_0 e^2 c}{2\hbar} \quad (1.147)$$

gives

$$\frac{e^2 \mu_0 c v}{2\hbar c} = 2\pi\alpha \frac{v}{c} \quad (1.148)$$

The fluxon treads the orbitsphere at $v=c$ (k is the lightlike k^0 , then $k = \omega_n/c$). Thus,

$$E_{mag}^{fluxon} = 2 \frac{\alpha}{2\pi} \mu_B B \quad (1.149)$$

Stored Electric Energy

The superposition of the vector projection of the orbitsphere angular momentum on the z-axis is $\frac{\hbar}{2}$ with an orthogonal component of $\frac{\hbar}{4}$. Excitation of a resonant Larmor precession gives rise to \hbar on an axis S that precesses about the spin axis at an angle of $\theta = \frac{\pi}{3}$. S rotates about the z-axis at the Larmor frequency. S_{\perp} , the transverse projection, is $\pm\sqrt{\frac{3}{4}}\hbar$ (Eq. (1.74a)), and S_{\parallel} , the projection onto the axis of the applied magnetic field, is $\pm\frac{\hbar}{2}$ (Eq. (1.74b)). As shown in the Spin Angular Momentum of the Orbitsphere with $\ell = 0$ section, the superposition of the $\frac{\hbar}{2}$ z-axis component of the orbitsphere angular momentum and the $\frac{\hbar}{2}$ z-axis component of S gives \hbar corresponding to the observed electron magnetic moment of a Bohr magneton, μ_B . The reorientation of S and the orbitsphere angular momentum from parallel to antiparallel to the magnetic field applied along the z-axis gives rise to a current. The current is acted on by the flux corresponding to Φ_0 , the magnetic flux quantum, linked by the electron during the transition which gives rise to a Hall voltage. The electric field corresponding to the Hall voltage corresponds to the electric power term, $\frac{\delta}{\delta t}\left[\frac{1}{2}\epsilon_0\mathbf{E}\cdot\mathbf{E}\right]$, of the Poynting power theorem (Eq. (1.138)).

Consider a conductor in a uniform magnetic field and assume that it carries a current driven by an electric field perpendicular to the magnetic field. The current in this case is not parallel to the electric field, but is deflected at an angle to it by the magnetic field. This is the Hall Effect, and it occurs in most conductors.

A spin-flip transition is analogous to Quantum Hall Effect given in the corresponding section wherein the applied magnetic field quantizes the Hall conductance. The current is then precisely perpendicular to the magnetic field, so that no dissipation (that is no ohmic loss) occurs. This is seen in two-dimensional systems, at cryogenic temperatures, in quite high magnetic fields. Furthermore, the ratio of the total electric potential drop to the total current, the Hall resistance, R_H , is precisely equal to

$$R_H = \frac{h}{ne^2} \quad (1.150)$$

The factor n is an integer in the case of the Integral Quantum Hall Effect, and n is a small rational fraction in the case of the Fractional Quantum

Hall Effect. In an experimental plot [23] as the function of the magnetic field, the Hall resistance exhibits flat steps precisely at these quantized resistance values; whereas, the regular resistance vanishes (or is very small) at these Hall steps. Thus, the quantized Hall resistance steps occur for a transverse superconducting state.

Consider the case that an external magnetic field is applied along the x-axis to a two dimensional superconductor in the yz-plane which exhibits the Integral Quantum Hall Effect. (See Figure 1.10.) Conduction electrons align with the applied field in the x direction as the field permeates the material. The normal current carrying electrons experience a Lorentzian force, F_L , due to the magnetic flux. The y-directed Lorentzian force on an electron having a velocity v in the z direction by an x-directed applied flux, B , is

$$F_L = ev \times B \quad (1.151)$$

The electron motion is a cycloid where the center of mass experiences an $E \times B$ drift [24]. Consequently, the normal Hall Effect occurs. Conduction electron energy states are altered by the applied field and by the electric field corresponding to the Hall Effect. The electric force, F_H , due to the Hall electric field, E_y , is

$$F_H = eE_y \quad (1.152)$$

When these two forces are equal and opposite, conduction electrons propagate in the z direction alone. For this special case, it is demonstrated in Jackson [24] that the ratio of the corresponding Hall electric field E_H and the applied magnetic flux is

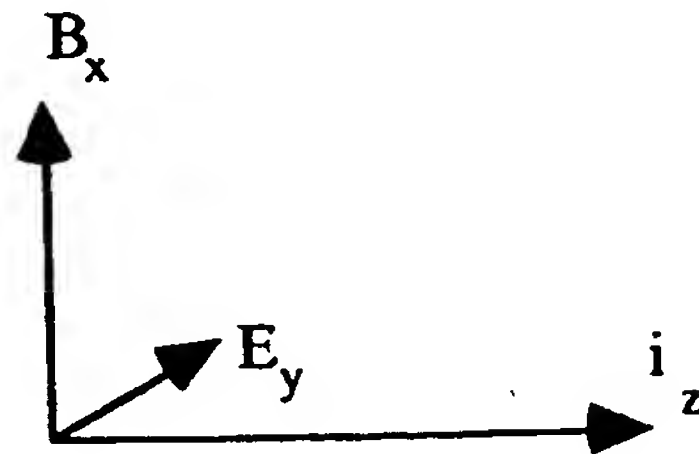
$$E_H/B = v \quad (1.153)$$

where v is the electron velocity. And, it is demonstrated in the Integral Quantum Hall Effect section that the Hall resistance, R_H , in the superconducting state is given by

$$R_H = \frac{h}{ne^2} \quad (1.154)$$

where n is an integer.

Figure 1.10. Coordinate system of crossed electric field, E_y , corresponding to the Hall voltage, magnetic flux, B_x , due to applied field, and superconducting current i_z .



Consider the case of the spin-flip transition of the electron. In the case of an exact balance between the Lorentzian force (Eq. (1.151)) and the electric force corresponding to the Hall voltage (Eq. (1.152)), each superconducting point mass of the electron propagates along a great circle where

$$E/B = v \quad (1.155)$$

where v is given by Eq. (1.47). Substitution of Eq. (1.47) into Eq. (1.155) gives

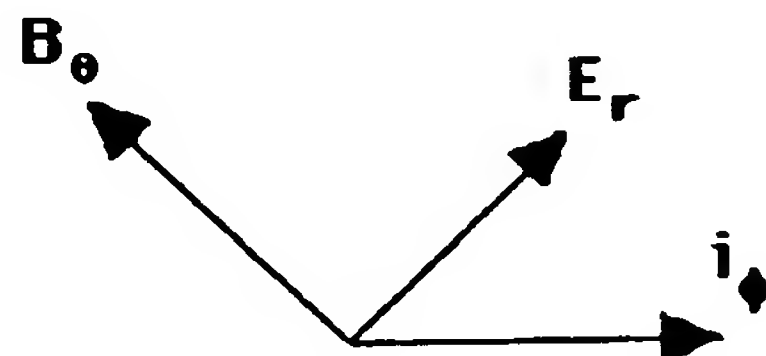
$$E/B = \frac{\hbar}{m_e r} \quad (1.156)$$

Eq. (1.156) is the condition for superconductivity in the presence of crossed electric and magnetic fields. The electric field corresponding to the Hall voltage corresponds to the electric energy term, E_{ele} , of the Poynting power theorem (Eq. (1.138)).

$$E_{ele} = \frac{1}{2} \int_0^{2\pi} \int_0^\pi \int_0^r \epsilon_0 \mathbf{E} \cdot \mathbf{E} r^2 \sin\theta dr d\theta d\phi \quad (1.157)$$

The electric term for this superconducting state is derived as follows using the coordinate system shown in Figure 1.11.

Figure 1.11. Coordinate system of crossed electric field, E_r , corresponding to the Hall voltage, magnetic flux, B_θ , due to applied field, and superconducting current i_ϕ .



The current is perpendicular to E_r , thus there is no dissipation. This occurs when

$$e\mathbf{E} = e\mathbf{v} \times \mathbf{B} \quad (1.158)$$

or

$$E/B = v \quad (1.159)$$

The electric field corresponding to the Hall voltage is

$$\mathbf{E} = \mathbf{v} \times \mathbf{B} \quad (1.160)$$

Substitution of Eq. (1.160) into Eq. (1.157) gives

$$E_{\text{elec}} = \frac{1}{2} \epsilon_0 \int_0^{2\pi} \int_0^\pi \int_0^r (vB)^2 r^2 \sin\theta dr d\theta d\phi \quad (1.161)$$

The spin flip transition may be induced by the absorption of a resonant photon. The velocity is determined from the distance traversed by each point and the time of the transition due to capture of a photon resonant with the spin-flip transition energy. The current i_ϕ corresponding to the Hall voltage and E_r is given by the product of the electron charge and the frequency f of the photon where the correspondence principle holds as given in the Photon Absorption section.

$$i = ef \quad (1.162)$$

The resistance of free space for the propagation of a photon is the radiation resistance of free space, η .

$$\eta = \sqrt{\frac{\mu_0}{\epsilon_0}} \quad (1.163)$$

The power P_r of the electron current induced by the photon as it transitions from free space to being captured by the electron is given by the product of the corresponding current and the resistance R which is given by Eq. (1.163).

$$P_r = i^2 R \quad (1.164)$$

Substitution of Eq. (1.162) and Eq. (1.163) gives

$$P_r = e^2 f^2 \sqrt{\frac{\mu_0}{\epsilon_0}} \quad (1.165)$$

It follows from the Poynting power theorem (Eq. (1.138)) with spherical radiation that the transition time τ is given by the ratio of the energy and the power of the transition [25].

$$\tau = \frac{\text{energy}}{\text{power}} \quad (1.166)$$

The energy of the transition which is equal to the energy of the resonant photon is given by Planck's equation.

$$E = \hbar\omega = hf \quad (1.167)$$

Substitution of Eq. (1.165) and Eq. (1.167) into Eq. (1.166) gives

$$\tau = \frac{hf}{e^2 f^2 \sqrt{\frac{\mu_0}{\epsilon_0}}} \quad (1.168)$$

The distance ℓ traversed by the electron with an kinetic angular momentum change of $\frac{\hbar}{2}$ is

$$\ell = \frac{2\pi r}{2} = \frac{\lambda}{2} \quad (1.169)$$

where the wavelength is given by Eq. (1.43). The velocity is given by the distance traversed divided by the transition time. Eq. (1.168) and Eq. (1.169) give

$$v = \frac{\lambda/2}{\tau} = \frac{\lambda/2}{\frac{hf}{e^2 f^2 \sqrt{\frac{\mu_0}{\epsilon_0}}}} = \frac{\sqrt{\frac{\mu_0}{\epsilon_0}} e^2}{2h} \lambda f \quad (1.170)$$

The relationship for a photon in free space is

$$c = \lambda f \quad (1.171)$$

As shown in the Unification of Spacetime, the Forces, Matter, and Energy section, the fine structure constant given by Eq. (1.147) is the dimensionless factor that corresponds to the relativistic invariance of charge.

$$\alpha = \frac{1}{4\pi} \sqrt{\frac{\mu_0}{\epsilon_0}} \frac{e^2}{\hbar} = \frac{1}{2} \frac{\sqrt{\frac{\mu_0}{\epsilon_0}}}{\frac{h}{e^2}} = \frac{\mu_0 e^2 c}{2h} \quad (1.172)$$

It is equivalent to one half the ratio of the radiation resistance of free space, $\sqrt{\frac{\mu_0}{\epsilon_0}}$, and the hall resistance, $\frac{h}{e^2}$. The radiation resistance of free space is equal to the ratio of the electric field and the magnetic field of the photon (Eq. (4.10)). Substitution of Eq. (1.171) and Eq. (1.172) into Eq. (1.170) gives

$$\nu = \alpha c \quad (1.173)$$

Substitution of Eq. (1.173) into Eq. (1.161) gives

$$E_{ele} = \frac{1}{2} \epsilon_0 \int_0^{2\pi} \int_0^\pi \int_0^r (\alpha c \mu_0 H)^2 r^2 \sin \theta dr d\theta d\phi \quad (1.174)$$

where

$$B = \mu_0 H \quad (1.175)$$

The relationship between the speed of light, c , and the permittivity of free space, ϵ_0 , and the permeability of free space, μ_0 , is

$$c = \frac{1}{\sqrt{\mu_0 \epsilon_0}} \quad (1.176)$$

Thus, Eq. (1.174) may be written as

$$E_{ele} = \frac{1}{2} \alpha^2 \int_0^{2\pi} \int_0^\pi \int_0^r \mu_0 H^2 r^2 \sin \theta dr d\theta d\phi \quad (1.177)$$

Substitution of Eq. (1.125) gives

$$E_{ele} = \alpha^2 \frac{2\pi \mu_0 e^2 \hbar^2}{3m_e^2 r_1^3} \quad (1.178)$$

The magnetic flux, B , is quantized in terms of the Bohr magneton because the electron links flux in units of the magnetic flux quantum,

$$\Phi_0 = \frac{h}{2e} \quad (1.179)$$

Substitution of Eqs. (1.139-1.149) gives

$$E_{ele} = 2 \left(\frac{2}{3} \alpha^2 \frac{\alpha}{2\pi} \mu_B B \right) \quad (1.180)$$

Dissipated Energy

The $\mathbf{J} \cdot \mathbf{E}$ energy over time is derived from the electron current corresponding to the Larmor excitation and the electric field given by Faraday's law due to the linkage of the magnetic flux of the fluxon during the spin-flip. Consider the electron current due the external field. The application of a magnetic field with a resonant Larmor excitation gives rise to a precessing angular momentum vector \mathbf{S} of magnitude \hbar directed from the origin of the orbitsphere at an angle of $\theta = \frac{\pi}{3}$ relative to the applied magnetic field. As given in the Spin Angular Momentum of the Orbitsphere with $\ell = 0$ section, \mathbf{S} rotates about the axis of the applied field

at the Larmor frequency. The magnitude of the components of \mathbf{S} that are parallel and orthogonal to the applied field (Eqs (1.74a-1.74b)) are $\frac{\hbar}{2}$ and $\sqrt{\frac{3}{4}}\hbar$, respectively. Since both the RF field and the orthogonal components shown in Figure 1.7 rotate at the Larmor frequency, the RF field that causes a Stern Gerlach transition produces a stationary magnetic field with respect to these components as described in Box 1.2. The corresponding central field at the orbitsphere surface given by the superposition of the central field of the proton and that of the photon follows from Eqs. (2.10-2.17) and Eq. (17) of Box 1.2:

$$\mathbf{E} = \frac{e}{4\pi\epsilon_0 r^2} \left[Y_0^0(\theta, \phi) \mathbf{i}_r + \text{Re} \{ Y_1^m(\theta, \phi) e^{i\omega t} \} \mathbf{i}_y \delta(r - r_1) \right] \quad (1.181)$$

where the spherical harmonic dipole $Y_1^m(\theta, \phi) = \sin\theta$ is with respect to the S-axis. The dipole spins about the S-axis at the angular velocity given by Eq. (1.55). The resulting current is nonradiative as shown by Eq. (1.39) and in Appendix I: Nonradiation Based on the Electromagnetic Fields and the Poynting Power Vector. Thus, the field in the RF rotating frame is magnetostatic as shown in Figure 1.9 but directed along the S-axis. Thus, the corresponding current given by Eq. (1.112) is

$$\mathbf{K}(\rho, \phi, z) = \frac{3}{2} \frac{e\hbar}{m_e r_n^3} \sin\theta \mathbf{i}_\phi \quad (1.182)$$

Next consider the Faraday's equation for the electric field

$$\oint_C \mathbf{E} \cdot d\mathbf{s} = -\frac{d}{dt} \int_S \mu_0 \mathbf{H} \cdot d\mathbf{a} \quad (1.183)$$

As demonstrated by Purcell [15], the velocity of the electron changes according to Lenz's law, but the change in centrifugal force is balanced by the change in the central field due to the applied field. The magnetic flux of the electron given by Eq. (1.120) is

$$\mathbf{B} = \mu_0 \mathbf{H} = \frac{\mu_0 e \hbar}{m_e r_1^3} (\mathbf{i}_r \cos\theta - \mathbf{i}_\theta \sin\theta) \quad \text{for } r < r_n \quad (1.184)$$

From Eq. (1.149), the magnetic flux $B_{J \cdot E}$ of the fluxon is

$$B_{J \cdot E} = \frac{\alpha}{2\pi} \frac{\mu_0 e \hbar}{m_e r_1^3} (\mathbf{i}_r \cos\theta - \mathbf{i}_\theta \sin\theta) = \frac{\alpha}{2\pi} \frac{\mu_0 e \hbar}{m_e r_1^3} \mathbf{i}_z \quad (1.185)$$

The electric field \mathbf{E} is constant about the line integral of the orbitsphere. Using Eq. (1.183) with the change in flux in units of fluxons along the z-axis given by Eq. (1.185) gives

$$\int_{-r_1}^{+r_1} \oint_C \mathbf{E} \cdot d\mathbf{s} dz = \int_{-r_1}^{+r_1} -\pi r^2 \frac{dB}{dt} dz \mathbf{i}_\phi \quad (1.186)$$

$$\begin{aligned} 2\pi \mathbf{E} \int_0^\pi r_1 \sin^2 \theta d\theta &= -\pi \frac{\Delta B}{\Delta t} r_1^2 \sin^3 \theta d\theta \mathbf{i}_\phi \\ &= -\pi r_1^2 \frac{2\Delta B}{3\Delta t} \mathbf{i}_\phi \end{aligned} \quad (1.187)$$

Substitution of Eq. (1.185) into Eq. (1.187) gives

$$\pi r_1 \mathbf{E} = -\pi r_1^2 \frac{2}{3} \frac{\alpha}{2\pi} \frac{\mu_0 e \hbar}{m_e r_1^3 \Delta t} \mathbf{i}_\phi \quad (1.188)$$

$$\pi r_1 \mathbf{E} = -\pi \frac{2}{3} \frac{\alpha}{2\pi} \frac{\mu_0 e \hbar}{m_e r_1 \Delta t} \mathbf{i}_\phi \quad (1.189)$$

Thus,

$$\mathbf{E} = -\frac{2}{3} \frac{\alpha}{2\pi} \frac{\mu_0 e \hbar}{m_e r_1^2 \Delta t} \mathbf{i}_\phi \quad (1.190)$$

The dissipative power density $\mathbf{E} \cdot \mathbf{J}$ can be expressed in terms of the surface current density \mathbf{K} as

$$\int_V (\mathbf{E} \cdot \mathbf{J}) \Delta t dv = \int_S (\mathbf{E} \cdot \mathbf{K}) \Delta t da \quad (1.191)$$

Using the electric field from Eq. (1.190) and the current density from Eq. (1.182) gives

$$\begin{aligned} \int_V (\mathbf{E} \cdot \mathbf{J}) \Delta t dv &= \int_0^{2\pi} \int_0^\pi \left(\frac{2}{3} \frac{\alpha}{2\pi} \frac{\mu_0 e \hbar}{m_e r_1^2 \Delta t} \frac{3}{2} \frac{e \hbar}{m_e r_1^3} \sin^2 \theta \right) \Delta t r_1^2 \sin \theta d\theta d\phi \\ &= \frac{4}{3} \frac{\alpha}{2\pi} \frac{\pi \mu_0 e^2 \hbar^2}{m_e^2 r_1^3} \end{aligned} \quad (1.192)$$

Substitution of Eqs. (1.139-1.149) into Eq. (1.192) gives

$$\int_V (\mathbf{E} \cdot \mathbf{J}) \Delta t dv = 2 \left(\frac{4}{3} \right) \left(\frac{\alpha}{2\pi} \right)^2 \mu_B B \quad (1.193)$$

Total Energy of Spin-Flip Transition

The principal energy of the transition corresponding to a reorientation of the orbitsphere is given by Eq. (1.136). And, the total energy of the flip transition is the sum of Eq. (1.136), and Eqs. (1.149), (1.180), and (1.193) corresponding to the electric energy, the magnetic energy, and the dissipated energy of a fluxon treading the orbitsphere, respectively.

$$\Delta E_{mag}^{spin} = 2 \left(1 + \frac{\alpha}{2\pi} + \frac{2}{3} \alpha^2 \left(\frac{\alpha}{2\pi} \right) - \frac{4}{3} \left(\frac{\alpha}{2\pi} \right)^2 \right) \mu_B B \quad (1.194)$$

$$\Delta E_{mag}^{spin} = g \mu_B B \quad (1.195)$$

where the stored magnetic energy corresponding to the $\frac{\partial}{\partial t}\left[\frac{1}{2}\mu_0\mathbf{H}\cdot\mathbf{H}\right]$ term increases, the stored electric energy corresponding to the $\frac{\partial}{\partial t}\left[\frac{1}{2}\epsilon_0\mathbf{E}\cdot\mathbf{E}\right]$ term increases, and the $\mathbf{J}\cdot\mathbf{E}$ term is dissipative. The magnetic moment of Eq. (1.136) is twice that from the gyromagnetic ratio as given by Eq. (28) of Box 1.2. The magnetic moment of the electron is the sum of the component corresponding to the kinetic angular momentum, $\frac{\hbar}{2}$, and the component corresponding to the vector potential angular momentum, $\frac{\hbar}{2}$, (Eq. (1.132)). The spin-flip transition can be considered as involving a magnetic moment of g times that of a Bohr magneton. The g factor is redesignated the fluxon g factor as opposed to the anomalous g factor, and it is given by Eq. (1.194).

$$\frac{g}{2} = 1 + \frac{\alpha}{2\pi} + \frac{2}{3}\alpha^2\left(\frac{\alpha}{2\pi}\right) - \frac{4}{3}\left(\frac{\alpha}{2\pi}\right)^2 \quad (1.196)$$

For $\alpha^{-1} = 137.03604(11)$ [26]

$$\frac{g}{2} = 1.001\,159\,652\,120 \quad (1.197)$$

The experimental value [27] is

$$\frac{g}{2} = 1.001\,159\,652\,188(4) \quad (1.198)$$

The calculated and experimental values are within the propagated error of the fine structure constant. Different values of the fine structure constant have been recorded from different experimental techniques, and α^{-1} depends on a circular argument between theory and experiment [28]. One measurement of the fine structure constant based on the electron g factor is $\alpha_g^{-1} = 137.036006(20)$ [29]. This value can be contrasted with equally precise measurements employing solid state techniques such as those based on the Josephson effect [30] ($\alpha_J^{-1} = 137.035963(15)$) or the quantized Hall effect [31] ($\alpha_H^{-1} = 137.035300(400)$). A method of the determination of α^{-1} that depends on the circular methodology between theory and experiment to a lesser extent is the substitution of the independently measured fundamental constants μ_0 , e , c , and h into Eq. (1.172). The following values of the fundamental constants are given by Weast [26]

$$\mu_0 = 4\pi \times 10^{-7} \text{ Hm}^{-1} \quad (1.199)$$

$$e = 1.6021892(46) \times 10^{-19} \text{ C} \quad (1.200)$$

$$c = 2.99792458(12) \times 10^8 \text{ ms}^{-1} \quad (1.201)$$

$$h = 6.626176(36) \times 10^{-34} \text{ JHz}^{-1} \quad (1.202)$$

For these constants,

$$\alpha^{-1} = 137.03603(82) \quad (1.203)$$

Substitution of the α^{-1} from Eq. (1.203) into Eq. (1.196) gives

$$\frac{g}{2} = 1.001\ 159\ 652\ 137 \quad (1.204)$$

The experimental value [27] is

$$\frac{g}{2} = 1.001\ 159\ 652\ 188(4) \quad (1.205)$$

Conversely, the fine structure calculated for the experimental $\frac{g}{2}$ and Eq. (1.196) is $\alpha^{-1} = 137.036\ 032\ 081$.

The *postulated* QED theory of $\frac{g}{2}$ is based on the determination of the terms of a *postulated* power series in α/π where each *postulated* virtual particle is a source of *postulated* vacuum polarization that gives rise to a *postulated* term. The algorithm involves scores of *postulated* Feynman diagrams corresponding to thousands of matrices with thousands of integrations per matrix requiring decades to reach a consensus on the "appropriate" *postulated* algorithm to remove the intrinsic infinities. The solution so obtained using the perturbation series further requires a *postulated* truncation since the series **diverges**. The remarkable agreement between Eqs. (1.204) and (1.205) demonstrates that $\frac{g}{2}$ may be derived in closed form from Maxwell's equations in a simple straightforward manner that yields a result with eleven figure agreement with experiment—the limit of the experimental capability of the measurement of the fundamental constants that determine α . In Appendix II: Quantum Electrodynamics is Purely Mathematical and Has No Basis in Reality, the Maxwellian result is contrasted with the QED algorithm of invoking virtual particles, zero point fluctuations of the vacuum, and negative energy states of the vacuum. Rather than an infinity of radically different QED models, an essential feature is that *Maxwellian solutions are unique*.

The muon, like the electron, is a lepton with \hbar of angular momentum. The magnetic moment of the muon is given by Eq. (1.136) with the electron mass replaced by the muon mass. It is twice that from

the gyromagnetic ratio as given by Eq. (2.36) of the Orbital and Spin Splitting section corresponding to the muon mass. As is the case with the electron, the magnetic moment of the muon is the sum of the component corresponding to the kinetic angular momentum, $\frac{\hbar}{2}$, and the component corresponding to the vector potential angular momentum, $\frac{\hbar}{2}$, (Eq. (1.132).

The spin-flip transition can be considered as involving a magnetic moment of g times that of a Bohr magneton of the muon. The g factor is equivalent to that of the electron given by Eq. (1.196).

The muon anomalous magnetic moment has been measured in a new experiment at Brookhaven National Laboratory (BNL) [32]. Polarized muons were stored in a superferric ring, and the angular frequency difference ω_a between the spin precession and orbital frequencies was determined by measuring the time distribution of high-energy decay positrons. The dependence of ω_a on the magnetic and electric fields is given by BMT equation which is the relativistic equation of motion for spin in uniform or slowly varying external fields [33]. The dependence on the electric field is eliminated by storing muons with the "magic" $\gamma=29.3$, which corresponds to a muon momentum $p=3.09 \text{ GeV}/c$. Hence measurement of ω_a and of B determines the anomalous magnetic moment.

The "magic" γ wherein the contribution to the change of the longitudinal polarization by the electric quadrupole focusing fields are eliminated occurs when

$$\frac{g_\mu \beta}{2} - \frac{1}{\beta} = 0 \quad (1.206)$$

where g_μ is the muon g factor which is required to be different from the electron g factor in the standard model due to the dependence of the mass dependent interaction of each lepton with vacuum polarizations due to virtual particles. For example, the muon is much heavier than the electron, and so high energy (short distance) effects due to strong and weak interactions are more important here [29]. The BNL Muon (g-2) Collaboration [32] used a "magic" $\gamma=29.3$ which satisfied Eq. (1.206)

identically for $\frac{g_\mu}{2}$; however, their assumption that this condition eliminated the affect of the electrostatic field on ω_a is flawed as shown in Appendix IV: Muon g Factor. Internal consistency was achieved during the determination of $\frac{g_\mu}{2}$ using the BMT equation with the flawed

assumption that $\frac{g_\mu}{2} \neq \frac{g_e}{2}$. The parameter measured by Carey et al. [32]

corresponding to $\frac{g_\mu}{2}$ was the sum of a finite electric term as well as a magnetic term. The calculated result based on the equivalence of the muon and electron g factors

$$\frac{g_\mu}{2} = 1.001\,165\,923 \quad (1.207)$$

is in agreement with the result of Carey et al. [32]:

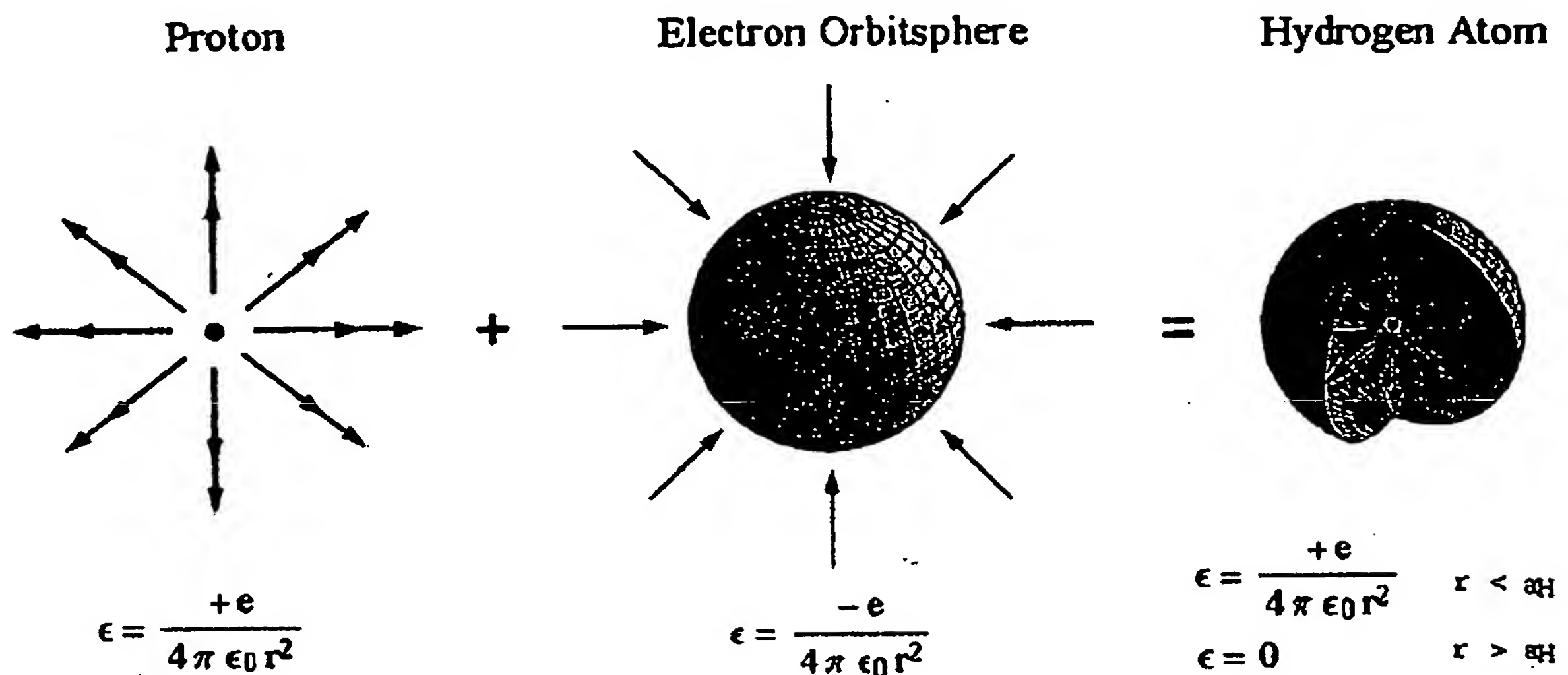
$$\frac{g_\mu}{2} = 1.001\,165\,925\,(15) \quad (1.208)$$

Rather than indicating an expanded plethora of postulated supersymmetry virtual particles which make contributions such as smuon-neutralino and sneutrino-chargino loops as suggested by Brown et al. [34], the deviation of the experimental value of $\frac{g_\mu}{2}$ from that of the standard model prediction simply indicates that the muon g factor is equivalent to the electron g factor.

DETERMINATION OF ORBITSPIHERE RADII

The one-electron orbitsphere is a spherical shell of negative charge (total charge = $-e$) of zero thickness at a distance r_n from the nucleus of charge $+Ze$. It is well known that the field of a spherical shell of charge is zero inside the shell and that of a point charge at the origin outside the shell [35]. See Figure 1.12.

Figure 1.12. The electric fields of a proton, a bound electron, and a hydrogen atom corresponding to a minimum energy and no electron self interaction where the bubble-like geometry of the orbitsphere requires the central field of the proton.



Thus, for a nucleus of charge Z , the force balance equation for the electron orbitsphere is obtained by equating the forces on the mass and charge densities. For the ground state, $n=1$, the centrifugal force of the electron is given by

$$F_{centrifugal} = \frac{m_e}{4\pi r_1^2} \frac{v_1^2}{r_1} \quad (1.209)$$

where $\frac{m_e}{4\pi r_1^2}$ is the mass density of the orbitsphere. The centripetal force is the electric force, F_{ele} , between the electron and the nucleus.

$$F_{ele} = \frac{e}{4\pi r_1^2} \frac{Ze}{4\pi\epsilon_0 r_1^2} \quad (1.210)$$

where ϵ_0 is the permittivity of free-space.

The second centripetal force is an electrodynamic force or radiation reaction force, a force dependent on the second derivative of charge position which respect to time, which arises between the electron and the nucleus. This force given in Sections 6.6, 12.10, and 17.3 of Jackson [36] achieves the condition that the sum of the mechanical momentum and electromagnetic momentum is conserved. The motion of each point in the magnetic field of the nucleus will cause a relativistic central force, F_{mag} , which acts on each point mass. The magnetic central force is derived as follows from the Lorentzian force which is relativistically corrected. Each infinitesimal point of the orbitsphere moves on a great circle, and each

point charge has the charge density $\frac{e}{4\pi r_n^2}$. As given in the Proton and Neutron section, the proton is comprised of a linear combination of three constant functions and three orthogonal spherical harmonic quark/gluon functions. The magnetic field front due to the motion of the electron propagates at the speed of light. From the photon inertial reference frame at the radius of each infinitesimal point of the electron orbitsphere, the proton charge distribution is given as the product of the quark and gluon functions which gives rise to a uniform distribution. The magnetic flux of the proton in the $v=c$ inertial frame at the electron radius follows from McQuarrie [19]:

$$\mathbf{B} = \frac{\mu_o e \hbar}{2m_p r_n^3} \quad (1.211)$$

And, the magnetic flux due to a nucleus of charge Z and mass m is

$$\mathbf{B} = \frac{\mu_o Z e \hbar}{2m r_n^3} \quad (1.212)$$

The motion of each point will cause a relativistic central force, F_{mag} , which acts on each point mass. The magnetic central force is derived as follows from the Lorentzian force which is relativistically corrected. The Lorentzian force density on each point moving at velocity v is

$$\mathbf{F}_{mag} = \frac{e}{4\pi r_n^2} \mathbf{v} \times \mathbf{B} \quad (1.213)$$

For the hydrogen atom with $Z=1$ and $m=m_p$, substitution of Eq. (1.47) for v and Eq. (1.212) for B gives

$$\mathbf{F}_{mag} = \frac{1}{4\pi r_n^2} \left[\frac{e^2 \mu_o}{2m_e r_n} \right] \frac{\hbar^2}{m r_n^3} \hat{r} \quad (1.214)$$

The term in brackets can be expressed in terms the fine structure constant α wherein the radius of the electron relative to the $v=c$ frame (k is the lightlike k^0 , then $k=\omega_n/c$), r_n^* , is the corresponding relativistic radius. From Eq. (1.43), the relationship between the radius and the electron wavelength is

$$2\pi r = \lambda \quad (1.215)$$

Using the de Broglie Eq. (1.46) with $v=c$

$$\lambda = \frac{h}{mv} = \frac{h}{mc} \quad (1.216)$$

With substitution of Eq. (1.216) into Eq. (1.215)

$$r_n^* = \frac{\hbar}{mc} = \lambda_c = \alpha a_o \quad (1.217)$$

The radius of the electron orbitsphere in the $v=c$ frame is λ_c , where $v=c$ corresponds to the magnetic field front propagation velocity which is the same in all inertial frames, independent of the electron velocity as shown

by the velocity addition formula of special relativity [37]. From Eqs. (1.147) and (1.217),

$$\frac{e^2 \mu_o}{2m_e r_n} = 2\pi\alpha \quad (1.218)$$

where λ_c is the Compton wavelength bar substituted for r_n , and a_o is the Bohr radius.

From Lorentz transformations with the electron's invariant angular momentum of \hbar (Eq. (1.57), it can be shown that the relativistic correction to Eq. (1.214) is the reciprocal of Eq. (1.218). Consider an inertial frame following a great circle of radius r_n with $v=c$. The motion is tangential to the radius; thus, r_n is Lorentzian invariant. But, as shown in the SPACETIME FOURIER TRANSFORM OF THE ELECTRON FUNCTION section and the Special Relativistic Correction to the Ionization Energies section, the tangential distance along a great circle is $2\pi r_n$ in the laboratory frame and r_n in the $v=c$ frame (k is the lightlike k^0 , then $k=\omega_n/c$). In addition, the corresponding radius is reduced by α for the light speed radial field. Thus, the term in brackets in Eq. (1.214) is the inverse of the relativistic correction γ' for the electrodynamic central force.

The electron's magnetic moment of a Bohr magneton μ_B given by Eq. (1.99) is also invariant as well as its angular momentum of \hbar . The electron is nonradiative due to its angular motion as shown in SPACETIME FOURIER TRANSFORM OF THE ELECTRON FUNCTION, Appendix I, and the Stability of Atoms and Hydrinos section. Furthermore, the angular momentum of the photon given in the Equation of the Photon section is $m = \int \frac{1}{8\pi c} \text{Re}[\mathbf{r} \times (\mathbf{E} \times \mathbf{B}^*)] dx^4 = \hbar$. It is conserved for the solutions for the resonant photons and excited state electron functions given in the Excited States of the One-Electron Atom (Quantization) section and the Equation of the Photon section. Thus, the electrodynamic angular momentum and the inertial angular momentum are matched such that the correspondence principle holds. It follows from the principle of conservation of angular momentum that $\frac{e}{m_e}$ of Eq. (1.99) is invariant.

The same applies for the intrinsic magnetic moment μ_B and angular momentum \hbar of the free electron since it is given by the projection of the bound electron into a plane as shown in the Electron in Free Space section. However, special relativity must be applied to physics relative to the electron's center of mass due to the invariance of charge and the invariant four momentum as given by Purcell [37].

The correction to the term in brackets of Eq. (1.214) also follows

from the Lorentz transformation of the electron's invariant magnetic moment as well as its invariant angular momentum of \hbar . Consider a great circle of the electron orbitsphere. As shown in the SPACETIME FOURIER TRANSFORM OF THE ELECTRON FUNCTION section, the tangential distance along a great circle is $2\pi r_n$ in the laboratory frame and r_n in the $v=c$ frame; thus, electron mass density along each great circle can be considered to contract to a point with an increase of the relativistic mass density by a factor of 2π . Furthermore, due to invariance of charge under Gauss' Integral Law, with the radius given by (1.217), the charge corresponding to the source current of the magnetic field must be corrected by α^{-1} . Thus, from the perspective of the invariance of μ_B , the term in brackets in Eq. (1.214) is inverse of the relativistic correction for the electrodynamic central force.

$$\frac{\alpha^{-1}e^2\mu_o}{2(2\pi m_e)r_n} = \frac{\alpha^{-1}e^2\mu_o}{2(2\pi m_e)\lambda} = \frac{2\pi\alpha^{-1}e^2\mu_o}{2(2\pi m_e)\frac{\hbar}{m_e c}} = 1 \quad (1.220)$$

Therefore, the force is given by

$$F_{mag} = -\frac{1}{4\pi r_1^2} \frac{\hbar^2}{m r_1^3} \hat{r} \quad (1.221)$$

The force balance equation is given by equating the centrifugal and centripetal force densities⁸:

⁸ In addition to the electrodynamic interaction between the electron and the nucleus, the self interaction of the electron must be considered. The bubble-like geometry of the orbitsphere requires the presence of the proton. As given in the Free Electron section, a free electron comprises a two-dimensional planar lamina with field lines that are discontinuous and orthogonal from opposite surfaces of the lamina such that the Maxwellian condition

$$\mathbf{n} \cdot (\mathbf{E}_1 - \mathbf{E}_2) = \frac{\sigma}{\epsilon_0} \quad (1)$$

is satisfied where \mathbf{n} is the radial normal unit vector, \mathbf{E}_1 and \mathbf{E}_2 are the electric field vectors that are discontinuous at the opposite surfaces, and σ is the charge density of the electron corresponding to a total charge of e . There is no self interaction for the free electron. Consider the transformation of the electron's field lines during binding due to the central field of the proton. The spherical symmetry requires that the field lines of the proton and the bound electron are radial. In order to minimize the energy, the continuous charge density function is a two-dimensional equipotential energy surface with an electric field that is strictly normal-radial (Eq. (2.11)) for $r > r_1$ according to Gauss' law and Faraday's law. The relationship between the electric field equation and the electron source charge-density function is also given by Eq. (1), Maxwell's equation in two dimensions [38-40]. As shown in Figure 1.12, \mathbf{E}_1 , the electric field inside of the orbitsphere, is zero, \mathbf{E}_2 , the electric field outside of the orbitsphere, is equivalent to that of a point charge at the origin, and σ is the surface charge density corresponding to a total charge of e . Eq. (1) applies to a perfect conductor. *The electron is a perfect conductor, and zero field inside of a perfect conductor is confirmed experimentally.* This relation

shows that only a 2-D geometry meets the criterion for a fundamental particle and is required for particle production in order to satisfy Maxwell's equations, special and general relativity, and other first principles such as conservation of energy and momentum as shown in the Gravity, Leptons, and Quarks sections. 2-D is the nonsingularity geometry which is no longer divisible. It is the dimension from which it is not possible to lower dimensionality. In this case, there is no electrostatic self interaction since the corresponding potential is continuous across the surface according to Faraday's law in the electrostatic limit, and the field is discontinuous, normal, and radial to the charge according to Gauss' law [38-40]. Thus, only the continuous current density function need be considered.

It was shown in the Electron g Factor section that as a requirement of the conservation of angular momentum, the magnetic momentum of the electron can only be parallel or antiparallel to an applied magnetic field. Similarly, in order to conserve angular momentum, any internal change in the bound-electron current distribution and its corresponding angular momentum requires emission of a photon that carries angular momentum in its electric and magnetic fields only in discrete units of \hbar as given in the Equation of the Photon section. Self interaction of the current of the bound electron having the angular momentum distribution given in the Spin Angular Momentum of the Orbitsphere with $\ell = 0$ section requires the emission of a photon having an angular momentum that is a fraction of \hbar which is not possible according to Maxwell's equations as given in the Excited States of the One-Electron Atom (Quantization) section. Thus, any self interaction is a radiation-reaction type wherein k is also the lightlike k^0 such that $k = \omega_n/c$. Any such light-like interaction can only be central. Since the velocity of each point of the electron is the same, the current of the orbitsphere is confined to a two-dimensional shell in the $v=c$ frame as well as the lab frame as given by Eq. (1.249). Since the current is orthogonal to the radial vector at the same radius for each great circle current density element, there is no self interaction.

Furthermore, since fundamental particles such as the electron are superconducting, nonresonant collisions cannot change the intrinsic angular momentum. Such collisions involve the entire particle. And, the intrinsic angular momentum remains unchanged, except when a resonant photon is emitted or absorbed according to the Maxwellian-based conservation rules given in the Excited States section and the Equation of the Photon section.

In contrast, QM is internally inconsistent. Electron shielding or self interaction of the electron cloud is ignored in cases involving one electron such as H and H_2^+ , but electron-electron repulsion terms as well as shielding are considered in multielectron problems such as He and H_2 ; even though, the charge densities occupy the same space whether there is one or more electrons—the only difference being the magnitude. The electron cloud model is also mandatory to achieve neutral scattering despite the internal inconsistency with scattering experiments that the momentum transfer is with the entire mass of the electron as pointed out by Max Born. The subsequent probability-wave model violates special relativity and causality by requiring a point electron to be over all space at once, weighted according to a "guiding" probability density function.

The electron spread over all space must interact with itself since Gauss' law applied to the volumetric charge density gives rise to a radial electric field from zero to infinity. Consequently, there is the inescapable problem that the electron cloud is unstable, not to mention the nonphysical nature of the infinities in the electric and magnetic fields of the point electron manifested as a probability cloud distribution.

$$\frac{m_e}{4\pi r_1^2} \frac{v_1^2}{r_1} = \frac{e}{4\pi r_1^2} \frac{Ze}{4\pi \epsilon_0 r_1^2} - \frac{1}{4\pi r_1^2} \frac{\hbar^2}{m r_1^3} \quad (1.222)$$

where $Z=1$ and $m=m_p$ for the hydrogen atom. (Since the surface-area factor cancels in all cases, this factor will be left out in subsequent force calculations throughout this book). Using Eq. (1.47),

$$r_1 = \frac{4\pi \epsilon_0 \hbar^2}{Ze^2 \mu_e} \quad (1.223)$$

where the reduced electron mass, μ_e , is

$$\mu_e = \frac{m_e m}{m_e + m} \quad (1.224)$$

The Bohr radius is

$$a_0 = \frac{4\pi \epsilon_0 \hbar^2}{e^2 m_e} \quad (1.225)$$

And, the radius given by force balance between the centrifugal force and central electrostatic force alone is

$$r_1 = \frac{4\pi \epsilon_0 \hbar^2}{Ze^2 m_e} = \frac{a_0}{Z} \quad (1.226)$$

And, for hydrogen, m of Eq. (1.224) is

$$m = m_p \quad (1.227)$$

Substitution of the reduced electron mass for the electron mass gives, a_H , the Bohr radius of the hydrogen atom.

$$a_H = \frac{4\pi \epsilon_0 \hbar^2}{e^2 \mu_e} \quad (1.228)$$

Thus, Eq. (1.223) becomes

$$r_1 = \frac{a_H}{Z} \quad (1.229)$$

where $Z=1$ for the hydrogen atom. The results can also be arrived at by the familiar minimization of the energy⁹.

⁹ The force balance equation can also be arrived at by the familiar minimization of the energy. The electron kinetic energy T_1 obtained by integration over the mass density at spherical position $r=r'$ (Eq. (1.64)) is

$$T_1 = \frac{1}{2} v^2 \int_0^{2\pi} \int_0^\pi \int_0^\infty \frac{m_e}{4\pi r'^2} \delta(r-r') r^2 \sin\theta dr d\theta d\phi = \frac{1}{2} m_e v^2 = \frac{1}{2} \frac{\hbar^2}{m_e r^2} \quad (1)$$

where the velocity is given by Eq. (1.47). The electron orbitsphere is a two-dimensional equipotential energy surface at spherical position $r=r'$. The potential energy is given by integrating Poisson's equation over the continuous two-dimensional surface charge density given by Eq. (1.64) at the equipotential due to the proton at spherical position $r=r'$ where the electric field of the electron is strictly normal-radial (Eq. (2.11)) for $r>r_1$ according to Gauss' law, and the potential is continuous across the surface according to Faraday's law in the electrostatic limit.

ENERGY CALCULATIONS

The potential energy V between the electron and the nucleus separated by the radial distance radius r_1 considering the force balance between the centrifugal force and central electrostatic force alone is

$$V = \frac{-Ze^2}{4\pi\epsilon_0 r_1} = \frac{-Z^2 e^2}{4\pi\epsilon_0 a_0} = -Z^2 \times 4.3598 \times 10^{-18} \text{ J} = -Z^2 \times 27.212 \text{ eV} \quad (1.230)$$

Because this is a central force problem, the kinetic energy, T , is $-\frac{1}{2}V$.

$$T = \frac{Z^2 e^2}{8\pi\epsilon_0 a_0} = Z^2 \times 13.606 \text{ eV} \quad (1.231)$$

The same result can be obtained from $T = \frac{1}{2}m_e v_1^2$ and Eq. (1.47).

Alternatively, the kinetic energy T and the binding energy E_B , which are each equal to the change in stored electric energy, ΔE_{ele} , can be calculated from

$$T = \Delta E_{ele} = -\frac{1}{2}\epsilon_0 Z \int_0^1 E^2 dv \text{ where } E = -\frac{e}{4\pi\epsilon_0 r^2} \hat{i}_r \quad (1.232)$$

$$V = -\frac{Ze}{4\pi\epsilon_0 r} \int_0^{2\pi} \int_0^\pi \int_0^\infty \frac{e}{4\pi r'^2} \delta(r-r') r'^2 \sin\theta dr' d\theta d\phi = -\frac{Ze^2}{4\pi\epsilon_0 r} \quad (2)$$

And, the energy due to the electrodynamic interaction of the electron and the proton T_2 due to their relative motion given by Eq. (1.47) is

$$T_2 = \frac{1}{2}mv^2 = \frac{1}{2} \frac{\hbar^2}{mr^2} \quad (3)$$

The total energy E is the sum of Eqs. (1-3).

$$E = T_1 + V + T_2 = \frac{1}{2} \frac{\hbar^2}{m_e r^2} - \frac{Ze^2}{4\pi\epsilon_0 r} + \frac{1}{2} \frac{\hbar^2}{mr^2} \quad (4)$$

Then, the minimum energy is obtained by taking the derivative of Eq. (4) and setting it to zero which is

$$\frac{\hbar^2}{m_e r^3} = \frac{Ze^2}{4\pi\epsilon_0 r^2} - \frac{\hbar^2}{mr^3} \quad (5)$$

Eq. (5) can be written in terms of the densities:

$$\frac{m_e}{4\pi r_1^2} \frac{v_1^2}{r_1} = \frac{e}{4\pi r_1^2} \frac{Ze}{4\pi\epsilon_0 r_1^2} - \frac{1}{4\pi r_1^2} \frac{\hbar^2}{mr_1^3} \quad (6)$$

where $Z=1$ and $m=m_p$ for the hydrogen atom. Then, Eq. (6) is the same as Eq. (1.222).

¹⁰ As shown in Figure 1.12, the electric field of the proton alone is over all space, and the electric field of the bound electron alone is finite only for $r > r_1$. The radius goes to infinity in the case of the ionized or free electron, and the corresponding charge and current density functions are given in the Free Electron Section. During binding of the free electron which is a two-dimensional disc lamina, the

Thus, as the orbitsphere shrinks from ∞ to r_1 ,

$$E_B = -\frac{Ze^2}{8\pi\epsilon_0 r_1} = -\frac{Z^2 e^2}{8\pi\epsilon_0 a_0} = -Z^2 \times 2.1799 \times 10^{-18} \text{ J} = -Z^2 \times 13.606 \text{ eV} \quad (1.233)$$

The calculated Rydberg constant R using Eq. (1.228) in Eqs. (1.230-1.233) which includes the relativistic correction corresponding to the magnetic force given by Eq. (1.221) is $10,967,758 \text{ m}^{-1}$. The experimental Rydberg constant is $10,967,758 \text{ m}^{-1}$. Furthermore, a host of parameters can be calculated for the hydrogen atom, as shown in Table 1.2.

electron charge distribution becomes that of a 2-D uniform spherical shell of charge, and the electric field of the electron superimposes and cancels part of that of the proton for $r > r_1$ as shown in Figure 1.12. The energy in the electric fields of each of the proton and the electron alone is given as

$$E_{ele} = \frac{1}{2} \epsilon_0 \int_0^\infty E^2 dv \quad (1)$$

where E is the electric field of each independently. The binding energy of the hydrogen atom which is released as photons is given as the change in the electric field energy due to the change in the electric field due to the superposition of the fields of the electron and proton.

$$\begin{aligned} T = \Delta E_{ele} &= \frac{1}{2} \epsilon_0 \int_0^\infty (\Delta E)^2 dv = -\frac{1}{2} \epsilon_0 \int_0^\infty \left(\frac{e}{4\pi\epsilon_0 r^2} \right)^2 dv \\ &= -\frac{1}{2} \epsilon_0 \int_0^\infty \int_0^{2\pi} \int_0^\pi \left(\frac{e}{4\pi\epsilon_0 r^2} \right)^2 r^2 \sin\theta dr d\theta d\Phi \\ &= -\int_0^\infty \frac{e^2}{8\pi\epsilon_0 r^2} dr \\ &= \frac{e^2}{8\pi\epsilon_0 r_1} \end{aligned} \quad (2)$$

For $r_1 = a_H$ as given by Eq. (1.229),

$$T = \Delta E_{ele} = \frac{e^2}{8\pi\epsilon_0 a_H} = 13.5984 \text{ eV} \quad (3)$$

In the case of nuclear charge Z , ΔE_{ele} increases by a factor of Z , and the radius given by Eq. (1.229) is $r_1 = \frac{a_H}{Z}$. These substitutions in Eq. (3) give Eq. (1.232).

Eq. (3), matches the experimental binding energy. Whereas, the corresponding energy does not match in the case of the solutions of the Schrödinger equation. Even if it is assumed that the electron is everywhere at once in order to achieve electroneutrality, which is impossible, the energy stored in the electric field of the electron does not match the binding energy since the average radius of the hydrogen atom in this case is $3/2$ the Bohr radius.

Table 1.2. Some calculated parameters for the hydrogen atom ($n=1$).

radius	$r_1 = a_H$	$5.2947 \times 10^{-11} \text{ m}$
potential energy	$V = \frac{-e^2}{4\pi\epsilon_0 a_H}$	-27.196 eV
kinetic energy	$T = \frac{e^2}{8\pi\epsilon_0 a_H}$	13.598 eV
angular velocity (spin)	$\omega_1 = \frac{\hbar}{m_e r_1^2}$	$4.13 \times 10^{16} \text{ rads}^{-1}$
linear velocity	$v_1 = r_1 \omega_1$	$2.19 \times 10^6 \text{ ms}^{-1}$
wavelength	$\lambda_1 = 2\pi r_1$	$3.325 \times 10^{-10} \text{ m}$
spin quantum number	$s = \frac{1}{2}$	$\frac{1}{2}$
moment of Inertia	$I = m_e r_1^2 \sqrt{s(s+1)}$	$2.209 \times 10^{-51} \text{ kgm}^2$
angular kinetic energy	$E_{angular} = \frac{1}{2} I \omega_1^2$	11.78 eV
magnitude of the angular momentum	\hbar	$1.0545 \times 10^{-34} \text{ Js}$
projection of the angular momentum onto the S-axis	$S = \hbar \sqrt{s(s+1)}$	$9.133 \times 10^{-35} \text{ Js}$
projection of the angular momentum onto the z-axis	$S_z = \frac{\hbar}{2}$	$5.273 \times 10^{-35} \text{ Js}$
mass density	$\frac{m_e}{4\pi r_1^2}$	$2.589 \times 10^{-11} \text{ kgm}^{-2}$
charge density	$\frac{e}{4\pi r_1^2}$	4.553 Cm^{-2}

Table 1.3 gives the radii and energies for some one-electron atoms. In addition to the energies, the wavelength, angular frequency, and the linear velocity can be calculated for any one-electron atom from Eqs. (1.46), (1.55), and (1.56). Values are given in Table 1.4.

Table 1.3. Calculated energies (non-relativistic) and calculated ionization energies for some one-electron atoms.

Atom	Calculated r_1^a (a_0)	Calculated Kinetic Energy ^b (eV)	Calculated Potential Energy ^c (eV)	Calculated Ionization Energy ^d (eV)	Experimental Ionization Energy ^e (eV)
<i>H</i>	1.000	13.61	-27.21	13.61	13.59
<i>He</i> ⁺	0.500	54.42	-108.85	54.42	54.42
<i>Li</i> ²⁺	0.333	122.45	-244.90	122.45	122.45
<i>Be</i> ³⁺	0.250	217.69	-435.39	217.69	217.71
<i>B</i> ⁴⁺	0.200	340.15	-680.29	340.15	340.22
<i>C</i> ⁵⁺	0.167	489.81	-979.62	489.81	489.98
<i>N</i> ⁶⁺	0.143	666.68	-1333.37	666.68	667.03
<i>O</i> ⁷⁺	0.125	870.77	-1741.54	870.77	871.39

^a from Equation (1.226)

^b from Equation (1.231)

^c from Equation (1.230)

^d from Equation (1.233)

^e experimental

It is noteworthy that the potential energy is a constant (at a given n) because the electron is at a fixed distance, r_n , from the nucleus. And, the kinetic energy and velocity squared are constant because the atom does not radiate at r_n and the potential energy is constant.

Table 1.4. Calculated radii, angular frequencies, linear velocities, and wavelengths for the $n=1$ state of some one-electron atoms (non-relativistic).

Atom	r_1^a (a_0)	angular ^b velocity ($10^{17} \text{ rad s}^{-1}$)	linear ^c velocity (10^6 ms^{-1})	wavelength ^d (10^{-10} m)
H	1.000	0.413	2.19	3.325
He^+	0.500	1.65	4.38	1.663
Li^{2+}	0.333	3.72	6.56	1.108
Be^{3+}	0.250	6.61	8.75	0.831
B^{4+}	0.200	10.3	10.9	0.665
C^{5+}	0.167	14.9	13.1	0.554
N^{6+}	0.143	20.3	15.3	0.475
O^{7+}	0.125	26.5	17.5	0.416

^a from Equation (1.226)
^b from Equation (1.55)
^c from Equation (1.56)
^d from Equation (1.46)

It should be noted that the linear velocity is an appreciable percentage of the velocity of light for some of the atoms in Table 1.3—5.9% for O^{7+} for example. Relativistic corrections must be applied before a comparison between the total energy and ionization energy (Table 1.3) is made.

SPECIAL RELATIVISTIC CORRECTION TO THE IONIZATION ENERGIES

The electron moves in an orbit relative to the laboratory frame. Time dilation of muonic decay due to motion in a cyclotron orbit relative to a stationary laboratory frame provides strong confirmation of special relativity and confirms that the electron's frame is an inertial frame. eB/m bunching of electrons in a gyrotron [41] occurs because the cyclotron frequency is inversely proportional to the relativistic electron mass. This further demonstrates that the electron frame is an inertial frame and that electron mass and time dilation occur. The special

relativistic relationship in polar coordinates is derived. The result of the treatment of the electron motion relative to the laboratory frame is in excellent agreement with numerous experimental observables such as the electron g factor, the invariance of the electron magnetic moment of μ_B and angular momentum of \hbar , the fine structure of the hydrogen atom, and the relativistically corrected ionization energies of one and two electron atoms found *infra.* and in the Excited States of the One-Electron Atom (Quantization) and The Two-Electron Atom sections.

The relativistic correction to the ionization energies is determined by determining the corrected radius in Eq. (1.233) corresponding to a decrease in the electron wavelength and period due to relativistic length contraction and time dilation of the electron motion in the laboratory inertial frame¹¹. Each infinitesimal point of the orbitsphere moves on a great circle as shown in the ORBITSphere EQUATION OF MOTION FOR $\ell = 0$ section. The electron motion is tangential to the radius; thus, r_n is Lorentzian invariant. A further consequence of the electron's motion always being perpendicular to its radius is that the electron's angular momentum of \hbar is invariant as shown by Eq. (1.57). The electron's magnetic moment of a Bohr magneton μ_B given by Eq. (1.99) is also invariant as well as its angular momentum of \hbar . Furthermore, the electron is nonradiative due to its angular motion as shown in the SPACETIME FOURIER TRANSFORM OF THE ELECTRON FUNCTION section, Appendix I, and the Stability of Atoms and Hydrinos section. The radiative instability of excited states is due to a radial dipole term in the function representative of the excited state due to the interaction of the photon and the excited state electron as shown in the Instability of Excited States section. The angular momentum of the photon given in the

¹¹ Many problems arise in the case of applying special relativity to standard quantum mechanical solutions for one-electron atoms as discussed in the Quantum Theory Past and Future section, the Shortcomings of Quantum Theory section, and Appendix II: Quantum Electrodynamics is Purely Mathematical and Has No Basis in Reality. Spin was missed entirely by the Schrödinger equation, and it was forced by spin matrices in the Dirac equation. It does not arise from first principles, and it results in nonsensical consequences such as infinities and "a sea of virtual particles". These are not consistent with observation and paradoxically the virtual particles constitute an ether, the elimination of which was the basis of special relativity and is the supposed basis of the Dirac equation. In addition, the electron motion in the Schrödinger and Dirac equations is in all directions; consequently, the relativistic increase in electron mass results in an instability since the electron radius is inversely proportional to the electron mass. Since the electron mass in special relativity is not invariant, but the charge is, the electron magnetic moment of a Bohr magneton μ_B as well as its angular momentum of \hbar can not be invariant in contradiction with experimental observations known to 14 figure accuracy [27].

Equation of the Photon section is $m = \int \frac{1}{8\pi c} \text{Re}[\mathbf{r} \times (\mathbf{E} \times \mathbf{B}^*)] dx^4 = \hbar$. It is conserved for the solutions for the resonant photons and excited state electron functions given in the Excited States of the One-Electron Atom (Quantization) section and the Equation of the Photon section. The photons emitted during the formation of each one-electron atom are its excited state photons. Thus, the electrodynamic angular momentum and the inertial angular momentum are matched such that the correspondence principle holds. It follows from the principle of conservation of angular momentum of \hbar that $\frac{e}{m_e}$ of Eq. (1.99) is invariant (See the Determination of Orbitsphere Radii section). Since charge is invariant according to special relativity, the electron mass of the orbitsphere must also be invariant. But, as shown in the SPACETIME FOURIER TRANSFORM OF THE ELECTRON FUNCTION section, the tangential distance along a great circle is $2\pi r_n$ in the $v=c$ frame is r_n in the laboratory frame. Thus, the effect of special relativity is to increase the mass and charge densities identically such that $\frac{e}{m_e}$ is a constant invariant.

In the present case, the electron mass density along each great circle can be considered to contract to a point with an increase of the relativistic mass density by a factor of 2π . The remarkable agreement between the calculated and observed value of the fine structure of the hydrogen atom which depends on the conditions of the invariance of the electron's charge and mass to charge ratio $\frac{e}{m_e}$ as given in the SPIN-ORBITAL COUPLING section further confirms the validity of this result.

Each infinitesimal point of the orbitsphere moves on a great circle, and each point charge has the charge density $\frac{e}{4\pi r_n^2}$ and mass density

$\frac{m_e}{4\pi r_n^2}$ as shown in the ORBITSPHERE EQUATION OF MOTION FOR $\ell = 0$

section. Consider a charge-density element (and correspondingly a mass-density element) of a great circle current loop of the electron orbitsphere in the $y'z'$ -plane as shown in Figure 1.4A. The distance on a great circle is given by

$$\int_0^{2\pi} r_n d\theta = r_n \theta \Big|_0^{2\pi} = 2\pi r_n \quad (1.234)$$

Due to relative motion, the distance along the great circle must contract and the time must dilate due to special relativity. The special relativistic length contraction relationship observed for a laboratory frame relative

to an inertial frame moving at constant velocity v in the direction of velocity v is

$$l = l_0 \sqrt{1 - \left(\frac{v}{c}\right)^2} \quad (1.235)$$

For Figure 1.4, the relationship between polar and Cartesian coordinates of special relativity (the Cartesian coordinate system as compared to general coordinates is special with regard to special relativity as discussed in the Relativity section) is given by Eq. (1.68)

$$x_1' = 0 \quad y_1' = -r_n \sin(\omega_n t) \quad z_1' = r_n \cos(\omega_n t) \quad (1.236)$$

where ω_n is given by Eq. (1.55), r_n is from Eq. (1.226) and

$$\phi = \omega_n t \quad (1.237)$$

Due to relativity, a contracted wavelength arises. The distance on the great circle undergoes length contraction only in the $\hat{\phi}$ direction as $v \rightarrow c$. Thus, as $v \rightarrow c$ the distance on a great circle approaches its radius which is the relativistically contracted electron wavelength since the relationship between the radius and the wavelength given by Eq. (1.43) is

$$2\pi r_n = \lambda_n \quad (1.238)$$

With $v = c$,

$$r^* = \lambda \quad (1.239)$$

where $*$ indicates the relativistically corrected parameter. Thus,

$$r^* = \frac{r_n}{2\pi} \quad (1.240)$$

The relativistically corrected mass m^* follows from Eq. (1.240) with maintenance of the invariance of the electron angular momentum of \hbar given by Eqs. (1.56) and (1.57).

$$m\mathbf{r} \times \mathbf{v} = m_e r \frac{\hbar}{m_e r} \quad (1.241)$$

With Eq. (1.240), the relativistically corrected mass m^* corresponding to an increase in its density only is

$$m^* = 2\pi m_e \quad (1.242)$$

The charge (mass) motion may be visualized. At light speed, there can be no motion transverse to the radius. The radial projection of the time harmonic motion of a point charge of a great circle becomes equivalent to a time harmonic oscillator moving along an axis of distance $2r_n$ in the direction of r . In spherical coordinates, the lab frame is at rest at the origin. Relativistic invariance of charge requires that all of the charge of a current loop be projected onto a line in the radial direction. For $n=1$, $\ell=0$, the charge is uniformly distributed. Consider, the radial projection of a point charge on a great circle at $\phi=0$ and a point charge at $\phi=\pi$. Both points move from opposite ends of a line of length $2r_n$

$(-r_n \leq r \leq +r_n)$ and are at the origin in a quarter of a period which is time $t = \frac{r_n}{2c}$. The points then cross. (The crossing is equivalent to elastic scattering at the origin which results in a momentum reversal for both points.) The points interchange roles and travel to the opposite starting points in a half of a period which is time $t = \frac{2r_n}{2c}$. So, with respect to each position, a point left and a point reappeared in $t = \frac{2r_n}{2c}$. Since $T = \frac{2\pi}{\omega} = \frac{\lambda}{c}$, the wavelength is r_n . This situation applies for any ϕ .

Thus, the effect of the relativistic contraction of the distance along a great circle loop is to change the angle of constant motion in Eq. (1.236) with a corresponding decrease in the electron wavelength. The relativistically corrected wavelength that follows from Eqs. (1.234-1.238) is given by the sum of the relativistic electron motion along the great circle (y' direction for point 1 of Figure 1.4A) and that projected along the radial axis (z' direction for point 1 of Figure 1.4):

$$\lambda_n = r_{n,y}^* \sin \phi^* \int_0^{2\pi} d\phi + \cos \phi^* \int_0^{r_n} dr \quad (1.243)$$

where the * indices corresponds to the relativistically corrected parameters in the y' and z' directions. The length contraction is only in the direction of motion which is orthogonal to the radius and constant as a function of angle. Thus, Eq. (1.237) is given by

$$\lambda_n = 2\pi r_n \sqrt{1 - \left(\frac{v}{c}\right)^2} \sin \phi^* + r_n \cos \phi^* \quad (1.244)$$

The projection of the angular motion onto the radial axis is determined by determining the relativistic angle ϕ^* corresponding to a decrease in the electron wavelength and period due to relativistic length contraction and time dilation of the electron motion in the laboratory inertial frame. Substitution of Eq. (1.55) into Eq. (1.237) gives

$$\phi = \omega_n t = \frac{\hbar}{m_e r_n^2} t \quad (1.245)$$

The correction for the time dilation and length contraction due to electron motion gives the relativistic angle ϕ^* as

$$\phi^* = \omega_n t = \frac{\hbar}{m_e \left[\frac{r_n}{\sqrt{1 - \left(\frac{v}{c}\right)^2}} \right]^2} t \sqrt{1 - \left(\frac{v}{c}\right)^2} = \frac{\hbar}{m_e r_n^2} t \left(1 - \left(\frac{v}{c}\right)^2 \right)^{3/2} \quad (1.246)$$

The period for a wavelength due to electron motion is

$$T = \frac{2\pi}{\omega} = \frac{\lambda}{\nu} \quad (1.247)$$

Only the elements of the second y'z'-quadrant need be considered due to symmetry and continuity of the motion. Thus, using Eqs. (1.245-1.246) for a quarter period of time, Eq. (1.244) becomes

$$\lambda_n = 2\pi r_n \sqrt{1 - \left(\frac{\nu}{c}\right)^2} \sin \left[\frac{\pi}{2} \left(1 - \left(\frac{\nu}{c}\right)^2 \right)^{3/2} \right] + r_n \cos \left[\frac{\pi}{2} \left(1 - \left(\frac{\nu}{c}\right)^2 \right)^{3/2} \right] \quad (1.248)$$

The relativistic correction to the ionization energies is determined by using the corrected radius in Eq. (1.233). Using a phase matching condition, the wavelengths of the electron (Eq. (1.238)) and laboratory (Eq. (1.248)) inertial frames are equated, and the corrected radius is given by

$$r_n = r_n \left[\sqrt{1 - \left(\frac{\nu}{c}\right)^2} \sin \left[\frac{\pi}{2} \left(1 - \left(\frac{\nu}{c}\right)^2 \right)^{3/2} \right] + \frac{1}{2\pi} \cos \left[\frac{\pi}{2} \left(1 - \left(\frac{\nu}{c}\right)^2 \right)^{3/2} \right] \right] \quad (1.249)$$

From Eqs. (1.233) and (1.249) the ionization energies are corrected by a factor γ^* of

$$\gamma^* = \frac{2\pi}{2\pi \sqrt{1 - \left(\frac{\nu}{c}\right)^2} \sin \left[\frac{\pi}{2} \left(1 - \left(\frac{\nu}{c}\right)^2 \right)^{3/2} \right] + \cos \left[\frac{\pi}{2} \left(1 - \left(\frac{\nu}{c}\right)^2 \right)^{3/2} \right]} \quad (1.250)$$

where the velocity is given by Eq. (1.56) with the radius given by Eq. (1.223). In Eq. (1.223), the reduced mass is that of the corresponding nucleus. Plots of ratio of the radii from Eq. (1.249) and the correction to the ionization energy γ^* (Eq. (1.250)) as a function of the electron velocity ν relative to the speed of light c are given in Figures 1.13 and 1.14, respectively.

Figure 1.13. The normalized radius as a function of v/c due to relativistic contraction.

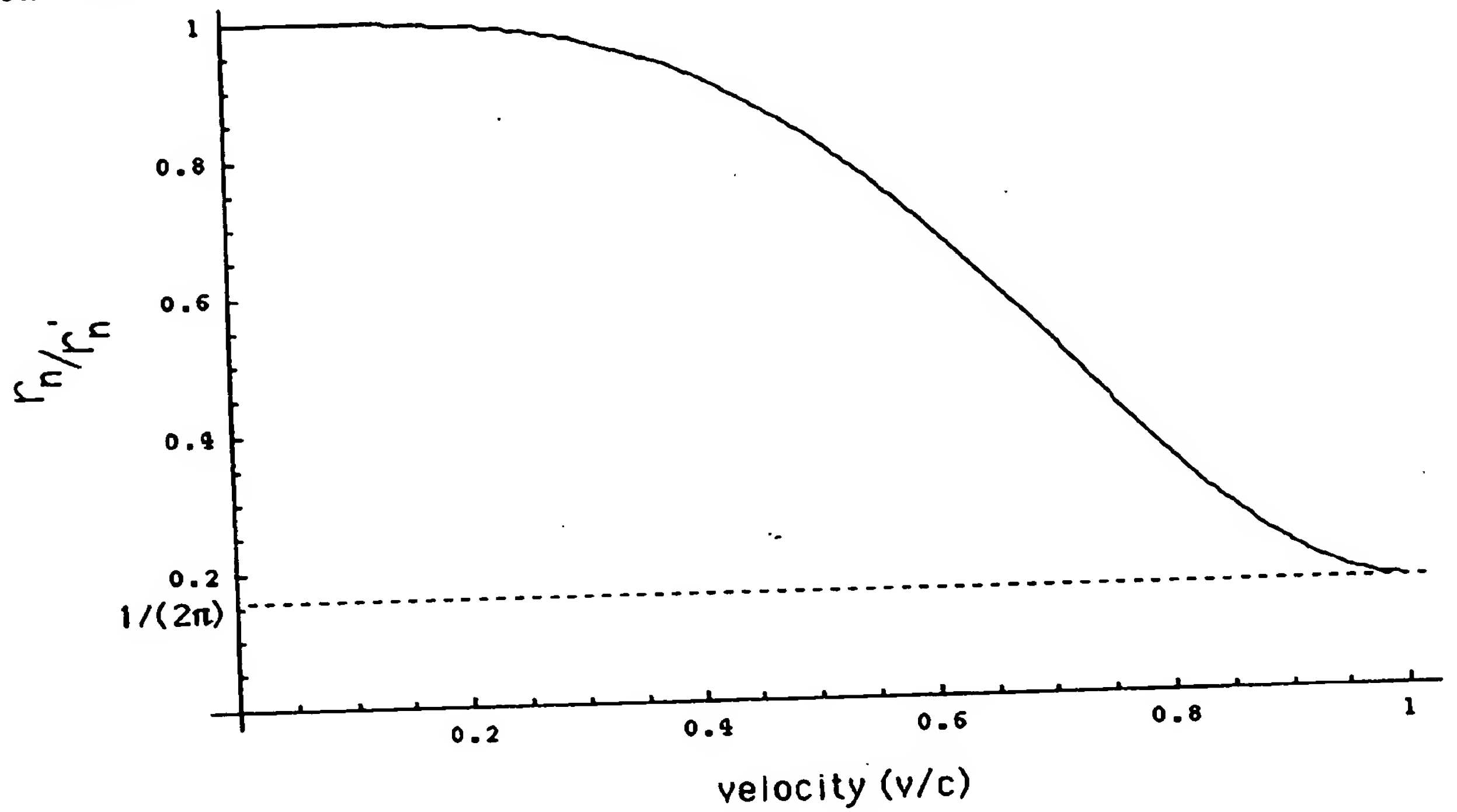
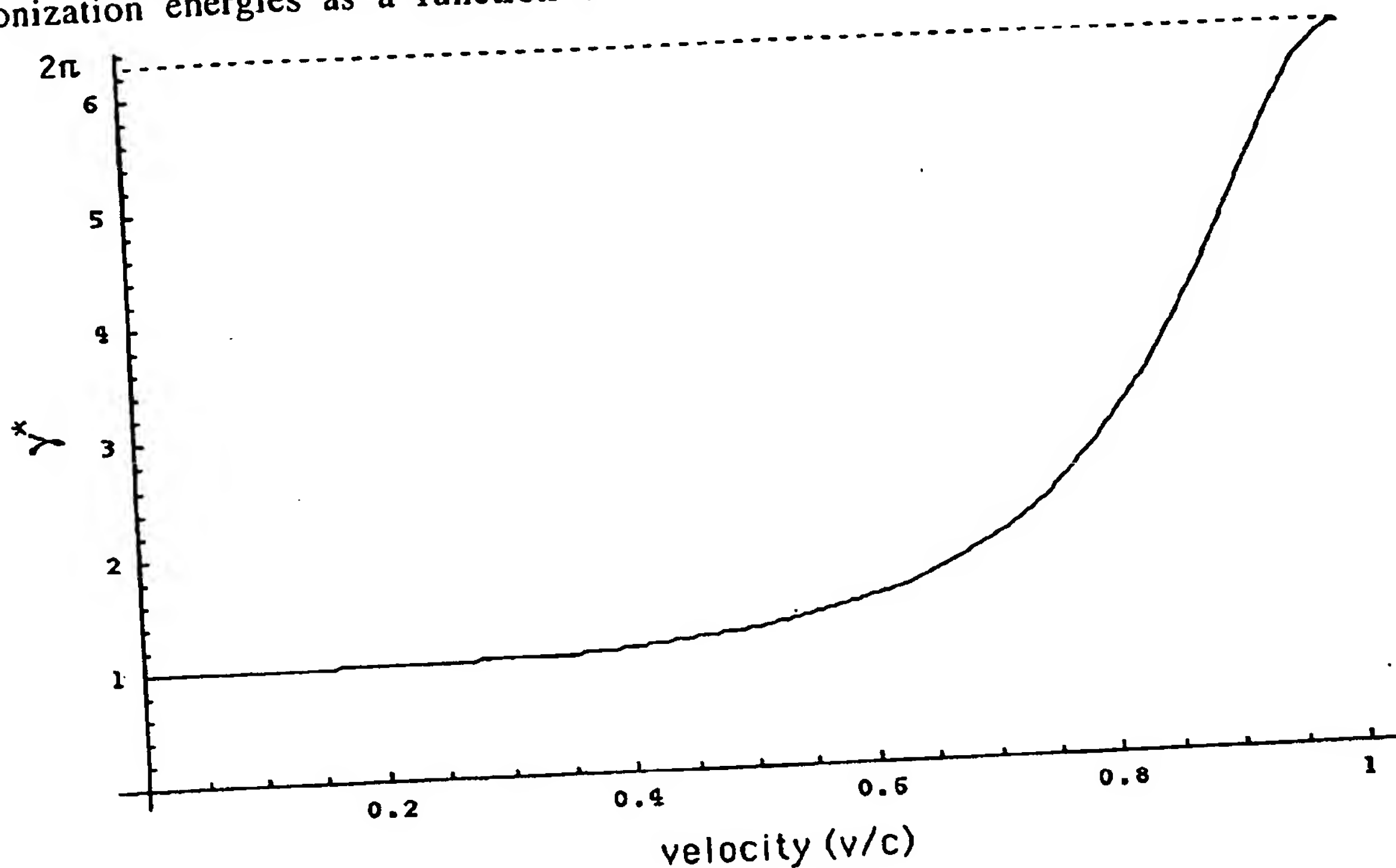


Figure 1.14. The relativistic correction to the one-atom-electron ionization energies as a function of v/c due to relativistic contraction.



The electron possesses an invariant angular momentum and magnetic moment of \hbar and a Bohr magneton, respectively. This invariance feature provides for the stability of multielectron atoms and the existence of excited states wherein electrons magnetically interact as shown in the Two-Electron Atom section, the Three, Four, Five, Six, Seven, Eight, Nine, Ten, Eleven, Twelve, Thirteen, Fourteen, Fifteen, Sixteen, Seventeen, Eighteen, Nineteen, and Twenty-Electron Atoms section, and the Excited States of Helium section. The electron's motion corresponds to a current which gives rise to a magnetic field with a field strength that is inversely proportional to its radius cubed wherein the magnetic field is a relativistic effect of the electric field as shown by Jackson [42]. As there is no electrostatic self-energy as shown in the Determination of Orbitsphere Radii section, there is also no magnetic self-energy for the bound electron since the magnetic moment is invariant for all states and the surface current is the source of the discontinuous field that does not exist inside of the electron as given by Eq. (1.104). No energy term is associated with the magnetic field unless another source of magnetic field is present. In general, the corresponding relativistic correction can be calculated from the effect of the electron's magnetic field on the force

balance and energies of other electrons and the nucleus which also produce magnetic fields. In the case of one-electron atoms, the nuclear-electron magnetic interaction is the only factor. Thus, for example, the effect of the proton was included in the derivation of Eq. (1.229) for the hydrogen atom. The relativistically corrected one electron ionization energies given by the product of Eqs. (1.233) and (1.250) is

$$E_{ele} = -\gamma \cdot \frac{Z^2 e^2}{8\pi\epsilon_0 a_0} \frac{\mu}{m_e} = -\gamma \cdot \frac{\mu}{m_e} Z^2 \times 2.1799 \times 10^{-18} \text{ J} = -\gamma \cdot \frac{\mu}{m_e} Z^2 \times 13.606 \text{ eV} \quad (1.251)$$

where the reduced mass term μ_e corresponds to the electron-nucleus relativistic correction and is only given by Eq. (1.224) for the hydrogen atom where $Z=1$. These energies are plotted in Figure 1.15 and are given in Table 1.5.

Figure 1.15. The relativistically corrected one-electron-atom ionization energies as a function of the nuclear charge Z .

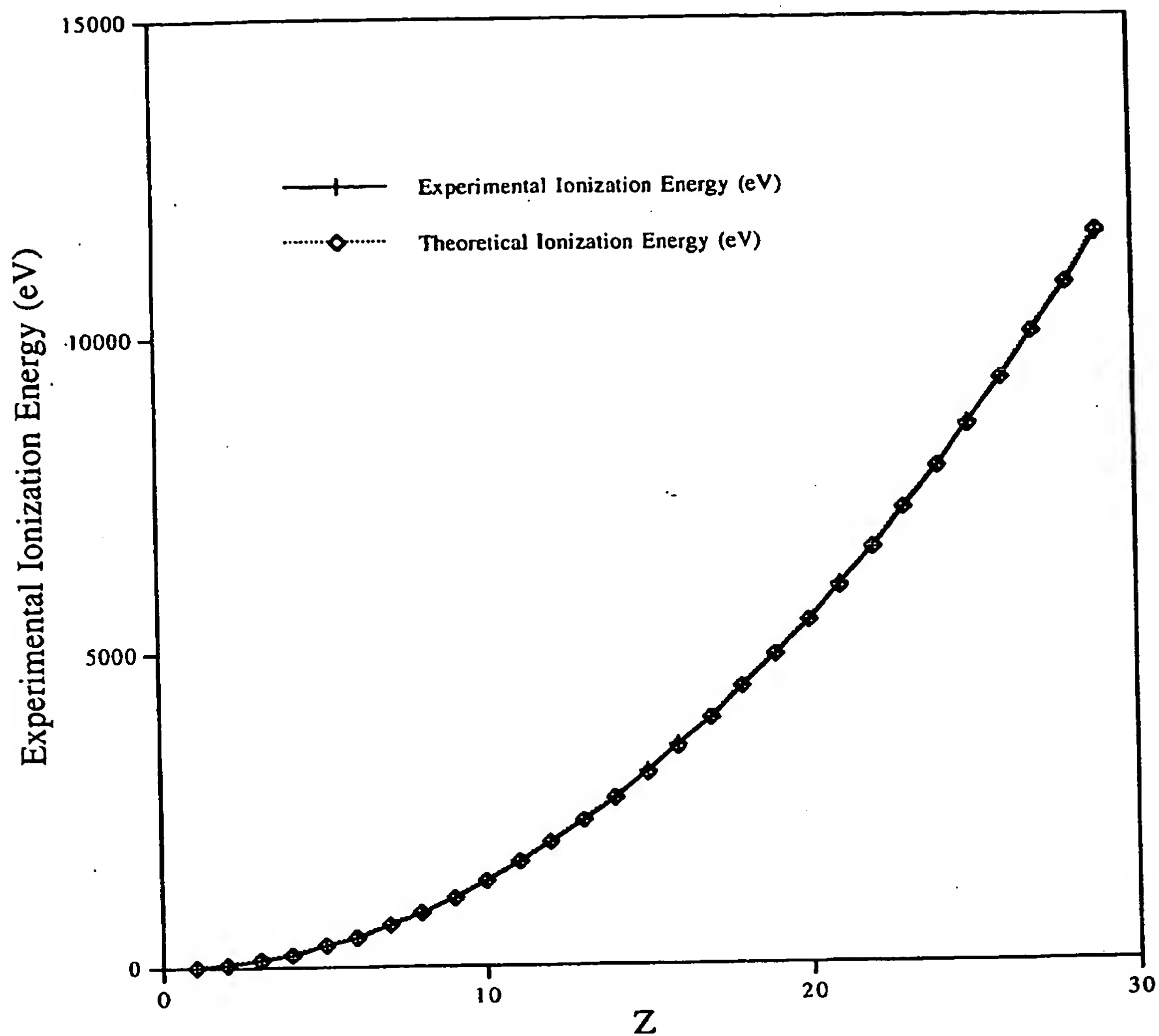


Table 1.5. Relativistically corrected ionization energies for some one-electron atoms.

Onee Atom	Z	γ^* ^a	Theoretical Ionization Energies (eV) ^b	Experimental Ionization Energies (eV) ^c	Relative Difference between Experimental and Calculated ^d
<i>H</i>	1	1.000007	13.59838	13.59844	0.00000
<i>He</i> ⁺	2	1.000027	54.40941	54.41778	0.00015
<i>Li</i> ²⁺	3	1.000061	122.43642	122.45429	0.00015
<i>Be</i> ³⁺	4	1.000109	217.68510	217.71865	0.00015
<i>B</i> ⁴⁺	5	1.000172	340.16367	340.2258	0.00018
<i>C</i> ⁵⁺	6	1.000251	489.88324	489.99334	0.00022
<i>N</i> ⁶⁺	7	1.000347	666.85813	667.046	0.00028
<i>O</i> ⁷⁺	8	1.000461	871.10635	871.4101	0.00035
<i>F</i> ⁸⁺	9	1.000595	1102.65013	1103.1176	0.00042
<i>Ne</i> ⁹⁺	10	1.000751	1361.51654	1362.1995	0.00050
<i>Na</i> ¹⁰⁺	11	1.000930	1647.73821	1648.702	0.00058
<i>Mg</i> ¹¹⁺	12	1.001135	1961.35405	1962.665	0.00067
<i>Al</i> ¹²⁺	13	1.001368	2302.41017	2304.141	0.00075
<i>Si</i> ¹³⁺	14	1.001631	2670.96078	2673.182	0.00083
<i>P</i> ¹⁴⁺	15	1.001927	3067.06918	3069.842	0.00090
<i>S</i> ¹⁵⁺	16	1.002260	3490.80890	3494.1892	0.00097
<i>Cl</i> ¹⁶⁺	17	1.002631	3942.26481	3946.296	0.00102
<i>Ar</i> ¹⁷⁺	18	1.003045	4421.53438	4426.2296	0.00106
<i>K</i> ¹⁸⁺	19	1.003505	4928.72898	4934.046	0.00108
<i>Ca</i> ¹⁹⁺	20	1.004014	5463.97524	5469.864	0.00108
<i>Sc</i> ²⁰⁺	21	1.004577	6027.41657	6033.712	0.00104
<i>Ti</i> ²¹⁺	22	1.005197	6619.21462	6625.82	0.00100
<i>V</i> ²²⁺	23	1.005879	7239.55091	7246.12	0.00091
<i>Cr</i> ²³⁺	24	1.006626	7888.62855	7894.81	0.00078
<i>Mn</i> ²⁴⁺	25	1.007444	8566.67392	8571.94	0.00061
<i>Fe</i> ²⁵⁺	26	1.008338	9273.93857	9277.69	0.00040
<i>Co</i> ²⁶⁺	27	1.009311	10010.70111	10012.12	0.00014
<i>Ni</i> ²⁷⁺	28	1.010370	10777.26918	10775.4	-0.00017
<i>Cu</i> ²⁸⁺	29	1.011520	11573.98161	11567.617	-0.00055

^a From theoretical calculations, interpolation of H isoelectronic and Rydberg series, and experimental data [43-44].

^b (Experimental-theoretical)/experimental.

The agreement between the experimental and calculated values of Table 1.5 is well within the experimental capability of the spectroscopic

determinations including the values at large Z which relies on X-ray spectroscopy. In this case, the experimental capability is three to four significant figures which is consistent with the last column. The hydrogen atom isoelectronic series is given in Table 1.5 [43-44] to much higher precision than the capability of X-ray spectroscopy, but these values are based on theoretical and interpolation techniques rather than data alone. Ionization energies are difficult to determine since the cut-off of the Rydberg series of lines at the ionization energy is often not observed, and the ionization energy must be determined from theoretical calculations, interpolation of H isoelectronic and Rydberg series, as well as direct experimental data.

APPENDIX I

NONRADIATION BASED ON THE ELECTROMAGNETIC FIELDS AND THE POYNTING POWER VECTOR

A point charge undergoing periodic motion accelerates and as a consequence radiates power P according to the Larmor formula:

$$P = \frac{1}{4\pi\epsilon_0} \frac{2e^2}{3c^3} a^2 \quad (1)$$

where e is the charge, a is its acceleration, ϵ_0 is the permittivity of free space, and c is the speed of light. Although an accelerated *point* particle radiates, an *extended distribution* modeled as a superposition of accelerating charges does not have to radiate [1, 11, 16, 45-46]. An ensemble of charges, all oscillating at the same frequency, create a radiation pattern with a number of nodes. The same applies to current patterns in phased array antenna design [47]. It is possible to have an infinite number of charges oscillating in such a way as to cause destructive interference or nodes in all directions. The electromagnetic far field is determined from the current distribution in order to obtain the condition, if it exists, that the electron current distribution given by Eq. (6) must satisfy such that the electron does not radiate.

The charge-density functions of the electron orbitsphere in spherical coordinates plus time are given by Eqs. (1.64-1.65). For $\ell = 0$, $N = \frac{-e}{8\pi r_n^2}$, and the charge-density function is

$$\rho(r, \theta, \phi, t) = \frac{e}{8\pi r_n^2} [\delta(r - r_n)] [Y_0^0(\theta, \phi) + Y_l^m(\theta, \phi)] \quad (2)$$

The equipotential, uniform or constant charge-density function (Eq. (1.64) and Eq. (2)) further comprises a current pattern given in the ORBITSphere EQUATION OF MOTION FOR $\ell = 0$ section. It also corresponds to the nonradiative $n=1, \ell = 0$ state of atomic hydrogen and to the spin function of the electron. The current-density function is given by multiplying Eq. (2) by the constant angular velocity ω_n . There is acceleration without radiation. In this case, centripetal acceleration. A static charge distribution exists even though each point on the surface is accelerating along a great circle. Haus' condition predicts no radiation for the entire ensemble. The same result is trivially predicted from consideration of the fields and the radiated power. Since the current is not time dependent, the fields are given by

$$\nabla \times \mathbf{H} = \mathbf{J}$$

(3)

and

$$\nabla \times \mathbf{E} = 0$$

(4)

which are the electrostatic and magnetostatic cases, respectively, with no radiation.

In cases of orbitals of heavier elements and excited states of one electron-atoms and atoms or ions of heavier elements which are not constant as given by Eq. (1.65), the constant spin function is modulated by a time and spherical harmonic function. The modulation or traveling charge-density wave corresponds to an orbital angular momentum in addition to a spin angular momentum. These states are typically referred to as p, d, f, etc. orbitals and correspond to an ℓ quantum number not equal to zero. Haus' condition also predicts nonradiation for a constant spin function modulated by a time and spherically harmonic orbital function. However, in the case that such a state arises as an excited state by photon absorption, it is radiative due to a radial dipole term in its current-density function since it possesses spacetime Fourier transform components synchronous with waves traveling at the speed of light as given in the INSTABILITY OF EXCITED STATES section.

The nonradiation condition given by Eqs. (1.44-1.45) may be confirmed by determining the fields and the current distribution condition that is nonradiative based on Maxwell's equations.

For $\ell \neq 0$, $N = \frac{-e}{4\pi r_n^2}$. The charge-density functions including the time-function factor are

$$\ell \neq 0$$

$$\rho(r, \theta, \phi, t) = \frac{e}{4\pi r^2} [\delta(r - r_n)] [Y_0^0(\theta, \phi) + \text{Re}\{Y_\ell^m(\theta, \phi)e^{i\omega_n t}\}] \quad (5)$$

where $\text{Re}\{Y_\ell^m(\theta, \phi)e^{i\omega_n t}\} = P_\ell^m(\cos\theta)\cos(m\phi + \omega_n t)$ and to keep the form of the spherical harmonic as a traveling wave about the z-axis, $\omega_n = m\omega_n$. Thus, $\omega_n = 0$ for $m=0$. In the cases that $m \neq 0$, Eq. (1.65) and Eq. (5) is a traveling charge-density wave that moves on the surface of the orbitsphere about the z-axis and modulates the orbitsphere corresponding to $\ell = 0$. Since the charge is moving time harmonically about the z-axis with frequency ω_n and the current-density function is given by the time derivative of the charge-density function, the current-density function is given by the normalized product of the constant angular velocity and the charge-density function. The first current term of Eq. (5) is static. Thus, it is trivially nonradiative.

The current due to the time dependent term is

$$\begin{aligned}
 \mathbf{J} &= \frac{\omega_n}{2\pi} \frac{e}{4\pi r_n^2} N[\delta(r-r_n)] \text{Re}\{Y_\ell^m(\theta, \phi)\} [\mathbf{u}(t) \times \mathbf{r}] \\
 &= \frac{\omega_n}{2\pi} \frac{e}{4\pi r_n^2} N[\delta(r-r_n)] \text{Re}\{Y_\ell^m(\theta, \phi) e^{i\omega_n t}\} [\mathbf{u} \times \mathbf{r}] \\
 &= \frac{\omega_n}{2\pi} \frac{e}{4\pi r_n^2} N[\delta(r-r_n)] \text{Re}\{P_\ell^m(\cos\theta) e^{im\phi} e^{i\omega_n t}\} [\mathbf{u} \times \mathbf{r}] \\
 &= \frac{\omega_n}{2\pi} \frac{e}{4\pi r_n^2} N[\delta(r-r_n)] (P_\ell^m(\cos\theta) \cos(m\phi + \omega_n t)) [\mathbf{u} \times \mathbf{r}] \\
 &= \frac{\omega_n}{2\pi} \frac{e}{4\pi r_n^2} N[\delta(r-r_n)] (P_\ell^m(\cos\theta) \cos(m\phi + \omega_n t)) \sin\theta \hat{\phi}
 \end{aligned} \tag{6}$$

where N and N' are normalization constants. The vectors are defined as

$$\hat{\phi} = \frac{\hat{\mathbf{u}} \times \hat{\mathbf{r}}}{|\hat{\mathbf{u}} \times \hat{\mathbf{r}}|} = \frac{\hat{\mathbf{u}} \times \hat{\mathbf{r}}}{\sin\theta}; \quad \hat{\mathbf{u}} = \hat{\mathbf{z}} = \text{orbital axis} \tag{7}$$

$$\hat{\theta} = \hat{\phi} \times \hat{\mathbf{r}} \tag{8}$$

"^" denotes the unit vectors $\hat{\mathbf{u}} \equiv \frac{\mathbf{u}}{|\mathbf{u}|}$, non-unit vectors are designed in bold,

and the current function is normalized. For time-varying electromagnetic fields, Jackson [48] gives a generalized expansion in vector spherical waves that are convenient for electromagnetic boundary-value problems possessing spherical symmetry properties and for analyzing multipole radiation from a localized source distribution. The Green function $G(\mathbf{x}', \mathbf{x})$ which is appropriate to the equation

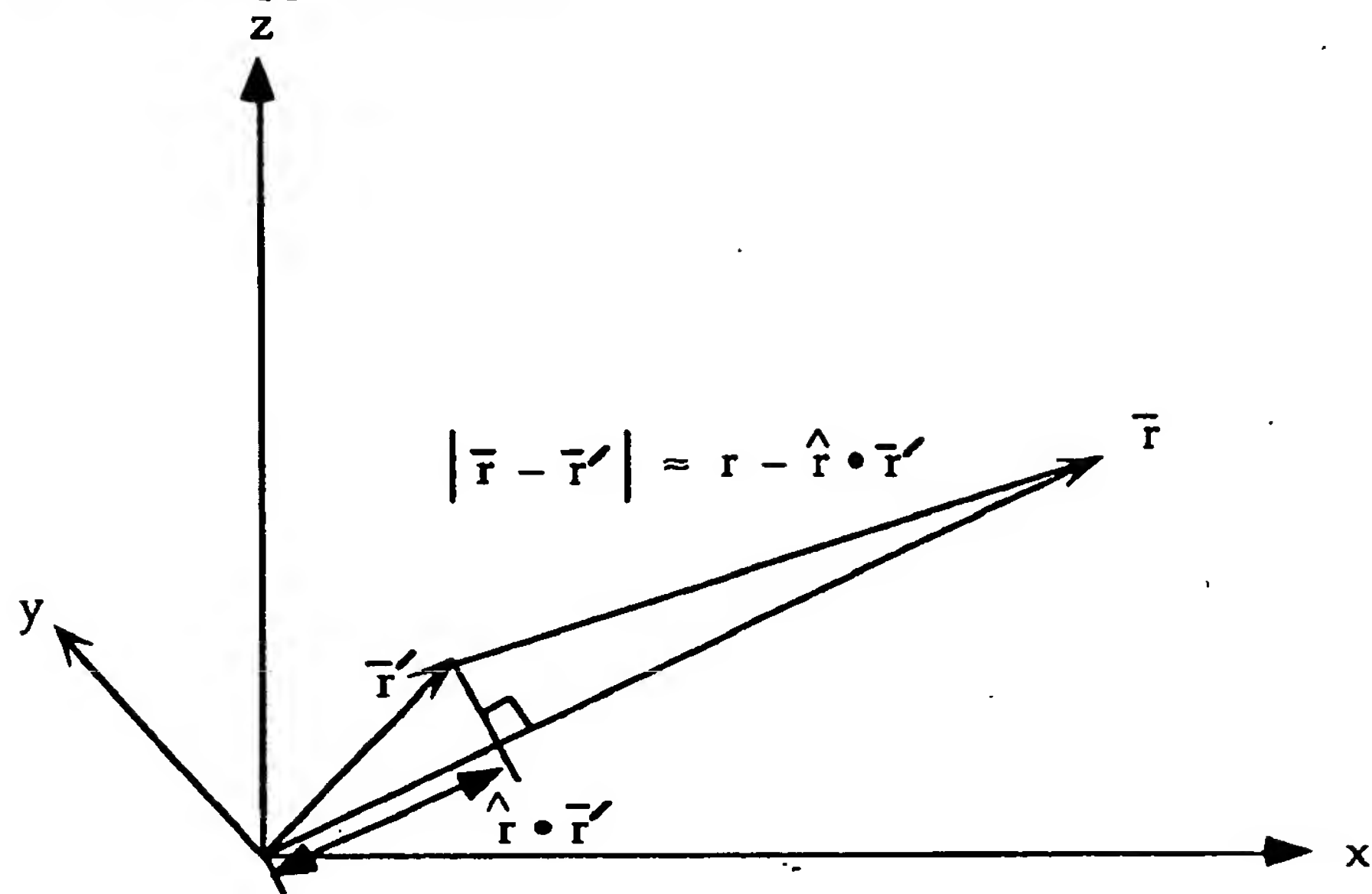
$$(\nabla^2 + k^2)G(\mathbf{x}', \mathbf{x}) = -\delta(\mathbf{x}' - \mathbf{x}) \tag{9}$$

in the infinite domain with the spherical wave expansion for the outgoing wave Green function is

$$G(\mathbf{x}', \mathbf{x}) = \frac{e^{-ik|\mathbf{x}-\mathbf{x}'|}}{|\mathbf{x}-\mathbf{x}'|} = ik \sum_{\ell=0}^{\infty} j_\ell(kr_<) h_\ell^{(1)}(kr_>) \sum_{m=-\ell}^{\ell} Y_{\ell,m}^*(\theta', \phi') Y_{\ell,m}(\theta, \phi) \tag{10}$$

General spherical coordinates are shown in Figure 1.

Figure 1. Far field approximation.



Jackson [48] further gives the general multipole field solution to Maxwell's equations in a source-free region of empty space with the assumption of a time dependence $e^{i\omega t}$:

$$\mathbf{B} = \sum_{\ell, m} \left[a_E(\ell, m) f_\ell(kr) \mathbf{X}_{\ell, m} - \frac{i}{k} a_M(\ell, m) \nabla \times g_\ell(kr) \mathbf{X}_{\ell, m} \right] \quad (11)$$

$$\mathbf{E} = \sum_{\ell, m} \left[\frac{i}{k} a_E(\ell, m) \nabla \times f_\ell(kr) \mathbf{X}_{\ell, m} + a_M(\ell, m) g_\ell(kr) \mathbf{X}_{\ell, m} \right]$$

where the cgs units used by Jackson are retained in this section. The radial functions $f_\ell(kr)$ and $g_\ell(kr)$ are of the form:

$$g_\ell(kr) = A_\ell^{(1)} h_\ell^{(1)} + A_\ell^{(2)} h_\ell^{(2)} \quad (12)$$

$\mathbf{X}_{\ell, m}$ is the vector spherical harmonic defined by

$$\mathbf{X}_{\ell, m}(\theta, \phi) = \frac{1}{\sqrt{\ell(\ell+1)}} \mathbf{L} Y_{\ell, m}(\theta, \phi) \quad (13)$$

where

$$\mathbf{L} = \frac{1}{i} (\mathbf{r} \times \nabla) \quad (14)$$

The coefficients $a_E(\ell, m)$ and $a_M(\ell, m)$ of Eq. (11) specify the amounts of electric (ℓ, m) multipole and magnetic (ℓ, m) multipole fields, and are determined by sources and boundary conditions as are the relative proportions in Eq. (12). Jackson gives the result of the electric and magnetic coefficients from the sources as

$$a_E(\ell, m) = \frac{4\pi k^2}{i\sqrt{\ell(\ell+1)}} \int Y_{\ell, m}^* \left\{ \rho \frac{\delta}{\delta r} [r j_\ell(kr)] + \frac{ik}{c} (\mathbf{r} \cdot \mathbf{J}) j_\ell(kr) - ik \nabla \cdot (\mathbf{r} \times \mathbf{M}) j_\ell(kr) \right\} d^3x \quad (15)$$

and

$$a_M(\ell, m) = \frac{-4\pi k^2}{\sqrt{\ell(\ell+1)}} \int j_\ell(kr) Y_\ell^m \mathbf{L} \cdot \left(\frac{\mathbf{J}}{c} + \nabla \times \mathbf{M} \right) d^3x \quad (16)$$

respectively, where the distribution of charge $\rho(\mathbf{x}, t)$, current $\mathbf{J}(\mathbf{x}, t)$, and intrinsic magnetization $\mathbf{M}(\mathbf{x}, t)$ are harmonically varying sources: $\rho(\mathbf{x})e^{-i\omega t}$, $\mathbf{J}(\mathbf{x})e^{-i\omega t}$, and $\mathbf{M}(\mathbf{x})e^{-i\omega t}$. From Eq. (6), the charge and intrinsic magnetization terms are zero. Also, the current $\mathbf{J}(\mathbf{x}, t)$ is in the $\hat{\phi}$ direction; thus, the $a_E(\ell, m)$ coefficient given by Eq. (15) is zero since $\mathbf{r} \cdot \mathbf{J} = 0$. Substitution of Eq. (6) into Eq. (16) gives the magnetic multipole coefficient $a_M(\ell, m)$:

$$a_M(\ell, m) = \frac{-4\pi k^2}{\sqrt{\ell(\ell+1)}} \int j_\ell(kr) Y_\ell^m \mathbf{L} \cdot \left(\frac{\frac{\omega_n}{2\pi} \frac{e}{4\pi r_n^2} N \delta(r - r_n) Y_\ell^m(\theta, \phi) \sin \theta \hat{\phi}}{c} \right) d^3x \quad (17)$$

Each mass-density element of the electron moves about the z-axis along a circular orbit of radius $r_n \sin \theta$ in such a way that ϕ , changes at a constant rate. That is $\phi = \omega t$ at time t where ω_n is the constant angular frequency given in Eq. (6), and

$$\mathbf{r}(t) = i r_n \sin \theta \cos \omega t + j r_n \sin \theta \sin \omega t \quad (18)$$

is the parametric equation of the circular orbit. Jackson gives the operator in the xy-plane corresponding to the current motion in this plane and the relations for $Y_\ell^m(\theta, \phi)$ [48].

$$L_+ = L_x + iL_y = e^{i\phi} \left(\frac{\partial}{\partial \theta} + i \cot \theta \frac{\partial}{\partial \phi} \right) \quad (19)$$

$$L_+ Y_\ell^m(\theta, \phi) = \sqrt{(\ell - m)(\ell + m + 1)} Y_\ell^{m+1}(\theta, \phi) \quad (20)$$

Using Eq. (19), $\mathbf{L} \cdot \mathbf{J}$ of Eq. (16) is

$$\begin{aligned} L_+(Y_\ell^m(\theta, \phi) \sin \theta) &= e^{i\phi} \left(\frac{\partial}{\partial \theta} + i \cot \theta \frac{\partial}{\partial \phi} \right) Y_\ell^m(\theta, \phi) \sin \theta \\ &= e^{i\phi} Y_\ell^m(\theta, \phi) \left(\frac{\partial}{\partial \theta} + i \cot \theta \frac{\partial}{\partial \phi} \right) \sin \theta + e^{i\phi} \sin \theta \left(\frac{\partial}{\partial \theta} + i \cot \theta \frac{\partial}{\partial \phi} \right) Y_\ell^m(\theta, \phi) \end{aligned} \quad (21)$$

Using Eq. (20) in Eq. (21) gives

$$L_+(Y_\ell^m(\theta, \phi) \sin \theta) = e^{i\phi} Y_\ell^m(\theta, \phi) \cos \theta + \sin \theta \sqrt{(\ell - m)(\ell + m + 1)} Y_\ell^{m+1}(\theta, \phi) \quad (22)$$

The spherical harmonic is given as

$$Y_\ell^m(\theta, \phi) = \sqrt{\frac{2\ell + 1}{4\pi} \frac{(\ell - m)!}{(\ell + m)!}} P_\ell^m(\cos \theta) e^{im\phi} = N_{\ell, m} P_\ell^m(\cos \theta) e^{im\phi} \quad (23)$$

Thus, Eq. (22) is given as

$$\begin{aligned} L_+(Y_\ell^m(\theta, \phi) \sin \theta) &= \\ &= e^{i\phi} N_{\ell, m} P_\ell^m(\cos \theta) e^{im\phi} \cos \theta + \sin \theta \sqrt{(\ell - m)(\ell + m + 1)} N_{\ell, m+1} P_\ell^{m+1}(\cos \theta) e^{i(m+1)\phi} \end{aligned} \quad (24)$$

Substitution of Eq. (24) into Eq. (17) gives

$$a_M(\ell, m) = \frac{-k^2}{c\sqrt{\ell(\ell+1)}} \frac{\omega_n}{2\pi} \frac{e}{r_n^2} N \int j_\ell(kr) Y_\ell^{m*}(\theta, \phi) \delta(r - r_n) \left\{ \begin{aligned} &e^{i\phi} N_{\ell, m} P_\ell^m(\cos\theta) e^{im\phi} \cos\theta \\ &+ \sin\theta \sqrt{(\ell-m)(\ell+m+1)} N_{\ell, m+1} P_\ell^{m+1}(\cos\theta) e^{i(m+1)\phi} \end{aligned} \right\} d^3x \quad (25)$$

Substitution of $Y_\ell^{-m}(\theta, \phi) = (-1)^m Y_\ell^{m*}(\theta, \phi)$ and Eq. (23) into Eq. (25) and integration with respect to dr gives

$$a_M(\ell, m) = \frac{-ek^2}{c\sqrt{\ell(\ell+1)}} \frac{\omega_n}{2\pi} N j_\ell(kr_n) \int_0^{2\pi} \int_0^\pi (-1)^m N_{\ell, -m} P_\ell^{-m}(\cos\theta) e^{-im\phi} \left\{ \begin{aligned} &e^{i\phi} N_{\ell, m} P_\ell^m(\cos\theta) e^{im\phi} \cos\theta \\ &+ \sin\theta \sqrt{(\ell-m)(\ell+m+1)} N_{\ell, m+1} P_\ell^{m+1}(\cos\theta) e^{i(m+1)\phi} \end{aligned} \right\} \sin\theta d\theta d\phi \quad (26)$$

The integral in Eq. (26) separated in terms of $d\theta$ and $d\phi$ is

$$a_M(\ell, m) = \frac{-ek^2}{c\sqrt{\ell(\ell+1)}} \frac{\omega_n}{2\pi} N j_\ell(kr_n) \int_0^\pi (-1)^m N_{\ell, -m} P_\ell^{-m}(\cos\theta) \left\{ \begin{aligned} &N_{\ell, m} P_\ell^m(\cos\theta) \cos\theta \\ &+ \sin\theta \sqrt{(\ell-m)(\ell+m+1)} N_{\ell, m+1} P_\ell^{m+1}(\cos\theta) \end{aligned} \right\} \sin\theta d\theta \int_0^{2\pi} e^{i\phi} d\phi \quad (27)$$

Consider that the $d\theta$ integral is finite and designated by Θ , then Eq. (27) is given as

$$a_M(\ell, m) = \frac{-ek^2}{c\sqrt{\ell(\ell+1)}} \frac{\omega_n}{2\pi} N j_\ell(kr_n) \Theta \int_0^{2\pi} e^{i\phi} d\phi \quad (28)$$

From Eq. (11), the far fields are given by

$$\mathbf{B} = -\frac{i}{k} a_M(\ell, m) \nabla \times g_\ell(kr) \mathbf{X}_{\ell, m} \quad (29)$$

$$\mathbf{E} = a_M(\ell, m) g_\ell(kr) \mathbf{X}_{\ell, m}$$

where $a_M(\ell, m)$ is given by Eq. (28).

The power density $P(t)$ given by the Poynting power vector is

$$P(t) = \mathbf{E} \times \mathbf{H} \quad (30)$$

For a pure multipole of order (ℓ, m) , the time-averaged power radiated per solid angle $\frac{dP(\ell, m)}{d\Omega}$ given by Jackson [48] is

$$\frac{dP(\ell, m)}{d\Omega} = \frac{c}{8\pi k^2} |a_M(\ell, m)|^2 |\mathbf{X}_{\ell, m}|^2 \quad (31)$$

where $a_M(\ell, m)$ is given by Eq. (30).

Since the modulation function $Y_{\ell, m}(\theta, \phi)$ is a traveling charge-density wave that moves time harmonically on the surface of the orbitsphere

about the z-axis with frequency ω_n , ϕ of the spherical harmonic function is a function of t as shown in Eq. (18). The time dependence of the source current must also be evaluated in Eq. (28), and it can be written as

$$a_M(\ell, m) = \frac{-ek^2}{c\sqrt{\ell(\ell+1)}} \frac{\omega_n}{2\pi} Nj_\ell(kr_n) \Theta \int_0^{vT_n} \cos(mks(t)) ds \quad (32)$$

where $s(t)$ is the angular displacement of the rotating modulation function during one period T_n and v is the linear velocity in the $\hat{\phi}$ direction. Thus,

$$a_M(\ell, m) = \frac{-ek^2}{c\sqrt{\ell(\ell+1)}} \frac{\omega_n}{2\pi} Nj_\ell(kr_n) \Theta \sin(mkvT_n) \quad (33)$$

$$a_M(\ell, m) = \frac{-ek^2}{c\sqrt{\ell(\ell+1)}} \frac{\omega_n}{2\pi} Nj_\ell(kr_n) \Theta \sin(mks) \quad (34)$$

In the case that k is the lightlike k^0 , then $k = \omega_n/c$, and the $\sin(mks)$ term in Eq. (34) vanishes for

$$R = cT_n \quad (35)$$

$$RT_n^{-1} = c \quad (36)$$

$$Rf = c \quad (37)$$

Thus,

$$s = vT_n = R = r_n = \lambda_n \quad (38)$$

as given by Eq. (1.248) which is identical to the Haus condition for nonradiation given by Eq. (1.45). Then, the multipole coefficient $a_M(\ell, m)$ is zero. For the condition given by Eq. (38), the time-averaged power radiated per solid angle $\frac{dP(\ell, m)}{d\Omega}$ given by Eqs (31) and (34) is zero. *There is no radiation.*

APPENDIX II

QUANTUM ELECTRODYNAMICS (QED) IS PURELY MATHEMATICAL AND HAS NO BASIS IN REALITY

The spin of the electron and the Lamb shift are calculated from first principles in closed form by Mills as shown in the Electron g Factor section and the Resonant Line Shape and Lamb Shift section, respectively. The spin angular momentum results from the motion of negatively charged mass moving systematically, and the equation for angular momentum, $\mathbf{r} \times \mathbf{p}$, can be applied directly to the wave function (a current-density function) that describes the electron. The Lamb shift results from conservation of linear momentum of the photon. The Casimir effect is predicted by Maxwell's equations. These results demonstrate that QED has no basis in reality.

Quantum mechanics failed to predict the results of the Stern-Gerlach experiment which indicated the need for an additional quantum number. Quantum electrodynamics was proposed by Dirac in 1926 to provide a generalization of quantum mechanics for high energies in conformity with the theory of special relativity and to provide a consistent treatment of the interaction of matter with radiation. It relies on the unfounded notions of negative energy states of the vacuum, virtual particles, and gamma factors. From Weisskopf [49], "Dirac's quantum electrodynamics gave a more consistent derivation of the results of the correspondence principle, but it also brought about a number of new and serious difficulties." Quantum electrodynamics; 1.) does not explain nonradiation of bound electrons; 2.) contains an internal inconsistency with special relativity regarding the classical electron radius—the electron mass corresponding to its electric energy is infinite; 3.) it admits solutions of negative rest mass and negative kinetic energy; 4.) the interaction of the electron with the predicted zero-point field fluctuations leads to infinite kinetic energy and infinite electron mass; 5.) Dirac used the unacceptable states of negative mass for the description of the vacuum; yet, infinities still arise. In 1947, contrary to Dirac's predictions, Lamb discovered a 1000 MHz shift between the $^2S_{1/2}$ state and the $^2P_{1/2}$ state of the hydrogen atom [50]. This so called Lamb Shift marked the beginning of modern quantum electrodynamics. In the words of Dirac [51], "No progress was made for 20 years. Then a development came initiated by Lamb's discovery and explanation of the Lamb Shift, which fundamentally changed the character of theoretical physics. It involved setting up rules for discarding ...infinities..." Renormalization is presently believed to be required of any fundamental

theory of physics [52]. However, dissatisfaction with renormalization has been expressed at various times by many physicists including Dirac [53] who felt that, "This is just not sensible mathematics. Sensible mathematics involves neglecting a quantity when it turns out to be small—not neglecting it just because it is infinitely great and you do not want it!"

Throughout the history of quantum theory, wherever there was an advance to a new application, it was necessary to repeat a trial-and-error experimentation to find which method of calculation gave the right answers. Often the textbooks present only the successful procedure as if it followed from first principles and do not mention the actual method by which it was found. In electromagnetic theory based on Maxwell's equations, one deduces the computational algorithm from the general principles. In quantum theory, the logic is just the opposite. One chooses the principle to fit the empirically successful algorithm. For example, we know that it required a great deal of art and tact over decades of effort to get correct predictions out of QED. The QED method of the determination of $(g-2)/2$ from the *postulated* Dirac equation is based on a *postulated* power series of α/π where each *postulated* virtual particle is a source of *postulated* vacuum polarization that gives rise to a *postulated* term which is processed over decades using ad hoc rules to remove infinities from each term that arises from *postulated* scores of *postulated* Feynman diagrams. The solution so obtained using the perturbation series further requires a *postulated* truncation since the series **diverges**. Mohr and Taylor reference some of the Herculean efforts to arrive at g using QED [54]:

"the sixth-order coefficient $A_1^{(6)}$ arises from 72 diagrams and is also known analytically after nearly 30 years of effort by many researchers [see Roskies, Remiddi, and Levine (1990) for a review of the early work]. It was not until 1996 that the last remaining distinct diagrams were calculated analytically, thereby completing the theoretical expression for $A_1^{(6)}$ ".

For the right experimental numbers to emerge, one must do the calculation (i.e. subtract off the infinities) in one particular way and not in some other way that appears in principle equally valid. For example, Milonni [55] presents a QED derivation of the magnetic moment of the electron which gives a result of the wrong sign and requires the introduction of an

"upper limit K in the integration over $k=\omega/c$ in order to avoid a

divergence."

A differential mass is arbitrarily added, then

"the choice $K = 0.42mc/\hbar$ yields $(g-2)/2 = \alpha/2\pi$ which is the relativistic QED result to first order in α . [...] However, the reader is warned not to take these calculations too seriously, for the result $(g-2)/2 = \alpha/2\pi$ could be obtained by retaining only the first (radiation reaction) term in (3.112) and choosing $K = 3mc/8\hbar$. It should also be noted that the solution $K \approx 0.42mc/\hbar$ of (3.112) with $(g-2)/2 = \alpha/2\pi$ is not unique."

Such an ad hoc nonphysical approach makes incredulous:

"the cliché that QED is the best theory we have!" [56]

or the statement that:

"The history of quantum electrodynamics (QED) has been one of unblemished triumph" [57].

There is a corollary, noted by Kallen: from an inconsistent theory, any result may be derived.

The QED determination of the postulated power series in α/π is based on scores of Feynman diagrams corresponding to thousands of matrices with thousands of integrations per matrix requiring decades to reach a consensus on the "appropriate" algorithm to remove the intrinsic infinities. Remarkably, $(g-2)/2$ may be derived in closed form from Maxwell's equations in a simple straightforward manner that yields a result with eleven figure agreement with experiment—the limit of experimental capability. Rather than an infinity of radically different QED models, an essential feature is that *Maxwellian solutions are unique*. The derivation from first principles without invoking virtual particles, zero point fluctuations of the vacuum, and negative energy states of the vacuum is given in the Electron g Factor section.

Furthermore, Oskar Klein pointed out a glaring paradox implied by the Dirac equation which was never resolved [58]. "Electrons may penetrate an electrostatic barrier even when their kinetic energy, $E - mc^2$ is lower than the barrier. Since in Klein's example the barrier was infinitely broad this could not be associated with wave mechanical tunnel effect. It is truly a paradox: Electrons too slow to surpass the potential, may still only be partially reflected. ...Even for an infinitely high barrier, i.e. $r_2 = 1$ and energies $\approx 1 \text{ MeV}$, (the reflection coefficient) R is less than

75%! From (2) and (3) it appears that as soon as the barrier is sufficiently high: $V > 2mc^2$, electrons may transgress the repulsive wall—seemingly defying conservation of energy. ...Nor is it possible by way of the positive energy spectrum of the free electron to achieve complete Einstein causality."

The Rutherford experiment demonstrated that even atoms are comprised of essentially empty space [59]. Zero-point field fluctuations, virtual particles, and states of negative energy and mass invoked to describe the vacuum are nonsensical and have no basis in reality since they have never been observed experimentally and would correspond to an essentially infinite cosmological constant throughout the entire universe including regions of no mass. As given by Waldrop [60], "What makes this problem into something more than metaphysics is that the cosmological constant is observationally zero to a very high degree of accuracy. And yet, ordinary quantum field theory predicts that it ought to be enormous, about 120 orders of magnitude larger than the best observational limit. Moreover, this prediction is almost inescapable because it is a straightforward application of the uncertainty principle, which in this case states that every quantum field contains a certain, irreducible amount of energy even in empty space. Electrons, photons, quarks—the quantum field of every particle contributes. And that energy is exactly equivalent to the kind of pressure described by the cosmological constant. The cosmological constant has accordingly been an embarrassment and a frustration to every physicist who has ever grappled with it."

Furthermore, a consequence of the Heisenberg Uncertainty principle and QED is that matter may be created from nothing, including vacuum. Taking quantum theory into account, Stephen Hawking [61-62] mathematically proved that blackholes must emit Hawking radiation comprising photons, neutrinos, and all sorts of massive particles. "The surface emits with equal probability all configurations of particles compatible with the observers limited knowledge. It is shown that the ignorance principle holds for quantum-mechanical evaporation of blackholes: The black hole creates particles in pairs, with one particle always falling into the hole and the other possibly escaping to infinity [62]." This QM theorem represents a perpetual motion machine with regard to spontaneous creation of mass and energy from the vacuum and with regard to gravitation. (QM also predicts a perpetual motion machine of the second kind [63-64]). Contrary to prediction, Hawking radiation has never been observed [65-67]. Classical laws including conservation of matter-energy are confirmed and QM is invalidated.

The Casimir effect is often touted as proof of that the vacuum is teeming with infinities of virtual particles. The experiment comprises a

feeble force between two plates with precision machined surfaces that are brought within microns of contacting each other. The QED explanation of the weak force that is observed between the two plates is that the plates serve to limit the number of virtual particle modes between the plates as opposed to those outside the plates and the resulting imbalance in pressure between two infinite quantities gives rise to the feeble force [68].

The Casimir effect is predicted by Maxwell's equations and is not due to virtual particles. There is no reality to electromagnetic field zero point fluctuations and the implication that the Casimir force is an intrinsic property of space. The attractive force is due only to the interactions of the material bodies themselves. Lifshitz [69-70] first developed the theory of the attractive force between two plane surfaces made of a material with a general susceptibility. The Lifshitz calculation is developed from considerations of charge and current fluctuations in a material body. These fluctuations serve as a source term for Maxwell's equations, i.e. classical fields, subject to the boundary conditions presented by the body surfaces. In the limiting case of rarefied media, the van der Waal force of interaction between individual atoms is obtained.

APPENDIX III

ANALYTICAL EQUATIONS TO GENERATE THE ORBITSphere CURRENT VECTOR FIELD AND THE UNIFORM CURRENT (CHARGE)- DENSITY FUNCTION $Y_0^0(\phi, \theta)$

STEP ONE BY THE ROTATION OF A GREAT CIRCLE ABOUT THE ($i_x, i_y, 0i_z$)-AXIS BY 2π

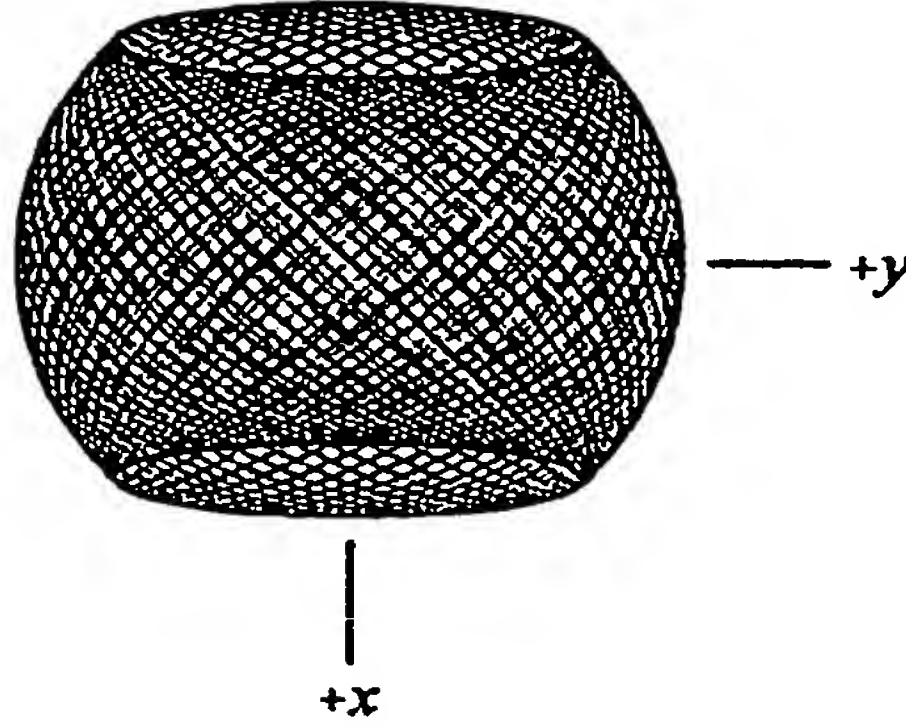
Great Circle in the yz-Plane about the ($i_x, i_y, 0i_z$)-Axis

Following the procedure given in Fowles [71], the orbitsphere-cvf component of STEP ONE is generated by the rotation of a great circle in the yz-plane about the ($i_x, i_y, 0i_z$)-axis by 2π . A first transformation matrix is generated by the combined rotation of a great circle in the yz-plane about the z-axis by $\frac{\pi}{4}$ then about the x-axis by θ where positive rotations about an axis are defined as clockwise:

$$\begin{bmatrix} x' \\ y' \\ z' \end{bmatrix} = \begin{bmatrix} \cos\left(\frac{\pi}{4}\right) & \sin\left(\frac{\pi}{4}\right) & 0 \\ -\sin\left(\frac{\pi}{4}\right)\cos\theta & \cos\left(\frac{\pi}{4}\right)\cos\theta & \sin\theta \\ \sin\left(\frac{\pi}{4}\right)\sin\theta & -\cos\left(\frac{\pi}{4}\right)\sin\theta & \cos\theta \end{bmatrix} \begin{bmatrix} 0 \\ r_n \cos\phi \\ r_n \sin\phi \end{bmatrix} \quad (1)$$

The transformation matrix about ($i_x, i_y, 0i_z$) is given by multiplication of the output of the matrix given by Eq. (1) by the matrix corresponding to a rotation about the z-axis of $-\frac{\pi}{4}$. The output of the matrix given by Eq. (1) is shown in Figure 1 wherein θ is varied from 0 to 2π .

Figure 1. The current pattern given by Eq. (1) shown with 6 degree increments of θ from the perspective of looking along the z-axis. The great circle current loop that served as a basis element that was initially in the yz-plane is shown as red.



The rotation matrix about the z-axis by $-\frac{\pi}{4}$, $zrot\left(-\frac{\pi}{4}\right)$, is given by

$$zrot\left(-\frac{\pi}{4}\right) = \begin{bmatrix} \cos\left(\frac{\pi}{4}\right) & -\sin\left(\frac{\pi}{4}\right) & 0 \\ \sin\left(\frac{\pi}{4}\right) & \cos\left(\frac{\pi}{4}\right) & 0 \\ 0 & 0 & 1 \end{bmatrix} \quad (2)$$

Thus,

$$\begin{bmatrix} x' \\ y' \\ z' \end{bmatrix} = zrot\left(-\frac{\pi}{4}\right) \cdot \begin{bmatrix} \cos\left(\frac{\pi}{4}\right) & \sin\left(\frac{\pi}{4}\right) & 0 \\ -\sin\left(\frac{\pi}{4}\right)\cos\theta & \cos\left(\frac{\pi}{4}\right)\cos\theta & \sin\theta \\ \sin\left(\frac{\pi}{4}\right)\sin\theta & -\cos\left(\frac{\pi}{4}\right)\sin\theta & \cos\theta \end{bmatrix} \begin{bmatrix} 0 \\ r_n \cos\phi \\ r_n \sin\phi \end{bmatrix} \quad (3)$$

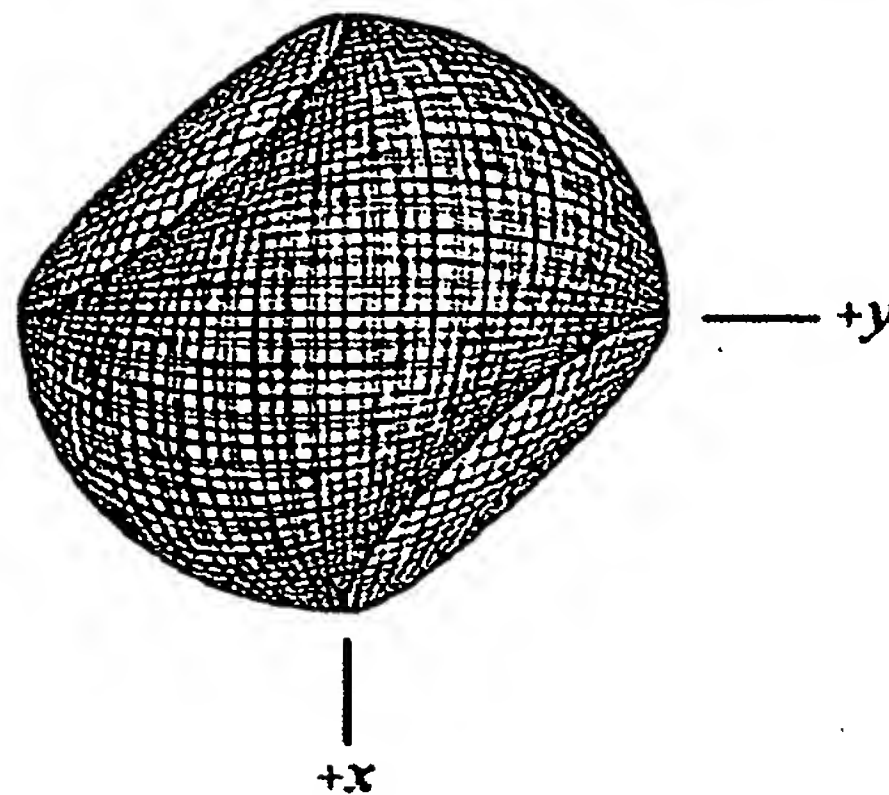
Substitution of the matrix given by Eq. (2) into Eq. (3) gives

$$\begin{bmatrix} x' \\ y' \\ z' \end{bmatrix} = \begin{bmatrix} \frac{1}{2} + \frac{\cos\theta}{2} & \frac{1}{2} - \frac{\cos\theta}{2} & -\frac{\sin\theta}{\sqrt{2}} \\ \frac{1}{2} - \frac{\cos\theta}{2} & \frac{1}{2} + \frac{\cos\theta}{2} & \frac{\sin\theta}{\sqrt{2}} \\ \frac{\sin\theta}{\sqrt{2}} & -\frac{\sin\theta}{\sqrt{2}} & \cos\theta \end{bmatrix} \begin{bmatrix} 0 \\ r_n \cos\phi \\ r_n \sin\phi \end{bmatrix} \quad (4)$$

$$\begin{bmatrix} x' \\ y' \\ z' \end{bmatrix} = \begin{bmatrix} \left(\frac{1}{2} - \frac{\cos \theta}{2}\right) r_n \cos \phi - \frac{\sin \theta}{\sqrt{2}} r_n \sin \phi \\ \left(\frac{1}{2} + \frac{\cos \theta}{2}\right) r_n \cos \phi + \frac{\sin \theta}{\sqrt{2}} r_n \sin \phi \\ -\frac{\sin \theta}{\sqrt{2}} r_n \cos \phi + \cos \theta r_n \sin \phi \end{bmatrix} \quad (5)$$

The orbitsphere-cvf component of STEP ONE that is generated by the rotation of a great circle in the yz -plane about the $(\mathbf{i}_x, \mathbf{i}_y, 0\mathbf{i}_z)$ -axis by 2π corresponding to the output of the matrix given by Eq. (5) is shown in Figure 2 wherein the sign of ϕ is positive for $0 \leq \theta \leq \pi$ and negative for $\pi < \theta \leq 2\pi$ in order to give the angular momentum projections given in the Orbitsphere Equation of Motion for $\ell = 0$ section.

Figure 2. The current pattern of the orbitsphere-cvf component of STEP ONE shown with 6 degree increments of θ from the perspective of looking along the z -axis. The yz -plane great circle current loop that served as a basis element that was initially in the yz -plane is shown as red.



Great Circle in the xz -Plane about the $(\mathbf{i}_x, \mathbf{i}_y, 0\mathbf{i}_z)$ -Axis

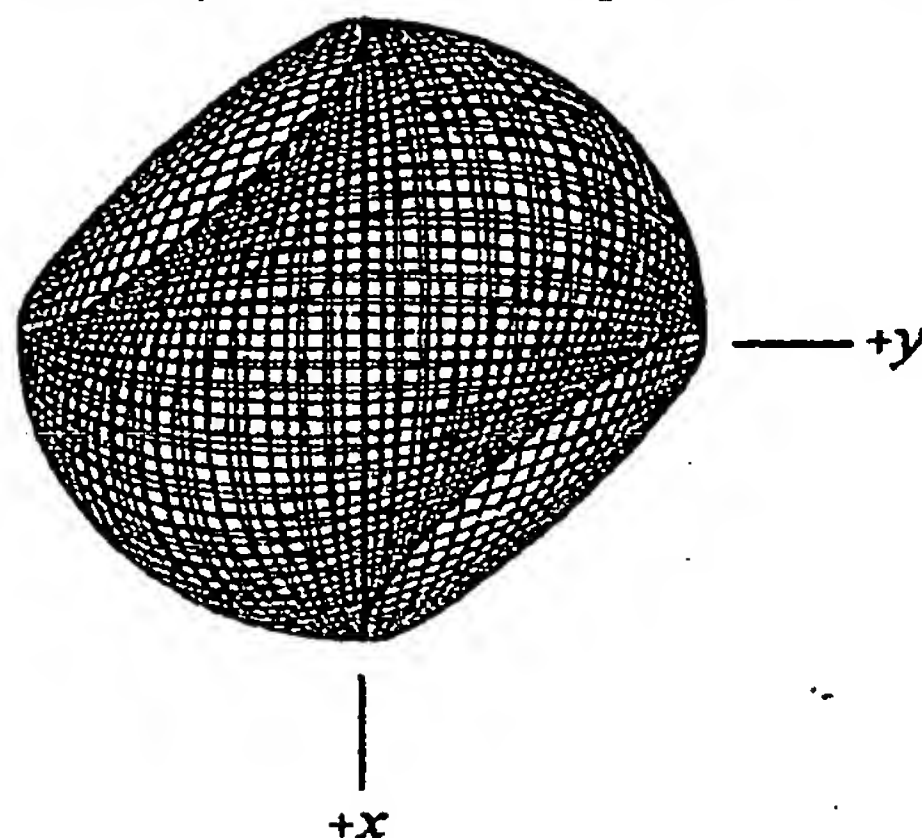
Alternatively, STEP ONE comprises the rotation of a great circle in the xz -plane about the $(\mathbf{i}_x, \mathbf{i}_y, 0\mathbf{i}_z)$ -axis by 2π . The coordinates of the great circle are given by the matrix:

$$\begin{bmatrix} x' \\ y' \\ z' \end{bmatrix} = \begin{bmatrix} r_n \cos \phi \\ 0 \\ r_n \sin \phi \end{bmatrix} \quad (6)$$

The matrix for the rotation about the $(\mathbf{i}_x, \mathbf{i}_y, 0\mathbf{i}_z)$ -axis is given by Eq. (4) wherein θ is varied from 0 to 2π and the sign of ϕ is positive for $0 \leq \theta \leq \pi$ and negative for $\pi < \theta \leq 2\pi$ in order to give the angular momentum projections given in the Orbitsphere Equation of Motion for $\ell = 0$ section.

The current pattern that is equivalent to that shown in Figure 2 is shown in Figure 3.

Figure 3. The current pattern of the orbitsphere-cvf component of STEP ONE shown with 6 degree increments of θ from the perspective of looking along the z-axis. The great circle current loop that served as a basis element that was initially in the xz-plane is shown as red.



It follows from the results shown in Figures 2 and 3 that the component orbitsphere-cvf for STEP ONE can further be generated by the rotation of the linear combination of the basis-element great circles in the yz- and xz-planes about the $(i_x, i_y, 0i_z)$ -axis by π using Eqs. (4) and (6) wherein θ is varied from 0 to π . It is a general feature for the generation of the components given in this Appendix that a linear combination of the orthogonal basis-element great circles can be used rather than a single element wherein the range of θ is varied from 0 to π rather than from 0 to 2π .

STEP TWO BY THE ROTATION OF A GREAT CIRCLE ABOUT THE $(-i_x, 0i_y, i_z)$ -AXIS BY 2π FOLLOWED BY A ROTATION ABOUT THE Z-AXIS BY $\frac{\pi}{4}$

Great Circle in the xy-Plane about the $(-i_x, 0i_y, i_z)$ -Axis by 2π Followed by a Rotation about the z-Axis by $\frac{\pi}{4}$

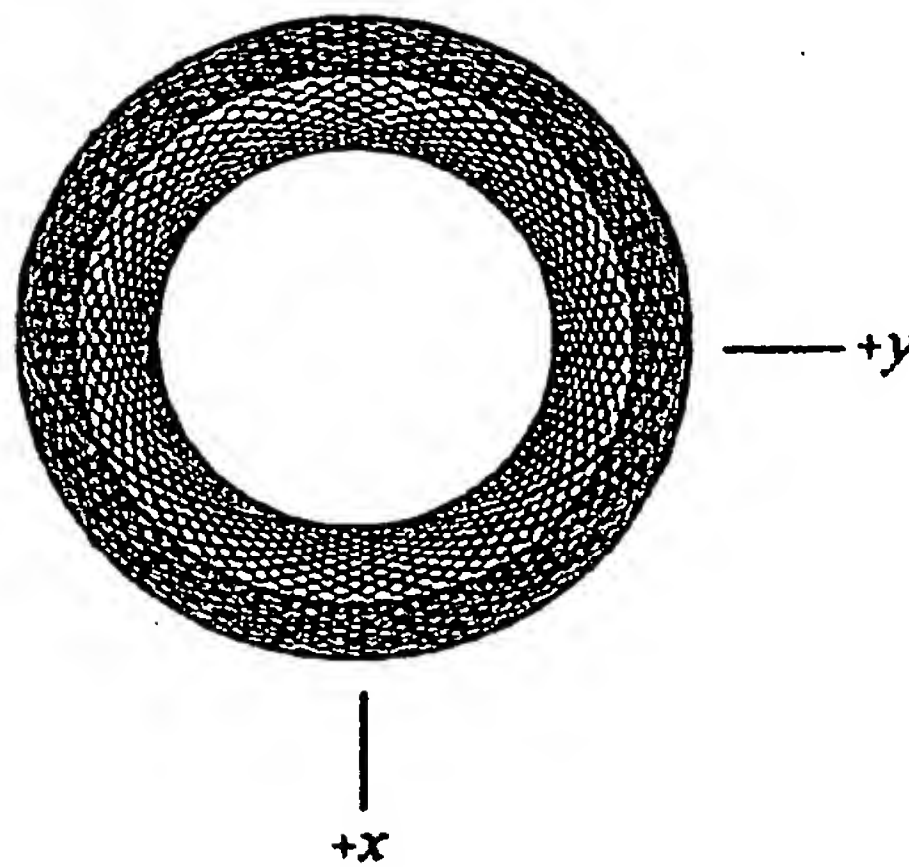
Following the procedure given in Fowles [71], the orbitsphere-cvf component of STEP TWO is generated by the rotation of a great circle in the xy-plane about the $(-i_x, 0i_y, i_z)$ -axis by 2π followed by a rotation about the z-axis by $\frac{\pi}{4}$. A first transformation matrix is generated by the

combined rotation of a great circle in the xy-plane about the y-axis by $-\frac{\pi}{4}$ then about the z-axis by θ :

$$\begin{bmatrix} x' \\ y' \\ z' \end{bmatrix} = \begin{bmatrix} \cos\left(\frac{\pi}{4}\right)\cos\theta & \sin\theta & \sin\left(\frac{\pi}{4}\right)\cos\theta \\ -\cos\left(\frac{\pi}{4}\right)\sin\theta & \cos\theta & -\sin\left(\frac{\pi}{4}\right)\sin\theta \\ -\sin\left(\frac{\pi}{4}\right) & 0 & \cos\left(\frac{\pi}{4}\right) \end{bmatrix} \begin{bmatrix} r_n \cos\phi \\ r_n \sin\phi \\ 0 \end{bmatrix} \quad (7)$$

The transformation matrix about $(-i_x, 0i_y, i_z)$ is given by multiplication of the output of the matrix given by Eq. (7) by the matrix corresponding to a rotation about the y-axis of $\frac{\pi}{4}$. The output of the matrix given by Eq. (7) is shown in Figure 4 wherein θ is varied from 0 to 2π .

Figure 4. The current pattern given by Eq. (7) shown with 6 degree increments of θ from the perspective of looking along the z-axis. The great circle current loop that served as a basis element that was initially in the xy-plane is shown as red.



The rotation matrix about the y-axis by $\frac{\pi}{4}$, $yrot\left(\frac{\pi}{4}\right)$, is given by

$$yrot\left(\frac{\pi}{4}\right) = \begin{bmatrix} \cos\left(\frac{\pi}{4}\right) & 0 & -\sin\left(\frac{\pi}{4}\right) \\ 0 & 1 & 0 \\ \sin\left(\frac{\pi}{4}\right) & 0 & \cos\left(\frac{\pi}{4}\right) \end{bmatrix} \quad (8)$$

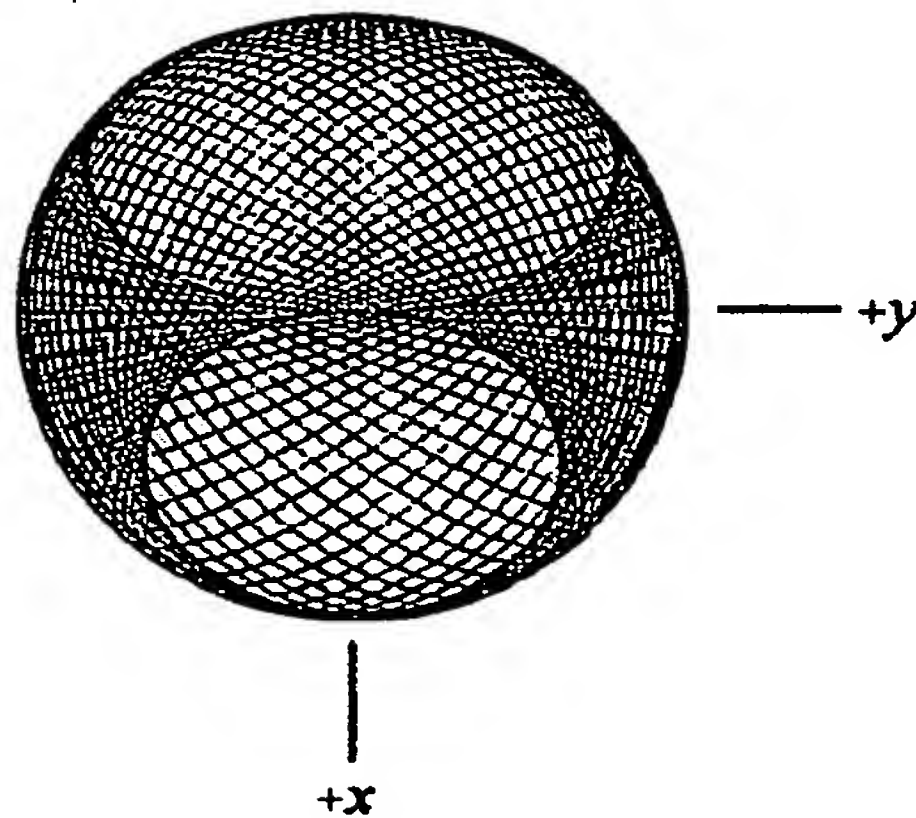
Thus,

$$\begin{bmatrix} x' \\ y' \\ z' \end{bmatrix} = yrot\left(\frac{\pi}{4}\right) \cdot \begin{bmatrix} \cos\left(\frac{\pi}{4}\right)\cos\theta & \sin\theta & \sin\left(\frac{\pi}{4}\right)\cos\theta \\ -\cos\left(\frac{\pi}{4}\right)\sin\theta & \cos\theta & -\sin\left(\frac{\pi}{4}\right)\sin\theta \\ -\sin\left(\frac{\pi}{4}\right) & 0 & \cos\left(\frac{\pi}{4}\right) \end{bmatrix} \begin{bmatrix} r_n \cos\phi \\ r_n \sin\phi \\ 0 \end{bmatrix} \quad (9)$$

Substitution of the matrix given by Eq. (8) into Eq. (9) gives the current pattern for the rotation of the xy-plane great circle about the $(-i_x, 0i_y, i_z)$ -axis as shown in Figure 5:

$$\begin{bmatrix} x' \\ y' \\ z' \end{bmatrix} = \begin{bmatrix} \frac{1}{2} + \frac{\cos\theta}{2} & \frac{\sin\theta}{\sqrt{2}} & -\frac{1}{2} + \frac{\cos\theta}{2} \\ -\frac{\sin\theta}{\sqrt{2}} & \cos\theta & -\frac{\sin\theta}{\sqrt{2}} \\ -\frac{1}{2} + \frac{\cos\theta}{2} & \frac{\sin\theta}{\sqrt{2}} & \frac{1}{2} + \frac{\cos\theta}{2} \end{bmatrix} \begin{bmatrix} r_n \cos\phi \\ r_n \sin\phi \\ 0 \end{bmatrix} \quad (10)$$

Figure 5. The current pattern for the rotation of the xy-plane great circle about the $(-i_x, 0i_y, i_z)$ -axis (Eq. (10)) shown with 6 degree increments of θ from the perspective of looking along the z-axis. The great circle current loop that served as a basis element that was initially in the xy-plane is shown as red.



STEP TWO is then given by a rotation of this result about z-axis by $\frac{\pi}{4}$ using $zrot\left(\frac{\pi}{4}\right)$ given by

$$zrot\left(\frac{\pi}{4}\right) = \begin{bmatrix} \cos\left(\frac{\pi}{4}\right) & \sin\left(\frac{\pi}{4}\right) & 0 \\ -\sin\left(\frac{\pi}{4}\right) & \cos\left(\frac{\pi}{4}\right) & 0 \\ 0 & 0 & 1 \end{bmatrix} \quad (11)$$

Thus, STEP TWO is given by

$$\begin{bmatrix} x' \\ y' \\ z' \end{bmatrix} = zrot\left(\frac{\pi}{4}\right) \cdot yrot\left(\frac{\pi}{4}\right) \cdot \begin{bmatrix} \cos\left(\frac{\pi}{4}\right)\cos\theta & \sin\theta & \sin\left(\frac{\pi}{4}\right)\cos\theta \\ -\cos\left(\frac{\pi}{4}\right)\sin\theta & \cos\theta & -\sin\left(\frac{\pi}{4}\right)\sin\theta \\ -\sin\left(\frac{\pi}{4}\right) & 0 & \cos\left(\frac{\pi}{4}\right) \end{bmatrix} \begin{bmatrix} r_n \cos\phi \\ r_n \sin\phi \\ 0 \end{bmatrix} \quad (12)$$

Substitution of the matrices given by Eqs. (8) and (11) into Eq. (12) gives

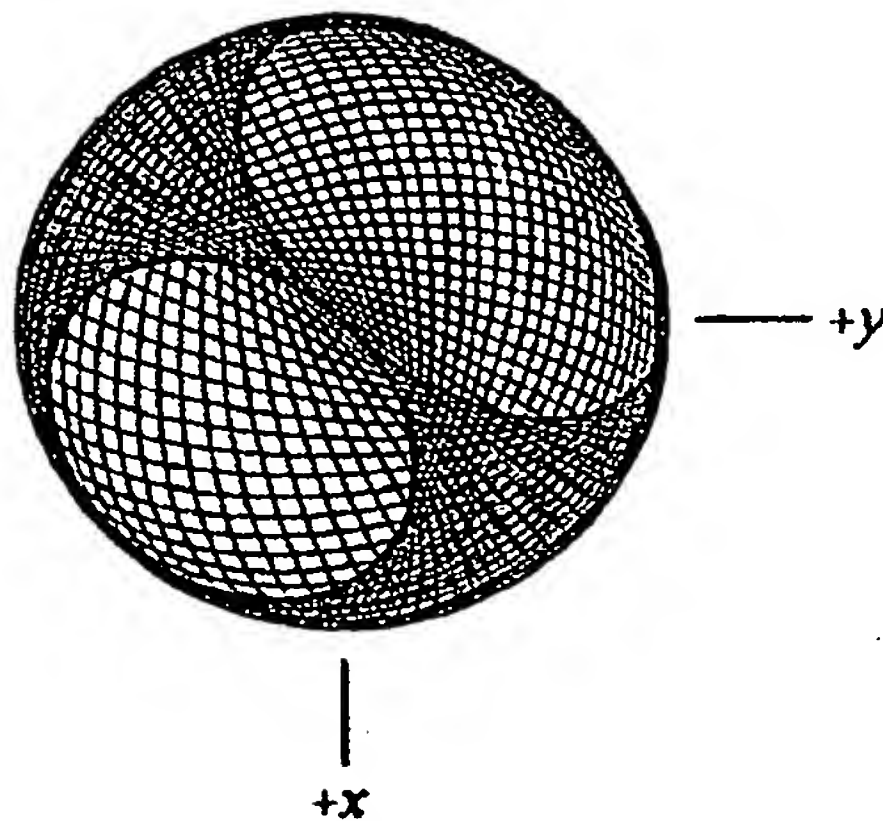
$$\begin{bmatrix} x' \\ y' \\ z' \end{bmatrix} = \begin{bmatrix} \frac{\frac{1}{2} + \frac{\cos\theta}{2}}{\sqrt{2}} - \frac{\sin\theta}{2} & \frac{\cos\theta}{\sqrt{2}} + \frac{\sin\theta}{2} & \frac{-\frac{1}{2} + \frac{\cos\theta}{2}}{\sqrt{2}} - \frac{\sin\theta}{2} \\ -\frac{\frac{1}{2} + \frac{\cos\theta}{2}}{\sqrt{2}} - \frac{\sin\theta}{2} & \frac{\cos\theta}{\sqrt{2}} - \frac{\sin\theta}{2} & -\frac{-\frac{1}{2} + \frac{\cos\theta}{2}}{\sqrt{2}} - \frac{\sin\theta}{2} \\ -\frac{1}{2} + \frac{\cos\theta}{2} & \frac{\sin\theta}{\sqrt{2}} & \frac{1}{2} + \frac{\cos\theta}{2} \end{bmatrix} \begin{bmatrix} r_n \cos\phi \\ r_n \sin\phi \\ 0 \end{bmatrix} \quad (13)$$

$$\begin{bmatrix} x' \\ y' \\ z' \end{bmatrix} = \begin{bmatrix} \left(\frac{\frac{1}{2} + \frac{\cos\theta}{2}}{\sqrt{2}} - \frac{\sin\theta}{2}\right)r_n \cos\phi + \left(\frac{\cos\theta}{\sqrt{2}} + \frac{\sin\theta}{2}\right)r_n \sin\phi \\ \left(-\frac{\frac{1}{2} + \frac{\cos\theta}{2}}{\sqrt{2}} - \frac{\sin\theta}{2}\right)r_n \cos\phi + \left(\frac{\cos\theta}{\sqrt{2}} - \frac{\sin\theta}{2}\right)r_n \sin\phi \\ \left(-\frac{1}{2} + \frac{\cos\theta}{2}\right)r_n \cos\phi + \frac{\sin\theta}{\sqrt{2}}r_n \sin\phi \end{bmatrix} \quad (14)$$

$$\begin{bmatrix} x' \\ y' \\ z' \end{bmatrix} = \begin{bmatrix} \frac{1}{4}r_n(\sqrt{2}\cos\phi + 2\sin\theta(-\cos\phi + \sin\phi) + \sqrt{2}\cos\theta(\cos\phi + 2\sin\phi)) \\ \frac{1}{4}r_n(-\sqrt{2}\cos\phi - \sqrt{2}\cos\theta(\cos\phi - 2\sin\phi) - 2\sin\theta(\cos\phi + \sin\phi)) \\ \frac{1}{2}r_n((-1 + \cos\theta)\cos\phi + \sqrt{2}\sin\theta\sin\phi) \end{bmatrix} \quad (15)$$

The orbitsphere-cvf component of STEP TWO that is generated by the rotation of a great circle in the xy-plane about the $(-i_x, 0i_y, i_z)$ -axis by 2π followed by a rotation about the z-axis by $\frac{\pi}{4}$ corresponding to the output of the matrix given by Eq. (15) is shown in Figure 6 wherein the sign of ϕ is positive for $0 \leq \theta \leq 2\pi$ in order to give the angular momentum projections given in the Orbitsphere Equation of Motion for $\ell = 0$ section.

Figure 6. The current pattern of the orbitsphere-cvf component of STEP TWO shown with 6 degree increments of θ from the perspective of looking along the z-axis. The great circle current loop that served as a basis element that was initially in the xy-plane is shown as red.



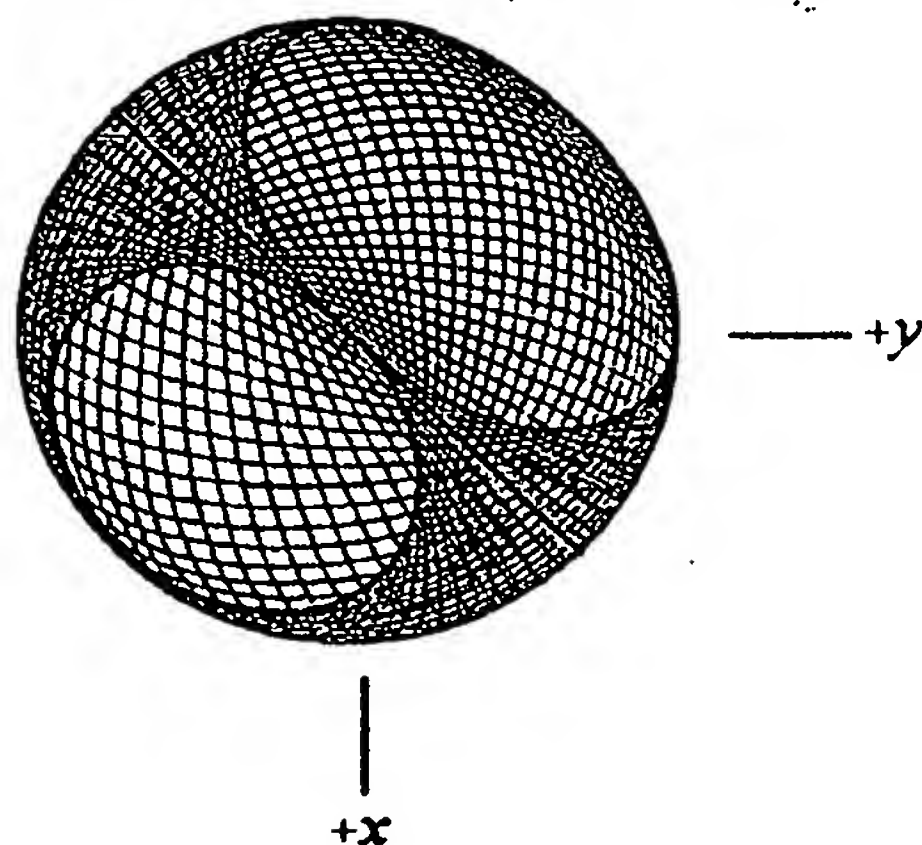
**Great Circle in the yz-Plane about the $(-i_x, 0i_y, i_z)$ -Axis by 2π
Followed by a Rotation about the z-Axis by $\frac{\pi}{4}$**

Alternatively, Step Two comprises the rotation of a great circle in the yz-plane about the $(-i_x, 0i_y, i_z)$ -axis by 2π followed by a rotation about the z-axis by $\frac{\pi}{4}$. The coordinates of the great circle are given by the matrix:

$$\begin{bmatrix} x' \\ y' \\ z' \end{bmatrix} = \begin{bmatrix} 0 \\ r_n \cos \phi \\ r_n \sin \phi \end{bmatrix} \quad (16)$$

The matrix for the rotation about the $(-i_x, 0i_y, i_z)$ -axis by 2π followed by a rotation about the z-axis by $\frac{\pi}{4}$ is given using Eq. (13) wherein θ is varied from 0 to 2π and the sign of ϕ is positive for $0 < \theta \leq 2\pi$ in order to give the angular momentum projections given in the Orbitsphere Equation of Motion for $\ell=0$ section. The current pattern that is equivalent to that shown in Figure 6 is shown in Figure 7.

Figure 7. The current pattern of the orbitsphere-cvf component of STEP TWO shown with 6 degree increments of θ from the perspective of looking along the z-axis. The great circle current loop that served as a basis element that was initially in the yz-plane is shown as red.



STEP TWO BY ROTATION OF A GREAT CIRCLE ABOUT THE $(-i_x, i_y, i_z)$ -AXIS BY 2π

The orbitsphere-cvf component of STEP TWO is also generated by the rotation of a great circle about the $(-i_x, i_y, i_z)$ -axis by 2π wherein the basis-element great circle bisects the xy-quadrant and is parallel to the z-axis. The coordinates of the great circle are given by the matrix that rotates a great circle in the yz-plane by $\frac{\pi}{4}$:

$$\begin{bmatrix} x' \\ y' \\ z' \end{bmatrix} = \begin{bmatrix} \cos\left(\frac{\pi}{4}\right) & \sin\left(\frac{\pi}{4}\right) & 0 \\ -\sin\left(\frac{\pi}{4}\right) & \cos\left(\frac{\pi}{4}\right) & 0 \\ 0 & 0 & 1 \end{bmatrix} \begin{bmatrix} 0 \\ r_n \cos \phi \\ r_n \sin \phi \end{bmatrix} \quad (17)$$

$$\begin{bmatrix} x' \\ y' \\ z' \end{bmatrix} = \begin{bmatrix} \sin\left(\frac{\pi}{4}\right) r_n \cos \phi \\ \cos\left(\frac{\pi}{4}\right) r_n \cos \phi \\ r_n \sin \phi \end{bmatrix} = \begin{bmatrix} \frac{r_n \cos \phi}{\sqrt{2}} \\ \frac{r_n \cos \phi}{\sqrt{2}} \\ r_n \sin \phi \end{bmatrix} \quad (18)$$

Since STEP TWO is given by the rotation of the yz-plane basis-element great circle (Eq. (16)) about the $(-i_x, 0i_y, i_z)$ -axis by 2π followed by a rotation about the z-axis by $\frac{\pi}{4}$ using Eq. (13), the equivalent result may be obtained by first rotating the great circle given by Eq. (18) about the z-axis by $-\frac{\pi}{4}$, $zrot\left(-\frac{\pi}{4}\right)$, then applying Eq. (13):

$$\begin{bmatrix} x' \\ y' \\ z' \end{bmatrix} = \begin{bmatrix} \frac{1 + \cos \theta}{2} - \frac{\sin \theta}{\sqrt{2}} & \frac{\cos \theta + \sin \theta}{\sqrt{2}} & -\frac{1 + \cos \theta}{2} - \frac{\sin \theta}{\sqrt{2}} \\ -\frac{1 + \cos \theta}{2} - \frac{\sin \theta}{\sqrt{2}} & \frac{\cos \theta - \sin \theta}{\sqrt{2}} & -\frac{1 + \cos \theta}{2} - \frac{\sin \theta}{\sqrt{2}} \\ -\frac{1 + \cos \theta}{2} & \frac{\sin \theta}{\sqrt{2}} & \frac{1 + \cos \theta}{2} \end{bmatrix} \cdot zrot\left(-\frac{\pi}{4}\right) \cdot \begin{bmatrix} \frac{r_n \cos \phi}{\sqrt{2}} \\ \frac{r_n \cos \phi}{\sqrt{2}} \\ r_n \sin \phi \end{bmatrix} \quad (19)$$

Using $zrot\left(-\frac{\pi}{4}\right)$ from Eq. (2) gives

$$\begin{bmatrix} x' \\ y' \\ z' \end{bmatrix} = \begin{bmatrix} \frac{1}{4}(1 + 3\cos \theta) & \frac{1}{4}(-1 + \cos \theta + 2\sqrt{2} \sin \theta) & \frac{1}{4}(-\sqrt{2} + \sqrt{2}\cos \theta - 2\sin \theta) \\ \frac{1}{4}(-1 + \cos \theta - 2\sqrt{2} \sin \theta) & \frac{1}{4}(1 + 3\cos \theta) & \frac{1}{4}(\sqrt{2} - \sqrt{2}\cos \theta - 2\sin \theta) \\ \frac{1}{2}\left(\frac{-1 + \cos \theta}{\sqrt{2}} + \sin \theta\right) & \frac{1}{4}(\sqrt{2} - \sqrt{2}\cos \theta + 2\sin \theta) & \cos^2 \frac{\theta}{2} \end{bmatrix} \begin{bmatrix} \frac{r_n \cos \phi}{\sqrt{2}} \\ \frac{r_n \cos \phi}{\sqrt{2}} \\ r_n \sin \phi \end{bmatrix} \quad (20)$$

$$\begin{bmatrix} x' \\ y' \\ z' \end{bmatrix} = \begin{bmatrix} \frac{(1+3\cos\theta)r_n \cos\phi}{4\sqrt{2}} + \frac{(-1+\cos\theta+2\sqrt{2}\sin\theta)r_n \cos\phi}{4\sqrt{2}} + \frac{1}{4}(-\sqrt{2}+\sqrt{2}\cos\theta-2\sin\theta)r_n \sin\phi \\ \frac{(1+3\cos\theta)r_n \cos\phi}{4\sqrt{2}} + \frac{(-1+\cos\theta-2\sqrt{2}\sin\theta)r_n \cos\phi}{4\sqrt{2}} + \frac{1}{4}(\sqrt{2}-\sqrt{2}\cos\theta-2\sin\theta)r_n \sin\phi \\ \frac{\left(\frac{-1+\cos\theta}{\sqrt{2}}+\sin\theta\right)r_n \cos\phi}{2\sqrt{2}} + \frac{(\sqrt{2}-\sqrt{2}\cos\theta+2\sin\theta)r_n \cos\phi}{4\sqrt{2}} + \cos^2\frac{\theta}{2}r_n \sin\phi \end{bmatrix} \quad (21)$$

$$\begin{bmatrix} x' \\ y' \\ z' \end{bmatrix} = \begin{bmatrix} \frac{1}{4}r_n(2\sin\theta(\cos\phi-\sin\phi)+\sqrt{2}(2\cos\theta\cos\phi+(-1+\cos\theta)\sin\phi)) \\ \frac{1}{4}r_n(-2\sin\theta(\cos\phi+\sin\phi)+\sqrt{2}(\cos\theta(2\cos\phi-\sin\phi)+\sin\phi)) \\ \frac{1}{2}r_n(\sqrt{2}\cos\phi\sin\theta+(1+\cos\theta)\sin\phi) \end{bmatrix} \quad (22)$$

where the sign of ϕ is positive for $0 < \theta \leq 2\pi$ in order to give the angular momentum projections given in the Orbitsphere Equation of Motion for $\ell = 0$ section. The current pattern of the orbitsphere-cvf component of STEP TWO that is generated by the rotation of a great circle in the xyz-plane about the $(-i_x, i_y, i_z)$ -axis by 2π corresponding to the output of the matrices given by Eqs. (20-22) is equivalent to that shown in Figures 6 and 7. In the $(-i_x, i_y, i_z)$ -rotational-axis case, the great circle current loop that serves as a basis element and initially and finally bisects the xy-quadrant and is parallel to the z-axis is shown as red in Figure 7.

The current pattern of the orbitsphere-cvf component of STEP TWO shown in Figure 6 is also generated by the rotation of a great circle in the xy-plane about the $(-i_x, i_y, i_z)$ -axis by 2π . Here, the great circle given by

$$\begin{bmatrix} x' \\ y' \\ z' \end{bmatrix} = \begin{bmatrix} r_n \cos\phi \\ r_n \sin\phi \\ 0 \end{bmatrix} \quad (23)$$

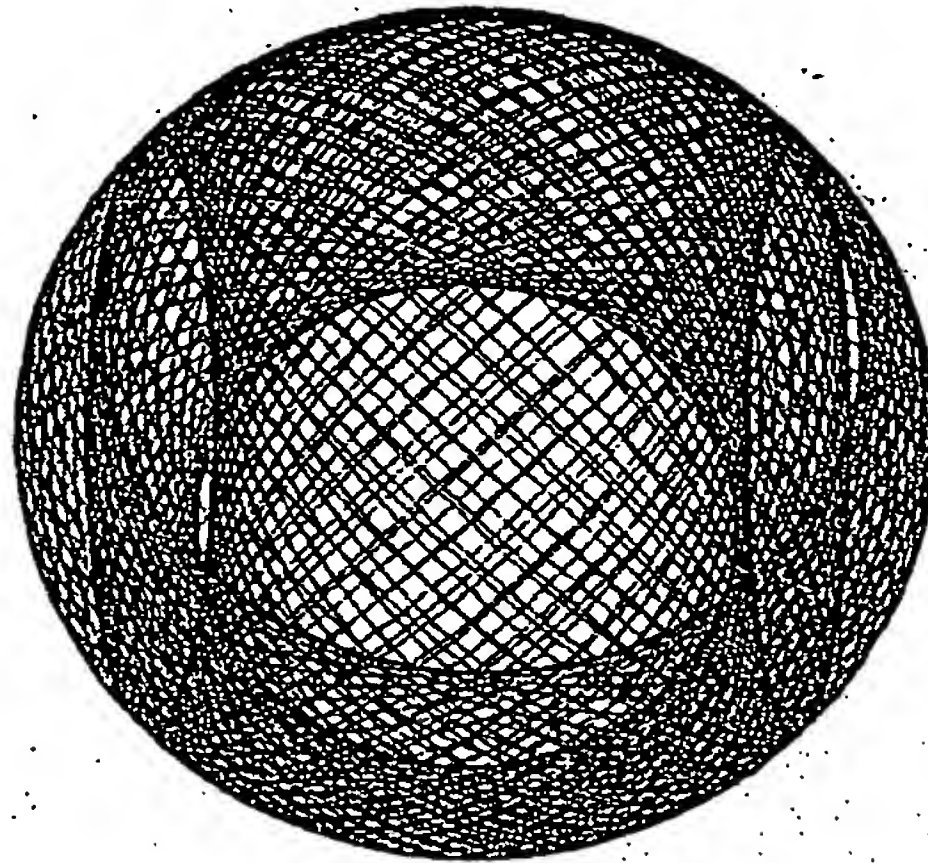
is input to transformational matrix given by Eq. (20), and the sign of ϕ is positive for $0 < \theta \leq 2\pi$ in order to give the angular momentum projections given in the Orbitsphere Equation of Motion for $\ell = 0$ section.

CHARACTERISTICS OF THE ORBITSPHERE-CVF

From Eqs. (1.73a) and (1.73b), angular momentum components of the orbitsphere-cvf are $L_x = \frac{\hbar}{4}$ and $L_z = \frac{\hbar}{2}$. The corresponding resultant

angular momentum vector, L_R , has magnitude $\frac{\sqrt{5}\hbar}{4}$ along the direction of the spherical-coordinate angles $\theta = 0.4636 \text{ rad}$, $\phi = \frac{3\pi}{4} \text{ rad}$. To obtain the view along L_R , the orbitsphere-cvf is first rotated counter clockwise about the vector $(i_x, i_y, 0i_z)$ by an angle -0.4636 rad using Eq. (4) or Eq. (1.70a) wherein $\Delta\alpha_x$ and $\Delta\alpha_y$ are each $-\sqrt{2}(0.4636) \text{ rad}$ to align L_R with the z-axis as shown in Figure 8.

Figure 8. The current pattern of the orbitsphere-cvf shown with 6 degree increments of the infinitesimal angular variables $\pm\Delta\alpha_x$ and $\pm\Delta\alpha_y$ from the perspective of looking along the z-axis onto which L_R , the resultant angular momentum vector of the L_{xy} and L_z components, was aligned.



The angular momentum is constant with respect to rotation of the orbitsphere-cvf about the axis of the resultant angular momentum vector, L_R . In this case, the corresponding component angular momentum L_{xy} is rotationally constant about the xy-axis, and the corresponding L_x and L_y components are rotationally constant about the x- and y-axes, respectively. The component L_z is further rotationally constant about the z-axis. The constancy of the angular momentum with respect to rotation of the orbitsphere-cvf about each of the principal axes determines that the corresponding rotational symmetry of each axis is C_∞ for the corresponding component even though the spatial symmetry of the current distribution is less. The angular-momentum axis of each component orbitsphere-cvf corresponding to either STEP ONE or STEP TWO is also a C_∞ -axis. Each component is comprised of great circles, and each great circle has a spatial and angular-momentum C_∞ -axis

perpendicular to the plane it defines. In addition, each component as well as the orbitsphere-cvf has the origin as a spatial inversion center (C_i) as shown in Figure 1.5A-F.

Each component orbitsphere-cvf has an infinite number of spatial C_2 -axes that lie in a symmetry plane (σ_v -plane) with a perpendicular spatial C_∞ -axis. Consider that the C_2 - and C_∞ -axes shown in Figure 9 are defined as the z-axis and the y-axis of the STEP-ONE component, respectively. The x-axis is perpendicular to the y- and z-axes. Then, the σ_v -plane is the xz-plane. The parameters of the width a from the center at the position of the σ_v -plane to the edge of the STEP-ONE component of the orbitsphere-cvf and the distance b from the edge to the apex of a circle defined by the orthogonal STEP-TWO component orbitsphere-cvf are shown in Figure 9. Also shown is the angle θ between the C_∞ -axis (y-axis) of the STEP-ONE component and the intersection of the edge of the two orthogonal component orbitsphere-cvfs. By symmetry, this is also the angle between the σ_v -plane and the edge. These parameters can be related to the radius r_n of the orbitsphere-cvf. From Figure 9, the relationship between the radius and the width is

$$a^2 + a^2 = r_n^2 \quad (24)$$

Thus, the width is

$$a = \frac{r_n}{\sqrt{2}} \quad (25)$$

Since

$$a + b = r_n \quad (26)$$

the distance from the edge of the STEP-ONE component to the to the apex at the STEP-TWO component using Eq. (25) is

$$b = r_n \left(1 - \frac{1}{\sqrt{2}} \right) \quad (27)$$

The angle θ is then

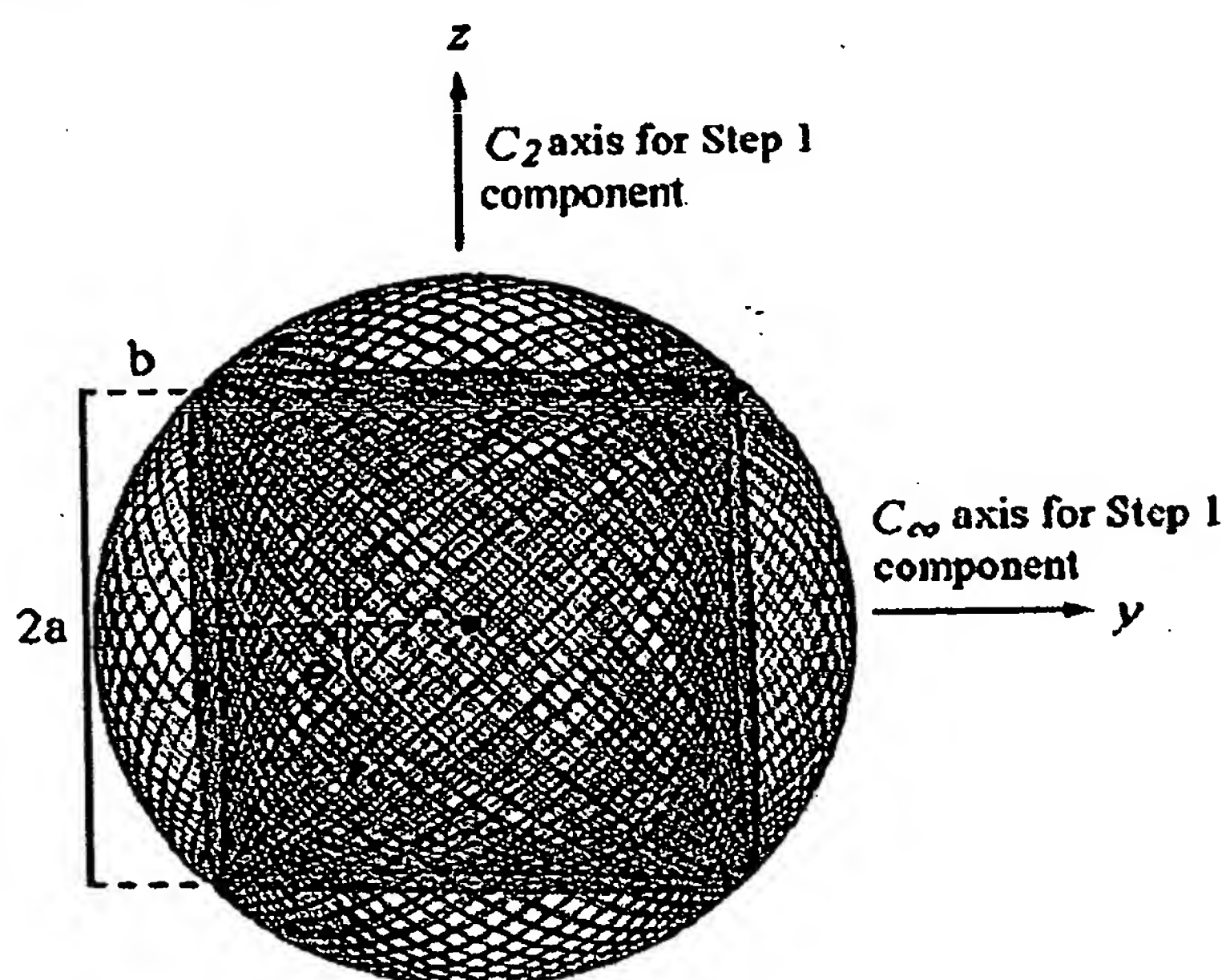
$$\theta = \cos^{-1} \frac{\frac{r_n}{\sqrt{2}}}{r_n} = \frac{\pi}{4} \quad (28)$$

As shown in Figure 9, the current density of the STEP-ONE component orbitsphere-cvf is constant along the C_2 -axis (z-axis) and increases from the origin to the edge along the C_∞ -axis. Since the current is on a sphere, the corresponding polar coordinates along this span are from $\phi = 0$ to $\phi = \frac{\pi}{4}$. It can be appreciated from Figure 2 that at $\phi = 0$, the great circles are initially at an angle of $\theta = \frac{\pi}{4}$ relative to the C_2 -axis as

defined in Figure 9 and are at an angle $\theta=0$ at $\phi=\frac{\pi}{4}$. Thus, the differential area per loop is given by the cosine of the angle $\phi+\frac{\pi}{4}$, and the density D is given by the inverse of the area function:

$$D = \sec\left(\phi + \frac{\pi}{4}\right) \quad (29)$$

Figure 9. Schematic of the relative dimensions of the component orbitsphere-cvfs (STEP-ONE component shown in blue and STEP-TWO component shown in red) that make-up the orbitsphere-cvf.



THE UNIFORM CURRENT (CHARGE)-DENSITY FUNCTION $Y_0^0(\phi, \theta)$

Boundary Constraints

The further constraint that the current density is uniform such that the charge density is uniform, corresponding to an equipotential, minimum energy surface is exactly satisfied by using the orbitsphere-cvf as a basis element to generate $Y_0^0(\phi, \theta)$. Utilizing the symmetry properties of each component of the orbitsphere-cvf corresponding to either STEP ONE or STEP TWO and the orthonormality of the trigonometric functions that generate the orbitsphere-cvf, a convolution operator comprising an autocorrelation-type function [72] gives rise to the spherically-symmetric current density, $Y_0^0(\phi, \theta)$. The operator comprises the convolution of each great circle current loop of the orbitsphere-cvf designated as the primary

orbitsphere-cvf with a second orbitsphere-cvf designated as the secondary orbitsphere-cvf. The angular momenta of the convolved elements are matched. The elements are also orientation matched by rotation of the secondary about the appropriate axis (axes), and the elements are phase matched using a rotation of each secondary orbitsphere-cvf element about its C_{∞} -axis. The convolution is over the angular span $\theta=0$ to $\theta=2\pi$ corresponding to the rotation of the basis-current loop which generated the primary orbitsphere-cvf. The angular momenta of the secondary elements project onto the resultant angular momentum axis, L_R -axis, of the primary orbitsphere-cvf equivalently to those of its great circles. The resulting exact uniform current distribution obtained from the convolution has the same angular momentum distribution, resultant, L_R , and components of $L_x = \frac{\hbar}{4}$ and $L_z = \frac{\hbar}{2}$ as those of the orbitsphere-cvf used as a primary basis element.

Properties of the Orbitsphere-cvf Permissive to Generate $Y_0^0(\phi, \theta)$

First, consider the symmetry properties of the each of the two orthogonal components the orbitsphere-cvf corresponding to STEP ONE and STEP TWO. As shown in the previous sections and the Orbitsphere Equation of Motion for $\ell=0$ section, a basis-element great circle is rotated by 2π to generate the same current pattern as that generated over the surface by a set of an infinite series of nested rotations of two orthogonal great circle current loops using Eqs. (1.70a-1.70b). The resulting component orbitsphere-cvf is always perpendicular to the 2π -axis of rotation used to generate the component from the great circle. This 2π -rotational axis defines a unique C_{∞} -axis which serves as a vector to characterize the angular momentum of the orbitsphere-cvf great circles. The resultant angular momentum of any given n th pair of great-circle elements defined by the rotational angle of the n th great circle at $\theta=\theta_n$ and its orthogonal partner at $\theta=\theta_n+\pi$ may be along the C_{∞} -axis or perpendicular to it depending on the current direction of the great circles for $0 \leq \theta \leq \pi$ and $\pi < \theta \leq 2\pi$. In the case that the angular momentum is perpendicular to the C_{∞} -axis, the angular momentum vector rotates about the C_{∞} -axis by π as a function of θ of Eq. (5) or as a function of θ of Eqs. (1.71a-1.71b) as shown in Figure 1.6. Also, shown in Figure 1.6 is an example of a stationary angular momentum vector that results when the angular momentum of each pair of great circles is along the C_{∞} -axis.

As a further example of a stationary orbitsphere-cvf angular momentum vector, consider the case of STEP ONE using the great circle current loops shown in Figure 1.4A as the basis elements. Each infinitesimal rotation of the infinite series of $\Delta\alpha$ is about the new i' -axis

and new j'-axis which results from the preceding such rotation wherein the angular sum of the rotations about each rotating i'-axis and j'-axis totals $\frac{\sqrt{2}}{2}\pi$ radians. When the $\Delta\alpha$ angles of Eq. (1.70a) have opposite signs, the resultant angular momentum vector of magnitude $\frac{\hbar}{2\sqrt{2}}$ shown in Figure 1.4A is stationary throughout the nested rotations that transform the axes as given in Table 1 during the generation of the component of the orbitsphere-cvf. The resulting component orbitsphere-cvf called STEP ONE \perp is orthogonal to that of STEP ONE given using $\Delta\alpha$ angles of the same sign as shown by comparing Figures 2 and 11.

Table 1. Summary of the results of the matrix transformations of two orthogonal current loops to generate a component orbitsphere-cvf with a stationary angular momentum vector.

Step	Initial Direction of Angular Momentum Components ($\hat{r} \times \hat{K}$) ^a	Final Direction of Angular Momentum Components ($\hat{r} \times \hat{K}$) ^a	Sign of $\Delta\alpha_i$	Sign of $\Delta\alpha_j$	Initial to Final Axis Transformation	L_x	L_y
1 \perp	$\hat{x}, -\hat{y}$	$\hat{x}, -\hat{y}$	$+\Delta\alpha_x$	$-\Delta\alpha_y$	$+x' \rightarrow -y$ $+y' \rightarrow -x$ $+z' \rightarrow -z$	$\frac{\hbar}{4}$	$-\frac{\hbar}{4}$

^a \mathbf{K} is the current density, \mathbf{r} is the polar vector of the great circle, and " \wedge " denotes the unit vectors $\hat{u} \equiv \frac{\mathbf{u}}{|\mathbf{u}|}$.

The nested rotations is also equivalent to rotating the orthogonal-great-circle basis set about the axis $(\mathbf{i}_x, -\mathbf{i}_y, 0\mathbf{i}_z)$ by an angle π or one of the great circles by 2π .

Component Orbitsphere-cvf Orthogonal to that of STEP ONE by the Rotation of a Great Circle about the $(\mathbf{i}_x, -\mathbf{i}_y, 0\mathbf{i}_z)$ -Axis by 2π

Great Circle in the yz-Plane about the $(\mathbf{i}_x, -\mathbf{i}_y, 0\mathbf{i}_z)$ -Axis

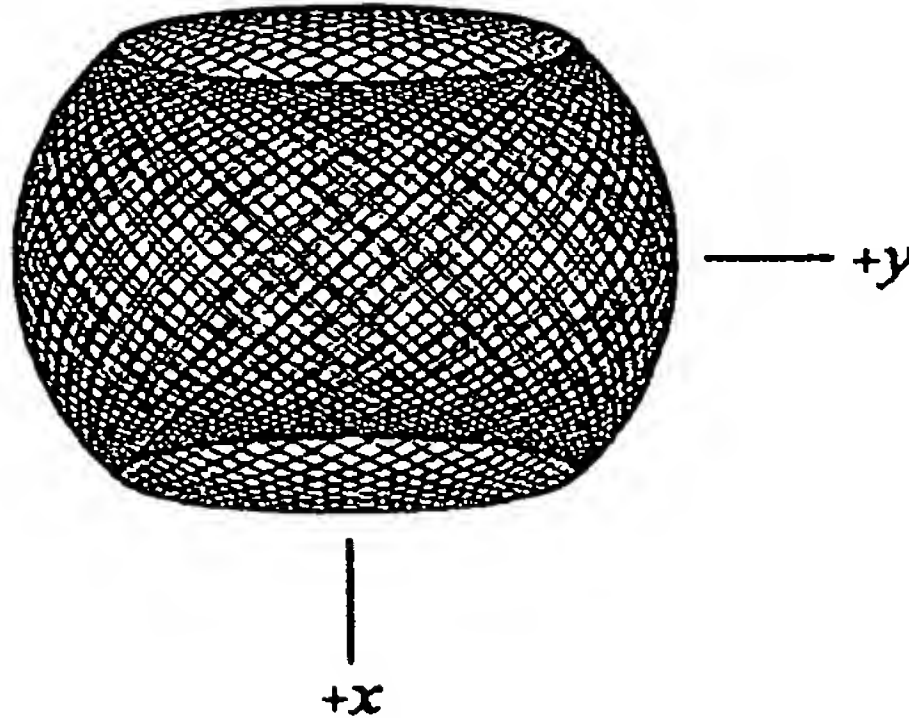
Following the procedure given in Fowles [71], the component orbitsphere-cvf that is orthogonal to that of STEP ONE (STEP ONE \perp) is generated by the rotation of a great circle in the yz-plane about the $(\mathbf{i}_x, -\mathbf{i}_y, 0\mathbf{i}_z)$ -axis by 2π . A first transformation matrix is generated by the

combined rotation of a great circle in the yz-plane about the z-axis by $-\frac{\pi}{4}$ then about the x-axis by θ where positive rotations about an axis are defined as clockwise:

$$\begin{bmatrix} x' \\ y' \\ z' \end{bmatrix} = \begin{bmatrix} \cos\left(\frac{\pi}{4}\right) & -\sin\left(\frac{\pi}{4}\right) & 0 \\ \sin\left(\frac{\pi}{4}\right)\cos\theta & \cos\left(\frac{\pi}{4}\right)\cos\theta & \sin\theta \\ -\sin\left(\frac{\pi}{4}\right)\sin\theta & -\cos\left(\frac{\pi}{4}\right)\sin\theta & \cos\theta \end{bmatrix} \begin{bmatrix} 0 \\ r_n \cos\phi \\ r_n \sin\phi \end{bmatrix} \quad (30)$$

The transformation matrix about $(\mathbf{i}_x, -\mathbf{i}_y, 0\mathbf{i}_z)$ is given by multiplication of the output of the matrix given by Eq. (30) by the matrix corresponding to a rotation about the z-axis of $\frac{\pi}{4}$. The output of the matrix given by Eq. (30) is shown in Figure 10 wherein θ is varied from 0 to 2π .

Figure 10. The current pattern given by Eq. (30) shown with 6 degree increments of θ from the perspective of looking along the z-axis. The great circle current loop that served as a basis element that was initially in the yz-plane is shown as red.



The rotation matrix about the z-axis by $\frac{\pi}{4}$, $zrot\left(\frac{\pi}{4}\right)$, is given by Eq. (11).

Thus,

$$\begin{bmatrix} x' \\ y' \\ z' \end{bmatrix} = zrot\left(\frac{\pi}{4}\right) \cdot \begin{bmatrix} \cos\left(\frac{\pi}{4}\right) & -\sin\left(\frac{\pi}{4}\right) & 0 \\ \sin\left(\frac{\pi}{4}\right)\cos\theta & \cos\left(\frac{\pi}{4}\right)\cos\theta & \sin\theta \\ -\sin\left(\frac{\pi}{4}\right)\sin\theta & -\cos\left(\frac{\pi}{4}\right)\sin\theta & \cos\theta \end{bmatrix} \begin{bmatrix} 0 \\ r_n \cos\phi \\ r_n \sin\phi \end{bmatrix} \quad (31)$$

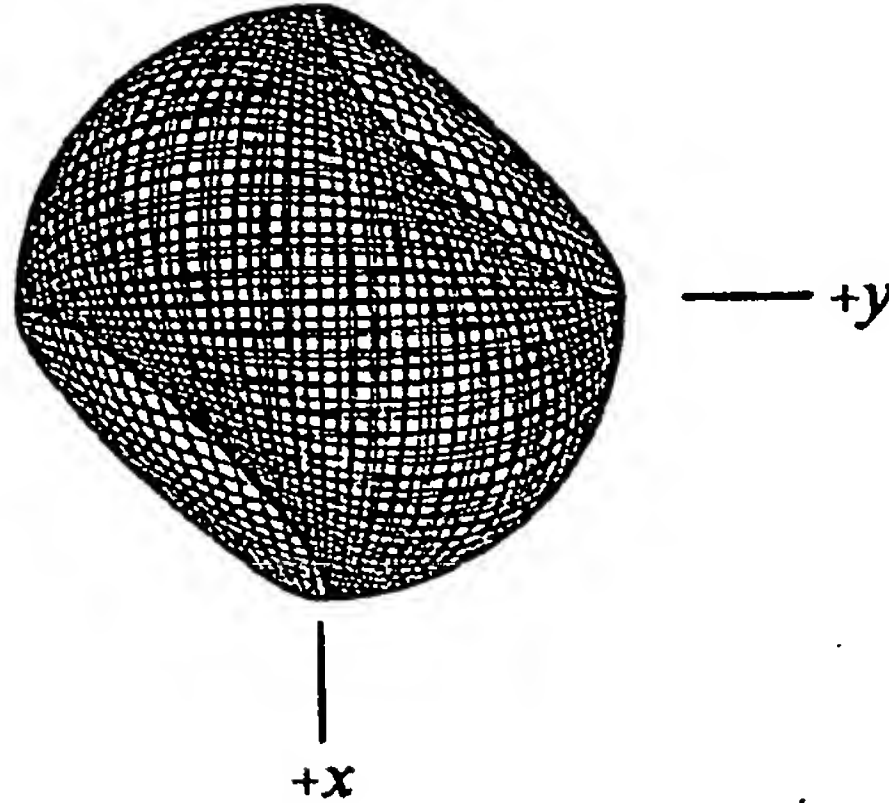
Substitution of the matrix given by Eq. (11) into Eq. (31) gives

$$\begin{bmatrix} x' \\ y' \\ z' \end{bmatrix} = \begin{bmatrix} \frac{1}{2} + \frac{\cos\theta}{2} & -\frac{1}{2} + \frac{\cos\theta}{2} & \frac{\sin\theta}{\sqrt{2}} \\ -\frac{1}{2} + \frac{\cos\theta}{2} & \frac{1}{2} + \frac{\cos\theta}{2} & \frac{\sin\theta}{\sqrt{2}} \\ -\frac{\sin\theta}{\sqrt{2}} & -\frac{\sin\theta}{\sqrt{2}} & \cos\theta \end{bmatrix} \begin{bmatrix} 0 \\ r_n \cos\phi \\ r_n \sin\phi \end{bmatrix} \quad (32)$$

$$\begin{bmatrix} x' \\ y' \\ z' \end{bmatrix} = \begin{bmatrix} \left(-\frac{1}{2} + \frac{\cos\theta}{2}\right)r_n \cos\phi + \frac{\sin\theta}{\sqrt{2}}r_n \sin\phi \\ \left(\frac{1}{2} + \frac{\cos\theta}{2}\right)r_n \cos\phi + \frac{\sin\theta}{\sqrt{2}}r_n \sin\phi \\ -\frac{\sin\theta}{\sqrt{2}}r_n \cos\phi + \cos\theta r_n \sin\phi \end{bmatrix} \quad (33)$$

The component orbitsphere-cvf that is orthogonal to that of STEP ONE that is generated by the rotation of a great circle in the yz-plane about the $(\mathbf{i}_x, -\mathbf{i}_y, 0\mathbf{i}_z)$ -axis by 2π corresponding to the output of the matrix given by Eq. (33) is shown in Figure 11 wherein the sign of ϕ is positive for $0 \leq \theta \leq \pi$ and negative for $\pi < \theta \leq 2\pi$ in order to give the currents directions shown in Figure 1.4A. The angular momentum vector is stationary along the $(\mathbf{i}_x, -\mathbf{i}_y, 0\mathbf{i}_z)$ -axis as shown in Figure 1.4A of the Orbitsphere Equation of Motion for $\ell = 0$ section. The same result is given by the rotation of a great circle in the xz-plane about the $(\mathbf{i}_x, -\mathbf{i}_y, 0\mathbf{i}_z)$ -axis by 2π using Eqs. (6) and (32).

Figure 11. The current pattern of the orbitsphere-cvf component given by Eq. (33) that is orthogonal to that of STEP ONE shown with 6 degree increments of θ from the perspective of looking along the z-axis. The yz-plane great circle current loop that served as a basis element that was initially in the yz-plane is shown as red.



Matching Phase, Angular Momentum, and Orientation

For STEP ONE \perp , the resultant angular momentum vector, \mathbf{L}_R , is along $(\mathbf{i}_x, -\mathbf{i}_y, 0\mathbf{i}_z)$. The angular momentum is constant for any rotation about the axis; thus, it is a C_∞ -axis relative to the angular momentum. However, rotation about this axis does change the phase (coordinate position relative to the starting position) of the component orbitsphere-cvf. For example, a rotation by π about the $(\mathbf{i}_x, -\mathbf{i}_y, 0\mathbf{i}_z)$ -axis using Eq. (32) causes the basis-element great circle to rotate by $\frac{\pi}{2}$ about the z-axis as shown in Figure 12. The rotation matrix about the $(\mathbf{i}_x, -\mathbf{i}_y, 0\mathbf{i}_z)$ -axis by π , $(\mathbf{i}_x, -\mathbf{i}_y, 0\mathbf{i}_z)\text{rot}(\pi)$, is given by

$$(\mathbf{i}_x, -\mathbf{i}_y, 0\mathbf{i}_z)\text{rot}(\pi) = \begin{bmatrix} \frac{1}{2} + \frac{\cos\pi}{2} & -\frac{1}{2} + \frac{\cos\pi}{2} & \frac{\sin\pi}{\sqrt{2}} \\ -\frac{1}{2} + \frac{\cos\pi}{2} & \frac{1}{2} + \frac{\cos\pi}{2} & \frac{\sin\pi}{\sqrt{2}} \\ -\frac{\sin\pi}{\sqrt{2}} & -\frac{\sin\pi}{\sqrt{2}} & \cos\pi \end{bmatrix} = \begin{bmatrix} 0 & -1 & 0 \\ -1 & 0 & 0 \\ 0 & 0 & -1 \end{bmatrix} \quad (34)$$

Thus,

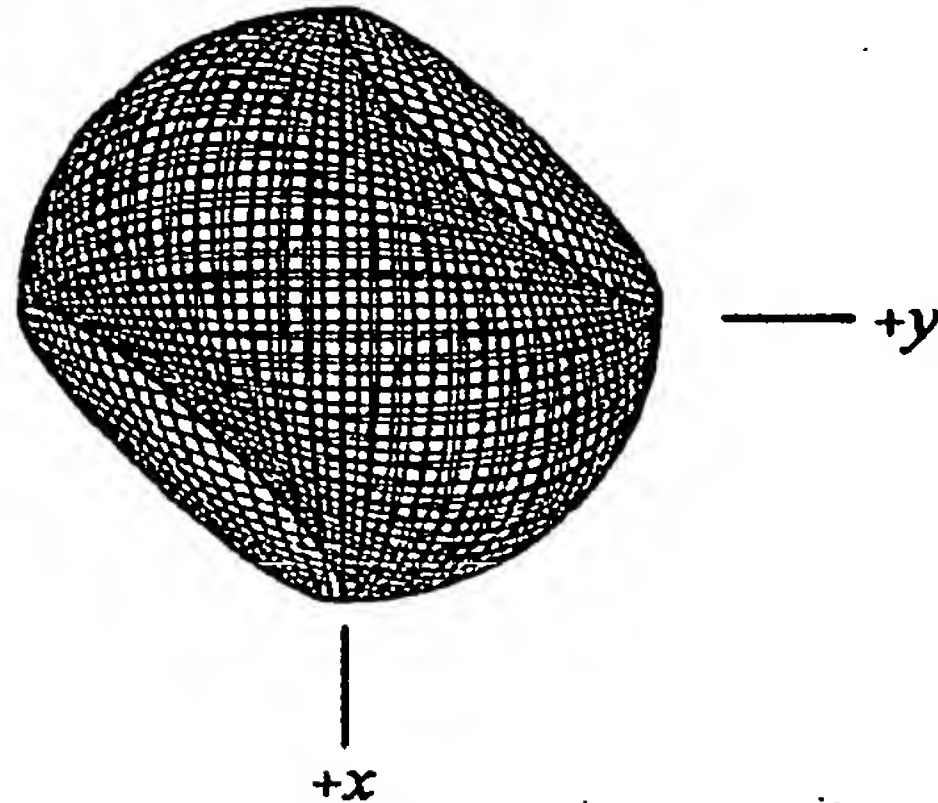
$$\begin{bmatrix} x' \\ y' \\ z' \end{bmatrix} = (\mathbf{i}_x, -\mathbf{i}_y, 0\mathbf{i}_z) \text{rot}(\pi) \cdot \begin{bmatrix} \frac{1}{2} + \frac{\cos\theta}{2} & -\frac{1}{2} + \frac{\cos\theta}{2} & \frac{\sin\theta}{\sqrt{2}} \\ -\frac{1}{2} + \frac{\cos\theta}{2} & \frac{1}{2} + \frac{\cos\theta}{2} & \frac{\sin\theta}{\sqrt{2}} \\ -\frac{\sin\theta}{\sqrt{2}} & -\frac{\sin\theta}{\sqrt{2}} & \cos\theta \end{bmatrix} \begin{bmatrix} 0 \\ r_n \cos\phi \\ r_n \sin\phi \end{bmatrix} \quad (35)$$

Substitution of the matrix given by Eq. (34) into Eq. (35) gives the current pattern for the $\frac{\pi}{2}$ phase shift relative to the z-axis corresponding to a rotation of the component orbitsphere-cvf given by Eq. (32) about the $(\mathbf{i}_x, -\mathbf{i}_y, 0\mathbf{i}_z)$ -axis by π as shown in Figure 12:

$$\begin{bmatrix} x' \\ y' \\ z' \end{bmatrix} = \begin{bmatrix} \sin^2 \frac{\theta}{2} & -\cos^2 \frac{\theta}{2} & -\frac{\sin\theta}{\sqrt{2}} \\ -\cos^2 \frac{\theta}{2} & \sin^2 \frac{\theta}{2} & -\frac{\sin\theta}{\sqrt{2}} \\ \frac{\sin\theta}{\sqrt{2}} & \frac{\sin\theta}{\sqrt{2}} & -\cos\theta \end{bmatrix} \begin{bmatrix} 0 \\ r_n \cos\phi \\ r_n \sin\phi \end{bmatrix} \quad (36)$$

$$\begin{bmatrix} x' \\ y' \\ z' \end{bmatrix} = \begin{bmatrix} -\cos^2 \frac{\theta}{2} r_n \cos\phi - \frac{\sin\theta}{\sqrt{2}} r_n \sin\phi \\ \sin^2 \frac{\theta}{2} r_n \cos\phi - \frac{\sin\theta}{\sqrt{2}} r_n \sin\phi \\ \frac{\sin\theta}{\sqrt{2}} r_n \cos\phi - \cos\theta r_n \sin\phi \end{bmatrix} \quad (37)$$

Figure 12. The current pattern given by Eq. (37) shown with 6 degree increments of θ from the perspective of looking along the z-axis obtained from Eq. (32) by rotation about the $(i_x, -i_y, 0i_z)$ -axis by π using Eq. (34). The great circle current loop that served as a basis element that was initially in the yz-plane is shown as red.



In general, for the stationary-angular-momentum-vector case, the angular momentum vector along the C_∞ -axis is always at an angle of $\frac{\pi}{4}$ relative to the plane of the basis-element great circle that generated the component orbitsphere-cvf. Thus, the plane of the great circle relative to the xyz coordinate system can be rotated over a span of $\pm\frac{\pi}{4}$ by rotation about L_R . The rotation of the basis-element great circle corresponds to changing the phase of the component orbitsphere-cvf in Eq. (38). The phase of the secondary component orbitsphere-cvf can be matched to that of the basis-element great circle of a primary component orbitsphere-cvf by rotation about L_R . Furthermore, each component orbitsphere-cvf is comprised of great circles, and each great circle has a C_∞ -axis perpendicular to the plane. This feature further permits the phase within the great circles of the secondary component orbitsphere-cvf to be matched to that of the basis element great circle of the primary.

Since the angular momentum vector is stationary and is a C_∞ -axis, the secondary component orbitsphere-cvf can be made to match the angular momentum of the basis-element great circle of any primary component orbitsphere-cvf by rotations that align the vector of the former with that of the latter. In addition to phase and angular momentum, the orientation of the secondary component orbitsphere-cvf is matched to that of the great circles elements of the primary, by rotation about the appropriate axis that aligns the angular momenta and orientation of the secondary component orbitsphere-cvf with the basis-element great circle of the primary. Thus, the secondary component

orbitsphere-cvf serves as a basis element in a convolution operator as shown in the Convolution Operator section.

CONVOLUTION OPERATOR

The orbitsphere-cvf comprises two components corresponding to each of STEP ONE and STEP TWO. In the case that the resultant angular momentum of each pair of orthogonal great circle current loops of the component orbitsphere-cvf is along the 2π -rotational axis, a secondary n th component orbitsphere-cvf can serve as a basis element to match the angular momentum of any given n th great circle of a primary component orbitsphere-cvf. The replacement of each great circle of the primary orbitsphere-cvf with a secondary orbitsphere-cvf of matching angular momentum, orientation, and phase comprises an autocorrelation-type function [72] that exactly gives rise to the spherically-symmetric current density, $Y_0^0(\phi, \theta)$.

The orbitsphere-cvf comprises the superposition or sum of the components corresponding to STEPS ONE and STEP TWO. Thus, the convolution is performed on each component. The convolution of a secondary component orbitsphere-cvf element with the each great circle current loop of a primary orbitsphere-cvf comprising two components is designated as the convolution operator, $A(\phi, \theta)$, given by

$$A(\phi, \theta) = \frac{1}{r_n^2} \lim_{\theta_2 \rightarrow 0} \sum_{m=1}^{2\pi} \lim_{\theta_1 \rightarrow 0} \sum_{m=1}^{2\pi} O(r_n, \phi, \theta) \otimes \left(\begin{array}{l} \delta(GC_{STEPONE}(\phi, \theta - \phi', \theta_1)) \\ + \delta(GC_{STEPTWO}(\phi, \theta - \phi', \theta_2)) \end{array} \right) \quad (38)$$

wherein the secondary component orbitsphere-cvf is defined by the symbol $O(r_n, \phi, \theta)$ -cvf) and each rotated great circle of each component orbitsphere-cvf of STEP M is defined by the symbol $GC_{STEPM}(\phi', \theta_M)$. In Eq. (38), the angular momentum of each secondary component orbitsphere-cvf is equal in magnitude and direction as that of the current loop with which it is convolved. Furthermore, the orientations and phases of the convolved elements are matched by rotating the secondary component orbitsphere-cvf about the appropriate principle axis (axes) and about the C_∞ -axis along its angular momentum vector, respectively. With the magnitude of the angular momentum of the secondary component orbitsphere-cvf matching that of the current loop which it replaces during the convolution and the loop then serving as a unit vector, the angular momentum resulting from the convolution operation is inherently normalized to that of the primary component orbitsphere-cvf.

The convolution of a sum is the sum of the convolutions. Thus, the convolution operation may be performed on each of STEP ONE and STEP TWO separately, and the result may be superposed in terms of the current densities and angular momenta.

$$A(\phi, \theta) = \frac{1}{r_n^2} \left(\lim_{\theta_1 \rightarrow 0} \sum_{m=1}^{\frac{2\pi}{|\Delta\theta_1|}} O(r_n, \phi, \theta) \otimes \delta(\phi, \theta - GC_{STEPONE}(\phi', \theta_1)) \right. \\ \left. + \lim_{\theta_2 \rightarrow 0} \sum_{m'=1}^{\frac{2\pi}{|\Delta\theta_2|}} O(r_n, \phi, \theta) \otimes \delta(\phi, \theta - GC_{STEPTWO}(\phi'', \theta_2)) \right) \quad (39)$$

Factoring out the secondary component orbitsphere-cvf gives

$$A(\phi, \theta) = \frac{1}{r_n^2} O(r_n, \phi, \theta) - cvf \left(\lim_{\theta_1 \rightarrow 0} \sum_{m=1}^{\frac{2\pi}{|\Delta\theta_1|}} GC_{STEPONE}(\phi', \theta_1) + \lim_{\theta_2 \rightarrow 0} \sum_{m'=1}^{\frac{2\pi}{|\Delta\theta_2|}} GC_{STEPTWO}(\phi'', \theta_2) \right) \quad (40)$$

The summation is the operator that generates the component orbitsphere-cvf of STEP M, $O_M(r_n, \phi, \theta) - cvf$. Thus, the current-density function is given by the primary orbitsphere-cvf squared comprised of two superimposed components.

$$A(\phi, \theta) = \frac{1}{r_n^2} (O_1^2 - cvf(r_n, \phi, \theta) + O_2^2 - cvf(r_n, \phi, \theta)) \quad (41)$$

COMPONENT ORBITSPIHERE-CVF SQUARED FOR STEP ONE USING THE ROTATION OF A GREAT CIRCLE ABOUT THE $(i_x, i_y, 0i_z)$ -AXIS BY 2π

From Eq. (5), the equation for the component orbitsphere-cvf squared for STEP ONE is given by

$$x^2 + y^2 + z^2 = \left[\left(\left(\frac{1}{2} - \frac{\cos\theta}{2} \right) r_n \cos\phi - \frac{\sin\theta}{\sqrt{2}} r_n \sin\phi \right)^2 \right. \\ \left(\left(\frac{1}{2} + \frac{\cos\theta}{2} \right) r_n \cos\phi + \frac{\sin\theta}{\sqrt{2}} r_n \sin\phi \right)^2 \\ \left. \left(-\frac{\sin\theta}{\sqrt{2}} r_n \cos\phi + \cos\theta r_n \sin\phi \right)^2 \right] \quad (42)$$

Multiplying out the squared terms gives

$$x^2 + y^2 + z^2 = \left[\begin{aligned} &\left(\frac{1}{2} - \frac{\cos\theta}{2}\right)^2 r_n^2 \cos^2 \phi + \frac{\sin^2 \theta}{2} r_n^2 \sin^2 \phi \\ &-2\left(\frac{1}{2} - \frac{\cos\theta}{2}\right) r_n \cos \phi \frac{\sin \theta}{\sqrt{2}} r_n \sin \phi \\ &+\left(\frac{1}{2} + \frac{\cos\theta}{2}\right)^2 r_n^2 \cos^2 \phi + \frac{\sin^2 \theta}{2} r_n^2 \sin^2 \phi \\ &+2\left(\frac{1}{2} + \frac{\cos\theta}{2}\right) r_n \cos \phi \frac{\sin \theta}{\sqrt{2}} r_n \sin \phi \\ &+\frac{\sin^2 \theta}{2} r_n^2 \cos^2 \phi + \cos^2 \theta r_n^2 \sin^2 \phi \\ &-2\frac{\sin \theta}{\sqrt{2}} r_n \cos \phi \cos \theta r_n \sin \phi \end{aligned} \right] \quad (43)$$

Further multiplying out the squared terms gives

$$x^2 + y^2 + z^2 = r_n^2 \left[\begin{aligned} &\left(\frac{1}{4} - \frac{\cos\theta}{2} + \frac{\cos^2 \theta}{4}\right) \cos^2 \phi + \frac{\sin^2 \theta}{2} \sin^2 \phi \\ &-2\left(\frac{1}{2} - \frac{\cos\theta}{2}\right) \cos \phi \frac{\sin \theta}{\sqrt{2}} \sin \phi \\ &+\left(\frac{1}{4} + \frac{\cos\theta}{2} + \frac{\cos^2 \theta}{4}\right) \cos^2 \phi + \frac{\sin^2 \theta}{2} \sin^2 \phi \\ &+2\left(\frac{1}{2} + \frac{\cos\theta}{2}\right) \cos \phi \frac{\sin \theta}{\sqrt{2}} \sin \phi \\ &+\frac{\sin^2 \theta}{2} \cos^2 \phi + \cos^2 \theta \sin^2 \phi \\ &-2\frac{\sin \theta}{\sqrt{2}} \cos \phi \cos \theta \sin \phi \end{aligned} \right] \quad (44)$$

Combining terms gives

$$x^2 + y^2 + z^2 = r_n^2 \left[\begin{aligned} &\left(\frac{1}{2} + \frac{\cos^2 \theta}{2} + \frac{\sin^2 \theta}{2}\right) \cos^2 \phi \\ &+(\sin^2 \theta + \cos^2 \theta) \sin^2 \phi \\ &+4\left(\frac{\cos \theta}{2}\right) \cos \phi \frac{\sin \theta}{\sqrt{2}} \sin \phi \\ &-2\frac{\sin \theta}{\sqrt{2}} \cos \phi \cos \theta \sin \phi \end{aligned} \right] \quad (45)$$

Using the trigonometric identity:

$$\sin^2 \theta + \cos^2 \theta = 1$$

gives

(46)

$$x^2 + y^2 + z^2 = r_n^2 \left[\left(\frac{1}{2} + \frac{1}{2} \right) \cos^2 \phi + \sin^2 \phi \right] \quad (47)$$

By using the trigonometric identity of Eq. (46) for ϕ , Eq. (47) becomes

$$x^2 + y^2 + z^2 = r_n^2 \quad (48)$$

which is the equation of a uniform sphere.

COMPONENT ORBITSPIHERE-CVF SQUARED FOR STEP TWO USING THE ROTATION OF A GREAT CIRCLE ABOUT THE $(-i_x, 0i_y, i_z)$ -AXIS BY 2π FOLLOWED BY A ROTATION ABOUT THE Z-AXIS BY $\frac{\pi}{4}$

From Eq. (14), the equation for the component orbitsphere-cvf squared for STEP TWO is given by

$$x^2 + y^2 + z^2 = \left\{ \begin{aligned} & \left(\left(\frac{\frac{1}{2} + \frac{\cos \theta}{2}}{\sqrt{2}} - \frac{\sin \theta}{2} \right) r_n \cos \phi + \left(\frac{\cos \theta}{\sqrt{2}} + \frac{\sin \theta}{2} \right) r_n \sin \phi \right)^2 \\ & + \left(\left(-\frac{\frac{1}{2} + \frac{\cos \theta}{2}}{\sqrt{2}} - \frac{\sin \theta}{2} \right) r_n \cos \phi + \left(\frac{\cos \theta}{\sqrt{2}} - \frac{\sin \theta}{2} \right) r_n \sin \phi \right)^2 \\ & + \left(\left(-\frac{1}{2} + \frac{\cos \theta}{2} \right) r_n \cos \phi + \frac{\sin \theta}{\sqrt{2}} r_n \sin \phi \right)^2 \end{aligned} \right\} \quad (49)$$

Multiplying out the squared terms gives

$$x^2 + y^2 + z^2 = \left[\begin{aligned} & \left(\frac{\frac{1}{2} + \frac{\cos \theta}{2}}{\sqrt{2}} - \frac{\sin \theta}{2} \right)^2 r_n^2 \cos^2 \phi + \left(\frac{\cos \theta}{\sqrt{2}} + \frac{\sin \theta}{2} \right)^2 r_n^2 \sin^2 \phi \\ & + 2 \left(\frac{\frac{1}{2} + \frac{\cos \theta}{2}}{\sqrt{2}} - \frac{\sin \theta}{2} \right) \left(\frac{\cos \theta}{\sqrt{2}} + \frac{\sin \theta}{2} \right) r_n^2 \cos \phi \sin \phi \\ & + \left(-\frac{\frac{1}{2} + \frac{\cos \theta}{2}}{\sqrt{2}} - \frac{\sin \theta}{2} \right)^2 r_n^2 \cos^2 \phi + \left(\frac{\cos \theta}{\sqrt{2}} - \frac{\sin \theta}{2} \right)^2 r_n^2 \sin^2 \phi \\ & + 2 \left(-\frac{\frac{1}{2} + \frac{\cos \theta}{2}}{\sqrt{2}} - \frac{\sin \theta}{2} \right) \left(\frac{\cos \theta}{\sqrt{2}} - \frac{\sin \theta}{2} \right) r_n^2 \cos \phi \sin \phi \\ & + \left(-\frac{1}{2} + \frac{\cos \theta}{2} \right)^2 r_n^2 \cos^2 \phi + \frac{\sin^2 \theta}{2} r_n^2 \sin^2 \phi \\ & + 2 \left(-\frac{1}{2} + \frac{\cos \theta}{2} \right) \frac{\sin \theta}{\sqrt{2}} r_n^2 \cos \phi \sin \phi \end{aligned} \right] \quad (50)$$

Further multiplying out the squared terms gives

$$\begin{aligned}
 x^2 + y^2 + z^2 = r_n^2 & \left\{ \left[\left(\left(\frac{1 + \cos \theta}{2} \right)^2 - \left(\frac{1 + \cos \theta}{2} \right) \sin \theta + \frac{\sin^2 \theta}{4} \right) \cos^2 \phi \right. \right. \\
 & + \left(\frac{\cos^2 \theta}{2} + \frac{\cos \theta \sin \theta}{\sqrt{2}} + \frac{\sin^2 \theta}{4} \right) \sin^2 \phi \\
 & + 2 \left(\frac{1 + \cos \theta}{2} - \frac{\sin \theta}{2} \right) \left(\frac{\cos \theta}{\sqrt{2}} + \frac{\sin \theta}{2} \right) \cos \phi \sin \phi \\
 & + \left(\left(\frac{1 + \cos \theta}{2} \right)^2 + \frac{1 + \cos \theta}{2} \sin \theta + \frac{\sin^2 \theta}{4} \right) \cos^2 \phi \\
 & + \left(\frac{\cos^2 \theta}{2} - \frac{\cos \theta \sin \theta}{\sqrt{2}} + \frac{\sin^2 \theta}{4} \right) \sin^2 \phi \\
 & + 2 \left(-\frac{1 + \cos \theta}{2} - \frac{\sin \theta}{2} \right) \left(\frac{\cos \theta}{\sqrt{2}} - \frac{\sin \theta}{2} \right) \cos \phi \sin \phi \\
 & + \left(\frac{1}{4} - \frac{\cos \theta}{2} + \frac{\cos^2 \theta}{4} \right) \cos^2 \phi + \frac{\sin^2 \theta}{2} \sin^2 \phi \\
 & \left. + 2 \left(-\frac{1}{2} + \frac{\cos \theta}{2} \right) \frac{\sin \theta}{\sqrt{2}} \cos \phi \sin \phi \right] \quad (51)
 \end{aligned}$$

Combining terms gives

$$x^2 + y^2 + z^2 = r_n^2 \left\{ \begin{aligned} & \left(2 \left(\frac{\frac{1}{2} + \frac{\cos \theta}{2}}{\sqrt{2}} \right)^2 + \frac{\sin^2 \theta}{2} + \left(\frac{1}{4} - \frac{\cos \theta}{2} + \frac{\cos^2 \theta}{4} \right) \right) \cos^2 \phi \\ & + \left(\cos^2 \theta + \frac{\sin^2 \theta}{2} + \frac{\sin^2 \theta}{2} \right) \sin^2 \phi \\ & + 2 \left(\frac{\frac{1}{2} + \frac{\cos \theta}{2}}{\sqrt{2}} - \frac{\sin \theta}{2} \right) \left(\frac{\cos \theta}{\sqrt{2}} + \frac{\sin \theta}{2} \right) \cos \phi \sin \phi \\ & + 2 \left(-\frac{\frac{1}{2} + \frac{\cos \theta}{2}}{\sqrt{2}} - \frac{\sin \theta}{2} \right) \left(\frac{\cos \theta}{\sqrt{2}} - \frac{\sin \theta}{2} \right) \cos \phi \sin \phi \\ & + 2 \left(-\frac{1}{2} + \frac{\cos \theta}{2} \right) \frac{\sin \theta}{\sqrt{2}} \cos \phi \sin \phi \end{aligned} \right\} \quad (52)$$

Using the trigonometric identity from Eq. (46) and multiplying out the trigonometric cross terms gives

$$x^2 + y^2 + z^2 = r_n^2 \left\{ \begin{aligned} & \left(\frac{1}{4} + \frac{\cos \theta}{2} + \frac{\cos^2 \theta}{4} + \frac{\sin^2 \theta}{2} + \left(\frac{1}{4} - \frac{\cos \theta}{2} + \frac{\cos^2 \theta}{4} \right) \right) \cos^2 \phi + \sin^2 \phi \\ & 2 \left(\begin{aligned} & \frac{\cos \theta}{4} + \frac{\cos^2 \theta}{4} - \frac{\sin \theta \cos \theta}{2\sqrt{2}} + \frac{\sin \theta}{4\sqrt{2}} + \frac{\sin \theta \cos \theta}{4\sqrt{2}} - \frac{\sin^2 \theta}{4} \\ & - \frac{\cos \theta}{4} - \frac{\cos^2 \theta}{4} - \frac{\sin \theta \cos \theta}{2\sqrt{2}} + \frac{\sin \theta}{4\sqrt{2}} + \frac{\sin \theta \cos \theta}{4\sqrt{2}} + \frac{\sin^2 \theta}{4} \\ & - \frac{\sin \theta}{2\sqrt{2}} + \frac{\sin \theta \cos \theta}{2\sqrt{2}} \end{aligned} \right) \cos \phi \sin \phi \end{aligned} \right\} \quad (53)$$

Combining terms gives

$$x^2 + y^2 + z^2 = r_n^2 \left\{ \begin{aligned} & \left(\frac{1}{2} + \frac{\cos^2 \theta}{2} + \frac{\sin^2 \theta}{2} \right) \cos^2 \phi + \sin^2 \phi \\ & 2(0) \cos \phi \sin \phi \end{aligned} \right\} \quad (54)$$

By using the trigonometric identity of Eq. (46) for θ and ϕ , Eq. (54) becomes

$$x^2 + y^2 + z^2 = r_n^2 \quad (55)$$

which is the equation of a uniform sphere.

COMPONENT ORBITSPIHERE-CVF SQUARED FOR STEP TWO BY THE ROTATION OF A GREAT CIRCLE ABOUT THE $(-i_x, i_y, i_z)$ -AXIS BY 2π

From Eq. (22), the equation for the component orbitsphere-cvf squared for STEP TWO is given by

$$x^2 + y^2 + z^2 = \frac{1}{16} r_n^2 \left\{ \begin{aligned} & \left(2 \sin \theta (\cos \phi - \sin \phi) + \sqrt{2} (2 \cos \theta \cos \phi + (-1 + \cos \theta) \sin \phi) \right)^2 \\ & + \left(-2 \sin \theta (\cos \phi + \sin \phi) + \sqrt{2} (\cos \theta (2 \cos \phi - \sin \phi) + \sin \phi) \right)^2 \\ & + 4 (\sqrt{2} \cos \phi \sin \theta + (1 + \cos \theta) \sin \phi)^2 \end{aligned} \right\} \quad (56)$$

Multiplying out the terms gives

$$x^2 + y^2 + z^2 = \frac{1}{16} r_n^2 \left\{ \begin{aligned} & 4 \sin^2 \theta (\cos \phi - \sin \phi)^2 + 2 (2 \cos \theta \cos \phi + (-1 + \cos \theta) \sin \phi)^2 \\ & + 4 \sqrt{2} \sin \theta (\cos \phi - \sin \phi) (2 \cos \theta \cos \phi + (-1 + \cos \theta) \sin \phi) \\ & + 4 \sin^2 \theta (\cos \phi + \sin \phi)^2 + 2 (\cos \theta (2 \cos \phi - \sin \phi) + \sin \phi)^2 \\ & - 4 \sqrt{2} \sin \theta (\cos \phi + \sin \phi) (\cos \theta (2 \cos \phi - \sin \phi) + \sin \phi) \\ & + 8 \cos^2 \phi \sin^2 \theta + 4 (1 + \cos \theta)^2 \sin^2 \phi \\ & + 8 \sqrt{2} \cos \phi \sin \theta (1 + \cos \theta) \sin \phi \end{aligned} \right\} \quad (57)$$

$$x^2 + y^2 + z^2 =$$

$$\frac{1}{16} r_n^2 \left\{ \begin{aligned} & 4 \sin^2 \theta (\cos^2 \phi - 2 \cos \phi \sin \phi + \sin^2 \phi) \\ & + 2 (4 \cos^2 \theta \cos^2 \phi + 4 \cos \theta \cos \phi (-1 + \cos \theta) \sin \phi + (-1 + \cos \theta)^2 \sin^2 \phi) \\ & + 4 \sqrt{2} \sin \theta (\cos \phi - \sin \phi) (2 \cos \theta \cos \phi + (-1 + \cos \theta) \sin \phi) \\ & + 4 \sin^2 \theta (\cos^2 \phi + 2 \cos \phi \sin \phi + \sin^2 \phi) + 2 \left(\cos^2 \theta (2 \cos \phi - \sin \phi)^2 \right. \\ & \quad \left. + 2 \cos \theta (2 \cos \phi - \sin \phi) \sin \phi + \sin^2 \phi \right) \\ & - 4 \sqrt{2} \sin \theta (\cos \phi + \sin \phi) (\cos \theta (2 \cos \phi - \sin \phi) + \sin \phi) \\ & + 8 \cos^2 \phi \sin^2 \theta + 4 (1 + 2 \cos \theta + \cos^2 \theta) \sin^2 \phi \\ & + 8 \sqrt{2} \cos \phi \sin \theta (1 + \cos \theta) \sin \phi \end{aligned} \right\} \quad (58)$$

$$x^2 + y^2 + z^2 =$$

$$\frac{1}{16} r_n^2 \left\{ \begin{aligned} &4 \sin^2 \theta \cos^2 \phi - 8 \sin^2 \theta \cos \phi \sin \phi + 4 \sin^2 \theta \sin^2 \phi \\ &+ 8 \cos^2 \theta \cos^2 \phi - 8 \cos \theta \cos \phi \sin \phi + 8 \cos^2 \theta \cos \phi \sin \phi + 2 \sin^2 \phi \\ &- 4 \cos \theta \sin^2 \phi + 2 \cos^2 \theta \sin^2 \phi \\ &+ 4 \sqrt{2} \sin \theta (\cos \phi - \sin \phi) (2 \cos \theta \cos \phi - \sin \phi + \cos \theta \sin \phi) \\ &+ 4 \sin^2 \theta \cos^2 \phi + 8 \sin^2 \theta \cos \phi \sin \phi + 4 \sin^2 \theta \sin^2 \phi \\ &+ 2 \cos^2 \theta (4 \cos^2 \phi - 4 \cos \phi \sin \phi + \sin^2 \phi) \\ &+ 8 \cos \theta \cos \phi \sin \phi - 4 \cos \theta \sin^2 \phi + 2 \sin^2 \phi \\ &- (\cos \phi + \sin \phi) (8 \sqrt{2} \sin \theta \cos \theta \cos \phi - 4 \sqrt{2} \sin \theta \cos \theta \sin \phi + 4 \sqrt{2} \sin \theta \sin \phi) \\ &+ 8 \cos^2 \phi \sin^2 \theta + 4 \sin^2 \phi + 8 \sin^2 \phi \cos \theta + 4 \sin^2 \phi \cos^2 \theta \\ &+ 8 \sqrt{2} \sin \theta \cos \phi \sin \phi + 8 \sqrt{2} \sin \theta \cos \theta \cos \phi \sin \phi \end{aligned} \right\} \quad (59)$$

$$x^2 + y^2 + z^2 =$$

$$\frac{1}{16} r_n^2 \left\{ \begin{aligned} &4 \sin^2 \theta \cos^2 \phi - 8 \sin^2 \theta \cos \phi \sin \phi + 4 \sin^2 \theta \sin^2 \phi \\ &+ 8 \cos^2 \theta \cos^2 \phi - 8 \cos \theta \cos \phi \sin \phi + 8 \cos^2 \theta \cos \phi \sin \phi + 2 \sin^2 \phi \\ &- 4 \cos \theta \sin^2 \phi + 2 \cos^2 \theta \sin^2 \phi \\ &+ 8 \sqrt{2} \cos \theta \sin \theta \cos^2 \phi - 4 \sqrt{2} \sin \theta \cos \phi \sin \phi + 4 \sqrt{2} \cos \theta \sin \theta \cos \phi \sin \phi \\ &- 8 \sqrt{2} \cos \theta \sin \theta \cos \phi \sin \phi + 4 \sqrt{2} \sin \theta \sin^2 \phi - 4 \sqrt{2} \cos \theta \sin \theta \sin^2 \phi \\ &+ 4 \sin^2 \theta \cos^2 \phi + 8 \sin^2 \theta \cos \phi \sin \phi + 4 \sin^2 \theta \sin^2 \phi \\ &+ 8 \cos^2 \theta \cos^2 \phi - 8 \cos^2 \theta \cos \phi \sin \phi + 2 \cos^2 \theta \sin^2 \phi \\ &+ 8 \cos \theta \cos \phi \sin \phi - 4 \cos \theta \sin^2 \phi + 2 \sin^2 \phi \\ &- 8 \sqrt{2} \cos \theta \sin \theta \cos^2 \phi + 4 \sqrt{2} \cos \theta \sin \theta \cos \phi \sin \phi - 4 \sqrt{2} \sin \theta \cos \phi \sin \phi \\ &- 8 \sqrt{2} \cos \theta \sin \theta \cos \phi \sin \phi + 4 \sqrt{2} \cos \theta \sin \theta \sin^2 \phi - 4 \sqrt{2} \sin \theta \sin^2 \phi \\ &+ 8 \sin^2 \theta \cos^2 \phi + 4 \sin^2 \phi + 8 \cos \theta \sin^2 \phi + 4 \cos^2 \theta \sin^2 \phi \\ &+ 8 \sqrt{2} \sin \theta \cos \phi \sin \phi + 8 \sqrt{2} \cos \theta \sin \theta \cos \phi \sin \phi \end{aligned} \right\} \quad (60)$$

$$x^2 + y^2 + z^2 =$$

$$\frac{1}{16} r_n^2 \left\{ \begin{array}{l} 4 \sin^2 \theta \cos^2 \phi - 8 \sin^2 \theta \cos \phi \sin \phi + 4 \sin^2 \theta \sin^2 \phi \\ + 8 \cos^2 \theta \cos^2 \phi - 8 \cos \theta \cos \phi \sin \phi + 8 \cos^2 \theta \cos \phi \sin \phi + 2 \sin^2 \phi \\ - 4 \cos \theta \sin^2 \phi + 2 \cos^2 \theta \sin^2 \phi \\ + 8 \sqrt{2} \cos \theta \sin \theta \cos^2 \phi - 4 \sqrt{2} \sin \theta \cos \phi \sin \phi + 4 \sqrt{2} \cos \theta \sin \theta \cos \phi \sin \phi \\ - 8 \sqrt{2} \cos \theta \sin \theta \cos \phi \sin \phi + 4 \sqrt{2} \sin \theta \sin^2 \phi - 4 \sqrt{2} \cos \theta \sin \theta \sin^2 \phi \\ + 4 \sin^2 \theta \cos^2 \phi + 8 \sin^2 \theta \cos \phi \sin \phi + 4 \sin^2 \theta \sin^2 \phi \\ + 8 \cos^2 \theta \cos^2 \phi - 8 \cos^2 \theta \cos \phi \sin \phi + 2 \cos^2 \theta \sin^2 \phi \\ + 8 \cos \theta \cos \phi \sin \phi - 4 \cos \theta \sin^2 \phi + 2 \sin^2 \phi \\ - 8 \sqrt{2} \cos \theta \sin \theta \cos^2 \phi + 4 \sqrt{2} \cos \theta \sin \theta \cos \phi \sin \phi - 4 \sqrt{2} \sin \theta \cos \phi \sin \phi \\ - 8 \sqrt{2} \cos \theta \sin \theta \cos \phi \sin \phi + 4 \sqrt{2} \cos \theta \sin \theta \sin^2 \phi - 4 \sqrt{2} \sin \theta \sin^2 \phi \\ + 8 \sin^2 \theta \cos^2 \phi + 4 \sin^2 \theta \sin^2 \phi + 8 \cos \theta \sin^2 \phi + 4 \cos^2 \theta \sin^2 \phi \\ + 8 \sqrt{2} \sin \theta \cos \phi \sin \phi + 8 \sqrt{2} \cos \theta \sin \theta \cos \phi \sin \phi \end{array} \right\} \quad (61)$$

Combining terms gives

$$x^2 + y^2 + z^2 =$$

$$\frac{1}{16} r_n^2 \left\{ \begin{array}{l} 4 \sin^2 \theta \sin^2 \phi + 4 \sin^2 \theta \sin^2 \phi \\ + 4 \sin^2 \theta \cos^2 \phi + 8 \sin^2 \theta \cos^2 \phi + 4 \sin^2 \theta \cos^2 \phi \\ + 4 \cos^2 \theta \sin^2 \phi + 2 \cos^2 \theta \sin^2 \phi + 2 \cos^2 \theta \sin^2 \phi \\ + 8 \cos^2 \theta \cos^2 \phi + 8 \cos^2 \theta \cos^2 \phi \\ + 2 \sin^2 \phi + 2 \sin^2 \phi + 4 \sin^2 \phi \\ - 8 \sin^2 \theta \cos \phi \sin \phi + 8 \sin^2 \theta \cos \phi \sin \phi \\ + 8 \cos^2 \theta \cos \phi \sin \phi - 8 \cos^2 \theta \cos \phi \sin \phi \\ - 4 \cos \theta \sin^2 \phi - 4 \cos \theta \sin^2 \phi + 8 \cos \theta \sin^2 \phi \\ - 8 \cos \theta \cos \phi \sin \phi + 8 \cos \theta \cos \phi \sin \phi \\ - 8 \sqrt{2} \cos \theta \sin \theta \cos^2 \phi + 8 \sqrt{2} \cos \theta \sin \theta \cos^2 \phi \\ - 4 \sqrt{2} \cos \theta \sin \theta \sin^2 \phi + 4 \sqrt{2} \cos \theta \sin \theta \sin^2 \phi \\ - 4 \sqrt{2} \sin \theta \cos \phi \sin \phi - 4 \sqrt{2} \sin \theta \cos \phi \sin \phi + 8 \sqrt{2} \sin \theta \cos \phi \sin \phi \\ - 8 \sqrt{2} \cos \theta \sin \theta \cos \phi \sin \phi + 8 \sqrt{2} \cos \theta \sin \theta \cos \phi \sin \phi \\ + 4 \sqrt{2} \cos \theta \sin \theta \cos \phi \sin \phi + 4 \sqrt{2} \cos \theta \sin \theta \cos \phi \sin \phi - 8 \sqrt{2} \cos \theta \sin \theta \cos \phi \sin \phi \\ + 4 \sqrt{2} \sin \theta \sin^2 \phi - 4 \sqrt{2} \sin \theta \sin^2 \phi \end{array} \right\} \quad (62)$$

$$x^2 + y^2 + z^2 = \frac{1}{16} r_n^2 \left\{ \begin{array}{l} 8\sin^2 \theta \sin^2 \phi \\ +16\sin^2 \theta \cos^2 \phi \\ +8\cos^2 \theta \sin^2 \phi \\ +16\cos^2 \theta \cos^2 \phi \\ +8\sin^2 \phi \end{array} \right\} \quad (63)$$

By using the trigonometric identity of Eq. (46) for θ and ϕ , Eq. (63) becomes

$$x^2 + y^2 + z^2 = \frac{1}{16} r_n^2 \left\{ \begin{array}{l} 8\sin^2 \phi (\sin^2 \theta + \cos^2 \theta) \\ +16\cos^2 \phi (\sin^2 \theta + \cos^2 \theta) \\ +8\sin^2 \phi \end{array} \right\} \quad (64)$$

$$x^2 + y^2 + z^2 = \frac{1}{16} r_n^2 \{ 16(\sin^2 \phi + \cos^2 \phi) \} \quad (65)$$

$$x^2 + y^2 + z^2 = r_n^2 \quad (66)$$

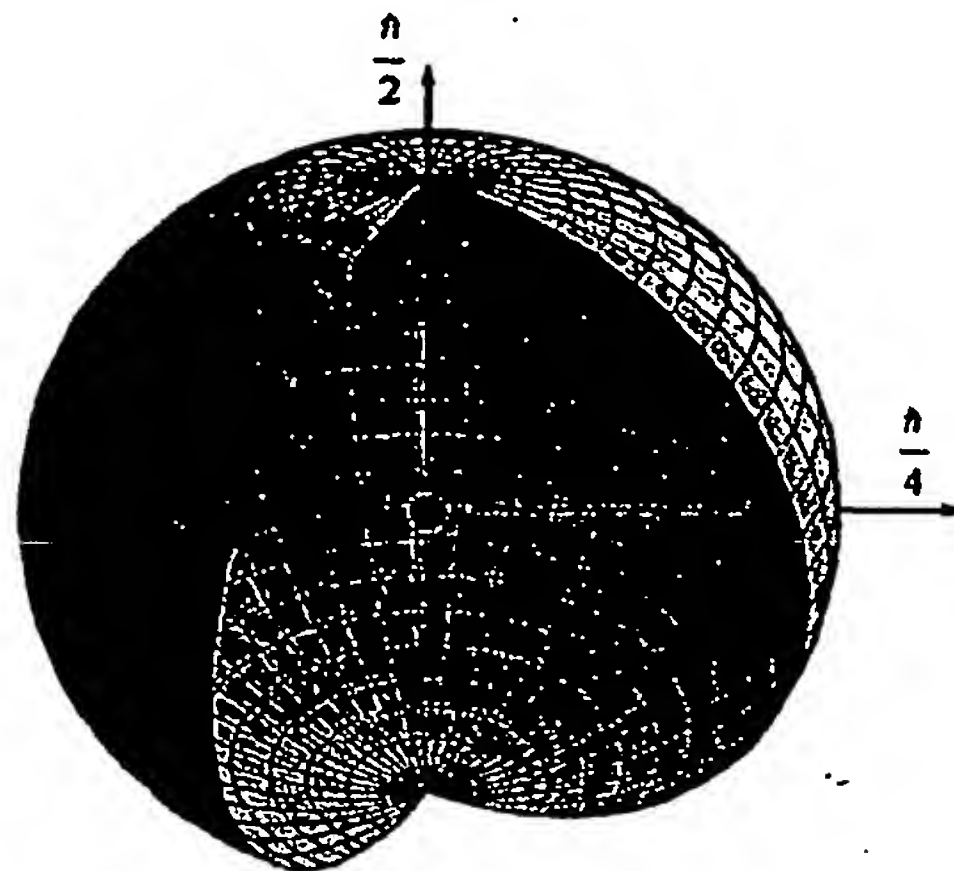
which is the equation of a uniform sphere.

ORBITSPIHERE-CVF SQUARED

Eqs. (48), (55), and (66) are each the equation of a uniform sphere. The superposition of the uniform distributions from STEP ONE and STEP TWO is the uniform current density function $Y_0^0(\phi, \theta)$ that is an equipotential, minimum energy surface shown in Figure 13. The angular momentum is identically that of the from the superposition of the primary component orbitsphere-cvfs of the orbitsphere-cvf, $L_{xy} = \frac{\hbar}{4}$ and $L_z = \frac{\hbar}{2}$. The spatially uniform electron current having the orthogonal angular momentum components given by Eqs. (1.73a-1.73b) can then be considered conceptually from two viewpoints regarding the basis element of the orbitsphere-cvf which is a two-dimensional vector field comprised of an infinite number of one-dimensional great circles having zero-dimensional crossings. The electron current, $Y_0^0(\phi, \theta)$, is a continuous uniform superposition of secondary orbitsphere-cvfs onto and over the two-dimensional surface wherein each secondary orbitsphere-cvf of equivalent angular momentum, orientation, and phase replaces a corresponding great-circle current loops of the primary orbitsphere-cvf. Or, equivalently, the primary orbitsphere-cvf is the compression of a secondary two-dimensional orbitsphere-cvf into each of the infinite number of one-dimensional great circles such that L_R , the orientation, and the phase of the former element matches that of the latter over a two-dimensional spherical shell to form a primary two-dimensional

vector field.

Figure 13. The orbitsphere-cvf is a two dimensional spherical shell of zero thickness with the Bohr radius of the hydrogen atom, $r = a_H$, having angular momentum components of $L_{xy} = \frac{\hbar}{4}$ and $L_z = \frac{\hbar}{2}$.



MATRICES TO DEMONSTRATE THE CONVOLUTION TO GENERATE THE UNIFORM CURRENT (CHARGE)-DENSITY FUNCTION $Y_0^0(\phi, \theta)$

Either one of the orthogonal basis-element great circles generates the component orbitsphere-cvf for STEP ONE and STEP TWO as given in the STEP ONE by the Rotation of a Great Circle about the $(\mathbf{i}_x, \mathbf{i}_y, 0\mathbf{i}_z)$ -Axis by 2π section and the STEP TWO by Rotation of a Great Circle About the $(-\mathbf{i}_x, \mathbf{i}_y, \mathbf{i}_z)$ -Axis by 2π section, respectively. Thus, either of the STEP ONE and the STEP TWO components can serve as the primary component orbitsphere-cvf for the convolution operation given by Eq. (38). Similarly, either one of the orthogonal basis-element great circles generates the component orbitsphere-cvf having a stationary angular momentum vector associated with STEP ONE and STEP TWO as given in the Orbitsphere-cvf Orthogonal to that of STEP ONE by the Rotation of a Great Circle about the $(\mathbf{i}_x, -\mathbf{i}_y, 0\mathbf{i}_z)$ -Axis by 2π section and the STEP TWO by Rotation of a Great Circle About the $(-\mathbf{i}_x, \mathbf{i}_y, \mathbf{i}_z)$ -Axis by 2π section, respectively. Thus, either of the STEP-ONE and the STEP-TWO-associated components can serve as the secondary component orbitsphere-cvf for the convolution operation given by Eq. (38).

STEP-ONE Matrices to Visualize the Currents of $Y_0^0(\phi, \theta)$

Consider the case that the STEP-ONE primary component orbitsphere-cvf is given by Eqs. (4) and (5) and the STEP-ONE-associated

secondary component orbitsphere-cvf is given by Eqs. (30-33). The basis-element great circle of the primary component orbitsphere-cvf is in the yz-plane as shown in Figure 2, and the current is counter clockwise. Thus, the angular momentum is along the x-axis. The angular-momentum-and-orientation-matched secondary component orbitsphere-cvf is shown in Figure 10 and is generated by Eq. (30). In this case, the secondary component orbitsphere-cvf is aligned on the yz-plane and the resultant angular momentum vector, L_R , of the secondary component orbitsphere-cvf is also along the x-axis.

Then, the uniform current distribution is given from Eq. (38) as a infinite sum of the convolved elements comprising the secondary component orbitsphere-cvf given by Eq. (30) rotated according to Eq. (4), the matrix which generated the primary component orbitsphere-cvf. The resulting constant function is exact as given by Eq. (48). A representation that shows the current elements can be generated by showing the basis-element secondary component orbitsphere-cvf as a sum of great circles using Eq. (30) and by showing the continuous convolution as a sum of discrete incremental rotations of the position of the secondary component orbitsphere-cvf using Eq. (4). In the case that the discrete representation of the secondary component orbitsphere-cvf comprises N great circles and the number of convolved secondary component orbitsphere-cvf elements is M , the representation of the uniform current density function showing current loops shown in Figures 14 and 15 is given by

$$\begin{bmatrix} x' \\ y' \\ z' \end{bmatrix} = \sum_{m=1}^{m=M} \begin{bmatrix} \frac{1}{2} + \frac{\cos\left(\frac{m2\pi}{M}\right)}{2} & \frac{1}{2} - \frac{\cos\left(\frac{m2\pi}{M}\right)}{2} & -\frac{\sin\left(\frac{m2\pi}{M}\right)}{\sqrt{2}} \\ \frac{1}{2} - \frac{\cos\left(\frac{m2\pi}{M}\right)}{2} & \frac{1}{2} + \frac{\cos\left(\frac{m2\pi}{M}\right)}{2} & \frac{\sin\left(\frac{m2\pi}{M}\right)}{\sqrt{2}} \\ \frac{\sin\left(\frac{m2\pi}{M}\right)}{\sqrt{2}} & -\frac{\sin\left(\frac{m2\pi}{M}\right)}{\sqrt{2}} & \cos\left(\frac{m2\pi}{M}\right) \end{bmatrix} \cdot \sum_{n=1}^{n=N} \begin{bmatrix} \cos\left(\frac{\pi}{4}\right) & -\sin\left(\frac{\pi}{4}\right) & 0 \\ \sin\left(\frac{\pi}{4}\right)\cos\left(\frac{n2\pi}{N}\right) & \cos\left(\frac{\pi}{4}\right)\cos\left(\frac{n2\pi}{N}\right) & \sin\left(\frac{n2\pi}{N}\right) \\ -\sin\left(\frac{\pi}{4}\right)\sin\left(\frac{n2\pi}{N}\right) & -\cos\left(\frac{\pi}{4}\right)\sin\left(\frac{n2\pi}{N}\right) & \cos\left(\frac{n2\pi}{N}\right) \end{bmatrix} \begin{bmatrix} 0 \\ r_n \cos \phi \\ r_n \sin \phi \end{bmatrix} \quad (67)$$

Figure 14. A representation of the uniform current pattern of the $Y_0^0(\phi, \theta)$ orbitsphere shown with 30 degree increments ($N=M=12$ in Eq. (67)) of the angle to generate the orbitsphere current-vector field corresponding to Eq. (30) and 30 degree increments of the rotation of this basis element about the $(i_x, i_y, 0i_z)$ -axis corresponding to Eq. (4). The perspective is along the z-axis. The great circle current loop that served as a basis element that was initially in the plane along the $(i_x, -i_y, 0i_z)$ - and z-axes of each secondary component orbitsphere-cvf is shown as red. Note that it is stationary over the convolution due to phase matching.

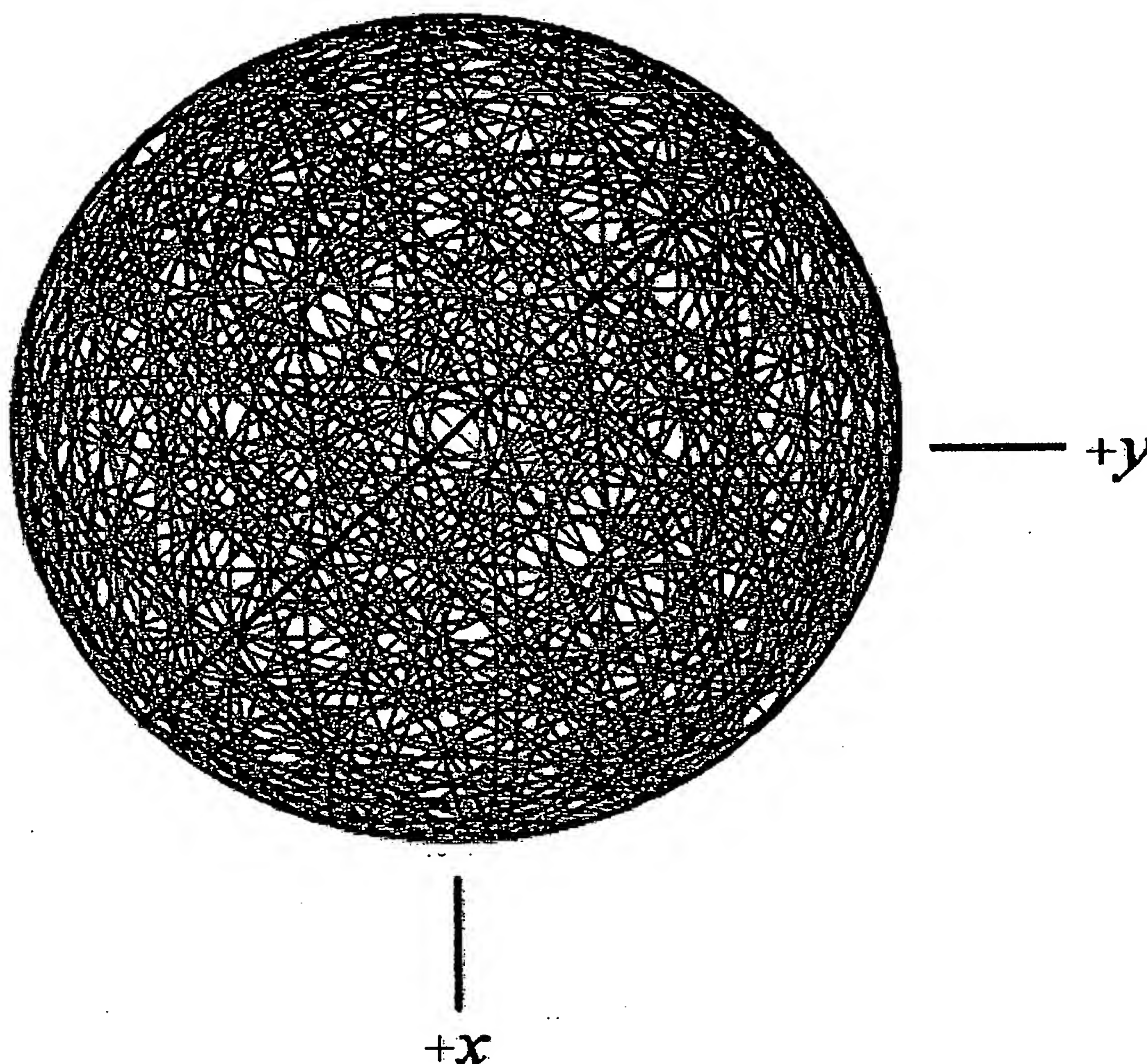
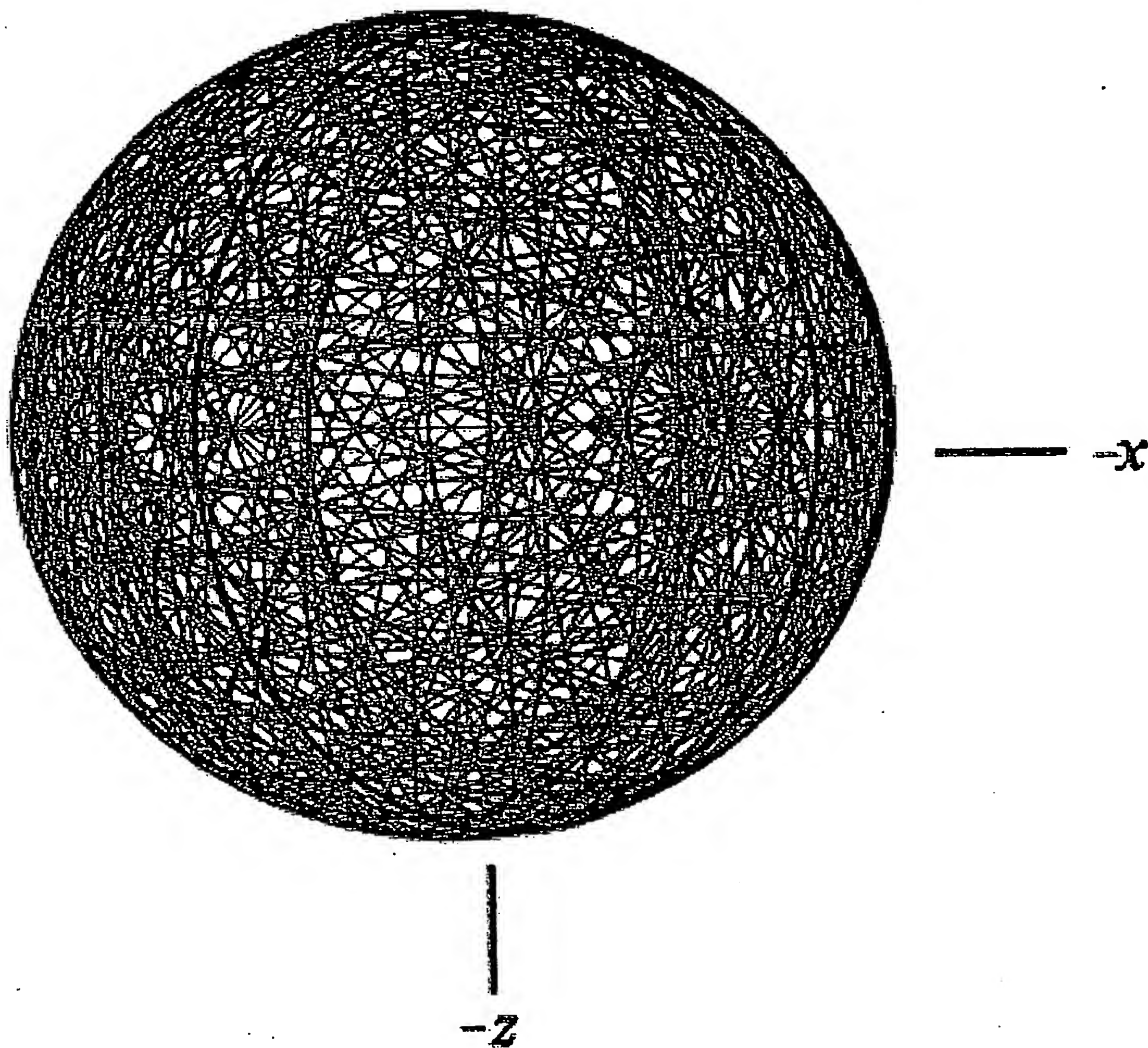


Figure 15. A representation of the uniform current pattern of the $Y_0^0(\phi, \theta)$ orbitsphere shown with 30 degree increments ($N=M=12$ in Eq. (67)) of the angle to generate the orbitsphere current-vector field corresponding to Eq. (30) and 30 degree increments of the rotation of this basis element about the $(\mathbf{i}_x, \mathbf{i}_y, 0\mathbf{i}_z)$ -axis corresponding to Eq. (4). The great circle current loop that served as a basis element that was initially in the plane along the $(\mathbf{i}_x, -\mathbf{i}_y, 0\mathbf{i}_z)$ - and z-axes of each secondary component orbitsphere-cvf is shown as red. The perspective is transverse to the z-axis.



STEP-Two Matrices to Visualize the Currents of $Y_0^0(\phi, \theta)$

Discrete Convolution with a Secondary Component Orbitsphere-cvf in a Plane Along the $(i_x, i_y, 0i_z)$ - and z-Axes (xyz-Plane)

The resultant angular momentum vector, L_R , of the secondary component orbitsphere-cvf given by Eq. (32) is along $(i_x, -i_y, 0i_z)$, corresponding to a basis-element great circle in the yz-plane having a counterclockwise current. The angular momentum direction is reversed by reversing the direction of the current to clockwise. Consider the case that the STEP-TWO primary component orbitsphere-cvf is given by Eqs. (20-23). Further, consider the case that the STEP-TWO-associated secondary component orbitsphere-cvf is given by Eq. (32). The basis-element great circle of the primary component orbitsphere-cvf shown in Figure 7 is in the xyz-plane, and the current is clockwise. Thus, the angular momentum is along the $(-i_x, i_y, 0i_z)$ -axis. The angular-momentum-and-orientation-matched secondary component orbitsphere-cvf is shown in Figure 11 and is generated by Eq. (32). In this case, the secondary component orbitsphere-cvf is aligned on the xyz-plane and the resultant angular momentum vector, L_R , of the secondary component orbitsphere-cvf is also along the $(-i_x, i_y, 0i_z)$ -axis.

Then, the uniform current distribution is given from Eq. (38) as a infinite sum of the convolved elements comprising the secondary component orbitsphere-cvf given by Eq. (32) rotated according to Eq. (20), the matrix which generated the primary component orbitsphere-cvf. The resulting constant function is exact as given by Eq. (66). A representation that shows the current elements can be generated by showing the basis-element secondary component orbitsphere-cvf as a sum of great circles using Eq. (32) and by showing the continuous convolution as a sum of discrete incremental rotations of the position of the secondary component orbitsphere-cvf using Eq. (20). In the case that the discrete representation of the secondary component orbitsphere-cvf comprises N great circles and the number of convolved secondary component orbitsphere-cvf elements is M , the representation of the uniform current density function showing current loops shown in Figures 16-18 is given by

$$\begin{bmatrix} x' \\ y \\ z' \end{bmatrix} = \sum_{m=1}^{m=M} \begin{bmatrix} \frac{1}{4} \left(1 + 3 \cos \left(\frac{m2\pi}{M} \right) \right) & \frac{1}{4} \left(-1 + \cos \left(\frac{m2\pi}{M} \right) + 2\sqrt{2} \sin \left(\frac{m2\pi}{M} \right) \right) & \frac{1}{4} \left(-\sqrt{2} + \sqrt{2} \cos \left(\frac{m2\pi}{M} \right) - 2 \sin \left(\frac{m2\pi}{M} \right) \right) \\ \frac{1}{4} \left(-1 + \cos \left(\frac{m2\pi}{M} \right) - 2\sqrt{2} \sin \left(\frac{m2\pi}{M} \right) \right) & \frac{1}{4} \left(1 + 3 \cos \left(\frac{m2\pi}{M} \right) \right) & \frac{1}{4} \left(\sqrt{2} - \sqrt{2} \cos \left(\frac{m2\pi}{M} \right) - 2 \sin \left(\frac{m2\pi}{M} \right) \right) \\ \frac{1}{2} \left(\frac{-1 + \cos \left(\frac{m2\pi}{M} \right)}{\sqrt{2}} + \sin \left(\frac{m2\pi}{M} \right) \right) & \frac{1}{4} \left(\sqrt{2} - \sqrt{2} \cos \left(\frac{m2\pi}{M} \right) + 2 \sin \left(\frac{m2\pi}{M} \right) \right) & \cos^2 \left(\frac{m2\pi}{M} \right) \frac{1}{2} \end{bmatrix} \\
 \cdot \sum_{n=1}^{n=N} \begin{bmatrix} \frac{1}{2} + \frac{\cos \left(\frac{n2\pi}{N} \right)}{2} & -\frac{1}{2} + \frac{\cos \left(\frac{n2\pi}{N} \right)}{2} & \frac{\sin \left(\frac{n2\pi}{N} \right)}{\sqrt{2}} \\ -\frac{1}{2} + \frac{\cos \left(\frac{n2\pi}{N} \right)}{2} & \frac{1}{2} + \frac{\cos \left(\frac{n2\pi}{N} \right)}{2} & \frac{\sin \left(\frac{n2\pi}{N} \right)}{\sqrt{2}} \\ -\frac{\sin \left(\frac{n2\pi}{N} \right)}{\sqrt{2}} & -\frac{\sin \left(\frac{n2\pi}{N} \right)}{\sqrt{2}} & \cos \left(\frac{n2\pi}{N} \right) \end{bmatrix} \begin{bmatrix} 0 \\ r_n \cos \phi \\ r_n \sin \phi \end{bmatrix}$$

(68)

Figure 16. A representation of the uniform current pattern of the $Y_0^0(\phi, \theta)$ orbitsphere shown with 30 degree increments ($N=M=12$ in Eq. (68)) of the angle to generate the orbitsphere current-vector field corresponding to Eq. (32) and 30 degree increments of the rotation of this basis element about the $(-i_x, i_y, i_z)$ -axis corresponding to Eq. (20). The great circle current loop that served as a basis element that was initially in the yz -plane of each secondary component orbitsphere-cvf is shown as red. Note that it is not stationary over the convolution due to phase matching. It is out of phase with the secondary component orbitsphere by a $-\frac{\pi}{4}$ rotation about the z -axis. The perspective is along the z -axis.

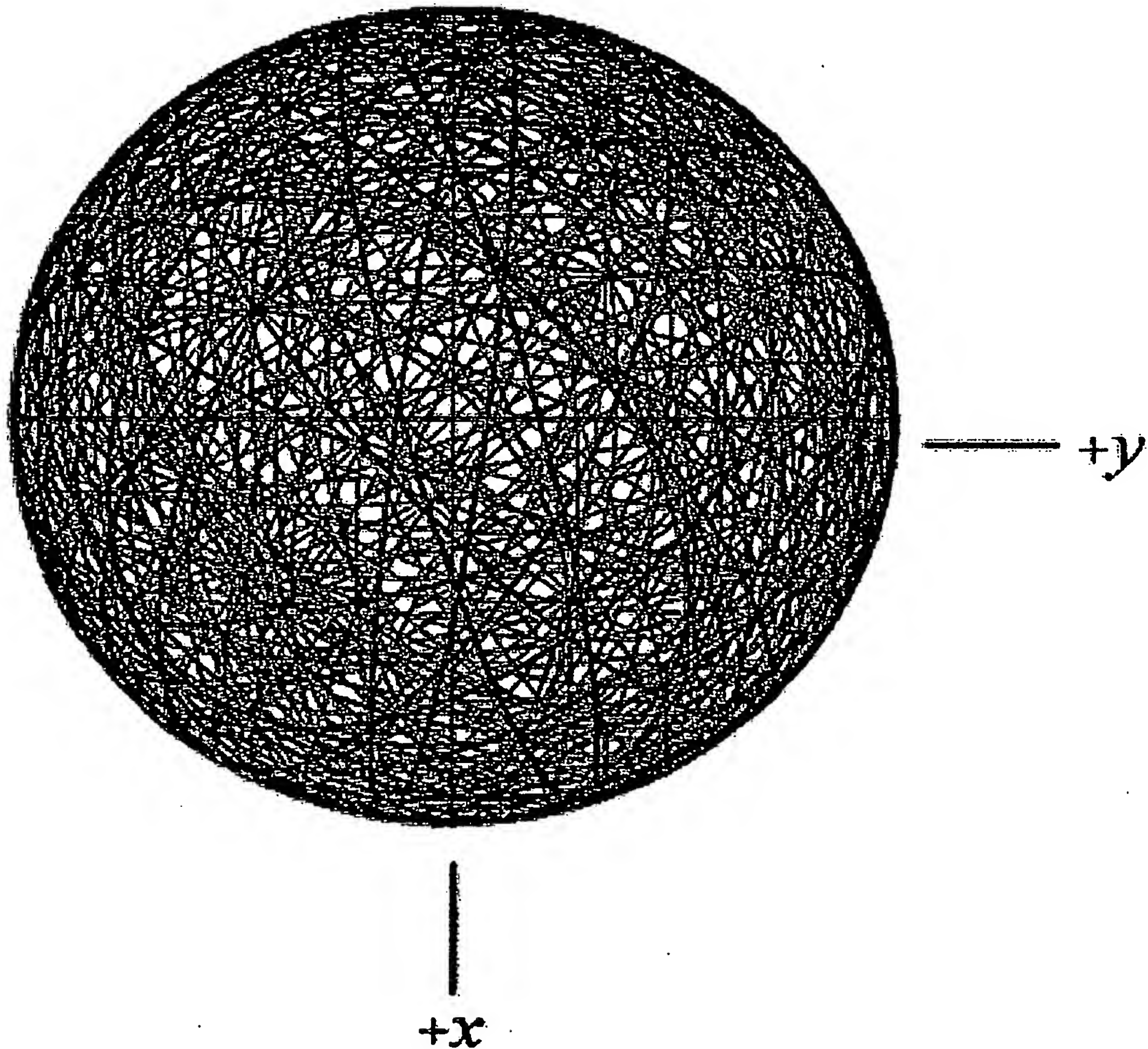


Figure 17. A representation of the uniform current pattern of the $Y_0^0(\phi, \theta)$ orbitsphere shown with 30 degree increments ($N=M=12$ in Eq. (68)) of the angle to generate the orbitsphere current-vector field corresponding to Eq. (32) and 30 degree increments of the rotation of this basis element about the $(-i_x, i_y, i_z)$ -axis corresponding to Eq. (20). The great circle current loop that served as a basis element that was initially in the yz -plane of each secondary component orbitsphere-cvf is shown as red. The perspective is transverse to the z -axis.

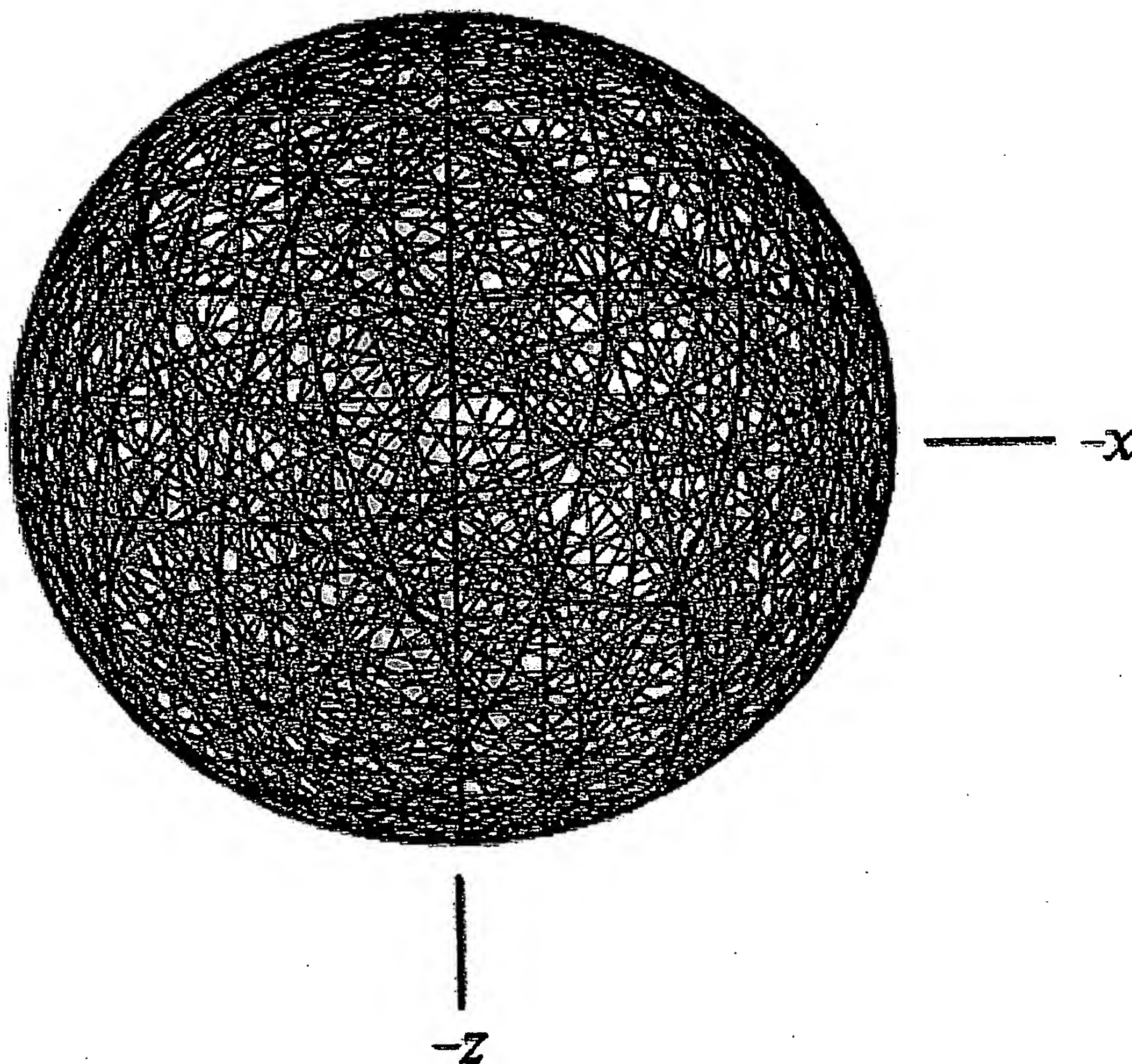
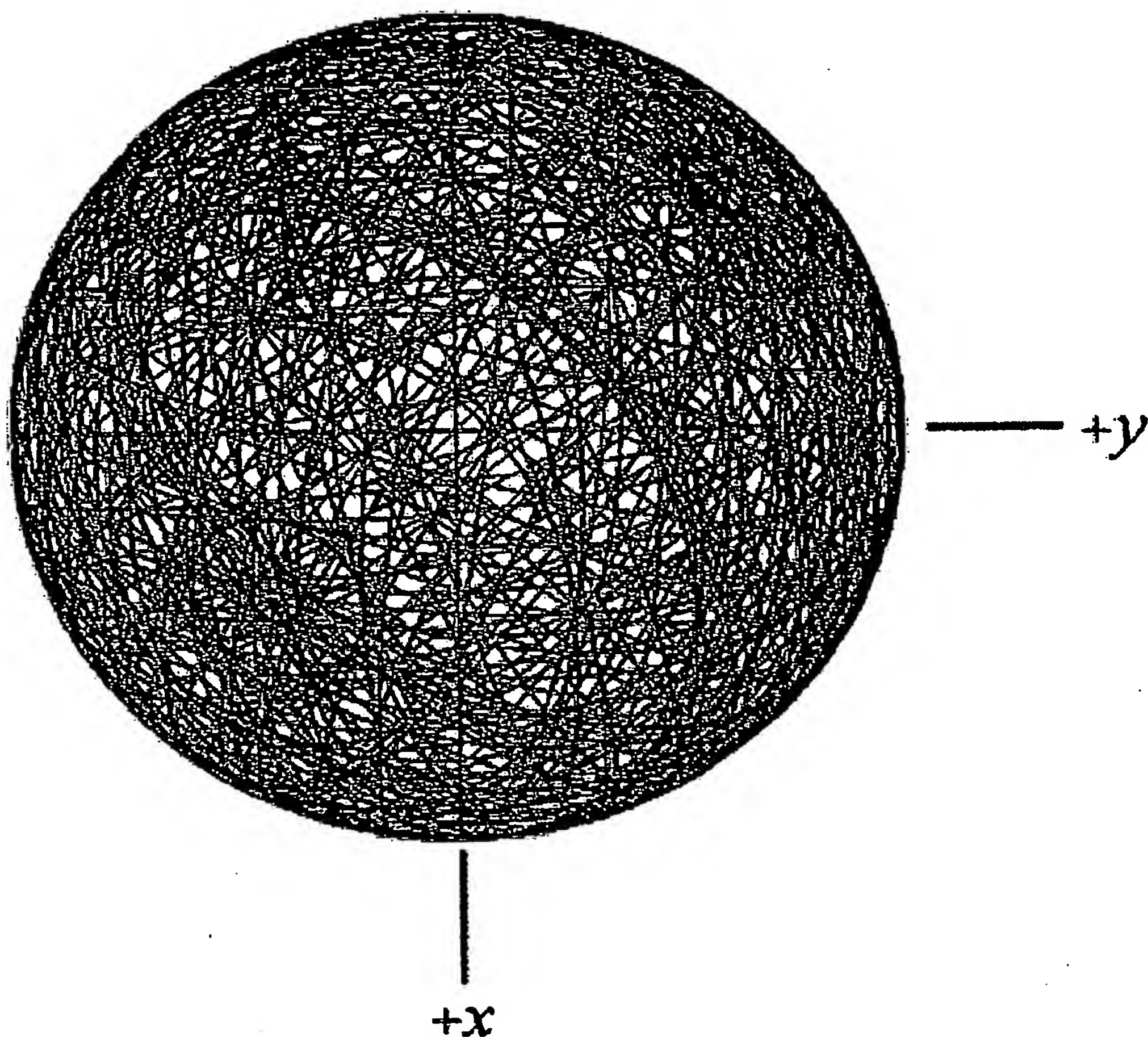


Figure 18. A representation of the uniform current pattern of the $Y_0^0(\phi, \theta)$ orbitsphere shown with 30 degree increments ($N=M=12$ in Eq. (68)) of the angle to generate the orbitsphere current-vector field corresponding to Eq. (32) and 30 degree increments of the rotation of this basis element about the $(-i_x, i_y, i_z)$ -axis corresponding to Eq. (20). The great circle current loop that served as a basis element that was initially in the yz -plane of each secondary component orbitsphere-cvf is not shown. The perspective is along the z -axis.



Discrete Convolution with a Secondary Component Orbitsphere-cvf in the xy -Plane

Consider the case that the STEP-TWO primary component orbitsphere-cvf is given by Eqs. (20-23). Further, consider the case that

the STEP-TWO associated secondary component orbitsphere-cvf is given by Eq. (7). The basis-element great circle of the primary component orbitsphere-cvf is in the xy-plane as shown in Figure 6, and the current is counter clockwise. Thus, the angular momentum is along the z-axis. The angular-momentum-and-orientation-matched secondary component orbitsphere-cvf is shown in Figure 4 and is generated by Eq. (7). In this case, the secondary component orbitsphere-cvf is aligned on the xy-plane and the resultant angular momentum vector, L_R , of the secondary component orbitsphere-cvf is also along the z-axis.

Then, the uniform current distribution is given from Eq. (38) as a infinite sum of the convolved elements comprising the secondary component orbitsphere-cvf given by Eq. (7) rotated according to Eq. (20), the matrix which generated the primary component orbitsphere-cvf using Eq. (23) with Eq. (20). The resulting constant function is exact as given by Eq. (66). A representation that shows the current elements can be generated by showing the basis-element secondary component orbitsphere-cvf as a sum of great circles using Eq. (7) and by showing the continuous convolution as a sum of discrete incremental rotations of the position of the secondary component orbitsphere-cvf using Eq. (20). In the case that the discrete representation of the secondary component orbitsphere-cvf comprises N great circles and the number of convolved secondary component orbitsphere-cvf elements is M , the representation of the uniform current density function showing current loops shown in Figures 19-21 is given by

$$\begin{bmatrix} x' \\ y' \\ z' \end{bmatrix} = \sum_{m=1}^{m=M} \begin{bmatrix} \frac{1}{4} \left(1 + 3 \cos \left(\frac{m2\pi}{M} \right) \right) & \frac{1}{4} \left(-1 + \cos \left(\frac{m2\pi}{M} \right) + 2\sqrt{2} \sin \left(\frac{m2\pi}{M} \right) \right) & \frac{1}{4} \left(-\sqrt{2} + \sqrt{2} \cos \left(\frac{m2\pi}{M} \right) - 2 \sin \left(\frac{m2\pi}{M} \right) \right) \\ \frac{1}{4} \left(-1 + \cos \left(\frac{m2\pi}{M} \right) - 2\sqrt{2} \sin \left(\frac{m2\pi}{M} \right) \right) & \frac{1}{4} \left(1 + 3 \cos \left(\frac{m2\pi}{M} \right) \right) & \frac{1}{4} \left(\sqrt{2} - \sqrt{2} \cos \left(\frac{m2\pi}{M} \right) - 2 \sin \left(\frac{m2\pi}{M} \right) \right) \\ \frac{1}{2} \left(\frac{-1 + \cos \left(\frac{m2\pi}{M} \right)}{\sqrt{2}} + \sin \left(\frac{m2\pi}{M} \right) \right) & \frac{1}{4} \left(\sqrt{2} - \sqrt{2} \cos \left(\frac{m2\pi}{M} \right) + 2 \sin \left(\frac{m2\pi}{M} \right) \right) & \cos^2 \left(\frac{m2\pi}{M} \right) \end{bmatrix} \\ \cdot \sum_{n=1}^{n=N} \begin{bmatrix} \cos \left(\frac{\pi}{4} \right) \cos \left(\frac{n2\pi}{N} \right) & \sin \left(\frac{n2\pi}{N} \right) & \sin \left(\frac{\pi}{4} \right) \cos \left(\frac{n2\pi}{N} \right) \\ -\cos \left(\frac{\pi}{4} \right) \sin \left(\frac{n2\pi}{N} \right) & \cos \left(\frac{n2\pi}{N} \right) & -\sin \left(\frac{\pi}{4} \right) \sin \left(\frac{n2\pi}{N} \right) \\ -\sin \left(\frac{\pi}{4} \right) & 0 & \cos \left(\frac{\pi}{4} \right) \end{bmatrix} \begin{bmatrix} r_n \cos \phi \\ r_n \sin \phi \\ 0 \end{bmatrix} \quad (69)$$

Figure 19. A representation of the uniform current pattern of the $Y_0^0(\phi, \theta)$ orbitsphere shown with 30 degree increments ($N=M=12$ in Eq. (69)) of the angle to generate the orbitsphere current-vector field corresponding to Eq. (7) and 30 degree increments of the rotation of this basis element about the $(-i_x, i_y, i_z)$ -axis corresponding to Eq. (20). The great circle current loop that served as a basis element that was initially in the plane along the $(i_x, 0i_y, -i_z)$ - and y-axes of each secondary component orbitsphere-cvf is shown as red. Note that it is not stationary over the convolution due to phase matching. It is out of phase with the secondary component orbitsphere by $-\frac{\pi}{4}$ about the y-axis. The perspective is along the z-axis.

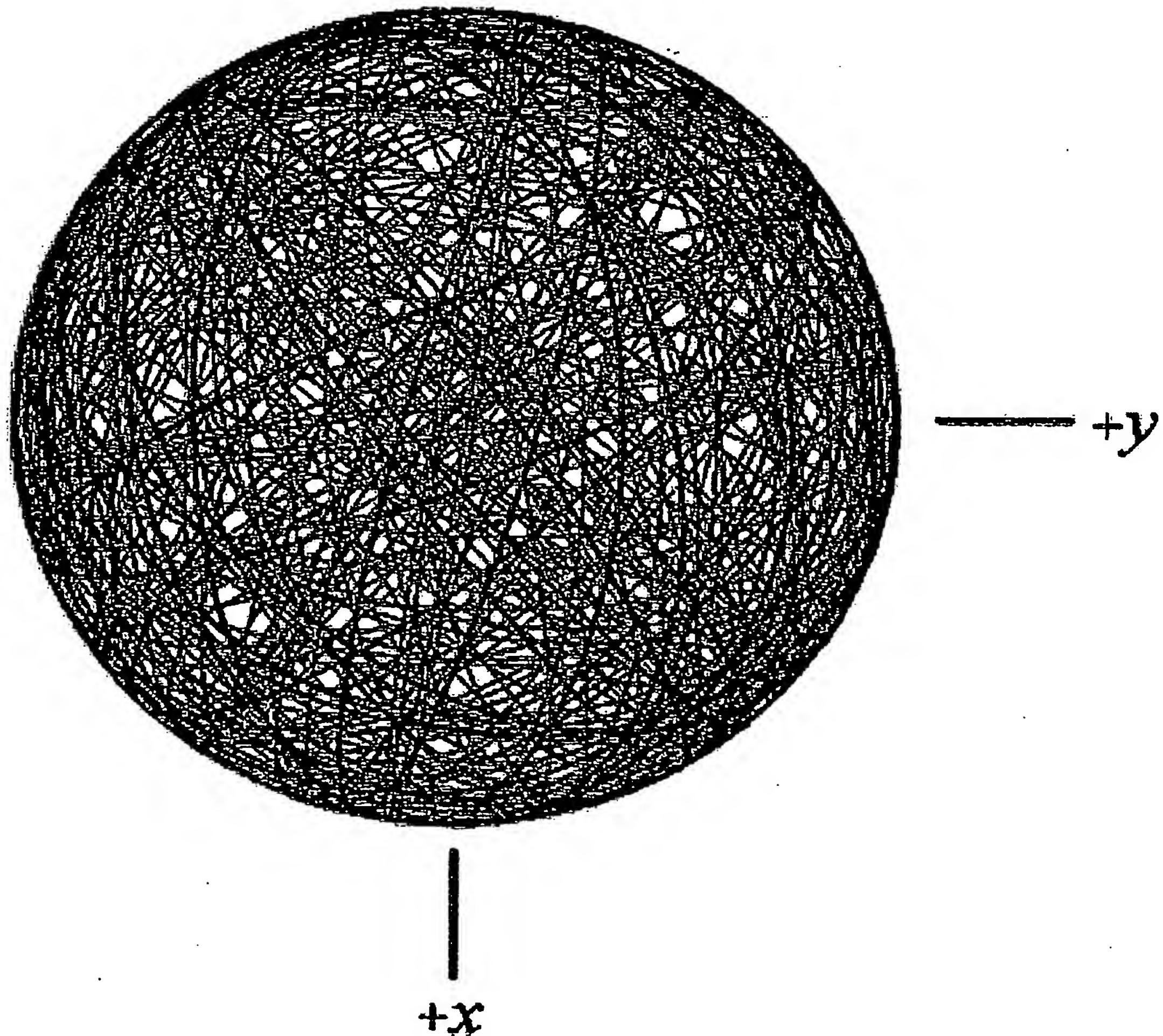


Figure 20. A representation of the uniform current pattern of the $\gamma_0^0(\phi, \theta)$ orbitsphere shown with 30 degree increments ($N=M=12$ in Eq. (69)) of the angle to generate the orbitsphere current-vector field corresponding to Eq. (7) and 30 degree increments of the rotation of this basis element about the $(-i_x, i_y, i_z)$ -axis corresponding to Eq. (20). The great circle current loop that served as a basis element that was initially in the plane along the $(i_x, 0i_y, -i_z)$ - and y-axes of each secondary component orbitsphere-cvf is shown as red. The perspective is transverse to the z-axis.

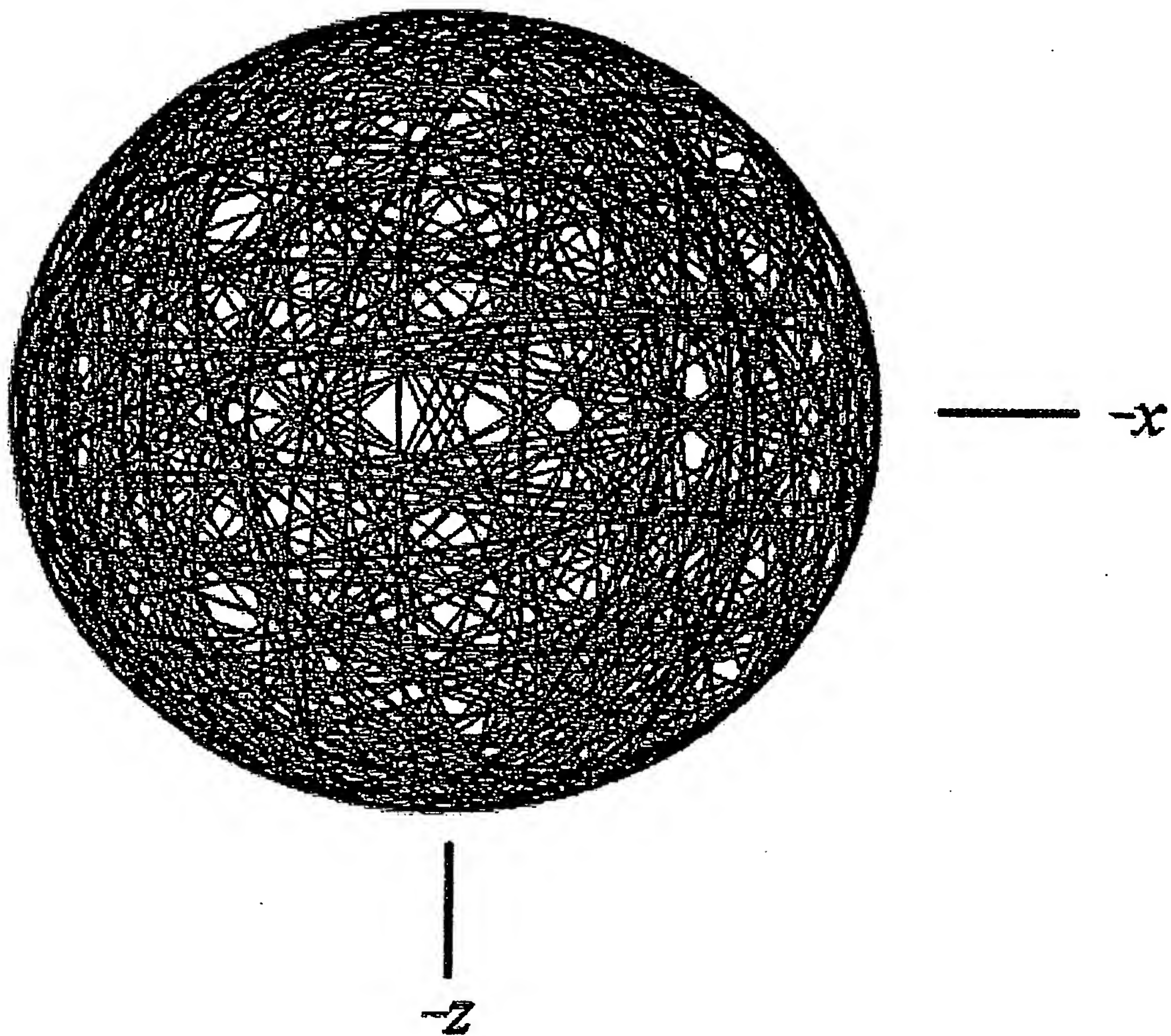
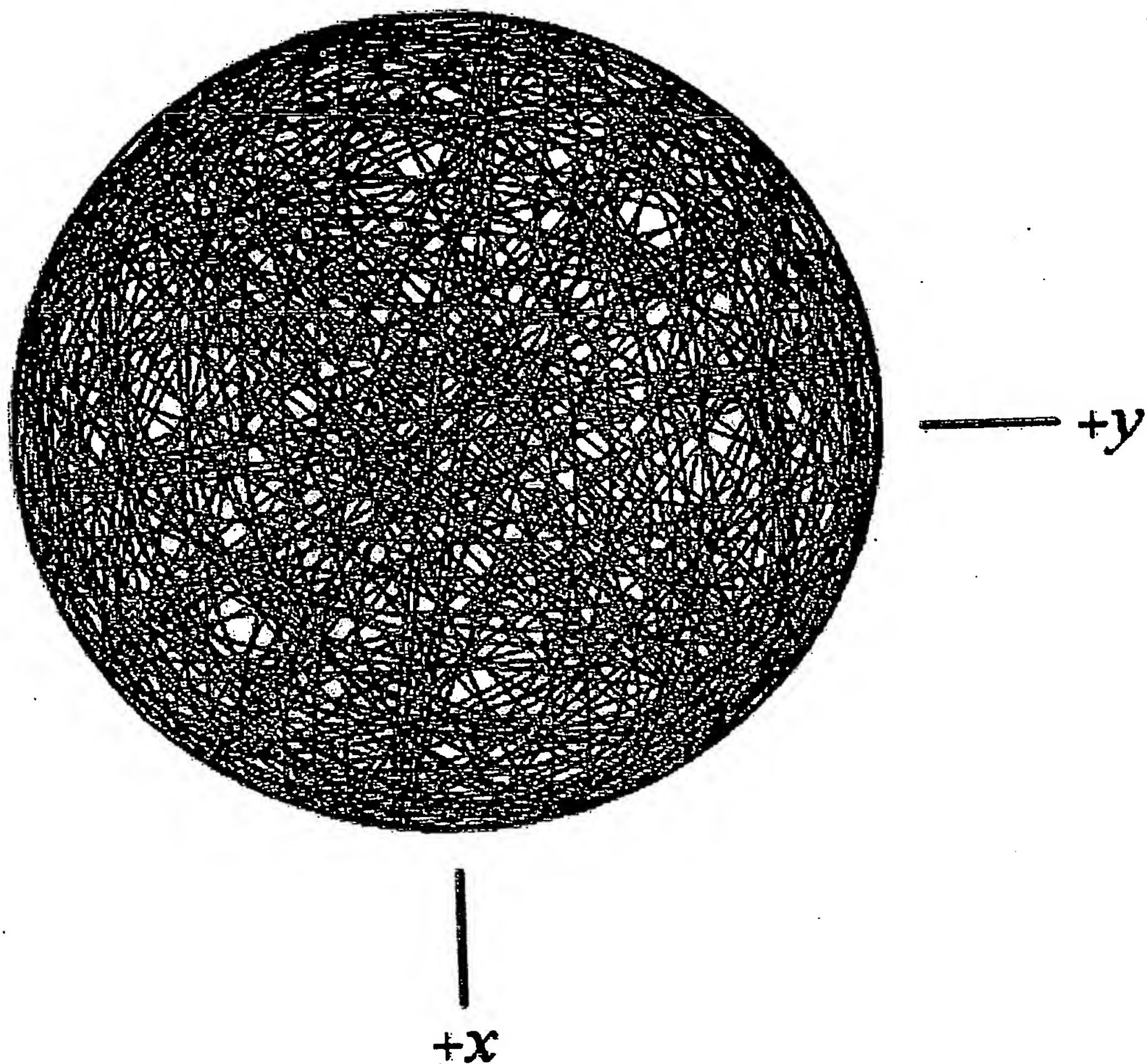


Figure 21. A representation of the uniform current pattern of the $Y_0^0(\phi, \theta)$ orbitsphere shown with 30 degree increments ($N=M=12$ in Eq. (69)) of the angle to generate the orbitsphere current-vector field corresponding to Eq. (7) and 30 degree increments of the rotation of this basis element about the $(-i_x, i_y, i_z)$ -axis corresponding to Eq. (20). The great circle current loop that served as a basis element that was initially in the plane along the $(i_x, 0i_y, -i_z)$ - and y-axes of each secondary component orbitsphere-cvf is not shown. The perspective is along the z-axis.



SIMPLE APPROXIMATION METHOD FOR VISUALIZING THE CURRENT PATTERN OF $Y_0^0(\phi, \theta)$ BY A DISCRETE CONVOLUTION ABOUT L_r

In addition, the angular momentum is constant with respect to

rotation of the orbitsphere-cvf about the axis of the resultant angular momentum vector, \mathbf{L}_R . In this case, the corresponding component angular momentum \mathbf{L}_x is rotationally constant about the xy-axis; thus, the corresponding \mathbf{L}_x and \mathbf{L}_y components are rotationally constant about the x-and y-axes, respectively. The component \mathbf{L}_z is further rotationally constant about the z-axis. The constancy of the angular momentum with respect to rotation about each of the principal axes determines that the corresponding rotational symmetry of each axes is C_∞ even though the spatial symmetry of the current distribution is less. Thus, a simple approximation of the convolution operation that preserves the angular momentum can be performed using the results of the Orbitsphere Equation of Motion for $\ell=0$ section by the superposition of orbitsphere-cvf at incremental angles about its resultant angular momentum axis shown in Figure 8 as given previously [73].

From Eqs. (1.73a) and (1.73b), the resultant angular momentum vector \mathbf{L}_R has magnitude $\frac{\sqrt{5}\hbar}{4}$ along the direction of the spherical-coordinate angles $\theta = 0.4636 \text{ rad}$, $\phi = \frac{3\pi}{4} \text{ rad}$. To perform the rotation about \mathbf{L}_R , the orbitsphere-cvf is first rotated counter clockwise about the vector $(\mathbf{i}_x, \mathbf{i}_y, 0\mathbf{i}_z)$ by an angle -0.4636 rad using Eq. (4) or using Eq. (1.70a) wherein $\Delta\alpha_x$ and $\Delta\alpha_y$ are each $-\sqrt{2}(0.4636) \text{ rad}$ to align \mathbf{L}_R with the z-axis as shown in Figure 8. Next, a series of n rotations are performed about the z-axis using Eq. (8) for a general angle, $\Delta\alpha_z = +q\frac{2\pi}{n}$ ($q=0,1,2,3,4\dots n$), or Eq. (1.70b) wherein $\Delta\alpha_z = +q\frac{2\pi}{n}$ ($q=0,1,2,3,4\dots n$) and $\Delta\alpha_x = 0$ to form $n+1$ orbitsphere-cvf elements. The superposition of the elements is normalized by $n+1$ and the final approximately uniform orbitsphere is rotated clockwise about the vector $(\mathbf{i}_x, \mathbf{i}_y, 0\mathbf{i}_z)$ by an angle 0.4636 rad using Eq. (4) or using Eq. (1.70a) wherein $\Delta\alpha_x$ and $\Delta\alpha_y$ are each $+\sqrt{2}(0.4636) \text{ rad}$.

A visual representation using an orbitsphere current-vector field generated with 12 degree increments of the infinitesimal angular variable $\pm\Delta\alpha_x$ and $\pm\Delta\alpha_y$ of Eqs. (1.70a) and (1.70b) as a basis element and using 24 degree increments of the rotation about \mathbf{L}_R from the perspective of along the axis of \mathbf{L}_R and perpendicular to \mathbf{L}_R are shown in Figures 22 and 23, respectively.

Figure 22. A quadrant of a simple approximation of the uniform current pattern of the $Y_0^0(\phi, \theta)$ orbitsphere shown with 12 degree increments of the infinitesimal angular variables $\pm\Delta\alpha_r$ and $\pm\Delta\alpha_\theta$ in Eqs. (1.70a) and (1.70b) to generate the orbitsphere current-vector field and 24 degree increments of the rotation of this basis element about L_R . The perspective is parallel to L_R .

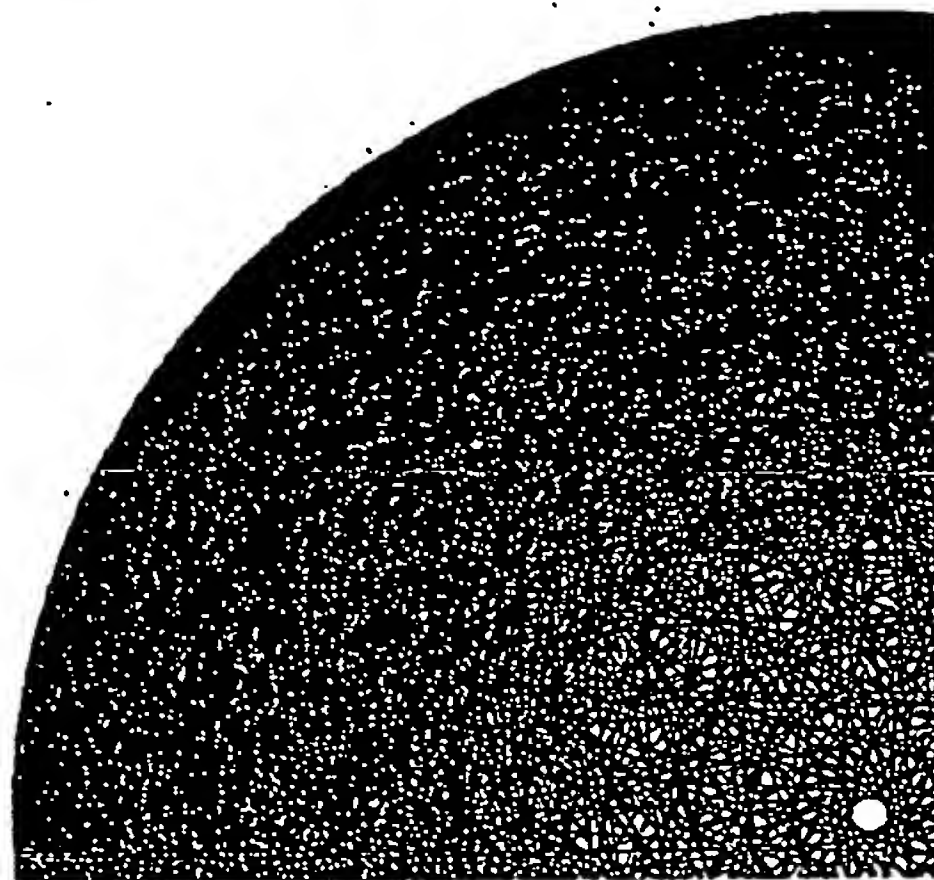
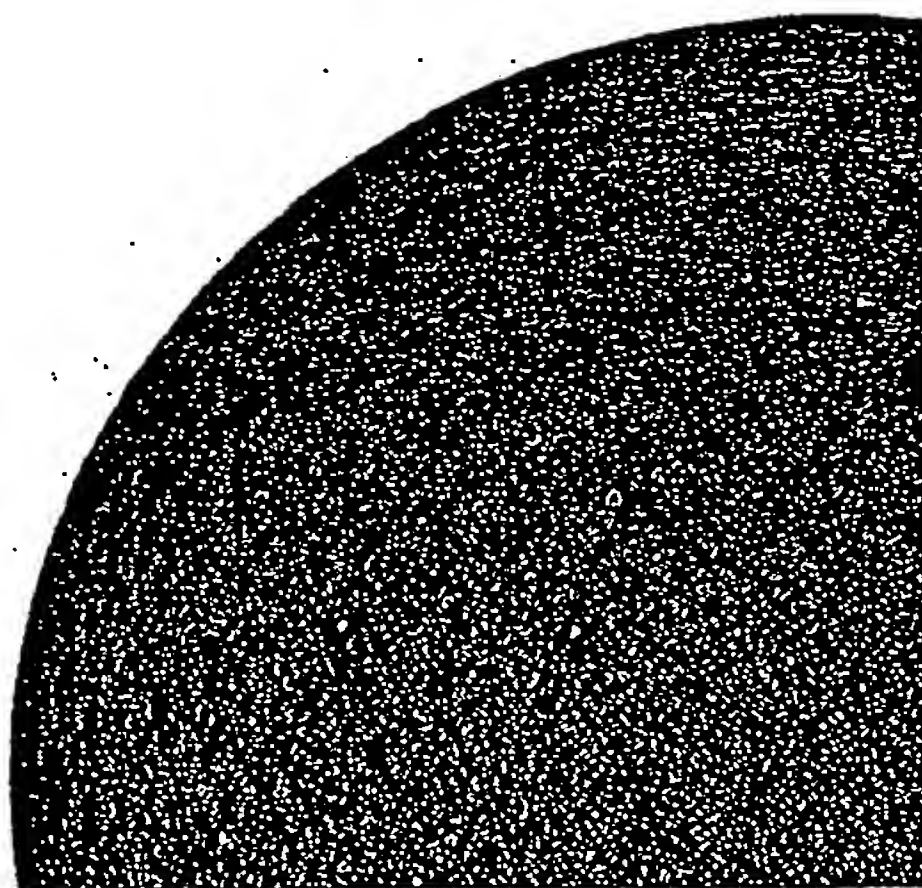


Figure 23. One quadrant of a simple approximation of the uniform current pattern of the $Y_0^0(\phi, \theta)$ orbitsphere shown with 12 degree increments of the infinitesimal angular variables $\pm\Delta\alpha_r$ and $\pm\Delta\alpha_\theta$ in Eqs. (1.70a) and (1.70b) to generate the orbitsphere current-vector field and 24 degree increments of the rotation of this basis element about L_R . The perspective is perpendicular to L_R .



APPENDIX IV

MUON g FACTOR

The muon, like the electron, is a lepton with \hbar of angular momentum. The magnetic moment of the muon is given by Eq. (1.136) with the electron mass replaced by the muon mass. It is twice that from the gyromagnetic ratio as given by Eq. (2.36) of the Orbital and Spin Splitting section corresponding to the muon mass. As is the case with the electron, the magnetic moment of the muon is the sum of the component corresponding to the kinetic angular momentum, $\frac{\hbar}{2}$, and the component corresponding to the vector potential angular momentum, $\frac{\hbar}{2}$, (Eq. (1.132)). The spin-flip transition can be considered as involving a magnetic moment of g times that of a Bohr magneton of the muon. The g factor (Eq. (1.196)) is

$$\frac{g}{2} = 1 + \frac{\alpha}{2\pi} + \frac{2}{3}\alpha^2 \left(\frac{\alpha}{2\pi} \right) - \frac{4}{3} \left(\frac{\alpha}{2\pi} \right)^2 \quad (1)$$

For $\alpha^{-1} = 137.03603(82)$ (Eq. 1.203)),

$$\frac{g}{2} = 1.001\,159\,652\,137 \quad (2)$$

The muon anomalous magnetic moment has been measured in a new experiment at Brookhaven National Laboratory (BNL) [32]. Polarized muons were stored in a superferric ring, and the angular frequency difference ω_a between the spin precession and orbital frequencies was determined by measuring the time distribution of high-energy decay positrons. The ratio R of ω_a to the Larmor precession frequency of free protons ω_p in the storage-ring magnetic field was measured. R is given by

$$R = \frac{\omega_a}{\omega_p} \quad (3)$$

The anomalous g value a_μ of the μ^+ was determined where the anomalous g value is related to the gyromagnetic ratio by

$$a_\mu = \frac{(g-2)}{2} \quad (4)$$

and

$$a_\mu = \frac{R}{\lambda - R} \quad (5)$$

where λ is the ratio of the muon and proton magnetic moments:

$$\lambda = \frac{\mu_\mu}{\mu_p} \quad (6)$$

According to Carey et al. [32], "For polarized muons moving in a uniform magnetic field \vec{B} , which is perpendicular to the muon spin direction and to the plane of the orbit, and with an electric quadrupole field \vec{E} for vertical focusing, the angular frequency difference, ω_a , between the spin precession frequency ω_s and the cyclotron frequency ω_c is given by

$$\bar{\omega}_a = -\frac{e}{m} \left[a_\mu \vec{B} - \left(a_\mu - \frac{1}{\gamma^2 - 1} \right) \vec{B} \times \vec{E} \right] \quad (7)$$

The dependence of ω_a on the electric field is eliminated by storing muons with the "magic" $\gamma=29.3$, which corresponds to a muon momentum $p=3.09 \text{ GeV}/c$. Hence measurement of ω_a and of B determines a_μ ."

Based on Lorentz covariance Jackson [33] gives the BMT equation which is the relativistic equation of motion for spin in uniform or slowly varying external fields. The rate of change of the component of spin s parallel to the velocity may be determined from the BMT equation. This is the longitudinal polarization or net helicity of the particle. If $\hat{\beta}$ is a unit vector in the direction of β , the longitudinal polarization is $\hat{\beta} \cdot s$. It changes in time because s changes and also β changes. The BMT equation in cgs units gives

$$\frac{d}{dt}(\hat{\beta} \cdot s) = -\frac{e}{mc} s_\perp \cdot \left[\left(\frac{g}{2} - 1 \right) \hat{\beta} \times \mathbf{B} + \left(\frac{g\beta}{2} - \frac{1}{\beta} \right) \mathbf{E} \right] \quad (8)$$

where s_\perp is the component of s perpendicular to the velocity. Eq. (8) demonstrates a remarkable property of a particle with $g=2$. In a purely magnetic field, the spin precesses in such a manner that the longitudinal polarization remains constant, whatever the motion of the particle. If the particle is relativistic ($\beta \rightarrow 1$), even the presence of an electric field causes the longitudinal polarization to change only very slowly, at a rate proportional to γ^{-2} times the electric field component perpendicular to v .

The "magic" γ given by Eq. (8) wherein the contribution to the change of the longitudinal polarization by the electric quadrupole focusing fields are eliminated occurs when

$$\frac{g_\mu \beta}{2} - \frac{1}{\beta} = 0 \quad (9)$$

where g_μ is the muon g factor which is required to be different from the electron g factor in the standard model due to the dependence of the mass dependent interaction of each lepton with vacuum polarizations due to virtual particles. For example, the muon is much heavier than the electron, and so high energy (short distance) effects due to strong and

weak interactions are more important here [29]. Also, according to the BNL collaboration [32]:

“The hadronic contribution and uncertainty are dominated by the single vacuum polarization loop with hadrons present, which is determined from a dispersion relationship using data from annihilation to hadrons and from hadronic decay. A contribution from higher order hadronic vacuum polarization and light-by-light scattering must be included”

The BNL Muon (g-2) Collaboration [32] used a “magic” $\gamma=29.3$ which satisfied Eq. (9) identically for $\frac{g_\mu}{2}$; however, their assumption that this condition eliminated the affect of the electrostatic field on ω_a is flawed as shown below. The relativistic factor γ is given by

$$\gamma = \frac{1}{\sqrt{1-\beta^2}} \quad (10)$$

where

$$\beta = \frac{v}{c} \quad (11)$$

Substitution of Eq. (9) into Eq. (10) gives

$$\gamma = \frac{1}{\sqrt{1-\frac{2}{g_\mu}}} \quad (12)$$

and

$$\beta_\mu = \sqrt{\frac{2}{g_\mu}} = \sqrt{1-\frac{1}{\gamma^2}} \quad (13)$$

From the BNL99 results and the average of the CERN and BNL97 results [32] an estimated value of $\frac{g_\mu}{2}$ is

$$\frac{g_\mu}{2} = 1.00116593 \quad (14)$$

Substitution of Eq. (14) into Eq. (12) gives the “magic” γ as

$$\gamma = 29.3033176 \quad (15)$$

and from Eq. (13),

$$\beta_\mu = 0.999417544 \quad (16)$$

As shown in the Electron g Factor section, in the case of an exact balance between the Lorentzian force (Eq. (1.151)) and the electric force corresponding to the Hall voltage (Eq. (1.152)), the superconducting condition is met when

$$\frac{E}{B} = v \quad (17)$$

which in cgs units is

$$E = \frac{Bv}{c} = B\beta_\mu \quad (18)$$

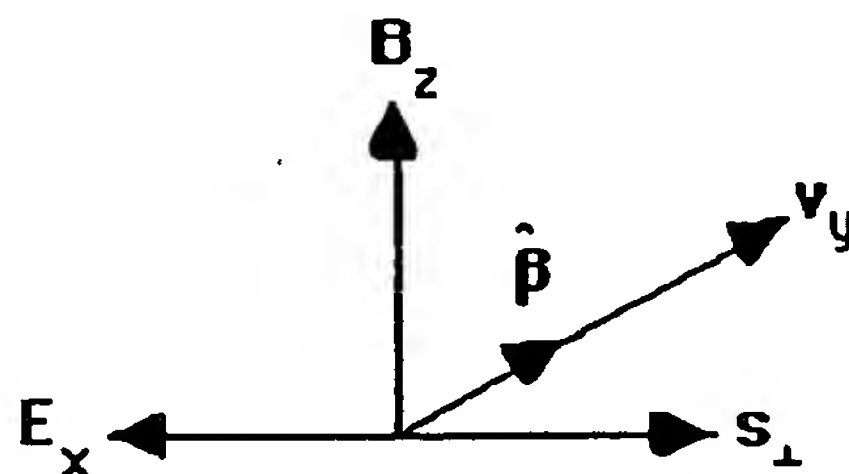
Consider the case that the g factor for the muon and the electron are the same and the “magic” $\gamma=29.3$ selected by the BNL Muon ($g-2$) Collaboration which satisfied Eq. (9) identically for $\frac{g_\mu}{2}$ (Eq. (1.197)) does not satisfy Eq. (9) for $\frac{g_e}{2}$ given by the experimental value (Eq. (27)). In this case, the second term of Eq. (8) contributes to ω_a . With $g=g_e$ and $\beta=\beta_\mu$, the BMT equation is

$$\frac{d}{dt}(\hat{\beta} \cdot s) = -\frac{e}{mc} s_\perp \cdot \left[\left(\frac{g_e}{2} - 1 \right) \hat{\beta} \times \mathbf{B} + \left(\frac{g_e \beta_\mu}{2} - \frac{1}{\beta_\mu} \right) \mathbf{E} \right] \quad (19)$$

Since \mathbf{B} is parallel to $s_\perp \times \hat{\beta}$ and since \mathbf{E} and s_\perp are anti-parallel, the electric field from Eq. (18) is

$$\mathbf{E} = -\beta_\mu \hat{\beta} \times \mathbf{B} \quad (20)$$

Figure 1. Coordinate system of crossed electric field, \mathbf{E}_x , corresponding to the Hall voltage, magnetic flux, \mathbf{B}_z , due to the applied field, the velocity, v_y , in the $\hat{\beta}$ direction, and s_\perp where $|\mathbf{E}| = \beta B$.



Then

$$\frac{d}{dt}(\hat{\beta} \cdot s) = -\frac{e}{mc} s_\perp \cdot \left[\left(\frac{g_e}{2} - 1 \right) - \left(\frac{g_e \beta_\mu^2}{2} - 1 \right) \right] \hat{\beta} \times \mathbf{B} \quad (21)$$

$$= -\frac{e}{mc} \left[\frac{g_e}{2} - \frac{g_e \beta_\mu^2}{2} \right] s_\perp \cdot (\hat{\beta} \times \mathbf{B}) \quad (22)$$

$$= -\frac{e}{mc} \left[\frac{g_e}{2} (1 - \beta_\mu^2) \right] s_\perp \cdot (\hat{\beta} \times \mathbf{B}) \quad (23)$$

In the case that $g = g_\mu \neq g_e$, the term in E of Eq. (8)

$$\frac{d}{dt}(\hat{\beta} \cdot \mathbf{s}) = -\frac{e}{mc} \left[\frac{g_\mu}{2} - 1 \right] \mathbf{s}_\perp \cdot (\hat{\beta} \times \mathbf{B}) \quad (24)$$

vanishes and a change in longitudinal polarization due to the finite electric term can be considered as an additional term to the electron g factor which gives rise to an effective g factor corresponding to $\frac{g_\mu}{2}$.

Comparison of Eq. (23) and Eq. (24) gives the effective value of $\frac{g_\mu}{2}$ which is the predicted experimental value for $\frac{g_\mu}{2}$:

$$\frac{g_\mu}{2} - 1 = \frac{g_e}{2} (1 - \beta_\mu^2) \quad (25)$$

$$\frac{g_\mu}{2} = 1 + \frac{g_e}{2} (1 - \beta_\mu^2) \quad (26)$$

Eq. (19) which gives the predicted experimental value for $\frac{g_\mu}{2}$ (Eq. (26)) corresponds to the experimental situation of the BNL measurement of $\frac{g_\mu}{2}$.

The experimental value of $\frac{g_e}{2}$ [27] is

$$\frac{g_e}{2} = 1.001\,159\,652\,188(4) \quad (27)$$

Substitution of $\frac{g_e}{2}$ and β_μ given by Eq. (27) and Eq. (16), respectively, into Eq. (26) gives the calculated effective muon g factor which is

$$\frac{g_\mu}{2} = 1.001\,165\,923 \quad (28)$$

The calculated result based on the equivalence of the muon and electron g factors is in agreement with the result of Carey et al. [32]:

$$\frac{g_\mu}{2} = 1.001\,165\,925\,(15) \quad (29)$$

Rather than indicating an expanded plethora of postulated supersymmetry virtual particles which make contributions such as smuon-neutralino and sneutrino-chargino loops as suggested by Brown et al. [34], the deviation of the experimental value of $\frac{g_\mu}{2}$ from that of the

standard model prediction simply indicates that the muon g factor is identical to the electron g factor. This could have been spotted immediately had the objectivity of the experimental design been given precedence over the assumption of the validity of the standard model. Given the ad hoc nonphysical nature of QED (See Appendix II: Quantum Electrodynamics is Purely Mathematical and Has No Basis in Reality) and the internal inconsistency of the theoretical basis of this experiment regarding using the classical BMT equation in a test of nonclassical QED, more scrutiny was especially warranted.

From Eqs. (26), (27), and (16), the difference between $\frac{g_\mu}{2}$ and $\frac{g_e}{2}$ due to the finite electric term of Eqs. (8) and (19) with $g = g_e$ is

$$\frac{g_\mu}{2} - \frac{g_e}{2} = 1 - \frac{g_e}{2} \beta_\mu^2 = 0.0000062705 \quad (30)$$

With the equivalence of the muon g factor and the electron g factor, the possibilities are limited for the occurrence of internal consistency during the determination of $\frac{g_\mu}{2}$ using the BMT equation with the flawed assumption that $\frac{g_\mu}{2} \neq \frac{g_e}{2}$. Consider the case of Eq. (9) with $g = g_e = g_\mu$ and $\beta = \beta_\mu$ with the corresponding “magic” γ given by Eqs. (10-13). An equation equivalent to Eq. (30) that gives rise to an internally consistent experimental observation of an effective muon g factor corresponding to $\beta = \beta_\mu$ is

$$\left[\frac{1}{\sqrt{\frac{2}{g_{\mu\gamma}}}} - \frac{g_e \sqrt{\frac{2}{g_{\mu\gamma}}}}{2} \right] \sqrt{\frac{2}{g_{\mu\gamma}}} = 0.0000062705 \quad (31)$$

$$1 - \frac{\frac{g_e}{2}}{\frac{g_{\mu\gamma}}{2}} = 0.0000062705 \quad (32)$$

where $g_{\mu\gamma}$ is the muon anomalous g factor selected before the experiment to fix the “magic” γ , 0.0000062705 given by Eq. (32) (also see Eq. (30)) is the difference between the projected experimental value of $\frac{g_\mu}{2}$ and the experimentally measured value of $\frac{g_e}{2}$. The experimental value of $\frac{g_e}{2}$ from Eq. (27) and the selected value of $\frac{g_{\mu\gamma}}{2}$ from Eq. (14) satisfy Eqs. (31-32)

and are in close agreement with the experimental value of $\frac{g_\mu}{2}$ determined by Carey et al. [32] (Eqs. (28-29)). The “magic” γ of BNL which gave an internally consistent but misinterpreted result was most likely arrived at by trial and error. Consider the following relationship between δ and $\frac{(g_{\mu\gamma}-2)}{2}$ of the “magic” γ that follows from Eq. (32):

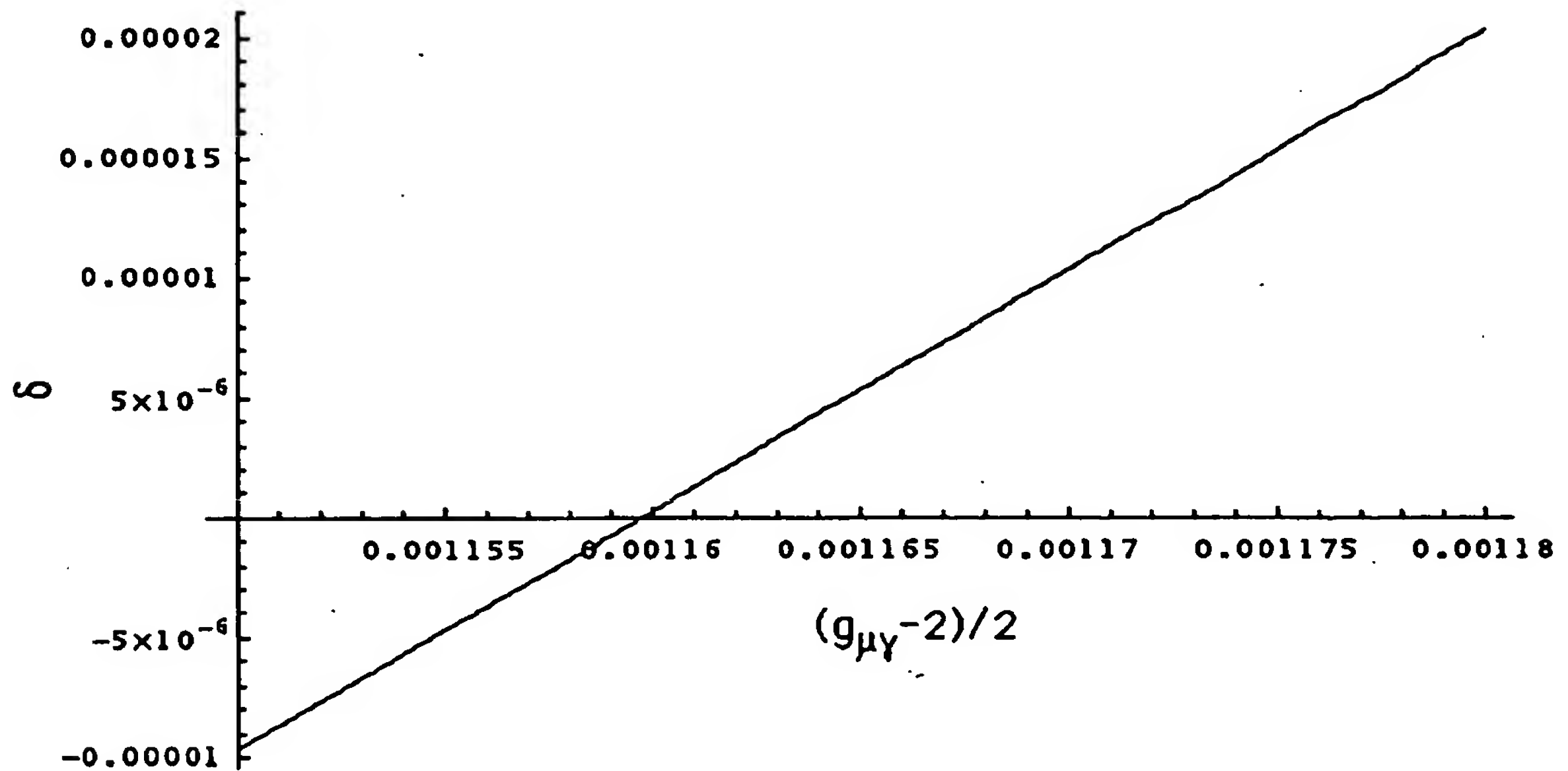
$$1 - \frac{\frac{g_e}{2}}{\frac{g_{\mu\gamma}}{2}} = \delta \quad (33)$$

where

$$\frac{(g_e-2)}{2} + \delta = \frac{(g_\mu-2)}{2} \quad (34)$$

and g_e is the experimentally measured electron anomalous g factor and g_μ is the projected experimental value of the muon anomalous g factor based on $g_{\mu\gamma}$, the selected value the muon anomalous g factor to fix the “magic” γ . A plot of δ versus $\frac{(g_{\mu\gamma}-2)}{2}$ from Eq. (33) is shown in Figure 2.

Figure 2. Plot of δ versus $\frac{(g_{\mu\gamma}-2)}{2}$ of the “magic” γ from Eq. (33).



Only a narrow range of values of $\frac{(g_{\mu\gamma}-2)}{2}$ about the value of $\frac{(g_{\mu}-2)}{2}$ measured by Carey et al. [32] are internally consistent.

Similar misinterpretations of data based on a bias towards quantum theory are described in the Schrödinger “Black” Cats section. For example, NIST claimed to have placed a ${}^9\text{Be}^+$ ion in two places at once when in reality an applied magnetic field and a potential well were found which forced a resonance between an oscillatory and a Stern-Gerlach transition. And, the resulting interference pattern in the fluorescence emission was misinterpreted as indicating that the ion was in two widely separated positions simultaneously [74]. The BNL experiment should be repeated to determine the dependence of ω_a on the “magic” γ . The current BNL results and classical theory support the equivalence of the electron and muon g factors.

Experimental determination of the proper β [75]

The angular frequency difference between the spin precession frequency and the cyclotron frequency, [27], is

$$\bar{\omega}_a = -\frac{e}{mc} \left[a_{\mu} \bar{\mathbf{B}} - \left(a_{\mu} - \frac{1}{\gamma^2 - 1} \right) \bar{\mathbf{B}} \times \bar{\mathbf{E}} \right] \quad (35)$$

Introducing the velocity ratio, β , and g ,

$$\gamma^2 - 1 = \frac{\beta^2}{1 - \beta^2}, \quad a_\mu = \frac{g}{2} - 1 \quad (36)$$

yields

$$\bar{\omega}_a = -\frac{e}{mc} \left[\left(\frac{g}{2} - 1 \right) \bar{\mathbf{B}} - \left(\frac{g}{2} - \frac{1}{\beta^2} \right) \bar{\mathbf{B}} \times \bar{\mathbf{E}} \right] \quad (37)$$

The unique value of β for which the term in \mathbf{E} vanishes is β^* :

$$\frac{g}{2} = \frac{1}{\beta^{*2}} \quad (38)$$

For $\beta = \beta^*$

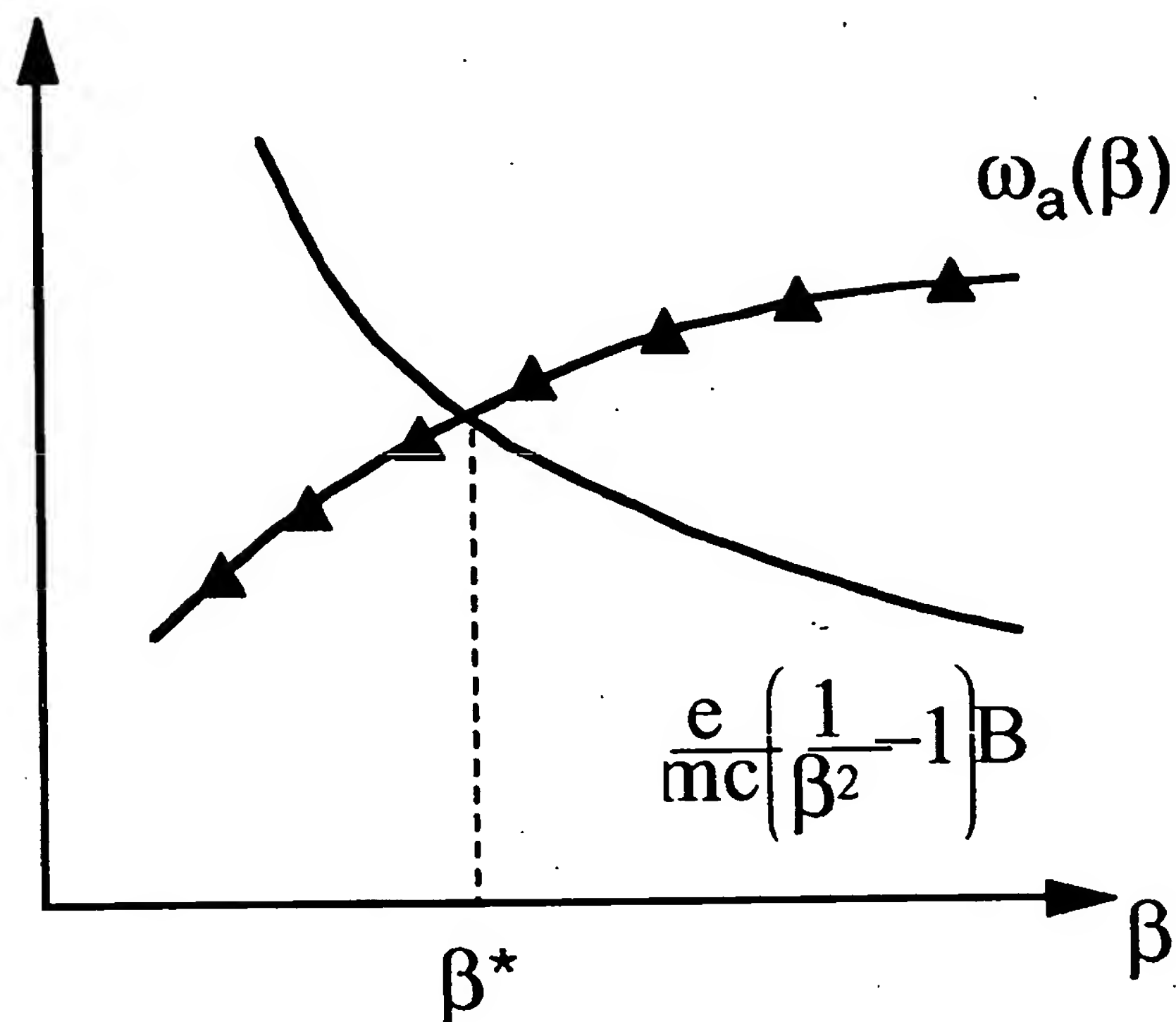
$$\bar{\omega}_a(\beta^*) = -\frac{e}{mc} \left(\frac{1}{\beta^{*2}} - 1 \right) \bar{\mathbf{B}} \quad (39)$$

Taking the magnitude results in

$$\omega_a(\beta^*) = \frac{e}{mc} \left(\frac{1}{\beta^{*2}} - 1 \right) B \quad (40)$$

The experimental measurement of the frequency difference for various β allows the graphical determination of β^* , (See Figure 3), with no assumption regarding g .

Figure 3. Plot of the experimental measurement of the frequency difference for various β which allows the graphical determination of β^* .



References

1. H. A. Haus, "On the radiation from point charges", American Journal of Physics, 54, (1986), pp. 1126-1129.
2. J. D. Jackson, Classical Electrodynamics, Second Edition, John Wiley & Sons, New York, (1975), p. 111.
3. R. N. Bracewell, The Fourier Transform and Its Applications, McGraw-Hill Book Company, New York, (1978), pp. 252-253.
4. W. McC. Siebert, Circuits, Signals, and Systems, The MIT Press, Cambridge, Massachusetts, (1986), p. 415.
5. Y. L. Luke, Integrals of Bessel Functions, McGrall-Hill, New York, (1962), p.22.
6. M. Abramowitz, I. Stegun (3rd Printing 1965), p. 366, eq. 9.1.10, and p. 255, eq. 6.1.6.
7. Y. L. Luke, Integrals of Bessel Functions, McGrall-Hill, New York, (1962), p.30.
8. H. Bateman, Tables of Integral Transforms, Vol. III, McGraw-Hill, New York, (1954), p. 33.

9. H. Bateman, Tables of Integral Transforms, Vol. III, McGraw-Hill, New York, (1954), p. 5.
10. G. O. Reynolds, J. B. DeVelis, G. B. Parrent, B. J. Thompson, The New Physical Optics Notebook, SPIE Optical Engineering Press, (1990).
11. T. A. Abbott, D. J. Griffiths, Am. J. Phys., Vol. 53, No. 12, (1985), pp. 1203-1211.
12. D. A. McQuarrie, Quantum Chemistry, University Science Books, Mill Valley, CA, (1983), pp. 206-221.
13. J. D. Jackson, Classical Electrodynamics, Second Edition, John Wiley & Sons, New York, (1975), p. 99.
14. B. Holverstott, R. Mills, "Modeling the Orbitsphere", posted at www.blacklightpower.com.
15. E. M. Purcell, Electricity and Magnetism, McGraw-Hill, New York, (1965), pp. 370-375, 447.
16. P. Pearle, Foundations of Physics, "Absence of radiationless motions of relativistically rigid classical electron", Vol. 7, Nos. 11/12, (1977), pp. 931-945.
17. G. R. Fowles, Analytical Mechanics, Third Edition, Holt, Rinehart, and Winston, New York, (1977), p. 196.
18. L. Pauling, E. B. Wilson, Introduction to Quantum Mechanics with Applications to Chemistry, McGraw-Hill Book Company, New York, (1935), pp. 118-121.
19. D. A. McQuarrie, Quantum Chemistry, University Science Books, Mill Valley, CA, (1983), pp. 238-241.
20. J. D. Jackson, Classical Electrodynamics, Second Edition, John Wiley & Sons, New York, (1975), p. 178.
21. J. D. Jackson, Classical Electrodynamics, Second Edition, John Wiley & Sons, New York, (1975), pp. 194-197.
22. C. E. Gough, M. S. Colclough, E. M. Forgan, R. G. Jordan, M. Keene, C. M. Muirhead, A. I. M. Rae, N. Thomas, J. S. Abell, S. Sutton, Nature, Vol. 326, (1987), p. 855.
23. S. Das Sarma, R. E. Prange, Science, Vol. 256, (1992), pp. 1284-1285.
24. J. D. Jackson, Classical Electrodynamics, Second Edition, John Wiley & Sons, New York, (1975), pp. 582-584.
25. J. D. Jackson, Classical Electrodynamics, Second Edition, John Wiley & Sons, New York, (1975), pp. 758-763.
26. R. C. Weast, CRC Handbook of Chemistry and Physics, 68 th Edition, CRC Press, Boca Raton, Florida, (1987-88), p. F-186 to p. F-187.
27. R. S. Van Dyck, Jr., P. Schwinberg, H. Dehmelt, "New high precision comparison of electron and positron g factors", Phys. Rev. Lett., Vol. 59, (1987), p. 26-29.
28. P. J. Mohr, B. N. Taylor, "CODATA recommended values of the fundamental physical constants: 1998", Reviews of Modern Physics,

- Vol. 72, No. 2, April, (2000), pp. 351-495.
29. G. P. Lepage, "Theoretical advances in quantum electrodynamics, International Conference on Atomic Physics, Atomic Physics; Proceedings, Singapore, World Scientific, Vol. 7, (1981), pp. 297-311.
 30. E. R. Williams and P. T. Olsen, Phys. Rev. Lett. Vol. 42, (1979), p. 1575.
 31. K. v. Klitzing et al., Phys. Rev. Lett. Vol. 45, (1980), p. 494.
 32. R. M. Carey et al., Muon (g-2) Collaboration, "New measurement of the anomalous magnetic moment of the positive muon", Phys. Rev. Lett., Vol. 82, (1999), pp. 1632-1635.
 33. J. D. Jackson, Classical Electrodynamics, Second Edition, John Wiley & Sons, New York, (1975), pp. 556-560.
 34. H. N. Brown et al., Muon (g-2) Collaboration, "Precise measurement of the positive muon anomalous magnetic moment", Phys. Rev. D62, 091101 (2000).
 35. F. Bueche, Introduction to Physics for Scientists and Engineers, McGraw-Hill, (1975), pp. 352-353.
 36. J. D. Jackson, *Classical Electrodynamics*, Second Edition, John Wiley & Sons, New York, (1975), pp. 236-240, 601-608, 786-790.
 37. E. M. Purcell, Electricity and Magnetism, McGraw-Hill, New York, (1985), Second Edition, pp. 451-458.
 38. J. D. Jackson, *Classical Electrodynamics*, Second Edition, John Wiley & Sons, New York, (1975), pp. 17-22
 39. H. A. Haus, J. R. Melcher, "Electromagnetic Fields and Energy", Department of Electrical engineering and Computer Science, Massachusetts Institute of Technology, (1985), Sec. 5.3.
 40. J. A. Stratton, *Electromagnetic Theory*, McGraw-Hill Book Company, (1941), p. 195.
 41. P. Sprangle and A. T. Drobot, "The linear and self-consistent nonlinear theory of the electron cyclotron maser instability", IEEE Transactions on Microwave Theory and Techniques, Vol. MTT-25, No. 6, June, (1977), pp. 528-544.
 42. J. D. Jackson, Classical Electrodynamics, Second Edition, John Wiley & Sons, New York, (1975), pp. 503-561.
 43. C. E. Moore, "Ionization Potentials and Ionization Limits Derived from the Analyses of Optical Spectra, Nat. Stand. Ref. Data Ser.-Nat. Bur. Stand. (U.S.), No. 34, 1970.
 44. D. R. Lide, *CRC Handbook of Chemistry and Physics*, 79 th Edition, CRC Press, Boca Raton, Florida, (1998-9), p. 10-175 to p. 10-177.
 45. G. Goedecke, Phys. Rev 135B, (1964), p. 281.
 46. J. Daboul and J. H. D. Jensen, Z. Physik, Vol. 265, (1973), pp. 455-478.
 47. L. C. Shi, J. A. Kong, Applied Electromagnetism, Brooks/Cole Engineering Division, Monterey, CA, (1983), pp. 170-209.
 48. J. D. Jackson, Classical Electrodynamics, Second Edition, John Wiley

- & Sons, New York, (1975), pp. 739-779.
49. V. F. Weisskopf, *Reviews of Modern Physics*, Vol. 21, No. 2, (1949), pp. 305-315.
 50. W. E. Lamb, R. C. Retherford, "Fine Structure of the Hydrogen Atom by a Microwave Method", *R. C., Phys. Rev.*, Vol. 72, No. 3, August 1, (1947), pp. 241-243.
 51. P. A. M. Dirac, From a Life of Physics, ed. A. Salam, et al., World Scientific, Singapore, (1989).
 52. P. W. Milonni, The Quantum Vacuum, Academic Press, Inc., Boston, p. 90.
 53. P. A. M. Dirac, Directions in Physics, ed. H. Hora and J. R. Shepanski, Wiley, New York, (1978), p. 36.
 54. P. J. Mohr and B. N. Taylor, "CODATA recommended values of the fundamental physical constants: 1998", *Reviews of Modern Physics*, Vol. 72, No. 2, April, (2000), p. 474.
 55. P. W. Milonni, The Quantum Vacuum An Introduction to Quantum Electrodynamics, Academic Press, Inc. Boston, pp. 107-111.
 56. P. W. Milonni, The Quantum Vacuum An Introduction to Quantum Electrodynamics, Academic Press, Inc. Boston, p. 108.
 57. G. P. Lepage, "Theoretical advances in quantum electrodynamics, International Conference on Atomic Physics, Atomic Physics; Proceedings, Singapore, World Scientific, Vol. 7, (1981), pp. 297-311.
 58. H. Wergeland, "The Klein Paradox Revisited", Old and New Questions in Physics, Cosmology, Philosophy, and Theoretical Biology, A. van der Merwe, Editor, Plenum Press, New York, (1983), pp. 503-515.
 59. Beiser, A., Concepts of Modern Physics, Fourth Edition, McGraw-Hill Book Company, New York, (1978), pp. 119-122.
 60. M. M. Waldrop, *Science*, Vol. 242, December, 2, (1988), pp. 1248-1250.
 61. S. W. Hawking, "Particle creation by black holes", *Commun. Math Phys.*, Vol. 43, (1975), pp. 199-220.
 62. S. W. Hawking, *Phys. Rev. D*, Vol. 14, (1976), pp. 2460-2473.
 63. P. F. Schewe and B. Stein, *Physic News Update*, The American Institute of Physics Bulletin of Physics News, Number 494, July 17, (2000).
 64. A. Allahverdyan, T. Nieuwenhuizen, *Phys. Rev. Lett.*, Vol. 85, No. 9, August 28, (2000), pp. 1799-1802.
 65. M. A. Seeds, Foundations of Astronomy, 1st Edition, Brooks/Cole, Pacific Grove, CA, (1980).
 66. *Sky and Telescope Magazine*, Feb. (1978), p. 113.
 67. *Sky and Telescope Magazine*, Aug. (1977), p. 84.
 68. P. W. Milonni, The Quantum Vacuum An Introduction to Quantum Electrodynamics, Academic Press, Inc. Boston, pp. 54-58.
 69. E. M. Lifshitz, "The theory of molecular attractive forces between

- solids", Soviet Physics, Vol. 2, No. 1, January, (1956), pp. 73-83.
70. S. K. Lamoreaux, "CF-1: Casimir Force", Am. J. Phys. Vol. 67, No. 10, October, (1999), p. 850-861.
 71. G. R. Fowles, Analytical Mechanics, Third Edition, Holt, Rinehart, and Winston, New York, (1977), pp. 17-20.
 72. W. McC. Siebert, Circuits, Signals, and Systems, The MIT Press, Cambridge, Massachusetts, (1986), p. 599.
 73. R. L. Mills, "Classical Quantum Mechanics", submitted.
 74. C. Monroe, D. M. Meekhof, B. E. King, D. J. Wineland, Science, Vol. 272, (1996), pp: 1131-1135.
 75. M. Nansteel, BlackLight Power, Inc., Cranbury, NJ, Personal Communication, May, (2001).

TWO-ELECTRON ATOMS

As is the case for one-electron atoms shown in the corresponding section, two-electron atoms can also be solved exactly. Two-electron atoms comprise two indistinguishable electrons bound to a nucleus of $+Z$. Each electron experiences a centrifugal force, and the balancing centripetal force (on each electron) is produced by the electric force between the electron and the nucleus and the magnetic force between the two electrons causing the electrons to pair.

DETERMINATION OF ORBITSPHERE RADII

As shown in the One-Electron Atom section, bound electrons are described by a charge-density (mass-density) function which is the product of a radial delta function ($f(r) = \delta(r - r_n)$), two angular functions (spherical harmonic functions), and a time harmonic function. Thus, an electron is a spinning, two-dimensional spherical surface, called an electron orbitsphere, that can exist in a bound state at only specified distances from the nucleus. More explicitly, the orbitsphere comprises a two-dimensional spherical shell of moving charge. The corresponding current pattern of the orbitsphere comprises an infinite series of correlated orthogonal great circle current loops. The current pattern (shown in Figure 1.5) is generated over the surface by two orthogonal sets of an infinite series of nested rotations of two orthogonal great circle current loops where the coordinate axes rotate with the two orthogonal great circles. Each infinitesimal rotation of the infinite series is about the new x-axis and new y-axis which results from the preceding such rotation. For each of the two sets of nested rotations, the angular sum of the rotations about each rotating x-axis and y-axis totals $\sqrt{2}\pi$ radians. The current pattern gives rise to the phenomenon corresponding to the spin quantum number. Each one-electron orbitsphere is a spherical shell of negative charge (total charge $= -e$) of zero thickness at a distance r_n from the nucleus (charge $= +Ze$). It is well known that the field of a spherical shell of charge is zero inside the shell and that of a point charge at the origin outside the shell [1] (See Figure 1.12). Thus, for a nucleus of charge Z , the force balance equation for the electron orbitsphere is obtained by equating the forces on the mass and charge densities. The centrifugal force of each electron is given by

$$F_{\text{centrifugal}} = \frac{m_e}{4\pi r_n^2} \frac{v_n^2}{r_n} \quad (7.1)$$

where r_n is the radius of electron n which has velocity v_n . In order to be nonradiative, the velocity for every point on the orbitsphere is given by Eq. (1.47).

$$v_n = \frac{\hbar}{m_e r_n} \quad (7.2)$$

Now, consider electron 1 initially at $r = r_1 = \frac{a_0}{Z}$ (the radius of the one-electron atom of charge Z given in the One-Electron Atom section where $a_0 = \frac{4\pi\epsilon_0\hbar^2}{e^2 m_e}$ and the spin-nuclear interaction corresponding to the electron reduced mass is not used here since the electrons have no field at the nucleus upon pairing) and electron 2 initially at $r_n = \infty$. Each electron can be treated as $-e$ charge at the nucleus with $E = \frac{-e}{4\pi\epsilon_0 r^2}$ for $r > r_n$ and $E = 0$ for $r < r_n$ where r_n is the radius of the electron orbitsphere. The centripetal force is the electric force, F_{ele} , between the electron and the nucleus. Thus, the electric force between electron 2 and the nucleus is

$$F_{ele(electron\ 2)} = \frac{(Z-1)e^2}{4\pi\epsilon_0 r_2^2} \quad (7.3)$$

where ϵ_0 is the permittivity of free-space. The second centripetal force, F_{mag} , on the electron 2 (initially at infinity) from electron 1 (at r_1) is the magnetic force. Each infinitesimal point (mass or charge-density element) of each orbitsphere moves on a great circle, and each point has the charge density $\frac{e}{4\pi r_n^2}$. Due to the relative motion of the charge-density elements of each electron, a radiation reaction force arises between the two electrons. This force given in Sections 6.6, 12.10, and 17.3 of Jackson [2] achieves the condition that the sum of the mechanical momentum and electromagnetic momentum is conserved. The magnetic central force is derived from the Lorentzian force which is relativistically corrected. The magnetic field of electron 2 at the radius of each infinitesimal point of electron 1 follows from Eq. (1.74b) after McQuarrie [3]:

$$B = \frac{\mu_0 e \hbar}{2m_e r_2^3} \quad (7.4)$$

where μ_0 is the permeability of free-space ($4\pi \times 10^{-7} \text{ N/A}^2$). The motion at each point of electron 1 in the presence of the magnetic field of electron 2 gives rise to a central force which acts at each point of electron 2. The Lorentzian force density at each point moving at velocity v given by Eq. (1.47) is

$$F_{mag} = \frac{e}{4\pi r_2^2} v \times B \quad (7.5)$$

Substitution of Eq. (1.47) for v and Eq. (7.4) for B gives

$$F_{mag} = \frac{1}{4\pi r_2^2} \left[\frac{e^2 \mu_o}{2m_e r_1} \right] \frac{\hbar^2}{m_e r_2^3} \quad (7.6)$$

Furthermore, the term in brackets can be expressed in terms of the fine structure constant α . The radius of the electron orbitsphere in the $v=c$ frame is λ_c , where $v=c$ corresponds to the magnetic field front propagation velocity which is the same in all inertial frames, independent of the electron velocity as shown by the velocity addition formula of special relativity [4]. From Eq. (1.57) and Eqs. (1.144-1.148)

$$\frac{e^2 \mu_o}{2m_e r_1} = 2\pi\alpha \frac{v}{c} \quad (7.7)$$

where $v=c$. Based on the relativistic invariance of the electron's magnetic moment of a Bohr magneton μ_B given by Eq. (1.99) as well as its invariant angular momentum of \hbar , it can be shown that the relativistic correction to Eq. (7.6) is $\frac{1}{Z}$ times the reciprocal of Eq. (7.7). As shown previously in the Atoms and Molecules—Determination of Orbitsphere Radii section, the radius term in the brackets of Eq. (7.6) is relativistically corrected due to invariance of charge under Gauss' Integral Law. The radius of the electron relative to the $v=c$ frame, r_a^* , is relativistically corrected as follows. The wave equation relationship is

$$v = \lambda \frac{\omega}{2\pi} \quad (7.8)$$

It can be demonstrated that the velocity of the electron orbitsphere satisfies the relationship for the velocity of a wave by substitution of Eqs. (1.43) and (1.55) into Eq. (7.8), which gives Eq. (1.47). The result of the substitution into Eq. (7.8) of c for v_n , of λ_n given by Eq. (2.2)

$$2\pi(kr_1) = 2\pi r_n = n\lambda_1 = \lambda_n \quad (7.9)$$

with r_1 given by Eq. (1.226)

$$r_1 = \frac{a_o}{Z} \quad (7.10)$$

for λ , and of ω_n given by Eq. (1.55)

$$\omega_n = \frac{\hbar}{m_e r_n^2} \quad (7.11)$$

for ω is

$$c = 2\pi \frac{\gamma^* a_o}{Z} \frac{\hbar}{m_e \left[\frac{\gamma^* a_o}{Z} \right]^2 2\pi} \quad (7.12)$$

$$\gamma^* = \frac{Zm_e c a_o}{\hbar} = \frac{Zm_e}{\hbar \sqrt{\epsilon_o \mu_o}} \frac{4\pi \epsilon_o \hbar^2}{e^2 m_e} = 4\pi Z \sqrt{\frac{\epsilon_o}{\mu_o}} \frac{\hbar}{e^2} = \alpha Z \quad (7.13)$$

where γ^* is the relativistic factor corresponding to the radius. It follows from Eq. (7.13) that the radius r_1 of Eq. (7.6) must be corrected by the

factor $(\alpha Z)^{-1}$.

Due to relativistic invariance of $\frac{e}{m_e}$ corresponding to the invariance of μ_B , the correction of the electron mass of the bracketed term of Eq. (7.6) is 2π as given in the Atoms and Molecules—Determination of Orbitsphere Radii section. By correcting the radius and the mass, the relativistic correction γ' due to the light speed electrodynamic central force is

$$\gamma' = \left(2\pi\alpha Z \frac{v}{c} \right)^{-1} \quad (7.14)$$

where $v=c$. Thus, $\frac{1}{Z}$ is substituted for the term in brackets in Eq. (7.6).

The force must be corrected for the vector projection of the velocity of electron 2 onto the z-axis. As given in the Spin Angular Momentum of the Orbitsphere with $\ell=0$ section, the application of a z directed magnetic field of electron 2 given by Eqs. (1.120) to the inner orbitsphere gives rise to a projection of the angular momentum of electron 1 onto an axis which precesses about the z-axis of $\sqrt{\frac{3}{4}}\hbar$. The projection of the force between electron 2 and electron 1 is equivalent to that of the angular momentum onto the axis which precesses about the z-axis, and is $\sqrt{s(s+1)} = \sqrt{\frac{3}{4}}$ times that of a point mass. Thus, Eq. (7.6) becomes

$$\mathbf{F}_{mag} = \frac{1}{4\pi r_2^2} \frac{1}{Z} \frac{\hbar^2}{m_e r_2^3} \sqrt{s(s+1)} \quad (7.15)$$

The outward centrifugal force on electron 2 is balanced by the electric force and the magnetic force (on electron 2),

$$\frac{m_e v_2^2}{4\pi r_2^2} = \frac{e}{4\pi r_2^2} \frac{(Z-1)e}{4\pi\epsilon_0 r_2^2} + \frac{1}{4\pi r_2^2} \frac{\hbar^2}{Z m_e r_2^3} \sqrt{s(s+1)} \quad (7.16)$$

From Eq. (1.47)

$$v_2^2 = \frac{\hbar^2}{m_e^2 r_2^2} \quad (7.17)$$

Then,

$$\frac{m_e v_2^2}{r_2} = \frac{\hbar^2}{m_e r_2^3} = \frac{(Z-1)e^2}{4\pi\epsilon_0 r_2^2} + \frac{1}{Z} \frac{\hbar^2}{m_e r_2^3} \sqrt{s(s+1)} \quad (7.18)$$

Solving for r_2 ,

$$r_2 = r_1 = a_0 \left(\frac{1}{Z-1} - \frac{\sqrt{s(s+1)}}{Z(Z-1)} \right); s = \frac{1}{2} \quad (7.19)$$

That is, the final radius of electron 2, r_2 , is given by Eq. (7.19); this is also the final radius of electron 1. The energies and radii of several two-

electron atoms are given in Table 7.1.

(Since the density factor always cancels, it will not be used in subsequent force balance equations).

ENERGY CALCULATIONS

The electric work to bring electron 2 to $r_2 = r_1$ is given by the integral of the electric force from infinity to r_1 ,

$$work(electric, electron2) = \frac{(Z-1)e^2}{8\pi\epsilon_0 r_1} \quad (7.20)$$

And, the electric energy is the negative of the electric work,

$$E(electric) = \frac{-(Z-1)e^2}{8\pi\epsilon_0 r_1} \quad (7.21)$$

The potential energy of each electron at $r = r_1$, is given as

$$V = \frac{-(Z-1)e^2}{4\pi\epsilon_0 r_1} \quad (7.22)$$

The kinetic energy is $\frac{1}{2}m_e v^2$, where v is given by Eq. (1.47).

$$T = \frac{1}{2} \frac{\hbar^2}{m_e r_1^2} \quad (7.23)$$

The magnetic work is the integral of the magnetic force from infinity to r_1 ,

$$work(magnetic, electron2) = -\frac{1}{2} \frac{1}{Z} \frac{\hbar^2}{m_e r_1^2} \sqrt{s(s+1)} \quad (7.24)$$

Conservation of Energy

Energy is conserved. Thus, the potential energy (electron 2 at r_1) with the nucleus plus the magnetic work (electron 2 going from infinity to r_1) must equal the sum of the negative of the electric work (electron 2 going from infinity to r_1) and the kinetic energy (electron 2 at r_1). This is shown below with Eq. (7.25) and Eq. (7.26).

$$-V(electron\ 2\ at\ r_1) = \frac{(Z-1)e^2}{8\pi\epsilon_0 r_1} + \frac{1}{2} \frac{1}{Z} \frac{\hbar^2}{m_e r_1^2} \sqrt{s(s+1)} - \frac{1}{2} \frac{\hbar^2}{m_e r_1^2} \quad (7.25)$$

and using r_1 for Eq. (7.19),

$$V(electron\ 2\ at\ r_1) = -\frac{(Z-1)e^2}{4\pi\epsilon_0 r_1} \quad (7.26)$$

This is also the potential energy of electron 1 where their potential energies are indistinguishable when $r_1 = r_2$.

Ionization Energies

During ionization, power must be conserved. Power flow is governed by the Poynting power theorem,

$$\nabla \cdot (\mathbf{E} \times \mathbf{H}) = -\frac{\partial}{\partial t} \left[\frac{1}{2} \mu_0 \mathbf{H} \cdot \mathbf{H} \right] - \frac{\partial}{\partial t} \left[\frac{1}{2} \epsilon_0 \mathbf{E} \cdot \mathbf{E} \right] - \mathbf{J} \cdot \mathbf{E} \quad (7.27)$$

Energy is superposable; thus, the calculation of the ionization energy is determined as a sum of the electric and magnetic contributions. Energy must be supplied to overcome the electric force of the nucleus, and this energy contribution is the negative of the electric work given by Eq. (7.21). Additionally, the electrons are initially spin paired at $r_1 = r_2 = 0.566987a_0$ producing no magnetic fields; whereas, following ionization, the electrons possess magnetic fields and corresponding energies. For helium, the contribution to the ionization energy is given as the energy stored in the magnetic fields of the two electrons at the initial radius where they become spin unpaired. Part of this energy and the corresponding relativistic term corresponds to the precession of the outer electron about the z-axis due to the spin angular momentum of the inner electron. These terms are the same as those of the corresponding terms of the hyperfine structure interval of muonium as given in the Muonium Hyperfine Structure Interval section. Thus, for helium, which has no electric field beyond r_1 the ionization energy is given by the general formula:

$$\text{Ionization Energy(He)} = -E(\text{electric}) + E(\text{magnetic}) \left(1 - \frac{1}{2} \left(\left(\frac{2}{3} \cos \frac{\pi}{3} \right)^2 + \alpha \right) \right) \quad (7.28)$$

where,

$$E(\text{electric}) = -\frac{(Z-1)e^2}{8\pi\epsilon_0 r_1} \quad (7.29)$$

$$E(\text{magnetic}) = \frac{2\pi\mu_0 e^2 \hbar^2}{m_e^2 r_1^3} = \frac{8\pi\mu_0 \mu_B^2}{r_1^3} \quad (7.30)$$

Eq. (7.30) is derived for each of the two electrons as Eq. (1.129) of the Magnetic Parameters of the Electron (Bohr Magnetron) section with the radius given by Eq. (7.19). With the substitution of the radius given by Eq. (7.19) into Eq. (1.47), the velocity v is given by

$$v = \frac{\hbar c}{\sqrt{\left(\frac{4\pi\epsilon_0 \hbar^2}{e^2} c \left(\frac{1}{Z-1} - \frac{\sqrt{3}}{Z(Z-1)} \right) \right)^2 + \hbar^2}} = \frac{\alpha c (Z-1)}{\sqrt{\left(1 - \frac{\sqrt{3}}{Z} \right)^2 + \alpha^2 (Z-1)^2}} \quad (7.31)$$

with $Z > 1$. For increasing Z , the velocity becomes a significant fraction of the speed of light; thus, special relativistic corrections were included in the calculation of the ionization energies of two-electron atoms given in

Table 7.1. The relativistic corrections follow from those given in the Special Relativistic Correction to the Ionization Energies section wherein the nuclear-electron magnetic interactions as well as the electron-electron interactions of two-electron atoms must be included to be precise.

For a nuclear charge Z greater than two, a quantized electric field exists outside of the orbitsphere of the unionized atom. During ionization, the energy contribution of the expansion of the orbitsphere of the ionized electron (electron 2) from r_1 to infinity in the presence of the electric fields present inside and outside of the orbitsphere is calculated as the $\mathbf{J} \cdot \mathbf{E}$ term of the Poynting theorem. This energy contribution can be determined by designing an energy cycle and considering the individual contributions of each electron (electron 1 and electron 2) in going from the initial unionized to the final ionized state. Consider two paired orbitspheres. Expansion of an orbitsphere in the presence of an electric field which is positive in the outward radial direction requires energy, and contraction of an orbitsphere in this field releases energy. Thus, the contribution of the $\mathbf{J} \cdot \mathbf{E}$ term to ionization is the difference in the energy required to expand one orbitsphere (electron 2) from r_1 to infinity and to contract one orbitsphere (electron 1) from infinity to r_1 . The energy contribution for the expanding orbitsphere follows the derivation of Eq. (1.193) of the ELECTRON g FACTOR section as follows (the vector direction is taken to give a positive dissipated energy):

Dissipated Energy

The $\mathbf{J} \cdot \mathbf{E}$ energy over time is derived from the central electric field from the nucleus against which electron 2 expands and the current of the expanding electron 2 wherein the latter is dependent of the magnetic field of the inner electron 1. The magnetic field of electron 1 gives rise to a Lorentz force on electron 2, and the dissipative current density of electron 2 depends on this force wherein the superconducting condition given by Eq. (1.155) is maintained with the electric field of electron 1. The magnetic flux at electron 2 due to electron 1 is given by that of Bohr magneton at the origin that follows from McQuarrie [3]:

$$\mathbf{B} = \frac{\mu_0 e \hbar}{2m_e r_2^3} \quad (7.32)$$

The magnetic force on electron 2 due to the magnetic field of electron 1 is the Lorentzian force given by Eq. (1.151). Substitution of Eq. (1.47) for \mathbf{v} and Eq. (7.32) for the magnetic flux into Eq. (1.151) gives

$$\mathbf{F}_{mag} = \frac{\mu_0 e^2 \hbar^2}{2m_e^2 r_2^4} \mathbf{i}_r \quad (7.33)$$

Furthermore, the velocity of electron 1 is inversely proportional to the

nuclear charge as given by Eqs. (1.56) and (1.226). Thus, in order to maintain the superconducting condition given by Eq. (1.155), the magnetic force corresponding to B must be given by

$$\mathbf{F}_{mag} = \frac{1}{Z} \frac{\mu_0 e^2 \hbar^2}{2m_e^2 r_2^4} \mathbf{i}_r \quad (7.34)$$

The expansion of the orbitsphere of electron 2 produces a current. The current over time $\Delta t \mathbf{J}$ is

$$\Delta t \mathbf{J} = \Delta t \sigma \mathbf{E}_f \quad (7.35)$$

where \mathbf{J} is the current density, Δt is the time interval, σ is the conductivity, and \mathbf{E}_f is the effective electric field defined as follows:

$$\mathbf{F} = q(\theta, \phi) \mathbf{E}_f \quad (7.36)$$

where \mathbf{F} is the magnetic force given by Eq. (7.34), and $q(\theta, \phi)$ is the angular charge density given as follows:

$$q(\theta, \phi) = \frac{e}{4\pi} \quad (7.37)$$

The orbit expands in free space; thus, the relation for the conductivity is

$$\Delta t \sigma = \epsilon_0 \quad (7.38)$$

The electric field provided by the nucleus for the expanding orbitsphere is

$$\mathbf{E} = \frac{(Z-2)e}{4\pi\epsilon_0 r_2^2} \mathbf{i}_r \quad (7.39)$$

where ϵ_0 is the permittivity of free space ($8.854 \times 10^{-12} \text{ C}^2 / \text{N} \cdot \text{m}^2$). Using Eqs. (7.34-7.39), the $\mathbf{J} \cdot \mathbf{E}$ energy density over time for the expansion of electron 2 with the contraction of electron 1 is

$$\Delta t(\mathbf{J} \cdot \mathbf{E}) = \frac{(Z-2)}{Z} \frac{\mu_0 e^2 \hbar^2}{2m_e^2 r_2^6} \quad (7.40)$$

The $\mathbf{J} \cdot \mathbf{E}$ energy over time is the volume integral of the energy density over time

$$[\Delta t(\mathbf{J} \cdot \mathbf{E})]_{\text{energy external}} = \int_0^{2\pi} \int_0^\pi \int_0^\infty \frac{(Z-2)}{Z} \frac{\mu_0 e^2 \hbar^2}{2m_e^2 r_2^6} r^2 \sin\theta dr d\theta d\Phi \quad (7.41)$$

$$[\Delta t(\mathbf{J} \cdot \mathbf{E})]_{\text{energy external}} = \frac{(Z-2)}{Z} \frac{2\pi\mu_0 e^2 \hbar^2}{3m_e^2 r_1^3} \quad (7.42)$$

The $\mathbf{J} \cdot \mathbf{E}$ energy over time involving the electric field external to the orbitsphere of electron 2 is $\frac{(Z-2)}{Z}$ times the magnetic energy stored in the space external to the orbitsphere as given by Eq. (1.127). The left and right sides of the Poynting theorem must balance. Given the form of the $\mathbf{J} \cdot \mathbf{E}$ energy over time involving the electric field external to the orbitsphere of electron 2 and given that the electric field inside of the orbitsphere is $Z-1$ times the electric field of a point charge, the $\mathbf{J} \cdot \mathbf{E}$

energy over time involving the electric field internal to the orbitsphere of electron 2 is $\frac{(Z-1)}{Z}$ times the magnetic energy stored inside of the orbitsphere as given by Eq. (1.125). This energy is

$$[\Delta t(\mathbf{J} \cdot \mathbf{E})]_{\text{energy internal}} = \frac{(Z-1)}{Z} \frac{4\pi\mu_0 e^2 \hbar^2}{3m_e^2 r_1^3} \quad (7.43)$$

Thus, the total $\mathbf{J} \cdot \mathbf{E}$ energy over time of electron 2 is the sum of Eqs. (7.42) and (7.43).

The $\mathbf{J} \cdot \mathbf{E}$ energy over time of electron 1 during contraction from infinity to r_1 is negative, and the equations for the external and internal contributions are of the same form as Eqs. (7.42) and (7.43) where the appropriate effective charge is substituted. The $\mathbf{J} \cdot \mathbf{E}$ energy over time involving the electric field external to the orbitsphere of electron 1 is

$$[\Delta t(\mathbf{J} \cdot \mathbf{E})]_{\text{energy external}} = \frac{(Z-1)}{Z} \frac{2\pi\mu_0 e^2 \hbar^2}{3m_e^2 r_1^3} \quad (7.44)$$

And, the $\mathbf{J} \cdot \mathbf{E}$ energy over time involving the electric field internal to the orbitsphere of electron 1 is

$$[\Delta t(\mathbf{J} \cdot \mathbf{E})]_{\text{energy internal}} = \frac{Z}{Z} \frac{4\pi\mu_0 e^2 \hbar^2}{3m_e^3 r_1^3} \quad (7.45)$$

The difference, Δ , between the $\mathbf{J} \cdot \mathbf{E}$ energy over time for expanding electron 2 from r_1 to infinity and contracting electron 1 from infinity to r_1 is $-\frac{1}{Z}$ times the stored magnetic energy given by Eq. (7.30).

$$\Delta = -\frac{1}{Z} \frac{2\pi\mu_0 e^2 \hbar^2}{m_e^2 r_1^3} \quad (7.46)$$

Thus, the ionization energies are given by

$$\text{Ionization Energy} = -\text{Electric Energy} - \frac{1}{Z} \text{Magnetic Energy} \quad (7.47)$$

The energies of several two-electron atoms are given in Table 7.1.

Table 7.1. Relativistically corrected ionization energies for some two-electron atoms.

2 e Atom	Z	r_1 (a_0) ^a	Electric Energy ^b (eV)	Magnetic Energy ^c (eV)	Velocity (m/s) ^d	γ ^e	Theoretical Ionization Energies ^f (eV)	Experimental Ionization Energies ^g (eV)	Relative Error ^h
He	2	0.566987	23.996467	0.590536	3.85845E+06	1.000021	24.58750	24.58741	-0.000004
Li ⁺	3	0.35566	76.509	2.543	6.15103E+06	1.00005	75.665	75.64018	-0.0003
Be ²⁺	4	0.26116	156.289	6.423	8.37668E+06	1.00010	154.699	153.89661	-0.0052
B ³⁺	5	0.20670	263.295	12.956	1.05840E+07	1.00016	260.746	259.37521	-0.0053
C ⁴⁺	6	0.17113	397.519	22.828	1.27836E+07	1.00024	393.809	392.087	-0.0044
N ⁵⁺	7	0.14605	558.958	36.728	1.49794E+07	1.00033	553.896	552.0718	-0.0033
O ⁶⁺	8	0.12739	747.610	55.340	1.71729E+07	1.00044	741.023	739.29	-0.0023
F ⁷⁺	9	0.11297	963.475	79.352	1.93649E+07	1.00057	955.211	953.9112	-0.0014
Ne ⁸⁺	10	0.10149	1206.551	109.451	2.15560E+07	1.00073	1196.483	1195.8286	-0.0005
Na ⁹⁺	11	0.09213	1476.840	146.322	2.37465E+07	1.00090	1464.871	1465.121	0.0002
Mg ¹⁰⁺	12	0.08435	1774.341	190.652	2.59364E+07	1.00110	1760.411	1761.805	0.0008
Al ¹¹⁺	13	0.07778	2099.05	243.13	2.81260E+07	1.00133	2083.15	2085.98	0.0014
Si ¹²⁺	14	0.07216	2450.98	304.44	3.03153E+07	1.00159	2433.13	2437.63	0.0018
P ¹³⁺	15	0.06730	2830.11	375.26	3.25043E+07	1.00188	2810.42	2816.91	0.0023
S ¹⁴⁺	16	0.06306	3236.46	456.30	3.46932E+07	1.00221	3215.09	3223.78	0.0027
Cl ¹⁵⁺	17	0.05932	3670.02	548.22	3.68819E+07	1.00258	3647.22	3658.521	0.0031
Ar ¹⁶⁺	18	0.05599	4130.79	651.72	3.90705E+07	1.00298	4106.91	4120.8857	0.0034
K ¹⁷⁺	19	0.05302	4618.77	767.49	4.12590E+07	1.00344	4594.25	4610.8	0.0036
Ca ¹⁸⁺	20	0.05035	5133.96	896.20	4.34475E+07	1.00394	5109.38	5128.8	0.0038
Sc ¹⁹⁺	21	0.04794	5676.37	1038.56	4.56358E+07	1.00450	5652.43	5674.8	0.0039
Ti ²⁰⁺	22	0.04574	6245.98	1195.24	4.78241E+07	1.00511	6223.55	6249	0.0041
V ²¹⁺	23	0.04374	6842.81	1366.92	5.00123E+07	1.00578	6822.93	6851.3	0.0041
Cr ²²⁺	24	0.04191	7466.85	1554.31	5.22005E+07	1.00652	7450.76	7481.7	0.0041
Mn ²³⁺	25	0.04022	8118.10	1758.08	5.43887E+07	1.00733	8107.25	8140.6	0.0041
Fe ²⁴⁺	26	0.03867	8796.56	1978.92	5.65768E+07	1.00821	8792.66	8828	0.0040
Co ²⁵⁺	27	0.03723	9502.23	2217.51	5.87649E+07	1.00917	9507.25	9544.1	0.0039
Ni ²⁶⁺	28	0.03589	10235.12	2474.55	6.09529E+07	1.01022	10251.33	10288.8	0.0036
Cu ²⁷⁺	29	0.03465	10995.21	2750.72	6.31409E+07	1.01136	11025.21	11062.38	0.0034

^a From Equation (7.19).^b From Equation (7.29).^c From Equation (7.30).^d From Equations (7.31).^e From Equation (1.250) with the velocity given by Eq. (7.31).^f From Equations (7.28) and (7.47) with $E(\text{electric})$ of Eq. (7.29) relativistically corrected by γ according to Eq.(1.251) except that the electron-nuclear electrodynamic relativistic factor corresponding to the reduced mass of Eqs. (1.213-1.223) was not included.^g From theoretical calculations for ions Ne^{8+} to Cu^{28+} [5-6].^h (Experimental-theoretical)/experimental.

The agreement between the experimental and calculated values of Table 7.1 is within the experimental capability of the spectroscopic determinations at large Z which relies on X-ray spectroscopy. In this case, the experimental capability is three to four significant figures which is consistent with the last column. The helium atom isoelectronic series is given in Table 7.1 [5-6] to much higher precision than the capability of X-ray spectroscopy, but these values are based on theoretical and interpolation techniques rather than data alone. Ionization energies are difficult to determine since the cut-off of the Rydberg series of lines at the ionization energy is often not observed, and the ionization energy must be determined from theoretical calculations, interpolation of He isoelectronic and Rydberg series, as well as direct experimental data.

The theoretical values for low Z can be improved by calculating the spin-nuclear relativistic factor which corresponds to the reduced mass for one-electron atoms given in the Determination of Orbitsphere Radii section.

HYDRIDE ION

The hydride ion comprises two indistinguishable electrons bound to a proton of $Z=+1$. Each electron experiences a centrifugal force, and the balancing centripetal force (on each electron) is produced by the electric force between the electron and the nucleus. In addition, a magnetic force exists between the two electrons causing the electrons to pair.

Determination of the Orbitsphere Radius

Consider the binding of a second electron to a hydrogen atom to form a hydride ion. The second electron experiences no central electric force because the electric field is zero outside of the radius of the first electron. However, the second electron experiences a magnetic force due to electron 1 causing it to pair with electron 1. Thus, electron 1 experiences the reaction force of electron 2 which acts as a centrifugal force. The force balance equation can be determined by equating the total forces acting on the two bound electrons taken together. The force balance equation for the paired electron orbitsphere is obtained by equating the forces on the mass and charge densities. The centrifugal force of both electrons is given by Eq. (7.1) and Eq. (7.2) where the mass is $2m_e$. Electric field lines end on charge. Since both electrons are paired at the same radius, the number of field lines ending on the charge density of electron 1 equals the number that end on the charge density of electron 2. The electric force is proportional to the number of field lines; thus, the centripetal electric force, F_{ele} , between the electrons and the nucleus is

$$F_{ele(electron\ 1,2)} = \frac{\frac{1}{2}e^2}{4\pi\epsilon_0 r_n^2} \quad (7.48)$$

where ϵ_0 is the permittivity of free-space. The outward magnetic force on the two paired electrons is given by the negative of Eq. (7.15) where the mass is $2m_e$. The outward centrifugal force and magnetic forces on electrons 1 and 2 are balanced by the electric force

$$\frac{\hbar^2}{2m_e r_2^3} = \frac{\frac{1}{2}e^2}{4\pi\epsilon_0 r_2^2} - \frac{1}{Z} \frac{\hbar^2}{2m_e r_2^3} \sqrt{s(s+1)} \quad (7.49)$$

where $Z=1$. Solving for r_2 ,

$$r_2 = r_1 = a_0 \left(1 + \sqrt{s(s+1)}\right); s = \frac{1}{2} \quad (7.50)$$

where a_0 is given by Eq. (1.225). That is, the final radius of electron 2, r_2 , is given by Eq. (7.50); this is also the final radius of electron 1.

Ionization Energy

Since the hydrogen atom is neutral, the ionization energy of the hydride ion is determined from the magnetic energy balance. During ionization, electron 2 is moved to infinity. By the selection rules for absorption of electromagnetic radiation dictated by conservation of angular momentum, absorption of a photon causes the spin axes of the antiparallel spin-paired electrons to become parallel. The unpairing energy, $E_{unpairing}(magnetic)$, is given by Eq. (7.30) and Eq. (7.50) multiplied by two because the magnetic energy is proportional to the square of the magnetic field as derived in Eqs. (1.122-1.129). The magnetic energy of electron 1 following ionization of the hydride ion, $E_{electron\ 1\ final}(magnetic)$, is given by Eq. (1.129) and Eq. (1.229).

In addition, a third ionization energy term arises from the interaction of the two electrons during ionization. A magnetic force exists on the electron to be ionized due to the spin-spin interaction. The energy to move electron 2 to a radius which is infinitesimally greater than that of electron 1 is zero. In this case, the only force acting on electron 2 is the magnetic force. Due to conservation of energy, the potential energy change to move electron 2 to infinity to ionize the hydride ion can be calculated from the magnetic force of Eq. (7.49). The magnetic work, $E_{magwork}$, is the negative integral of the magnetic force (the second term on the right side of Eq. (7.49)) from r_2 to infinity,

$$E_{magwork} = \int_{r_2}^{\infty} \frac{\hbar^2}{2m_e r^3} \sqrt{s(s+1)} dr \quad (7.51)$$

where r_2 is given by Eq. (7.50). The result of the integration is

$$E_{magwork} = \frac{\hbar^2 \sqrt{s(s+1)}}{4m_e a_0^2 [1 + \sqrt{s(s+1)}]^2} \quad (7.52)$$

where $s = \frac{1}{2}$. By moving electron 2 to infinity, electron 1 moves to the radius $r_1 = a_H$, and the corresponding magnetic energy, $E_{electron\ 1\ final}(magnetic)$, is given by Eq. (7.30). In the present case of an inverse squared central field corresponding to the reaction force on electron 1, the magnitude of the binding energy is one half the magnitude of the potential energy [7] which is equivalent to that of Eq. (7.52). Thus, the ionization energy is given by subtracting the two magnetic energy terms from one half the magnetic work (Eq. (7.52)) wherein m_e is the electron reduced mass

$$\mu_e = \frac{m_e m_p}{\frac{m_e}{\sqrt{3}} + m_p}$$

due to the electrodynamic magnetic energy that arises from the force between the unpaired electrons and the nucleus which follows from Eqs. (1.222-1.224) and Eq. (7.51)¹. The electrodynamic force goes to zero as the two electrons pair due to the cancellation of the electron currents and magnetic fields. Thus, the corresponding reduced mass only appears in the $E_{magwork}$ term and in the magnetic energy of the free hydrogen atom term, $E_{electron\ 1\ final}(magnetic)$. Thus, the ionization energy of the hydride ion is given by

¹ The electrodynamic force between the unpaired electrons and the nucleus which follows from Eqs. (1.222-1.224) goes to zero as the two electrons pair due to the cancellation of the electron currents and magnetic fields. During ionization, the corresponding energy due to the unpaired electrons is given by

$$E_{electrodynamic\ magwork} = \frac{\hbar^2}{2m_p r_1^2} \sqrt{s(s+1)} - \int_{r_2}^{\infty} \frac{\hbar^2}{2m_p r^3} \sqrt{s(s+1)} dr \quad (1)$$

where the mass in Eq. (1.214) is $2m_e$. Eq. (7.51) with the inclusion of the electrodynamic energy given by Eq. (1) is

$$E_{magwork} = \int_{r_2}^{\infty} \frac{\hbar^2}{2r^3} \sqrt{s(s+1)} \left(\frac{1}{m_e} + \frac{1}{m_p \sqrt{s(s+1)}} \right) dr \quad (2)$$

Thus, Eq. (7.52) with the electrodynamic energy is given by

$$E_{magwork} = \frac{\hbar^2 \sqrt{s(s+1)}}{4\mu_e a_0^2 [1 + \sqrt{s(s+1)}]^2} \quad (3)$$

where the electron reduced mass is

$$\mu_e = \frac{m_e m_p}{\frac{m_e}{\sqrt{3}} + m_p} \quad (4)$$

$$\begin{aligned} \text{Ionization Energy} &= \frac{1}{2} E_{\text{magwork}} - E_{\text{electron 1 final}}(\text{magnetic}) - E_{\text{unpairing}}(\text{magnetic}) \\ &= \frac{\hbar^2 \sqrt{s(s+1)}}{8\mu_e a_0^2 [1 + \sqrt{s(s+1)}]^2} - \frac{\pi\mu_0 e^2 \hbar^2}{m_e^2} \left(\frac{1}{a_H^3} + \frac{2^2}{a_0^3 [1 + \sqrt{s(s+1)}]^3} \right) \end{aligned} \quad (7.53)$$

From Eq. (7.53), the calculated ionization energy of the hydride ion is 0.75418 eV.

The experimental value given by Lykke [8] is $6082.99 \pm 0.15 \text{ cm}^{-1}$ (0.75418 eV).

Without deriving the details of the nuclear structure of the deuterium nucleus and its magnetic moment, the electrodynamic magnetic energy term of the deuterium hydride ion due to the corresponding force between the interacting electrons and the nucleus with two nucleons may be taken as twice that of hydrogen which has only one nucleon. From Eqs. (1.222-1.224) and Eq. (7.52), the

corresponding reduced electron mass in Eq. (7.53) is $\mu_e = \frac{m_e m_p}{\frac{2m_e}{\sqrt{\frac{3}{4}}} + m_p}$.

From Eq. (7.53), the calculated ionization energy of the deuterium hydride ion is 0.75471 eV.

The experimental value given by Lykke [8] is $6086.2 \pm 0.6 \text{ cm}^{-1}$ (0.75457 eV).

HYDRINO HYDRIDE ION

The hydrino atom $H(1/2)$ can form a stable hydride ion. The central field is twice that of the hydrogen atom, and it follows from Eq. (7.49) that the radius of the hydrino hydride ion $H^-(n=1/2)$ is one half that of atomic hydrogen hydride, $H^-(n=1)$, given by Eq. (7.50).

$$r_2 = r_1 = \frac{a_0}{2} (1 + \sqrt{s(s+1)}); s = \frac{1}{2} \quad (7.54)$$

The energy follows from Eq. (7.53) and Eq. (7.54) where due to the invariance of e/m and \hbar for lower-energy states as well as excited states as shown in the SPIN-ORBITAL COUPLING section, the relativistic correction to the binding of the electron to a hydrogen atom or hydrino atom is the energy stored in the magnetic field of the hydrogen atom.

$$\begin{aligned} \text{Ionization Energy} &= \frac{1}{2} E_{\text{magwork}} - E_{\text{electron 1 final}}(\text{magnetic}) - E_{\text{unpairing}}(\text{magnetic}) \\ &= \frac{\hbar^2 \sqrt{s(s+1)}}{8\mu_e a_0^2 \left[\frac{1 + \sqrt{s(s+1)}}{2} \right]^2} - \frac{\pi\mu_0 e^2 \hbar^2}{m_e^2} \left(\frac{1}{a_H^3} + \frac{2^2}{a_0^3 \left[\frac{1 + \sqrt{s(s+1)}}{2} \right]^3} \right) \end{aligned} \quad (7.55)$$

From Eq. (7.55), the calculated ionization energy of the hydrino hydride ion $H^-(n=1/2)$ is 3.047 eV which corresponds to a wavelength of $\lambda = 407 \text{ nm}$.

In general, the central field of hydrino atom $H(n=1/p)$; $p = \text{integer}$ is p times that of the hydrogen atom. Thus, the force balance equation is

$$\frac{\hbar^2}{2m_e r_2^3} = \frac{\frac{p}{2} e^2}{4\pi\epsilon_0 r_2^2} - \frac{1}{Z} \frac{\hbar^2}{2m_e r_2^3} \sqrt{s(s+1)} \quad (7.56)$$

where $Z=1$ because the field is zero for $r > r_1$. Solving for r_2 ,

$$r_2 = r_1 = \frac{a_0}{p} (1 + \sqrt{s(s+1)}); s = \frac{1}{2} \quad (7.57)$$

From Eq. (7.57), the radius of the hydrino hydride ion $H^-(n=1/p)$; $p = \text{integer}$ is $\frac{1}{p}$ that of atomic hydrogen hydride, $H^-(n=1)$, given by Eq. (7.50). The energy follows from Eq. (7.53) and Eq. (7.57).

$$\begin{aligned} \text{Ionization Energy} &= \frac{1}{2} E_{\text{magwork}} - E_{\text{electron 1 final}}(\text{magnetic}) - E_{\text{unpairing}}(\text{magnetic}) \\ &= \frac{\hbar^2 \sqrt{s(s+1)}}{8\mu_e a_0^2 \left[\frac{1 + \sqrt{s(s+1)}}{p} \right]^2} - \frac{\pi\mu_0 e^2 \hbar^2}{m_e^2} \left(\frac{1}{a_H^3} + \frac{2^2}{a_0^3 \left[\frac{1 + \sqrt{s(s+1)}}{p} \right]^3} \right) \end{aligned} \quad (7.58)$$

From Eq. (7.58), the calculated ionization energy of the hydrino hydride ion $H^-(n=1/p)$ as a function of p is given in Table 7.2.

Table 7.2. The ionization energy of the hydrino hydride ion $H^-(n=1/p)$ as a function of p .

Hydride Ion	r_1 (a_0) ^a	Calculated Ionization Energy ^b (eV)	Calculated Wavelength (nm)
$H^-(n=1)$	1.8660	0.7542	1644
$H^-(n=1/2)$	0.9330	3.047	406.9
$H^-(n=1/3)$	0.6220	6.610	187.6
$H^-(n=1/4)$	0.4665	11.23	110.4
$H^-(n=1/5)$	0.3732	16.70	74.23
$H^-(n=1/6)$	0.3110	22.81	54.35
$H^-(n=1/7)$	0.2666	29.34	42.25
$H^-(n=1/8)$	0.2333	36.09	34.46
$H^-(n=1/9)$	0.2073	42.84	28.94
$H^-(n=1/10)$	0.1866	49.38	25.11
$H^-(n=1/11)$	0.1696	55.50	22.34
$H^-(n=1/12)$	0.1555	60.98	20.33
$H^-(n=1/13)$	0.1435	65.63	18.89
$H^-(n=1/14)$	0.1333	69.22	17.91
$H^-(n=1/15)$	0.1244	71.55	17.33
$H^-(n=1/16)$	0.1166	72.40	17.12
$H^-(n=1/17)$	0.1098	71.56	17.33
$H^-(n=1/18)$	0.1037	68.83	18.01
$H^-(n=1/19)$	0.0982	63.98	19.38
$H^-(n=1/20)$	0.0933	56.81	21.82
$H^-(n=1/21)$	0.0889	47.11	26.32
$H^-(n=1/22)$	0.0848	34.66	35.76
$H^-(n=1/23)$	0.0811	19.26	64.36
$H^-(n=1/24)$	0.0778	0.6945	1785
$H^-(n=1/25)$		not stable	

^a from Equation (7.57)

^b from Equation (7.58)

HYDRINO HYDRIDE ION NUCLEAR MAGNETIC RESONANCE SHIFT

The proton gyromagnetic ratio $\gamma_p/2\pi$ is

$$\gamma_p / 2\pi = 42.57602 \text{ MHz } T^{-1} \quad (7.59)$$

The NMR frequency f is the product of the proton gyromagnetic ratio given by Eq. (7.59) and the magnetic flux B .

$$f = \gamma_p / 2\pi B = 42.57602 \text{ MHz } T^{-1} B \quad (7.60)$$

A typical flux for a superconducting NMR magnet is 1.5 T . According to Eq. (7.60) this corresponds to a radio frequency (RF) of 63.86403 MHz . With a constant magnetic field, the frequency is scanned to yield the spectrum. Or, in a common type of NMR spectrometer, the radiofrequency is held constant (e.g. 60 MHz), the applied magnetic field H_0 ($H_0 = \frac{B}{\mu_0}$) is varied

over a small range, and the frequency of energy absorption is recorded at the various values for H_0 . The spectrum is typically scanned and displayed as a function of increasing H_0 . The protons that absorb energy at a lower H_0 give rise to a downfield absorption peak; whereas, the protons that absorb energy at a higher H_0 give rise to an upfield absorption peak. The electrons of the compound of a sample influence the field at the nucleus such that it deviates slightly from the applied value. For the case that the chemical environment has no NMR effect, the value of H_0 at resonance with the radiofrequency held constant at 60 MHz is

$$\frac{2\pi f}{\mu_0 \gamma_p} = \frac{(2\pi)(60 \text{ MHz})}{\mu_0 42.57602 \text{ MHz } T^{-1}} = H_0 \quad (7.61)$$

In the case that the chemical environment has a NMR effect, a different value of H_0 is required for resonance. This chemical shift is proportional to the electronic magnetic flux change at the nucleus due to the applied field which in the case of each hydride ion is a function of its radius.

The change in the magnetic moment, Δm , of each electron of the hydride ion due to an applied magnetic flux B is [9]

$$\Delta m = -\frac{e^2 r^2 B}{4m_e} \quad (7.62)$$

The two electrons are spin-paired and the velocities are mirror opposites. Thus, the change in velocity of each electron treated individually (Eq. (10.3)) due to the applied field would be equal and opposite. However, as shown in the Three Electron Atom section, the two paired electrons may be treated as one with twice the mass where m_e is replaced by $2m_e$ in Eq. (7.62). In this case, the paired electrons spin together about the applied field axis, the z-axis, to cause a reduction in the applied field according to Lenz's law. Then, the radius in Eq. (7.62) corresponds to the coordinate ρ in cylindrical coordinates since it is perpendicular to the direction of the

applied field along the z-axis. The integral over the entire flux linked by the hydride ion orbitsphere is given by

$$\Delta m = -\frac{e^2 B}{8m_e} \frac{\int_0^{r_1} (r_1^2 - z^2) dz}{2r_1} = -\frac{2}{3} \frac{e^2 r_1^2 B}{8m_e} \quad (7.63)$$

where r_1 is the radius of the hydride ion [10]. The change in magnetic flux ΔB at the nucleus due to the change in magnetic moment, Δm , given by Eq. (7.63) follows from Eq. (1.100).

$$\Delta B = \mu_0 \frac{\Delta m}{r_1^3} (i_r \cos \theta - i_\theta \sin \theta) \quad \text{for } r < r_n \quad (7.64)$$

where μ_0 is the permeability of vacuum. Substitution of Eq. (7.63) into Eq. (7.64) gives the absolute upfield chemical shift $\frac{\Delta B}{B}$ of $H^-(1/1)$ relative to a bare proton:

$$\begin{aligned} \frac{\Delta B_r}{B} &= -\mu_0 \frac{pe^2}{12m_e a_0 (1 + \sqrt{s(s+1)})} \\ &= -p29.9 \text{ ppm} \end{aligned} \quad (7.65)$$

where $p=1$ for $H^-(1/1)$.

It follows from Eqs. (7.57) and (7.65) that the diamagnetic flux (flux opposite to the applied field) at the nucleus is inversely proportional to the radius, $r_1 = \frac{a_0}{p} (1 + \sqrt{s(s+1)})$. For resonance to occur, ΔH_0 , the change in applied field from that given by Eq. (7.61), must compensate by an equal and opposite amount as the field due to the electrons of the hydrino hydride ion.

According to Eq. (7.57), the ratio of the radius of the hydrino hydride ion $H^-(1/p)$ to that of the hydride ion $H^-(1/1)$ is the reciprocal of an integer p . It follows from Eqs. (7.59-7.65) that compared to a proton with no chemical shift, the ratio of ΔH_0 for resonance of the proton of the hydrino hydride ion $H^-(1/p)$ to that of the hydride ion $H^-(1/1)$ is a positive integer. That is, if only the radius is considered, the absorption peak of the hydrino hydride ion occurs at a value of ΔH_0 that is a multiple of p times the value that is resonant for the hydride ion compared to that of a proton with no shift. However, a hydrino hydride ion is equivalent to the ordinary hydride ion except that it is in a lower energy state. The source current of the state must be considered in addition to the reduced radius.

As shown in the Stability of "Ground" and Hydrino States section, for the below "ground" (fractional quantum number) energy states of the hydrogen atom, σ_{photon} , the two-dimensional surface charge due to the

"trapped photon" at the electron orbitsphere and phase-locked with the electron orbitsphere current, is given by Eqs. (5.13) and (2.11).

$$\sigma_{\text{photon}} = \frac{e}{4\pi(r_n)^2} \left[Y_0^0(\theta, \phi) - \frac{1}{n} \left[Y_0^0(\theta, \phi) + \text{Re}\{Y_l^m(\theta, \phi)e^{i\omega_{s,l}}\} \right] \right] \delta(r - r_n)$$

$$n = \frac{1}{p} = 1, \frac{1}{2}, \frac{1}{3}, \frac{1}{4}, \dots, \quad (7.66)$$

And, σ_{electron} , the two-dimensional surface charge of the electron orbitsphere is

$$\sigma_{\text{electron}} = \frac{-e}{4\pi(r_n)^2} \left[Y_0^0(\theta, \phi) + \text{Re}\{Y_l^m(\theta, \phi)e^{i\omega_{s,l}}\} \right] \delta(r - r_n) \quad (7.67)$$

The superposition of σ_{photon} (Eq. (7.66)) and σ_{electron} , (Eq. (7.67)) where the spherical harmonic functions satisfy the conditions given in the Angular Function section is

$$\sigma_{\text{photon}} + \sigma_{\text{electron}} = \frac{-e}{4\pi(r_n)^2} \left[\frac{1}{n} Y_0^0(\theta, \phi) + \left(1 + \frac{1}{n} \right) \text{Re}\{Y_l^m(\theta, \phi)e^{i\omega_{s,l}}\} \right] \delta(r - r_n)$$

$$n = \frac{1}{p} = 1, \frac{1}{2}, \frac{1}{3}, \frac{1}{4}, \dots, \quad (7.68)$$

The ratio of the total charge distributed over the surface at the radius of the hydride ion of the hydrino hydride ion $H^-(1/p)$ to that of the hydride ion $H^-(1/1)$ is an integer p , and the corresponding total source current of the hydrino hydride ion is equivalent to an integer p times that of an electron. The "trapped photon" obeys the phase-matching condition given in Excited States of the One-Electron Atom (Quantization) section, but does not interact with the applied flux directly. Only each electron does; thus, Δv of Purcell [9] that gives rise to the change in the magnetic moment, Δm , of Eq. (7.62) must be corrected by a factor of $1/p$ corresponding to the normalization of the electron source current according to the invariance of charge under Gauss' Integral Law. As also shown by Eqs. (7.8-7.14) and (7.57), the "trapped photon" gives rise to a correction to the change in magnetic moment due to the interaction of each electron with the applied flux. The correction factor of $1/p$ consequently cancels the NMR effect of the reduced radius for $H^-(1/p)$ in Eq. (7.65) which is consistent with general observations on diamagnetism [11]. This is consistent with the $E_{\text{electron} + \text{final}}(\text{magnetic})$ term of Eq. (7.53).

The cancellation of the chemical shift due to the reduced radius or the reduced semiminor and semimajor axes in the case of $H^-(1/p)$ and $H_2(1/p)$, respectively, by the corresponding source current is exact except for an additional relativistic effect. The relativistic effect for $H^-(1/p)$ arises due to the interaction of the currents corresponding to the angular momenta of the "trapped photon" and the electrons and is analogous to

that of the fine structure of the hydrogen atom involving the $^2P_{3/2} \rightarrow ^2P_{1/2}$ transition. The derivation follows that of the fine structure given in the Spin-Orbital Coupling section.

$\frac{e}{m_e}$ of the electron, the electron angular momentum of \hbar , and the electron magnetic momentum of μ_B are invariant for any electronic state. The same applies for the paired electrons of hydrino hydride ions. The condition that flux must be linked by the electron in units of the magnetic flux quantum in order to conserve the invariant electron angular momentum of \hbar gives the additional chemical shift due to relativistic effects. Using Eqs. (2.95-2.96), Eq. (2.102) may be written as

$$E_{s/o} = \frac{\alpha\pi\mu_0 e^2 \hbar^2}{m_e^2 r^3} \sqrt{\frac{3}{4}} = \alpha 2\pi 2 \frac{e\hbar}{2m_e} \frac{\mu_0 e\hbar}{2m_e a_0^3} \sqrt{\frac{3}{4}} = \alpha 2\pi 2 \mu_B B \quad (7.69)$$

From Eq. (7.69) and Eq. (1.194), the relativistic stored magnetic energy contributes a factor of $\alpha 2\pi$. The relativistic change in flux ΔB_{SR} may be calculated using Eq. (7.64) and the relativistic factor of $2\pi\alpha$ which is the same as that given by Eq. (1.218):

$$\Delta B_{SR} = -2\pi\alpha\mu_0 \frac{\Delta m}{r_n^3} (\mathbf{i}_r \cos\theta - \mathbf{i}_\theta \sin\theta) \quad \text{for } r < r_n \quad (7.70)$$

Thus, using Eqs. (7.57), (7.63), and (7.70), the upfield chemical shift $\frac{\Delta B_{SR}}{B}$ due to the relativistic effect of the ion $H^-(1/p)$ corresponding to the lower-energy state with principal quantum energy state p is given by

$$\frac{\Delta B_{SR}}{B} = -2\pi\alpha\mu_0 \frac{pe^2}{12m_e a_0 (1 + \sqrt{s(s+1)})} \quad (7.71)$$

The total shift $\frac{\Delta B_T}{B}$ for $H^-(1/p)$ is given by the sum of that of $H^-(1/1)$ given by Eqs. (7.65) plus that given by Eq. (7.71):

$$\frac{\Delta B_T}{B} = -\mu_0 \frac{e^2}{12m_e a_0 (1 + \sqrt{s(s+1)})} (1 + 2\pi\alpha p) = -(29.9 + 1.37p) \text{ ppm} \quad (7.72)$$

where $p = \text{integer} > 1$.

Alkali and alkaline earth hydrides and hydrino hydrides have been characterized by NMR [12-14] where the field was fixed and the NMR frequency was scanned. The experimental frequency of $H^-(1/1)$ compared to that of a proton and the upfield shifted peaks of $H^-(1/p)$ were consistent with Eqs. (7.65) and (7.72), respectively. For example, 1H MAS NMR was performed on novel hydrino hydride compound KH^*Cl synthesized with K as the catalyst, and the spectrum was compared to that of KH [12]. The 1H MAS NMR spectrum of KH^*Cl relative to external tetramethylsilane (TMS) showed a resonance at 1.3 ppm that

matched ordinary hydride ion. A large distinct upfield resonance at -4.4 identified a novel hydride ion of KH^*Cl . The experimental absolute resonance shift of TMS is -31.5 ppm relative to the proton's gyromagnetic frequency [15-16]. The KH experimental shift of +1.3 ppm relative to TMS corresponding to absolute resonance shift of -30.2 ppm matches very well the predicted shift of $H^-(1/1)$ of -30 ppm given by Eq. (7.65). The novel peak at -4.4 ppm relative to TMS corresponding to an absolute resonance shift of -35.9 ppm indicates that $p = 4$ in Eq. (7.72). $H^-(1/4)$ is the hydride ion predicted by using K as the catalyst according to Eqs. (5.19-5.21). This assignment was further supported by the XPS spectrum of KH^*I that was also synthesized by using K as the catalyst. It differed from that of KI by having additional features at 9.1 eV and 11.1 eV [14]. The XPS peaks centered at 9.0 eV and 11.1 eV that do not correspond to any other primary element peaks corresponded to the $H^-(n=1/4)E_b=11.2\text{ eV}$ hydride ion (Eq. (7.58)) in two different chemical environments where E_b is the predicted vacuum binding energy.

Extreme ultraviolet spectroscopy was performed on the potassium catalysis reaction [17]. Intense extreme ultraviolet (EUV) emission was observed from incandescently heated atomic hydrogen and the atomized potassium catalyst that generated an anomalous plasma at low temperatures (e.g. $\approx 10^3\text{ K}$) and an extraordinary low field strength of about 1-2 V/cm. No emission was observed with potassium or hydrogen alone or when sodium replaced potassium with hydrogen. Emission was observed from K^{3+} that confirmed the resonant nonradiative energy transfer of $3\cdot27.2\text{ eV}$ from atomic hydrogen to atomic potassium. The catalysis product, a lower-energy hydrogen atom, was predicted to be a highly reactive intermediate which further reacts to form a novel hydride ion. The predicted hydride ion of hydrogen catalysis by atomic potassium is the hydride ion $H^-(1/4)$. This ion was observed spectroscopically at 110 nm corresponding to its predicted binding energy of 11.2 eV .

HYDRINO HYDRIDE ION HYPERFINE LINES

For ordinary hydride ion H^- , a continuum is observed at shorter wavelengths of the ionization or binding energy referred to as the bound-free continuum. For typical conditions in the photosphere, Figure 4.5 of Stix [18] shows the continuous absorption coefficient $\kappa_c(\lambda)$ of the Sun. In the visible and infrared spectrum, the hydride ion H^- is the dominant absorber. Its free-free continuum starts at $\lambda=1.645\text{ }\mu\text{m}$, corresponding to the ionization energy of 0.745 eV for H^- with strongly increasing absorption towards the far infrared. The ordinary hydride spectrum

recorded on the Sun is representative of the hydride spectrum in a very hot plasma.

Hydride ions formed by the reaction of hydrogen or hydrino atoms with free electrons with a kinetic energy distribution give rise to the bound-free emission band to shorter wavelengths than the ionization or binding energy due to the release of the electron kinetic energy and the hydride ion binding energy. As shown by Eq. (7.55), the energies for the formation of hydrino hydride ions are much greater, and with sufficient spectroscopic resolution, it may be possible to resolve hyperfine structure in the corresponding bound-free band due to interactions of the free and bound electrons. The derivation of the hyperfine lines follows.

Consider a free electron binding to a hydrino atom to form a hydrino hydride ion. The total angular momentum of an electron is \hbar . During binding of the free electron, the bound electron produces a magnetic field at the free electron given by Eq. (1.101). Thus, for radial distances greater than the radius of the hydride ion, the magnetic field is equivalent to that of a magnetic dipole of a Bohr magneton at the origin. The energy of interaction of a magnetic dipole with the magnetic field of the bound electron E_{ss} , the spin-spin energy, is given by Eq. (1.195)—the product of the electron g factor given by Eq. (1.194), the magnetic moment of the free electron, a Bohr magneton given by Eq. (1.99), and the magnetic flux which follows from Eq. (1.101).

$$E_{ss} = g\mu_B\mu_0 H = g\mu_B B = g\frac{\mu_0}{r^3}\left(\frac{e\hbar}{2m_e}\right)^2 \quad (7.73)$$

where μ_0 is the permeability of free space, r is the radius of hydride ion $H^-(n=1/p)$ given by Eq. (7.56), and p is an integer. E_{ss} for $H^-(1/2)$ is given by

$$E_{ss} = 0.011223 \text{ eV} \quad (7.74)$$

where the radius given by Eq. (7.56) is

$$r_1 = 0.93301a_0 \quad (7.75)$$

where $p=2$. From Eqs. (7.55) and (7.56), the binding energy E_b of $H^-(1/2)$ is

$$E_b = 3.0471 \text{ eV} (4069.0 \text{ Å}) \quad (7.76)$$

When a free electron binds to the hydrino atom $H(1/2)$ to form a hydride ion $H^-(1/2)$, a photon is emitted with a minimum energy equal to the binding energy ($E_b = 3.0471 \text{ eV}$). Any kinetic energy that the free electron possess must increase the energy of the emitted photon. The interaction of the two electrons quantizes this emission by the same mechanism as that observed in the Stern Gerlach experiment—quantization of flux linkage. Superconducting Quantum Interference Devices (SQUIDs) or wire loops linked to SQUIDs also show quantization of flux and the

corresponding energies as shown in the Schrödinger Fat Cats—Another Flawed Interpretation section.

In the Stern-Gerlach experiment, a magnetic field is applied along the z-axis called the spin axis. The superposition of the vector projection of the orbitsphere angular momentum on the z-axis is $\frac{\hbar}{2}$ with an orthogonal component of $\frac{\hbar}{4}$. Excitation of a resonant Larmor precession gives rise to \hbar on an axis S that precesses about the spin axis at an angle of $\theta = \frac{\pi}{3}$. S rotates about the z-axis at the Larmor frequency. S_{\perp} , the transverse projection (Y_R -axis of Figure 1.7), is $\pm\sqrt{\frac{3}{4}}\hbar$, and S_{\parallel} , the projection onto the axis of the applied magnetic field (z-axis), is $\pm\frac{\hbar}{2}$. As shown in the Spin Angular Momentum of the Orbitsphere with $\ell = 0$ section, the superposition of the $\frac{\hbar}{2}$ z-axis component of the orbitsphere angular momentum and the $\frac{\hbar}{2}$ z-axis component of S gives \hbar corresponding to the observed electron magnetic moment of a Bohr magneton, μ_B . As given in the Electron g Factor section, the electron links flux in units of the magnetic flux quantum $\Phi_0 = \frac{h}{2e}$ during a Stern-Gerlach transition which conserves the angular momentum of the electron of \hbar . Due to the field of the bound electron, the free electron possessing kinetic energy will precess about the z-axis as it orbits the bound electron giving an additional component of angular momentum. A resonance exists when the transverse precessional angular momentum along the Y_R -axis of Figure 1.7 is an integer number of $\frac{\hbar}{\sqrt{s(s+1)}}$ such that its projection onto the S-axis is \hbar . In order to conserve angular momentum of both electrons as the bound electron links an integer number of fluxons due to the free electron, the corresponding fluxon energy E_Φ due the free electron's Y_R -axis component of $j\frac{\hbar}{\sqrt{s(s+1)}}$ follows from Eq. (1.194) wherein the angular momentum corresponding to the Bohr magneton, \hbar , is replaced by $j\frac{\hbar}{\sqrt{s(s+1)}}$, and the magnetic flux density B is given by the ratio of the flux to the area.

$$E_{\Phi} = j(g-2) \frac{\mu_B}{\sqrt{s(s+1)}} B = j(g-2) \frac{\mu_B}{\sqrt{s(s+1)}} \left(\frac{j\Phi_0}{A} \right) = j^2(g-2) \frac{\mu_B}{\sqrt{s(s+1)}} B \quad (7.77)$$

$$= j^2(g-2) \frac{\mu_B}{\sqrt{s(s+1)}} \frac{\mu_0}{r^3} \left(\frac{e\hbar}{2m_e} \right)$$

where j is an integer, $s=1/2$, and A is the area linked by the integer number of fluxons as given in the Electron g Factor section. The additional angular momentum due to the kinetic energy of the binding free electron is conserved in rotational energy of the resulting hydride ion. The flux linkage energy applies to each of the two electrons; thus, a factor of two in Eq. (7.77) is required. This is analogous to mutual induction. The electrons flip in opposite directions and conserve angular momentum by linking flux in integer units of the magnetic flux quantum which corresponds to the term $(g-2)$. With the radius given by Eq. (7.75), the fluxon energy E_{Φ} of $H^-(1/2)$ for both electrons is given by

$$E_{\Phi} = j^2 2(g-2) \frac{\mu_B}{\sqrt{s(s+1)}} \frac{\mu_0}{r^3} \left(\frac{e\hbar}{2m_e} \right) = j^2 3.00213 \times 10^{-5} \text{ eV} \quad (7.78)$$

The energies of the hyperfine lines E_{HF} , are given by the sum of the binding energy (Eqs. (7.55) and (7.76)), the spin-spin energy (Eqs. (7.73) and (7.74)), and the fluxon energy (Eqs. (7.77) and (7.78)).

$$E_{HF} = E_{\Phi} + E_{ss} + E_B = (j^2 3.00213 \times 10^{-5} + 0.011223 + 3.0471) \text{ eV} \quad (j \text{ is an integer}) \quad (7.79)$$

$$= (j^2 3.00213 \times 10^{-5} + 3.0583) \text{ eV}$$

The observation of bound-free hyperfine peaks requires an electron binding threshold with a large cross section. Ordinary hydride ion does not have a fine structure transition; thus, it shows only a hydride binding energy continuum [19]. The existence of fine structure transitions in $H(1/2)$ provides a mechanism to observe a peak corresponding to the formation of a free hydride ion by the binding of an electron. The predicted energy difference between the $1/2P_{1/2}$, $1/2S_{1/2}$ and $1/2P_{3/2}$ levels of the hydrogen atom, the fine structure splitting given by Eq. (2.102), is

$$E_{s/o} = 8\alpha^5 (2\pi)^2 m_e c^2 \sqrt{\frac{3}{4}} = 2.8922 \times 10^{-3} \text{ eV} \quad (7.80)$$

From Eq. (2.40) and the Spin-Nuclear Coupling section, the spin-orbital coupling is proportional to the applied flux due to spin and orbital angular momenta. With the requirement of the quantization of flux in integer units of the magnetic flux quantum during binding as shown in the Electron g Factor section, the corresponding emission is at a longer wavelength having an energy of the binding energy minus an integer

times the fine structure energy. The peak due to the binding energy (Eq. (7.76)) with excitation the fine structure splitting (Eq. (7.80)) is given by

$$E_{s/o} = E_B - E_{s/o} = 3.0471 \text{ eV} - 2.8922 \times 10^{-3} \text{ eV} = 3.0442 \text{ eV} \quad (\lambda_{air} = 4071.7 \text{ Å}) \quad (7.81)$$

The $1/2P_{3/2}$, $1/2P_{1/2}$, and $1/2S_{1/2}$ levels are also split by spin-nuclear and orbital-nuclear coupling. $1/2S_{1/2} \rightarrow 1/2P_{3/2}$ and $1/2P_{1/2} \rightarrow 1/2P_{3/2}$ transitions occur between hyperfine levels; thus, the transition energy is the sum of the fine structure and the corresponding hyperfine energy. The hyperfine splittings of $H(1/2)$ given in the SPIN-NUCLEAR COUPLING section are $1.197 \times 10^{-4} \text{ eV}$ and $3.153 \times 10^{-4} \text{ eV}$ for $\ell=0$ and $\ell=1$, respectively. In addition to a continuum, the binding of an electron to $H(1/2)$ has a resonance emission with excitation of transitions between hyperfine levels of the fine structure levels.

The catalyst product of Rb^+ and two K^+ , $H(1/2)$, was predicted to be a highly reactive intermediate which further reacts to form a novel hydride ion $H^-(1/2)$. This hydride ion with a predicted binding energy of 3.0471 eV was observed by high resolution visible spectroscopy as a continuum threshold at 3.047 eV ($\lambda_{air} = 4068 \text{ Å}$), and a structured, strong emission peak was observed at 4071 Å corresponding to the fine structure and hyperfine structure of $H(1/2)$ [20]. The experimental $H^-(1/2)$ peak at 4070.6 Å (air wavelength) was used to calculate the peak positions of the bound-free hyperfine lines. Substitution of the corresponding energy of 3.0451 eV into Eq. (7.79) for E_B gives

$$\begin{aligned} E_{HF} &= E_\phi + E_s + E_B = (j^2 3.00213 \times 10^{-5} + 0.011223 + 3.0451) \text{ eV} \\ &\quad (j \text{ is an integer}) \quad (7.82) \\ &= (j^2 3.00213 \times 10^{-5} + 3.0563) \text{ eV} \end{aligned}$$

Bound-free hyperfine structure lines of $H^-(1/2)$ were predicted with energies E_{HF} given by Eq. (7.82) as an inverse Rydberg-type series from 3.0563 eV to 3.1012 eV —the hydride binding energy peak plus one and five times the spin-pairing energy, respectively. The high resolution visible plasma emission spectra in the region of 3995 Å to 4060 Å matched the predicted emission lines for $j=1$ to $j=39$ with the series edge at 3996.3 Å up to 1 part in 10^5 [20]. The structure of these peaks matched that of $H(1/2)$ which corresponded to the predicted hyperfine splitting. All species present in the reaction or possible contaminants were eliminated as the source of the 4071 Å peak, the series of 39 lines, and series the edge. In particular, nitrogen, air, and hydrogen were eliminated.

The high resolution visible spectroscopy results were supported by the NMR of the reaction product. A novel peak at -1.5 ppm relative to TMS corresponding to an absolute resonance shift of -33.0 ppm indicates

that $p = 2$ in Eq. (7.72) [12, 14]. $H^-(1/2)$ is the hydride ion predicted by using K^+/K^+ as the catalyst according to Eqs. (5.28-5.30). In addition to spectroscopy on the $H^-(1/2)$ hydride ion product, the energetic reaction of K^+/K^+ catalyst with atomic hydrogen has been characterized. Each of the ionization of Rb^+ and cesium and an electron transfer between two K^+ ions (K^+/K^+) provide a reaction with a net enthalpy of an integer multiple of the potential energy of atomic hydrogen, 27.2 eV . The corresponding Group I nitrates provide these reactants as volatilized ions directly or as atoms by undergoing decomposition or reduction to the corresponding metal. The presence of each of the reactants identified as providing an enthalpy of 27.2 eV formed a low applied temperature, extremely low voltage plasma in atomic hydrogen called a resonant transfer or rt-plasma having strong vacuum ultraviolet (VUV) emission. In contrast, magnesium and aluminum atoms or ions do not ionize at integer multiples of the potential energy of atomic hydrogen. $Mg(NO_3)_2$ or $Al(NO_3)_3$ did not form a plasma and caused no emission [20-24]. Anomalous afterglow durations of plasmas formed by catalysts providing a net enthalpy of reaction within thermal energies of $m \cdot 27.28\text{ eV}$ including hydrogen-potassium mixtures were observed [22-24]. Emission from rt-plasmas occurred even when the electric field applied to the plasma was zero.

For further characterization, the width of the 6563 \AA Balmer α line on light emitted from rt-plasmas was recorded. Significant line broadening of 18, 12, and 12 eV was observed from a rt-plasma of hydrogen with KNO_3 , $RbNO_3$, and $CsNO_3$, respectively, compared to 3 eV from a hydrogen microwave plasma. These results could not be explained by Stark or thermal broadening or electric field acceleration of charged species since the measured field of the incandescent heater was extremely weak, 1 V/cm , corresponding to a broadening of much less than 1 eV . Rather the source of the excessive line broadening is consistent with that of the observed VUV emission, an energetic reaction caused by a resonant energy transfer between hydrogen atoms and K^+/K^+ , Rb^+ , and cesium, which serve as catalysts.

KNO_3 and $RbNO_3$ formed the most intense plasma. Remarkably, a stationary inverted Lyman population was observed in the case of an rt-plasma formed with potassium and rubidium catalysts. These catalytic reactions may pump a cw H I laser as predicted by a collisional radiative model used to determine that the observed overpopulation was above threshold [21].

References

1. Bueche, F., Introduction to Physics for Scientists and Engineers, McGraw-Hill, (1975), pp. 352-353.
2. J. D. Jackson, Classical Electrodynamics, Second Edition, John Wiley & Sons, New York, (1975), pp. 236-240, 601-608, 786-790.
3. McQuarrie, D. A., Quantum Chemistry, University Science Books, Mill Valley, CA, (1983), pp. 238-241.
4. Purcell, E. M., Electricity and Magnetism, McGraw-Hill, New York, (1985), Second Edition, pp. 451-458.
5. C. E. Moore, "Ionization Potentials and Ionization Limits Derived from the Analyses of Optical Spectra, Nat. Stand. Ref. Data Ser.-Nat. Bur. Stand. (U.S.), No. 34, 1970.
6. Robert C. Weast, CRC Handbook of Chemistry and Physics, 58 Edition, CRC Press, West Palm Beach, Florida, (1977), p. E-68.
7. Fowles, G. R., Analytical Mechanics, Third Edition, Holt, Rinehart, and Winston, New York, (1977), pp. 154-156.
8. K. R. Lykke, K. K. Murray, W. C. Lineberger, "Threshold photodetachment of H^- ", Phys. Rev. A, Vol. 43, No. 11, (1991), pp. 6104-6107.
9. Purcell, E., Electricity and Magnetism, McGraw-Hill, New York, (1965), pp. 370-389.
10. Fowles, G. R., Analytical Mechanics, Third Edition, Holt, Rinehart, and Winston, New York, (1977), p. 195-196.
11. E. Purcell, Electricity and Magnetism, McGraw-Hill, New York, (1985), pp. 417-418.
12. R. Mills, B. Dhandapani, M. Nansteel, J. He, A. Voigt, "Identification of Compounds Containing Novel Hydride Ions by Nuclear Magnetic Resonance Spectroscopy", Int. J. Hydrogen Energy, Vol. 26, No. 9, (2001); pp. 965-979.
13. R. Mills, B. Dhandapani, M. Nansteel, J. He, T. Shannon, A. Echezuria, "Synthesis and Characterization of Novel Hydride Compounds", Int. J. of Hydrogen Energy, Vol. 26, No. 4, (2001), pp. 339-367.
14. R. Mills, B. Dhandapani, N. Greenig, J. He, "Synthesis and Characterization of Potassium Iodo Hydride", Int. J. of Hydrogen Energy, Vol. 25, Issue 12, December, (2000), pp. 1185-1203.
15. K. K. Baldrige, J. S. Siegel, "Correlation of empirical $\delta(\text{TMS})$ and absolute NMR chemical shifts predicted by ab initio computations", J. Phys. Chem. A, Vol. 103, (1999), pp. 4038-4042.
16. J. Mason, Editor, Multinuclear NMR, Plenum Press, New York, (1987), Chp. 3.
17. R. Mills, P. Ray, "Spectroscopic Identification of a Novel Catalytic Reaction of Potassium and Atomic Hydrogen and the Hydride Ion Product", Int. J. Hydrogen Energy, Vol. 27, No. 2, (2002), pp. 183-192.
18. M. Stix, The Sun, Springer-Verlag, Berlin, (1991), p. 136
19. K. R. Lykke, K. K. Murray, W. C. Lineberger, "Threshold photodetachment

- of H^- ", Phys. Rev. A, Vol. 43, No. 11, (1991), pp. 6104-6107
20. R. L. Mills, P. Ray, "A Comprehensive Study of Spectra of the Bound-Free Hyperfine Levels of Novel Hydride Ion $H^-(1/2)$, Hydrogen, Nitrogen, and Air", Int. J. Hydrogen Energy, Vol. 28, No. 8, (2003), pp. 825-871.
 21. R. Mills, P. Ray, R. M. Mayo, "CW HI Laser Based on a Stationary Inverted Lyman Population Formed from Incandescently Heated Hydrogen Gas with Certain Group I Catalysts", submitted.
 22. H. Conrads, R. Mills, Th. Wrubel, "Emission in the Deep Vacuum Ultraviolet from a Plasma Formed by Incandescently Heating Hydrogen Gas with Trace Amounts of Potassium Carbonate", submitted.
 23. R. Mills, "Temporal Behavior of Light-Emission in the Visible Spectral Range from a Ti-K₂CO₃-H-Cell", Int. J. Hydrogen Energy, Vol. 26, No. 4, (2001), pp. 327-332.
 24. R. Mills, T. Onuma, and Y. Lu, "Formation of a Hydrogen Plasma from an Incandescently Heated Hydrogen-Catalyst Gas Mixture with an Anomalous Afterglow Duration", Int. J. Hydrogen Energy, Vol. 26, No. 7, July, (2001), pp. 749-762.

THREE, FOUR, FIVE, SIX, SEVEN, EIGHT, NINE, TEN, ELEVEN, TWELVE, THIRTEEN, FOURTEEN, FIFTEEN, SIXTEEN, SEVENTEEN, EIGHTEEN, NINETEEN, AND TWENTY-ELECTRON ATOMS

THREE-ELECTRON ATOMS

As is the case for one and two-electron atoms shown in the corresponding sections, three through ten-electron atoms can also be solved exactly using the results of the solutions of the preceding atoms. For example, three-electron atoms can be solved exactly using the results of the solutions of the one and two-electron atoms.

THE LITHIUM ATOM

For Li^+ , there are two spin-paired electrons in an orbitsphere with

$$r_1 = r_2 = a_0 \left[\frac{1}{2} - \frac{\sqrt{3}}{6} \right] \quad (10.1)$$

as given by Eq. (7.19) where r_n is the radius of electron n which has velocity v_n . The next electron is added to a new orbitsphere because of the repulsive diamagnetic force between the two spin-paired electrons and the spin-unpaired electron. This repulsive diamagnetic force is due to the interaction of the magnetic field of the outer spin-unpaired electron on the electron current of the two spin-paired electrons of the inner shell. The diamagnetic force on the outer electron is determined by first considering the central force on each electron of the inner shell due to the magnetic flux B of the outer electron that follows from Purcell [1]

$$\mathbf{F} = \frac{2m_e v_n \Delta v}{r} \mathbf{i}_r \quad (10.2)$$

where \mathbf{i}_r is defined as the radial vector in the direction of the central electric field of the nucleus and

$$\frac{\Delta v}{r} = \frac{eB}{2m_e} \quad (10.3)$$

The velocity v_n is given by the boundary condition for no radiation as follows:

$$v_1 = \frac{\hbar}{m_e r_1} \quad (10.4)$$

where r_1 is the radius of the first orbitsphere; therefore, the force on each of the inner electrons is given as follows:

$$\mathbf{F} = \frac{\hbar e B}{m_e r_1} \mathbf{i}_r \quad (10.5)$$

The change in magnetic moment, Δm , of each electron of the inner shell

due to the magnetic flux B of the outer electron is [1]

$$\Delta m = -\frac{e^2 r_1^2 B}{4m_e} \quad (10.6)$$

The diamagnetic force on the outer electron due to the two inner shell electrons is in the opposite direction of the force given by Eq. (10.5), and this diamagnetic force on the outer electron is proportional to the sum of the changes in magnetic moments of the two inner electrons due to the magnetic flux B of the outer electron. The two electrons are spin-paired and the, . Thus, the change in velocity of each electron treated individually (Eq. (10.3)) due to the magnetic flux B would be equal and opposite. However, the two paired electrons may be treated as one with twice the mass where m_e is replaced by $2m_e$ in Eq. (10.6). In this case, the paired electrons spin together about the field axis to cause a reduction in the flux according to Lenz's law. It is then apparent that the force given by Eq. (10.5) is proportional to the flux B of the outer electron; whereas, the total of the change in magnetic moments of the inner shell electrons given by Eq. (10.6) applied to the combination of the inner electrons is proportional to one eighth of the flux, B . Thus, the force on the outer electron due to the reaction of the inner shell to the flux of the outer electron is given as follows:

$$\mathbf{F}_{\text{diamagnetic}} = -\frac{\hbar}{8r_1} \frac{eB}{m_e} \mathbf{i}_r \quad (10.7)$$

where r_1 is the radial distance of the first orbitsphere from the nucleus. The magnetic flux, B , is supplied by the constant field inside the orbitsphere of the outer electron at radius r_3 and is given by the product of μ_o times Eq. (1.120).

$$B = \frac{\mu_o e \hbar}{m_e r_3^3} \quad (10.8)$$

The result of substitution of Eq. (10.8) into Eq. (10.7) is

$$\mathbf{F}_{\text{diamagnetic}} = -\left[\frac{e^2 \mu_o}{2m_e r_3} \right] \frac{\hbar^2}{4m_e r_1 r_3^2} \mathbf{i}_r \quad (10.9)$$

The term in brackets can be expressed in terms of the fine structure constant, α . From Eqs. (1.144-1.148)

$$\frac{e^2 \mu_o}{2m_e r_3} = 2\pi\alpha \frac{v}{c} \quad (10.10)$$

It is demonstrated in the Two-Electron Atom section that the relativistic correction to Eq. (10.9) is $\frac{1}{Z}$ times the reciprocal of Eq. (10.10). Z for electron three is one; thus, one is substituted for the term in brackets in Eq. (10.9).

The force must be corrected for the vector projection of the velocity

onto the z-axis. As given in the Spin Angular Momentum of the Orbitsphere with $\ell=0$ section, the application of a z directed magnetic field of electron three given by Eq. (1.120) to the two inner orbitspheres gives rise to a diamagnetic field and a projection of the angular momentum of electron three onto an axis which precesses about the z-axis of $\sqrt{\frac{3}{4}}\hbar$. The projection of the force between electron three and electron one and two is equivalent to that of the angular momentum onto the axis which precesses about the z-axis, and is $\sqrt{s(s+1)} = \sqrt{\frac{3}{4}}$ times that of a point mass. Thus, Eq. (10.9) becomes

$$\mathbf{F}_{\text{diamagnetic}} = -\frac{\hbar^2}{4m_e r_3^2 r_1} \sqrt{s(s+1)} \mathbf{i}_r \quad (10.11)$$

THE RADIUS OF THE OUTER ELECTRON OF THE LITHIUM ATOM

The radius for the outer electron is calculated by equating the outward centrifugal force to the sum of the electric and diamagnetic forces as follows:

$$\frac{m_e v_3^2}{r_3} = \frac{e^2}{4\pi\epsilon_0 r_3^2} - \frac{\hbar^2}{4m_e r_3^2 r_1} \sqrt{s(s+1)} \quad (10.12)$$

With $v_3 = \frac{\hbar}{m_e r_3}$ (Eq. (1.56)), $r_1 = a_0 \left[\frac{1}{2} - \frac{\sqrt{\frac{3}{4}}}{6} \right]$ (Eq. (7.19)), and $s = \frac{1}{2}$, we solve for r_3 .

$$r_3 = \frac{a_0}{\left[1 - \frac{\sqrt{3/4}}{4 \left(\frac{1}{2} - \frac{\sqrt{3/4}}{6} \right)} \right]} \quad (10.13)$$

$$r_3 = 2.5559 a_0$$

THE IONIZATION ENERGY OF LITHIUM

From Eq. (1.233), the magnitude of the energy stored in the electric field is

$$\frac{e^2}{8\pi\epsilon_0 r_3} = 5.318 \text{ eV} \quad (10.14)$$

The magnetic field of the outer electron changes the angular velocities of the inner electrons. However, the magnetic field of the outer electron

provides a central Lorentzian force which exactly balances the change in centrifugal force because of the change in angular velocity [1]. Thus, the electric energy of the inner orbitsphere is unchanged upon ionization. The magnetic field of the outer electron, however, also changes the magnetic moment, m , of each of the inner orbitsphere electrons. From Eq. (10.6), the change in magnetic moment, Δm , (per electron) is

$$\Delta m = -\frac{e^2 r_1^2}{4m_e} B \quad (10.15)$$

where B is the magnetic flux of the outer electron given by the product of μ_o times Eq. (1.120).

$$B = \frac{\mu_o e \hbar}{m_e r_3^3} \quad (10.16)$$

Substitution of Eq. (10.16) and $2m_e$ for m_e (because there are two electrons) into Eq. (10.15) gives

$$\Delta m = -\left[\frac{e^2 \mu_o}{2m_e r_3} \right] \frac{e \hbar r_1^2}{4m_e r_3^2} \quad (10.17)$$

Furthermore, we know from Eqs. (10.9) and (10.11) that the term in brackets is replaced by $\sqrt{s(s+1)}$.

$$\Delta m = -\frac{e \hbar r_1^2}{4m_e r_3^2} \sqrt{s(s+1)} \quad (10.18)$$

Substitution of Eq. (10.1) for r_1 , Eq. (10.13) for r_3 , and given that the magnetic moment of an electron is one Bohr magneton according to Eq. (1.99),

$$\mu_B = \frac{e \hbar}{2m_e} \quad (10.19)$$

the fractional change in magnetic moment of an inner shell electron, Δm_f , is given as follows:

$$\Delta m_f = \frac{\frac{e \hbar r_1^2 \sqrt{s(s+1)}}{4m_e r_3^2}}{\frac{e \hbar}{2m_e}} \quad (10.20)$$

$$= \frac{1}{2} \frac{r_1^2}{r_3^2} \sqrt{s(s+1)} \quad (10.21)$$

With r_1 given by Eq. (10.1), r_3 given by Eq. (10.13), and $s = \frac{1}{2}$, the fractional change in magnetic moment of the two inner shell electrons is

$$\Delta m_f = \frac{\left[a_o \left[\frac{1}{2} - \frac{\sqrt{3}}{6} \right] \right]^2 \sqrt{\frac{3}{4}}}{\left[\frac{a_o}{1 - \frac{\sqrt{3}}{4}} \left(\frac{1}{2} - \frac{\sqrt{3}}{6} \right) \right]^2} \quad (10.22)$$

$$\Delta m_f = 0.01677$$

We add one (corresponding to m_f) to Δm_f which is the fractional change in the magnetic moment. The energy stored in the magnetic field is proportional to the magnetic field strength squared as given by Eq. (1.122); thus, the sum is squared

$$(1.0168)^2 = 1.03382 \quad (10.23)$$

Thus, the change in magnetic energy of the inner orbitsphere is 3.382 %, so that the corresponding energy ΔE_{mag} is

$$\Delta E_{mag} = 0.03382 \times 2.543 \text{ eV} = 0.0860 \text{ eV} \quad (10.24)$$

where the magnetic energy of the inner electrons given in Table 7.1 is 2.543 eV. Then the ionization energy of the lithium atom is given by Eqs. (10.13-10.14) and (10.24):

$$E(\text{ionization}; \text{Li}) = \frac{(Z-2)e^2}{8\pi\epsilon_o r_3} + \Delta E_{mag} \quad (10.25)$$

$$= 5.3178 \text{ eV} + 0.0860 \text{ eV} = 5.4038 \text{ eV}$$

The experimental ionization energy of lithium is 5.392 eV [2-3].

THREE-ELECTRON ATOMS WITH A NUCLEAR CHARGE $Z > 3$

Three-electron atoms having $Z > 3$ possess an electric field of

$$\mathbf{E} = \frac{(Z-3)e}{4\pi\epsilon_o r^2} \mathbf{i}_r \quad (10.26)$$

for $r > r_3$. For three-electron atoms having $Z > 3$, the diamagnetic force given by Eq. (10.11) is unchanged. However, for three-electron atoms having $Z > 3$, an electric field exists for $r > r_3$. This electric field gives rise

to an additional diamagnetic force term which adds to Eq. (10.11). The additional diamagnetic force is derived as follows. The diamagnetic force repels the third (outer) electron, and the electric force attracts the third electron. Consider the reverse of ionization where the third electron is at infinity and the two spin-paired electrons are at $r_1 = r_2$ given by Eq. (7.19).

Power must be conserved as the net force of the diamagnetic and electric forces cause the third electron to move from infinity to its final radius. Power flow is given by the Poynting Power Theorem:

$$\nabla \cdot (\mathbf{E} \times \mathbf{H}) = -\frac{\delta}{\delta t} \left[\frac{1}{2} \mu_o \mathbf{H} \cdot \mathbf{H} \right] - \frac{\delta}{\delta t} \left[\frac{1}{2} \epsilon_o \mathbf{E} \cdot \mathbf{E} \right] - \mathbf{J} \cdot \mathbf{E} \quad (10.27)$$

During binding, the radius of electron three decreases. The electric force

$$\mathbf{F}_{ele} = \frac{(Z-2)e^2}{4\pi\epsilon_o r_3^2} \mathbf{i}_r \quad (10.28)$$

increases the stored electric energy which corresponds to the power term, $-\frac{\delta}{\delta t} \left[\frac{1}{2} \epsilon_o \mathbf{E} \cdot \mathbf{E} \right]$, of Eq. (10.27). The diamagnetic force given by Eq. (10.7) changes the stored magnetic energy which corresponds to the power term, $-\frac{\delta}{\delta t} \left[\frac{1}{2} \mu_o \mathbf{H} \cdot \mathbf{H} \right]$, of Eq. (10.27). An additional diamagnetic force arises when $Z-3 > 0$. This diamagnetic force corresponds to that given by Purcell [1] for a charge moving in a central field having an imposed magnetic field perpendicular to the plane of motion. The second diamagnetic force $\mathbf{F}_{diamagnetic\ 2}$ is given by

$$\mathbf{F}_{diamagnetic\ 2} = -2 \frac{m_e \Delta v^2}{r_1} \mathbf{i}_r \quad (10.29)$$

where Δv is derived from Eq. (10.3). The result of substitution of Δv into Eq. (10.29) is

$$\mathbf{F}_{diamagnetic\ 2} = -\frac{2m_e}{r_1} \left[\frac{er_1 B}{2m_e} \right]^2 \mathbf{i}_r \quad (10.30)$$

The magnetic flux, B , at electron three for $r < r_3$ is given by the product of μ_o times Eq. (1.120). The result of the substitution of the flux into Eq. (10.30) is

$$\mathbf{F}_{diamagnetic\ 2} = -2 \left[\frac{e^2 \mu_o}{2m_e r_3} \right]^2 \frac{r_1 \hbar^2}{m_e r_3^4} \mathbf{i}_r \quad (10.31)$$

The term in brackets can be expressed in terms of the fine structure constant, α . From Eqs. (1.144-1.148)

$$\frac{Z_1 e^2 \mu_o}{2m_e r_3} = 2\pi\alpha Z_1 \frac{v}{c} \quad (10.32)$$

It is demonstrated in the Two-Electron Atom section that the relativistic

correction to Eq. (10.31) is $\frac{1}{Z}$ times the reciprocal of Eq. (10.32). Consider the case wherein Z_1 of Eq. (10.32) is different from $Z = Z_2$ of Eq. (7.13) in order to maintain relativistic invariance of the electron angular momentum and magnetic moment. The relativistic correction to Eq. (10.31) can be considered the product of two corrections—a correction of electron three relative to electron one and two, and electron one and two relative to electron three. In the former case, Z_1 and $Z_2 = 1$ which corresponds to electron three. In the latter case, $Z_1 = Z - 3$, and $Z_2 = Z - 2$ which corresponds to r_3^+ , infinitesimally greater than the radius of the outer orbitsphere and r_3^- , infinitesimally less than the radius of the outer orbitsphere, respectively, where Z is the nuclear charge. Thus, $\frac{Z-3}{Z-2}$ is substituted for the term in brackets in Eq. (10.31). The force must be corrected for the vector projection of the velocity onto the z-axis. As given in the Spin Angular Momentum of the Orbitsphere with $\ell = 0$ section, the application of a z directed magnetic field of electron three given by Eq. (1.120) to the two inner orbitspheres gives rise to a diamagnetic field and a projection of the angular momentum of electron three onto an axis which precesses about the z-axis of $\sqrt{\frac{3}{4}}\hbar$. The projection of the force between electron three and electron one and two is equivalent to that of the angular momentum onto the axis which precesses about the z-axis, and is $\sqrt{s(s+1)} = \sqrt{\frac{3}{4}}$ times that of a point mass.

Thus, Eq. (10.31) becomes

$$\mathbf{F}_{\text{diamagnetic } 2} = -2 \frac{(Z-3)r_1\hbar^2}{(Z-2)m_e r_3^4} \sqrt{s(s+1)} \mathbf{i}_r, \quad (10.33)$$

As given previously in the Two Electron section, this force corresponds to the dissipation term of Eq. (10.27), $\mathbf{J} \cdot \mathbf{E}$. The current \mathbf{J} is proportional to the sum of one for the outer electron and two times two—the number of spin-paired electrons. For the inner electrons, the factor of two arises because they possess mutual inductance which doubles their contribution to \mathbf{J} . (Recall the general relationship that the current is equal to the flux divided by the inductance.) Thus, the second diamagnetic force is

$$\mathbf{F}_{\text{diamagnetic } 2} = -2 \left[\frac{Z-3}{Z-2} \right] \frac{(1+4)r_1\hbar^2}{m_e r_3^4} \sqrt{s(s+1)} \mathbf{i}_r; \quad s = \frac{1}{2} \quad (10.34)$$

$$\mathbf{F}_{\text{diamagnetic } 2} = - \left[\frac{Z-3}{Z-2} \right] \frac{r_1\hbar^2}{m_e r_3^4} 10\sqrt{3/4} \mathbf{i}_r, \quad (10.35)$$

THE RADIUS OF THE OUTER ELECTRON OF THREE-ELECTRON

ATOMS WITH A NUCLEAR CHARGE $Z > 3$

The radius of the outer electron is calculated by equating the outward centrifugal force to the sum of the electric and diamagnetic forces as follows:

$$\frac{m_e v_3^2}{r_3} = \frac{(Z-2)e^2}{4\pi\epsilon_0 r_3^2} - \frac{\hbar^2}{4m_e r_3^2 r_1} \sqrt{s(s+1)} - \left[\frac{Z-3}{Z-2} \right] \frac{r_1 \hbar^2}{r_3^4 m_e} 10 \sqrt{s(s+1)} \quad (10.36)$$

With $v_3 = \frac{\hbar}{m_e r_3}$ (Eq. (1.56)), $r_1 = a_0 \left(\frac{1}{Z-1} - \frac{\sqrt{s(s+1)}}{Z(Z-1)} \right)$ (Eq. (7.19)), and $s = \frac{1}{2}$, we solve for r_3 using the quadratic formula or reiteratively.

$$r_3 = \frac{\left[1 + \left[\frac{Z-3}{Z-2} \right] \frac{r_1}{r_3} 10 \sqrt{\frac{3}{4}} \right]}{\left[\frac{(Z-2)}{a_0} - \frac{\sqrt{\frac{3}{4}}}{4r_1} \right]} \quad (10.37)$$

The quadratic equation corresponding to Eq. (10.37) is

$$r_3^2 - \frac{r_3}{\left[\frac{(Z-2)}{a_0} - \frac{\sqrt{\frac{3}{4}}}{4r_1} \right]} - \frac{\left[\frac{Z-3}{Z-2} \right] r_1 10 \sqrt{\frac{3}{4}}}{\left[\frac{(Z-2)}{a_0} - \frac{\sqrt{\frac{3}{4}}}{4r_1} \right]} = 0 \quad (10.38)$$

The solution of Eq. (10.38) using the quadratic formula is

$$r_3 = \frac{\left[\frac{a_0}{(Z-2) - \frac{\sqrt{\frac{3}{4}}}{4r_1}} \right] \pm a_0 \sqrt{\frac{1}{\left[\frac{(Z-2)}{a_0} - \frac{\sqrt{\frac{3}{4}}}{4r_1} \right]^2} + 4 \left[\frac{Z-3}{Z-2} \right] \frac{r_1 10 \sqrt{\frac{3}{4}}}{\left[\frac{(Z-2)}{a_0} - \frac{\sqrt{\frac{3}{4}}}{4r_1} \right]}}}{2}, \quad r_1 \text{ in units of } a_0 \quad (10.39)$$

$$r_3 = \frac{\left[\frac{a_0}{(Z-2) - \frac{\sqrt{\frac{3}{4}}}{4r_1}} \right] \left[1 \pm \sqrt{1 + 4 \left[\frac{Z-3}{Z-2} \right] \frac{r_1 10 \sqrt{\frac{3}{4}}}{\left[\frac{(Z-2)}{a_0} - \frac{\sqrt{\frac{3}{4}}}{4r_1} \right]}} \right]}{2}, \quad r_1 \text{ in units of } a_0 \quad (10.40)$$

$$r_3 = \frac{a_o \left[(Z-2) - \frac{\sqrt{3}}{4r_1} \right] \left[1 \pm \sqrt{1 + 4(Z-3)r_1 10 \sqrt{\frac{3}{4}} - \left[\frac{Z-3}{Z-2} \right] \frac{30}{4}} \right]}{2}, \quad r_1 \text{ in units of } a_o \quad (10.41)$$

$$r_3 = \frac{a_o \left[(Z-2) - \frac{\sqrt{3}}{4 \left(\frac{1}{Z-1} - \frac{\sqrt{3/4}}{Z(Z-1)} \right)} \right] \left[1 \pm \sqrt{1 + 4(Z-3) \left(\frac{1}{Z-1} - \frac{\sqrt{3/4}}{Z(Z-1)} \right) 10 \sqrt{\frac{3}{4}} - \left[\frac{Z-3}{Z-2} \right] \frac{30}{4}} \right]}{2} \quad (10.42)$$

The positive root of Eq. (10.42) must be taken in order that $r_3 > 0$.

THE IONIZATION ENERGIES OF THREE-ELECTRON ATOMS WITH A NUCLEAR CHARGE $Z > 3$

The energy stored in the electric field, $E(\text{electric})$, is

$$E(\text{electric}) = -\frac{(Z-2)e^2}{8\pi\epsilon_o r_3} \quad (10.43)$$

where r_3 is given by Eq. (10.42). The magnetic field of the outer electron changes the velocities of the inner electrons. However, the magnetic field of the outer electron provides a central Lorentzian field which balances the change in centrifugal force because of the change in velocity. Thus, the electric energy of the inner orbitsphere is unchanged upon ionization. The change in the velocities of the inner electrons upon ionization gives rise to a change in kinetic energies of the inner electrons. The change in velocity, Δv , is given by Eq. (10.3)

$$\Delta v = \frac{er_1 B}{2m_e} \quad (10.44)$$

Substitution of the flux, B , given by the product of μ_o and Eq. (1.120), into Eq. (10.43) is

$$\Delta v = \left[\frac{e^2 \mu_o}{2m_e r_1} \right] \frac{r_1^2 \hbar}{m_e r_3^3} \quad (10.45)$$

It is demonstrated in the One-Electron Atom section and the Two-Electron Atom section (at Eq. (7.14)) that the relativistic correction to Eq. (10.45) is $\frac{1}{Z}$ times the reciprocal of the term in brackets. In this case, Z corresponding to electron three is one; thus, one is substituted for the

term in brackets in Eq. (10.45). Thus, Eq. (10.45) becomes,

$$\Delta v = \frac{r_1^2 \hbar}{r_3^3 m_e} \quad (10.46)$$

where r_1 is given by Eq. (7.19), and r_3 is given by Eq. (10.42). The change in kinetic energy, ΔE_T , of the two inner shell electrons is given by

$$\Delta E_T = 2 \frac{1}{2} m_e \Delta v^2 \quad (10.47)$$

The ionization energy is the sum of the electric energy, Eq. (10.43), and the change in the kinetic energy, Eq. (10.47), of the inner electrons.

$$E(\text{Ionization}) = E(\text{Electric}) + E_T \quad (10.48)$$

The relativistic correction to Eq. (10.48) is given by 1.) relativistically correcting the radius of the inner paired electrons r_1 , 2.) using the relativistically corrected r_1 to determine r_3 which is then relativistically corrected. The relativistically corrected r_1 is given by dividing the radius given Eq. (7.19) by γ^* of Eq. (1.250)

$$r_2 = r_1 = \frac{r_1}{\gamma^*} = \frac{a_0 \left(\frac{1}{Z-1} - \frac{\sqrt{s(s+1)}}{Z(Z-1)} \right)}{2\pi \sqrt{1 - \left(\frac{v}{c} \right)^2} \sin \left[\frac{\pi}{2} \left(1 - \left(\frac{v}{c} \right)^2 \right)^{3/2} \right] + \cos \left[\frac{\pi}{2} \left(1 - \left(\frac{v}{c} \right)^2 \right)^{3/2} \right]}, \quad s = \frac{1}{2} \quad (10.49)$$

where the velocity is given by Eq. (1.56) with the radius given by Eq. (7.19). Similarly, the relativistically corrected r_3 is given by dividing the radius given Eq. (10.41) by γ^* of Eq. (1.250)

$$r_3 = \frac{r_3}{\gamma^*} = \frac{\frac{a_0}{\left(Z-2 - \frac{\sqrt{3}}{4} \right)} \left[1 + \sqrt{1 + 4(Z-3)r_1 10 \sqrt{\frac{3}{4} - \left[\frac{Z-3}{Z-2} \right] \frac{30}{4}}} \right]}{2\pi \sqrt{1 - \left(\frac{v}{c} \right)^2} \sin \left[\frac{\pi}{2} \left(1 - \left(\frac{v}{c} \right)^2 \right)^{3/2} \right] + \cos \left[\frac{\pi}{2} \left(1 - \left(\frac{v}{c} \right)^2 \right)^{3/2} \right]}, \quad r_1 \text{ in units of } a_0 \quad (10.50)$$

where r_1 is given by Eq. (10.49) and the velocity is given by Eq. (1.56) with the radius given by Eq. (10.42). The ionization energies are given by Eq. (10.48) wherein the relativistically corrected radii given by Eqs. (10.49-10.50) are used in the sum of the electric energy, Eq. (10.43), and the change in the kinetic energy, Eq. (10.47), of the inner electrons. The ionization energies for several three-electron atoms are given in Table 10.1.

Table 10.1. Ionization energies for some three-electron atoms.

3 e Atom	Z	r_1 (a_0) ^a	r_3 (a_0) ^b	Electric Energy ^c (eV)	Δv ^d (m/s)	ΔE_T ^e (eV)	Theoretical Ionization Energies ^f (eV)	Experimental Ionization Energies ^g (eV)	Relative Error ^h
Li	3	0.35566	2.55606	5.3230	1.6571E+04	1.5613E-03	5.40381	5.39172	-0.00224
Be ⁺	4	0.26116	1.49849	18.1594	4.4346E+04	1.1181E-02	18.1706	18.21116	0.00223
B ²⁺	5	0.20670	1.07873	37.8383	7.4460E+04	3.1523E-02	37.8701	37.93064	0.00160
C ³⁺	6	0.17113	0.84603	64.3278	1.0580E+05	6.3646E-02	64.3921	64.4939	0.00158
N ⁴⁺	7	0.14605	0.69697	97.6067	1.3782E+05	1.0800E-01	97.7160	97.8902	0.00178
O ⁵⁺	8	0.12739	0.59299	137.6655	1.7026E+05	1.6483E-01	137.8330	138.1197	0.00208
F ⁶⁺	9	0.11297	0.51621	184.5001	2.0298E+05	2.3425E-01	184.7390	185.186	0.00241
Ne ⁷⁺	10	0.10149	0.45713	238.1085	2.3589E+05	3.1636E-01	238.4325	239.0989	0.00279
Na ⁸⁺	11	0.09213	0.41024	298.4906	2.6894E+05	4.1123E-01	298.9137	299.864	0.00317
Mg ⁹⁺	12	0.08435	0.37210	365.6469	3.0210E+05	5.1890E-01	366.1836	367.5	0.00358
Al ¹⁰⁺	13	0.07778	0.34047	439.5790	3.3535E+05	6.3942E-01	440.2439	442	0.00397
Si ¹¹⁺	14	0.07216	0.31381	520.2888	3.6868E+05	7.7284E-01	521.0973	523.42	0.00444
P ¹²⁺	15	0.06730	0.29102	607.7792	4.0208E+05	9.1919E-01	608.7469	611.74	0.00489
S ¹³⁺	16	0.06306	0.27132	702.0535	4.3554E+05	1.0785E+00	703.1966	707.01	0.00539
Cl ¹⁴⁺	17	0.05932	0.25412	803.1158	4.6905E+05	1.2509E+00	804.4511	809.4	0.00611
Ar ¹⁵⁺	18	0.05599	0.23897	910.9708	5.0262E+05	1.4364E+00	912.5157	918.03	0.00601
K ¹⁶⁺	19	0.05302	0.22552	1025.6241	5.3625E+05	1.6350E+00	1027.3967	1033.4	0.00581
Ca ¹⁷⁺	20	0.05035	0.21350	1147.0819	5.6993E+05	1.8468E+00	1149.1010	1157.8	0.00751
Sc ¹⁸⁺	21	0.04794	0.20270	1275.3516	6.0367E+05	2.0720E+00	1277.6367	1287.97	0.00802
Ti ¹⁹⁺	22	0.04574	0.19293	1410.4414	6.3748E+05	2.3106E+00	1413.0129	1425.4	0.00869
V ²⁰⁺	23	0.04374	0.18406	1552.3606	6.7135E+05	2.5626E+00	1555.2398	1569.6	0.00915
Cr ²¹⁺	24	0.04191	0.17596	1701.1197	7.0530E+05	2.8283E+00	1704.3288	1721.4	0.00992
Mn ²²⁺	25	0.04022	0.16854	1856.7301	7.3932E+05	3.1077E+00	1860.2926	1879.9	0.01043
Fe ²³⁺	26	0.03867	0.16172	2019.2050	7.7342E+05	3.4011E+00	2023.1451	2023	-0.00007
Co ²⁴⁺	27	0.03723	0.15542	2188.5585	8.0762E+05	3.7084E+00	2192.9020	2219	0.01176
Ni ²⁵⁺	28	0.03589	0.14959	2364.8065	8.4191E+05	4.0300E+00	2369.5803	2399.2	0.01235
Cu ²⁶⁺	29	0.03465	0.14418	2547.9664	8.7630E+05	4.3661E+00	2553.1987	2587.5	0.01326

^a Radius of the paired inner electrons of three-electron atoms from Eq. (10.49).

^b Radius of the unpaired outer electron of three-electron atoms from Eq. (10.50).

^c Electric energy of the outer electron of three-electron atoms from Eq. (10.43).

^d Change in the velocity of the paired inner electrons due to the unpaired outer electron of three-electron atoms from Eq. (10.46).

^e Change in the kinetic energy of the paired inner electrons due to the unpaired outer electron of three-electron atoms from Eq. (10.47).

^f Calculated ionization energies of three-electron atoms from Eq. (10.48) for $Z > 3$ and Eq. (10.25) for Li .

^g From theoretical calculations, interpolation of isoelectronic and spectral series, and experimental data [2-3].

^h (Experimental-theoretical)/experimental.

The agreement between the experimental and calculated values of Table 10.1 is well within the experimental capability of the spectroscopic determinations including the values at large Z which relies on X-ray spectroscopy. In this case, the experimental capability is three to four significant figures which is consistent with the last column. The lithium atom isoelectronic series is given in Table 10.1 [2-3] to much higher precision than the capability of X-ray spectroscopy, but these values are based on theoretical and interpolation techniques rather than data alone. Ionization energies are difficult to determine since the cut-off of the Rydberg series of lines at the ionization energy is often not observed, and the ionization energy must be determined from theoretical calculations, interpolation of Li isoelectronic and Rydberg series, as well as direct experimental data.

FOUR-ELECTRON ATOMS

Four-electron atoms can be solved exactly using the results of the solutions of one, two, and three-electron atoms.

RADI OF THE OUTER ELECTRONS OF FOUR-ELECTRON ATOMS

For each three-electron atom having a central charge of Z times that of the proton, there are two indistinguishable spin-paired electrons in an orbitsphere with radii r_1 and r_2 both given by Eq. (7.19):

$$r_1 = r_2 = a_0 \left[\frac{1}{Z-1} - \frac{\sqrt{3}}{Z(Z-1)} \right] \quad (10.51)$$

and an unpaired electron with a radius r_3 given by Eq. (10.42). For $Z \geq 4$, the next electron which binds to form the corresponding four-electron atom becomes spin-paired with the outer electron such that they become indistinguishable with the same radius $r_3 = r_4$. The corresponding spin-pairing force F_{mag} is given by Eq. (7.15):

$$F_{mag} = \frac{1}{Z} \frac{\hbar^2}{m_e r_4^3} \sqrt{s(s+1)} \mathbf{i}_r \quad (10.52)$$

The central forces given by Eq. (10.36) and Eq. (10.52) act on the outer electron to cause it to bind wherein the electric force on the outermost electron due to the nucleus and the inner three electrons is given by Eq. (10.28) with the appropriate charge and radius:

$$F_{ele} = \frac{(Z-3)e^2}{4\pi\epsilon_0 r_4^2} \mathbf{i}_r \quad (10.53)$$

for $r > r_3$.

In addition to the paramagnetic spin-pairing force between the third electron initially at radius r_3 , the pairing causes the diamagnetic interaction between the outer electrons and the inner electrons given by Eq. (10.11) to vanish, except for an electrodynamic effect for $Z > 4$ described in the Two-Electron Atoms section, since upon pairing the magnetic field of the outer electrons becomes zero. Therefore, the force F_{mag2} is in the same direction as the spin-pairing force and is given by substitution of Eq. (7.4) with the radius r_4 into Eq. (10.5):

$$F_{mag2} = \frac{\hbar e B}{2m_e r_1} = \frac{\mu_o e^2 \hbar^2}{2m_e^2 r_1 r_4^3} \mathbf{i}_r \quad (10.54)$$

Then, from Eqs. (10.54) and (7.6-7.15), the diamagnetic force is given by

$$F_{mag2} = \frac{1}{Z} \frac{\hbar^2}{m_e r_1 r_4^2} \sqrt{s(s+1)} \mathbf{i}_r \quad (10.55)$$

The outward centrifugal force on electron 4 is balanced by the electric force and the magnetic forces (on electron 4). The radius of the outer electron is calculated by equating the outward centrifugal force to the sum of the electric (Eq. (10.53)), diamagnetic (Eqs. (10.11) and (10.35) for r_4), and paramagnetic (Eqs. (10.52) and (10.54)) forces as follows:

$$\frac{m_e v_4^2}{r_4} = \frac{(Z-3)e^2}{4\pi\epsilon_o r_4^2} - \frac{\hbar^2}{4m_e r_4^2 r_1} \sqrt{s(s+1)} + \frac{\hbar^2}{Zm_e r_4^2 r_1} \sqrt{s(s+1)} - \left[\frac{Z-3}{Z-2} \right] \frac{r_1 \hbar^2}{r_4^4 m_e} 10 \sqrt{s(s+1)} + \frac{\hbar^2}{Zm_e r_4^3} \sqrt{s(s+1)} \quad (10.56)$$

Substitution of $v_4 = \frac{\hbar}{m_e r_4}$ (Eq. (1.56) and $s = \frac{1}{2}$ into Eq. (10.56) gives:

$$\frac{\hbar^2}{m_e r_4^3} = \frac{(Z-3)e^2}{4\pi\epsilon_o r_4^2} - \frac{\hbar^2}{4m_e r_4^2 r_1} \sqrt{\frac{3}{4}} + \frac{\hbar^2}{Zm_e r_4^2 r_1} \sqrt{\frac{3}{4}} - \left[\frac{Z-3}{Z-2} \right] \frac{r_1 \hbar^2}{r_4^4 m_e} 10 \sqrt{\frac{3}{4}} + \frac{\hbar^2}{Zm_e r_4^3} \sqrt{\frac{3}{4}} \quad (10.57)$$

$$\left(\frac{(Z-3)e^2}{4\pi\epsilon_o} - \left(\frac{1}{4} - \frac{1}{Z} \right) \frac{\hbar^2}{m_e r_1} \sqrt{\frac{3}{4}} \right) \frac{1}{r_4^2} - \left[\frac{Z-3}{Z-2} \right] \frac{r_1 \hbar^2}{r_4^4 m_e} 10 \sqrt{\frac{3}{4}} - \frac{\hbar^2}{m_e r_4^3} \left(1 - \frac{\sqrt{\frac{3}{4}}}{Z} \right) = 0 \quad (10.58)$$

The quadratic equation corresponding to Eq. (10.58) is

$$\left(\frac{(Z-3)e^2}{4\pi\epsilon_o} - \left(\frac{1}{4} - \frac{1}{Z} \right) \frac{\hbar^2}{m_e r_1} \sqrt{\frac{3}{4}} \right) r_4^2 - \frac{\hbar^2}{m_e} \left(1 - \frac{\sqrt{\frac{3}{4}}}{Z} \right) r_4 - \left[\frac{Z-3}{Z-2} \right] \frac{r_1 \hbar^2}{m_e} 10 \sqrt{\frac{3}{4}} = 0 \quad (10.59)$$

$$r_4^2 - \frac{\frac{\hbar^2}{m_e} \left(1 - \frac{\sqrt{3}}{Z}\right)}{\left(\frac{(Z-3)e^2}{4\pi\epsilon_0} - \left(\frac{1}{4} - \frac{1}{Z}\right) \frac{\hbar^2}{m_e r_1} \sqrt{\frac{3}{4}}\right)} r_4 - \frac{\left[\frac{Z-3}{Z-2}\right] \frac{r_1 \hbar^2}{m_e} 10 \sqrt{\frac{3}{4}}}{\left(\frac{(Z-3)e^2}{4\pi\epsilon_0} - \left(\frac{1}{4} - \frac{1}{Z}\right) \frac{\hbar^2}{m_e r_1} \sqrt{\frac{3}{4}}\right)} = 0 \quad (10.60)$$

$$r_4^2 - \frac{\left(1 - \frac{\sqrt{3}}{Z}\right)}{\left(\frac{(Z-3)}{a_0} - \left(\frac{1}{4} - \frac{1}{Z}\right) \frac{\sqrt{3}}{r_1}\right)} r_4 - \frac{\left[\frac{Z-3}{Z-2}\right] r_1 10 \sqrt{\frac{3}{4}}}{\left(\frac{(Z-3)}{a_0} - \left(\frac{1}{4} - \frac{1}{Z}\right) \frac{\sqrt{3}}{r_1}\right)} = 0 \quad (10.61)$$

The solution of Eq. (10.61) using the quadratic formula is:

$$r_4 = r_3 = \frac{a_0 \left(1 - \frac{\sqrt{3}}{Z}\right) \pm a_0 \sqrt{\frac{\left(1 - \frac{\sqrt{3}}{Z}\right)^2}{\left(\frac{(Z-3)}{a_0} - \left(\frac{1}{4} - \frac{1}{Z}\right) \frac{\sqrt{3}}{r_1}\right)^2} + 4 \frac{\left[\frac{Z-3}{Z-2}\right] r_1 10 \sqrt{\frac{3}{4}}}{\left(\frac{(Z-3)}{a_0} - \left(\frac{1}{4} - \frac{1}{Z}\right) \frac{\sqrt{3}}{r_1}\right)}}}{2} \quad (10.62)$$

r_1 in units of a_0

where r_1 is given by Eq. (10.51) and also Eq. (7.19). The positive root of Eq. (10.62) must be taken in order that $r_4 > 0$. The final radius of electron 4, r_4 , is given by Eq. (10.62); this is also the final radius of electron 3. The radii of several four-electron atoms are given in Table 10.2.

ENERGIES OF THE BERYLLIUM ATOM

The energy stored in the electric field, $E(\text{electric})$, is given by Eq. (10.43) with the appropriate charge and radius:

$$E(\text{electric}) = -\frac{(Z-3)e^2}{8\pi\epsilon_0 r_4} \quad (10.63)$$

The ionization energy is given by the sum of the electric energy and the diamagnetic and paramagnetic energy terms. The magnetic energy, $E(\text{magnetic})$, for an electron corresponding to a radius r_n given by Eq. (7.30) is

$$E(\text{magnetic}) = \frac{2\pi\mu_0 e^2 \hbar^2}{m_e^2 r_n^3} \quad (10.64)$$

Since there is no source of dissipative power, $\mathbf{J} \cdot \mathbf{E}$ of Eq. (10.27), to compensate for any potential change in the magnetic moments, Δm , of the inner electrons due to the ionization of an outer electron of the beryllium atom, there is a diamagnetic energy term in the ionization energy for this atom that follows from the corresponding term for the lithium atom. This term is given by Eqs. (10.15-10.24) wherein r_1 is given by Eq. (10.51) with $Z=4$ and $r_3=r_4$ is given by Eq. (10.62). Thus, the change in magnetic energy of the inner orbitsphere is 5.144 %, so that the corresponding energy ΔE_{mag} is

$$\Delta E_{mag} = 0.05144 \times 6.42291 \text{ eV} = 0.33040 \text{ eV} \quad (10.65)$$

where the magnetic energy of the inner electrons is 6.42291 eV. In addition, there is a paramagnetic energy term $E(\text{magnetic})$ corresponding to the ionization of a spin-paired electron from a neutral atom with a closed s-shell. The energy follows from that given for helium by Eqs. (7.28) and (7.30) wherein the electron radius for helium is replaced by the radius r_4 of Eq. (10.62). Then, the ionization energy of the beryllium atom is given by Eqs. (7.28), (7.30), (10.25), and (10.62-10.65):

$$\begin{aligned} E(\text{ionization}; Be) &= \frac{(Z-3)e^2}{8\pi\epsilon_0 r_4} + \frac{2\pi\mu_0 e^2 \hbar^2}{m_e^2 r_4^3} + \Delta E_{mag} \\ &= 8.9216 \text{ eV} + 0.03226 \text{ eV} + 0.33040 \text{ eV} = 9.28430 \text{ eV} \end{aligned} \quad (10.66)$$

The experimental ionization energy of beryllium is 9.32263 eV [3].

THE IONIZATION ENERGIES OF FOUR-ELECTRON ATOMS WITH A NUCLEAR CHARGE $Z>4$

The ionization energies for the four-electron atoms with $Z>4$ are given by the sum of the electric energy, $E(\text{electric})$, given by Eq. (10.63) and the magnetic energies. The paramagnetic energy term corresponding to the ionization of a spin-paired electron from an atom with an external electric field is given by Eqs. (7.30) and (7.47) wherein the electron radius for helium is replaced by the radius r_4 of Eq. (10.62):

$$\text{Ionization Energy} = -\text{Electric Energy} - \frac{1}{Z} \text{Magnetic Energy} \quad (10.67)$$

Once the outer electrons of four-electron atoms with $Z>4$ become spin unpaired during ionization, the corresponding magnetic field changes the velocities of the inner electrons in the same manner as shown for the case of the outer electron of three-electron atoms with $Z>3$. The magnetic effect is calculated for the remaining electron 3 at the radius r_4 corresponding to condition of the derivation of Eq. (10.67) that follows from Eqs. (7.30) and (7.47). Thus, change in velocity, Δv , in the four-

electron-atom case is that of three-electron atoms given by Eq. (10.46) wherein the electron radius r_3 is replaced by the radius r_4 of Eq. (10.62).

Since the velocities of electrons one and two decrease during ionization in the case of four-electron atoms rather than increase as in the case of three-electron atoms, the corresponding kinetic energy decreases and the kinetic energy term given by Eq. (10.47) is the opposite sign in Eq. (10.48). Thus, the ionization energies of four-electron atoms with $Z > 4$ given by Eqs. (10.48) and (10.67) with the electric energy (Eq. (10.63)), the magnetic energy (Eq. (10.64)), and the change in the kinetic energy of the inner electrons (Eq. (10.47)) are

$$E(\text{Ionization}) = -\text{Electric Energy} - \frac{1}{Z} \text{Magnetic Energy} - E_r \quad (10.68)$$

The ionization energies for several four-electron atoms are given in Table 10.2. Since the radii, r_4 , are greater than 10% of a_0 corresponding to a velocity of less than $1.5 \times 10^7 \text{ m/s}$, the relativistic corrections are negligible and are not included in Table 10.2.

Table 10.2. Ionization energies for some four-electron atoms.

4 e Atom	Z	r_1 (a_0) ^a	r_3 (a_0) ^b	Electric Energy ^c (eV)	Magnetic Energy ^d (eV)	Δv ^e (m/s X 10^{-3})	ΔE_T ^f (eV)	Theoretical Ionization Energies ^g (eV)	Experimental Ionization Energies ^h (eV)	Relative Error ⁱ
<i>Be</i>	4	0.26116	1.52503	8.9178	0.03226	0.4207	0.0101	9.28430	9.32263	0.0041
<i>B</i> ⁺	5	0.20670	1.07930	25.2016	0.0910	0.7434	0.0314	25.1627	25.15484	-0.0003
<i>C</i> ²⁺	6	0.17113	0.84317	48.3886	0.1909	1.0688	0.0650	48.3125	47.8878	-0.0089
<i>N</i> ³⁺	7	0.14605	0.69385	78.4029	0.3425	1.3969	0.1109	78.2765	77.4735	-0.0104
<i>O</i> ⁴⁺	8	0.12739	0.59020	115.2148	0.5565	1.7269	0.1696	115.0249	113.899	-0.0099
<i>F</i> ⁵⁺	9	0.11297	0.51382	158.8102	0.8434	2.0582	0.2409	158.5434	157.1651	-0.0088
<i>Ne</i> ⁶⁺	10	0.10149	0.45511	209.1813	1.2138	2.3904	0.3249	208.8243	207.2759	-0.0075
<i>Na</i> ⁷⁺	11	0.09213	0.40853	266.3233	1.6781	2.7233	0.4217	265.8628	264.25	-0.0061
<i>Mg</i> ⁸⁺	12	0.08435	0.37065	330.2335	2.2469	3.0567	0.5312	329.6559	328.06	-0.0049
<i>Al</i> ⁹⁺	13	0.07778	0.33923	400.9097	2.9309	3.3905	0.6536	400.2017	398.75	-0.0036
<i>Si</i> ¹⁰⁺	14	0.07216	0.31274	478.3507	3.7404	3.7246	0.7888	477.4989	476.36	-0.0024
<i>P</i> ¹¹⁺	15	0.06730	0.29010	562.5555	4.6861	4.0589	0.9367	561.5464	560.8	-0.0013
<i>S</i> ¹²⁺	16	0.06306	0.27053	653.5233	5.7784	4.3935	1.0975	652.3436	652.2	-0.0002
<i>Cl</i> ¹³⁺	17	0.05932	0.25344	751.2537	7.0280	4.7281	1.2710	749.8899	749.76	-0.0002
<i>Ar</i> ¹⁴⁺	18	0.05599	0.23839	855.7463	8.4454	5.0630	1.4574	854.1849	854.77	0.0007
<i>K</i> ¹⁵⁺	19	0.05302	0.22503	967.0007	10.0410	5.3979	1.6566	965.2283	968	0.0029
<i>Ca</i> ¹⁶⁺	20	0.05035	0.21308	1085.0167	11.8255	5.7329	1.8687	1083.0198	1087	0.0037
<i>Sc</i> ¹⁷⁺	21	0.04794	0.20235	1209.7940	13.8094	6.0680	2.0935	1207.5592	1213	0.0045
<i>Ti</i> ¹⁸⁺	22	0.04574	0.19264	1341.3326	16.0032	6.4032	2.3312	1338.8465	1346	0.0053
<i>V</i> ¹⁹⁺	23	0.04374	0.18383	1479.6323	18.4174	6.7384	2.5817	1476.8813	1486	0.0061
<i>Cr</i> ²⁰⁺	24	0.04191	0.17579	1624.6929	21.0627	7.0737	2.8450	1621.6637	1634	0.0075
<i>Mn</i> ²¹⁺	25	0.04022	0.16842	1776.5144	23.9495	7.4091	3.1211	1773.1935	1788	0.0083
<i>Fe</i> ²²⁺	26	0.03867	0.16165	1935.0968	27.0883	7.7444	3.4101	1931.4707	1950	0.0095
<i>Co</i> ²³⁺	27	0.03723	0.15540	2100.4398	30.4898	8.0798	3.7118	2096.4952	2119	0.0106
<i>Ni</i> ²⁴⁺	28	0.03589	0.14961	2272.5436	34.1644	8.4153	4.0264	2268.2669	2295	0.0116
<i>Cu</i> ²⁵⁺	29	0.03465	0.14424	2451.4080	38.1228	8.7508	4.3539	2446.7858	2478	0.0126

^a Radius of the paired inner electrons of four-electron atoms from Eq. (10.51).^b Radius of the paired outer electrons of four-electron atoms from Eq. (10.62).^c Electric energy of the outer electrons of four-electron atoms from Eq. (10.63).^d Magnetic energy of the outer electrons of four-electron atoms upon unpairing from Eq. (7.30) and Eq. (10.64).^e Change in the velocity of the paired inner electrons due to the unpaired outer electron of four-electron atoms during ionization from Eq. (10.46).^f Change in the kinetic energy of the paired inner electrons due to the unpaired outer electron of four-electron atoms during ionization from Eq. (10.47).^g Calculated ionization energies of four-electron atoms from Eq. (10.68) for $Z > 4$ and Eq. (10.66) for *Be*.^h From theoretical calculations, interpolation of isoelectronic and spectral series, and experimental data [2-3].ⁱ (Experimental-theoretical)/experimental.

The agreement between the experimental and calculated values of Table 10.2 is well within the experimental capability of the spectroscopic determinations including the values at large Z which relies on X-ray spectroscopy. In this case, the experimental capability is three to four significant figures which is consistent with the last column. The beryllium atom isoelectronic series is given in Table 10.2 [2-3] to much higher precision than the capability of X-ray spectroscopy, but these values are based on theoretical and interpolation techniques rather than data alone. Ionization energies are difficult to determine since the cut-off of the Rydberg series of lines at the ionization energy is often not observed, and the ionization energy must be determined from theoretical calculations, interpolation of Be isoelectronic and Rydberg series, as well as direct experimental data.

2P-ORBITAL ELECTRONS BASED ON AN ENERGY MINIMUM

For each four-electron atom having a central charge of Z times that of the proton, there are two indistinguishable spin-paired electrons in an orbitsphere with radii r_1 and r_2 both given by Eq. (7.19) (Eq. (10.51)) and two indistinguishable spin-paired electrons in an orbitsphere with radii r_3 and r_4 both given by Eq. (10.62). For $Z \geq 5$, the next electron which binds to form the corresponding five-electron atom is attracted by the central Coulomb field and is repelled by diamagnetic force due to the spin-paired inner electrons such that it forms an unpaired orbitsphere at radius r_5 .

The central Coulomb force, F_{ele} , acts on the outer electron to cause it to bind wherein this electric force on the outer-most electron due to the nucleus and the inner four electrons is given by Eq. (10.28) with the appropriate charge and radius:

$$F_{ele} = \frac{(Z-4)e^2}{4\pi\epsilon_0 r_5^2} \mathbf{i}_r \quad (10.69)$$

for $r > r_4$. The same form of force equation also applies to six through ten-electron atoms as well as five-electron atoms:

$$F_{ele} = \frac{(Z-n)e^2}{4\pi\epsilon_0 r_n^2} \mathbf{i}_r \quad (10.70)$$

for $r > r_{n-1}$ where n corresponds to the number of electrons of the atom and Z is its atomic number. In each case, the magnetic field of the binding outer electron changes the angular velocities of the inner electrons. However, in each case, the magnetic field of the outer electron provides a central Lorentzian force which exactly balances the change in centrifugal force because of the change in angular velocity [1]. The inner electrons remain at their initial radii, but cause a diamagnetic force

according to Lenz's law.

The diamagnetic force, $F_{\text{diamagnetic}}$, for the formation of an s orbital given by Eq. (10.11) with the appropriate radii is

$$F_{\text{diamagnetic}} = -\frac{\hbar^2}{4m_e r_n^2 r_3} \sqrt{s(s+1)} \mathbf{i}_r \quad (10.71)$$

However, with the formation of a third shell, a nonuniform distribution of charge is possible that achieves an energy minimum. Minimum energy configurations are given by solutions to Laplace's Equation. The general form of the solution (Eq. (11.1)) is

$$\Phi(r, \theta, \phi) = \sum_{\ell=0}^{\infty} \sum_{m=-\ell}^{\ell} B_{\ell,m} r^{-(\ell+1)} Y_{\ell}^m(\theta, \phi) \quad (10.72)$$

As shown in the Excited States of the One-Electron Atom (Quantization) section, this general solution in the form of a wave-equation gives the functions of the resonant photons of excited states. From Eqs. (2.15-2.16):

$$\begin{aligned} E_{r_{\text{photon } n,l,m}} &= \frac{e(na_H)^{\ell}}{4\pi\epsilon_0} \frac{1}{r^{(\ell+2)}} \left[-Y_0^0(\theta, \phi) + \frac{1}{n} \left[Y_0^0(\theta, \phi) + \text{Re}\{Y_{\ell}^m(\theta, \phi)e^{i\omega_{\ell}t}\} \right] \right] \delta(r - r_n) \\ \omega_n &= 0 \text{ for } m = 0 \\ n &= 1, 2, 3, 4, \dots \\ \ell &= 1, 2, \dots, n-1 \\ m &= -\ell, -\ell+1, \dots, 0, \dots, +\ell \end{aligned} \quad (10.73)$$

$E_{r_{\text{total}}}$ is the sum of the "trapped photon" and proton electric fields,

$$\begin{aligned} E_{r_{\text{total}}} &= \frac{e}{4\pi\epsilon_0 r^2} + \frac{e(na_H)^{\ell}}{4\pi\epsilon_0} \frac{1}{r^{(\ell+2)}} \left[-Y_0^0(\theta, \phi) + \frac{1}{n} \left[Y_0^0(\theta, \phi) + \text{Re}\{Y_{\ell}^m(\theta, \phi)e^{i\omega_{\ell}t}\} \right] \right] \delta(r - r_n) \\ \omega_n &= 0 \text{ for } m = 0 \end{aligned} \quad (10.74)$$

As shown in the Angular Function section and the Instability of Excited States section, the charge-density functions including the time-function factor are also solutions of Laplace's equation in the form of a wave-equation (Eqs. (1.48-1.49)):

$$\ell = 0$$

$$\rho(r, \theta, \phi, t) = \frac{e}{8\pi r^2} [\delta(r - r_n)] [Y_0^0(\theta, \phi) + Y_{\ell}^m(\theta, \phi)] \quad (10.75)$$

$$\ell \neq 0$$

$$\rho(r, \theta, \phi, t) = \frac{e}{4\pi r^2} [\delta(r - r_n)] \left[Y_0^0(\theta, \phi) + \text{Re}\{Y_{\ell}^m(\theta, \phi)[1 + e^{i\omega_{\ell}t}]\} \right] \quad (10.76)$$

$$\rho(r, \theta, \phi, t) = \frac{e}{4\pi r^2} [\delta(r - r_n)] [Y_0^0(\theta, \phi) + \text{Re}\{Y_\ell^m(\theta, \phi)e^{i\omega_n t}\}] \quad (10.77)$$

where

$$\text{Re}\{Y_\ell^m(\theta, \phi)[1 + e^{i\omega_n t}]\} = \text{Re}\{Y_\ell^m(\theta, \phi) + Y_\ell^m(\theta, \phi)e^{i\omega_n t}\} = P_\ell^m(\cos\theta)\cos m\phi + P_\ell^m(\cos\theta)\cos(m\phi + \omega_n t)$$

or $\text{Re}\{Y_\ell^m(\theta, \phi)e^{i\omega_n t}\} = P_\ell^m(\cos\theta)\cos(m\phi + \omega_n t)$ and to keep the form of the spherical harmonic as a traveling wave about the z-axis, $\omega_n = m\omega_n$. In the cases that $m \neq 0$, Eq. (1.65) is a traveling charge-density wave that moves on the surface of the orbitsphere about the z-axis with frequency ω_n and modulates the orbitsphere corresponding to $\ell = 0$. These functions comprise the well known s, p, d, f, etc. orbitals wherein the constant function $Y_0^0(\theta, \phi)$ corresponds to the spin function having spin angular momentum and the modulation function $\text{Re}\{Y_\ell^m(\theta, \phi)e^{i\omega_n t}\}$ corresponds to the orbital function having orbital angular momentum as given in the Angular Function section and the Rotational Parameters of the Electron (Angular Momentum, Rotational Energy, Moment of Inertia) section.

Similar to the phenomenon observed for spherical conductors [4-5], spherical harmonic charge-density waves may be induced in the inner electron orbitspheres with the addition of one or more outer electrons, each having an orbital quantum number $\ell \neq 0$ as given by Eq. (10.77). With $Z > 5$, an energy minimum is achieved when the fifth through tenth electrons of each five through ten-electron atom fills a p orbital with the formation of orthogonal complementary charge-density waves in the inner shell electrons. To maintain the symmetry of the central charge and the energy minimum condition given by solutions to Laplace's equation (Eq. (10.72)), the charge-density waves on electron orbitspheres at r_1 and r_3 complement those of the outer orbitals when the outer p orbitals are not all occupied by at least one electron, and the complementary charge-density waves are provided by electrons at r_3 when this condition is met. Since the angular harmonic charge-density waves are nonradiative as shown in the Spacetime Fourier Transform of the Electron Function section and Appendix I: Nonradiation Based on the Electromagnetic Fields and the Poynting Power Vector, the time-averaged central field is inverse r -squared even though the central field is modulated by the concentric charge-density waves. The modulated central field maintains the spherical harmonic orbitals that maintain the spherical-harmonic phase according to Eq. (10.72). For $\ell=1$ and $m=\pm 1$, the spherical harmonics $Y_\ell^m(\theta, \phi)$ given by Eqs. (1.66-1.67) are

$$Y_{1,x} = \sin\theta \cos\phi \quad (10.78)$$

$$Y_{1,y} = \sin\theta \sin\phi \quad (10.79)$$

wherein the x and y designation corresponds, respectively, to the historical p_x and p_y probability-density functions of quantum mechanics. The p_x and p_y charge-density waves rotate in the same direction such that their individual contributions to the diamagnetic force add, or they rotate in opposite directions such that their contributions cancel. In addition, for $\ell=1$ and $m=0$, the spherical harmonic $Y_\ell^m(\theta, \phi)$ is

$$Y_{1,z} = \cos\theta \quad (10.80)$$

wherein the z designation corresponds to the historical p_z probability-density function of quantum mechanics. The demonstration that the modulated orbitsphere solutions are solutions of the wave equation appears in Box 1.1.

As shown by Eq. (10.9), the diamagnetic force is dependent on the integral of the charge-density squared over the surface of the orbitsphere with the further constant of the invariance of charge under Gauss's integral law. The correction to the force due to a time and spatially-dependent spherical harmonic current-density wave is given by the normalization term for spherical harmonics given by Eq. (3.53) of Jackson [6] and Eq. (6-76) of McQuarrie [7]:

$$\frac{(\ell + |m|)!}{(2\ell + 1)(\ell - |m|)!} \quad (10.81)$$

Since the spin function is constant and the orbital function is a traveling wave, only the latter contributes to the diamagnetic and paramagnetic-force contributions of an unpaired electron. Substitution of Eq. (10.81) into Eq. (10.11) gives the contribution of each orbital to the diamagnetic force, $F_{\text{diamagnetic}}$, which is summed over the orbitals:

$$F_{\text{diamagnetic}} = -\sum_m \frac{(\ell + |m|)!}{(2\ell + 1)(\ell - |m|)!} \frac{\hbar^2}{4m_e r_n^2 r_3} \sqrt{s(s+1)} \mathbf{i}_r \quad (10.82)$$

where the contributions from orbitals having $|m|=1$ add positively or negatively.

For each five-electron atom having a central charge of Z times that of the proton, there are two indistinguishable spin-paired electrons in an orbitsphere with radii r_1 and r_2 both given by Eq. (7.19) (Eq. (10.51)), two indistinguishable spin-paired electrons in an orbitsphere with radii r_3 and r_4 both given by Eq. (10.62), and an unpaired electron is in an orbitsphere at r_5 given by Eq. (10.113). For $Z \geq 6$, the next electron which binds to form the corresponding six-electron atom is attracted by the central Coulomb field and is repelled by diamagnetic force due to the spin-paired inner electrons. A paramagnetic spin-pairing force to form a filled s orbital is also possible, but the force due to the spin-pairing of the electrons (Eq. (7.15) with the radius r_6) reduces the energy of the atom

less than that due to the alternative forces on two unpaired p electrons in an orbitsphere at the same radius r_6 .

In general, a nonuniform distribution of charge achieves an energy minimum with the formation of a third shell due to the dependence of the magnetic forces on the nuclear charge and orbital energy (Eqs. (10.52), (10.55), and (10.93)). The outer electrons of atoms and ions that are isoelectronic with the series boron through neon half-fill a 2p level with unpaired electrons at nitrogen, then fill the level with paired electrons at neon. *Thus, it is found that the purely postulated Hund's Rule and the Pauli Exclusion Principle of the assignment of unique quantum numbers to all electrons are not "weird spooky action" phenomena unique to quantum mechanics that require all electrons in the universe to have instantaneous communication and coordination with no basis in physical laws such as Maxwell's equations. Rather they are phenomenological consequences of those laws.*

Each outer 2p electron contributes spin as well as orbital angular momentum. The former gives rise to spin pairing to another 2p electron when an energy minimum is achieved. The corresponding force, $F_{mag 2}$, given by Eq. (10.52) is:

$$F_{mag 2} = \frac{1}{Z} \frac{\hbar^2}{m_e r_n^2 r_3} \sqrt{s(s+1)} \mathbf{i}_r \quad (10.83)$$

The orbital angular momenta of spin-paired electrons may add to double the spin-pairing force of each individual p electron such that the resultant force is four times that of Eq. (10.83) in agreement with the energy (and force) relationship of magnetic fields (Eq. (1.122)):

$$F_{mag 2} = \frac{1}{Z} \frac{4\hbar^2}{m_e r_n^2 r_3} \sqrt{s(s+1)} \mathbf{i}_r \quad (10.84)$$

Or, the orbital angular momenta of spin-paired electrons may add negatively to cancel such that $F_{mag 2}$ due to the contribution from spin-pairing alone is equivalent to that given by Eq. (10.83).

Since the electron velocity given by Eq. (1.47) is

$$v_n = \frac{\hbar}{m_e r_n} \quad (10.85)$$

The scalar sum of the magnitude of the angular momentum of each infinitesimal point of the orbitsphere L_i of mass m_i must be constant. The constant is \hbar .

$$\sum |L_i| = \sum |\mathbf{r} \times m_i \mathbf{v}| = m_e r_n \frac{\hbar}{m_e r_n} = \hbar \quad (10.86)$$

where the velocity is given by Eq. (1.47). The sum of the magnitude of the angular momentum of the electron is \hbar in any inertial frame and is relativistically invariant. The vector projections of the orbitsphere spin

angular momentum relative to the Cartesian coordinates are given in the Spin Angular Momentum of the Orbitsphere with $\ell = 0$ section. The orbital and spin angular momentum of excited states is also quantized in units of \hbar as shown in the Orbital and Spin Splitting section. The orbital moment of inertia, $I_{orbital}$, corresponding to orbital quantum number ℓ (Eq. (1.96)) is

$$I_{orbital} = m_e r_n^2 \left[\frac{\ell(\ell+1)}{\ell^2 + 2\ell + 1} \right]^{\frac{1}{2}} = m_e r_n^2 \sqrt{\frac{\ell}{\ell+1}} \quad (10.87)$$

The spin and orbital angular momentum can superimpose positively or negatively:

$$L_{z\ total} = L_{z\ spin} + L_{z\ orbital} \quad (10.88)$$

Thus, the contribution of the orbital angular momentum to the paramagnetic force is also that given by Eq. (10.83):

$$\mathbf{F}_{mag\ 2} = \frac{1}{Z} \frac{\hbar^2}{m_e r_n^2 r_3} \sqrt{s(s+1)} \mathbf{i}_r \quad (10.89)$$

And, the total force is given as the sum over the orbital and spin angular momenta that may add positively or negatively to achieve an energy minimum while maintaining the conservation of angular momentum.

The amplitude of the corresponding rotational energy, $E_{rotational\ orbital}$, given by Eqs. (1.95-1.96) is

$$E_{rotational\ orbital} = \frac{\hbar^2}{2m_e r_n^2} \left[\frac{\ell(\ell+1)}{\ell^2 + 2\ell + 1} \right]^{\frac{1}{2}} = \frac{\hbar^2}{2m_e r_n^2} \sqrt{\frac{\ell}{\ell+1}} \quad (10.90)$$

Since the orbital rotational energy arises from a spin function (spin angular momentum) modulated by a spherical harmonic angular function (orbital angular momentum), the time-averaged orbital rotational energy having an amplitude given by Eq. (1.95) (Eq. (10.90)) is zero:

$$\langle E_{rotational\ orbital} \rangle = 0 \quad (10.91)$$

However, the orbital energy is nonzero in the presence of a magnetic field.

N-electron atoms having $Z > n$ possess an electric field of

$$\mathbf{E} = \frac{(Z-n)e}{4\pi\epsilon_0 r^2} \mathbf{i}_r \quad (10.92)$$

for $r > r_n$. Since there is a source of dissipative, $\mathbf{J} \cdot \mathbf{E}$ of Eq. (10.27), the magnetic moments of the inner electrons may change due to the outer electron such that the energy of the n-electron atom is lowered. The diamagnetic force, $\mathbf{F}_{diamagnetic\ 2}$, due to a relativistic effect with an electric field for $r > r_n$ (Eq. (10.35)) is dependent on the amplitude of the orbital energy. Using the orbital energy with $\ell=1$ (Eq. (10.90)), the energy $m_e \Delta v^2$

of Eq. (10.29) is reduced by the factor of $\left(1 - \frac{\sqrt{2}}{2}\right)$ due to the contribution of the charge-density wave of the inner electrons at r_3 . Thus, $F_{\text{diamagnetic } 2}$ is given by

$$F_{\text{diamagnetic } 2} = -\left[\frac{Z-n}{Z-(n-1)}\right]\left(1 - \frac{\sqrt{2}}{2}\right)\frac{r_3\hbar^2}{m_e r_n^4}10\sqrt{s(s+1)}\mathbf{i}_r \quad (10.93)$$

Using the forces given by Eqs. (10.70), (10.82-10.84), (10.89), (10.93), and the radii r_3 given by Eq. (10.62), the radii of the 2p electrons of all five through ten-electron atoms may be solved exactly. The electric energy given by Eq. (10.102) gives the corresponding exact ionization energies. F_{ele} and $F_{\text{diamagnetic } 2}$ given by Eqs. (10.70) and (10.93), respectively, are of the same form for all atoms with the appropriate nuclear charges and atomic radii. $F_{\text{diamagnetic}}$ given by Eq. (10.82) and $F_{\text{mag } 2}$ given by Eqs. (10.83-10.84) and (10.89) are of the same form with the appropriate factors that depend on the minimum-energy electron configuration. The general equation and the summary of the parameters that determine the exact radii and ionization energies of all five through ten-electron atoms are given the General Equation For The Ionization Energies of Five Through Ten-Electron Atoms section and in Table 10.9.

FIVE-ELECTRON ATOMS

Five-electron atoms can be solved exactly using the results of the solutions of one, two, three, and four-electron atoms.

RADIUS AND IONIZATION ENERGY OF THE OUTER ELECTRON OF THE BORON ATOM

For each four-electron atom having a central charge of Z times that of the proton, there are two indistinguishable spin-paired electrons in an orbitsphere with radii r_1 and r_2 both given by Eq. (7.19) (Eq. (10.51)) and two indistinguishable spin-paired electrons in an orbitsphere with radii r_3 and r_4 both given by Eq. (10.62). For $Z \geq 5$, the next electron which binds to form the corresponding five-electron atom is attracted by the central Coulomb field and is repelled by diamagnetic force due to the spin-paired inner electrons such that it forms an unpaired orbitsphere at radius r_5 . The resulting electron configuration is $1s^2 2s^2 2p^1$, and the orbital arrangement is

$$\begin{array}{ccc} \uparrow & _ & _ \\ 1 & 0 & -1 \end{array} \quad (10.94)$$

corresponding to the ground state $^2P_{1/2}^0$.

The central Coulomb force acts on the outer electron to cause it to bind wherein this electric force on the outer-most electron due to the nucleus and the inner four electrons is given by Eq. (10.70) with the appropriate charge and radius:

$$\mathbf{F}_{ele} = \frac{(Z-4)e^2}{4\pi\epsilon_0 r_5^2} \mathbf{i}_r \quad (10.95)$$

for $r > r_4$.

The single p orbital of the boron atom produces a diamagnetic force equivalent to that of the formation of an s orbital due to the induction of complementary and spherically symmetrical charge-density waves on electron orbitspheres at r_1 and r_3 in order to achieve a solution of Laplace's equation (Eq. (10.72)). The inner electrons remain at their initial radii, but cause a diamagnetic force according to Lenz's law that is two times that of Eqs. (10.11) and (10.71) since the two electrons at $r_1 = r_2$ act on the two electrons at $r_3 = r_4$ which in turn act of the outer electron. $\mathbf{F}_{diamagnetic}$ is also given by Eq. (10.82) with the appropriate radii when the contributions from the three orthogonal spherical harmonics are summed over including those induced:

$$\mathbf{F}_{diamagnetic} = -\frac{2\hbar^2}{4m_e r_5^2 r_3} \sqrt{s(s+1)} \mathbf{i}_r \quad (10.96)$$

The charge induction forms complementary mirror charge-density waves which must have opposing angular momenta such that momentum is conserved. In this case, \mathbf{F}_{mag2} given by Eq. (10.89) is zero:

$$\mathbf{F}_{mag2} = 0 \quad (10.97)$$

The outward centrifugal force on electron 5 is balanced by the electric force and the magnetic force (on electron 5). The radius of the outer electron is calculated by equating the outward centrifugal force to the sum of the electric (Eq. (10.95)) and diamagnetic (Eq. (10.96)) forces as follows:

$$\frac{m_e v_5^2}{r_5} = \frac{(Z-4)e^2}{4\pi\epsilon_0 r_5^2} - \frac{2\hbar^2}{4m_e r_5^2 r_3} \sqrt{s(s+1)} \quad (10.98)$$

Substitution of $v_5 = \frac{\hbar}{m_e r_5}$ (Eq. (1.56)) and $s = \frac{1}{2}$ into Eq. (10.98) gives:

$$\frac{\hbar^2}{m_e r_5^3} = \frac{(Z-4)e^2}{4\pi\epsilon_0 r_5^2} - \frac{\hbar^2}{2m_e r_5^2 r_3} \sqrt{\frac{3}{4}} \quad (10.99)$$

$$r_5 = \frac{a_0}{\left((Z-4) - \frac{\sqrt{3/4}}{2r_3} \right)}, \quad r_3 \text{ in units of } a_0 \quad (10.100)$$

Substitution of $\frac{r_3}{a_0} = 1.07930$ (Eq. (10.62) with $Z=5$) into Eq. (10.100) gives

$$r_3 = 1.67000351a_0 \quad (10.101)$$

In general, the energy stored in the electric field, $E(\text{electric})$, is given by Eq. (10.43) with the appropriate charge and radius:

$$E(\text{electric}) = -\frac{(Z-(n-1))e^2}{8\pi\epsilon_0 r_n} \quad (10.102)$$

where n corresponds to the number of electrons of the atom and Z is its atomic number. The ionization energy is given by the sum of the electric energy and the energy corresponding to the change in magnetic-moments of the inner shell electrons. Since there is no source of dissipative power, $\mathbf{J} \cdot \mathbf{E}$ of Eq. (10.27), to compensate for any potential change in the magnetic moments, Δm , of the inner electrons due to the ionization of the outer electron of the boron atom, there is a diamagnetic energy term in the ionization energy for this atom that follows from the corresponding term for the lithium atom. Since the diamagnetic force for the boron atom (Eq. (10.96)) is twice that of the corresponding force (Eq. (10.11)) of the lithium atom, this term is given by twice that of Eqs. (10.15-10.24), with $Z=5$, r_3 given by Eq. (10.62), and r_5 given by Eq. (10.101). Thus, the change in magnetic energy of the inner orbitsphere at r_3 is 85.429321%, so that the corresponding energy ΔE_{mag} is

$$\Delta E_{mag} = 2(0.85429321 \times 0.09100214 \text{ eV}) = 0.15548501 \text{ eV} \quad (10.103)$$

where the magnetic energy of the inner electrons is 0.09100214 eV (Eqs. (10.64) and (10.101)). Then, the ionization energy of the boron atom is given by Eqs. (10.101-10.102) and (10.103):

$$\begin{aligned} E(\text{ionization}; B) &= \frac{(Z-4)e^2}{8\pi\epsilon_0 r_3} + \Delta E_{mag} \\ &= 8.147170901 \text{ eV} + 0.15548501 \text{ eV} = 8.30265592 \text{ eV} \end{aligned} \quad (10.104)$$

The experimental ionization energy of the boron atom is 8.29803 eV [3].

THE IONIZATION ENERGIES OF FIVE-ELECTRON ATOMS WITH A NUCLEAR CHARGE $Z>5$

Five-electron atoms having $Z>5$ possess an external electric field given by Eq. (10.92). In this case, an energy minimum is achieved with conservation of momentum when the orbital angular momentum is such that $\mathbf{F}_{\text{diamagnetic}}$ is minimized while $\mathbf{F}_{\text{mag } 2}$ is maximized. From Eq. (10.82), the diamagnetic force, $\mathbf{F}_{\text{diamagnetic}}$, is given by the sum of the contributions from the p_x , p_y , and p_z orbitals corresponding to $m = 1, -1$, and 0, respectively:

$$\mathbf{F}_{\text{diamagnetic}} = -\left(\frac{2}{3} + \frac{2}{3} + \frac{1}{3}\right) \frac{\hbar^2}{4m_e r_3^2 r_5} \sqrt{s(s+1)} \mathbf{i}_r = -\left(\frac{5}{3}\right) \frac{\hbar^2}{4m_e r_3^2 r_5} \sqrt{s(s+1)} \mathbf{i}_r \quad (10.105)$$

With $Z > 5$, the charge induction forms complementary mirror charge-density waves such that the angular momenta do not cancel. From Eq. (10.89), $F_{mag\ 2}$ corresponding to the orbital angular momentum of the single p_x electron is

$$F_{mag\ 2} = \frac{1}{Z} \frac{\hbar^2}{m_e r_5^2 r_3} \sqrt{s(s+1)} \mathbf{i}_r \quad (10.106)$$

The second diamagnetic force, $F_{diamagnetic\ 2}$, due to the binding of the p-orbital electron having an electric field outside of its radius is given by Eq. (10.93):

$$F_{diamagnetic\ 2} = -\left[\frac{Z-5}{Z-4} \right] \left(1 - \frac{\sqrt{2}}{2} \right) \frac{r_3 \hbar^2}{m_e r_5^4} 10 \sqrt{s(s+1)} \mathbf{i}_r \quad (10.107)$$

In the case that $Z > 5$, the radius of the outer electron is calculated by equating the outward centrifugal force to the sum of the electric (Eq. (10.95)) and diamagnetic (Eqs. (10.105) and (10.107)), and paramagnetic (Eq. (10.106)) forces as follows:

$$\frac{m_e v_s^2}{r_5} = \frac{(Z-4)e^2}{4\pi\epsilon_0 r_5^2} - \frac{5\hbar^2}{12m_e r_5^2 r_3} \sqrt{s(s+1)} + \frac{\hbar^2}{Zm_e r_5^2 r_3} \sqrt{s(s+1)} - \left[\frac{Z-5}{Z-4} \right] \left(1 - \frac{\sqrt{2}}{2} \right) \frac{r_3 \hbar^2}{r_5^4 m_e} 10 \sqrt{s(s+1)} \quad (10.108)$$

Substitution of $v_s = \frac{\hbar}{m_e r_5}$ (Eq. (1.56)) and $s = \frac{1}{2}$ into Eq. (10.108) gives:

$$\frac{\hbar^2}{m_e r_5^3} = \frac{(Z-4)e^2}{4\pi\epsilon_0 r_5^2} - \frac{5\hbar^2}{12m_e r_5^2 r_3} \sqrt{\frac{3}{4}} + \frac{\hbar^2}{Zm_e r_5^2 r_3} \sqrt{\frac{3}{4}} - \left[\frac{Z-5}{Z-4} \right] \left(1 - \frac{\sqrt{2}}{2} \right) \frac{r_3 \hbar^2}{r_5^4 m_e} 10 \sqrt{\frac{3}{4}} \quad (10.109)$$

The quadratic equation corresponding to Eq. (10.109) is

$$\left(\frac{(Z-4)e^2}{4\pi\epsilon_0} - \left(\frac{5}{12} - \frac{1}{Z} \right) \frac{\hbar^2}{m_e r_3} \sqrt{\frac{3}{4}} \right) r_5^2 - \frac{\hbar^2}{m_e} r_5 - \left[\frac{Z-5}{Z-4} \right] \left(1 - \frac{\sqrt{2}}{2} \right) \frac{r_3 \hbar^2}{m_e} 10 \sqrt{\frac{3}{4}} = 0 \quad (10.110)$$

$$r_5^2 - \frac{\frac{\hbar^2}{m_e}}{\left(\frac{(Z-4)e^2}{4\pi\epsilon_0} - \left(\frac{5}{12} - \frac{1}{Z} \right) \frac{\hbar^2}{m_e r_3} \sqrt{\frac{3}{4}} \right)} r_5 - \frac{\frac{\hbar^2}{m_e} \left[\frac{Z-5}{Z-4} \right] \left(1 - \frac{\sqrt{2}}{2} \right) r_3 10 \sqrt{\frac{3}{4}}}{\left(\frac{(Z-4)e^2}{4\pi\epsilon_0} - \left(\frac{5}{12} - \frac{1}{Z} \right) \frac{\hbar^2}{m_e r_3} \sqrt{\frac{3}{4}} \right)} = 0 \quad (10.111)$$

The solution of Eq. (10.111) using the quadratic formula is:

$$r_5 = \frac{\frac{\hbar^2}{m_e} \left(\frac{(Z-4)e^2}{4\pi\epsilon_0} - \left(\frac{5}{12} - \frac{1}{Z} \right) \frac{\hbar^2}{m_e r_3} \sqrt{\frac{3}{4}} \right) \pm \sqrt{\left(\frac{\hbar^2}{m_e} \left(\frac{(Z-4)e^2}{4\pi\epsilon_0} - \left(\frac{5}{12} - \frac{1}{Z} \right) \frac{\hbar^2}{m_e r_3} \sqrt{\frac{3}{4}} \right) \right)^2 + 4 \frac{\frac{\hbar^2}{m_e} \left[\frac{Z-5}{Z-4} \right] \left(1 - \frac{\sqrt{2}}{2} \right) r_3 10 \sqrt{\frac{3}{4}} \left(\frac{(Z-4)e^2}{4\pi\epsilon_0} - \left(\frac{5}{12} - \frac{1}{Z} \right) \frac{\hbar^2}{m_e r_3} \sqrt{\frac{3}{4}} \right)}}{2} \quad (10.112)$$

$$r_5 = \frac{\frac{a_0}{\left((Z-4) - \left(\frac{5}{24} - \frac{1}{2Z} \right) \frac{\sqrt{3}}{r_3} \right)} \pm a_0 \sqrt{\left(\frac{1}{\left((Z-4) - \left(\frac{5}{24} - \frac{1}{2Z} \right) \frac{\sqrt{3}}{r_3} \right)} \right)^2 + \frac{20\sqrt{3} \left(\left[\frac{Z-5}{Z-4} \right] \left(1 - \frac{\sqrt{2}}{2} \right) r_3 \right)}{\left((Z-4) - \left(\frac{5}{24} - \frac{1}{2Z} \right) \frac{\sqrt{3}}{r_3} \right)}}}{2} \quad (10.113)$$

r_3 in units of a_0

where r_3 is given by Eq. (10.62). The positive root of Eq. (10.113) must be taken in order that $r_5 > 0$. The radii of several five-electron atoms are given in Table 10.3.

The ionization energies for the five-electron atoms with $Z > 5$ are given by the electric energy, $E(\text{electric})$, (Eq. (10.102) with the radii, r_5 , given by Eq. (10.113)):

$$E(\text{ionization}) = -\text{Electric Energy} = \frac{(Z-4)e^2}{8\pi\epsilon_0 r_5} \quad (10.114)$$

Since the relativistic corrections were small, the nonrelativistic ionization energies for experimentally measured five-electron atoms are given in Table 10.3.

Table 10.3. Ionization energies for some five-electron atoms.

5 e Atom	Z	r_1 (a_0) ^a	r_3 (a_0) ^b	r_5 (a_0) ^c	Theoretical Ionization Energies ^d (eV)	Experimental Ionization Energies ^e (eV)	Relative Error ^f
B	5	0.20670	1.07930	1.67000	8.30266	8.29803	-0.00056
C ⁺	6	0.17113	0.84317	1.12092	24.2762	24.38332	0.0044
N ²⁺	7	0.14605	0.69385	0.87858	46.4585	47.44924	0.0209
O ³⁺	8	0.12739	0.59020	0.71784	75.8154	77.41353	0.0206
F ⁴⁺	9	0.11297	0.51382	0.60636	112.1922	114.2428	0.0179
Ne ⁵⁺	10	0.10149	0.45511	0.52486	155.5373	157.93	0.0152
Na ⁶⁺	11	0.09213	0.40853	0.46272	205.8266	208.5	0.0128
Mg ⁷⁺	12	0.08435	0.37065	0.41379	263.0469	265.96	0.0110
Al ⁸⁺	13	0.07778	0.33923	0.37425	327.1901	330.13	0.0089
Si ⁹⁺	14	0.07216	0.31274	0.34164	398.2509	401.37	0.0078
P ¹⁰⁺	15	0.06730	0.29010	0.31427	476.2258	479.46	0.0067
S ¹¹⁺	16	0.06306	0.27053	0.29097	561.1123	564.44	0.0059
Cl ¹²⁺	17	0.05932	0.25344	0.27090	652.9086	656.71	0.0058
Ar ¹³⁺	18	0.05599	0.23839	0.25343	751.6132	755.74	0.0055
K ¹⁴⁺	19	0.05302	0.22503	0.23808	857.2251	861.1	0.0045
Ca ¹⁵⁺	20	0.05035	0.21308	0.22448	969.7435	974	0.0044
Sc ¹⁶⁺	21	0.04794	0.20235	0.21236	1089.1678	1094	0.0044
Ti ¹⁷⁺	22	0.04574	0.19264	0.20148	1215.4975	1221	0.0045
V ¹⁸⁺	23	0.04374	0.18383	0.19167	1348.7321	1355	0.0046
Cr ¹⁹⁺	24	0.04191	0.17579	0.18277	1488.8713	1496	0.0048
Mn ²⁰⁺	25	0.04022	0.16842	0.17466	1635.9148	1644	0.0049
Fe ²¹⁺	26	0.03867	0.16165	0.16724	1789.8624	1799	0.0051
Co ²²⁺	27	0.03723	0.15540	0.16042	1950.7139	1962	0.0058
Ni ²³⁺	28	0.03589	0.14961	0.15414	2118.4690	2131	0.0059
Cu ²⁴⁺	29	0.03465	0.14424	0.14833	2293.1278	2308	0.0064

^a Radius of the first set of paired inner electrons of five-electron atoms from Eq. (10.51).^b Radius of the second set of paired inner electrons of five-electron atoms from Eq. (10.62).^c Radius of the outer electron of five-electron atoms from Eq. (10.113) for $Z > 5$ and Eq. (10.101) for B .^d Calculated ionization energies of five-electron atoms given by the electric energy (Eq. (10.114)) for $Z > 5$ and Eq. (10.104) for B .^e From theoretical calculations, interpolation of isoelectronic and spectral series, and experimental data [2-3].^f (Experimental-theoretical)/experimental.

The agreement between the experimental and calculated values of Table 10.3 is well within the experimental capability of the spectroscopic determinations including the values at large Z which relies on X-ray

spectroscopy. In this case, the experimental capability is three to four significant figures which is consistent with the last column. The boron atom isoelectronic series is given in Table 10.3 [2-3] to much higher precision than the capability of X-ray spectroscopy, but these values are based on theoretical and interpolation techniques rather than data alone. Ionization energies are difficult to determine since the cut-off of the Rydberg series of lines at the ionization energy is often not observed, and the ionization energy must be determined from theoretical calculations, interpolation of B isoelectronic and Rydberg series, as well as direct experimental data.

SIX-ELECTRON ATOMS

Six-electron atoms can be solved exactly using the results of the solutions of one, two, three, four, and five-electron atoms.

RADIUS AND IONIZATION ENERGY OF AN OUTER ELECTRON OF THE CARBON ATOM

For each five-electron atom having a central charge of Z times that of the proton, there are two indistinguishable spin-paired electrons in an orbitsphere with radii r_1 and r_2 both given by Eq. (7.19) (Eq. (10.51)), two indistinguishable spin-paired electrons in an orbitsphere with radii r_3 and r_4 both given by Eq. (10.62), and an unpaired electron is in an orbitsphere at r_5 given by Eq. (10.113). For $Z \geq 6$, the next electron which binds to form the corresponding six-electron atom is attracted by the central Coulomb field and is repelled by diamagnetic force due to the spin-paired inner electrons. A paramagnetic spin-pairing force to form a filled s orbital is also possible, but the force due to the spin-pairing of the electrons (Eq. (7.15) with the radius r_6) reduces the energy of the atom less than that due to the alternative forces on two unpaired p electrons in an orbitsphere at the same radius r_6 . The resulting electron configuration is $1s^2 2s^2 2p^2$, and the orbital arrangement is

$$\begin{array}{ccc} \uparrow & \uparrow & _ \\ \hline 1 & 0 & -1 \end{array} \quad (10.115)$$

corresponding to the ground state 3P_0 .

The central Coulomb force acts on the outer electron to cause it to bind wherein this electric force on the outer-most electron due to the nucleus and the inner five electrons is given by Eq. (10.70) with the appropriate charge and radius:

$$\mathbf{F}_{ele} = \frac{(Z-5)e^2}{4\pi\epsilon_0 r_6^2} \mathbf{i}_r \quad (10.116)$$

for $r > r_3$.

The two orthogonal electrons form charge-density waves such that the total angular momentum of the two outer electrons is conserved which determines the diamagnetic force according to Eq. (10.82). $F_{diamagnetic}$ is

$$F_{diamagnetic} = -\left(\frac{2}{3}\right) \frac{\hbar^2}{4m_e r_6^2 r_3} \sqrt{s(s+1)} \mathbf{i}, \quad (10.117)$$

corresponding to $m=1$.

The charge induction forms complementary mirror charge-density waves which must have opposing angular momenta such that momentum is conserved. In this case, F_{mag2} given by Eq. (10.89) is zero:

$$F_{mag2} = 0 \quad (10.118)$$

The outward centrifugal force on electron 6 is balanced by the electric force and the magnetic forces (on electron 6). The radius of the outer electron is calculated by equating the outward centrifugal force to the sum of the electric (Eq. (10.116)) and diamagnetic (Eq. (10.117)) forces as follows:

$$\frac{m_e v_6^2}{r_6} = \frac{(Z-5)e^2}{4\pi\epsilon_0 r_6^2} - \frac{\hbar^2}{6m_e r_6^2 r_3} \sqrt{s(s+1)} \quad (10.119)$$

Substitution of $v_6 = \frac{\hbar}{m_e r_6}$ (Eq. (1.56)) and $s = \frac{1}{2}$ into Eq. (10.119) gives:

$$\frac{\hbar^2}{m_e r_6^3} = \frac{(Z-5)e^2}{4\pi\epsilon_0 r_6^2} - \frac{\hbar^2}{6m_e r_6^2 r_3} \sqrt{\frac{3}{4}} \quad (10.120)$$

$$r_6 = \frac{a_0}{\left((Z-5) - \frac{\sqrt{\frac{3}{4}}}{6r_3} \right)}, \quad r_3 \text{ in units of } a_0 \quad (10.121)$$

Substitution of $\frac{r_3}{a_0} = 0.84317$ (Eq. (10.62) with $Z=6$) into Eq. (10.121) gives

$$r_6 = 1.20654a_0 \quad (10.122)$$

The ionization energy of the carbon atom is given by the electric energy, $E(electric)$, (Eq. (10.102) with the radius, r_6 , given by Eq. (10.122)):

$$E(ionization; C) = -Electric\ Energy = \frac{(Z-5)e^2}{8\pi\epsilon_0 r_6} = 11.27671\ eV \quad (10.123)$$

where $r_6 = 1.20654a_0$ (Eq. (10.122)) and $Z=6$. The experimental ionization energy of the carbon atom is 11.2603 eV [3].

THE IONIZATION ENERGIES OF SIX-ELECTRON ATOMS WITH A NUCLEAR CHARGE $Z>6$

Six-electron atoms having $Z > 6$ possess an external electric field given by Eq. (10.92). In this case, an energy minimum is achieved with conservation of momentum when the orbital angular momentum is such that $F_{\text{diamagnetic}}$ is minimized while $F_{\text{mag } 2}$ is maximized. From Eq. (10.82), the diamagnetic force, $F_{\text{diamagnetic}}$, is given by the sum of the contributions from the p_x , p_y , and p_z orbitals corresponding to $m = 1, -1$, and 0 , respectively:

$$F_{\text{diamagnetic}} = -\left(\frac{2}{3} + \frac{2}{3} + \frac{1}{3}\right) \frac{\hbar^2}{4m_e r_6^2 r_3} \sqrt{s(s+1)} \mathbf{i}_r = -\left(\frac{5}{3}\right) \frac{\hbar^2}{4m_e r_6^2 r_3} \sqrt{s(s+1)} \mathbf{i}_r \quad (10.124)$$

With $Z > 6$, the charge induction forms complementary mirror charge-density waves such that the angular momenta do not cancel. From Eq. (10.89), $F_{\text{mag } 2}$ corresponding to the orbital angular momentum of the two p electrons in addition to complementary charge-density waves is

$$F_{\text{mag } 2} = 2 \frac{1}{Z} \frac{2\hbar^2}{m_e r_6^2 r_3} \sqrt{s(s+1)} \mathbf{i}_r = \frac{1}{Z} \frac{4\hbar^2}{m_e r_6^2 r_3} \sqrt{s(s+1)} \mathbf{i}_r \quad (10.125)$$

The second diamagnetic force, $F_{\text{diamagnetic } 2}$, due to the binding of the p -orbital electron having an electric field outside of its radius is given by Eq. (10.93):

$$F_{\text{diamagnetic } 2} = -\left[\frac{Z-6}{Z-5}\right] \left(1 - \frac{\sqrt{2}}{2}\right) \frac{r_3 \hbar^2}{m_e r_6^4} 10 \sqrt{s(s+1)} \mathbf{i}_r \quad (10.126)$$

In the case that $Z > 6$, the radius of the outer electron is calculated by equating the outward centrifugal force to the sum of the electric (Eq. (10.116)), diamagnetic (Eqs. (10.124) and (10.126)), and paramagnetic (Eq. (10.125)) forces as follows:

$$\frac{m_e v_6^2}{r_6} = \frac{(Z-5)e^2}{4\pi\epsilon_0 r_6^2} - \frac{5\hbar^2}{12m_e r_6^2 r_3} \sqrt{s(s+1)} + \frac{4\hbar^2}{Zm_e r_6^2 r_3} \sqrt{s(s+1)} - \left[\frac{Z-6}{Z-5}\right] \left(1 - \frac{\sqrt{2}}{2}\right) \frac{r_3 \hbar^2}{m_e r_6^4} 10 \sqrt{s(s+1)} \quad (10.127)$$

Substitution of $v_6 = \frac{\hbar}{m_e r_6}$ (Eq. (1.56)) and $s = \frac{1}{2}$ into Eq. (10.127) gives:

$$\frac{\hbar^2}{m_e r_6^3} = \frac{(Z-5)e^2}{4\pi\epsilon_0 r_6^2} - \frac{5\hbar^2}{12m_e r_6^2 r_3} \sqrt{\frac{3}{4}} + \frac{4\hbar^2}{Zm_e r_6^2 r_3} \sqrt{\frac{3}{4}} - \left[\frac{Z-6}{Z-5}\right] \left(1 - \frac{\sqrt{2}}{2}\right) \frac{r_3 \hbar^2}{r_6^4 m_e} 10 \sqrt{\frac{3}{4}} \quad (10.128)$$

The quadratic equation corresponding to Eq. (10.128) is

$$\left(\frac{(Z-5)e^2}{4\pi\epsilon_0} - \left(\frac{5}{12} - \frac{4}{Z}\right) \frac{\hbar^2}{m_e r_3} \sqrt{\frac{3}{4}}\right) r_6^2 - \frac{\hbar^2}{m_e} r_6 - \left[\frac{Z-6}{Z-5}\right] \left(1 - \frac{\sqrt{2}}{2}\right) \frac{r_3 \hbar^2}{m_e} 10 \sqrt{\frac{3}{4}} = 0 \quad (10.129)$$

$$r_6^2 - \frac{\frac{\hbar^2}{m_e}}{\left(\frac{(Z-5)e^2}{4\pi\epsilon_0} - \left(\frac{5}{12} - \frac{4}{Z}\right)\frac{\hbar^2}{m_e r_3} \sqrt{\frac{3}{4}}\right)} r_6 - \frac{\frac{\hbar^2}{m_e} \left[\frac{Z-6}{Z-5}\right] \left(1 - \frac{\sqrt{2}}{2}\right) r_3 10 \sqrt{\frac{3}{4}}}{\left(\frac{(Z-5)e^2}{4\pi\epsilon_0} - \left(\frac{5}{12} - \frac{4}{Z}\right)\frac{\hbar^2}{m_e r_3} \sqrt{\frac{3}{4}}\right)} = 0 \quad (10.130)$$

The solution of Eq. (10.130) using the quadratic formula is:

$$r_6 = \frac{\frac{\hbar^2}{m_e}}{\left(\frac{(Z-5)e^2}{4\pi\epsilon_0} - \left(\frac{5}{12} - \frac{4}{Z}\right)\frac{\hbar^2}{m_e r_3} \sqrt{\frac{3}{4}}\right)} \pm \frac{\sqrt{\left(\frac{\hbar^2}{m_e}\right)^2 - 4 \left(\frac{(Z-5)e^2}{4\pi\epsilon_0} - \left(\frac{5}{12} - \frac{4}{Z}\right)\frac{\hbar^2}{m_e r_3} \sqrt{\frac{3}{4}}\right) \frac{\hbar^2}{m_e} \left[\frac{Z-6}{Z-5}\right] \left(1 - \frac{\sqrt{2}}{2}\right) r_3 10 \sqrt{\frac{3}{4}}}}{2} \quad (10.131)$$

$$r_6 = \frac{\frac{a_0}{\left((Z-5) - \left(\frac{5}{24} - \frac{2}{Z}\right)\frac{\sqrt{3}}{r_3}\right)} \pm a_0 \sqrt{\left(\frac{1}{\left((Z-5) - \left(\frac{5}{24} - \frac{2}{Z}\right)\frac{\sqrt{3}}{r_3}\right)}\right)^2 - 20\sqrt{3} \left[\frac{Z-6}{Z-5}\right] \left(1 - \frac{\sqrt{2}}{2}\right) r_3}}{2} \quad (10.132)$$

r_3 in units of a_0

where r_3 is given by Eq. (10.62). The positive root of Eq. (10.132) must be taken in order that $r_6 > 0$. The final radius of electron 6, r_6 , is given by Eq. (10.132); this is also the final radius of electron 5. The radii of several six-electron atoms are given in Table 10.4.

The ionization energies for the six-electron atoms with $Z > 6$ are given by the electric energy, $E(\text{electric})$, (Eq. (10.102) with the radii r_6 , given by Eq. (10.132)):

$$E(\text{Ionization}) = -\text{Electric Energy} = \frac{(Z-5)e^2}{8\pi\epsilon_0 r_6} \quad (10.133)$$

Since the relativistic corrections were small, the nonrelativistic ionization energies for experimentally measured six-electron atoms are given in

Table 10.4.

Table 10.4. Ionization energies for some six-electron atoms.

6 e Atom	Z	r_1 (a_0) ^a	r_3 (a_0) ^b	r_6 (a_0) ^c	Theoretical Ionization Energies ^d (eV)	Experimental Ionization Energies ^e (eV)	Relative Error ^f
C	6	0.17113	0.84317	1.20654	11.27671	11.2603	-0.0015
N ⁺	7	0.14605	0.69385	0.90119	30.1950	29.6013	-0.0201
O ²⁺	8	0.12739	0.59020	0.74776	54.5863	54.9355	0.0064
F ³⁺	9	0.11297	0.51382	0.63032	86.3423	87.1398	0.0092
Ne ⁴⁺	10	0.10149	0.45511	0.54337	125.1986	126.21	0.0080
Na ⁵⁺	11	0.09213	0.40853	0.47720	171.0695	172.18	0.0064
Mg ⁶⁺	12	0.08435	0.37065	0.42534	223.9147	225.02	0.0049
Al ⁷⁺	13	0.07778	0.33923	0.38365	283.7121	284.66	0.0033
Si ⁸⁺	14	0.07216	0.31274	0.34942	350.4480	351.12	0.0019
P ⁹⁺	15	0.06730	0.29010	0.32081	424.1135	424.4	0.0007
S ¹⁰⁺	16	0.06306	0.27053	0.29654	504.7024	504.8	0.0002
Cl ¹¹⁺	17	0.05932	0.25344	0.27570	592.2103	591.99	-0.0004
Ar ¹²⁺	18	0.05599	0.23839	0.25760	686.6340	686.1	-0.0008
K ¹³⁺	19	0.05302	0.22503	0.24174	787.9710	786.6	-0.0017
Ca ¹⁴⁺	20	0.05035	0.21308	0.22772	896.2196	894.5	-0.0019
Sc ¹⁵⁺	21	0.04794	0.20235	0.21524	1011.3782	1009	-0.0024
Ti ¹⁶⁺	22	0.04574	0.19264	0.20407	1133.4456	1131	-0.0022
V ¹⁷⁺	23	0.04374	0.18383	0.19400	1262.4210	1260	-0.0019
Cr ¹⁸⁺	24	0.04191	0.17579	0.18487	1398.3036	1396	-0.0017
Mn ¹⁹⁺	25	0.04022	0.16842	0.17657	1541.0927	1539	-0.0014
Fe ²⁰⁺	26	0.03867	0.16165	0.16899	1690.7878	1689	-0.0011
Co ²¹⁺	27	0.03723	0.15540	0.16203	1847.3885	1846	-0.0008
Ni ²²⁺	28	0.03589	0.14961	0.15562	2010.8944	2011	0.0001
Cu ²³⁺	29	0.03465	0.14424	0.14970	2181.3053	2182	0.0003

^a Radius of the first set of paired inner electrons of six-electron atoms from Eq. (10.51).^b Radius of the second set of paired inner electrons of six-electron atoms from Eq. (10.62).^c Radius of the two unpaired outer electrons of six-electron atoms from Eq. (10.132) for $Z > 6$ and Eq. (10.122) for C.^d Calculated ionization energies of six-electron atoms given by the electric energy (Eq. (10.133)).^e From theoretical calculations, interpolation of isoelectronic and spectral series, and experimental data [2-3].^f (Experimental-theoretical)/experimental.

The agreement between the experimental and calculated values of Table 10.4 is well within the experimental capability of the spectroscopic

determinations including the values at large Z which relies on X-ray spectroscopy. In this case, the experimental capability is three to four significant figures which is consistent with the last column. The carbon atom isoelectronic series is given in Table 10.4 [2-3] to much higher precision than the capability of X-ray spectroscopy, but these values are based on theoretical and interpolation techniques rather than data alone. Ionization energies are difficult to determine since the cut-off of the Rydberg series of lines at the ionization energy is often not observed, and the ionization energy must be determined from theoretical calculations, interpolation of C isoelectronic and Rydberg series, as well as direct experimental data.

SEVEN-ELECTRON ATOMS

Seven-electron atoms can be solved exactly using the results of the solutions of one, two, three, four, five, and six-electron atoms.

RADIUS AND IONIZATION ENERGY OF AN OUTER ELECTRON OF THE NITROGEN ATOM

For each six-electron atom having a central charge of Z times that of the proton, there are two indistinguishable spin-paired electrons in an orbitsphere with radii r_1 and r_2 both given by Eq. (7.19) (Eq. (10.51)), two indistinguishable spin-paired electrons in an orbitsphere with radii r_3 and r_4 both given by Eq. (10.62), and two unpaired electrons in an orbitsphere at r_6 given by Eq. (10.132). For $Z \geq 7$, the next electron which binds to form the corresponding seven-electron atom is attracted by the central Coulomb field and is repelled by diamagnetic force due to the spin-paired inner electrons. A paramagnetic spin-pairing force is also possible, but the force due to the spin-pairing of the electrons (Eq. (7.15) with the radius r_7) reduces the energy of the atom less than that due to the alternative forces on three unpaired p electrons in an orbitsphere at the same radius r_7 . The resulting electron configuration is $1s^2 2s^2 2p^3$, and the orbital arrangement is

$$\begin{array}{ccc} \text{2p state} & & \\ \uparrow & \uparrow & \uparrow \\ \hline 1 & 0 & -1 \end{array} \quad (10.134)$$

corresponding to the ground state $^4S_{3/2}^0$.

The central Coulomb force acts on the outer electron to cause it to bind wherein this electric force on the outer-most electron due to the nucleus and the inner six electrons is given by Eq. (10.70) with the appropriate charge and radius:

$$\mathbf{F}_{ele} = \frac{(Z-6)e^2}{4\pi\epsilon_0 r_7^2} \mathbf{i}_r \quad (10.135)$$

for $r > r_6$.

The energy is minimized with conservation of angular momentum when the angular momenta of the two orthogonal p_x and p_y electrons cancel such that the diamagnetic force (Eq. (10.82)), $\mathbf{F}_{diamagnetic}$, is

$$\mathbf{F}_{diamagnetic} = -\left(\frac{1}{3}\right) \frac{\hbar^2}{4m_e r_7^2 r_3} \sqrt{s(s+1)} \mathbf{i}_r \quad (10.136)$$

corresponding to $m=0$.

From Eq. (10.89), \mathbf{F}_{mag2} corresponding to the orbital angular momentum of the p_z electron is

$$\mathbf{F}_{mag2} = \frac{1}{Z} \frac{\hbar^2}{m_e r_7^2 r_3} \sqrt{s(s+1)} \mathbf{i}_r \quad (10.137)$$

The outward centrifugal force on electron 7 is balanced by the electric force and the magnetic forces (on electron 7). The radius of the outer electron is calculated by equating the outward centrifugal force to the sum of the electric (Eq. (10.135)), diamagnetic (Eq. (10.136)), and paramagnetic (Eq. (10.137)) forces as follows:

$$\frac{m_e v_7^2}{r_7} = \frac{(Z-6)e^2}{4\pi\epsilon_0 r_7^2} - \frac{\hbar^2}{12m_e r_7^2 r_3} \sqrt{s(s+1)} + \frac{\hbar^2}{Zm_e r_7^2 r_3} \sqrt{s(s+1)} \quad (10.138)$$

Substitution of $v_7 = \frac{\hbar}{m_e r_7}$ (Eq. (1.56)) and $s = \frac{1}{2}$ into Eq. (10.138) gives:

$$\frac{\hbar^2}{m_e r_7^3} = \frac{(Z-6)e^2}{4\pi\epsilon_0 r_7^2} - \frac{\hbar^2}{12m_e r_7^2 r_3} \sqrt{\frac{3}{4}} + \frac{\hbar^2}{Zm_e r_7^2 r_3} \sqrt{\frac{3}{4}} \quad (10.139)$$

$$r_7 = \frac{\frac{\hbar^2}{m_e}}{\frac{(Z-6)e^2}{4\pi\epsilon_0} - \frac{\hbar^2}{12m_e r_3} \sqrt{\frac{3}{4}} + \frac{\hbar^2}{Zm_e r_3} \sqrt{\frac{3}{4}}} \quad (10.140)$$

$$r_7 = \frac{a_0}{(Z-6) - \left(\frac{1}{12} - \frac{1}{Z}\right) \frac{\sqrt{3}}{r_3}}, \quad r_3 \text{ in units of } a_0 \quad (10.141)$$

Substitution of $\frac{r_3}{a_0} = 0.69385$ (Eq. (10.62) with $Z=7$) into Eq. (10.141) gives

$$r_7 = 0.93084a_0 \quad (10.142)$$

The ionization energy of the nitrogen atom is given by the electric energy, $E(electric)$, (Eq. (10.102) with the radius, r_7 , given by Eq. (10.142)):

$$E(\text{ionization}; N) = -\text{Electric Energy} = \frac{(Z-6)e^2}{8\pi\epsilon_0 r_7} = 14.61664 \text{ eV} \quad (10.143)$$

where $r_7 = 0.93084a_0$ (Eq. (10.142)) and $Z=7$. The experimental ionization energy of the nitrogen atom is 14.53414 eV [3].

THE IONIZATION ENERGIES OF SEVEN-ELECTRON ATOMS WITH A NUCLEAR CHARGE $Z>7$

Seven-electron atoms having $Z>7$ possess an external electric field given by Eq. (10.92). In this case, an energy minimum is achieved with conservation of momentum when the orbital angular momentum is such that $F_{\text{diamagnetic}}$ is minimized while $F_{\text{mag } 2}$ is maximized. From Eq. (10.82), the diamagnetic force, $F_{\text{diamagnetic}}$, is given by the sum of the contributions from the p_x , p_y , and p_z orbitals corresponding to $m = 1, -1$, and 0, respectively:

$$F_{\text{diamagnetic}} = -\left(\frac{2}{3} + \frac{2}{3} + \frac{1}{3}\right) \frac{\hbar^2}{4m_e r_7^2 r_3} \sqrt{s(s+1)} \mathbf{i}_r = -\left(\frac{5}{3}\right) \frac{\hbar^2}{4m_e r_7^2 r_3} \sqrt{s(s+1)} \mathbf{i}_r \quad (10.144)$$

With $Z>6$, the charge induction forms complementary mirror charge-density waves such that the angular momenta do not cancel. From Eq. (10.89), $F_{\text{mag } 2}$ corresponding to the orbital angular momentum of the three p electrons in addition complementary charge-density waves is

$$F_{\text{mag } 2} = 2 \frac{1}{Z} \frac{3\hbar^2}{m_e r_7^2 r_3} \sqrt{s(s+1)} \mathbf{i}_r \quad (10.145)$$

The second diamagnetic force, $F_{\text{diamagnetic } 2}$, due to the binding of the p-orbital electron having an electric field outside of its radius is given by Eq. (10.93):

$$F_{\text{diamagnetic } 2} = -\left[\frac{Z-7}{Z-6}\right] \left(1 - \frac{\sqrt{2}}{2}\right) \frac{r_3 \hbar^2}{m_e r_7^4} 10 \sqrt{s(s+1)} \mathbf{i}_r \quad (10.146)$$

In the case that $Z>7$, the radius of the outer electron is calculated by equating the outward centrifugal force to the sum of the electric (Eq. (10.135)), diamagnetic (Eqs. (10.10.144) and (10.146)), and paramagnetic (Eq. (10.145)) forces as follows:

$$\frac{m_e v_7^2}{r_7} = \frac{(Z-6)e^2}{4\pi\epsilon_0 r_7^2} - \frac{5\hbar^2}{12m_e r_7^2 r_3} \sqrt{s(s+1)} + \frac{6\hbar^2}{Zm_e r_7^2 r_3} \sqrt{s(s+1)} - \left[\frac{Z-7}{Z-6}\right] \left(1 - \frac{\sqrt{2}}{2}\right) \frac{r_3 \hbar^2}{m_e r_7^4} 10 \sqrt{s(s+1)} \quad (10.147)$$

Substitution of $v_7 = \frac{\hbar}{m_e r_7}$ (Eq. (1.56)) and $s = \frac{1}{2}$ into Eq. (10.147) gives:

$$\frac{\hbar^2}{m_e r_7^3} = \frac{(Z-6)e^2}{4\pi\epsilon_0 r_7^2} - \frac{5\hbar^2}{12m_e r_7^2 r_3} \sqrt{\frac{3}{4}} + \frac{6\hbar^2}{Zm_e r_7^2 r_3} \sqrt{\frac{3}{4}} - \left[\frac{Z-7}{Z-6}\right] \left(1 - \frac{\sqrt{2}}{2}\right) \frac{r_3 \hbar^2}{r_7^4 m_e} 10 \sqrt{\frac{3}{4}} \quad (10.148)$$

The quadratic equation corresponding to Eq. (10.148) is

$$\left(\frac{(Z-6)e^2}{4\pi\epsilon_0} - \left(\frac{5}{12} - \frac{6}{Z}\right) \frac{\hbar^2}{m_e r_3} \sqrt{\frac{3}{4}}\right) r_7^2 - \frac{\hbar^2}{m_e} r_7 - \left[\frac{Z-7}{Z-6}\right] \left(1 - \frac{\sqrt{2}}{2}\right) \frac{r_3 \hbar^2}{m_e} 10 \sqrt{\frac{3}{4}} = 0$$

$$r_7^2 - \frac{\frac{\hbar^2}{m_e}}{\left(\frac{(Z-6)e^2}{4\pi\epsilon_0} - \left(\frac{5}{12} - \frac{6}{Z}\right)\frac{\hbar^2}{m_e r_3} \sqrt{\frac{3}{4}}\right)} r_7 - \frac{\frac{\hbar^2}{m_e} \left[\frac{Z-7}{Z-6}\right] \left(1 - \frac{\sqrt{2}}{2}\right) r_3 10 \sqrt{\frac{3}{4}}}{\left(\frac{(Z-6)e^2}{4\pi\epsilon_0} - \left(\frac{5}{12} - \frac{6}{Z}\right)\frac{\hbar^2}{m_e r_3} \sqrt{\frac{3}{4}}\right)} = 0 \quad (10.149)$$

$$(10.150)$$

The solution of Eq. (10.150) using the quadratic formula is:

$$r_7 = \frac{\frac{\hbar^2}{m_e}}{\left(\frac{(Z-6)e^2}{4\pi\epsilon_0} - \left(\frac{5}{12} - \frac{6}{Z}\right)\frac{\hbar^2}{m_e r_3} \sqrt{\frac{3}{4}}\right)} \pm \frac{\sqrt{\left(\frac{\hbar^2}{m_e}\right)^2 - 4 \left(\frac{(Z-6)e^2}{4\pi\epsilon_0} - \left(\frac{5}{12} - \frac{6}{Z}\right)\frac{\hbar^2}{m_e r_3} \sqrt{\frac{3}{4}}\right) \frac{\hbar^2}{m_e} \left[\frac{Z-7}{Z-6}\right] \left(1 - \frac{\sqrt{2}}{2}\right) r_3 10 \sqrt{\frac{3}{4}}}}{2} \quad (10.151)$$

$$r_7 = \frac{\frac{a_0}{\left((Z-6) - \left(\frac{5}{24} - \frac{3}{Z}\right)\frac{\sqrt{3}}{r_3}\right)} \pm a_0 \sqrt{\frac{1}{\left((Z-6) - \left(\frac{5}{24} - \frac{3}{Z}\right)\frac{\sqrt{3}}{r_3}\right)}^2 - 20\sqrt{3} \left[\frac{Z-7}{Z-6}\right] \left(1 - \frac{\sqrt{2}}{2}\right) r_3}}{2} \quad (10.152)$$

r_3 in units of a_0

where r_3 is given by Eq. (10.62). The positive root of Eq. (10.152) must be taken in order that $r_7 > 0$. The final radius of electron 7, r_7 , is given by Eq. (10.152); this is also the final radius of electrons 5 and 6. The radii of several seven-electron atoms are given in Table 10.5.

The ionization energies for the seven-electron atoms with $Z > 7$ are given by the electric energy, $E(\text{electric})$, (Eq. (10.102) with the radii, r_7 , given by Eq. (10.152)):

$$E(\text{Ionization}) = -\text{Electric Energy} = \frac{(Z-6)e^2}{8\pi\epsilon_0 r_7} \quad (10.153)$$

Since the relativistic corrections were small, the nonrelativistic ionization

energies for experimentally measured seven-electron atoms are given in Table 10.5.

Table 10.5. Ionization energies for some seven-electron atoms.

7 e Atom	Z	r_1 (a_0) ^a	r_3 (a_0) ^b	r_7 (a_0) ^c	Theoretical Ionization Energies ^d (eV)	Experimental Ionization Energies ^e (eV)	Relative Error ^f
<i>N</i>	7	0.14605	0.69385	0.93084	14.61664	14.53414	-0.0057
<i>O</i> ⁺	8	0.12739	0.59020	0.78489	34.6694	35.1173	0.0128
<i>F</i> ²⁺	9	0.11297	0.51382	0.67084	60.8448	62.7084	0.0297
<i>Ne</i> ³⁺	10	0.10149	0.45511	0.57574	94.5279	97.12	0.0267
<i>Na</i> ⁴⁺	11	0.09213	0.40853	0.50250	135.3798	138.4	0.0218
<i>Mg</i> ⁵⁺	12	0.08435	0.37065	0.44539	183.2888	186.76	0.0186
<i>Al</i> ⁶⁺	13	0.07778	0.33923	0.39983	238.2017	241.76	0.0147
<i>Si</i> ⁷⁺	14	0.07216	0.31274	0.36271	300.0883	303.54	0.0114
<i>P</i> ⁸⁺	15	0.06730	0.29010	0.33191	368.9298	372.13	0.0086
<i>S</i> ⁹⁺	16	0.06306	0.27053	0.30595	444.7137	447.5	0.0062
<i>Cl</i> ¹⁰⁺	17	0.05932	0.25344	0.28376	527.4312	529.28	0.0035
<i>Ar</i> ¹¹⁺	18	0.05599	0.23839	0.26459	617.0761	618.26	0.0019
<i>K</i> ¹²⁺	19	0.05302	0.22503	0.24785	713.6436	714.6	0.0013
<i>Ca</i> ¹³⁺	20	0.05035	0.21308	0.23311	817.1303	817.6	0.0006
<i>Sc</i> ¹⁴⁺	21	0.04794	0.20235	0.22003	927.5333	927.5	0.0000
<i>Ti</i> ¹⁵⁺	22	0.04574	0.19264	0.20835	1044.8504	1044	-0.0008
<i>V</i> ¹⁶⁺	23	0.04374	0.18383	0.19785	1169.0800	1168	-0.0009
<i>Cr</i> ¹⁷⁺	24	0.04191	0.17579	0.18836	1300.2206	1299	-0.0009
<i>Mn</i> ¹⁸⁺	25	0.04022	0.16842	0.17974	1438.2710	1437	-0.0009
<i>Fe</i> ¹⁹⁺	26	0.03867	0.16165	0.17187	1583.2303	1582	-0.0008
<i>Co</i> ²⁰⁺	27	0.03723	0.15540	0.16467	1735.0978	1735	-0.0001
<i>Ni</i> ²¹⁺	28	0.03589	0.14961	0.15805	1893.8726	1894	0.0001
<i>Cu</i> ²²⁺	29	0.03465	0.14424	0.15194	2059.5543	2060	0.0002

^a Radius of the first set of paired inner electrons of seven-electron atoms from Eq. (10.51).

^b Radius of the second set of paired inner electrons of seven-electron atoms from Eq. (10.62).

^c Radius of the three unpaired paired outer electrons of seven-electron atoms from Eq. (10.152) for $Z > 7$ and Eq. (10.142) for N .

^d Calculated ionization energies of seven-electron atoms given by the electric energy (Eq. (10.153)).

^e From theoretical calculations, interpolation of isoelectronic and spectral series, and experimental data [2-3].

^f (Experimental-theoretical)/experimental.

The agreement between the experimental and calculated values of Table 10.5 is well within the experimental capability of the spectroscopic

determinations including the values at large Z which relies on X-ray spectroscopy. In this case, the experimental capability is three to four significant figures which is consistent with the last column. The nitrogen atom isoelectronic series is given in Table 10.5 [2-3] to much higher precision than the capability of X-ray spectroscopy, but these values are based on theoretical and interpolation techniques rather than data alone. Ionization energies are difficult to determine since the cut-off of the Rydberg series of lines at the ionization energy is often not observed, and the ionization energy must be determined from theoretical calculations, interpolation of N isoelectronic and Rydberg series, as well as direct experimental data.

EIGHT-ELECTRON ATOMS

Eight-electron atoms can be solved exactly using the results of the solutions of one, two, three, four, five, six, and seven-electron atoms.

RADIUS AND IONIZATION ENERGY OF AN OUTER ELECTRON OF THE OXYGEN ATOM

For each seven-electron atom having a central charge of Z times that of the proton, there are two indistinguishable spin-paired electrons in an orbitsphere with radii r_1 and r_2 both given by Eq. (7.19) (Eq. (10.51)), two indistinguishable spin-paired electrons in an orbitsphere with radii r_3 and r_4 both given by Eq. (10.62), and three unpaired electrons in an orbitsphere at r_7 given by Eq. (10.152). For $Z \geq 8$, the next electron which binds to form the corresponding eight-electron atom is attracted by the central Coulomb field and is repelled by diamagnetic force due to the spin-paired inner electrons. A paramagnetic spin-pairing force that results in the formation of a filled s orbital is also possible, but the force due to the spin-pairing of the electrons (Eq. (7.15) with the radius r_8) reduces the energy of the atom less than that due to the alternative forces on two paired electrons in a p_x orbital and two unpaired electrons in p_z and p_y orbitals of an orbitsphere at the same radius r_8 . The resulting electron configuration is $1s^2 2s^2 2p^4$, and the orbital arrangement is

$$\begin{array}{c} \text{2p state} \\ \uparrow \downarrow \quad \uparrow \quad \uparrow \\ \hline 1 \quad 0 \quad -1 \end{array} \quad (10.154)$$

corresponding to the ground state 3P_2 .

The central Coulomb force acts on the outer electron to cause it to bind wherein this electric force on the outer-most electron due to the nucleus and the inner seven electrons is given by Eq. (10.70) with the

appropriate charge and radius:

$$\mathbf{F}_{ele} = \frac{(Z-7)e^2}{4\pi\epsilon_0 r_8^2} \mathbf{i}_r \quad (10.155)$$

for $r > r_7$.

The energy is minimized with conservation of angular momentum by the cancellation of the orbital angular momentum of a p_x electron by that of the p_y electron with the pairing of electron eight to fill the p_x orbital. Then, the diamagnetic force is that of N given by Eq. (10.136) corresponding to the p_z -orbital electron (Eq. (10.82) with $m=0$) as the source of diamagnetism with an additional contribution from the uncanceled p_x electron (Eq. (10.82) with $m=1$). $\mathbf{F}_{diamagnetic}$ for the oxygen atom is

$$\mathbf{F}_{diamagnetic} = -\left(\frac{1}{3} + \frac{2}{3}\right) \frac{\hbar^2}{4m_e r_8^2 r_3} \sqrt{s(s+1)} \mathbf{i}_r = -\frac{\hbar^2}{4m_e r_8^2 r_3} \sqrt{s(s+1)} \mathbf{i}_r \quad (10.156)$$

From Eqs. (10.83) and (10.89), \mathbf{F}_{mag2} is

$$\mathbf{F}_{mag2} = (1+1) \frac{1}{Z} \frac{\hbar^2}{m_e r_8^2 r_3} \sqrt{s(s+1)} \mathbf{i}_r = \frac{1}{Z} \frac{2\hbar^2}{m_e r_8^2 r_3} \sqrt{s(s+1)} \mathbf{i}_r \quad (10.157)$$

corresponding to the spin-angular-momentum contribution alone of the p_x electron and the orbital angular momentum of the p_z electron, respectively.

The outward centrifugal force on electron 8 is balanced by the electric force and the magnetic forces (on electron 8). The radius of the outer electron is calculated by equating the outward centrifugal force to the sum of the electric (Eq. (10.155)), diamagnetic (Eq. (10.156)), and paramagnetic (Eq. (10.157)) forces as follows:

$$\frac{m_e v_8^2}{r_8} = \frac{(Z-7)e^2}{4\pi\epsilon_0 r_8^2} - \frac{\hbar^2}{4m_e r_8^2 r_3} \sqrt{s(s+1)} + \frac{2\hbar^2}{Zm_e r_8^2 r_3} \sqrt{s(s+1)} \quad (10.158)$$

Substitution of $v_8 = \frac{\hbar}{m_e r_8}$ (Eq. (1.56)) and $s = \frac{1}{2}$ into Eq. (10.158) gives:

$$\frac{\hbar^2}{m_e r_8^3} = \frac{(Z-7)e^2}{4\pi\epsilon_0 r_8^2} - \frac{\hbar^2}{4m_e r_8^2 r_3} \sqrt{\frac{3}{4}} + \frac{2\hbar^2}{Zm_e r_8^2 r_3} \sqrt{\frac{3}{4}} \quad (10.159)$$

$$r_8 = \frac{\frac{\hbar^2}{m_e}}{\frac{(Z-7)e^2}{4\pi\epsilon_0} - \frac{\hbar^2}{4m_e r_3} \sqrt{\frac{3}{4}} + \frac{2\hbar^2}{Zm_e r_3} \sqrt{\frac{3}{4}}} \quad (10.160)$$

$$r_8 = \frac{a_0}{(Z-7) - \left(\frac{1}{4} - \frac{2}{Z}\right) \frac{\sqrt{3}}{r_3}}, \quad r_3 \text{ in units of } a_0 \quad (10.161)$$

Substitution of $\frac{r_3}{a_0} = 0.59020$ (Eq. (10.62) with $Z=8$) into Eq. (10.161) gives

$$r_8 = a_0 \quad (10.162)$$

The ionization energy of the oxygen atom is given by the negative of $E(\text{electric})$ given by Eq. (10.102) with the appropriate charge and radius:

$$E(\text{ionization}; O) = -\text{Electric Energy} = \frac{(Z-7)e^2}{8\pi\epsilon_0 r_8} = 13.60580 \text{ eV} \quad (10.163)$$

where $r_8 = a_0$ (Eq. (10.162)) and $Z=8$. The experimental ionization energy of the oxygen atom is 13.6181 eV [3].

THE IONIZATION ENERGIES OF EIGHT-ELECTRON ATOMS WITH A NUCLEAR CHARGE $Z>8$

Eight-electron atoms having $Z>8$ possess an external electric field given by Eq. (10.92). In this case, an energy minimum is achieved with conservation of momentum when the orbital angular momentum is such that $F_{\text{diamagnetic}}$ is minimized while $F_{\text{mag } 2}$ is maximized. From Eq. (10.82), the diamagnetic force, $F_{\text{diamagnetic}}$, is given by the sum of the contributions from the p_x , p_y , and p_z orbitals corresponding to $m = 1, -1$, and 0 , respectively:

$$F_{\text{diamagnetic}} = -\left(\frac{2}{3} + \frac{2}{3} + \frac{1}{3}\right) \frac{\hbar^2}{4m_e r_8^2 r_3} \sqrt{s(s+1)} \mathbf{i}_r = -\left(\frac{5}{3}\right) \frac{\hbar^2}{4m_e r_8^2 r_3} \sqrt{s(s+1)} \mathbf{i}_r \quad (10.164)$$

The filled p orbitals with the maintenance of symmetry according to Eq. (10.72) requires that the diamagnetic force is only due to the electrons at r_3 . From Eqs. (10.84) and (10.89), $F_{\text{mag } 2}$ is

$$F_{\text{mag } 2} = (4+1+1) \frac{1}{Z} \frac{\hbar^2}{m_e r_8^2 r_3} \sqrt{s(s+1)} \mathbf{i}_r = \frac{1}{Z} \frac{6\hbar^2}{m_e r_8^2 r_3} \sqrt{s(s+1)} \mathbf{i}_r \quad (10.165)$$

corresponding to the spin and orbital angular momenta of the paired p_x electrons and the orbital angular momentum of each of the p_y and p_z electrons, respectively.

The second diamagnetic force, $F_{\text{diamagnetic } 2}$, due to the binding of the p-orbital electron having an electric field outside of its radius is given by Eq. (10.93):

$$F_{\text{diamagnetic } 2} = -\left[\frac{Z-8}{Z-7}\right] \left(1 - \frac{\sqrt{2}}{2}\right) \frac{r_3 \hbar^2}{m_e r_8^4} 10 \sqrt{s(s+1)} \mathbf{i}_r \quad (10.166)$$

In the case that $Z>8$, the radius of the outer electron is calculated by equating the outward centrifugal force to the sum of the electric (Eq. (10.155)), diamagnetic (Eqs. (10.164) and (10.166)), and paramagnetic (Eq. (10.165)) forces as follows:

$$\frac{m_e v_8^2}{r_8} = \frac{(Z-7)e^2}{4\pi\epsilon_0 r_8^2} - \frac{5\hbar^2}{12m_e r_8^2 r_3} \sqrt{s(s+1)} + \frac{6\hbar^2}{Zm_e r_8^2 r_3} \sqrt{s(s+1)} - \left[\frac{Z-8}{Z-7}\right] \left(1 - \frac{\sqrt{2}}{2}\right) \frac{r_3 \hbar^2}{m_e r_8^4} 10 \sqrt{s(s+1)}$$

(10.167)

Substitution of $\nu_8 = \frac{\hbar}{m_e r_8}$ (Eq. (1.56)) and $s = \frac{1}{2}$ into Eq. (10.167) gives:

$$\frac{\hbar^2}{m_e r_8^3} = \frac{(Z-7)e^2}{4\pi\epsilon_0 r_8^2} - \frac{5\hbar^2}{12m_e r_8^2 r_3} \sqrt{\frac{3}{4}} + \frac{6\hbar^2}{Zm_e r_8^2 r_3} \sqrt{\frac{3}{4}} - \left[\frac{Z-8}{Z-7} \right] \left(1 - \frac{\sqrt{2}}{2} \right) \frac{r_3 \hbar^2}{r_8^4 m_e} 10 \sqrt{\frac{3}{4}} \quad (10.168)$$

The quadratic equation corresponding to Eq. (10.168) is

$$\left(\frac{(Z-7)e^2}{4\pi\epsilon_0} - \left(\frac{5}{12} - \frac{6}{Z} \right) \frac{\hbar^2}{m_e r_3} \sqrt{\frac{3}{4}} \right) r_8^2 - \frac{\hbar^2}{m_e} r_8 - \left[\frac{Z-8}{Z-7} \right] \left(1 - \frac{\sqrt{2}}{2} \right) \frac{r_3 \hbar^2}{m_e} 10 \sqrt{\frac{3}{4}} = 0 \quad (10.169)$$

$$r_8^2 - \frac{\frac{\hbar^2}{m_e}}{\left(\frac{(Z-7)e^2}{4\pi\epsilon_0} - \left(\frac{5}{12} - \frac{6}{Z} \right) \frac{\hbar^2}{m_e r_3} \sqrt{\frac{3}{4}} \right)} r_8 - \frac{\frac{\hbar^2}{m_e} \left[\frac{Z-8}{Z-7} \right] \left(1 - \frac{\sqrt{2}}{2} \right) r_3 10 \sqrt{\frac{3}{4}}}{\left(\frac{(Z-7)e^2}{4\pi\epsilon_0} - \left(\frac{5}{12} - \frac{6}{Z} \right) \frac{\hbar^2}{m_e r_3} \sqrt{\frac{3}{4}} \right)} = 0 \quad (10.170)$$

The solution of Eq. (10.170) using the quadratic formula is:

$$r_8 = \frac{\frac{\hbar^2}{m_e}}{\left(\frac{(Z-7)e^2}{4\pi\epsilon_0} - \left(\frac{5}{12} - \frac{6}{Z} \right) \frac{\hbar^2}{m_e r_3} \sqrt{\frac{3}{4}} \right)} \pm \frac{\sqrt{\left(\frac{\hbar^2}{m_e} \right)^2 - 4 \left(\frac{(Z-7)e^2}{4\pi\epsilon_0} - \left(\frac{5}{12} - \frac{6}{Z} \right) \frac{\hbar^2}{m_e r_3} \sqrt{\frac{3}{4}} \right) \frac{\hbar^2}{m_e} \left[\frac{Z-8}{Z-7} \right] \left(1 - \frac{\sqrt{2}}{2} \right) r_3 10 \sqrt{\frac{3}{4}}}}{2} \quad (10.171)$$

$$r_8 = \frac{\frac{a_0}{\left((Z-7) - \left(\frac{5}{24} - \frac{3}{Z} \right) \frac{\sqrt{3}}{r_3} \right)} \pm a_0}{2} \sqrt{\frac{1}{\left((Z-7) - \left(\frac{5}{24} - \frac{3}{Z} \right) \frac{\sqrt{3}}{r_3} \right)} + \frac{20\sqrt{3} \left[\frac{Z-8}{Z-7} \right] \left(1 - \frac{\sqrt{2}}{2} \right) r_3}{\left((Z-7) - \left(\frac{5}{24} - \frac{3}{Z} \right) \frac{\sqrt{3}}{r_3} \right)}} \quad (10.172)$$

r_3 in units of a_0

where r_3 is given by Eq. (10.62). The positive root of Eq. (10.172) must be taken in order that $r_8 > 0$. The final radius of electron 8, r_8 , is given by Eq. (10.172); this is also the final radius of electrons 5, 6, and 7. The radii of several eight-electron atoms are given in Table 10.6.

The ionization energies for the eight-electron atoms with $Z > 8$ are given by the electric energy, $E(\text{electric})$, (Eq. (10.102) with the radii, r_8 , given by Eq. (10.172)):

$$E(\text{Ionization}) = -\text{Electric Energy} = \frac{(Z-7)e^2}{8\pi\epsilon_0 r_8} \quad (10.173)$$

Since the relativistic corrections were small, the nonrelativistic ionization energies for experimentally measured eight-electron atoms are given in Table 10.6.

Table 10.6. Ionization energies for some eight-electron atoms.

8 e Atom	Z	r_1 (a_0) ^a	r_3 (a_0) ^b	r_8 (a_0) ^c	Theoretical Ionization Energies ^d (eV)	Experimental Ionization Energies ^e (eV)	Relative Error ^f
O	8	0.12739	0.59020	1.00000	13.60580	13.6181	0.0009
F ⁺	9	0.11297	0.51382	0.7649	35.5773	34.9708	-0.0173
Ne ²⁺	10	0.10149	0.45511	0.6514	62.6611	63.45	0.0124
Na ³⁺	11	0.09213	0.40853	0.5592	97.3147	98.91	0.0161
Mg ⁴⁺	12	0.08435	0.37065	0.4887	139.1911	141.27	0.0147
Al ⁵⁺	13	0.07778	0.33923	0.4338	188.1652	190.49	0.0122
Si ⁶⁺	14	0.07216	0.31274	0.3901	244.1735	246.5	0.0094
P ⁷⁺	15	0.06730	0.29010	0.3543	307.1791	309.6	0.0078
S ⁸⁺	16	0.06306	0.27053	0.3247	377.1579	379.55	0.0063
Cl ⁹⁺	17	0.05932	0.25344	0.2996	454.0940	455.63	0.0034
Ar ¹⁰⁺	18	0.05599	0.23839	0.2782	537.9756	538.96	0.0018
K ¹¹⁺	19	0.05302	0.22503	0.2597	628.7944	629.4	0.0010
Ca ¹²⁺	20	0.05035	0.21308	0.2434	726.5442	726.6	0.0001
Sc ¹³⁺	21	0.04794	0.20235	0.2292	831.2199	830.8	-0.0005
Ti ¹⁴⁺	22	0.04574	0.19264	0.2165	942.8179	941.9	-0.0010
V ¹⁵⁺	23	0.04374	0.18383	0.2051	1061.3351	1060	-0.0013
Cr ¹⁶⁺	24	0.04191	0.17579	0.1949	1186.7691	1185	-0.0015
Mn ¹⁷⁺	25	0.04022	0.16842	0.1857	1319.1179	1317	-0.0016
Fe ¹⁸⁺	26	0.03867	0.16165	0.1773	1458.3799	1456	-0.0016
Co ¹⁹⁺	27	0.03723	0.15540	0.1696	1604.5538	1603	-0.0010
Ni ²⁰⁺	28	0.03589	0.14961	0.1626	1757.6383	1756	-0.0009
Cu ²¹⁺	29	0.03465	0.14424	0.1561	1917.6326	1916	-0.0009

^a Radius of the first set of paired inner electrons of eight-electron atoms from Eq. (10.51).^b Radius of the second set of paired inner electrons of eight-electron atoms from Eq. (10.62).^c Radius of the two paired and two unpaired outer electrons of eight-electron atoms from Eq. (10.172) for $Z > 8$ and Eq. (10.162) for O.^d Calculated ionization energies of eight-electron atoms given by the electric energy (Eq. (10.173)).^e From theoretical calculations, interpolation of isoelectronic and spectral series, and experimental data [2-3].^f (Experimental-theoretical)/experimental.

The agreement between the experimental and calculated values of Table 10.6 is well within the experimental capability of the spectroscopic determinations including the values at large Z which relies on X-ray spectroscopy. In this case, the experimental capability is three to four significant figures which is consistent with the last column. The oxygen atom isoelectronic series is given in Table 10.6 [2-3] to much higher

precision than the capability of X-ray spectroscopy, but these values are based on theoretical and interpolation techniques rather than data alone. Ionization energies are difficult to determine since the cut-off of the Rydberg series of lines at the ionization energy is often not observed, and the ionization energy must be determined from theoretical calculations, interpolation of O isoelectronic and Rydberg series, as well as direct experimental data.

NINE-ELECTRON ATOMS

Nine-electron atoms can be solved exactly using the results of the solutions of one, two, three, four, five, six, seven, and eight-electron atoms.

RADIUS AND IONIZATION ENERGY OF AN OUTER ELECTRON OF THE FLUORINE ATOM

For each eight-electron atom having a central charge of Z times that of the proton, there are two indistinguishable spin-paired electrons in an orbitsphere with radii r_1 and r_2 both given by Eq. (7.19) (Eq. (10.51)), two indistinguishable spin-paired electrons in an orbitsphere with radii r_3 and r_4 both given by Eq. (10.62), and two paired and unpaired electrons in an orbitsphere at r_8 given by Eq. (10.172). For $Z \geq 9$, the next electron which binds to form the corresponding nine-electron atom is attracted by the central Coulomb field and is repelled by diamagnetic force due to the spin-paired inner electrons. A paramagnetic spin-pairing force that results in the formation of a filled s orbital is also possible, but the force due to the spin-pairing of the electrons (Eq. (7.15) with the radius r_9) reduces the energy of the atom less than that due to the alternative forces on an unpaired electron in a p_y orbital and two pairs of electrons of opposite spin in p_x and p_z orbitals of an orbitsphere at the same radius r_9 . The resulting electron configuration is $1s^2 2s^2 2p^5$, and the orbital arrangement is

$$\begin{array}{ccc} \uparrow \downarrow & \uparrow \downarrow & \uparrow \\ 1 & 0 & -1 \end{array} \quad (10.174)$$

corresponding to the ground state $^2P_{3/2}^0$.

The central Coulomb force acts on the outer electron to cause it to bind wherein this electric force on the outer-most electron due to the nucleus and the inner eight electrons is given by Eq. (10.70) with the appropriate charge and radius:

$$F_{ele} = \frac{(Z-8)e^2}{4\pi\epsilon_0 r_9^2} \mathbf{i}_r \quad (10.175)$$

for $r > r_8$.

The energy is minimized and the angular momentum is conserved with the pairing of electron nine to fill the p_z orbital when the orbital angular momenta of each set of p_x and p_z spin-paired electrons adds negatively to cancel. Then, the diamagnetic force (Eq. (10.82)), $F_{\text{diamagnetic}}$, is

$$F_{\text{diamagnetic}} = -\left(\frac{2}{3}\right) \frac{\hbar^2}{4m_e r_9^2 r_3} \sqrt{s(s+1)} \mathbf{i}_r \quad (10.176)$$

corresponding to $m = -1$ for the unpaired p_y electron.

From Eqs. (10.83) and (10.89), $F_{\text{mag}2}$ is

$$F_{\text{mag}2} = (1+1+1) \frac{1}{Z} \frac{\hbar^2}{m_e r_9^2 r_3} \sqrt{s(s+1)} \mathbf{i}_r = \frac{1}{Z} \frac{3\hbar^2}{m_e r_9^2 r_3} \sqrt{s(s+1)} \mathbf{i}_r \quad (10.177)$$

corresponding to the spin-angular-momentum contribution alone from each of the p_x and p_z orbitals and the orbital-angular-momentum contribution of the p_z electron, respectively.

The outward centrifugal force on electron 9 is balanced by the electric force and the magnetic forces (on electron 9). The radius of the outer electron is calculated by equating the outward centrifugal force to the sum of the electric (Eq. (10.175)), diamagnetic (Eq. (10.176)), and paramagnetic (Eq. (10.177)) forces as follows:

$$\frac{m_e v_9^2}{r_9} = \frac{(Z-8)e^2}{4\pi\epsilon_0 r_9^2} - \frac{\hbar^2}{6m_e r_9^2 r_3} \sqrt{s(s+1)} + \frac{3\hbar^2}{Zm_e r_9^2 r_3} \sqrt{s(s+1)} \quad (10.178)$$

Substitution of $v_9 = \frac{\hbar}{m_e r_9}$ (Eq. (1.56)) and $s = \frac{1}{2}$ into Eq. (10.178) gives:

$$\frac{\hbar^2}{m_e r_9^3} = \frac{(Z-8)e^2}{4\pi\epsilon_0 r_9^2} - \frac{\hbar^2}{6m_e r_9^2 r_3} \sqrt{\frac{3}{4}} + \frac{3\hbar^2}{Zm_e r_9^2 r_3} \sqrt{\frac{3}{4}} \quad (10.179)$$

$$r_9 = \frac{\frac{\hbar^2}{m_e}}{\frac{(Z-8)e^2}{4\pi\epsilon_0} - \frac{\hbar^2}{6m_e r_3} \sqrt{\frac{3}{4}} + \frac{3\hbar^2}{Zm_e r_3} \sqrt{\frac{3}{4}}} \quad (10.180)$$

$$r_9 = \frac{a_0}{(Z-8) - \left(\frac{1}{6} - \frac{3}{Z}\right) \sqrt{\frac{3}{4}} \frac{a_0}{r_3}}, \quad r_3 \text{ in units of } a_0 \quad (10.181)$$

Substitution of $\frac{r_3}{a_0} = 0.51382$ (Eq. (10.62) with $Z=9$) into Eq. (10.181) gives

$$r_9 = 0.78069 a_0 \quad (10.182)$$

The ionization energy of the fluorine atom is given by the negative of $E(\text{electric})$ given by Eq. (10.102) with the appropriate charge and radius:

$$E(\text{ionization}; F) = -\text{Electric Energy} = \frac{(Z-8)e^2}{8\pi\epsilon_0 r_9} = 17.42782 \text{ eV} \quad (10.183)$$

where $r_9 = 0.78069a_0$ (Eq. (10.183)) and $Z=9$. The experimental ionization energy of the fluorine atom is 17.42282 eV [3].

THE IONIZATION ENERGIES OF NINE-ELECTRON ATOMS WITH A NUCLEAR CHARGE $Z>9$

Nine-electron atoms having $Z>9$ possess an external electric field given by Eq. (10.92). In this case, an energy minimum is achieved with conservation of momentum when the orbital angular momentum is such that $F_{\text{diamagnetic}}$ is minimized while $F_{\text{mag } 2}$ is maximized. From Eq. (10.82), the diamagnetic force, $F_{\text{diamagnetic}}$, is given by the sum of the contributions from the p_x , p_y , and p_z orbitals corresponding to $m = 1, -1$, and 0, respectively:

$$F_{\text{diamagnetic}} = -\left(\frac{2}{3} + \frac{2}{3} + \frac{1}{3}\right) \frac{\hbar^2}{4m_e r_9^2 r_3} \sqrt{s(s+1)} \mathbf{i}_r = -\left(\frac{5}{3}\right) \frac{\hbar^2}{4m_e r_9^2 r_3} \sqrt{s(s+1)} \mathbf{i}_r \quad (10.184)$$

The filled p orbitals with the maintenance of symmetry according to Eq. (10.72) requires that the diamagnetic force is only due to the electrons at r_3 . From Eqs. (10.84) and (10.89), $F_{\text{mag } 2}$ is

$$F_{\text{mag } 2} = (4 + 4 + 1) \frac{1}{Z} \frac{\hbar^2}{m_e r_9^2 r_3} \sqrt{s(s+1)} \mathbf{i}_r = \frac{1}{Z} \frac{9\hbar^2}{m_e r_9^2 r_3} \sqrt{s(s+1)} \mathbf{i}_r \quad (10.185)$$

corresponding to the spin and orbital angular momenta of the paired p_x and p_z electrons and the orbital angular momentum of the unpaired p_y electron, respectively.

The second diamagnetic force, $F_{\text{diamagnetic } 2}$, due to the binding of the p-orbital electron having an electric field outside of its radius is given by Eq. (10.93):

$$F_{\text{diamagnetic } 2} = -\left[\frac{Z-9}{Z-8}\right] \left(1 - \frac{\sqrt{2}}{2}\right) \frac{r_3 \hbar^2}{m_e r_9^4} 10 \sqrt{s(s+1)} \mathbf{i}_r \quad (10.186)$$

In the case that $Z>9$, the radius of the outer electron is calculated by equating the outward centrifugal force to the sum of the electric (Eq. (10.175)), diamagnetic (Eqs. (10.184) and (10.186)), and paramagnetic (Eq. (10.185)) forces as follows:

$$\frac{m_e v_9^2}{r_9} = \frac{(Z-8)e^2}{4\pi\epsilon_0 r_9^2} - \frac{5\hbar^2}{12m_e r_9^2 r_3} \sqrt{s(s+1)} + \frac{9\hbar^2}{Zm_e r_9^2 r_3} \sqrt{s(s+1)} - \left[\frac{Z-9}{Z-8}\right] \left(1 - \frac{\sqrt{2}}{2}\right) \frac{r_3 \hbar^2}{m_e r_9^4} 10 \sqrt{s(s+1)} \quad (10.187)$$

Substitution of $v_9 = \frac{\hbar}{m_e r_9}$ (Eq. (1.56)) and $s = \frac{1}{2}$ into Eq. (10.187) gives:

$$\frac{\hbar^2}{m_e r_9^3} = \frac{(Z-8)e^2}{4\pi\epsilon_0 r_9^2} - \frac{5\hbar^2}{12m_e r_9^2 r_3} \sqrt{\frac{3}{4}} + \frac{9\hbar^2}{Zm_e r_9^2 r_3} \sqrt{\frac{3}{4}} - \left[\frac{Z-9}{Z-8}\right] \left(1 - \frac{\sqrt{2}}{2}\right) \frac{r_3 \hbar^2}{r_9^4 m_e} 10 \sqrt{\frac{3}{4}}$$

(10.188)

The quadratic equation corresponding to Eq. (10.188) is

$$\left(\frac{(Z-8)e^2}{4\pi\epsilon_0} - \left(\frac{5}{12} - \frac{9}{Z} \right) \frac{\hbar^2}{m_e r_3} \sqrt{\frac{3}{4}} \right) r_9^2 - \frac{\hbar^2}{m_e} r_9 - \left[\frac{Z-9}{Z-8} \right] \left(1 - \frac{\sqrt{2}}{2} \right) \frac{r_3 \hbar^2}{m_e} 10 \sqrt{\frac{3}{4}} = 0 \quad (10.189)$$

$$r_9^2 - \frac{\frac{\hbar^2}{m_e}}{\left(\frac{(Z-8)e^2}{4\pi\epsilon_0} - \left(\frac{5}{12} - \frac{9}{Z} \right) \frac{\hbar^2}{m_e r_3} \sqrt{\frac{3}{4}} \right)} r_9 - \frac{\frac{\hbar^2}{m_e} \left[\frac{Z-9}{Z-8} \right] \left(1 - \frac{\sqrt{2}}{2} \right) r_3 10 \sqrt{\frac{3}{4}}}{\left(\frac{(Z-8)e^2}{4\pi\epsilon_0} - \left(\frac{5}{12} - \frac{9}{Z} \right) \frac{\hbar^2}{m_e r_3} \sqrt{\frac{3}{4}} \right)} = 0 \quad (10.190)$$

The solution of Eq. (10.190) using the quadratic formula is:

$$r_9 = \frac{\frac{\hbar^2}{m_e}}{\left(\frac{(Z-8)e^2}{4\pi\epsilon_0} - \left(\frac{5}{12} - \frac{9}{Z} \right) \frac{\hbar^2}{m_e r_3} \sqrt{\frac{3}{4}} \right)} \pm \frac{\sqrt{\left(\frac{\hbar^2}{m_e} \right)^2 + 4 \frac{\frac{\hbar^2}{m_e} \left[\frac{Z-9}{Z-8} \right] \left(1 - \frac{\sqrt{2}}{2} \right) r_3 10 \sqrt{\frac{3}{4}}}{\left(\frac{(Z-8)e^2}{4\pi\epsilon_0} - \left(\frac{5}{12} - \frac{9}{Z} \right) \frac{\hbar^2}{m_e r_3} \sqrt{\frac{3}{4}} \right)}}}{2} \quad (10.191)$$

$$r_9 = \frac{\frac{a_0}{\left((Z-8) - \left(\frac{5}{24} - \frac{9}{2Z} \right) \frac{\sqrt{3}}{r_3} \right)}}{2} \pm \frac{a_0 \sqrt{\left(\frac{1}{\left((Z-8) - \left(\frac{5}{24} - \frac{9}{2Z} \right) \frac{\sqrt{3}}{r_3} \right)} \right)^2 + \frac{20\sqrt{3} \left[\frac{Z-9}{Z-8} \right] \left(1 - \frac{\sqrt{2}}{2} \right) r_3}{\left((Z-8) - \left(\frac{5}{24} - \frac{9}{2Z} \right) \frac{\sqrt{3}}{r_3} \right)}}}{2} \quad (10.192)$$

r_3 in units of a_0

where r_3 is given by Eq. (10.62). The positive root of Eq. (10.192) must be taken in order that $r_9 > 0$. The final radius of electron 9, r_9 , is given by Eq. (10.192); this is also the final radius of electrons 5, 6, 7, and 8. The radii of several nine-electron atoms are given in Table 10.7.

The ionization energies for the nine-electron atoms with $Z > 9$ are given by the electric energy, $E(\text{electric})$, (Eq. (10.102) with the radii, r_9 ,

given by Eq. (10.192)):

$$E(\text{Ionization}) = -\text{Electric Energy} = \frac{(Z-8)e^2}{8\pi\epsilon_0 r_0} \quad (10.193)$$

Since the relativistic corrections were small, the nonrelativistic ionization energies for experimentally measured nine-electron atoms are given in Table 10.7.

Table 10.7. Ionization energies for some nine-electron atoms.

9 e Atom	Z	r_1 (a_0) ^a	r_3 (a_0) ^b	r_9 (a_0) ^c	Theoretical Ionization Energies ^d (eV)	Experimental Ionization Energies ^e (eV)	Relative Error ^f
<i>F</i>	9	0.11297	0.51382	0.78069	17.42782	17.42282	-0.0003
<i>Ne</i> ⁺	10	0.10149	0.45511	0.64771	42.0121	40.96328	-0.0256
<i>Na</i> ²⁺	11	0.09213	0.40853	0.57282	71.2573	71.62	0.0051
<i>Mg</i> ³⁺	12	0.08435	0.37065	0.50274	108.2522	109.2655	0.0093
<i>Al</i> ⁴⁺	13	0.07778	0.33923	0.44595	152.5469	153.825	0.0083
<i>Si</i> ⁵⁺	14	0.07216	0.31274	0.40020	203.9865	205.27	0.0063
<i>P</i> ⁶⁺	15	0.06730	0.29010	0.36283	262.4940	263.57	0.0041
<i>S</i> ⁷⁺	16	0.06306	0.27053	0.33182	328.0238	328.75	0.0022
<i>Cl</i> ⁸⁺	17	0.05932	0.25344	0.30571	400.5466	400.06	-0.0012
<i>Ar</i> ⁹⁺	18	0.05599	0.23839	0.28343	480.0424	478.69	-0.0028
<i>K</i> ¹⁰⁺	19	0.05302	0.22503	0.26419	566.4968	564.7	-0.0032
<i>Ca</i> ¹¹⁺	20	0.05035	0.21308	0.24742	659.8992	657.2	-0.0041
<i>Sc</i> ¹²⁺	21	0.04794	0.20235	0.23266	760.2415	756.7	-0.0047
<i>Ti</i> ¹³⁺	22	0.04574	0.19264	0.21957	867.5176	863.1	-0.0051
<i>V</i> ¹⁴⁺	23	0.04374	0.18383	0.20789	981.7224	976	-0.0059
<i>Cr</i> ¹⁵⁺	24	0.04191	0.17579	0.19739	1102.8523	1097	-0.0053
<i>Mn</i> ¹⁶⁺	25	0.04022	0.16842	0.18791	1230.9038	1224	-0.0056
<i>Fe</i> ¹⁷⁺	26	0.03867	0.16165	0.17930	1365.8746	1358	-0.0058
<i>Co</i> ¹⁸⁺	27	0.03723	0.15540	0.17145	1507.7624	1504.6	-0.0021
<i>Ni</i> ¹⁹⁺	28	0.03589	0.14961	0.16427	1656.5654	1648	-0.0052
<i>Cu</i> ²⁰⁺	29	0.03465	0.14424	0.15766	1812.2821	1804	-0.0046

^a Radius of the first set of paired inner electrons of nine-electron atoms from Equation (10.51).

^b Radius of the second set of paired inner electrons of nine-electron atoms from Equation (10.62).

^c Radius of the one unpaired and two sets of paired outer electrons of nine-electron atoms from Eq. (10.192) for $Z > 9$ and Eq. (10.182) for F .

^d Calculated ionization energies of nine-electron atoms given by the electric energy (Eq. (10.193)).

^e From theoretical calculations, interpolation of isoelectronic and spectral series, and experimental data [2-3].

^f (Experimental-theoretical)/experimental.

The agreement between the experimental and calculated values of Table 10.7 is well within the experimental capability of the spectroscopic determinations including the values at large Z which relies on X-ray spectroscopy. In this case, the experimental capability is three to four significant figures which is consistent with the last column. The fluorine atom isoelectronic series is given in Table 10.7 [2-3] to much higher

precision than the capability of X-ray spectroscopy, but these values are based on theoretical and interpolation techniques rather than data alone. Ionization energies are difficult to determine since the cut-off of the Rydberg series of lines at the ionization energy is often not observed, and the ionization energy must be determined from theoretical calculations, interpolation of F isoelectronic and Rydberg series, as well as direct experimental data.

TEN-ELECTRON ATOMS

Ten-electron atoms can be solved exactly using the results of the solutions of one, two, three, four, five, six, seven, eight, and nine-electron atoms.

RADIUS AND IONIZATION ENERGY OF AN OUTER ELECTRON OF THE NEON ATOM

For each nine-electron atom having a central charge of Z times that of the proton, there are two indistinguishable spin-paired electrons in an orbitsphere with radii r_1 and r_2 both given by Eq. (7.19) (Eq. (10.51)), two indistinguishable spin-paired electrons in an orbitsphere with radii r_3 and r_4 both given by Eq. (10.62), and two sets of paired and an unpaired electron is in an orbitsphere at r_5 given by Eq. (10.192). For $Z \geq 10$, the next electron which binds to form the corresponding ten-electron atom is attracted by the central Coulomb field and is repelled by diamagnetic force due to the spin-paired inner electrons. A paramagnetic spin-pairing force that results in the formation of a filled s orbital is also possible, but the force due to the spin-pairing of the electrons (Eq. (7.15) with the radius r_{10}) reduces the energy of the atom less than that due to the alternative forces on three pairs of electrons of opposite spin in p_x , p_y , and p_z orbitals of an orbitsphere at the same radius r_{10} . The resulting electron configuration is $1s^2 2s^2 2p^6$, and the orbital arrangement is

$$\begin{array}{ccc} \uparrow \downarrow & \uparrow \downarrow & \uparrow \downarrow \\ 1 & 0 & -1 \end{array} \quad (10.194)$$

corresponding to the ground state 1S_0 .

The central Coulomb force acts on the outer electron to cause it to bind wherein this electric force on the outer-most electron due to the nucleus and the inner nine electrons is given by Eq. (10.70) with the appropriate charge and radius:

$$\mathbf{F}_{ele} = \frac{(Z-9)e^2}{4\pi\epsilon_0 r_{10}^2} \mathbf{i}_r \quad (10.195)$$

for $r > r_9$.

The energy is minimized and the angular momentum is conserved with the pairing of electron ten to fill the p_y orbital when the orbital angular momenta of each set of the p_x , p_y , and p_z spin-paired electrons add negatively to cancel. Then, the diamagnetic force (Eq. (10.82)), $F_{\text{diamagnetic}}$, is zero:

$$F_{\text{diamagnetic}} = 0 \quad (10.196)$$

From Eq. (10.83), $F_{\text{mag } 2}$ is

$$F_{\text{mag } 2} = (1+1+1) \frac{1}{Z} \frac{\hbar^2}{m_e r_{10}^2 r_3} \sqrt{s(s+1)} \mathbf{i}_r = \frac{1}{Z} \frac{3\hbar^2}{m_e r_{10}^2 r_3} \sqrt{s(s+1)} \mathbf{i}_r, \quad (10.197)$$

corresponding to the spin-angular-momentum contribution alone from each of the p_x , p_y , and p_z orbitals.

The outward centrifugal force on electron 10 is balanced by the electric force and the magnetic forces (on electron 10). The radius of the outer electron is calculated by equating the outward centrifugal force to the sum of the electric (Eq. (10.195)), diamagnetic (Eq. (10.196)), and paramagnetic (Eq. (10.197)) forces as follows:

$$\frac{m_e v_{10}^2}{r_{10}} = \frac{(Z-9)e^2}{4\pi\epsilon_0 r_{10}^2} + \frac{3\hbar^2}{Z m_e r_{10}^2 r_3} \sqrt{s(s+1)} \quad (10.198)$$

Substitution of $v_{10} = \frac{\hbar}{m_e r_{10}}$ (Eq. (1.56)) and $s = \frac{1}{2}$ into Eq. (10.198) gives:

$$\frac{\hbar^2}{m_e r_{10}^3} = \frac{(Z-9)e^2}{4\pi\epsilon_0 r_{10}^2} + \frac{3\hbar^2}{Z m_e r_{10}^2 r_3} \sqrt{\frac{3}{4}} \quad (10.199)$$

$$r_{10} = \frac{\frac{\hbar^2}{m_e}}{\frac{(Z-9)e^2}{4\pi\epsilon_0} + \frac{3\hbar^2}{Z m_e r_3} \sqrt{\frac{3}{4}}} \quad (10.200)$$

$$r_{10} = \frac{a_0}{(Z-9) + \frac{3}{Z} \sqrt{\frac{3}{4}}}, \quad r_3 \text{ in units of } a_0 \quad (10.201)$$

Substitution of $\frac{r_3}{a_0} = 0.45511$ (Eq. (10.62) with $Z=10$) into Eq. (10.201) gives

$$r_{10} = 0.63659 a_0 \quad (10.202)$$

The ionization energy of the neon atom is given by the negative of $E(\text{electric})$ given by Eq. (10.102) with the appropriate charge and radius:

$$E(\text{ionization}; \text{Ne}) = -\text{Electric Energy} = \frac{(Z-9)e^2}{8\pi\epsilon_0 r_{10}} = 21.37296 \text{ eV} \quad (10.203)$$

where $r_{10} = 0.63659 a_0$ (Eq. (10.202)) and $Z=10$. The experimental ionization energy of the neon atom is 21.56454 eV [3].

THE IONIZATION ENERGIES OF TEN-ELECTRON ATOMS WITH A NUCLEAR CHARGE $Z > 10$

Ten-electron atoms having $Z > 10$ possess an external electric field given by Eq. (10.92). In this case, an energy minimum is achieved with conservation of momentum when the orbital angular momentum is such that $F_{\text{diamagnetic}}$ is minimized while $F_{\text{mag } 2}$ is maximized. From Eq. (10.82), the diamagnetic force, $F_{\text{diamagnetic}}$, is given by the sum of the contributions from the p_x , p_y , and p_z orbitals corresponding to $m = 1, -1$, and 0 , respectively:

$$F_{\text{diamagnetic}} = -\left(\frac{2}{3} + \frac{2}{3} + \frac{1}{3}\right) \frac{\hbar^2}{4m_e r_{10}^2 r_3} \sqrt{s(s+1)} \mathbf{i}_r = -\left(\frac{5}{3}\right) \frac{\hbar^2}{4m_e r_{10}^2 r_3} \sqrt{s(s+1)} \mathbf{i}_r \quad (10.204)$$

The filled p orbitals with the maintenance of symmetry according to Eq. (10.72) requires that the diamagnetic force is only due to the electrons at r_3 . From Eq. (10.84), $F_{\text{mag } 2}$ is

$$F_{\text{mag } 2} = (4 + 4 + 4) \frac{1}{Z} \frac{\hbar^2}{m_e r_{10}^2 r_3} \sqrt{s(s+1)} \mathbf{i}_r = \frac{1}{Z} \frac{12\hbar^2}{m_e r_{10}^2 r_3} \sqrt{s(s+1)} \mathbf{i}_r \quad (10.205)$$

corresponding to the spin and orbital angular momenta of the paired p_x , p_y , and p_z electrons.

The second diamagnetic force, $F_{\text{diamagnetic } 2}$, due to the binding of the p-orbital electron having an electric field outside of its radius is given by Eq. (10.93):

$$F_{\text{diamagnetic } 2} = -\left[\frac{Z-10}{Z-9}\right] \left(1 - \frac{\sqrt{2}}{2}\right) \frac{r_3 \hbar^2}{m_e r_{10}^4} 10 \sqrt{s(s+1)} \mathbf{i}_r \quad (10.206)$$

In the case that $Z > 10$, the radius of the outer electron is calculated by equating the outward centrifugal force to the sum of the electric (Eq. (10.195)), diamagnetic (Eqs. (10.204) and (10.206)), and paramagnetic (Eq. (10.205)) forces as follows:

$$\frac{m_e v_{10}^2}{r_{10}} = \frac{(Z-9)e^2}{4\pi\epsilon_0 r_{10}^2} - \frac{5\hbar^2}{12m_e r_{10}^2 r_3} \sqrt{s(s+1)} + \frac{12\hbar^2}{Zm_e r_{10}^2 r_3} \sqrt{s(s+1)} - \left[\frac{Z-10}{Z-9}\right] \left(1 - \frac{\sqrt{2}}{2}\right) \frac{r_3 \hbar^2}{m_e r_{10}^4} 10 \sqrt{s(s+1)} \quad (10.207)$$

Substitution of $v_{10} = \frac{\hbar}{m_e r_{10}}$ (Eq. (1.56)) and $s = \frac{1}{2}$ into Eq. (10.207) gives:

$$\frac{\hbar^2}{m_e r_{10}^3} = \frac{(Z-9)e^2}{4\pi\epsilon_0 r_{10}^2} - \frac{5\hbar^2}{12m_e r_{10}^2 r_3} \sqrt{\frac{3}{4}} + \frac{12\hbar^2}{Zm_e r_{10}^2 r_3} \sqrt{\frac{3}{4}} - \left[\frac{Z-10}{Z-9}\right] \left(1 - \frac{\sqrt{2}}{2}\right) \frac{r_3 \hbar^2}{m_e r_{10}^4} 10 \sqrt{\frac{3}{4}} \quad (10.208)$$

The quadratic equation corresponding to Eq. (10.208) is

$$\left(\frac{(Z-9)e^2}{4\pi\epsilon_0} - \left(\frac{5}{12} - \frac{12}{Z}\right) \frac{\hbar^2}{m_e r_3} \sqrt{\frac{3}{4}}\right) r_{10}^2 - \frac{\hbar^2}{m_e} r_{10} - \left[\frac{Z-10}{Z-9}\right] \left(1 - \frac{\sqrt{2}}{2}\right) \frac{r_3 \hbar^2}{m_e} 10 \sqrt{\frac{3}{4}} = 0 \quad (10.209)$$

$$r_{10}^2 - \frac{\frac{\hbar^2}{m_e}}{\left(\frac{(Z-9)e^2}{4\pi\epsilon_0} - \left(\frac{5}{12} - \frac{12}{Z}\right)\frac{\hbar^2}{m_e r_3} \sqrt{\frac{3}{4}}\right)} r_{10} - \frac{\frac{\hbar^2}{m_e} \left[\frac{Z-10}{Z-9}\right] \left(1 - \frac{\sqrt{2}}{2}\right) r_3 10 \sqrt{\frac{3}{4}}}{\left(\frac{(Z-9)e^2}{4\pi\epsilon_0} - \left(\frac{5}{12} - \frac{12}{Z}\right)\frac{\hbar^2}{m_e r_3} \sqrt{\frac{3}{4}}\right)} = 0 \quad (10.210)$$

The solution of Eq. (10.210) using the quadratic formula is:

$$r_{10} = \frac{\frac{\hbar^2}{m_e}}{\left(\frac{(Z-9)e^2}{4\pi\epsilon_0} - \left(\frac{5}{12} - \frac{12}{Z}\right)\frac{\hbar^2}{m_e r_3} \sqrt{\frac{3}{4}}\right)} \pm \frac{\sqrt{\left(\frac{\hbar^2}{m_e}\right)^2 - 4 \frac{\frac{\hbar^2}{m_e} \left[\frac{Z-10}{Z-9}\right] \left(1 - \frac{\sqrt{2}}{2}\right) r_3 10 \sqrt{\frac{3}{4}}}{\left(\frac{(Z-9)e^2}{4\pi\epsilon_0} - \left(\frac{5}{12} - \frac{12}{Z}\right)\frac{\hbar^2}{m_e r_3} \sqrt{\frac{3}{4}}\right)}}}{2} \quad (10.211)$$

$$r_{10} = \frac{\frac{a_0}{\left((Z-9) - \left(\frac{5}{24} - \frac{6}{Z}\right)\frac{\sqrt{3}}{r_3}\right)} \pm a_0}{2} \sqrt{\frac{1}{\left((Z-9) - \left(\frac{5}{24} - \frac{6}{Z}\right)\frac{\sqrt{3}}{r_3}\right)} + \frac{20\sqrt{3} \left[\frac{Z-10}{Z-9}\right] \left(1 - \frac{\sqrt{2}}{2}\right) r_3}{\left((Z-9) - \left(\frac{5}{24} - \frac{6}{Z}\right)\frac{\sqrt{3}}{r_3}\right)}} \quad (10.212)$$

r_3 in units of a_0

where r_3 is given by Eq. (10.62). The positive root of Eq. (10.212) must be taken in order that $r_{10} > 0$. The final radius of electron 10, r_{10} , is given by Eq. (10.62); this is also the final radius of electrons 5, 6, 7, 8, and 9. The radii of several ten-electron atoms are given in Table 10.8.

The ionization energies for the ten-electron atoms with $Z > 10$ are given by the electric energy, $E(\text{electric})$, (Eq. (10.102) with the radii, r_{10} , given by Eq. (10.212)):

$$E(\text{ionization}) = -\text{Electric Energy} = \frac{(Z-9)e^2}{8\pi\epsilon_0 r_{10}} \quad (10.213)$$

Since the relativistic corrections were small, the nonrelativistic ionization energies for experimentally measured ten-electron atoms are given in

Table 10.8.

Table 10.8. Ionization energies for some ten-electron atoms.

10 e Atom	Z	r_1 (a_0) ^a	r_3 (a_0) ^b	r_{10} (a_0) ^c	Theoretical Ionization Energies ^d (eV)	Experimental Ionization Energies ^e (eV)	Relative Error ^f
Ne	10	0.10149	0.45511	0.63659	21.37296	21.56454	0.00888
Na ⁺	11	0.09213	0.40853	0.560945	48.5103	47.2864	-0.0259
Mg ²⁺	12	0.08435	0.37065	0.510568	79.9451	80.1437	0.0025
Al ³⁺	13	0.07778	0.33923	0.456203	119.2960	119.992	0.0058
Si ⁴⁺	14	0.07216	0.31274	0.409776	166.0150	166.767	0.0045
P ⁵⁺	15	0.06730	0.29010	0.371201	219.9211	220.421	0.0023
S ⁶⁺	16	0.06306	0.27053	0.339025	280.9252	280.948	0.0001
Cl ⁷⁺	17	0.05932	0.25344	0.311903	348.9750	348.28	-0.0020
Ar ⁸⁺	18	0.05599	0.23839	0.288778	424.0365	422.45	-0.0038
K ⁹⁺	19	0.05302	0.22503	0.268844	506.0861	503.8	-0.0045
Ca ¹⁰⁺	20	0.05035	0.21308	0.251491	595.1070	591.9	-0.0054
Sc ¹¹⁺	21	0.04794	0.20235	0.236251	691.0866	687.36	-0.0054
Ti ¹²⁺	22	0.04574	0.19264	0.222761	794.0151	787.84	-0.0078
V ¹³⁺	23	0.04374	0.18383	0.210736	903.8853	896	-0.0088
Cr ¹⁴⁺	24	0.04191	0.17579	0.19995	1020.6910	1010.6	-0.0100
Mn ¹⁵⁺	25	0.04022	0.16842	0.19022	1144.4276	1134.7	-0.0086
Fe ¹⁶⁺	26	0.03867	0.16165	0.181398	1275.0911	1266	-0.0072
Co ¹⁷⁺	27	0.03723	0.15540	0.173362	1412.6783	1397.2	-0.0111
Ni ¹⁸⁺	28	0.03589	0.14961	0.166011	1557.1867	1541	-0.0105
Cu ¹⁹⁺	29	0.03465	0.14424	0.159261	1708.6139	1697	-0.0068
Zn ²⁰⁺	30	0.03349	0.13925	0.153041	1866.9581	1856	-0.0059

^a Radius of the first set of paired inner electrons of ten-electron atoms from Equation (10.51).

^b Radius of the second set of paired inner electrons of ten-electron atoms from Equation (10.62).

^c Radius of three sets of paired outer electrons of ten-electron atoms from Eq. (10.212) for $Z > 10$ and Eq. (10.202) for Ne.

^d Calculated ionization energies of ten-electron atoms given by the electric energy (Eq. (10.213)).

^e From theoretical calculations, interpolation of isoelectronic and spectral series, and experimental data [2-3].

^f (Experimental-theoretical)/experimental.

The agreement between the experimental and calculated values of Table 10.8 is well within the experimental capability of the spectroscopic determinations including the values at large Z which relies on X-ray spectroscopy. In this case, the experimental capability is three to four

significant figures which is consistent with the last column. The neon atom isoelectronic series is given in Table 10.8 [2-3] to much higher precision than the capability of X-ray spectroscopy, but these values are based on theoretical and interpolation techniques rather than data alone. Ionization energies are difficult to determine since the cut-off of the Rydberg series of lines at the ionization energy is often not observed, and the ionization energy must be determined from theoretical calculations, interpolation of Ne isoelectronic and Rydberg series, as well as direct experimental data.

GENERAL EQUATION FOR THE IONIZATION ENERGIES OF FIVE THROUGH TEN-ELECTRON ATOMS

Using the forces given by Eqs. (10.70), (10.82-10.84), (10.89), (10.93), and the radii r_3 given by Eq. (10.62), the radii of the 2p electrons of all five through ten-electron atoms may be solved exactly. The electric energy given by Eq. (10.102) gives the corresponding exact ionization energies. A summary of the parameters of the equations that determine the exact radii and ionization energies of all five through ten-electron atoms is given in Table 10.9.

F_{ele} and $F_{diamagnetic\ 2}$ given by Eqs. (10.70) and (10.93), respectively, are of the same form for all atoms with the appropriate nuclear charges and atomic radii. $F_{diamagnetic}$ given by Eq. (10.82) and $F_{mag\ 2}$ given by Eqs. (10.83-10.84) and (10.89) are of the same form with the appropriate factors that depend on the electron configuration wherein the electron configuration must be a minimum of energy.

For each n-electron atom having a central charge of Z times that of the proton and an electron configuration $1s^2 2s^2 2p^{n-4}$, there are two indistinguishable spin-paired electrons in an orbitsphere with radii r_1 and r_2 both given by Eqs. (7.19) and (10.51):

$$r_1 = r_2 = a_0 \left[\frac{1}{Z-1} - \frac{\sqrt{\frac{3}{4}}}{Z(Z-1)} \right] \quad (10.214)$$

two indistinguishable spin-paired electrons in an orbitsphere with radii r_3 and r_4 both given by Eq. (10.62):

$$r_4 = r_3 = \frac{a_0 \left(1 - \frac{\sqrt{3}}{4Z}\right)}{\left((Z-3) - \left(\frac{1}{4} - \frac{1}{Z}\right) \frac{\sqrt{3}}{r_1}\right)} \pm a_0 \sqrt{\frac{\left(1 - \frac{\sqrt{3}}{4Z}\right)^2}{\left((Z-3) - \left(\frac{1}{4} - \frac{1}{Z}\right) \frac{\sqrt{3}}{r_1}\right)^2} + 4 \frac{\left[\frac{Z-3}{Z-2}\right] r_1 10 \sqrt{\frac{3}{4}}}{\left((Z-3) - \left(\frac{1}{4} - \frac{1}{Z}\right) \frac{\sqrt{3}}{r_1}\right)}}} \quad (10.215)$$

r_1 in units of a_0

where r_1 is given by Eq. (10.214), and $n-4$ electrons in an orbitsphere with radius r_n given by

$$r_n = \frac{a_0}{\left((Z-(n-1)) - \left(\frac{A}{8} - \frac{B}{2Z}\right) \frac{\sqrt{3}}{r_3}\right)} \pm a_0 \sqrt{\frac{1}{\left((Z-(n-1)) - \left(\frac{A}{8} - \frac{B}{2Z}\right) \frac{\sqrt{3}}{r_3}\right)^2} + \frac{20\sqrt{3} \left(\left[\frac{Z-n}{Z-(n-1)}\right] \left(1 - \frac{\sqrt{2}}{2}\right) r_3\right)}{\left((Z-(n-1)) - \left(\frac{A}{8} - \frac{B}{2Z}\right) \frac{\sqrt{3}}{r_3}\right)}}} \quad (10.216)$$

r_3 in units of a_0

where r_3 is given by Eq. (10.215), the parameter A given in Table 10.9 corresponds to the diamagnetic force, $F_{\text{diamagnetic}}$, (Eq. (10.82)), and the parameter B given in Table 10.9 corresponds to the paramagnetic force, $F_{\text{mag}2}$ (Eqs. (10.83-10.84) and (10.89)). The positive root of Eq. (10.216) must be taken in order that $r_n > 0$. The radii of several n -electron atoms are given in Tables 10.3-10.8.

The ionization energy for the boron atom is given by Eq. (10.104). The ionization energies for the n -electron atoms are given by the negative of the electric energy, $E(\text{electric})$, (Eq. (10.102) with the radii, r_n , given by Eq. (10.216)):

$$E(\text{ionization}) = -\text{Electric Energy} = \frac{(Z-(n-1))e^2}{8\pi\epsilon_0 r_n} \quad (10.217)$$

Since the relativistic corrections were small, the nonrelativistic ionization energies for experimentally measured n -electron atoms are given by Eqs. (10.217) and (10.216) in Tables 10.3-10.8.

Table 10.9. Summary of the parameters of five through ten-electron atoms.

Atom Type	Electron Configuration	Ground State Term ^a	Orbital Arrangement of 2p Electrons (2p state)	Diamagnetic Force Factor A^b	Paramagnetic Force Factor B^c
Neutral 5 e Atom <i>B</i>	$1s^2 2s^2 2p^1$	$^2P_{1/2}^0$	$\begin{array}{ccc} \uparrow & \text{---} & \text{---} \\ 1 & 0 & -1 \end{array}$	2	0
Neutral 6 e Atom <i>C</i>	$1s^2 2s^2 2p^2$	3P_0	$\begin{array}{ccc} \uparrow & \uparrow & \text{---} \\ 1 & 0 & -1 \end{array}$	$\frac{2}{3}$	0
Neutral 7 e Atom <i>N</i>	$1s^2 2s^2 2p^3$	$^4S_{3/2}^0$	$\begin{array}{ccc} \uparrow & \uparrow & \uparrow \\ 1 & 0 & -1 \end{array}$	$\frac{1}{3}$	1
Neutral 8 e Atom <i>O</i>	$1s^2 2s^2 2p^4$	3P_2	$\begin{array}{ccc} \uparrow \downarrow & \uparrow & \uparrow \\ 1 & 0 & -1 \end{array}$	1	2
Neutral 9 e Atom <i>F</i>	$1s^2 2s^2 2p^5$	$^2P_{3/2}^0$	$\begin{array}{ccc} \uparrow \downarrow & \uparrow \downarrow & \uparrow \\ 1 & 0 & -1 \end{array}$	$\frac{2}{3}$	3
Neutral 10 e Atom <i>Ne</i>	$1s^2 2s^2 2p^6$	1S_0	$\begin{array}{ccc} \uparrow \downarrow & \uparrow \downarrow & \uparrow \downarrow \\ 1 & 0 & -1 \end{array}$	0	3
5 e Ion	$1s^2 2s^2 2p^1$	$^2P_{1/2}^0$	$\begin{array}{ccc} \uparrow & \text{---} & \text{---} \\ 1 & 0 & -1 \end{array}$	$\frac{5}{3}$	1
6 e Ion	$1s^2 2s^2 2p^2$	3P_0	$\begin{array}{ccc} \uparrow & \uparrow & \text{---} \\ 1 & 0 & -1 \end{array}$	$\frac{5}{3}$	4
7 e Ion	$1s^2 2s^2 2p^3$	$^4S_{3/2}^0$	$\begin{array}{ccc} \uparrow & \uparrow & \uparrow \\ 1 & 0 & -1 \end{array}$	$\frac{5}{3}$	6
8 e Ion	$1s^2 2s^2 2p^4$	3P_2	$\begin{array}{ccc} \uparrow \downarrow & \uparrow & \uparrow \\ 1 & 0 & -1 \end{array}$	$\frac{5}{3}$	6
9 e Ion	$1s^2 2s^2 2p^5$	$^2P_{3/2}^0$	$\begin{array}{ccc} \uparrow \downarrow & \uparrow \downarrow & \uparrow \\ 1 & 0 & -1 \end{array}$	$\frac{5}{3}$	9
10 e Ion	$1s^2 2s^2 2p^6$	1S_0	$\begin{array}{ccc} \uparrow \downarrow & \uparrow \downarrow & \uparrow \downarrow \\ 1 & 0 & -1 \end{array}$	$\frac{5}{3}$	12

^a The theoretical ground state terms match those given by NIST [8].^b Eq. (10.82).^c Eqs. (10.83-10.84) and (10.89).

ELEVEN-ELECTRON ATOMS

Eleven-electron atoms can be solved exactly using the results of the solutions of one, two, three, four, five, six, seven, eight, nine, and ten-electron atoms.

RADIUS AND IONIZATION ENERGY OF THE OUTER ELECTRON OF THE SODIUM ATOM

For each ten-electron atom having a central charge of Z times that of the proton, there are two indistinguishable spin-paired electrons in an orbitsphere with radii r_1 and r_2 both given by Eq. (7.19) (Eq. (10.51)), two indistinguishable spin-paired electrons in an orbitsphere with radii r_3 and r_4 both given by Eq. (10.62), and three sets of paired electrons in an orbitsphere at r_{10} given by Eq. (10.212). For $Z \geq 11$, the next electron which binds to form the corresponding eleven-electron atom is attracted by the central Coulomb field and is repelled by diamagnetic forces due to the 3 sets of spin-paired inner electrons such that it forms an unpaired orbitsphere at radius r_{11} .

The central Coulomb force acts on the outer electron to cause it to bind wherein this electric force on the outer-most electron due to the nucleus and the inner ten electrons is given by Eq. (10.70) with the appropriate charge and radius:

$$F_{ele} = \frac{(Z-10)e^2}{4\pi\epsilon_0 r_{11}^2} \mathbf{i}_r \quad (10.218)$$

for $r > r_{10}$.

The spherically symmetrical closed 2p shell of eleven-electron atoms produces a diamagnetic force, $F_{diamagnetic}$, that is equivalent to that of a closed s shell given by Eq. (10.11) with the appropriate radii. The inner electrons remain at their initial radii, but cause a diamagnetic force according to Lenz's law that is

$$F_{diamagnetic} = -\frac{\hbar^2}{4m_e r_{11}^2 r_{10}} \sqrt{s(s+1)} \mathbf{i}_r \quad (10.219)$$

In addition to the spin-spin interaction between electron pairs, the three sets of 2p electrons are orbitally paired. The single s orbital of the sodium atom produces a magnetic field at the position of the three sets of spin-paired 2p electrons. In order for the electrons to remain spin and orbitally paired, a corresponding diamagnetic force, $F_{diamagnetic 3}$, on electron eleven from the three sets of spin-paired electrons is given by

$$F_{diamagnetic 3} = -8 \left[\frac{e^2 \mu_0}{2m_e r_{10}} \right] \frac{\hbar^2}{m_e r_{11}^3} \mathbf{i}_r \quad (10.220)$$

corresponding to the p_x and p_y electrons with no interaction from the

orthogonal p_i electrons (Eq. (10.84)). As demonstrated by Eqs. (7.6-7.15), the maintenance of the invariance of the electron's angular momentum of \hbar , mass to charge ratio, $\frac{e}{m_e}$, and corresponding magnetic moment of a Bohr magneton, μ_B , requires that the term in brackets is be replaced by $\frac{1}{Z}$ corresponding to the relativistic correction given by Eq. (7.14). Thus, $F_{\text{diamagnetic } 3}$ is given by

$$F_{\text{diamagnetic } 3} = -\frac{1}{Z} \frac{8\hbar^2}{m_e r_{11}^3} \sqrt{s(s+1)} \mathbf{i}_r \quad (10.221)$$

where the vector projection of the spin interaction of $\sqrt{s(s+1)} = \sqrt{\frac{3}{4}}$ is given by Eq. (7.15).

The outward centrifugal force on electron 11 is balanced by the electric force and the magnetic forces (on electron 11). The radius of the outer electron is calculated by equating the outward centrifugal force to the sum of the electric (Eq. (10.218)) and diamagnetic (Eqs. (10.219) and (10.221)) forces as follows:

$$\frac{m_e v_{11}^2}{r_{11}} = \frac{(Z-10)e^2}{4\pi\epsilon_0 r_{11}^2} - \frac{\hbar^2}{4m_e r_{11}^2 r_{10}} \sqrt{s(s+1)} - \frac{8\hbar^2}{Zm_e r_{11}^3} \sqrt{s(s+1)} \quad (10.222)$$

Substitution of $v_{11} = \frac{\hbar}{m_e r_{11}}$ (Eq. (1.56)) and $s = \frac{1}{2}$ into Eq. (10.222) gives:

$$\frac{\hbar^2}{m_e r_{11}^3} = \frac{(Z-10)e^2}{4\pi\epsilon_0 r_{11}^2} - \frac{\hbar^2}{4m_e r_{11}^2 r_{10}} \sqrt{\frac{3}{4}} - \frac{8\hbar^2}{Zm_e r_{11}^3} \sqrt{\frac{3}{4}} \quad (10.223)$$

$$r_{11} = \frac{\frac{\hbar^2}{m_e} \left(1 + \frac{8}{Z} \sqrt{\frac{3}{4}} \right)}{\frac{(Z-10)e^2}{4\pi\epsilon_0} - \frac{\hbar^2}{4m_e r_{10}} \sqrt{\frac{3}{4}}} \quad (10.224)$$

$$r_{11} = \frac{a_0 \left(1 + \frac{8}{Z} \sqrt{\frac{3}{4}} \right)}{(Z-10) - \frac{\sqrt{\frac{3}{4}}}{4r_{10}}}, \quad r_{10} \text{ in units of } a_0 \quad (10.225)$$

Substitution of $\frac{r_{10}}{a_0} = 0.56094$ (Eq. (10.212) with $Z=11$) into Eq. (10.225) gives

$$r_{11} = 2.65432a_0 \quad (10.226)$$

The ionization energy of the sodium atom is given by the negative of $E(\text{electric})$ given by Eq. (10.102) with the appropriate charge and radius:

$$E(\text{ionization}; \text{Na}) = -\text{Electric Energy} = \frac{(Z-10)e^2}{8\pi\epsilon_0 r_{11}} = 5.12592 \text{ eV} \quad (10.227)$$

where $r_{11} = 2.65432a_0$ (Eq. (10.226)) and $Z=11$. The experimental ionization energy of the sodium atom is 5.13908 eV [3].

THE IONIZATION ENERGIES OF ELEVEN-ELECTRON ATOMS WITH A NUCLEAR CHARGE $Z>11$

Eleven-electron atoms having $Z>11$ possess an external electric field given by Eq. (10.92). Since there is a source of dissipative, $\mathbf{J} \cdot \mathbf{E}$ of Eq. (10.27), the magnetic moments of the inner electrons may change due to the outer electron such that the energy of the eleven-electron atom is lowered. The orbital angular momenta of the paired p_x and p_y electrons give rise to the paramagnetic force given by Eq. (10.89) which is also equivalent to that given by Eq. (10.55):

$$\mathbf{F}_{\text{mag } 2} = \frac{1}{Z} \frac{4\hbar^2}{m_e r_{11}^2 r_{10}} \sqrt{s(s+1)} \mathbf{i}_r \quad (10.228)$$

The diamagnetic force, $\mathbf{F}_{\text{diamagnetic } 2}$, due to a relativistic effect with an electric field for $r > r_n$ (Eq. (10.35)) may be determined by considering the corresponding force due to the binding of a 2p electron. It was shown in the Five-Electron Atom section, that $\mathbf{F}_{\text{diamagnetic } 2}$ for five through ten-electron atoms, is dependent on the amplitude of the orbital energy. Using the orbital energy with $\ell=1$ (Eq. (10.90)), the energy $m_e \Delta v^2$ of Eq. (10.29) is reduced by the factor of $\left(1 - \frac{\sqrt{2}}{2}\right)$ due to the contribution of the charge-density wave of the inner electrons at r_3 . Thus, $\mathbf{F}_{\text{diamagnetic } 2}$ is given by Eq. (10.93). Conversely, the binding of a 3s electron increases the energy $m_e \Delta v^2$ of Eq. (10.29) by the factor of $\left(1 + \frac{\sqrt{2}}{2}\right)$ such that $\mathbf{F}_{\text{diamagnetic } 2}$ becomes

$$\mathbf{F}_{\text{diamagnetic } 2} = -\left[\frac{Z-11}{Z-10}\right] \left(1 + \frac{\sqrt{2}}{2}\right) \frac{r_{10} \hbar^2}{m_e r_{11}^4} 10 \sqrt{s(s+1)} \mathbf{i}_r \quad (10.229)$$

In the case that $Z>11$, the radius of the outer electron is calculated by equating the outward centrifugal force to the sum of the electric (Eq. (10.218)), diamagnetic (Eq. (10.229)), and paramagnetic (Eq. (10.228)) forces as follows:

$$\begin{aligned} \frac{m_e v_{11}^2}{r_{11}} = & \frac{(Z-10)e^2}{4\pi\epsilon_0 r_{11}^2} - \frac{\hbar^2}{4m_e r_{11}^2 r_{10}} \sqrt{s(s+1)} + \frac{4\hbar^2}{Zm_e r_{11}^2 r_{10}} \sqrt{s(s+1)} \\ & - \frac{8\hbar^2}{Zm_e r_{11}^3} \sqrt{s(s+1)} - \left[\frac{Z-11}{Z-10}\right] \left(1 + \frac{\sqrt{2}}{2}\right) \frac{r_{10} \hbar^2}{m_e r_{11}^4} 10 \sqrt{s(s+1)} \end{aligned} \quad (10.230)$$

Substitution of $v_{11} = \frac{\hbar}{m_e r_{11}}$ (Eq. (1.56)) and $s = \frac{1}{2}$ into Eq. (10.230) gives:

$$\frac{\hbar^2}{m_e r_{11}^3} = \frac{(Z-10)e^2}{4\pi\epsilon_0 r_{11}^2} - \frac{\hbar^2}{4m_e r_{11}^2 r_{10}} \sqrt{\frac{3}{4}} + \frac{4\hbar^2}{Zm_e r_{11}^2 r_{10}} \sqrt{\frac{3}{4}} - \frac{8\hbar^2}{Zm_e r_{11}^3} \sqrt{\frac{3}{4}} - \left[\frac{Z-11}{Z-10} \right] \left(1 + \frac{\sqrt{2}}{2} \right) \frac{r_{10}\hbar^2}{m_e r_{11}^4} 10 \sqrt{\frac{3}{4}} \quad (10.231)$$

The quadratic equation corresponding to Eq. (10.231) is

$$\left(\frac{(Z-10)e^2}{4\pi\epsilon_0} - \left(\frac{1}{4} - \frac{4}{Z} \right) \frac{\hbar^2}{m_e r_{10}} \sqrt{\frac{3}{4}} \right) r_{11}^2 - \frac{\hbar^2}{m_e} \left(1 + \frac{8\sqrt{\frac{3}{4}}}{Z} \right) r_{11} - \left[\frac{Z-11}{Z-10} \right] \left(1 + \frac{\sqrt{2}}{2} \right) \frac{r_{10}\hbar^2}{m_e} 10 \sqrt{\frac{3}{4}} = 0 \quad (10.232)$$

$$r_{11}^2 - \frac{\frac{\hbar^2}{m_e} \left(1 + \frac{8\sqrt{\frac{3}{4}}}{Z} \right)}{\left(\frac{(Z-10)e^2}{4\pi\epsilon_0} - \left(\frac{1}{4} - \frac{4}{Z} \right) \frac{\hbar^2}{m_e r_{10}} \sqrt{\frac{3}{4}} \right)} r_{11} - \frac{\left[\frac{Z-11}{Z-10} \right] \left(1 + \frac{\sqrt{2}}{2} \right) \frac{r_{10}\hbar^2}{m_e} 10 \sqrt{\frac{3}{4}}}{\left(\frac{(Z-10)e^2}{4\pi\epsilon_0} - \left(\frac{1}{4} - \frac{4}{Z} \right) \frac{\hbar^2}{m_e r_{10}} \sqrt{\frac{3}{4}} \right)} = 0 \quad (10.233)$$

The solution of Eq. (10.233) using the quadratic formula is:

$$r_{11} = \frac{\frac{\hbar^2}{m_e} \left(1 + \frac{8\sqrt{\frac{3}{4}}}{Z} \right)}{\left(\frac{(Z-10)e^2}{4\pi\epsilon_0} - \left(\frac{1}{4} - \frac{4}{Z} \right) \frac{\hbar^2}{m_e r_{10}} \sqrt{\frac{3}{4}} \right)} \pm \frac{\sqrt{\left(\frac{\hbar^2}{m_e} \left(1 + \frac{8\sqrt{\frac{3}{4}}}{Z} \right) \right)^2 - 4 \frac{\left[\frac{Z-11}{Z-10} \right] \left(1 + \frac{\sqrt{2}}{2} \right) \frac{r_{10}\hbar^2}{m_e} 10 \sqrt{\frac{3}{4}}}{\left(\frac{(Z-10)e^2}{4\pi\epsilon_0} - \left(\frac{1}{4} - \frac{4}{Z} \right) \frac{\hbar^2}{m_e r_{10}} \sqrt{\frac{3}{4}} \right)}}}{2} \quad (10.234)$$

$$r_{11} = \frac{a_0 \left(1 + \frac{4\sqrt{3}}{Z}\right)}{\left((Z-10) - \left(\frac{1}{8} - \frac{2}{Z}\right)\frac{\sqrt{3}}{r_{10}}\right)} \pm a_0 \sqrt{\frac{\left(1 + \frac{4\sqrt{3}}{Z}\right)^2}{\left((Z-10) - \left(\frac{1}{8} - \frac{2}{Z}\right)\frac{\sqrt{3}}{r_{10}}\right)} + \frac{20\sqrt{3}\left(\left[\frac{Z-11}{Z-10}\right]\left(1 + \frac{\sqrt{2}}{2}\right)r_{10}\right)}{\left((Z-10) - \left(\frac{1}{8} - \frac{2}{Z}\right)\frac{\sqrt{3}}{r_{10}}\right)}} \quad (10.235)$$

r_{10} in units of a_0

where r_{10} is given by Eq. (10.212). The positive root of Eq. (10.235) must be taken in order that $r_{11} > 0$. The radii of several eleven-electron atoms are given in Table 10.10.

The ionization energies for the eleven-electron atoms with $Z > 11$ are given by the electric energy, $E(\text{electric})$, (Eq. (10.102) with the radii, r_{11} , given by Eq. (10.235)):

$$E(\text{Ionization}) = -\text{Electric Energy} = \frac{(Z-10)e^2}{8\pi\epsilon_0 r_{11}} \quad (10.236)$$

Since the relativistic corrections were small, the nonrelativistic ionization energies for experimentally measured eleven-electron atoms are given in Table 10.10.

Table 10.10. Ionization energies for some eleven-electron atoms.

11 e Atom	Z	r_1 (a_0) ^a	r_3 (a_0) ^b	r_{10} (a_0) ^c	r_{11} (a_0) ^d	Theoretical Ionization Energies ^e (eV)	Experimenta l Ionization Energies ^f (eV)	Relative Error ^g
<i>Na</i>	11	0.09213	0.40853	0.560945	2.65432	5.12592	5.13908	0.0026
<i>Mg</i> ⁺	12	0.08435	0.37065	0.510568	1.74604	15.5848	15.03528	-0.0365
<i>Al</i> ²⁺	13	0.07778	0.33923	0.456203	1.47399	27.6918	28.44765	0.0266
<i>Si</i> ³⁺	14	0.07216	0.31274	0.409776	1.25508	43.3624	45.14181	0.0394
<i>P</i> ⁴⁺	15	0.06730	0.29010	0.371201	1.08969	62.4299	65.0251	0.0399
<i>S</i> ⁵⁺	16	0.06306	0.27053	0.339025	0.96226	84.8362	88.0530	0.0365
<i>Cl</i> ⁶⁺	17	0.05932	0.25344	0.311903	0.86151	110.5514	114.1958	0.0319
<i>Ar</i> ⁷⁺	18	0.05599	0.23839	0.288778	0.77994	139.5577	143.460	0.0272
<i>K</i> ⁸⁺	19	0.05302	0.22503	0.268844	0.71258	171.8433	175.8174	0.0226
<i>Ca</i> ⁹⁺	20	0.05035	0.21308	0.251491	0.65602	207.3998	211.275	0.0183
<i>Sc</i> ¹⁰⁺	21	0.04794	0.20235	0.236251	0.60784	246.2213	249.798	0.0143
<i>Ti</i> ¹¹⁺	22	0.04574	0.19264	0.222761	0.56631	288.3032	291.500	0.0110
<i>V</i> ¹²⁺	23	0.04374	0.18383	0.210736	0.53014	333.6420	336.277	0.0078
<i>Cr</i> ¹³⁺	24	0.04191	0.17579	0.19995	0.49834	382.2350	384.168	0.0050
<i>Mn</i> ¹⁴⁺	25	0.04022	0.16842	0.19022	0.47016	434.0801	435.163	0.0025
<i>Fe</i> ¹⁵⁺	26	0.03867	0.16165	0.181398	0.44502	489.1753	489.256	0.0002
<i>Co</i> ¹⁶⁺	27	0.03723	0.15540	0.173362	0.42245	547.5194	546.58	-0.0017
<i>Ni</i> ¹⁷⁺	28	0.03589	0.14961	0.166011	0.40207	609.1111	607.06	-0.0034
<i>Cu</i> ¹⁸⁺	29	0.03465	0.14424	0.159261	0.38358	673.9495	670.588	-0.0050
<i>Zn</i> ¹⁹⁺	30	0.03349	0.13925	0.153041	0.36672	742.0336	738	-0.0055

^a Radius of the first set of paired inner electrons of eleven-electron atoms from Eq. (10.51).^b Radius of the second set of paired inner electrons of eleven-electron atoms from Eq. (10.62).^c Radius of three sets of paired inner electrons of eleven-electron atoms from Eq. (10.212)).^d Radius of unpaired outer electron of eleven-electron atoms from Eq. (10.235)) for $Z > 11$ and Eq. (10.226) for *Na*.^e Calculated ionization energies of eleven-electron atoms given by the electric energy (Eq. (10.236)).^f From theoretical calculations, interpolation of isoelectronic and spectral series, and experimental data [2-3].^g (Experimental-theoretical)/experimental.

The agreement between the experimental and calculated values of Table 10.10 is well within the experimental capability of the spectroscopic determinations including the values at large Z which relies on X-ray spectroscopy. In this case, the experimental capability is three to four significant figures which is consistent with the last column. The sodium atom isoelectronic series is given in Table 10.10 [2-3] to much higher precision than the capability of X-ray spectroscopy, but these

values are based on theoretical and interpolation techniques rather than data alone. Ionization energies are difficult to determine since the cut-off of the Rydberg series of lines at the ionization energy is often not observed, and the ionization energy must be determined from theoretical calculations, interpolation of Na isoelectronic and Rydberg series, as well as direct experimental data.

TWELVE-ELECTRON ATOMS

Twelve-electron atoms can be solved exactly using the results of the solutions of one, two, three, four, five, six, seven, eight, nine, ten, and eleven-electron atoms.

RADIUS AND IONIZATION ENERGY OF AN OUTER ELECTRON OF THE MAGNESIUM ATOM

For each eleven-electron atom having a central charge of Z times that of the proton, there are two indistinguishable spin-paired electrons in an orbitsphere with radii r_1 and r_2 both given by Eq. (7.19) (Eq. (10.51)), two indistinguishable spin-paired electrons in an orbitsphere with radii r_3 and r_4 both given by Eq. (10.62), three sets of paired electrons in an orbitsphere at r_{10} given by Eq. (10.212), and an unpaired electron in an orbitsphere at r_{11} . For $Z \geq 12$, the next electron which binds to form the corresponding twelve-electron atom is attracted by the central Coulomb field and the spin-pairing force with the unpaired 3s inner electron and is repelled by diamagnetic forces due to the 3 sets of spin-paired inner electrons such that it forms an unpaired orbitsphere at radius r_{12} .

The central Coulomb force acts on the outer electron to cause it to bind wherein this electric force on the outer-most electron due to the nucleus and the inner eleven electrons is given by Eq. (10.70) with the appropriate charge and radius:

$$\mathbf{F}_{ele} = \frac{(Z-11)e^2}{4\pi\epsilon_0 r_{12}^2} \mathbf{i}_r \quad (10.237)$$

for $r > r_{11}$.

The outer electron which binds to form the corresponding twelve-electron atom becomes spin-paired with the unpaired inner electron such that they become indistinguishable with the same radius $r_{11} = r_{12}$ corresponding to a filled 3s shell. The corresponding spin-pairing force \mathbf{F}_{mag} is given by Eq. (7.15):

$$\mathbf{F}_{mag} = \frac{1}{Z} \frac{\hbar^2}{m_e r_{12}^3} \sqrt{s(s+1)} \mathbf{i}_r \quad (10.238)$$

The spherically symmetrical closed 2p shell of twelve-electron

atoms produces a diamagnetic force, $F_{\text{diamagnetic}}$, that is equivalent to that of a closed s shell given by Eq. (10.11) with the appropriate radii. The inner electrons remain at their initial radii, but cause a diamagnetic force according to Lenz's law that is

$$F_{\text{diamagnetic}} = -\frac{\hbar^2}{4m_e r_{12}^2 r_{10}} \sqrt{s(s+1)} \mathbf{i}_r \quad (10.239)$$

In addition to the paramagnetic spin-pairing force between the eleventh electron initially at radius r_{11} , the pairing causes the diamagnetic interaction between the outer electrons and the inner electrons given by Eq. (10.11) to vanish, except for an electrodynamic effect for $Z > 12$ described in the Two-Electron Atoms section, since upon pairing the magnetic field of the outer electrons becomes zero. Using Eq. (10.55), $F_{\text{mag } 2}$ due to the three 2p orbitals is given by:

$$F_{\text{mag } 2} = \frac{3}{Z} \frac{\hbar^2}{m_e r_{10} r_{12}^2} \sqrt{s(s+1)} \mathbf{i}_r \quad (10.240)$$

In addition to the spin-spin interactions between electron pairs, the three sets of 2p electrons are orbitally paired. The s electrons of the magnesium atom produce a magnetic field at the position of the three sets of spin-paired 2p electrons. In order for the electrons to remain spin and orbitally paired, the corresponding diamagnetic force, $F_{\text{diamagnetic } 3}$ (Eq. (10.221)), on electron twelve from the three sets of spin-paired electrons is given by

$$F_{\text{diamagnetic } 3} = -\frac{1}{Z} \frac{12\hbar^2}{m_e r_{12}^3} \sqrt{s(s+1)} \mathbf{i}_r \quad (10.241)$$

corresponding to the p_x , p_y , and p_z electrons.

The outward centrifugal force on electron 12 is balanced by the electric force and the magnetic forces (on electron 12). The radius of the outer electron is calculated by equating the outward centrifugal force to the sum of the electric (Eq. (10.237)), diamagnetic (Eqs. (10.239) and (10.241)) and paramagnetic (Eqs. (10.238) and (10.240)) forces as follows:

$$\begin{aligned} \frac{m_e v_{12}^2}{r_{12}} = & \frac{(Z-11)e^2}{4\pi\epsilon_0 r_{12}^2} - \frac{\hbar^2}{4m_e r_{12}^2 r_{10}} \sqrt{s(s+1)} + \frac{3\hbar^2}{Zm_e r_{12}^2 r_{10}} \sqrt{s(s+1)} \\ & - \frac{12\hbar^2}{Zm_e r_{12}^3} \sqrt{s(s+1)} + \frac{\hbar^2}{Zm_e r_{12}^3} \sqrt{s(s+1)} \end{aligned} \quad (10.242)$$

Substitution of $v_{12} = \frac{\hbar}{m_e r_{12}}$ (Eq. (1.56)) and $s = \frac{1}{2}$ into Eq. (10.242) gives:

$$\frac{\hbar^2}{m_e r_{12}^3} = \frac{(Z-11)e^2}{4\pi\epsilon_0 r_{12}^2} - \frac{\hbar^2}{4m_e r_{12}^2 r_{10}} \sqrt{\frac{3}{4}} + \frac{3\hbar^2}{Zm_e r_{12}^2 r_{10}} \sqrt{\frac{3}{4}} - \frac{12\hbar^2}{Zm_e r_{12}^3} \sqrt{\frac{3}{4}} + \frac{\hbar^2}{Zm_e r_{12}^3} \sqrt{\frac{3}{4}} \quad (10.243)$$

$$r_{12} = \frac{\frac{\hbar^2}{m_e} \left(1 + \frac{11\sqrt{\frac{3}{4}}}{Z} \right)}{\frac{(Z-11)e^2}{4\pi\epsilon_0} - \left(\frac{1}{4} - \frac{3}{Z} \right) \frac{\hbar^2}{m_e r_{10}} \sqrt{\frac{3}{4}}} \quad (10.244)$$

$$r_{12} = \frac{a_0 \left(1 + \frac{11\sqrt{\frac{3}{4}}}{Z} \right)}{(Z-11) - \left(\frac{1}{4} - \frac{3}{Z} \right) \frac{\sqrt{\frac{3}{4}}}{r_{10}}}, \quad r_{10} \text{ in units of } a_0 \quad (10.245)$$

Substitution of $\frac{r_{10}}{a_0} = 0.51057$ (Eq. (10.212) with $Z=12$) into Eq. (10.245) gives

$$r_{12} = 1.79386a_0 \quad (10.246)$$

The ionization energy of the magnesium atom is given by the electric energy, $E(\text{electric})$, (Eq. (10.102) with the radius, r_{12} , given by Eq. (10.246)):

$$E(\text{ionization}; \text{Mg}) = -\text{Electric Energy} = \frac{(Z-11)e^2}{8\pi\epsilon_0 r_{12}} = 7.58467 \text{ eV} \quad (10.247)$$

where $r_{12} = 1.79386a_0$ (Eq. (10.246)) and $Z=12$. The experimental ionization energy of the magnesium atom is 7.64624 eV [3].

THE IONIZATION ENERGIES OF TWELVE-ELECTRON ATOMS WITH A NUCLEAR CHARGE $Z>12$

Twelve-electron atoms having $Z>12$ possess an external electric field given by Eq. (10.92). Since there is a source of dissipative, $\mathbf{J} \cdot \mathbf{E}$ of Eq. (10.27), the magnetic moments of the inner electrons may change due to the outer electron such that the energy of the twelve-electron atom is lowered with conservation of angular momentum. Of the possible forces based on Maxwell's equations, those which give rise to an energy minimum are used to calculate the atomic radii and energies. With this constraint, the only paramagnetic force is that given by Eq. (10.89) due to the spin angular momenta of the paired $2p_x$, p_y , and p_z electrons interacting with equivalently with each of the 3s electrons. This force which is also equivalent to that given by Eq. (10.145) is:

$$\mathbf{F}_{\text{mag } 2} = 2 \frac{1}{Z} \frac{3\hbar^2}{m_e r_{12}^2 r_{10}} \sqrt{s(s+1)} \mathbf{i}_r \quad (10.248)$$

From Eq. (10.229), the diamagnetic force, $F_{\text{diamagnetic } 2}$, due to a relativistic effect with an electric field for $r > r_{12}$ (Eq. (10.35)) is

$$F_{\text{diamagnetic } 2} = -\left[\frac{Z-12}{Z-11}\right]\left(1 + \frac{\sqrt{2}}{2}\right)\frac{r_{10}\hbar^2}{m_e r_{12}^4} 10\sqrt{s(s+1)}\mathbf{i}_r \quad (10.249)$$

In the case that $Z > 12$, the radius of the outer electron is calculated by equating the outward centrifugal force to the sum of the electric (Eq. (10.237)), diamagnetic (Eq. (10.249)), and paramagnetic (Eq. (10.248)) forces as follows:

$$\frac{m_e v_{12}^2}{r_{12}} = \frac{(Z-11)e^2}{4\pi\epsilon_0 r_{12}^2} - \frac{\hbar^2}{4m_e r_{12}^2 r_{10}} \sqrt{s(s+1)} + \frac{6\hbar^2}{Zm_e r_{12}^2 r_{10}} \sqrt{s(s+1)} - \left[\frac{Z-12}{Z-11}\right]\left(1 + \frac{\sqrt{2}}{2}\right)\frac{r_{10}\hbar^2}{m_e r_{12}^4} 10\sqrt{s(s+1)} \quad (10.250)$$

Substitution of $v_{12} = \frac{\hbar}{m_e r_{12}}$ (Eq. (1.56)) and $s = \frac{1}{2}$ into Eq. (10.250) gives:

$$\frac{\hbar^2}{m_e r_{12}^3} = \frac{(Z-11)e^2}{4\pi\epsilon_0 r_{12}^2} - \frac{\hbar^2}{4m_e r_{12}^2 r_{10}} \sqrt{\frac{3}{4}} + \frac{6\hbar^2}{Zm_e r_{12}^2 r_{10}} \sqrt{\frac{3}{4}} - \left[\frac{Z-12}{Z-11}\right]\left(1 + \frac{\sqrt{2}}{2}\right)\frac{r_{10}\hbar^2}{m_e r_{12}^4} 10\sqrt{\frac{3}{4}} \quad (10.251)$$

The quadratic equation corresponding to Eq. (10.251) is

$$\left(\frac{(Z-11)e^2}{4\pi\epsilon_0} - \left(\frac{1}{4} - \frac{6}{Z}\right)\frac{\hbar^2}{m_e r_{10}} \sqrt{\frac{3}{4}}\right)r_{12}^2 - \frac{\hbar^2}{m_e} r_{12} - \left[\frac{Z-12}{Z-11}\right]\left(1 + \frac{\sqrt{2}}{2}\right)\frac{r_{10}\hbar^2}{m_e} 10\sqrt{\frac{3}{4}} = 0 \quad (10.252)$$

$$r_{12}^2 - \frac{\frac{\hbar^2}{m_e}}{\left(\frac{(Z-11)e^2}{4\pi\epsilon_0} - \left(\frac{1}{4} - \frac{6}{Z}\right)\frac{\hbar^2}{m_e r_{10}} \sqrt{\frac{3}{4}}\right)} r_{12} - \frac{\left[\frac{Z-12}{Z-11}\right]\left(1 + \frac{\sqrt{2}}{2}\right)\frac{r_{10}\hbar^2}{m_e} 10\sqrt{\frac{3}{4}}}{\left(\frac{(Z-11)e^2}{4\pi\epsilon_0} - \left(\frac{1}{4} - \frac{6}{Z}\right)\frac{\hbar^2}{m_e r_{10}} \sqrt{\frac{3}{4}}\right)} = 0 \quad (10.253)$$

The solution of Eq. (10.253) using the quadratic formula is:

$$r_{12} = \frac{\frac{\hbar^2}{m_e}}{\left(\frac{(Z-11)e^2}{4\pi\epsilon_0} - \left(\frac{1}{4} - \frac{6}{Z}\right)\frac{\hbar^2}{m_e r_{10}} \sqrt{\frac{3}{4}}\right)} \pm \frac{\sqrt{\left(\frac{\hbar^2}{m_e}\right)^2 - 4\left(\frac{(Z-11)e^2}{4\pi\epsilon_0} - \left(\frac{1}{4} - \frac{6}{Z}\right)\frac{\hbar^2}{m_e r_{10}} \sqrt{\frac{3}{4}}\right)\left[\frac{Z-12}{Z-11}\right]\left(1 + \frac{\sqrt{2}}{2}\right)\frac{r_{10}\hbar^2}{m_e} 10\sqrt{\frac{3}{4}}}}{2} \quad (10.254)$$

$$r_{12} = \frac{\left(\frac{a_0}{\left((Z-11) - \left(\frac{1}{8} - \frac{3}{Z} \right) \frac{\sqrt{3}}{r_{10}} \right)} \pm a_0 \right) \sqrt{\frac{1}{\left((Z-11) - \left(\frac{1}{8} - \frac{3}{Z} \right) \frac{\sqrt{3}}{r_{10}} \right)^2} + \frac{20\sqrt{3} \left(\left[\frac{Z-12}{Z-11} \right] \left(1 + \frac{\sqrt{2}}{2} \right) r_{10} \right)}{\left((Z-11) - \left(\frac{1}{8} - \frac{3}{Z} \right) \frac{\sqrt{3}}{r_{10}} \right)}}}{2} \quad (10.255)$$

r_{10} in units of a_0

where r_{10} is given by Eq. (10.212). The positive root of Eq. (10.255) must be taken in order that $r_{12} > 0$. The radii of several twelve-electron atoms are given in Table 10.11.

The ionization energies for the twelve-electron atoms with $Z > 12$ are given by the electric energy, $E(\text{electric})$, (Eq. (10.102) with the radii, r_{12} , given by Eq. (10.255)):

$$E(\text{Ionization}) = -\text{Electric Energy} = \frac{(Z-11)e^2}{8\pi\epsilon_0 r_{12}} \quad (10.256)$$

Since the relativistic corrections were small, the nonrelativistic ionization energies for experimentally measured twelve-electron atoms are given in Table 10.11.

Table 10.11. Ionization energies for some twelve-electron atoms.

12 e Atom	Z	r_1 (a_0) ^a	r_3 (a_0) ^b	r_{10} (a_0) ^c	r_{12} (a_0) ^d	Theoretical Ionization Energies ^e (eV)	Experimental Ionization Energies ^f (eV)	Relative Error ^g
<i>Mg</i>	12	0.08435	0.37065	0.51057	1.79386	7.58467	7.64624	0.0081
<i>Al</i> ⁺	13	0.07778	0.33923	0.45620	1.41133	19.2808	18.82856	-0.0240
<i>Si</i> ²⁺	14	0.07216	0.31274	0.40978	1.25155	32.6134	33.49302	0.0263
<i>P</i> ³⁺	15	0.06730	0.29010	0.37120	1.09443	49.7274	51.4439	0.0334
<i>S</i> ⁴⁺	16	0.06306	0.27053	0.33902	0.96729	70.3296	72.5945	0.0312
<i>Cl</i> ⁵⁺	17	0.05932	0.25344	0.31190	0.86545	94.3266	97.03	0.0279
<i>Ar</i> ⁶⁺	18	0.05599	0.23839	0.28878	0.78276	121.6724	124.323	0.0213
<i>K</i> ⁷⁺	19	0.05302	0.22503	0.26884	0.71450	152.3396	154.88	0.0164
<i>Ca</i> ⁸⁺	20	0.05035	0.21308	0.25149	0.65725	186.3102	188.54	0.0118
<i>Sc</i> ⁹⁺	21	0.04794	0.20235	0.23625	0.60857	223.5713	225.18	0.0071
<i>Ti</i> ¹⁰⁺	22	0.04574	0.19264	0.22276	0.56666	264.1138	265.07	0.0036
<i>V</i> ¹¹⁺	23	0.04374	0.18383	0.21074	0.53022	307.9304	308.1	0.0006
<i>Cr</i> ¹²⁺	24	0.04191	0.17579	0.19995	0.49822	355.0157	354.8	-0.0006
<i>Mn</i> ¹³⁺	25	0.04022	0.16842	0.19022	0.46990	405.3653	403.0	-0.0059
<i>Fe</i> ¹⁴⁺	26	0.03867	0.16165	0.18140	0.44466	458.9758	457	-0.0043
<i>Co</i> ¹⁵⁺	27	0.03723	0.15540	0.17336	0.42201	515.8442	511.96	-0.0076
<i>Ni</i> ¹⁶⁺	28	0.03589	0.14961	0.16601	0.40158	575.9683	571.08	-0.0086
<i>Cu</i> ¹⁷⁺	29	0.03465	0.14424	0.15926	0.38305	639.3460	633	-0.0100
<i>Zn</i> ¹⁸⁺	30	0.03349	0.13925	0.15304	0.36617	705.9758	698	-0.0114

^a Radius of the first set of paired inner electrons of twelve-electron atoms from Eq. (10.51).

^b Radius of the second set of paired inner electrons of twelve-electron atoms from Eq. (10.62).

^c Radius of three sets of paired inner electrons of twelve-electron atoms from Eq. (10.212)).

^d Radius of paired outer electrons of twelve-electron atoms from Eq. (10.255)) for $Z > 12$ and Eq. (10.246) for *Mg*.

^e Calculated ionization energies of twelve-electron atoms given by the electric energy (Eq. (10.256)).

^f From theoretical calculations, interpolation of isoelectronic and spectral series, and experimental data [2-3].

^g (Experimental-theoretical)/experimental.

The agreement between the experimental and calculated values of Table 10.11 is well within the experimental capability of the spectroscopic determinations including the values at large Z which relies on X-ray spectroscopy. In this case, the experimental capability is three to four significant figures which is consistent with the last column. The magnesium atom isoelectronic series is given in Table 10.11 [2-3] to much higher precision than the capability of X-ray spectroscopy, but these values are based on theoretical and interpolation techniques rather

than data alone. Ionization energies are difficult to determine since the cut-off of the Rydberg series of lines at the ionization energy is often not observed, and the ionization energy must be determined from theoretical calculations, interpolation of Mg isoelectronic and Rydberg series, as well as direct experimental data.

3P-ORBITAL ELECTRONS BASED ON AN ENERGY MINIMUM

For each thirteen through eighteen-electron atom having a central charge of Z times that of the proton, there are two indistinguishable spin-paired electrons in an orbitsphere with radii r_1 and r_2 both given by Eq. (7.19) (Eq. (10.51)), two indistinguishable spin-paired electrons in an orbitsphere with radii r_3 and r_4 both given by Eq. (10.62), three sets of paired electrons in an orbitsphere at r_{10} given by Eq. (10.212), and two indistinguishable spin-paired electrons in an orbitsphere with radii r_{11} and r_{12} both given by Eq. (10.255). For $Z \geq 12$, the next electron which binds to form the corresponding n -electron atom ($13 \leq n \leq 18$) is attracted by the central Coulomb field and is repelled by diamagnetic forces and attracted by paramagnetic forces due to the 3 sets of spin-paired inner 2p electrons and two spin-paired inner 3s electrons such that it forms an orbitsphere comprising all of the 3p electrons at radius r_n . The resulting electron configuration is $1s^2 2s^2 2p^6 3s^2 3p^{n-12}$.

The central Coulomb force, F_{ele} , acts on the outer electron to cause it to bind wherein this electric force on the outer-most electron due to the nucleus and the inner $n-1$ electrons is given by Eq. (10.70):

$$F_{ele} = \frac{(Z - (n-1))e^2}{4\pi\epsilon_0 r_n^2} \mathbf{i}_r \quad (10.257)$$

for $r > r_{n-1}$ where n corresponds to the number of electrons of the atom and Z is its atomic number. In each case, the magnetic field of the binding outer electron changes the angular velocities of the inner electrons. However, in each case, the magnetic field of the outer electron provides a central Lorentzian force which exactly balances the change in centrifugal force because of the change in angular velocity [1]. The inner electrons remain at their initial radii, but cause a diamagnetic force according to Lenz's law.

As shown in the 2P-Orbital Electrons Based on an Energy Minimum section the quantum numbers $\ell=1$ $m=\pm 1$ and $\ell=1$ $m=0$ correspond to spherical harmonics solutions, $Y_\ell^m(\theta, \phi)$, of Laplace's equation designated the $2p_x$, $2p_y$, and $2p_z$ orbitals, respectively. Similarly, for $13 \leq n \leq 18$, the energy may be lowered by filling 3p orbitals in the same manner to achieve an energy minimum relative to other configurations and arrangements. In general, a nonuniform distribution of charge achieves

an energy minimum with the formation of a fifth shell due to the dependence of the magnetic forces on the nuclear charge and orbital energy (Eqs. (10.70), (10.258-10.264), and (10.268)). The outer electrons of atoms and ions that are isoelectronic with the series aluminum through argon half-fill a 3p level with unpaired electrons at phosphorous, then fill the level with paired electrons at argon.

Similarly to the case of the 2p orbitals, spherical harmonic charge-density waves may be induced in the inner electron orbitspheres with the addition of one or more outer electrons to the 3p orbitals. An energy minimum is achieved when the thirteenth through eighteenth electrons of each thirteen through eighteen-electron atom fills a 3p orbital with the formation of orthogonal complementary charge-density waves in the inner shell 2p and 3s electrons. To maintain the symmetry of the central charge and the energy minimum condition given by solutions to Laplace's equation (Eq. (10.72)), the charge-density waves on electron orbitspheres at r_{10} and r_{12} complement those of the outer orbitals when the outer 3p orbitals are not all occupied by at least one electron, and the complementary charge-density waves are provided by electrons at r_{12} when this condition is met. In the case of the 3p electrons, an exception to the trends in 2p orbital forces arises due to the interaction between the 2p, 3s, and 3p electrons due to magnetic fields independent of induced complementary charge-density waves. The spin and angular momenta of the 2p electrons give rise to corresponding magnetic fields that interact with the two 3s electrons. The filled 2p orbitals with the maintenance of symmetry according to Laplace's equation (Eq. (10.72)) requires that the 2p as well as the 3s electrons contribute forces to the 3p electrons due to the electrons at r_{10} acting on the electrons at r_{12} which complies with the reactive force, $F_{\text{diamagnetic } 2}$, having the factor $\left(1 + \frac{\sqrt{2}}{2}\right)$ and given by Eq. (10.229).

The total orbital contribution to the diamagnetic force, $F_{\text{diamagnetic}}$, given by Eq. (10.82) is:

$$F_{\text{diamagnetic}} = -\sum_m \frac{(\ell + |m|)!}{(2\ell + 1)(\ell - |m|)!} \frac{\hbar^2}{4m_e r_n^2 r_{12}} \sqrt{s(s+1)} \mathbf{i}_r \quad (10.258)$$

where the contributions from orbitals having $|m|=1$ add positively or negatively. From Eq. (10.204), the diamagnetic force, $F_{\text{diamagnetic}}$, contribution from the 2p electrons is given by the sum of the contributions from the p_x , p_y , and p_z orbitals corresponding to $m = 1, -1$, and 0, respectively:

$$F_{\text{diamagnetic}} = -\left(\frac{2}{3} + \frac{2}{3} + \frac{1}{3}\right) \frac{\hbar^2}{4m_e r_n^2 r_{12}} \sqrt{s(s+1)} \mathbf{i}_r = -\left(\frac{5}{3}\right) \frac{\hbar^2}{4m_e r_n^2 r_{12}} \sqrt{s(s+1)} \mathbf{i}_r \quad (10.259)$$

where r_{12} is given by Eq. (10.255). Due to the 2p-3s-3p interaction, the 3s electrons provide spin or orbital angular momentum in order conserve angular momentum of the interacting orbitals. In the case that an energy minimum is achieved with 3s orbital angular momentum, the diamagnetic force, $F_{\text{diamagnetic}}$, contribution is given by Eqs. (10.82) and (10.258) where $m = 1, -1$, or 0 corresponding to induced charge-density waves. The contribution from the 3s orbital is added to the contributions from the 3p and the 2p orbitals until the 3p orbitals are at least half filled. Then the diamagnetic force is only due to 3p and 3s electrons since the induced charge-density waves only involve the inner-most shell, the 3s orbital.

As given by Eq. (10.89), the contribution of the orbital angular momentum of an unpaired 3p electron to the paramagnetic force, $F_{\text{mag } 2}$, is

$$F_{\text{mag } 2} = \frac{1}{Z} \frac{\hbar^2}{m_e r_n^2 r_{12}} \sqrt{s(s+1)} \mathbf{i}_r \quad (10.260)$$

Each outer 3p electron contributes spin as well as orbital angular momentum. The former gives rise to spin pairing to another 3p electron when an energy minimum is achieved. In the case that the orbital angular momenta of paired 3p electrons cancel, the contribution to $F_{\text{mag } 2}$ due to spin alone given by Eq. (10.83) is equivalent to that due to orbital angular momentum alone (Eq. (10.260)). Due to the 2p-3s-3p interaction, the 3s electrons can also provide a paramagnetic force, $F_{\text{mag } 2}$, contribution given by Eqs. (10.82) and (10.260) due to spin angular momentum corresponding to induced charge-density waves.

N-electron atoms having $Z > n$ possess an electric field given by Eq. (10.92) for $r > r_n$. Since there is a source of dissipative, $\mathbf{J} \cdot \mathbf{E}$ of Eq. (10.27), the magnetic moments of the inner electrons may change due to the outer electron such that the energy of the n-electron atom is lowered. $F_{\text{diamagnetic}}$ is given by Eqs. (10.82) and (10.258). Due to the 2p-3s-3p interaction, the 2p level contributes to the forces even when the filling of the 3p level is half or greater, and the 3s electrons may provide orbital angular momentum in order conserve angular momentum of the interacting orbitals. In the case that an energy minimum is achieved with 3s orbital angular momentum, the diamagnetic force, $F_{\text{diamagnetic}}$, contribution is given by Eqs. (10.82) and (10.258) where $m = 1, -1$, or 0 corresponding to induced charge-density waves. The contribution from the 3s orbital is added to the contributions from the 3p and the 2p orbitals.

Due to the 2p-3s-3p interaction with $Z > n$, $F_{\text{mag } 2}$ has a contribution from the 2p, 3s, and 3p orbitals. The filled 2p orbitals with the maintenance of symmetry according to Eq. (10.72) requires that the

diamagnetic force, $F_{mag 2}$, contribution is

$$F_{mag 2} = (4 + 4 + 4) \frac{1}{Z} \frac{\hbar^2}{m_e r_n^2 r_{12}} \sqrt{s(s+1)} \mathbf{i}_r = \frac{1}{Z} \frac{12\hbar^2}{m_e r_n^2 r_{12}} \sqrt{s(s+1)} \mathbf{i}_r \quad (10.261)$$

corresponding to the spin and orbital angular momenta of the paired $2p_x$, p_y , and p_z electrons (Eq. (10.205)). The 3s electrons can provide a $F_{mag 2}$ contribution of

$$F_{mag 2} = \frac{1}{Z} \frac{4\hbar^2}{m_e r_n^2 r_{12}} \sqrt{s(s+1)} \mathbf{i}_r \quad (10.262)$$

corresponding to coupling to the spin and induced orbital angular momentum wherein the orbitals interact such that this contribution superimposes negatively or positively to the contributions from the 2p and 3p orbitals. Each outer 3p electron contributes spin as well as orbital angular momentum. Each unpaired 3p electron can spin and orbitally pair with a 2p orbital. The corresponding force, $F_{mag 2}$, contribution given by Eq. (10.84) is:

$$F_{mag 2} = \frac{1}{Z} \frac{4\hbar^2}{m_e r_n^2 r_{12}} \sqrt{s(s+1)} \mathbf{i}_r \quad (10.263)$$

The 3p electrons spin-pair upon further filling of the 3p orbital. Two spin-paired 3p electrons interacting with two spin-paired 2p orbital electrons double the corresponding force, $F_{mag 2}$, contribution:

$$F_{mag 2} = \frac{1}{Z} \frac{8\hbar^2}{m_e r_n^2 r_{12}} \sqrt{s(s+1)} \mathbf{i}_r \quad (10.264)$$

The sum of the magnitude of the angular momentum of the electron is \hbar in any inertial frame and is relativistically invariant. The vector projections of the orbitsphere spin angular momentum relative to the Cartesian coordinates are given in the Spin Angular Momentum of the Orbitsphere with $\mathbf{l} = 0$ section. The magnitude of the z-axis projection of the spin angular momentum, $|L_z|$, the moment of inertia about the z-axis, I_z , and the rotational energy about the z-axis, $E_{rotational \ spin}$, given by Eqs. (1.78-1.82) are

$$|L_z| = I \frac{\hbar}{m_e r^2} = \frac{\hbar}{2} \quad (10.265)$$

$$I_z = I_{spin} = \frac{m_e r_n^2}{2} \quad (10.266)$$

$$E_{rotational} = E_{rotational \ spin} = \frac{1}{4} \left[\frac{\hbar^2}{2I_{spin}} \right] = \frac{1}{4} \left[\frac{\hbar^2}{m_e r_n^2} \right] \quad (10.267)$$

N-electron atoms having $Z > n$ possess an electric field given by Eq. (10.92) for $r > r_n$. Since there is a source of dissipative, $\mathbf{J} \cdot \mathbf{E}$ of Eq. (10.27), the magnetic moments of the inner electrons may change due to the

outer electron such that the energy of the n -electron atom is lowered. As shown in the P-Orbital Electrons Based on an Energy Minimum section for $F_{\text{diamagnetic } 2}$ given by Eq. (10.93), the corresponding diamagnetic force for 2p electrons, $F_{\text{diamagnetic } 2}$, due to a relativistic effect with an electric field for $r > r_n$ (Eq. (10.35)) is dependent on the amplitude of the orbital energy. Using the orbital energy with $\ell=1$ (Eq. (10.90)), the energy $m_e \Delta v^2$ of Eq. (10.29) is reduced by the factor of $\left(1 - \frac{\sqrt{2}}{2}\right)$ due to the contribution of the charge-density wave of the inner electrons at r_{12} . In addition, the two 3s electrons contribute an energy factor based on Eq. (1.82) since the filled 2p orbitals with the maintenance of symmetry according to Eq. (10.72) requires that the diamagnetic force is due to the electrons at r_{10} acting on the electrons at r_{12} which complies with the reactive force, $F_{\text{diamagnetic } 2}$, given by Eq. (10.229). Thus, $F_{\text{diamagnetic } 2}$ for 3p electrons with $Z > n$ is given by

$$F_{\text{diamagnetic } 2} = - \left[\frac{Z-n}{Z-(n-1)} \right] \left(1 - \frac{\sqrt{2}}{2} + \frac{1}{2} \right) \frac{r_{12} \hbar^2}{m_e r_n^4} 10 \sqrt{s(s+1)} \mathbf{i}_r \quad (10.268)$$

The total diamagnetic and paramagnetic forces are given as the sum over the orbital and spin angular momenta that may add positively or negatively while maintaining the conservation of angular momentum. Of the possible forces based on Maxwell's equations, those which give rise to an energy minimum are used to calculate the atomic radii and energies. In general, an energy minimum is achieved by minimizing $F_{\text{diamagnetic}}$ while maximizing $F_{\text{mag } 2}$ with conservation of angular momentum.

Using the forces given by Eqs. (10.257-10.264), (10.268), and the radii r_{12} given by Eq. (10.255), the radii of the 3p electrons of all thirteen through eighteen-electron atoms may be solved exactly. The electric energy given by Eq. (10.102) gives the corresponding exact ionization energies. F_{ele} and $F_{\text{diamagnetic } 2}$ given by Eqs. (10.257) and (10.268), respectively, are of the same form for all atoms with the appropriate nuclear charges and atomic radii. $F_{\text{diamagnetic}}$ given by Eq. (10.258) and $F_{\text{mag } 2}$ given by Eqs. (10.260-10.264) are of the same form with the appropriate factors that depend on the minimum-energy electron configuration. The general equation and the summary of the parameters that determine the exact radii and ionization energies of all thirteen through eighteen-electron atoms are given in the General Equation For The Ionization Energies of Thirteen Through Eighteen-Electron Atoms section and in Table 10.18.

THIRTEEN-ELECTRON ATOMS

Thirteen-electron atoms can be solved exactly using the results of the solutions of one, two, three, four, five, six, seven, eight, nine, ten,

eleven, and twelve-electron atoms.

RADIUS AND IONIZATION ENERGY OF THE OUTER ELECTRON OF THE ALUMINUM ATOM

For each twelve-electron atom having a central charge of Z times that of the proton, there are two indistinguishable spin-paired electrons in an orbitsphere with radii r_1 and r_2 both given by Eq. (7.19) (Eq. (10.51)), two indistinguishable spin-paired electrons in an orbitsphere with radii r_3 and r_4 both given by Eq. (10.62), three sets of paired electrons in an orbitsphere at r_{10} given by Eq. (10.212), and two indistinguishable spin-paired electrons in an orbitsphere with radii r_{11} and r_{12} both given by Eq. (10.255). For $Z \geq 13$, the next electron which binds to form the corresponding thirteen-electron atom is attracted by the central Coulomb field and is repelled by diamagnetic forces due to the 3 sets of spin-paired inner 2p electrons and two spin-paired inner 3s electrons such that it forms an unpaired orbitsphere at radius r_{13} . The resulting electron configuration is $1s^2 2s^2 2p^6 3s^2 3p^1$, and the orbital arrangement is

$$\begin{array}{ccc} \uparrow & \text{---} & \text{---} \\ 1 & 0 & -1 \end{array} \quad (10.269)$$

corresponding to the ground state $^2P_{1/2}^0$.

The central Coulomb force acts on the outer electron to cause it to bind wherein this electric force on the outer-most electron due to the nucleus and the inner twelve electrons is given by Eq. (10.70) with the appropriate charge and radius:

$$\mathbf{F}_{ele} = \frac{(Z-12)e^2}{4\pi\epsilon_0 r_{13}^2} \mathbf{i}_r \quad (10.270)$$

for $r > r_{12}$.

As in the case of the boron atom given in the Five-Electron Atom section, the single p orbital of the aluminum atom produces a diamagnetic force equivalent to that of the formation of an s orbital due to the induction of complementary and spherically symmetrical charge-density waves on electron orbitspheres at r_{10} and r_{12} in order to achieve a solution of Laplace's equation (Eq. (10.72)). The inner electrons remain at their initial radii, but cause a diamagnetic force according to Lenz's law that is given by Eq. (10.96) with the appropriate radii. In addition, the contribution of the diamagnetic force, $\mathbf{F}_{diamagnetic}$, due to the 2p electrons is given by Eqs. (10.105) and (10.259) as the sum of the contributions from the p_x , p_y , and p_z orbitals corresponding to $m = 1, -1$, and 0, respectively.

Thus, $F_{\text{diamagnetic}}$ is given by

$$F_{\text{diamagnetic}} = -\left(2 + \frac{2}{3} + \frac{2}{3} + \frac{1}{3}\right) \frac{\hbar^2}{4m_e r_{13}^2 r_{12}} \sqrt{s(s+1)} \mathbf{i}_r = -\left(\frac{11}{3}\right) \frac{\hbar^2}{4m_e r_{13}^2 r_{12}} \sqrt{s(s+1)} \mathbf{i}_r \quad (10.271)$$

The charge induction forms complementary mirror charge-density waves which must have opposing angular momenta such that momentum is conserved. In this case, $F_{\text{mag } 2}$ given by Eq. (10.260) is zero:

$$F_{\text{mag } 2} = 0 \quad (10.272)$$

The outward centrifugal force on electron 13 is balanced by the electric force and the magnetic force (on electron 13). The radius of the outer electron is calculated by equating the outward centrifugal force to the sum of the electric (Eq. (10.270)) and diamagnetic (Eq. (10.271)) forces as follows:

$$\frac{m_e v_{13}^2}{r_{13}} = \frac{(Z-12)e^2}{4\pi\epsilon_0 r_{13}^2} - \frac{\frac{11}{3}\hbar^2}{4m_e r_{13}^2 r_{12}} \sqrt{s(s+1)} \quad (10.273)$$

Substitution of $v_{13} = \frac{\hbar}{m_e r_{13}}$ (Eq. (1.56)) and $s = \frac{1}{2}$ into Eq. (10.273) gives:

$$\frac{\hbar^2}{m_e r_{13}^3} = \frac{(Z-12)e^2}{4\pi\epsilon_0 r_{13}^2} - \frac{11\hbar^2}{12m_e r_{13}^2 r_{12}} \sqrt{\frac{3}{4}} \quad (10.274)$$

$$r_{13} = \frac{a_0}{\left((Z-12) - \frac{11\sqrt{3}}{12r_{12}} \right)}, \quad r_{12} \text{ in units of } a_0 \quad (10.275)$$

Substitution of $\frac{r_{12}}{a_0} = 1.41133$ (Eq. (10.255) with $Z=13$) into Eq. (10.275) gives

$$r_{13} = 2.28565a_0 \quad (10.276)$$

The energy stored in the electric field of the aluminum atom, $E(\text{electric})$, is given by Eq. (10.102) with the appropriate with the radius, r_{13} , given by Eq. (10.276):

$$E(\text{electric}); \text{Al} = -\frac{(Z-12)e^2}{8\pi\epsilon_0 r_{13}} = 5.95270 \text{ eV} \quad (10.277)$$

where $r_{13} = 2.28565a_0$ (Eq. (10.276)) and $Z=13$. The ionization energy is given by the sum of the electric energy and the energy corresponding to the change in magnetic-moments of the inner shell electrons. Since there is no source of dissipative power, $\mathbf{J} \cdot \mathbf{E}$ of Eq. (10.27), to compensate for any potential change in the magnetic moments, Δm , of the inner electrons due to the ionization of the outer electron of the aluminum atom, there is a diamagnetic energy term in the ionization energy for this atom that

follows from the corresponding term for the lithium atom given by Eqs. (10.15-10.24), with $Z=13$, r_{12} given by Eq. (10.255), and r_{13} given by Eq. (10.276). Thus, the change in magnetic energy of the inner orbitsphere at r_{12} is 76.94147 %, so that the corresponding energy ΔE_{mag} is

$$\Delta E_{mag} = 0.7694147 \times 0.04069938 \text{ eV} = 0.0313147 \text{ eV} \quad (10.278)$$

where the magnetic energy of the inner electrons is 0.04069938 eV (Eqs. (10.64) and (10.276)). Then, the ionization energy of the aluminum atom is given by Eqs. (10.276-10.278):

$$\begin{aligned} E(\text{ionization; Al}) &= \frac{(Z-12)e^2}{8\pi\epsilon_0 r_{13}} + \Delta E_{mag} \\ &= 5.95270 \text{ eV} + 0.031315 \text{ eV} = 5.98402 \text{ eV} \end{aligned} \quad (10.279)$$

The experimental ionization energy of the boron atom is 5.98577 eV [3].

THE IONIZATION ENERGIES OF THIRTEEN-ELECTRON ATOMS WITH A NUCLEAR CHARGE $Z>13$

Thirteen-electron atoms having $Z>13$ possess an external electric field given by Eq. (10.92). In this case, an energy minimum is achieved with conservation of momentum when the orbital angular momentum is such that $F_{diamagnetic}$ is minimized while $F_{mag 2}$ is maximized. From Eq. (10.258), the diamagnetic force, $F_{diamagnetic}$, is given by the sum of the contributions from the $2p_x$, p_y , and p_z orbitals corresponding to $m = 1, -1$, and 0, respectively:

$$F_{diamagnetic} = -\left(\frac{2}{3} + \frac{2}{3} + \frac{1}{3}\right) \frac{\hbar^2}{4m_e r_{13}^2 r_{12}} \sqrt{s(s+1)} \mathbf{i}_r = -\left(\frac{5}{3}\right) \frac{\hbar^2}{4m_e r_{13}^2 r_{12}} \sqrt{s(s+1)} \mathbf{i}_r \quad (10.280)$$

wherein the contribution due to the $3p_x$ ($m = 1$) is canceled by the mirror charge-density wave with $m = -1$ induced in the 3s orbital according to Eq. (10.258).

With $Z>13$, the charge induction forms complementary mirror charge-density waves such that the angular momenta do not cancel. The filled 2p orbitals with the maintenance of symmetry according to Eq. (10.72) requires that the diamagnetic force is due to the electrons at r_{10} acting on the electrons at r_{12} which complies with the reactive force, $F_{diamagnetic 2}$, given by Eq. (10.249). From Eq. (10.261), $F_{mag 2}$ is

$$F_{mag 2} = (4 + 4 + 4) \frac{1}{Z} \frac{\hbar^2}{m_e r_{13}^2 r_{12}} \sqrt{s(s+1)} \mathbf{i}_r = \frac{12\hbar^2}{Z m_e r_{13}^2 r_{12}} \sqrt{s(s+1)} \mathbf{i}_r \quad (10.281)$$

corresponding to the spin and orbital angular momenta of the paired $2p_x$, p_y , and p_z electrons wherein the contribution due to the $3p_x$ ($m = 1$) is canceled by the mirror charge-density wave with $m = -1$ induced in the 3s orbital according to Eq. (10.262).

The diamagnetic force, $F_{diamagnetic 2}$, due to the binding of the 3p-orbital

electron having an electric field outside of its radius is given by Eq. (10.268):

$$\mathbf{F}_{\text{diamagnetic 2}} = -\left[\frac{Z-13}{Z-12}\right]\left(1 - \frac{\sqrt{2}}{2} + \frac{1}{2}\right)\frac{r_{12}\hbar^2}{m_e r_{13}^4} 10\sqrt{s(s+1)}\mathbf{i}_r \quad (10.282)$$

In the case that $Z > 13$, the radius of the outer electron is calculated by equating the outward centrifugal force to the sum of the electric (Eq. (10.270)) and diamagnetic (Eqs. (10.280) and (10.282)), and paramagnetic (Eq. (10.281)) forces as follows:

$$\begin{aligned} \frac{m_e v_{13}^2}{r_{13}} = & \frac{(Z-12)e^2}{4\pi\epsilon_0 r_{13}^2} - \frac{5\hbar^2}{12m_e r_{13}^2 r_{12}} \sqrt{s(s+1)} + \frac{12\hbar^2}{Zm_e r_{13}^2 r_{12}} \sqrt{s(s+1)} \\ & - \left[\frac{Z-13}{Z-12}\right]\left(1 - \frac{\sqrt{2}}{2} + \frac{1}{2}\right)\frac{r_{12}\hbar^2}{r_{13}^4 m_e} 10\sqrt{s(s+1)} \end{aligned} \quad (10.283)$$

Substitution of $v_{13} = \frac{\hbar}{m_e r_{13}}$ (Eq. (1.56)) and $s = \frac{1}{2}$ into Eq. (10.283) gives:

$$\frac{\hbar^2}{m_e r_{13}^3} = \frac{(Z-12)e^2}{4\pi\epsilon_0 r_{13}^2} - \frac{5\hbar^2}{12m_e r_{13}^2 r_{12}} \sqrt{\frac{3}{4}} + \frac{12\hbar^2}{Zm_e r_{13}^2 r_{12}} \sqrt{\frac{3}{4}} - \left[\frac{Z-13}{Z-12}\right]\left(1 - \frac{\sqrt{2}}{2} + \frac{1}{2}\right)\frac{r_{12}\hbar^2}{r_{13}^4 m_e} 10\sqrt{\frac{3}{4}} \quad (10.284)$$

The quadratic equation corresponding to Eq. (10.284) is

$$\left(\frac{(Z-12)e^2}{4\pi\epsilon_0} - \left(\frac{5}{12} - \frac{12}{Z}\right)\frac{\hbar^2}{m_e r_{12}} \sqrt{\frac{3}{4}}\right)r_{13}^2 - \frac{\hbar^2}{m_e} r_{13} - \left[\frac{Z-13}{Z-12}\right]\left(1 - \frac{\sqrt{2}}{2} + \frac{1}{2}\right)\frac{r_{12}\hbar^2}{m_e} 10\sqrt{\frac{3}{4}} = 0 \quad (10.285)$$

$$r_{13}^2 - \frac{\frac{\hbar^2}{m_e}}{\left(\frac{(Z-12)e^2}{4\pi\epsilon_0} - \left(\frac{5}{12} - \frac{12}{Z}\right)\frac{\hbar^2}{m_e r_{12}} \sqrt{\frac{3}{4}}\right)} r_{13} - \frac{\left[\frac{Z-13}{Z-12}\right]\left(1 - \frac{\sqrt{2}}{2} + \frac{1}{2}\right)\frac{r_{12}\hbar^2}{m_e} 10\sqrt{\frac{3}{4}}}{\left(\frac{(Z-12)e^2}{4\pi\epsilon_0} - \left(\frac{5}{12} - \frac{12}{Z}\right)\frac{\hbar^2}{m_e r_{12}} \sqrt{\frac{3}{4}}\right)} = 0 \quad (10.286)$$

The solution of Eq. (10.286) using the quadratic formula is:

$$r_{13} = \frac{\frac{\hbar^2}{m_e}}{\left(\frac{(Z-12)e^2}{4\pi\epsilon_0} - \left(\frac{5}{12} - \frac{12}{Z}\right)\frac{\hbar^2}{m_e r_{12}} \sqrt{\frac{3}{4}}\right)} \pm \sqrt{\frac{\left(\frac{\hbar^2}{m_e}\right)^2}{\left(\frac{(Z-12)e^2}{4\pi\epsilon_0} - \left(\frac{5}{12} - \frac{12}{Z}\right)\frac{\hbar^2}{m_e r_{12}} \sqrt{\frac{3}{4}}\right)^2} + 4\frac{\left[\frac{Z-13}{Z-12}\right]\left(1 - \frac{\sqrt{2}}{2} + \frac{1}{2}\right)\frac{r_{12}\hbar^2}{m_e} 10\sqrt{\frac{3}{4}}}{\left(\frac{(Z-12)e^2}{4\pi\epsilon_0} - \left(\frac{5}{12} - \frac{12}{Z}\right)\frac{\hbar^2}{m_e r_{12}} \sqrt{\frac{3}{4}}\right)}} \quad (10.287)$$

$$r_{13} = \frac{\frac{a_0}{\left((Z-12) - \left(\frac{5}{24} - \frac{6}{Z}\right)\frac{\sqrt{3}}{r_{12}}\right)} \pm a_0}{2} \sqrt{\frac{1}{\left((Z-12) - \left(\frac{5}{24} - \frac{6}{Z}\right)\frac{\sqrt{3}}{r_{12}}\right)}^2 + \frac{20\sqrt{3}\left(\left[\frac{Z-13}{Z-12}\right]\left(1 - \frac{\sqrt{2}}{2} + \frac{1}{2}\right)r_{12}\right)}{\left((Z-12) - \left(\frac{5}{24} - \frac{6}{Z}\right)\frac{\sqrt{3}}{r_{12}}\right)}} \quad (10.288)$$

r_{12} in units of a_0

where r_{12} is given by Eq. (10.255). The positive root of Eq. (10.288) must be taken in order that $r_{13} > 0$. The radii of several thirteen-electron atoms are given in Table 10.12.

The ionization energies for the thirteen-electron atoms with $Z > 13$ are given by the electric energy, $E(\text{electric})$, (Eq. (10.102) with the radii, r_{13} , given by Eq. (10.288)):

$$E(\text{Ionization}) = -\text{Electric Energy} = \frac{(Z-12)e^2}{8\pi\epsilon_0 r_{13}} \quad (10.289)$$

Since the relativistic corrections were small, the nonrelativistic ionization energies for experimentally measured thirteen-electron atoms are given in Table 10.12.

Table 10.12. Ionization energies for some thirteen-electron atoms.

13 e Atom	Z	r_1 (a_0) ^a	r_3 (a_0) ^b	r_{10} (a_0) ^c	r_{12} (a_0) ^d	r_{13} (a_0) ^e	Theoretical Ionization Energies ^f (eV)	Experimental Ionization Energies ^g (eV)	Relative Error ^h
<i>Al</i>	13	0.07778	0.33923	0.45620	1.41133	2.28565	5.98402	5.98577	0.0003
<i>Si</i> ⁺	14	0.07216	0.31274	0.40978	1.25155	1.5995	17.0127	16.34585	-0.0408
<i>P</i> ²⁺	15	0.06730	0.29010	0.37120	1.09443	1.3922	29.3195	30.2027	0.0292
<i>S</i> ³⁺	16	0.06306	0.27053	0.33902	0.96729	1.1991	45.3861	47.222	0.0389
<i>Cl</i> ⁴⁺	17	0.05932	0.25344	0.31190	0.86545	1.0473	64.9574	67.8	0.0419
<i>Ar</i> ⁵⁺	18	0.05599	0.23839	0.28878	0.78276	0.9282	87.9522	91.009	0.0336
<i>K</i> ⁶⁺	19	0.05302	0.22503	0.26884	0.71450	0.8330	114.3301	117.56	0.0275
<i>Ca</i> ⁷⁺	20	0.05035	0.21308	0.25149	0.65725	0.7555	144.0664	147.24	0.0216
<i>Sc</i> ⁸⁺	21	0.04794	0.20235	0.23625	0.60857	0.6913	177.1443	180.03	0.0160
<i>Ti</i> ⁹⁺	22	0.04574	0.19264	0.22276	0.56666	0.6371	213.5521	215.92	0.0110
<i>V</i> ¹⁰⁺	23	0.04374	0.18383	0.21074	0.53022	0.5909	253.2806	255.7	0.0095
<i>Cr</i> ¹¹⁺	24	0.04191	0.17579	0.19995	0.49822	0.5510	296.3231	298.0	0.0056
<i>Mn</i> ¹²⁺	25	0.04022	0.16842	0.19022	0.46990	0.5162	342.6741	343.6	0.0027
<i>Fe</i> ¹³⁺	26	0.03867	0.16165	0.18140	0.44466	0.4855	392.3293	392.2	-0.0003
<i>Co</i> ¹⁴⁺	27	0.03723	0.15540	0.17336	0.42201	0.4583	445.2849	444	-0.0029
<i>Ni</i> ¹⁵⁺	28	0.03589	0.14961	0.16601	0.40158	0.4341	501.5382	499	-0.0051
<i>Cu</i> ¹⁶⁺	29	0.03465	0.14424	0.15926	0.38305	0.4122	561.0867	557	-0.0073
<i>Zn</i> ¹⁷⁺	30	0.03349	0.13925	0.15304	0.36617	0.3925	623.9282	619	-0.0080

^a Radius of the paired 1s inner electrons of thirteen-electron atoms from Eq. (10.51).

^b Radius of the paired 2s inner electrons of thirteen-electron atoms from Eq. (10.62).

^c Radius of the three sets of paired 2p inner electrons of thirteen-electron atoms from Eq. (10.212)).

^d Radius of the paired 3s inner electrons of thirteen-electron atoms from Eq. (10.255)).

^e Radius of the unpaired 3p outer electron of thirteen-electron atoms from Eq. (10.288) for $Z > 13$ and Eq. (10.276) for *Al*.

^f Calculated ionization energies of thirteen-electron atoms given by the electric energy (Eq. (10.289)) for $Z > 13$ and Eq. (10.279) for *Al*.

^g From theoretical calculations, interpolation of isoelectronic and spectral series, and experimental data [2-3].

^h (Experimental-theoretical)/experimental.

The agreement between the experimental and calculated values of Table 10.12 is well within the experimental capability of the spectroscopic determinations including the values at large Z which relies on X-ray spectroscopy. In this case, the experimental capability is three to four significant figures which is consistent with the last column. The aluminum atom isoelectronic series is given in Table 10.12 [2-3] to much higher precision than the capability of X-ray spectroscopy, but these values are based on theoretical and interpolation techniques rather than

data alone. Ionization energies are difficult to determine since the cut-off of the Rydberg series of lines at the ionization energy is often not observed, and the ionization energy must be determined from theoretical calculations, interpolation of Al isoelectronic and Rydberg series, as well as direct experimental data.

FOURTEEN-ELECTRON ATOMS

Fourteen-electron atoms can be solved exactly using the results of the solutions of one, two, three, four, five, six, seven, eight, nine, ten, eleven, twelve, and thirteen-electron atoms.

RADIUS AND IONIZATION ENERGY OF AN OUTER ELECTRON OF THE SILICON ATOM

For each thirteen-electron atom having a central charge of Z times that of the proton, there are two indistinguishable spin-paired electrons in an orbitsphere with radii r_1 and r_2 both given by Eq. (7.19) (Eq. (10.51)), two indistinguishable spin-paired electrons in an orbitsphere with radii r_3 and r_4 both given by Eq. (10.62), three sets of paired electrons in an orbitsphere at r_{10} given by Eq. (10.212), two indistinguishable spin-paired electrons in an orbitsphere with radii r_{11} and r_{12} both given by Eq. (10.255), and an unpaired electron in an orbitsphere with radius r_{13} given by Eq. (10.288). For $Z \geq 14$, the next electron which binds to form the corresponding fourteen-electron atom is attracted by the central Coulomb field and is repelled by diamagnetic forces due to the 3 sets of spin-paired inner 2p electrons and two spin-paired inner 3s electrons. A paramagnetic spin-pairing force to form a filled s orbital is also possible, but the force due to the spin-pairing of the electrons (Eq. (7.15) with the radius r_{14}) reduces the energy of the atom less than that due to the alternative forces on two unpaired 3p electrons in an orbitsphere at the same radius r_{14} . The resulting electron configuration is $1s^2 2s^2 2p^6 3s^2 3p^2$, and the orbital arrangement is

$$\begin{array}{ccc} \uparrow & \uparrow & _ \\ \hline 1 & 0 & -1 \end{array} \quad (10.290)$$

corresponding to the ground state 3P_0 .

The central Coulomb force acts on the outer electron to cause it to bind wherein this electric force on the outer-most electron due to the nucleus and the inner thirteen electrons is given by Eq. (10.70) with the appropriate charge and radius:

$$F_{ele} = \frac{(Z-13)e^2}{4\pi\epsilon_0 r_{14}^2} \mathbf{i}_r \quad (10.291)$$

for $r > r_{13}$.

As in the case of the carbon atom given in the Six-Electron Atom section, the two orthogonal 3p electrons form charge-density waves such that the total angular momentum of the two outer electrons is conserved which determines the diamagnetic force according to Eq. (10.82) (Eq. (10.258)). The contribution is given by Eq. (10.117) corresponding to $m=1$. In addition, the contribution of the diamagnetic force, $F_{\text{diamagnetic}}$, due to the 2p electrons is given by Eq. (10.105) (Eq. (10.259)) as the sum of the contributions from the 2 p_x , p_y , and p_z orbitals corresponding to $m = 1, -1$, and 0, respectively. Thus, $F_{\text{diamagnetic}}$ is given by

$$\begin{aligned} F_{\text{diamagnetic}} &= -\left(\frac{2}{3} + \frac{2}{3} + \frac{2}{3} + \frac{1}{3}\right) \frac{\hbar^2}{4m_e r_{14}^2 r_{12}} \sqrt{s(s+1)} \mathbf{i}_r \\ &= -\left(\frac{7}{3}\right) \frac{\hbar^2}{4m_e r_{14}^2 r_{12}} \sqrt{s(s+1)} \mathbf{i}_r \end{aligned} \quad (10.292)$$

The charge induction forms complementary mirror charge-density waves which must have opposing angular momenta such that momentum is conserved. In this case, $F_{\text{mag}2}$ given by Eq. (10.89) (Eq. (10.260)) is zero:

$$F_{\text{mag}2} = 0 \quad (10.293)$$

The outward centrifugal force on electron 14 is balanced by the electric force and the magnetic forces (on electron 14). The radius of the outer electron is calculated by equating the outward centrifugal force to the sum of the electric (Eq. (10.291)) and diamagnetic (Eq. (10.292)) forces as follows:

$$\frac{m_e v_{14}^2}{r_{14}} = \frac{(Z-13)e^2}{4\pi\epsilon_0 r_{14}^2} - \frac{7\hbar^2}{12m_e r_{14}^2 r_{12}} \sqrt{s(s+1)} \quad (10.294)$$

Substitution of $v_{14} = \frac{\hbar}{m_e r_{14}}$ (Eq. (1.56)) and $s = \frac{1}{2}$ into Eq. (10.294) gives:

$$\frac{\hbar^2}{m_e r_{14}^3} = \frac{(Z-13)e^2}{4\pi\epsilon_0 r_{14}^2} - \frac{7\hbar^2}{12m_e r_{14}^2 r_{12}} \sqrt{s(s+1)} \quad (10.295)$$

$$r_{14} = \frac{a_0}{\left((Z-13) - \frac{7\sqrt{3}}{12r_{12}} \right)}, \quad r_{12} \text{ in units of } a_0 \quad (10.296)$$

Substitution of $\frac{r_{12}}{a_0} = 1.25155$ (Eq. (10.255) with $Z=14$) into Eq. (10.296) gives

$$r_{14} = 1.67685a_0 \quad (10.297)$$

The ionization energy of the silicon atom is given by the electric energy, $E(\text{electric})$, (Eq. (10.102) with the radius, r_{14} , given by Eq. (10.297)):

$$E(\text{ionization}; \text{Si}) = -\text{Electric Energy} = \frac{(Z-13)e^2}{8\pi\epsilon_0 r_{14}} = 8.11391 \text{ eV} \quad (10.298)$$

where $r_{14} = 1.67685a_0$ (Eq. (10.297)) and $Z=14$. The experimental ionization energy of the silicon atom is 8.15169 eV [3].

THE IONIZATION ENERGIES OF FOURTEEN-ELECTRON ATOMS WITH A NUCLEAR CHARGE $Z>14$

Fourteen-electron atoms having $Z>14$ possess an external electric field given by Eq. (10.92). In this case, an energy minimum is achieved with conservation of momentum when the orbital angular momentum is such that $F_{\text{diamagnetic}}$ is minimized while $F_{\text{mag } 2}$ is maximized. With a half-filled 3p shell, the diamagnetic force due to the orbital angular momenta of the 3p electrons cancels that of the 2p electrons. Thus, $F_{\text{diamagnetic}}$ is minimized by the formation of a charge-density wave in the 3s orbital corresponding to $m = -1$ in Eq. (10.258) to form the equivalent of a half-filled 3p shell such that the contribution due to the 2p shell is canceled. From Eq. (10.258), the diamagnetic force, $F_{\text{diamagnetic}}$, is given by the sum of the contributions from the $3p_x$ and p_z orbitals corresponding to $m = 1$ and 0, respectively, and the negative contribution due to the charge-density wave with $m = -1$ induced in the 3s orbital according to Eq. (10.258):

$$F_{\text{diamagnetic}} = -\left(\frac{2}{3} + \frac{1}{3} - \frac{2}{3}\right) \frac{\hbar^2}{4m_e r_{14}^2 r_{12}} \sqrt{s(s+1)} \mathbf{i}_r = -\left(\frac{1}{3}\right) \frac{\hbar^2}{4m_e r_{14}^2 r_{12}} \sqrt{s(s+1)} \mathbf{i}_r \quad (10.299)$$

From Eq. (10.261), $F_{\text{mag } 2}$ corresponding to the spin and orbital angular momenta of the paired $2p_x$, p_y , and p_z electrons is

$$F_{\text{mag } 2} = (4 + 4 + 4) \frac{1}{Z} \frac{\hbar^2}{m_e r_{14}^2 r_{12}} \sqrt{s(s+1)} \mathbf{i}_r = \frac{1}{Z} \frac{12\hbar^2}{m_e r_{14}^2 r_{12}} \sqrt{s(s+1)} \mathbf{i}_r \quad (10.300)$$

and the contribution from the 3p shell is

$$F_{\text{mag } 2} = (4 + 4 - 4) \frac{1}{Z} \frac{\hbar^2}{m_e r_{14}^2 r_{12}} \sqrt{s(s+1)} \mathbf{i}_r = \frac{1}{Z} \frac{4\hbar^2}{m_e r_{14}^2 r_{12}} \sqrt{s(s+1)} \mathbf{i}_r \quad (10.301)$$

corresponding to the $3p_x$ and p_z electrons wherein the contribution due to the $3p_x$ ($m = 1$) electron is canceled by the mirror charge-density wave with $m = -1$ induced in the 3s orbital (Eq. (10.262)). Thus, the total of $F_{\text{mag } 2}$ is

$$F_{\text{mag } 2} = \frac{1}{Z} \frac{16\hbar^2}{m_e r_{14}^2 r_{12}} \sqrt{s(s+1)} \mathbf{i}_r \quad (10.302)$$

The diamagnetic force, $F_{\text{diamagnetic } 2}$, due to the binding of the 3p-orbital electron having an electric field outside of its radius is given by Eq. (10.268):

$$\mathbf{F}_{\text{diamagnetic } 2} = -\left[\frac{Z-14}{Z-13}\right]\left(1 - \frac{\sqrt{2}}{2} + \frac{1}{2}\right)\frac{r_{12}\hbar^2}{m_e r_{14}^4} 10\sqrt{s(s+1)}\mathbf{i}_r \quad (10.303)$$

In the case that $Z > 14$, the radius of the outer electron is calculated by equating the outward centrifugal force to the sum of the electric (Eq. (10.291)), diamagnetic (Eqs. (10.299) and (10.303)), and paramagnetic (Eq. (10.302)) forces as follows:

$$\begin{aligned} \frac{m_e v_{14}^2}{r_{14}} = & \frac{(Z-13)e^2}{4\pi\epsilon_0 r_{14}^2} - \frac{\hbar^2}{12m_e r_{14}^2 r_{12}} \sqrt{s(s+1)} + \frac{16\hbar^2}{Zm_e r_{14}^2 r_{12}} \sqrt{s(s+1)} \\ & - \left[\frac{Z-14}{Z-13}\right]\left(1 - \frac{\sqrt{2}}{2} + \frac{1}{2}\right)\frac{r_{12}\hbar^2}{m_e r_{14}^4} 10\sqrt{s(s+1)} \end{aligned} \quad (10.304)$$

Substitution of $v_{14} = \frac{\hbar}{m_e r_{14}}$ (Eq. (1.56)) and $s = \frac{1}{2}$ into Eq. (10.304) gives:

$$\frac{\hbar^2}{m_e r_{14}^3} = \frac{(Z-13)e^2}{4\pi\epsilon_0 r_{14}^2} - \frac{\hbar^2}{12m_e r_{14}^2 r_{12}} \sqrt{\frac{3}{4}} + \frac{16\hbar^2}{Zm_e r_{14}^2 r_{12}} \sqrt{\frac{3}{4}} - \left[\frac{Z-14}{Z-13}\right]\left(1 - \frac{\sqrt{2}}{2} + \frac{1}{2}\right)\frac{r_{12}\hbar^2}{m_e r_{14}^4} 10\sqrt{\frac{3}{4}} \quad (10.305)$$

The quadratic equation corresponding to Eq. (10.305) is

$$\left(\frac{(Z-13)e^2}{4\pi\epsilon_0} - \left(\frac{1}{12} - \frac{16}{Z}\right)\frac{\hbar^2}{m_e r_{12}} \sqrt{\frac{3}{4}}\right)r_{14}^2 - \frac{\hbar^2}{m_e} r_{14} - \left[\frac{Z-14}{Z-13}\right]\left(1 - \frac{\sqrt{2}}{2} + \frac{1}{2}\right)\frac{r_{12}\hbar^2}{m_e} 10\sqrt{\frac{3}{4}} = 0 \quad (10.306)$$

$$r_{14}^2 - \frac{\frac{\hbar^2}{m_e}}{\left(\frac{(Z-13)e^2}{4\pi\epsilon_0} - \left(\frac{1}{12} - \frac{16}{Z}\right)\frac{\hbar^2}{m_e r_{12}} \sqrt{\frac{3}{4}}\right)} r_{14} - \frac{\frac{\hbar^2}{m_e} \left[\frac{Z-14}{Z-13}\right]\left(1 - \frac{\sqrt{2}}{2} + \frac{1}{2}\right)r_{12} 10\sqrt{\frac{3}{4}}}{\left(\frac{(Z-13)e^2}{4\pi\epsilon_0} - \left(\frac{1}{12} - \frac{16}{Z}\right)\frac{\hbar^2}{m_e r_{12}} \sqrt{\frac{3}{4}}\right)} = 0 \quad (10.307)$$

The solution of Eq. (10.307) using the quadratic formula is:

$$r_{14} = \frac{\frac{\hbar^2}{m_e}}{\left(\frac{(Z-13)e^2}{4\pi\epsilon_0} - \left(\frac{1}{12} - \frac{16}{Z}\right)\frac{\hbar^2}{m_e r_{12}} \sqrt{\frac{3}{4}}\right)} \pm \sqrt{\left(\frac{\frac{\hbar^2}{m_e}}{\left(\frac{(Z-13)e^2}{4\pi\epsilon_0} - \left(\frac{1}{12} - \frac{16}{Z}\right)\frac{\hbar^2}{m_e r_{12}} \sqrt{\frac{3}{4}}\right)}\right)^2 + 4 \frac{\frac{\hbar^2}{m_e} \left[\frac{Z-14}{Z-13}\right]\left(1 - \frac{\sqrt{2}}{2} + \frac{1}{2}\right)r_{12} 10\sqrt{\frac{3}{4}}}{\left(\frac{(Z-13)e^2}{4\pi\epsilon_0} - \left(\frac{1}{12} - \frac{16}{Z}\right)\frac{\hbar^2}{m_e r_{12}} \sqrt{\frac{3}{4}}\right)}} \quad (10.308)$$

$$r_{14} = \frac{\left((Z-13) - \left(\frac{1}{24} - \frac{8}{Z} \right) \frac{\sqrt{3}}{r_{12}} \right) \pm a_0}{2} \sqrt{\frac{1}{\left((Z-13) - \left(\frac{1}{24} - \frac{8}{Z} \right) \frac{\sqrt{3}}{r_{12}} \right)^2} + \frac{20\sqrt{3} \left(\left[\frac{Z-14}{Z-13} \right] \left(1 - \frac{\sqrt{2}}{2} + \frac{1}{2} \right) r_{12} \right)}{\left((Z-13) - \left(\frac{1}{24} - \frac{8}{Z} \right) \frac{\sqrt{3}}{r_{12}} \right)}} \quad (10.309)$$

r_{12} in units of a_0

where r_{12} is given by Eq. (10.255). The positive root of Eq. (10.309) must be taken in order that $r_{14} > 0$. The final radius of electron 14, r_{14} , is given by Eq. (10.309); this is also the final radius of electron 13. The radii of several fourteen-electron atoms are given in Table 10.13.

The ionization energies for the fourteen-electron atoms with $Z > 14$ are given by the electric energy, $E(\text{electric})$, (Eq. (10.102) with the radii r_{14} , given by Eq. (10.309)):

$$E(\text{Ionization}) = -\text{Electric Energy} = \frac{(Z-13)e^2}{8\pi\epsilon_0 r_{14}} \quad (10.310)$$

Since the relativistic corrections were small, the nonrelativistic ionization energies for experimentally measured fourteen-electron atoms are given in Table 10.13.

Table 10.13. Ionization energies for some fourteen-electron atoms.

14 e Atom	Z	r_1 (a_0) ^a	r_3 (a_0) ^b	r_{10} (a_0) ^c	r_{12} (a_0) ^d	r_{14} (a_0) ^e	Theoretical Ionization Energies ^f (eV)	Experimental Ionization Energies ^g (eV)	Relative Error ^h
Si	14	0.07216	0.31274	0.40978	1.25155	1.67685	8.11391	8.15169	0.0046
P ⁺	15	0.06730	0.29010	0.37120	1.09443	1.35682	20.0555	19.7694	-0.0145
S ²⁺	16	0.06306	0.27053	0.33902	0.96729	1.21534	33.5852	34.790	0.0346
Cl ³⁺	17	0.05932	0.25344	0.31190	0.86545	1.06623	51.0426	53.4652	0.0453
Ar ⁴⁺	18	0.05599	0.23839	0.28878	0.78276	0.94341	72.1094	75.020	0.0388
K ⁵⁺	19	0.05302	0.22503	0.26884	0.71450	0.84432	96.6876	99.4	0.0273
Ca ⁶⁺	20	0.05035	0.21308	0.25149	0.65725	0.76358	124.7293	127.2	0.0194
Sc ⁷⁺	21	0.04794	0.20235	0.23625	0.60857	0.69682	156.2056	158.1	0.0120
Ti ⁸⁺	22	0.04574	0.19264	0.22276	0.56666	0.64078	191.0973	192.10	0.0052
V ⁹⁺	23	0.04374	0.18383	0.21074	0.53022	0.59313	229.3905	230.5	0.0048
Cr ¹⁰⁺	24	0.04191	0.17579	0.19995	0.49822	0.55211	271.0748	270.8	-0.0010
Mn ¹¹⁺	25	0.04022	0.16842	0.19022	0.46990	0.51644	316.1422	314.4	-0.0055
Fe ¹²⁺	26	0.03867	0.16165	0.18140	0.44466	0.48514	364.5863	361	-0.0099
Co ¹³⁺	27	0.03723	0.15540	0.17336	0.42201	0.45745	416.4021	411	-0.0131
Ni ¹⁴⁺	28	0.03589	0.14961	0.16601	0.40158	0.43277	471.5854	464	-0.0163
Cu ¹⁵⁺	29	0.03465	0.14424	0.15926	0.38305	0.41064	530.1326	520	-0.0195
Zn ¹⁶⁺	30	0.03349	0.13925	0.15304	0.36617	0.39068	592.0410	579	-0.0225

^a Radius of the paired 1s inner electrons of fourteen-electron atoms from Eq. (10.51).^b Radius of the paired 2s inner electrons of fourteen-electron atoms from Eq. (10.62).^c Radius of the three sets of paired 2p inner electrons of fourteen-electron atoms from Eq. (10.212)).^d Radius of the paired 3s inner electrons of fourteen-electron atoms from Eq. (10.255)).^e Radius of the two unpaired 3p outer electrons of fourteen-electron atoms from Eq. (10.309) for $Z > 14$ and Eq. (10.297) for Si.^f Calculated ionization energies of fourteen-electron atoms given by the electric energy (Eq. (10.310)).^g From theoretical calculations, interpolation of isoelectronic and spectral series, and experimental data [2-3].^h (Experimental-theoretical)/experimental.

The agreement between the experimental and calculated values of Table 10.13 is well within the experimental capability of the spectroscopic determinations including the values at large Z which relies on X-ray spectroscopy. In this case, the experimental capability is three to four significant figures which is consistent with the last column. The silicon atom isoelectronic series is given in Table 10.13 [2-3] to much higher precision than the capability of X-ray spectroscopy, but these values are based on theoretical and interpolation techniques rather than data alone. Ionization energies are difficult to determine since the cut-off

of the Rydberg series of lines at the ionization energy is often not observed, and the ionization energy must be determined from theoretical calculations, interpolation of Si isoelectronic and Rydberg series, as well as direct experimental data.

FIFTEEN-ELECTRON ATOMS

Fifteen-electron atoms can be solved exactly using the results of the solutions of one, two, three, four, five, six, seven, eight, nine, ten, eleven, twelve, thirteen and fourteen-electron atoms.

RADIUS AND IONIZATION ENERGY OF AN OUTER ELECTRON OF THE PHOSPHOROUS ATOM

For each fourteen-electron atom having a central charge of Z times that of the proton, there are two indistinguishable spin-paired electrons in an orbitsphere with radii r_1 and r_2 both given by Eq. (7.19) (Eq. (10.51)), two indistinguishable spin-paired electrons in an orbitsphere with radii r_3 and r_4 both given by Eq. (10.62), three sets of paired electrons in an orbitsphere at r_{10} given by Eq. (10.212), two indistinguishable spin-paired electrons in an orbitsphere with radii r_{11} and r_{12} both given by Eq. (10.255), and two unpaired electrons in an orbitsphere with radius r_{14} given by Eq. (10.288). For $Z \geq 15$, the next electron which binds to form the corresponding fifteen-electron atom is attracted by the central Coulomb field and is repelled by diamagnetic forces due to the 3 sets of spin-paired inner 2p electrons and two spin-paired inner 3s electrons. A paramagnetic spin-pairing force to form a filled s orbital is also possible, but the force due to the spin-pairing of the electrons (Eq. (7.15) with the radius r_{15}) reduces the energy of the atom less than that due to the alternative forces on three unpaired 3p electrons in an orbitsphere at the same radius r_{15} . The resulting electron configuration is $1s^2 2s^2 2p^6 3s^2 3p^3$, and the orbital arrangement is

3p state

$$\begin{array}{ccc} \uparrow & \uparrow & \uparrow \\ \hline 1 & 0 & -1 \end{array} \quad (10.311)$$

corresponding to the ground state $^4S_{3/2}$.

The central Coulomb force acts on the outer electron to cause it to bind wherein this electric force on the outer-most electron due to the nucleus and the inner fourteen electrons is given by Eq. (10.70) with the appropriate charge and radius:

$$\mathbf{F}_{ele} = \frac{(Z-14)e^2}{4\pi\epsilon_0 r_{15}^2} \mathbf{i}_r \quad (10.312)$$

for $r > r_{14}$.

The diamagnetic force, $F_{\text{diamagnetic}}$, is only due to 3p and 3s electrons when the 3p shell is at least half filled since the induced charge-density waves only involve the inner-most shell, the 3s orbital. Thus, $F_{\text{diamagnetic}}$ is given by Eq. (10.259) as the sum of the contributions from the $3p_x$, p_y , and p_z orbitals corresponding to $m = 1, -1$, and 0 , respectively:

$$F_{\text{diamagnetic}} = -\left(\frac{2}{3} + \frac{2}{3} + \frac{1}{3}\right) \frac{\hbar^2}{4m_e r_{15}^2 r_{12}} \sqrt{s(s+1)} \mathbf{i}_r = -\left(\frac{5}{3}\right) \frac{\hbar^2}{4m_e r_{15}^2 r_{12}} \sqrt{s(s+1)} \mathbf{i}_r \quad (10.313)$$

The energy is minimized with conservation of angular momentum when the spin angular momentum of the 3s orbital superimposes negatively with the orbital angular momentum of the 3p orbitals. From Eq. (10.260), $F_{\text{mag } 2}$ corresponding to the orbital angular momentum of the $3p_x$, p_y , and p_z orbitals minus the contribution from the 3s orbital is

$$F_{\text{mag } 2} = (1+1+1-1) \frac{1}{Z} \frac{\hbar^2}{m_e r_{15}^2 r_{12}} \sqrt{s(s+1)} \mathbf{i}_r = \frac{1}{Z} \frac{2\hbar^2}{m_e r_{15}^2 r_{12}} \sqrt{s(s+1)} \mathbf{i}_r \quad (10.314)$$

The outward centrifugal force on electron 15 is balanced by the electric force and the magnetic forces (on electron 15). The radius of the outer electron is calculated by equating the outward centrifugal force to the sum of the electric (Eq. (10.312)), diamagnetic (Eq. (10.313)), and paramagnetic (Eq. (10.314)) forces as follows:

$$\frac{m_e v_{15}^2}{r_{15}} = \frac{(Z-14)e^2}{4\pi\epsilon_0 r_{15}^2} - \frac{5\hbar^2}{12m_e r_{15}^2 r_{12}} \sqrt{s(s+1)} + \frac{2\hbar^2}{Zm_e r_{15}^2 r_{12}} \sqrt{s(s+1)} \quad (10.315)$$

Substitution of $v_{15} = \frac{\hbar}{m_e r_{15}}$ (Eq. (1.56)) and $s = \frac{1}{2}$ into Eq. (10.315) gives:

$$\frac{\hbar^2}{m_e r_{15}^3} = \frac{(Z-14)e^2}{4\pi\epsilon_0 r_{15}^2} - \frac{5\hbar^2}{12m_e r_{15}^2 r_{12}} \sqrt{\frac{3}{4}} + \frac{2\hbar^2}{Zm_e r_{15}^2 r_{12}} \sqrt{\frac{3}{4}} \quad (10.316)$$

$$r_{15} = \frac{\frac{\hbar^2}{m_e}}{\frac{(Z-14)e^2}{4\pi\epsilon_0} - \frac{5\hbar^2}{12m_e r_{12}} \sqrt{\frac{3}{4}} + \frac{2\hbar^2}{Zm_e r_{12}} \sqrt{\frac{3}{4}}} \quad (10.317)$$

$$r_{15} = \frac{a_0}{(Z-14) - \left(\frac{5}{12} - \frac{2}{Z}\right) \sqrt{\frac{3}{4}} \frac{1}{r_{12}}}, \quad r_{12} \text{ in units of } a_0 \quad (10.318)$$

Substitution of $\frac{r_{12}}{a_0} = 1.09443$ (Eq. (10.255) with $Z=15$) into Eq. (10.318) gives

$$r_{15} = 1.28900a_0 \quad (10.319)$$

The ionization energy of the phosphorous atom is given by the electric energy, $E(\text{electric})$, (Eq. (10.102) with the radius, r_{15} , given by Eq.

(10.319)):

$$E(\text{ionization}; P) = -\text{Electric Energy} = \frac{(Z-14)e^2}{8\pi\epsilon_0 r_{15}} = 10.5554 \text{ eV} \quad (10.320)$$

where $r_{15} = 1.28900a_0$ (Eq. (10.319)) and $Z = 15$. The experimental ionization energy of the phosphorous atom is 10.48669 eV [3].

THE IONIZATION ENERGIES OF FIFTEEN-ELECTRON ATOMS WITH A NUCLEAR CHARGE $Z > 15$

Fifteen-electron atoms having $Z > 15$ possess an external electric field given by Eq. (10.92). In this case, an energy minimum is achieved with conservation of momentum when the orbital angular momentum is such that $F_{\text{diamagnetic}}$ is minimized while $F_{\text{mag } 2}$ is maximized. With a half-filled 3p shell, the diamagnetic force due to the orbital angular momenta of the 3p electrons cancels that of the 2p electrons. Thus, the diamagnetic force (Eq. (10.258)), $F_{\text{diamagnetic}}$, is zero:

$$F_{\text{diamagnetic}} = 0 \quad (10.321)$$

From Eqs. (10.205) and (10.261), $F_{\text{mag } 2}$ corresponding to the spin and orbital angular momenta of the paired $2p_x$, p_y , and p_z electrons is

$$F_{\text{mag } 2} = (4 + 4 + 4) \frac{1}{Z} \frac{\hbar^2}{m_e r_{15}^2 r_{12}} \sqrt{s(s+1)} \mathbf{i}_r = \frac{1}{Z} \frac{12\hbar^2}{m_e r_{15}^2 r_{12}} \sqrt{s(s+1)} \mathbf{i}_r \quad (10.322)$$

and the contribution from the 3p level is

$$F_{\text{mag } 2} = (4 + 4 + 4) \frac{1}{Z} \frac{\hbar^2}{m_e r_{15}^2 r_{12}} \sqrt{s(s+1)} \mathbf{i}_r = \frac{1}{Z} \frac{12\hbar^2}{m_e r_{15}^2 r_{12}} \sqrt{s(s+1)} \mathbf{i}_r \quad (10.323)$$

corresponding to the $3p_x$, p_y , and p_z electrons. Thus, the total of $F_{\text{mag } 2}$ is

$$F_{\text{mag } 2} = \frac{1}{Z} \frac{24\hbar^2}{m_e r_{15}^2 r_{12}} \sqrt{s(s+1)} \mathbf{i}_r \quad (10.324)$$

The diamagnetic force, $F_{\text{diamagnetic } 2}$, due to the binding of the 3p-orbital electron having an electric field outside of its radius is given by Eq. (10.268):

$$F_{\text{diamagnetic } 2} = -\left[\frac{Z-15}{Z-14} \right] \left(1 - \frac{\sqrt{2}}{2} + \frac{1}{2} \right) \frac{r_{12}\hbar^2}{m_e r_{15}^4} 10\sqrt{s(s+1)} \mathbf{i}_r \quad (10.325)$$

In the case that $Z > 15$, the radius of the outer electron is calculated by equating the outward centrifugal force to the sum of the electric (Eq. (10.312)), diamagnetic (Eqs. (10.321) and (10.325)), and paramagnetic (Eq. (10.324)) forces as follows:

$$\frac{m_e v_{15}^2}{r_{15}} = \frac{(Z-14)e^2}{4\pi\epsilon_0 r_{15}^2} + \frac{24\hbar^2}{Z m_e r_{15}^2 r_{12}} \sqrt{s(s+1)} - \left[\frac{Z-15}{Z-14} \right] \left(1 - \frac{\sqrt{2}}{2} + \frac{1}{2} \right) \frac{r_{12}\hbar^2}{m_e r_{15}^4} 10\sqrt{s(s+1)} \quad (10.326)$$

Substitution of $v_{15} = \frac{\hbar}{m_e r_{15}}$ (Eq. (1.56)) and $s = \frac{1}{2}$ into Eq. (10.326) gives:

$$\frac{\hbar^2}{m_e r_{15}^3} = \frac{(Z-14)e^2}{4\pi\epsilon_0 r_{15}^2} + \frac{24\hbar^2}{Zm_e r_{15}^2 r_{12}} \sqrt{\frac{3}{4}} - \left[\frac{Z-15}{Z-14} \right] \left(1 - \frac{\sqrt{2}}{2} + \frac{1}{2} \right) \frac{r_{12} \hbar^2}{m_e r_{15}^4} 10 \sqrt{\frac{3}{4}} \quad (10.327)$$

The quadratic equation corresponding to Eq. (10.327) is

$$\left(\frac{(Z-14)e^2}{4\pi\epsilon_0} + \frac{24\hbar^2}{Zm_e r_{12}} \sqrt{\frac{3}{4}} \right) r_{15}^2 - \frac{\hbar^2}{m_e} r_{15} - \left[\frac{Z-15}{Z-14} \right] \left(1 - \frac{\sqrt{2}}{2} + \frac{1}{2} \right) \frac{r_{12} \hbar^2}{m_e} 10 \sqrt{\frac{3}{4}} = 0 \quad (10.328)$$

$$r_{15}^2 - \frac{\frac{\hbar^2}{m_e}}{\left(\frac{(Z-14)e^2}{4\pi\epsilon_0} + \frac{24\hbar^2}{Zm_e r_{12}} \sqrt{\frac{3}{4}} \right)} r_{15} - \frac{\frac{\hbar^2}{m_e} \left[\frac{Z-15}{Z-14} \right] \left(1 - \frac{\sqrt{2}}{2} + \frac{1}{2} \right) r_{12} 10 \sqrt{\frac{3}{4}}}{\left(\frac{(Z-14)e^2}{4\pi\epsilon_0} + \frac{24\hbar^2}{Zm_e r_{12}} \sqrt{\frac{3}{4}} \right)} = 0 \quad (10.329)$$

The solution of Eq. (10.329) using the quadratic formula is:

$$r_{15} = \frac{\frac{\hbar^2}{m_e} \left(\frac{(Z-14)e^2}{4\pi\epsilon_0} + \frac{24\hbar^2}{Zm_e r_{12}} \sqrt{\frac{3}{4}} \right) \pm \sqrt{\left(\frac{\hbar^2}{m_e} \left(\frac{(Z-14)e^2}{4\pi\epsilon_0} + \frac{24\hbar^2}{Zm_e r_{12}} \sqrt{\frac{3}{4}} \right) \right)^2 + 4 \frac{\frac{\hbar^2}{m_e} \left[\frac{Z-15}{Z-14} \right] \left(1 - \frac{\sqrt{2}}{2} + \frac{1}{2} \right) r_{12} 10 \sqrt{\frac{3}{4}}}{\left(\frac{(Z-14)e^2}{4\pi\epsilon_0} + \frac{24\hbar^2}{Zm_e r_{12}} \sqrt{\frac{3}{4}} \right)}}}{2} \quad (10.330)$$

$$r_{15} = \frac{\frac{a_0}{\left((Z-14) - \frac{12\sqrt{3}}{Zr_{12}} \right)} \pm a_0 \sqrt{\left(\frac{1}{\left((Z-14) - \frac{12\sqrt{3}}{Zr_{12}} \right)} \right)^2 + \frac{20\sqrt{3} \left(\left[\frac{Z-15}{Z-14} \right] \left(1 - \frac{\sqrt{2}}{2} + \frac{1}{2} \right) r_{12} \right)}{\left((Z-14) - \frac{12\sqrt{3}}{Zr_{12}} \right)}}}{2} \quad (10.331)$$

where r_{12} is given by Eq. (10.255). The positive root of Eq. (10.331) must
 r_{12} in units of a_0

be taken in order that $r_{15} > 0$. The final radius of electron 15, r_{15} , is given by Eq. (10.331); this is also the final radius of electrons 13 and 14. The radii of several fifteen-electron atoms are given in Table 10.14.

The ionization energies for the fifteen-electron atoms with $Z > 15$ are given by the electric energy, $E(\text{electric})$, (Eq. (10.102) with the radii r_{15} , given by Eq. (10.331)):

$$E(\text{ionization}) = -\text{Electric Energy} = \frac{(Z-14)e^2}{8\pi\epsilon_0 r_{15}} \quad (10.332)$$

Since the relativistic corrections were small, the nonrelativistic ionization energies for experimentally measured fifteen-electron atoms are given in Table 10.14.

Table 10.14. Ionization energies for some fifteen-electron atoms.

15 e Atom	Z	r_1 (a_0) ^a	r_3 (a_0) ^b	r_{10} (a_0) ^c	r_{12} (a_0) ^d	r_{15} (a_0) ^e	Theoretical Ionization Energies ^f (eV)	Experimental Ionization Energies ^g (eV)	Relative Error ^h
P	15	0.06730	0.29010	0.37120	1.09443	1.28900	10.55536	10.48669	-0.0065
S ⁺	16	0.06306	0.27053	0.33902	0.96729	1.15744	23.5102	23.3379	-0.0074
Cl ²⁺	17	0.05932	0.25344	0.31190	0.86545	1.06759	38.2331	39.61	0.0348
Ar ³⁺	18	0.05599	0.23839	0.28878	0.78276	0.95423	57.0335	59.81	0.0464
K ⁴⁺	19	0.05302	0.22503	0.26884	0.71450	0.85555	79.5147	82.66	0.0381
Ca ⁵⁺	20	0.05035	0.21308	0.25149	0.65725	0.77337	105.5576	108.78	0.0296
Sc ⁶⁺	21	0.04794	0.20235	0.23625	0.60857	0.70494	135.1046	138.0	0.0210
Ti ⁷⁺	22	0.04574	0.19264	0.22276	0.56666	0.64743	168.1215	170.4	0.0134
V ⁸⁺	23	0.04374	0.18383	0.21074	0.53022	0.59854	204.5855	205.8	0.0059
Cr ⁹⁺	24	0.04191	0.17579	0.19995	0.49822	0.55652	244.4799	244.4	-0.0003
Mn ¹⁰⁺	25	0.04022	0.16842	0.19022	0.46990	0.52004	287.7926	286.0	-0.0063
Fe ¹¹⁺	26	0.03867	0.16165	0.18140	0.44466	0.48808	334.5138	330.8	-0.0112
Co ¹²⁺	27	0.03723	0.15540	0.17336	0.42201	0.45985	384.6359	379	-0.0149
Ni ¹³⁺	28	0.03589	0.14961	0.16601	0.40158	0.43474	438.1529	430	-0.0190
Cu ¹⁴⁺	29	0.03465	0.14424	0.15926	0.38305	0.41225	495.0596	484	-0.0229
Zn ¹⁵⁺	30	0.03349	0.13925	0.15304	0.36617	0.39199	555.3519	542	-0.0246

^a Radius of the paired 1s inner electrons of fifteen-electron atoms from Eq. (10.51).

^b Radius of the paired 2s inner electrons of fifteen-electron atoms from Eq. (10.62).

^c Radius of the three sets of paired 2p inner electrons of fifteen-electron atoms from Eq. (10.212)).

^d Radius of the paired 3s inner electrons of fifteen-electron atoms from Eq. (10.255)).

^e Radius of the three unpaired 3p outer electrons of fifteen-electron atoms from Eq. (10.331) for $Z > 15$ and Eq. (10.319) for P.

^f Calculated ionization energies of fifteen-electron atoms given by the electric energy (Eq. (10.332)).

^g From theoretical calculations, interpolation of isoelectronic and spectral series, and

experimental data [2-3].

^h (Experimental-theoretical)/experimental.

The agreement between the experimental and calculated values of Table 10.14 is well within the experimental capability of the spectroscopic determinations including the values at large Z which relies on X-ray spectroscopy. In this case, the experimental capability is three to four significant figures which is consistent with the last column. The phosphorous atom isoelectronic series is given in Table 10.14 [2-3] to much higher precision than the capability of X-ray spectroscopy, but these values are based on theoretical and interpolation techniques rather than data alone. Ionization energies are difficult to determine since the cut-off of the Rydberg series of lines at the ionization energy is often not observed, and the ionization energy must be determined from theoretical calculations, interpolation of P isoelectronic and Rydberg series, as well as direct experimental data.

SIXTEEN-ELECTRON ATOMS

Sixteen-electron atoms can be solved exactly using the results of the solutions of one, two, three, four, five, six, seven, eight, nine, ten, eleven, twelve, thirteen, fourteen, and fifteen-electron atoms.

RADIUS AND IONIZATION ENERGY OF AN OUTER ELECTRON OF THE SULFUR ATOM

For each fifteen-electron atom having a central charge of Z times that of the proton, there are two indistinguishable spin-paired electrons in an orbitsphere with radii r_1 and r_2 both given by Eq. (7.19) (Eq. (10.51)), two indistinguishable spin-paired electrons in an orbitsphere with radii r_3 and r_4 both given by Eq. (10.62), three sets of paired electrons in an orbitsphere at r_{10} given by Eq. (10.212), two indistinguishable spin-paired electrons in an orbitsphere with radii r_{11} and r_{12} both given by Eq. (10.255), and three unpaired electrons in an orbitsphere with radius r_{15} given by Eq. (10.331). For $Z \geq 16$, the next electron which binds to form the corresponding sixteen-electron atom is attracted by the central Coulomb field and is repelled by diamagnetic forces due to the 3 sets of spin-paired inner 2p electrons and two spin-paired inner 3s electrons. A paramagnetic spin-pairing force to form a filled s orbital is also possible, but the force due to the spin-pairing of the electrons (Eq. (7.15) with the radius r_{16}) reduces the energy of the atom less than that due to the alternative forces on a set of paired and two unpaired 3p electrons in an orbitsphere at the same radius r_{16} . The resulting electron configuration is $1s^2 2s^2 2p^6 3s^2 3p^4$, and the orbital

arrangement is

$$\begin{array}{ccc} & \text{3p state} & \\ \uparrow \downarrow & \uparrow & \uparrow \\ 1 & 0 & -1 \end{array} \quad (10.333)$$

corresponding to the ground state 3P_2 .

The central Coulomb force acts on the outer electron to cause it to bind wherein this electric force on the outer-most electron due to the nucleus and the inner fifteen electrons is given by Eq. (10.70) with the appropriate charge and radius:

$$\mathbf{F}_{ele} = \frac{(Z-15)e^2}{4\pi\epsilon_0 r_{16}^2} \mathbf{i}_r \quad (10.334)$$

for $r > r_{15}$.

The diamagnetic force, $\mathbf{F}_{diamagnetic}$, is only due to 3p and 3s electrons when the 3p shell is at least half filled since the induced charge-density waves only involve the inner-most shell, the 3s orbital. The energy is minimized with conservation of angular momentum when the induced orbital angular momentum of the 3s orbital superimposes positively with the orbital angular momenta of the other $3p_x$ and the $3p_z$ -orbital electrons and the orbital angular momentum of one of the spin-paired $3p_x$ electrons is canceled by the $3p_y$ electron. Thus, $\mathbf{F}_{diamagnetic}$ is given by Eq. (10.258) as the sum of the contributions from the $3p_x$ and p_z orbitals corresponding to $m = 1$ and 0, respectively, and the induced contribution from the 3s orbital corresponding to $m = 0$:

$$\mathbf{F}_{diamagnetic} = -\left(\frac{2}{3} + \frac{1}{3} + \frac{1}{3}\right) \frac{\hbar^2}{4m_e r_{16}^2 r_{12}} \sqrt{s(s+1)} \mathbf{i}_r = -\left(\frac{4}{3}\right) \frac{\hbar^2}{4m_e r_{16}^2 r_{12}} \sqrt{s(s+1)} \mathbf{i}_r \quad (10.335)$$

The energy is minimized with conservation of angular momentum when the spin angular momentum the 3s orbital superimposes negatively with the spin angular momentum of the $3p_x$ orbital-electron and the orbital angular momentum of the $3p_z$ -orbital electron. From Eq. (10.260), \mathbf{F}_{mag2} corresponding to the orbital angular momentum of the $3p_x$, p_y , and p_z orbitals minus the contribution from the 3s orbital is

$$\mathbf{F}_{mag2} = (1+1-1) \frac{1}{Z} \frac{\hbar^2}{m_e r_{16}^2 r_3} \sqrt{s(s+1)} \mathbf{i}_r = \frac{1}{Z} \frac{\hbar^2}{m_e r_{16}^2 r_{12}} \sqrt{s(s+1)} \mathbf{i}_r \quad (10.336)$$

The outward centrifugal force on electron 16 is balanced by the electric force and the magnetic forces (on electron 16). The radius of the outer electron is calculated by equating the outward centrifugal force to the sum of the electric (Eq. (10.334)), diamagnetic (Eq. (10.335)), and paramagnetic (Eq. (10.336)) forces as follows:

$$\frac{m_e v_{16}^2}{r_{16}} = \frac{(Z-15)e^2}{4\pi\epsilon_0 r_{16}^2} - \frac{4\hbar^2}{12m_e r_{16}^2 r_{12}} \sqrt{s(s+1)} + \frac{\hbar^2}{Zm_e r_{16}^2 r_{12}} \sqrt{s(s+1)} \quad (10.337)$$

Substitution of $v_{16} = \frac{\hbar}{m_e r_{16}}$ (Eq. (1.56)) and $s = \frac{1}{2}$ into Eq. (10.337) gives:

$$\frac{\hbar^2}{m_e r_{16}^3} = \frac{(Z-15)e^2}{4\pi\epsilon_0 r_{16}^2} - \frac{4\hbar^2}{12m_e r_{16}^2 r_{12}} \sqrt{\frac{3}{4}} + \frac{\hbar^2}{Zm_e r_{16}^2 r_{12}} \sqrt{\frac{3}{4}} \quad (10.338)$$

$$r_{16} = \frac{\frac{\hbar^2}{m_e}}{\frac{(Z-15)e^2}{4\pi\epsilon_0} - \frac{4\hbar^2}{12m_e r_{12}} \sqrt{\frac{3}{4}} + \frac{\hbar^2}{Zm_e r_{12}} \sqrt{\frac{3}{4}}} \quad (10.339)$$

$$r_{16} = \frac{a_0}{(Z-15) - \left(\frac{4}{12} - \frac{1}{Z}\right) \sqrt{\frac{3}{4}}}, \quad r_{12} \text{ in units of } a_0 \quad (10.340)$$

Substitution of $\frac{r_{12}}{a_0} = 0.96729$ (Eq. (10.255) with $Z=16$) into Eq. (10.340) gives

$$r_{16} = 1.32010a_0 \quad (10.341)$$

The ionization energy of the sulfur atom is given by the electric energy, $E(\text{electric})$, (Eq. (10.102) with the radius, r_{16} , given by Eq. (10.341)):

$$E(\text{ionization}; S) = -\text{Electric Energy} = \frac{(Z-15)e^2}{8\pi\epsilon_0 r_{16}} = 10.30666 \text{ eV} \quad (10.342)$$

where $r_{16} = 1.32010a_0$ (Eq. (10.341)) and $Z=16$. The experimental ionization energy of the sulfur atom is 10.36001 eV [3].

THE IONIZATION ENERGIES OF SIXTEEN-ELECTRON ATOMS WITH A NUCLEAR CHARGE $Z>16$

Sixteen-electron atoms having $Z>16$ possess an external electric field given by Eq. (10.92). In this case, an energy minimum is achieved with conservation of momentum when the orbital angular momentum is such that $F_{\text{diamagnetic}}$ is minimized while $F_{\text{mag } 2}$ is maximized. With a half-filled 3p shell, the diamagnetic force due to the orbital angular momenta of the 3p electrons cancels that of the 2p electrons. Thus, $F_{\text{diamagnetic}}$ is minimized by the formation of a charge-density wave in the 3s orbital corresponding to $m = 1$ in Eq. (10.258) that cancels the orbital angular momentum of one of the $3p_x$ electrons to form the equivalent of a half-filled 3p shell. Then, the contribution due to the 2p level is canceled. From Eq. (10.82), the diamagnetic force, $F_{\text{diamagnetic}}$, is given by the sum of the contributions from the $3p_y$ and p_z orbitals corresponding to $m = -1$ and 0, respectively, and the negative contribution due to the charge-density wave with $m = 1$ induced in the 3s orbital (Eq. (10.258)):

$$\mathbf{F}_{\text{diamagnetic}} = -\left(\frac{2}{3} + \frac{1}{3} - \frac{2}{3}\right) \frac{\hbar^2}{4m_e r_{16}^2 r_{12}} \sqrt{s(s+1)} \mathbf{i}_r = -\left(\frac{1}{3}\right) \frac{\hbar^2}{4m_e r_{16}^2 r_{12}} \sqrt{s(s+1)} \mathbf{i}_r \quad (10.343)$$

From Eq. (10.261), $\mathbf{F}_{\text{mag } 2}$ corresponding to the spin and orbital angular momenta of the paired $2p_x$, p_y , and p_z electrons is

$$\mathbf{F}_{\text{mag } 2} = (4 + 4 + 4) \frac{1}{Z} \frac{\hbar^2}{m_e r_{16}^2 r_{12}} \sqrt{s(s+1)} \mathbf{i}_r = \frac{1}{Z} \frac{12\hbar^2}{m_e r_{16}^2 r_{12}} \sqrt{s(s+1)} \mathbf{i}_r \quad (10.344)$$

and the contribution from the 3p level is

$$\mathbf{F}_{\text{mag } 2} = (8 + 4 + 4 - 4) \frac{1}{Z} \frac{\hbar^2}{m_e r_{16}^2 r_{12}} \sqrt{s(s+1)} \mathbf{i}_r = \frac{1}{Z} \frac{12\hbar^2}{m_e r_{16}^2 r_{12}} \sqrt{s(s+1)} \mathbf{i}_r \quad (10.345)$$

corresponding to the $3p_x$ (Eq. (10.264)) and p_z (Eq. (10.263)) electrons wherein the contribution due to the $3p_x$ ($m = 1$) electron is canceled by the mirror charge-density wave with $m = 1$ induced in the 3s orbital (Eq. (10.262)). Thus, the total of $\mathbf{F}_{\text{mag } 2}$ is

$$\mathbf{F}_{\text{mag } 2} = \frac{1}{Z} \frac{24\hbar^2}{m_e r_{16}^2 r_{12}} \sqrt{s(s+1)} \mathbf{i}_r \quad (10.346)$$

The diamagnetic force, $\mathbf{F}_{\text{diamagnetic } 2}$, due to the binding of the 3p-orbital electron having an electric field outside of its radius is given by Eq. (10.268):

$$\mathbf{F}_{\text{diamagnetic } 2} = -\left[\frac{Z-16}{Z-15}\right] \left(1 - \frac{\sqrt{2}}{2} + \frac{1}{2}\right) \frac{r_{12} \hbar^2}{m_e r_{16}^4} 10 \sqrt{s(s+1)} \mathbf{i}_r \quad (10.347)$$

In the case that $Z > 16$, the radius of the outer electron is calculated by equating the outward centrifugal force to the sum of the electric (Eq. (10.334)), diamagnetic (Eqs. (10.343) and (10.347)), and paramagnetic (Eq. (10.346)) forces as follows:

$$\begin{aligned} \frac{m_e v_{16}^2}{r_{16}} = & \frac{(Z-15)e^2}{4\pi\epsilon_0 r_{16}^2} - \frac{\hbar^2}{12m_e r_{16}^2 r_{12}} \sqrt{s(s+1)} + \frac{24\hbar^2}{Zm_e r_{16}^2 r_{12}} \sqrt{s(s+1)} \\ & - \left[\frac{Z-16}{Z-15}\right] \left(1 - \frac{\sqrt{2}}{2} + \frac{1}{2}\right) \frac{r_{12} \hbar^2}{m_e r_{16}^4} 10 \sqrt{s(s+1)} \end{aligned} \quad (10.348)$$

Substitution of $v_{16} = \frac{\hbar}{m_e r_{16}}$ (Eq. (1.56)) and $s = \frac{1}{2}$ into Eq. (10.348) gives:

$$\frac{\hbar^2}{m_e r_{16}^3} = \frac{(Z-15)e^2}{4\pi\epsilon_0 r_{16}^2} - \frac{\hbar^2}{12m_e r_{16}^2 r_{12}} \sqrt{\frac{3}{4}} + \frac{24\hbar^2}{Zm_e r_{16}^2 r_{12}} \sqrt{\frac{3}{4}} - \left[\frac{Z-16}{Z-15}\right] \left(1 - \frac{\sqrt{2}}{2} + \frac{1}{2}\right) \frac{r_{12} \hbar^2}{m_e r_{16}^4} 10 \sqrt{\frac{3}{4}} \quad (10.349)$$

The quadratic equation corresponding to Eq. (10.349) is

$$\left(\frac{(Z-15)e^2}{4\pi\epsilon_0} - \left(\frac{1}{12} - \frac{24}{Z}\right) \frac{\hbar^2}{m_e r_{12}} \sqrt{\frac{3}{4}}\right) r_{16}^2 - \frac{\hbar^2}{m_e} r_{16} - \left[\frac{Z-16}{Z-15}\right] \left(1 - \frac{\sqrt{2}}{2} + \frac{1}{2}\right) \frac{r_{12} \hbar^2}{m_e} 10 \sqrt{\frac{3}{4}} = 0 \quad (10.350)$$

$$r_{16}^2 - \frac{\frac{\hbar^2}{m_e}}{\left(\frac{(Z-15)e^2}{4\pi\epsilon_0} - \left(\frac{1}{12} - \frac{24}{Z}\right)\frac{\hbar^2}{m_e r_{12}}\sqrt{\frac{3}{4}}\right)} r_{16} - \frac{\frac{\hbar^2}{m_e} \left[\frac{Z-16}{Z-15}\right] \left(1 - \frac{\sqrt{2}}{2} + \frac{1}{2}\right) r_{12} 10\sqrt{\frac{3}{4}}}{\left(\frac{(Z-15)e^2}{4\pi\epsilon_0} - \left(\frac{1}{12} - \frac{24}{Z}\right)\frac{\hbar^2}{m_e r_{12}}\sqrt{\frac{3}{4}}\right)} = 0 \quad (10.351)$$

The solution of Eq. (10.351) using the quadratic formula is:

$$r_{16} = \frac{\frac{\hbar^2}{m_e}}{\left(\frac{(Z-15)e^2}{4\pi\epsilon_0} - \left(\frac{1}{12} - \frac{24}{Z}\right)\frac{\hbar^2}{m_e r_{12}}\sqrt{\frac{3}{4}}\right)} \pm \frac{\sqrt{\left(\frac{\hbar^2}{m_e}\right)^2 - 4 \left(\frac{(Z-15)e^2}{4\pi\epsilon_0} - \left(\frac{1}{12} - \frac{24}{Z}\right)\frac{\hbar^2}{m_e r_{12}}\sqrt{\frac{3}{4}}\right) \frac{\hbar^2}{m_e} \left[\frac{Z-16}{Z-15}\right] \left(1 - \frac{\sqrt{2}}{2} + \frac{1}{2}\right) r_{12} 10\sqrt{\frac{3}{4}}}}{2} \quad (10.352)$$

$$r_{16} = \frac{\frac{a_0}{\left((Z-15) - \left(\frac{1}{24} - \frac{12}{Z}\right)\frac{\sqrt{3}}{r_{12}}\right)} \pm a_0 \sqrt{\left(\frac{1}{\left((Z-15) - \left(\frac{1}{24} - \frac{12}{Z}\right)\frac{\sqrt{3}}{r_{12}}\right)}\right)^2 - 20\sqrt{3} \left[\frac{Z-16}{Z-15}\right] \left(1 - \frac{\sqrt{2}}{2} + \frac{1}{2}\right) r_{12}}}{2} \quad (10.353)$$

r_{12} in units of a_0

where r_{12} is given by Eq. (10.255). The positive root of Eq. (10.353) must be taken in order that $r_{16} > 0$. The final radius of electron 16, r_{16} , is given by Eq. (10.353); this is also the final radius of electrons 13, 14, and 15. The radii of several sixteen-electron atoms are given in Table 10.15.

The ionization energies for the sixteen-electron atoms with $Z > 16$ are given by the electric energy, $E(\text{electric})$, (Eq. (10.102) with the radii r_{16} , given by Eq. (10.353)):

$$E(\text{Ionization}) = -\text{Electric Energy} = \frac{(Z-15)e^2}{8\pi\epsilon_0 r_{16}} \quad (10.354)$$

Since the relativistic corrections were small, the nonrelativistic ionization energies for experimentally measured sixteen-electron atoms are given

in Table 10.15.

Table 10.15. Ionization energies for some sixteen-electron atoms.

16 e Atom	Z	r_1 (a_o) ^a	r_3 (a_o) ^b	r_{10} (a_o) ^c	r_{12} (a_o) ^d	r_{16} (a_o) ^e	Theoretical Ionization Energies ^f (eV)	Experimental Ionization Energies ^g (eV)	Relative Error ^h
S	16	0.06306	0.27053	0.33902	0.96729	1.32010	10.30666	10.36001	0.0051
Cl ⁺	17	0.05932	0.25344	0.31190	0.86545	1.10676	24.5868	23.814	-0.0324
Ar ²⁺	18	0.05599	0.23839	0.28878	0.78276	1.02543	39.8051	40.74	0.0229
K ³⁺	19	0.05302	0.22503	0.26884	0.71450	0.92041	59.1294	60.91	0.0292
Ca ⁴⁺	20	0.05035	0.21308	0.25149	0.65725	0.82819	82.1422	84.50	0.0279
Sc ⁵⁺	21	0.04794	0.20235	0.23625	0.60857	0.75090	108.7161	110.68	0.0177
Ti ⁶⁺	22	0.04574	0.19264	0.22276	0.56666	0.68622	138.7896	140.8	0.0143
V ⁷⁺	23	0.04374	0.18383	0.21074	0.53022	0.63163	172.3256	173.4	0.0062
Cr ⁸⁺	24	0.04191	0.17579	0.19995	0.49822	0.58506	209.2996	209.3	0.0000
Mn ⁹⁺	25	0.04022	0.16842	0.19022	0.46990	0.54490	249.6938	248.3	-0.0056
Fe ¹⁰⁺	26	0.03867	0.16165	0.18140	0.44466	0.50994	293.4952	290.2	-0.0114
Co ¹¹⁺	27	0.03723	0.15540	0.17336	0.42201	0.47923	340.6933	336	-0.0140
Ni ¹²⁺	28	0.03589	0.14961	0.16601	0.40158	0.45204	391.2802	384	-0.0190
Cu ¹³⁺	29	0.03465	0.14424	0.15926	0.38305	0.42781	445.2492	435	-0.0236
Zn ¹⁴⁺	30	0.03349	0.13925	0.15304	0.36617	0.40607	502.5950	490	-0.0257

^a Radius of the paired 1s inner electrons of sixteen-electron atoms from Eq. (10.51).

^b Radius of the paired 2s inner electrons of sixteen-electron atoms from Eq. (10.62).

^c Radius of the three sets of paired 2p inner electrons of sixteen-electron atoms from Eq. (10.212)).

^d Radius of the paired 3s inner electrons of sixteen-electron atoms from Eq. (10.255)).

^e Radius of the two paired and two unpaired 3p outer electrons of sixteen-electron atoms from Eq. (10.353) for $Z > 16$ and Eq. (10.341) for S.

^f Calculated ionization energies of sixteen-electron atoms given by the electric energy (Eq. (10.354)).

^g From theoretical calculations, interpolation of isoelectronic and spectral series, and experimental data [2-3].

^h (Experimental-theoretical)/experimental.

The agreement between the experimental and calculated values of Table 10.15 is well within the experimental capability of the spectroscopic determinations including the values at large Z which relies on X-ray spectroscopy. In this case, the experimental capability is three to four significant figures which is consistent with the last column. The sulfur atom isoelectronic series is given in Table 10.15 [2-3] to much higher precision than the capability of X-ray spectroscopy, but these values are based on theoretical and interpolation techniques rather than data alone. Ionization energies are difficult to determine since the cut-off

of the Rydberg series of lines at the ionization energy is often not observed, and the ionization energy must be determined from theoretical calculations, interpolation of S isoelectronic and Rydberg series, as well as direct experimental data.

SEVENTEEN-ELECTRON ATOMS

Seventeen-electron atoms can be solved exactly using the results of the solutions of one, two, three, four, five, six, seven, eight, nine, ten, eleven, twelve, thirteen, fourteen, fifteen, and sixteen-electron atoms.

RADIUS AND IONIZATION ENERGY OF AN OUTER ELECTRON OF THE CHLORINE ATOM

For each sixteen-electron atom having a central charge of Z times that of the proton, there are two indistinguishable spin-paired electrons in an orbitsphere with radii r_1 and r_2 both given by Eq. (7.19) (Eq. (10.51)), two indistinguishable spin-paired electrons in an orbitsphere with radii r_3 and r_4 both given by Eq. (10.62), three sets of paired electrons in an orbitsphere at r_{10} given by Eq. (10.212), two indistinguishable spin-paired electrons in an orbitsphere with radii r_{11} and r_{12} both given by Eq. (10.255), and two paired and two unpaired electrons in an orbitsphere with radius r_{16} given by Eq. (10.353). For $Z \geq 17$, the next electron which binds to form the corresponding seventeen-electron atom is attracted by the central Coulomb field and is repelled by diamagnetic forces due to the 3 sets of spin-paired inner 2p electrons and two spin-paired inner 3s electrons. A paramagnetic spin-pairing force to form a filled s orbital is also possible, but the force due to the spin-pairing of the electrons (Eq. (7.15) with the radius r_{17}) reduces the energy of the atom less than that due to the alternative forces on two sets of paired electrons and an unpaired 3p electron in an orbitsphere at the same radius r_{17} . The resulting electron configuration is $1s^2 2s^2 2p^6 3s^2 3p^5$, and the orbital arrangement is

$$\begin{array}{ccc} \uparrow \downarrow & \uparrow \downarrow & \uparrow \\ 1 & 0 & -1 \end{array} \quad (10.355)$$

corresponding to the ground state $^2P_{3/2}^0$.

The central Coulomb force acts on the outer electron to cause it to bind wherein this electric force on the outer-most electron due to the nucleus and the inner sixteen electrons is given by Eq. (10.70) with the appropriate charge and radius:

$$\mathbf{F}_{ele} = \frac{(Z-16)e^2}{4\pi\epsilon_0 r_{17}^2} \mathbf{i}_r \quad (10.356)$$

for $r > r_{16}$.

The diamagnetic force, $F_{\text{diamagnetic}}$, is only due to 3p and 3s electrons when the 3p shell is at least half filled since the induced charge-density waves only involve the inner-most shell, the 3s orbital. Thus, $F_{\text{diamagnetic}}$ is given by Eq. (10.258) as the contribution from the $3p_y$ orbital corresponding to $m = -1$ with the cancellation of the orbital angular momenta of the spin-paired $3p_x$ and p_z electrons:

$$F_{\text{diamagnetic}} = -\left(\frac{2}{3}\right) \frac{\hbar^2}{4m_e r_{17}^2 r_{12}} \sqrt{s(s+1)} \mathbf{i}_r \quad (10.357)$$

The energy is minimized with conservation of angular momentum when the spin angular momentum of the 3s orbital superimposes negatively with the angular momenta of the 3p orbitals. From Eq. (10.260), $F_{\text{mag } 2}$ corresponding to the sum of the spin angular momenta of the $3p_x$ and $3p_z$ orbitals and the orbital angular momentum of the $3p_y$ orbital, minus the contribution from the 3s orbital is

$$F_{\text{mag } 2} = (1+1+1-1) \frac{1}{Z} \frac{\hbar^2}{m_e r_{17}^2 r_{12}} \sqrt{s(s+1)} \mathbf{i}_r = \frac{1}{Z} \frac{2\hbar^2}{m_e r_{17}^2 r_{12}} \sqrt{s(s+1)} \mathbf{i}_r \quad (10.358)$$

The outward centrifugal force on electron 17 is balanced by the electric force and the magnetic forces (on electron 17). The radius of the outer electron is calculated by equating the outward centrifugal force to the sum of the electric (Eq. (10.356)), diamagnetic (Eq. (10.357)), and paramagnetic (Eq. (10.358)) forces as follows:

$$\frac{m_e v_{17}^2}{r_{17}} = \frac{(Z-16)e^2}{4\pi\epsilon_0 r_{17}^2} - \frac{2\hbar^2}{12m_e r_{17}^2 r_{12}} \sqrt{s(s+1)} + \frac{2\hbar^2}{Zm_e r_{17}^2 r_{12}} \sqrt{s(s+1)} \quad (10.359)$$

Substitution of $v_{17} = \frac{\hbar}{m_e r_{17}}$ (Eq. (1.56)) and $s = \frac{1}{2}$ into Eq. (10.359) gives:

$$\frac{\hbar^2}{m_e r_{17}^3} = \frac{(Z-16)e^2}{4\pi\epsilon_0 r_{17}^2} - \frac{2\hbar^2}{12m_e r_{17}^2 r_{12}} \sqrt{\frac{3}{4}} + \frac{2\hbar^2}{Zm_e r_{17}^2 r_{12}} \sqrt{\frac{3}{4}} \quad (10.360)$$

$$r_{17} = \frac{\frac{\hbar^2}{m_e}}{\frac{(Z-16)e^2}{4\pi\epsilon_0} - \frac{2\hbar^2}{12m_e r_{12}} \sqrt{\frac{3}{4}} + \frac{2\hbar^2}{Zm_e r_{12}} \sqrt{\frac{3}{4}}} \quad (10.361)$$

$$r_{17} = \frac{a_0}{(Z-16) - \left(\frac{2}{12} - \frac{2}{Z}\right) \frac{\sqrt{\frac{3}{4}}}{r_{12}}}, \quad r_{12} \text{ in units of } a_0 \quad (10.362)$$

Substitution of $\frac{r_{12}}{a_0} = 0.86545$ (Eq. (10.255) with $Z=17$) into Eq. (10.362) gives

$$r_{17} = 1.05158a_0 \quad (10.363)$$

The ionization energy of the chlorine atom is given by the electric energy, $E(\text{electric})$, (Eq. (10.102) with the radius, r_{17} , given by Eq. (10.363)):

$$E(\text{ionization}; \text{Cl}) = -\text{Electric Energy} = \frac{(Z-16)e^2}{8\pi\epsilon_0 r_{17}} = 12.93841 \text{ eV} \quad (10.364)$$

where $r_{17} = 1.05158a_0$ (Eq. (10.363)) and $Z=17$. The experimental ionization energy of the chlorine atom is 12.96764 eV [3].

THE IONIZATION ENERGIES OF SEVENTEEN-ELECTRON ATOMS WITH A NUCLEAR CHARGE $Z>17$

Seventeen-electron atoms having $Z>17$ possess an external electric field given by Eq. (10.92). In this case, an energy minimum is achieved with conservation of momentum when the orbital angular momentum is such that $F_{\text{diamagnetic}}$ is minimized while $F_{\text{mag } 2}$ is maximized. With a filled 3p shell, the diamagnetic force due to the orbital angular momenta of the 3p electrons cancels that of the 2p electrons. Thus, $F_{\text{diamagnetic}}$ is minimized by the formation of a charge-density wave in the 3s orbital corresponding to two electrons with $m = -1$ in Eq. (10.258) to form the equivalent of a filled 3p level such that the contribution due to the 2p level is canceled. From Eq. (10.82), the diamagnetic force, $F_{\text{diamagnetic}}$, is given by the contribution due to the charge-density wave with $m = -1$ induced in the 3s orbital according to Eq. (10.258):

$$F_{\text{diamagnetic}} = -\left(\frac{2}{3}\right) \frac{\hbar^2}{4m_e r_{17}^2 r_{12}} \sqrt{s(s+1)} \mathbf{i}_r \quad (10.365)$$

From Eqs. (10.205) and (10.261), $F_{\text{mag } 2}$ corresponding to the spin and orbital angular momenta of the paired $2p_x$, p_y , and p_z electrons is

$$F_{\text{mag } 2} = (4+4+4) \frac{1}{Z} \frac{\hbar^2}{m_e r_{17}^2 r_{12}} \sqrt{s(s+1)} \mathbf{i}_r = \frac{1}{Z} \frac{12\hbar^2}{m_e r_{17}^2 r_{12}} \sqrt{s(s+1)} \mathbf{i}_r \quad (10.366)$$

and the contribution from the paired $3p_x$, p_y , and p_z electrons given by Eq. (10.264) is

$$F_{\text{mag } 2} = (8+8+8) \frac{1}{Z} \frac{\hbar^2}{m_e r_{17}^2 r_{12}} \sqrt{s(s+1)} \mathbf{i}_r = \frac{1}{Z} \frac{24\hbar^2}{m_e r_{17}^2 r_{12}} \sqrt{s(s+1)} \mathbf{i}_r \quad (10.367)$$

wherein the contribution due to the charge-density wave with $m = -1$ induced in the 3s orbital (Eq. (10.262)) provides the equivalent of a filled $3p_y$ orbital and adds a negative contribution of

$$F_{\text{mag } 2} = -\frac{1}{Z} \frac{4\hbar^2}{m_e r_{17}^2 r_{12}} \sqrt{s(s+1)} \mathbf{i}_r \quad (10.368)$$

Thus, the total of $F_{\text{mag } 2}$ is

$$\mathbf{F}_{mag 2} = \frac{1}{Z} \frac{32\hbar^2}{m_e r_{17}^2 r_{12}} \sqrt{s(s+1)} \mathbf{i}_r \quad (10.369)$$

The diamagnetic force, $\mathbf{F}_{diamagnetic 2}$, due to the binding of the 3p-orbital electron having an electric field outside of its radius is given by Eq. (10.268):

$$\mathbf{F}_{diamagnetic 2} = -\left[\frac{Z-17}{Z-16} \right] \left(1 - \frac{\sqrt{2}}{2} + \frac{1}{2} \right) \frac{r_{12} \hbar^2}{m_e r_{17}^4} 10 \sqrt{s(s+1)} \mathbf{i}_r \quad (10.370)$$

In the case that $Z > 17$, the radius of the outer electron is calculated by equating the outward centrifugal force to the sum of the electric (Eq. (10.356)), diamagnetic (Eqs. (10.365) and (10.370)), and paramagnetic (Eq. (10.369)) forces as follows:

$$\begin{aligned} \frac{m_e v_{17}^2}{r_{17}} = & \frac{(Z-16)e^2}{4\pi\epsilon_0 r_{17}^2} - \frac{2\hbar^2}{12m_e r_{17}^2 r_{12}} \sqrt{s(s+1)} + \frac{32\hbar^2}{Zm_e r_{17}^2 r_{12}} \sqrt{s(s+1)} \\ & - \left[\frac{Z-17}{Z-16} \right] \left(1 - \frac{\sqrt{2}}{2} + \frac{1}{2} \right) \frac{r_{12} \hbar^2}{m_e r_{17}^4} 10 \sqrt{s(s+1)} \end{aligned} \quad (10.371)$$

Substitution of $v_{17} = \frac{\hbar}{m_e r_{17}}$ (Eq. (1.56)) and $s = \frac{1}{2}$ into Eq. (10.371) gives:

$$\frac{\hbar^2}{m_e r_{17}^3} = \frac{(Z-16)e^2}{4\pi\epsilon_0 r_{17}^2} - \frac{2\hbar^2}{12m_e r_{17}^2 r_{12}} \sqrt{\frac{3}{4}} + \frac{32\hbar^2}{Zm_e r_{17}^2 r_{12}} \sqrt{\frac{3}{4}} - \left[\frac{Z-17}{Z-16} \right] \left(1 - \frac{\sqrt{2}}{2} + \frac{1}{2} \right) \frac{r_{12} \hbar^2}{m_e r_{17}^4} 10 \sqrt{\frac{3}{4}} \quad (10.372)$$

The quadratic equation corresponding to Eq. (10.372) is

$$\left(\frac{(Z-16)e^2}{4\pi\epsilon_0} - \left(\frac{2}{12} - \frac{32}{Z} \right) \frac{\hbar^2}{m_e r_{12}} \sqrt{\frac{3}{4}} \right) r_{17}^2 - \frac{\hbar^2}{m_e} r_{17} - \left[\frac{Z-17}{Z-16} \right] \left(1 - \frac{\sqrt{2}}{2} + \frac{1}{2} \right) \frac{r_{12} \hbar^2}{m_e} 10 \sqrt{\frac{3}{4}} = 0 \quad (10.373)$$

$$r_{17}^2 - \frac{\frac{\hbar^2}{m_e}}{\left(\frac{(Z-16)e^2}{4\pi\epsilon_0} - \left(\frac{2}{12} - \frac{32}{Z} \right) \frac{\hbar^2}{m_e r_{12}} \sqrt{\frac{3}{4}} \right)} r_{17} - \frac{\frac{\hbar^2}{m_e} \left[\frac{Z-17}{Z-16} \right] \left(1 - \frac{\sqrt{2}}{2} + \frac{1}{2} \right) r_{12} 10 \sqrt{\frac{3}{4}}}{\left(\frac{(Z-16)e^2}{4\pi\epsilon_0} - \left(\frac{2}{12} - \frac{32}{Z} \right) \frac{\hbar^2}{m_e r_{12}} \sqrt{\frac{3}{4}} \right)} = 0 \quad (10.374)$$

The solution of Eq. (10.374) using the quadratic formula is:

$$r_{17} = \frac{\frac{\hbar^2}{m_e} \left(\frac{(Z-16)e^2}{4\pi\epsilon_0} - \left(\frac{2}{12} - \frac{32}{Z} \right) \frac{\hbar^2}{m_e r_{12}} \sqrt{\frac{3}{4}} \right) \pm \sqrt{\left(\frac{\hbar^2}{m_e} \left(\frac{(Z-16)e^2}{4\pi\epsilon_0} - \left(\frac{2}{12} - \frac{32}{Z} \right) \frac{\hbar^2}{m_e r_{12}} \sqrt{\frac{3}{4}} \right) \right)^2 + 4 \frac{\hbar^2}{m_e} \left[\frac{Z-17}{Z-16} \right] \left(1 - \frac{\sqrt{2}}{2} + \frac{1}{2} \right) r_{12}^{10} \sqrt{\frac{3}{4}} \left(\frac{(Z-16)e^2}{4\pi\epsilon_0} - \left(\frac{2}{12} - \frac{32}{Z} \right) \frac{\hbar^2}{m_e r_{12}} \sqrt{\frac{3}{4}} \right)}}{2} \quad (10.375)$$

$$r_{17} = \frac{\frac{a_0}{\left((Z-16) - \left(\frac{1}{12} - \frac{16}{Z} \right) \frac{\sqrt{3}}{r_{12}} \right)} \pm a_0 \sqrt{\left(\frac{1}{\left((Z-16) - \left(\frac{1}{12} - \frac{16}{Z} \right) \frac{\sqrt{3}}{r_{12}} \right)} \right)^2 + 20\sqrt{3} \left[\frac{Z-17}{Z-16} \right] \left(1 - \frac{\sqrt{2}}{2} + \frac{1}{2} \right) r_{12} \left((Z-16) - \left(\frac{1}{12} - \frac{16}{Z} \right) \frac{\sqrt{3}}{r_{12}} \right)}}{2} \quad (10.376)$$

r_{12} in units of a_0

where r_{12} is given by Eq. (10.255). The positive root of Eq. (10.376) must be taken in order that $r_{17} > 0$. The final radius of electron 17, r_{17} , is given by Eq. (10.376); this is also the final radius of electrons 13, 14, 15, and 16. The radii of several seventeen-electron atoms are given in Table 10.16.

The ionization energies for the seventeen-electron atoms with $Z > 17$ are given by the electric energy, $E(\text{electric})$, (Eq. (10.102) with the radii r_{17} , given by Eq. (10.376)):

$$E(\text{ionization}) = -\text{Electric Energy} = \frac{(Z-16)e^2}{8\pi\epsilon_0 r_{17}} \quad (10.377)$$

Since the relativistic corrections were small, the nonrelativistic ionization energies for experimentally measured seventeen-electron atoms are given in Table 10.16.

Table 10.16. Ionization energies for some seventeen-electron atoms.

17 e Atom	Z	r_1 (a_0) ^a	r_3 (a_0) ^b	r_{10} (a_0) ^c	r_{12} (a_0) ^d	r_{17} (a_0) ^e	Theoretical Ionization Energies ^f (eV)	Experimental Ionization Energies ^g (eV)	Relative Error ^h
<i>Cl</i>	17	0.05932	0.25344	0.31190	0.86545	1.05158	12.93841	12.96764	0.0023
<i>Ar</i> ⁺	18	0.05599	0.23839	0.28878	0.78276	0.98541	27.6146	27.62967	0.0005
<i>K</i> ²⁺	19	0.05302	0.22503	0.26884	0.71450	0.93190	43.8001	45.806	0.0438
<i>Ca</i> ³⁺	20	0.05035	0.21308	0.25149	0.65725	0.84781	64.1927	67.27	0.0457
<i>Sc</i> ⁴⁺	21	0.04794	0.20235	0.23625	0.60857	0.77036	88.3080	91.65	0.0365
<i>Ti</i> ⁵⁺	22	0.04574	0.19264	0.22276	0.56666	0.70374	116.0008	119.53	0.0295
<i>V</i> ⁶⁺	23	0.04374	0.18383	0.21074	0.53022	0.64701	147.2011	150.6	0.0226
<i>Cr</i> ⁷⁺	24	0.04191	0.17579	0.19995	0.49822	0.59849	181.8674	184.7	0.0153
<i>Mn</i> ⁸⁺	25	0.04022	0.16842	0.19022	0.46990	0.55667	219.9718	221.8	0.0082
<i>Fe</i> ⁹⁺	26	0.03867	0.16165	0.18140	0.44466	0.52031	261.4942	262.1	0.0023
<i>Co</i> ¹⁰⁺	27	0.03723	0.15540	0.17336	0.42201	0.48843	306.4195	305	-0.0047
<i>Ni</i> ¹¹⁺	28	0.03589	0.14961	0.16601	0.40158	0.46026	354.7360	352	-0.0078
<i>Cu</i> ¹²⁺	29	0.03465	0.14424	0.15926	0.38305	0.43519	406.4345	401	-0.0136
<i>Zn</i> ¹³⁺	30	0.03349	0.13925	0.15304	0.36617	0.41274	461.5074	454	-0.0165

^a Radius of the paired 1s inner electrons of seventeen-electron atoms from Eq. (10.51).^b Radius of the paired 2s inner electrons of seventeen-electron atoms from Eq. (10.62).^c Radius of the three sets of paired 2p inner electrons of seventeen-electron atoms from Eq. (10.212)).^d Radius of the paired 3s inner electrons of seventeen-electron atoms from Eq. (10.255)).^e Radius of the two sets of paired and an unpaired 3p outer electron of seventeen-electron atoms from Eq. (10.376) for $Z > 17$ and Eq. (10.363) for *Cl*.^f Calculated ionization energies of seventeen-electron atoms given by the electric energy (Eq. (10.377)).^g From theoretical calculations, interpolation of isoelectronic and spectral series, and experimental data [2-3].^h (Experimental-theoretical)/experimental.

The agreement between the experimental and calculated values of Table 10.16 is well within the experimental capability of the spectroscopic determinations including the values at large Z which relies on X-ray spectroscopy. In this case, the experimental capability is about two to four significant figures which is consistent with the last column. Ionization energies are difficult to determine since the cut-off of the Rydberg series of lines at the ionization energy is often not observed. Thus, the chlorine atom isoelectronic series given in Table 10.16 [2-3] relies on theoretical calculations and interpolation of the Cl isoelectronic and Rydberg series as well as direct experimental data to extend the precision beyond the capability of X-ray spectroscopy. But, no assurances can be given that these techniques are correct, and they may not improve

the results. The error given in the last column is very reasonable given the quality of the data.

EIGHTEEN-ELECTRON ATOMS

Eighteen-electron atoms can be solved exactly using the results of the solutions of one, two, three, four, five, six, seven, eight, nine, ten, eleven, twelve, thirteen, fourteen, fifteen, sixteen, and seventeen-electron atoms.

RADIUS AND IONIZATION ENERGY OF AN OUTER ELECTRON OF THE ARGON ATOM

For each seventeen-electron atom having a central charge of Z times that of the proton, there are two indistinguishable spin-paired electrons in an orbitsphere with radii r_1 and r_2 both given by Eq. (7.19) (Eq. (10.51)), two indistinguishable spin-paired electrons in an orbitsphere with radii r_3 and r_4 both given by Eq. (10.62), three sets of paired electrons in an orbitsphere at r_5 given by Eq. (10.212), two indistinguishable spin-paired electrons in an orbitsphere with radii r_{11} and r_{12} both given by Eq. (10.255), and two sets of paired and an unpaired electron in an orbitsphere with radius r_{17} given by Eq. (10.376). For $Z \geq 18$, the next electron which binds to form the corresponding eighteen-electron atom is attracted by the central Coulomb field and is repelled by diamagnetic forces due to the 3 sets of spin-paired inner 2p electrons and two spin-paired inner 3s electrons. A paramagnetic spin-pairing force to form a filled s orbital is also possible, but the force due to the spin-pairing of the electrons (Eq. (7.15) with the radius r_{18}) reduces the energy of the atom less than that due to the alternative forces on three sets of paired 3p electrons in an orbitsphere at the same radius r_{18} . The resulting electron configuration is $1s^2 2s^2 2p^6 3s^2 3p^6$, and the orbital arrangement is

$$\begin{array}{ccc} \uparrow \downarrow & \uparrow \downarrow & \uparrow \downarrow \\ 1 & 0 & -1 \end{array} \quad (10.378)$$

corresponding to the ground state 1S_0 .

The central Coulomb force acts on the outer electron to cause it to bind wherein this electric force on the outer-most electron due to the nucleus and the inner seventeen electrons is given by Eq. (10.70) with the appropriate charge and radius:

$$\mathbf{F}_{ele} = \frac{(Z-17)e^2}{4\pi\epsilon_0 r_{18}^2} \mathbf{j}_r \quad (10.379)$$

for $r > r_{17}$.

As in the case on the neon atom, the energy of the argon atom is minimized and the angular momentum is conserved with the pairing of electron eighteen to fill the $3p_y$ orbital when the orbital angular momenta of each set of the $3p_x$, p_y , and p_z spin-paired electrons adds negatively to cancel. Then, the diamagnetic force (Eq. (10.258)), $F_{\text{diamagnetic}}$, is given by the induced orbital angular momentum of the $3s$ orbital alone which conserves angular momentum.

$$F_{\text{diamagnetic}} = -\left(\frac{1}{3}\right) \frac{\hbar^2}{4m_e r_{18}^2 r_{12}} \sqrt{s(s+1)} \mathbf{i}_r \quad (10.380)$$

From Eq. (10.260), $F_{\text{mag } 2}$ is

$$F_{\text{mag } 2} = (1+1+1+1) \frac{1}{Z} \frac{\hbar^2}{m_e r_{18}^2 r_{12}} \sqrt{s(s+1)} \mathbf{i}_r = \frac{1}{Z} \frac{4\hbar^2}{m_e r_{18}^2 r_{12}} \sqrt{s(s+1)} \mathbf{i}_r \quad (10.381)$$

corresponding to the spin-angular-momentum contribution alone from each of the $3p_x$, p_y , and p_z orbitals and the spin angular momentum of the $3s$ orbital.

The outward centrifugal force on electron 18 is balanced by the electric force and the magnetic forces (on electron 18). The radius of the outer electron is calculated by equating the outward centrifugal force to the sum of the electric (Eq. (10.379)), diamagnetic (Eq. (10.380)), and paramagnetic (Eq. (10.381)) forces as follows:

$$\frac{m_e v_{18}^2}{r_{18}} = \frac{(Z-17)e^2}{4\pi\epsilon_0 r_{18}^2} - \frac{\hbar^2}{12m_e r_{18}^2 r_{12}} \sqrt{s(s+1)} + \frac{4\hbar^2}{Zm_e r_{18}^2 r_{12}} \sqrt{s(s+1)} \quad (10.382)$$

Substitution of $v_{18} = \frac{\hbar}{m_e r_{18}}$ (Eq. (1.56)) and $s = \frac{1}{2}$ into Eq. (10.382) gives:

$$\frac{\hbar^2}{m_e r_{18}^3} = \frac{(Z-17)e^2}{4\pi\epsilon_0 r_{18}^2} - \frac{\hbar^2}{12m_e r_{18}^2 r_{12}} \sqrt{\frac{3}{4}} + \frac{4\hbar^2}{Zm_e r_{18}^2 r_{12}} \sqrt{\frac{3}{4}} \quad (10.383)$$

$$r_{18} = \frac{\frac{\hbar^2}{m_e}}{\frac{(Z-17)e^2}{4\pi\epsilon_0} - \frac{\hbar^2}{12m_e r_{12}} \sqrt{\frac{3}{4}} + \frac{4\hbar^2}{Zm_e r_{12}} \sqrt{\frac{3}{4}}} \quad (10.384)$$

$$r_{18} = \frac{a_0}{(Z-17) - \left(\frac{1}{12} - \frac{4}{Z}\right) \sqrt{\frac{3}{4}} \frac{1}{r_{12}}}, \quad r_{12} \text{ in units of } a_0 \quad (10.385)$$

Substitution of $\frac{r_{12}}{a_0} = 0.78276$ (Eq. (10.255) with $Z=18$) into Eq. (10.385) gives

$$r_{18} = 0.86680 a_0 \quad (10.386)$$

The ionization energy of the argon atom is given by the electric

energy, $E(\text{electric})$, (Eq. (10.102) with the radius, r_{18} , given by Eq. (10.386)):

$$E(\text{ionization}; \text{Ar}) = -\text{Electric Energy} = \frac{(Z-17)e^2}{8\pi\epsilon_0 r_{18}} = 15.69651 \text{ eV} \quad (10.387)$$

where $r_{18} = 0.86680a_0$ (Eq. (10.386)) and $Z=18$. The experimental ionization energy of the argon atom is 15.75962 eV [3].

THE IONIZATION ENERGIES OF EIGHTEEN-ELECTRON ATOMS WITH A NUCLEAR CHARGE $Z>18$

Eighteen-electron atoms having $Z>18$ possess an external electric field given by Eq. (10.92). In this case, an energy minimum is achieved with conservation of momentum when the orbital angular momentum is such that $F_{\text{diamagnetic}}$ is minimized while $F_{\text{mag } 2}$ is maximized. With a filled 3p shell, the diamagnetic force due to the orbital angular momenta of the 3p electrons cancels that of the 2p electrons. Thus, the diamagnetic force (Eq. (10.258)), $F_{\text{diamagnetic}}$, is zero:

$$F_{\text{diamagnetic}} = 0 \quad (10.388)$$

From Eqs. (10.205) and (10.261), $F_{\text{mag } 2}$ corresponding to the spin and orbital angular momenta of the paired $2p_x$, p_y , and p_z electrons is

$$F_{\text{mag } 2} = (4+4+4) \frac{1}{Z} \frac{\hbar^2}{m_e r_{18}^2 r_{12}} \sqrt{s(s+1)} \mathbf{i}_r = \frac{1}{Z} \frac{12\hbar^2}{m_e r_{18}^2 r_{12}} \sqrt{s(s+1)} \mathbf{i}_r, \quad (10.389)$$

the contribution from the 3p level (Eq. (10.264)) is

$$F_{\text{mag } 2} = (8+8+8) \frac{1}{Z} \frac{\hbar^2}{m_e r_{18}^2 r_{12}} \sqrt{s(s+1)} \mathbf{i}_r = \frac{1}{Z} \frac{24\hbar^2}{m_e r_{18}^2 r_{12}} \sqrt{s(s+1)} \mathbf{i}_r, \quad (10.390)$$

and the contribution due to the spin and induced orbital angular momentum of the 3s orbital that achieves conservation of angular momentum given by Eq. (10.262) is

$$F_{\text{mag } 2} = \frac{1}{Z} \frac{4\hbar^2}{m_e r_{18}^2 r_{12}} \sqrt{s(s+1)} \mathbf{i}_r, \quad (10.391)$$

Thus, the total of $F_{\text{mag } 2}$ is

$$F_{\text{mag } 2} = \frac{1}{Z} \frac{40\hbar^2}{m_e r_{18}^2 r_{12}} \sqrt{s(s+1)} \mathbf{i}_r, \quad (10.392)$$

The diamagnetic force, $F_{\text{diamagnetic } 2}$, due to the binding of the 3p-orbital electron having an electric field outside of its radius is given by Eq. (10.268):

$$F_{\text{diamagnetic } 2} = -\left[\frac{Z-18}{Z-17} \right] \left(1 - \frac{\sqrt{2}}{2} + \frac{1}{2} \right) \frac{r_{12}\hbar^2}{m_e r_{18}^4} 10\sqrt{s(s+1)} \mathbf{i}_r, \quad (10.393)$$

In the case that $Z>18$, the radius of the outer electron is calculated by equating the outward centrifugal force to the sum of the electric (Eq. (10.379)), diamagnetic (Eqs. (10.388) and (10.393)), and paramagnetic

(Eq. (10.392)) forces as follows:

$$\frac{m_e v_{18}^2}{r_{18}} = \frac{(Z-17)e^2}{4\pi\epsilon_o r_{18}^2} + \frac{40\hbar^2}{Zm_e r_{18}^2 r_{12}} \sqrt{s(s+1)} - \left[\frac{Z-18}{Z-17} \right] \left(1 - \frac{\sqrt{2}}{2} + \frac{1}{2} \right) \frac{r_{12}\hbar^2}{m_e r_{18}^4} 10\sqrt{s(s+1)} \quad (10.394)$$

Substitution of $v_{18} = \frac{\hbar}{m_e r_{18}}$ (Eq. (1.56)) and $s = \frac{1}{2}$ into Eq. (10.394) gives:

$$\frac{\hbar^2}{m_e r_{18}^3} = \frac{(Z-17)e^2}{4\pi\epsilon_o r_{18}^2} + \frac{40\hbar^2}{Zm_e r_{18}^2 r_{12}} \sqrt{\frac{3}{4}} - \left[\frac{Z-18}{Z-17} \right] \left(1 - \frac{\sqrt{2}}{2} + \frac{1}{2} \right) \frac{r_{12}\hbar^2}{m_e r_{18}^4} 10\sqrt{\frac{3}{4}} \quad (10.395)$$

The quadratic equation corresponding to Eq. (10.395) is

$$\left(\frac{(Z-17)e^2}{4\pi\epsilon_o} + \frac{40\hbar^2}{Zm_e r_{12}} \sqrt{\frac{3}{4}} \right) r_{18}^2 - \frac{\hbar^2}{m_e} r_{18} - \left[\frac{Z-18}{Z-17} \right] \left(1 - \frac{\sqrt{2}}{2} + \frac{1}{2} \right) \frac{r_{12}\hbar^2}{m_e} 10\sqrt{\frac{3}{4}} = 0 \quad (10.396)$$

$$r_{18}^2 - \frac{\frac{\hbar^2}{m_e}}{\left(\frac{(Z-17)e^2}{4\pi\epsilon_o} + \frac{40\hbar^2}{Zm_e r_{12}} \sqrt{\frac{3}{4}} \right)} r_{18} - \frac{\frac{\hbar^2}{m_e} \left[\frac{Z-18}{Z-17} \right] \left(1 - \frac{\sqrt{2}}{2} + \frac{1}{2} \right) r_{12} 10\sqrt{\frac{3}{4}}}{\left(\frac{(Z-17)e^2}{4\pi\epsilon_o} + \frac{40\hbar^2}{Zm_e r_{12}} \sqrt{\frac{3}{4}} \right)} = 0$$

(10.397)

The solution of Eq. (10.397) using the quadratic formula is:

$$r_{18} = \frac{\frac{\hbar^2}{m_e}}{\left(\frac{(Z-17)e^2}{4\pi\epsilon_o} + \frac{40\hbar^2}{Zm_e r_{12}} \sqrt{\frac{3}{4}} \right)} \pm \frac{\sqrt{\left(\frac{\hbar^2}{m_e} \right)^2 - 4 \frac{\frac{\hbar^2}{m_e} \left[\frac{Z-18}{Z-17} \right] \left(1 - \frac{\sqrt{2}}{2} + \frac{1}{2} \right) r_{12} 10\sqrt{\frac{3}{4}}}{\left(\frac{(Z-17)e^2}{4\pi\epsilon_o} + \frac{40\hbar^2}{Zm_e r_{12}} \sqrt{\frac{3}{4}} \right)}}}{2}$$

(10.398)

$$r_{18} = \frac{\frac{a_0}{\left((Z-17) + \frac{20\sqrt{3}}{Zr_{12}}\right)} \pm a_0}{2} \sqrt{\frac{1}{\left((Z-17) + \frac{20\sqrt{3}}{Zr_{12}}\right)} + \frac{20\sqrt{3} \left(\left[\frac{Z-18}{Z-17} \right] \left(1 - \frac{\sqrt{2}}{2} + \frac{1}{2} \right) r_{12} \right)}{\left((Z-17) + \frac{20\sqrt{3}}{Zr_{12}}\right)}}} \quad (10.399)$$

r_{12} in units of a_0

where r_{12} is given by Eq. (10.255). The positive root of Eq. (10.399) must be taken in order that $r_{18} > 0$. The final radius of electron 18, r_{18} , is given by Eq. (10.399); this is also the final radius of electrons 13, 14, 15, 16, and 17. The radii of several eighteen-electron atoms are given in Table 10.17.

The ionization energies for the eighteen-electron atoms with $Z > 18$ are given by the electric energy, $E(\text{electric})$, (Eq. (10.102) with the radii r_{18} , given by Eq. (10.399)):

$$E(\text{Ionization}) = -\text{Electric Energy} = \frac{(Z-17)e^2}{8\pi\epsilon_0 r_{18}} \quad (10.400)$$

Since the relativistic corrections were small, the nonrelativistic ionization energies for experimentally measured eighteen-electron atoms are given in Table 10.17.

Table 10.17. Ionization energies for some eighteen-electron atoms.

18 e Atom	Z	r_1 (a_0) ^a	r_3 (a_0) ^b	r_{10} (a_0) ^c	r_{12} (a_0) ^d	r_{18} (a_0) ^e	Theoretical Ionization Energies ^f (eV)	Experimental Ionization Energies ^g (eV)	Relative Error ^h
Ar	18	0.05599	0.23839	0.28878	0.78276	0.86680	15.69651	15.75962	0.0040
K ⁺	19	0.05302	0.22503	0.26884	0.71450	0.85215	31.9330	31.63	-0.0096
Ca ²⁺	20	0.05035	0.21308	0.25149	0.65725	0.82478	49.4886	50.9131	0.0280
Sc ³⁺	21	0.04794	0.20235	0.23625	0.60857	0.76196	71.4251	73.4894	0.0281
Ti ⁴⁺	22	0.04574	0.19264	0.22276	0.56666	0.70013	97.1660	99.30	0.0215
V ⁵⁺	23	0.04374	0.18383	0.21074	0.53022	0.64511	126.5449	128.13	0.0124
Cr ⁶⁺	24	0.04191	0.17579	0.19995	0.49822	0.59718	159.4836	160.18	0.0043
Mn ⁷⁺	25	0.04022	0.16842	0.19022	0.46990	0.55552	195.9359	194.5	-0.0074
Fe ⁸⁺	26	0.03867	0.16165	0.18140	0.44466	0.51915	235.8711	233.6	-0.0097
Co ⁹⁺	27	0.03723	0.15540	0.17336	0.42201	0.48720	279.2670	275.4	-0.0140
Ni ¹⁰⁺	28	0.03589	0.14961	0.16601	0.40158	0.45894	326.1070	321.0	-0.0159
Cu ¹¹⁺	29	0.03465	0.14424	0.15926	0.38305	0.43379	376.3783	369	-0.0200
Zn ¹²⁺	30	0.03349	0.13925	0.15304	0.36617	0.41127	430.0704	419.7	-0.0247

^a Radius of the paired 1s inner electrons of eighteen-electron atoms from Eq. (10.51).^b Radius of the paired 2s inner electrons of eighteen-electron atoms from Eq. (10.62).^c Radius of the three sets of paired 2p inner electrons of eighteen-electron atoms from Eq. (10.212)).^d Radius of the paired 3s inner electrons of eighteen-electron atoms from Eq. (10.255)).^e Radius of the three sets of paired 3p outer electrons of eighteen-electron atoms from Eq. (10.399) for $Z > 18$ and Eq. (10.386) for Ar.^f Calculated ionization energies of eighteen-electron atoms given by the electric energy (Eq. (10.400)).^g From theoretical calculations, interpolation of isoelectronic and spectral series, and experimental data [2-3].^h (Experimental-theoretical)/experimental.

The agreement between the experimental and calculated values of Table 10.17 is well within the experimental capability of the spectroscopic determinations including the values at large Z which relies on X-ray spectroscopy. In this case, the experimental capability is about two to four significant figures which is consistent with the last column. Ionization energies are difficult to determine since the cut-off of the Rydberg series of lines at the ionization energy is often not observed. Thus, the argon atom isoelectronic series given in Table 10.17 [2-3] relies on theoretical calculations and interpolation of the Ar isoelectronic and Rydberg series as well as direct experimental data to extend the precision beyond the capability of X-ray spectroscopy. But, no assurances can be given that these techniques are correct, and they may not improve the results. The error given in the last column is very reasonable given the

quality of the data.

GENERAL EQUATION FOR THE IONIZATION ENERGIES OF THIRTEEN THROUGH EIGHTEEN-ELECTRON ATOMS

Using the forces given by Eqs. (10.257-10.264), (10.268), and the radii r_{12} given by Eq. (10.255), the radii of the 3p electrons of all thirteen through eighteen-electron atoms may be solved exactly. The electric energy given by Eq. (10.102) gives the corresponding exact ionization energies. A summary of the parameters of the equations that determine the exact radii and ionization energies of all thirteen through eighteen-electron atoms is given in Table 10.18.

F_{ele} and $F_{diamagnetic\ 2}$ given by Eqs. (10.257) and (10.268), respectively, are of the same form for all atoms with the appropriate nuclear charges and atomic radii. $F_{diamagnetic}$ given by Eq. (10.258) and $F_{mag\ 2}$ given by Eqs. (10.259-10.264) are of the same form with the appropriate factors that depend on the electron configuration wherein the electron configuration must be a minimum of energy.

For each n-electron atom having a central charge of Z times that of the proton and an electron configuration $1s^2 2s^2 2p^6 3s^2 3p^{n-12}$, there are two indistinguishable spin-paired electrons in an orbitsphere with radii r_1 and r_2 both given by Eq. (7.19) and (10.51):

$$r_1 = r_2 = a_0 \left[\frac{1}{Z-1} - \frac{\sqrt{\frac{3}{4}}}{Z(Z-1)} \right] \quad (10.401)$$

two indistinguishable spin-paired electrons in an orbitsphere with radii r_3 and r_4 both given by Eq. (10.62):

$$r_4 = r_3 = \frac{a_0 \left(1 - \frac{\sqrt{\frac{3}{4}}}{Z} \right)}{\left((Z-3) - \left(\frac{1}{4} - \frac{1}{Z} \right) \frac{\sqrt{\frac{3}{4}}}{r_1} \right)} \pm a_0 \frac{\left(1 - \frac{\sqrt{\frac{3}{4}}}{Z} \right)^2}{\left((Z-3) - \left(\frac{1}{4} - \frac{1}{Z} \right) \frac{\sqrt{\frac{3}{4}}}{r_1} \right)^2} + 4 \frac{\left[\frac{Z-3}{Z-2} \right] r_1 10 \sqrt{\frac{3}{4}}}{\left((Z-3) - \left(\frac{1}{4} - \frac{1}{Z} \right) \frac{\sqrt{\frac{3}{4}}}{r_1} \right)} \quad (10.402)$$

r_1 in units of a_0

where r_1 is given by Eqs. (10.51) and (10.401), three sets of paired indistinguishable electrons in an orbitsphere with radius r_{10} given by Eq.

(10.212):

$$r_{10} = \frac{\frac{a_0}{\left((Z-9) - \left(\frac{5}{24} - \frac{6}{Z}\right)\frac{\sqrt{3}}{r_3}\right)} \pm a_0}{2} \sqrt{\frac{1}{\left((Z-9) - \left(\frac{5}{24} - \frac{6}{Z}\right)\frac{\sqrt{3}}{r_3}\right)} + \frac{20\sqrt{3}\left(\left[\frac{Z-10}{Z-9}\right]\left(1 - \frac{\sqrt{2}}{2}\right)r_3\right)}{\left((Z-9) - \left(\frac{5}{24} - \frac{6}{Z}\right)\frac{\sqrt{3}}{r_3}\right)}}^2 \quad (10.403)$$

r₃ in units of a₀

where r_3 is given by Eqs. (10.62) and (10.402), two indistinguishable spin-paired electrons in an orbitsphere with radius r_{12} given by Eq. (10.255):

$$r_{12} = \frac{\frac{a_0}{\left((Z-11) - \left(\frac{1}{8} - \frac{3}{Z}\right)\frac{\sqrt{3}}{r_{10}}\right)} \pm a_0}{2} \sqrt{\frac{1}{\left((Z-11) - \left(\frac{1}{8} - \frac{3}{Z}\right)\frac{\sqrt{3}}{r_{10}}\right)} + \frac{20\sqrt{3}\left(\left[\frac{Z-12}{Z-11}\right]\left(1 + \frac{\sqrt{2}}{2}\right)r_{10}\right)}{\left((Z-11) - \left(\frac{1}{8} - \frac{3}{Z}\right)\frac{\sqrt{3}}{r_{10}}\right)}}^2 \quad (10.404)$$

r₁₀ in units of a₀

where r_{10} is given by Eq. (10.212), and $n-12$ electrons in a 3p orbitsphere with radius r_n given by

$$r_n = \frac{\left((Z - (n - 1)) - \left(\frac{A}{8} - \frac{B}{2Z} \right) \frac{\sqrt{3}}{r_{12}} \right) \pm a_0 \sqrt{\frac{1}{\left((Z - (n - 1)) - \left(\frac{A}{8} - \frac{B}{2Z} \right) \frac{\sqrt{3}}{r_{12}} \right)^2} + \frac{20\sqrt{3} \left[\frac{Z - n}{Z - (n - 1)} \right] \left(1 - \frac{\sqrt{2}}{2} + \frac{1}{2} \right) r_{12}}{\left((Z - (n - 1)) - \left(\frac{A}{8} - \frac{B}{2Z} \right) \frac{\sqrt{3}}{r_{12}} \right)}}}{2} \quad (10.405)$$

r_{12} in units of a_0

where r_{12} is given by Eqs. (10.255) and (10.404), the parameter A given in Table 10.18 corresponds to the diamagnetic force, $F_{\text{diamagnetic}}$, (Eq. (10.258)), and the parameter B given in Table 10.18 corresponds to the paramagnetic force, $F_{\text{mag}2}$ (Eqs. (10.260-10.264)). The positive root of Eq. (10.405) must be taken in order that $r_n > 0$. The radii of several n -electron 3p atoms are given in Tables 10.10-10.17.

The ionization energy for the aluminum atom is given by Eq. (10.227). The ionization energies for the n -electron 3p atoms are given by the negative of the electric energy, $E(\text{electric})$, (Eq. (10.102) with the radii, r_n , given by Eq. (10.405)):

$$E(\text{Ionization}) = -\text{Electric Energy} = \frac{(Z - (n - 1))e^2}{8\pi\epsilon_0 r_n} \quad (10.406)$$

Since the relativistic corrections were small, the nonrelativistic ionization energies for experimentally measured n -electron 3p atoms are given by Eqs. (10.405) and (10.406) in Tables 10.10-10.17.

Table 10.18. Summary of the parameters of thirteen through eighteen-electron atoms.

Atom Type	Electron Configuration	Ground State Term ^a	Orbital Arrangement of 3p Electrons (3p state)			Diamagnetic Force Factor A^b	Paramagnetic Force Factor B^c
Neutral 13 e Atom <i>Al</i>	$1s^2 2s^2 2p^6 3s^2 3p^1$	$^2P_{1/2}^0$	\uparrow 1	$\underline{\hspace{0.5em}}$ 0	$\underline{\hspace{0.5em}}$ -1	$\frac{11}{3}$	0
Neutral 14 e Atom <i>Si</i>	$1s^2 2s^2 2p^6 3s^2 3p^2$	3P_0	\uparrow 1	\uparrow 0	$\underline{\hspace{0.5em}}$ -1	$\frac{7}{3}$	0
Neutral 15 e Atom <i>P</i>	$1s^2 2s^2 2p^6 3s^2 3p^3$	$^4S_{3/2}^0$	\uparrow 1	\uparrow 0	\uparrow -1	$\frac{5}{3}$	2
Neutral 16 e Atom <i>S</i>	$1s^2 2s^2 2p^6 3s^2 3p^4$	3P_2	$\uparrow \downarrow$ 1	\uparrow 0	\uparrow -1	$\frac{4}{3}$	1
Neutral 17 e Atom <i>Cl</i>	$1s^2 2s^2 2p^6 3s^2 3p^5$	$^2P_{3/2}^0$	$\uparrow \downarrow$ 1	$\uparrow \downarrow$ 0	\uparrow -1	$\frac{2}{3}$	2
Neutral 18 e Atom <i>Ar</i>	$1s^2 2s^2 2p^6 3s^2 3p^6$	1S_0	$\uparrow \downarrow$ 1	$\uparrow \downarrow$ 0	$\uparrow \downarrow$ -1	$\frac{1}{3}$	4
13 e Ion	$1s^2 2s^2 2p^6 3s^2 3p^1$	$^2P_{1/2}^0$	\uparrow 1	$\underline{\hspace{0.5em}}$ 0	$\underline{\hspace{0.5em}}$ -1	$\frac{5}{3}$	12
14 e Ion	$1s^2 2s^2 2p^6 3s^2 3p^2$	3P_0	\uparrow 1	\uparrow 0	$\underline{\hspace{0.5em}}$ -1	$\frac{1}{3}$	16
15 e Ion	$1s^2 2s^2 2p^6 3s^2 3p^3$	$^4S_{3/2}^0$	\uparrow 1	\uparrow 0	\uparrow -1	0	24
16 e Ion	$1s^2 2s^2 2p^6 3s^2 3p^4$	3P_2	$\uparrow \downarrow$ 1	\uparrow 0	\uparrow -1	$\frac{1}{3}$	24
17 e Ion	$1s^2 2s^2 2p^6 3s^2 3p^5$	$^2P_{3/2}^0$	$\uparrow \downarrow$ 1	$\uparrow \downarrow$ 0	\uparrow -1	$\frac{2}{3}$	32
18 e Ion	$1s^2 2s^2 2p^6 3s^2 3p^6$	1S_0	$\uparrow \downarrow$ 1	$\uparrow \downarrow$ 0	$\uparrow \downarrow$ -1	0	40

^a The theoretical ground state terms match those given by NIST [8].^b Eq. (10.258).^c Eqs. (10.260-10.264).

NINETEEN-ELECTRON ATOMS

Nineteen-electron atoms can be solved exactly using the results of the solutions of one, two, three, four, five, six, seven, eight, nine, ten, eleven, twelve, thirteen, fourteen, fifteen, sixteen, seventeen, and eighteen-electron atoms.

RADIUS AND IONIZATION ENERGY OF THE OUTER ELECTRON OF THE POTASSIUM ATOM

For each eighteen-electron atom having a central charge of Z times that of the proton, there are two indistinguishable spin-paired electrons in an orbitsphere with radii r_1 and r_2 both given by Eq. (7.19) (Eq. (10.51)), two indistinguishable spin-paired electrons in an orbitsphere with radii r_3 and r_4 both given by Eq. (10.62), three sets of paired electrons in an orbitsphere at r_{10} given by Eq. (10.212), two indistinguishable spin-paired electrons in an orbitsphere with radii r_{11} and r_{12} both given by Eq. (10.255), and three sets of paired electrons in an orbitsphere with radius r_{18} given by Eq. (10.399). For $Z \geq 19$, the next electron which binds to form the corresponding nineteen-electron atom is attracted by the central Coulomb field and is repelled by diamagnetic forces due to the 3 sets of spin-paired inner 3p electrons such that it forms an unpaired orbitsphere at radius r_{19} .

The central Coulomb force acts on the outer electron to cause it to bind wherein this electric force on the outer-most electron due to the nucleus and the inner eighteen electrons is given by Eq. (10.70) with the appropriate charge and radius:

$$\mathbf{F}_{ele} = \frac{(Z-18)e^2}{4\pi\epsilon_0 r_{19}^2} \mathbf{i}_r \quad (10.407)$$

for $r > r_{18}$.

The spherically symmetrical closed 3p shell of eighteen-electron atoms produces a diamagnetic force, $\mathbf{F}_{diamagnetic}$, that is equivalent to that of a closed s shell given by Eq. (10.11) with the appropriate radii except that the force is doubled due to the interaction of the 4s and 3p electrons as given by Eq. (10.96). The inner electrons remain at their initial radii, but cause a diamagnetic force according to Lenz's law that is

$$\mathbf{F}_{diamagnetic} = -\frac{2\hbar^2}{4m_e r_{19}^2 r_{18}} \sqrt{s(s+1)} \mathbf{i}_r \quad (10.408)$$

In addition to the spin-spin interaction between electron pairs, the three sets of 3p electrons are orbitally paired. As in the case of the sodium atom with the corresponding radii, the single 4s orbital of the potassium atom produces a magnetic field at the position of the three sets

of spin-paired 3p electrons. In order for the electrons to remain spin and orbitally paired, a corresponding diamagnetic force, $\mathbf{F}_{\text{diamagnetic } 3}$, on electron eighteen from the three sets of spin-paired electrons that follows from the deviation given in the Eleven-Electron Atom section (Eq. (10.221)) is

$$\mathbf{F}_{\text{diamagnetic } 3} = -\frac{1}{Z} \frac{12\hbar^2}{m_e r_{19}^3} \sqrt{s(s+1)} \mathbf{i}_r \quad (10.409)$$

corresponding to the $3p_x$, p_y , and p_z electrons.

The outward centrifugal force on electron 19 is balanced by the electric force and the magnetic forces (on electron 19). The radius of the outer electron is calculated by equating the outward centrifugal force to the sum of the electric (Eq. (10.407)) and diamagnetic (Eqs. (10.408) and (10.409)) forces as follows:

$$\frac{m_e v_{19}^2}{r_{19}} = \frac{(Z-18)e^2}{4\pi\epsilon_0 r_{19}^2} - \frac{2\hbar^2}{4m_e r_{19}^2 r_{18}} \sqrt{s(s+1)} - \frac{12\hbar^2}{Zm_e r_{19}^3} \sqrt{s(s+1)} \quad (10.410)$$

Substitution of $v_{19} = \frac{\hbar}{m_e r_{19}}$ (Eq. (1.56)) and $s = \frac{1}{2}$ into Eq. (10.410) gives:

$$\frac{\hbar^2}{m_e r_{19}^3} = \frac{(Z-18)e^2}{4\pi\epsilon_0 r_{19}^2} - \frac{2\hbar^2}{4m_e r_{19}^2 r_{18}} \sqrt{\frac{3}{4}} - \frac{12\hbar^2}{Zm_e r_{19}^3} \sqrt{\frac{3}{4}} \quad (10.411)$$

$$r_{19} = \frac{\frac{\hbar^2}{m_e} \left(1 + \frac{12}{Z} \sqrt{\frac{3}{4}} \right)}{\frac{(Z-18)e^2}{4\pi\epsilon_0} - \frac{\hbar^2}{2m_e r_{18}} \sqrt{\frac{3}{4}}} \quad (10.412)$$

$$r_{19} = \frac{a_0 \left(1 + \frac{12}{Z} \sqrt{\frac{3}{4}} \right)}{(Z-18) - \frac{\sqrt{\frac{3}{4}}}{2r_{18}}}, \quad r_{18} \text{ in units of } a_0 \quad (10.413)$$

Substitution of $\frac{r_{18}}{a_0} = 0.85215$ (Eq. (10.399) with $Z=19$) into Eq. (10.413) gives

$$r_{19} = 3.14515a_0 \quad (10.414)$$

The ionization energy of the potassium atom is given by the electric energy, $E(\text{electric})$, (Eq. (10.102) with the radius, r_{19} , given by Eq. (10.414)):

$$E(\text{ionization}; K) = -\text{Electric Energy} = \frac{(Z-18)e^2}{8\pi\epsilon_0 r_{19}} = 4.32596 \text{ eV} \quad (10.415)$$

where $r_{19} = 3.14515a_0$ (Eq. (10.414)) and $Z=19$. The experimental ionization energy of the potassium atom is 4.34066 eV [3].

THE IONIZATION ENERGIES OF NINETEEN-ELECTRON ATOMS

WITH A NUCLEAR CHARGE $Z > 19$

Nineteen-electron atoms having $Z > 19$ possess an external electric field given by Eq. (10.92). Since there is a source of dissipative, $\mathbf{J} \cdot \mathbf{E}$ of Eq. (10.27), the magnetic moments of the inner electrons may change due to the outer electron such that the energy of the nineteen-electron atom is lowered. The spherically symmetrical closed 3p shell of eighteen-electron atoms produces a diamagnetic force, $\mathbf{F}_{\text{diamagnetic}}$, that is equivalent to that of a closed s shell given by Eq. (10.11) with the appropriate radii except that the force is tripled due to the interaction of the 2p, 3s, and 3p electrons as discussed in the 3P-Orbital Electrons Based on an Energy Minimum section. The inner electrons remain at their initial radii, but cause a diamagnetic force according to Lenz's law that is

$$\mathbf{F}_{\text{diamagnetic}} = -\frac{3\hbar^2}{4m_e r_{19}^2 r_{18}} \sqrt{s(s+1)} \mathbf{i}_r \quad (10.416)$$

In addition to the spin-spin interaction between electron pairs, the six sets of 2p and 3p electrons are orbitally paired. As in given in the Eleven-Electron Atom section, the single 4s orbital of each nineteen-electron atoms having $Z > 19$ produces a magnetic field at the position of the six sets of spin-paired 2p and 3p electrons. In order for the electrons to remain spin and orbitally paired, a corresponding diamagnetic force, $\mathbf{F}_{\text{diamagnetic } 3}$, on electron nineteen from the six sets of spin-paired electrons that follows from the deviation given in the Eleven-Electron Atom section (Eq. (10.221)) is

$$\mathbf{F}_{\text{diamagnetic } 3} = -\frac{1}{Z} \frac{24\hbar^2}{m_e r_{19}^3} \sqrt{s(s+1)} \mathbf{i}_r \quad (10.417)$$

corresponding to the 2 and 3 p_x , p_y , and p_z electrons.

As shown in the P-Orbital Electrons Based on an Energy Minimum section for $\mathbf{F}_{\text{diamagnetic } 2}$ given by Eq. (10.93), the corresponding diamagnetic force for 2p electrons due to a relativistic effect with an electric field for $r > r_n$ (Eq. (10.35)) is dependent on the amplitude of the orbital energy. Using the orbital energy with $\ell=1$ (Eq. (10.90)), the energy $m_e \Delta v^2$ of Eq. (10.29) is reduced by the factor of $\left(1 - \frac{\sqrt{2}}{2}\right)$ due to the contribution of the charge-density wave of the inner electrons at r_3 . In addition, it was shown in the 3P-Orbital Electrons Based on an Energy Minimum section that the two 3s electrons contribute an energy factor based on Eq. (1.82) since the filled 2p orbitals with the maintenance of symmetry according to Eq. (10.72) requires that the diamagnetic force is due to the electrons at r_{10} acting on the electrons at r_{12} which complies with the reactive force, $\mathbf{F}_{\text{diamagnetic } 2}$, given by Eq. (10.229). Thus, $\mathbf{F}_{\text{diamagnetic } 2}$ for the factor from 3p

electrons with $Z > n$ is reduced by the factor of $\left(1 - \frac{\sqrt{2}}{2} + \frac{1}{2}\right)$. Similarly, the factor for 4s electrons due to the inner 2p, 3s, and 3p electrons is cumulative. Thus, $F_{\text{diamagnetic } 2}$ for 4s electrons with $Z > n$ is

$$F_{\text{diamagnetic } 2} = -\left[\frac{Z-n}{Z-(n-1)}\right]\left(1 - \frac{\sqrt{2}}{2} + \frac{1}{2} - \frac{\sqrt{2}}{2} + \frac{1}{2}\right)\frac{r_{18}\hbar^2}{m_e r_n^4}10\sqrt{s(s+1)}\mathbf{i}_r \quad (10.418)$$

For $n=19$, $F_{\text{diamagnetic } 2}$ is

$$F_{\text{diamagnetic } 2} = -\left[\frac{Z-19}{Z-18}\right]\left(1 - \frac{\sqrt{2}}{2} + \frac{1}{2} - \frac{\sqrt{2}}{2} + \frac{1}{2}\right)\frac{r_{18}\hbar^2}{m_e r_{19}^4}10\sqrt{s(s+1)}\mathbf{i}_r \quad (10.419)$$

In the case that $Z > 19$, the radius of the outer electron is calculated by equating the outward centrifugal force to the sum of the electric (Eq. (10.407)) and diamagnetic (Eqs. (10.416), (10.417), and (10.419)) forces as follows:

$$\begin{aligned} \frac{m_e v_{19}^2}{r_{19}} = & \frac{(Z-18)e^2}{4\pi\epsilon_0 r_{19}^2} - \frac{3\hbar^2}{4m_e r_{19}^2 r_{18}}\sqrt{s(s+1)} - \frac{24\hbar^2}{Zm_e r_{19}^3}\sqrt{s(s+1)} \\ & - \left[\frac{Z-19}{Z-18}\right]\left(1 - \frac{\sqrt{2}}{2} + \frac{1}{2} - \frac{\sqrt{2}}{2} + \frac{1}{2}\right)\frac{r_{18}\hbar^2}{m_e r_{19}^4}10\sqrt{s(s+1)} \end{aligned} \quad (10.420)$$

Substitution of $v_{19} = \frac{\hbar}{m_e r_{19}}$ (Eq. (1.56)) and $s = \frac{1}{2}$ into Eq. (10.420) gives:

$$\frac{\hbar^2}{m_e r_{19}^3} = \frac{(Z-18)e^2}{4\pi\epsilon_0 r_{19}^2} - \frac{3\hbar^2}{4m_e r_{19}^2 r_{18}}\sqrt{\frac{3}{4}} - \frac{24\hbar^2}{Zm_e r_{19}^3}\sqrt{\frac{3}{4}} - \left[\frac{Z-19}{Z-18}\right]\left(1 - \frac{\sqrt{2}}{2} + \frac{1}{2} - \frac{\sqrt{2}}{2} + \frac{1}{2}\right)\frac{r_{18}\hbar^2}{m_e r_{19}^4}10\sqrt{\frac{3}{4}} \quad (10.421)$$

The quadratic equation corresponding to Eq. (10.421) is

$$\left(\frac{(Z-18)e^2}{4\pi\epsilon_0} - \frac{3\hbar^2}{4m_e r_{18}}\sqrt{\frac{3}{4}}\right)r_{19}^2 - \frac{\hbar^2}{m_e}\left(1 + \frac{24\sqrt{\frac{3}{4}}}{Z}\right)r_{19} - \left[\frac{Z-19}{Z-18}\right]\left(1 - \frac{\sqrt{2}}{2} + \frac{1}{2} - \frac{\sqrt{2}}{2} + \frac{1}{2}\right)\frac{r_{18}\hbar^2}{m_e}10\sqrt{\frac{3}{4}} = 0 \quad (10.422)$$

$$r_{19}^2 - \frac{\frac{\hbar^2}{m_e}\left(1 + \frac{24\sqrt{\frac{3}{4}}}{Z}\right)}{\left(\frac{(Z-18)e^2}{4\pi\epsilon_0} - \frac{3\hbar^2}{4m_e r_{18}}\sqrt{\frac{3}{4}}\right)}r_{19} - \frac{\left[\frac{Z-19}{Z-18}\right]\left(1 - \frac{\sqrt{2}}{2} + \frac{1}{2} - \frac{\sqrt{2}}{2} + \frac{1}{2}\right)\frac{r_{18}\hbar^2}{m_e}10\sqrt{\frac{3}{4}}}{\left(\frac{(Z-18)e^2}{4\pi\epsilon_0} - \frac{3\hbar^2}{4m_e r_{18}}\sqrt{\frac{3}{4}}\right)} = 0 \quad (10.423)$$

The solution of Eq. (10.423) using the quadratic formula is:

$$r_{19} = \frac{\frac{\hbar^2}{m_e} \left(1 + \frac{24\sqrt{\frac{3}{4}}}{Z} \right)}{\left(\frac{(Z-18)e^2}{4\pi\epsilon_0} - \frac{3\hbar^2}{4m_e r_{18}} \sqrt{\frac{3}{4}} \right)} \pm \sqrt{\left(\frac{\frac{\hbar^2}{m_e} \left(1 + \frac{24\sqrt{\frac{3}{4}}}{Z} \right)}{\left(\frac{(Z-18)e^2}{4\pi\epsilon_0} - \frac{3\hbar^2}{4m_e r_{18}} \sqrt{\frac{3}{4}} \right)} \right)^2 + 4 \frac{\left[\frac{Z-19}{Z-18} \right] \left(1 - \frac{\sqrt{2}}{2} + \frac{1}{2} - \frac{\sqrt{2}}{2} + \frac{1}{2} \right) \frac{r_{18}\hbar^2}{m_e} 10\sqrt{\frac{3}{4}}}{\left(\frac{(Z-18)e^2}{4\pi\epsilon_0} - \frac{3\hbar^2}{4m_e r_{18}} \sqrt{\frac{3}{4}} \right)}} \quad (10.424)$$

$$r_{19} = \frac{a_0 \left(1 + \frac{12\sqrt{3}}{Z} \right)}{\left((Z-18) - \frac{3\sqrt{3}}{8r_{18}} \right)} \pm a_0 \sqrt{\left(\frac{1 + \frac{12\sqrt{3}}{Z}}{\left((Z-18) - \frac{3\sqrt{3}}{8r_{18}} \right)} \right)^2 + \frac{20\sqrt{3} \left[\frac{Z-19}{Z-18} \right] \left(1 - \frac{\sqrt{2}}{2} + \frac{1}{2} - \frac{\sqrt{2}}{2} + \frac{1}{2} \right) r_{18}}{\left((Z-18) - \frac{3\sqrt{3}}{8r_{18}} \right)}} \quad (10.425)$$

r_{18} in units of a_0

where r_{18} is given by Eq. (10.399). The positive root of Eq. (10.425) must be taken in order that $r_{19} > 0$. The radii of several nineteen-electron atoms are given in Table 10.19.

The ionization energies for the nineteen-electron atoms with $Z > 19$ are given by the electric energy, $E(\text{electric})$, (Eq. (10.102) with the radii r_{19} , given by Eq. (10.425)):

$$E(\text{ionization}) = -\text{Electric Energy} = \frac{(Z-18)e^2}{8\pi\epsilon_0 r_{19}} \quad (10.426)$$

Since the relativistic corrections were small, the nonrelativistic ionization energies for experimentally measured nineteen-electron atoms are given in Table 10.19.

Table 10.19. Ionization energies for some nineteen-electron atoms.

19 e Atom	Z	r_1 (a_0) ^a	r_3 (a_0) ^b	r_{10} (a_0) ^c	r_{12} (a_0) ^d	r_{18} (a_0) ^e	r_{19} (a_0) ^f	Theoretical Ionization Energies ^g (eV)	Experimental Ionization Energies ^h (eV)	Relative Error ⁱ
<i>K</i>	19	0.05302	0.22503	0.26884	0.71450	0.85215	3.14515	4.32596	4.34066	0.0034
<i>Ca</i> ⁺	20	0.05035	0.21308	0.25149	0.65725	0.82478	2.40060	11.3354	11.87172	0.0452
<i>Sc</i> ²⁺	21	0.04794	0.20235	0.23625	0.60857	0.76196	1.65261	24.6988	24.75666	0.0023
<i>Ti</i> ³⁺	22	0.04574	0.19264	0.22276	0.56666	0.70013	1.29998	41.8647	43.2672	0.0324
<i>V</i> ⁴⁺	23	0.04374	0.18383	0.21074	0.53022	0.64511	1.08245	62.8474	65.2817	0.0373
<i>Cr</i> ⁵⁺	24	0.04191	0.17579	0.19995	0.49822	0.59718	0.93156	87.6329	90.6349	0.0331
<i>Mn</i> ⁶⁺	25	0.04022	0.16842	0.19022	0.46990	0.55552	0.81957	116.2076	119.203	0.0251
<i>Fe</i> ⁷⁺	26	0.03867	0.16165	0.18140	0.44466	0.51915	0.73267	148.5612	151.06	0.0165
<i>Co</i> ⁸⁺	27	0.03723	0.15540	0.17336	0.42201	0.48720	0.66303	184.6863	186.13	0.0078
<i>Ni</i> ⁹⁺	28	0.03589	0.14961	0.16601	0.40158	0.45894	0.60584	224.5772	224.6	0.0001
<i>Cu</i> ¹⁰⁺	29	0.03465	0.14424	0.15926	0.38305	0.43379	0.55797	268.2300	265.3	-0.0110
<i>Zn</i> ¹¹⁺	30	0.03349	0.13925	0.15304	0.36617	0.41127	0.51726	315.6418	310.8	-0.0156

^a Radius of the paired 1s inner electrons of nineteen-electron atoms from Eq. (10.51).

^b Radius of the paired 2s inner electrons of nineteen-electron atoms from Eq. (10.62).

^c Radius of the three sets of paired 2p inner electrons of nineteen-electron atoms from Eq. (10.212)).

^d Radius of the paired 3s inner electrons of nineteen-electron atoms from Eq. (10.255)).

^e Radius of the three sets of paired 3p inner electrons of nineteen-electron atoms from Eq. (10.399).

^f Radius of the unpaired 4s outer electron of nineteen-electron atoms from Eq. (10.425) for $Z > 19$ and Eq. (10.414) for K .

^g Calculated ionization energies of nineteen-electron atoms given by the electric energy (Eq. (10.426)).

^h From theoretical calculations, interpolation of isoelectronic and spectral series, and experimental data [2-3].

ⁱ (Experimental-theoretical)/experimental.

The agreement between the experimental and calculated values of Table 10.19 is well within the experimental capability of the spectroscopic determinations including the values at large Z which relies on X-ray spectroscopy. In this case, the experimental capability is about three to four significant figures which is consistent with the last column. Ionization energies are difficult to determine since the cut-off of the Rydberg series of lines at the ionization energy is often not observed. Thus, the potassium atom isoelectronic series given in Table 10.19 [2-3] relies on theoretical calculations and interpolation of the K isoelectronic and Rydberg series as well as direct experimental data to extend the precision beyond the capability of X-ray spectroscopy. But, no assurances can be given that these techniques are correct, and they may not improve

the results. The error given in the last column is very reasonable given the quality of the data.

TWENTY-ELECTRON ATOMS

Twenty-electron atoms can be solved exactly using the results of the solutions of one, two, three, four, five, six, seven, eight, nine, ten, eleven, twelve, thirteen, fourteen, fifteen, sixteen, seventeen, eighteen, and nineteen-electron atoms.

RADIUS AND IONIZATION ENERGY OF AN OUTER ELECTRON OF THE CALCIUM ATOM

For each nineteen-electron atom having a central charge of Z times that of the proton, there are two indistinguishable spin-paired electrons in an orbitsphere with radii r_1 and r_2 both given by Eq. (7.19) (Eq. (10.51)), two indistinguishable spin-paired electrons in an orbitsphere with radii r_3 and r_4 both given by Eq. (10.62), three sets of paired electrons in an orbitsphere at r_{10} given by Eq. (10.212), two indistinguishable spin-paired electrons in an orbitsphere with radii r_{11} and r_{12} both given by Eq. (10.255), three sets of paired electrons in an orbitsphere with radius r_{18} given by Eq. (10.399), and an unpaired electron in an orbitsphere with radius r_{19} given by Eq. (10.425). For $Z \geq 20$, the next electron which binds to form the corresponding twenty-electron atom is attracted by the central Coulomb field and the spin-pairing force with the unpaired 4s inner electron and is repelled by diamagnetic forces due to the 3 sets of spin-paired inner 3p electrons such that it forms an unpaired orbitsphere at radius r_{20} .

The central Coulomb force acts on the outer electron to cause it to bind wherein this electric force on the outer-most electron due to the nucleus and the inner nineteen electrons is given by Eq. (10.70) with the appropriate charge and radius:

$$\mathbf{F}_{ele} = \frac{(Z-19)e^2}{4\pi\epsilon_0 r_{20}^2} \mathbf{i}_r \quad (10.427)$$

for $r > r_{19}$.

The forces for the calcium atom follow from those of the magnesium atom given in the Twelve-Electron Atom section. The outer electron which binds to form the corresponding twenty-electron atom becomes spin-paired with the unpaired inner electron such that they become indistinguishable with the same radius $r_{19} = r_{20}$ corresponding to a filled 4s shell. The corresponding spin-pairing force F_{mag} is given by Eqs. (7.15) and (10.239):

$$\mathbf{F}_{mag} = \frac{1}{Z} \frac{\hbar^2}{m_e r_{20}^3} \sqrt{s(s+1)} \mathbf{i}_r \quad (10.428)$$

The spherically symmetrical closed 3p shell of twenty-electron atoms produces a diamagnetic force, $\mathbf{F}_{diamagnetic}$, that is equivalent to that of a closed s shell given by Eq. (10.11) with the appropriate radii. The inner electrons remain at their initial radii, but cause a diamagnetic force according to Lenz's law that is

$$\mathbf{F}_{diamagnetic} = -\frac{\hbar^2}{4m_e r_{20}^2 r_{18}} \sqrt{s(s+1)} \mathbf{i}_r \quad (10.429)$$

In addition to the paramagnetic spin-pairing force between the nineteenth electron initially at radius r_{19} , the pairing causes the diamagnetic interaction between the outer electrons and the inner electrons given by Eq. (10.11) to vanish, except for an electrodynamic effect for $Z > 20$ described in the Two-Electron Atoms section, since upon pairing the magnetic field of the outer electrons becomes zero. Using Eqs. (10.55) and (10.240), $\mathbf{F}_{mag 2}$ due to the three 3p orbitals is given by:

$$\mathbf{F}_{mag 2} = \frac{3}{Z} \frac{\hbar^2}{m_e r_{20} r_{18}^2} \sqrt{s(s+1)} \mathbf{i}_r \quad (10.430)$$

In addition to the spin-spin interactions between electron pairs, the three sets of 2p and 3p electrons are orbitally paired. The 4s electrons of the calcium atom produce a magnetic field at the position of the six sets of spin-paired 2p and 3p electrons which interact as described in the P-Orbital Electrons Based on an Energy Minimum section. In order for the electrons to remain spin and orbitally paired, the corresponding diamagnetic force, $\mathbf{F}_{diamagnetic 3}$, on electron twenty from the six sets of spin-paired electrons that follows from the deviation given in the Eleven-Electron Atom section (Eq. (10.221)) is

$$\mathbf{F}_{diamagnetic 3} = -\frac{1}{Z} \frac{24\hbar^2}{m_e r_{20}^3} \sqrt{s(s+1)} \mathbf{i}_r \quad (10.431)$$

corresponding to the 2 and 3 p_x , p_y , and p_z electrons.

The outward centrifugal force on electron 20 is balanced by the electric force and the magnetic forces (on electron 20). The radius of the outer electron is calculated by equating the outward centrifugal force to the sum of the electric (Eq. (10.427)), diamagnetic (Eq. (10.428-10.429) and (10.431)), and paramagnetic (Eq. (10.430)) forces as follows:

$$\begin{aligned} \frac{m_e v_{20}^2}{r_{20}} = & \frac{(Z-19)e^2}{4\pi\epsilon_0 r_{20}^2} - \frac{\hbar^2}{4m_e r_{20}^2 r_{18}} \sqrt{s(s+1)} + \frac{3\hbar^2}{Zm_e r_{20}^2 r_{18}} \sqrt{s(s+1)} \\ & - \frac{24\hbar^2}{Zm_e r_{20}^3} \sqrt{s(s+1)} + \frac{\hbar^2}{Zm_e r_{20}^3} \sqrt{s(s+1)} \end{aligned} \quad (10.432)$$

Substitution of $v_{20} = \frac{\hbar}{m_e r_{20}}$ (Eq. (1.56)) and $s = \frac{1}{2}$ into Eq. (10.432) gives:

$$\frac{\hbar^2}{m_e r_{20}^3} = \frac{(Z-18)e^2}{4\pi\epsilon_0 r_{20}^2} - \frac{\hbar^2}{4m_e r_{20}^2 r_{18}} \sqrt{\frac{3}{4}} + \frac{3\hbar^2}{Zm_e r_{20}^2 r_{18}} \sqrt{\frac{3}{4}} - \frac{24\hbar^2}{Zm_e r_{20}^3} \sqrt{\frac{3}{4}} + \frac{\hbar^2}{Zm_e r_{20}^3} \sqrt{\frac{3}{4}} \quad (10.433)$$

$$r_{20} = \frac{\frac{\hbar^2}{m_e} \left(1 + \frac{23\sqrt{\frac{3}{4}}}{Z} \right)}{\frac{(Z-19)e^2}{4\pi\epsilon_0} - \left(\frac{1}{4} - \frac{3}{Z} \right) \frac{\hbar^2}{m_e r_{18}} \sqrt{\frac{3}{4}}} \quad (10.434)$$

$$r_{20} = \frac{a_0 \left(1 + \frac{23\sqrt{\frac{3}{4}}}{Z} \right)}{(Z-19) - \left(\frac{1}{4} - \frac{3}{Z} \right) \frac{\sqrt{\frac{3}{4}}}{r_{18}}}, \quad r_{18} \text{ in units of } a_0 \quad (10.435)$$

Substitution of $\frac{r_{18}}{a_0} = 0.82478$ (Eq. (10.399) with $Z=20$) into Eq. (10.435) gives

$$r_{20} = 2.23009a_0 \quad (10.436)$$

The ionization energy of the calcium atom is given by the electric energy, $E(\text{electric})$, (Eq. (10.102) with the radius, r_{20} , given by Eq. (10.435)):

$$E(\text{ionization; Ca}) = -\text{Electric Energy} = \frac{(Z-19)e^2}{8\pi\epsilon_0 r_{20}} = 6.10101 \text{ eV} \quad (10.437)$$

where $r_{20} = 2.23009a_0$ (Eq. (10.435)) and $Z=20$. The experimental ionization energy of the calcium atom is 6.11316 eV [3].

THE IONIZATION ENERGIES OF TWENTY-ELECTRON ATOMS WITH A NUCLEAR CHARGE $Z > 20$

Nineteen-electron atoms having $Z > 20$ possess an external electric field given by Eq. (10.92). Since there is a source of dissipative, $\mathbf{J} \cdot \mathbf{E}$ of Eq. (10.27), the magnetic moments of the inner electrons may change due to the outer electron such that the energy of the nineteen-electron atom is lowered. The spherically symmetrical closed 3p shell of twenty-electron atoms produces a diamagnetic force, $\mathbf{F}_{\text{diamagnetic}}$, that is equivalent to that of a closed s shell given by Eq. (10.11) with the appropriate radii except that the force is doubled (Eq. (10.96)) due to the interaction of the

2p, 3s, and 3p electrons as discussed in the 3P-Orbital Electrons Based on an Energy Minimum section with the cancellation of the contribution of the 3s orbital by the 4s orbital. The inner electrons remain at their initial radii, but cause a diamagnetic force according to Lenz's law that is

$$\mathbf{F}_{\text{diamagnetic}} = -\frac{2\hbar^2}{4m_e r_{20}^2 r_{18}} \sqrt{s(s+1)} \mathbf{i}_r \quad (10.438)$$

In addition to the spin-spin interaction between electron pairs, the six sets of 2p and 3p electrons are orbitally paired. As in given in the Eleven-Electron Atom section, the single 4s orbital of each twenty-electron atoms having $Z > 20$ produces a magnetic field at the position of the six sets of spin-paired 2p and 3p electrons. In order for the electrons to remain spin and orbitally paired, the corresponding diamagnetic force, $\mathbf{F}_{\text{diamagnetic } 3}$, on electron twenty from the six sets of spin-paired electrons given by Eq. (10.221) is

$$\mathbf{F}_{\text{diamagnetic } 3} = -\frac{1}{Z} \frac{24\hbar^2}{m_e r_{20}^3} \sqrt{s(s+1)} \mathbf{i}_r \quad (10.439)$$

corresponding to the 2 and 3 p_x , p_y , and p_z electrons.

From Eq. (10.418), the diamagnetic force, $\mathbf{F}_{\text{diamagnetic } 2}$, due to a relativistic effect with an electric field for $r > r_{20}$ (Eq. (10.35)) is

$$\mathbf{F}_{\text{diamagnetic } 2} = -\left[\frac{Z-20}{Z-19} \right] \left(1 - \frac{\sqrt{2}}{2} + \frac{1}{2} - \frac{\sqrt{2}}{2} + \frac{1}{2} \right) \frac{r_{18} \hbar^2}{m_e r_{20}^4} 10 \sqrt{s(s+1)} \mathbf{i}_r \quad (10.440)$$

In the case that $Z > 20$, the radius of the outer electron is calculated by equating the outward centrifugal force to the sum of the electric (Eq. (10.427)) and diamagnetic (Eqs. (10.438-10.440)) forces as follows:

$$\begin{aligned} \frac{m_e v_{20}^2}{r_{20}} = & \frac{(Z-19)e^2}{4\pi\epsilon_0 r_{20}^2} - \frac{2\hbar^2}{4m_e r_{20}^2 r_{18}} \sqrt{s(s+1)} - \frac{24\hbar^2}{Zm_e r_{20}^3} \sqrt{s(s+1)} \\ & - \left[\frac{Z-20}{Z-19} \right] \left(1 - \frac{\sqrt{2}}{2} + \frac{1}{2} - \frac{\sqrt{2}}{2} + \frac{1}{2} \right) \frac{r_{18} \hbar^2}{m_e r_{20}^4} 10 \sqrt{s(s+1)} \end{aligned} \quad (10.441)$$

Substitution of $v_{20} = \frac{\hbar}{m_e r_{20}}$ (Eq. (1.56)) and $s = \frac{1}{2}$ into Eq. (10.441) gives:

$$\begin{aligned} \frac{\hbar^2}{m_e r_{20}^3} = & \frac{(Z-19)e^2}{4\pi\epsilon_0 r_{20}^2} - \frac{2\hbar^2}{4m_e r_{20}^2 r_{18}} \sqrt{\frac{3}{4}} - \frac{24\hbar^2}{Zm_e r_{20}^3} \sqrt{\frac{3}{4}} \\ & - \left[\frac{Z-20}{Z-19} \right] \left(1 - \frac{\sqrt{2}}{2} + \frac{1}{2} - \frac{\sqrt{2}}{2} + \frac{1}{2} \right) \frac{r_{18} \hbar^2}{m_e r_{20}^4} 10 \sqrt{\frac{3}{4}} \end{aligned} \quad (10.442)$$

The quadratic equation corresponding to Eq. (10.442) is

$$r_{20}^2 - \frac{\frac{\hbar^2}{m_e} \left(1 + \frac{24\sqrt{\frac{3}{4}}}{Z} \right)}{\left(\frac{(Z-19)e^2}{4\pi\epsilon_0} - \frac{2\hbar^2}{4m_e r_{18}} \sqrt{\frac{3}{4}} \right)} r_{20} - \frac{\left[\frac{Z-20}{Z-19} \right] \left(1 - \frac{\sqrt{2}}{2} + \frac{1}{2} - \frac{\sqrt{2}}{2} + \frac{1}{2} \right) \frac{r_{18}\hbar^2}{m_e} 10\sqrt{\frac{3}{4}}}{\left(\frac{(Z-19)e^2}{4\pi\epsilon_0} - \frac{2\hbar^2}{4m_e r_{18}} \sqrt{\frac{3}{4}} \right)} = 0 \quad (10.443)$$

The solution of Eq. (10.443) using the quadratic formula is:

$$r_{20} = \frac{\frac{\hbar^2}{m_e} \left(1 + \frac{24\sqrt{\frac{3}{4}}}{Z} \right)}{\left(\frac{(Z-19)e^2}{4\pi\epsilon_0} - \frac{2\hbar^2}{4m_e r_{18}} \sqrt{\frac{3}{4}} \right)} \pm \frac{\sqrt{\left(\frac{\hbar^2}{m_e} \left(1 + \frac{24\sqrt{\frac{3}{4}}}{Z} \right) \right)^2 - 4 \frac{\left[\frac{Z-20}{Z-19} \right] \left(1 - \frac{\sqrt{2}}{2} + \frac{1}{2} - \frac{\sqrt{2}}{2} + \frac{1}{2} \right) \frac{r_{18}\hbar^2}{m_e} 10\sqrt{\frac{3}{4}}}{\left(\frac{(Z-19)e^2}{4\pi\epsilon_0} - \frac{2\hbar^2}{4m_e r_{18}} \sqrt{\frac{3}{4}} \right)}}}{2} \quad (10.444)$$

$$r_{20} = \frac{a_0 \left(1 + \frac{12\sqrt{3}}{Z} \right)}{\left((Z-19) - \frac{\sqrt{3}}{4r_{18}} \right)} \pm a_0 \frac{\sqrt{\left(1 + \frac{12\sqrt{3}}{Z} \right)^2 - \frac{20\sqrt{3} \left[\frac{Z-20}{Z-19} \right] \left(1 - \frac{\sqrt{2}}{2} + \frac{1}{2} - \frac{\sqrt{2}}{2} + \frac{1}{2} \right) r_{18}}{\left((Z-19) - \frac{\sqrt{3}}{4r_{18}} \right)}}}{2} \quad (10.445)$$

r_{18} in units of a_0

where r_{18} is given by Eq. (10.399). The positive root of Eq. (10.445) must be taken in order that $r_{20} > 0$. The final radius of electron 20, r_{20} , is given by Eq. (10.445); this is also the final radius of electron 19. The radii of several twenty-electron atoms are given in Table 10.20. The general equation for the ionization energies of atoms having an outer s-shell is

given in the General Equation for the Ionization Energies of Atoms Having an Outer S-Shell section.

The ionization energies for the twenty-electron atoms with $Z > 20$ are given by the electric energy, $E(\text{electric})$, (Eq. (10.102) with the radii r_{20} , given by Eq. (10.445)):

$$E(\text{Ionization}) = -\text{Electric Energy} = \frac{(Z-19)e^2}{8\pi\epsilon_0 r_{20}} \quad (10.446)$$

Since the relativistic corrections were small, the nonrelativistic ionization energies for experimentally measured twenty-electron atoms are given in Table 10.20.

Table 10.20. Ionization energies for some twenty-electron atoms.

20 e Atom	Z	r_1 (a_0) ^a	r_3 (a_0) ^b	r_{10} (a_0) ^c	r_{12} (a_0) ^d	r_{18} (a_0) ^e	r_{20} (a_0) ^f	Theoretical Ionization Energies ^g (eV)	Experimental Ionization Energies ^h (eV)	Relative Error ⁱ
Ca	20	0.05035	0.21308	0.25149	0.65725	0.82478	2.23009	6.10101	6.11316	0.0020
Sc ⁺	21	0.04794	0.20235	0.23625	0.60857	0.76196	2.04869	13.2824	12.79967	-0.0377
Ti ²⁺	22	0.04574	0.19264	0.22276	0.56666	0.70013	1.48579	27.4719	27.4917	0.0007
V ³⁺	23	0.04374	0.18383	0.21074	0.53022	0.64511	1.19100	45.6956	46.709	0.0217
Cr ⁴⁺	24	0.04191	0.17579	0.19995	0.49822	0.59718	1.00220	67.8794	69.46	0.0228
Mn ⁵⁺	25	0.04022	0.16842	0.19022	0.46990	0.55552	0.86867	93.9766	95.6	0.0170
Fe ⁶⁺	26	0.03867	0.16165	0.18140	0.44466	0.51915	0.76834	123.9571	124.98	0.0082
Co ⁷⁺	27	0.03723	0.15540	0.17336	0.42201	0.48720	0.68977	157.8012	157.8	0.0000
Ni ⁸⁺	28	0.03589	0.14961	0.16601	0.40158	0.45894	0.62637	195.4954	193	-0.0129
Cu ⁹⁺	29	0.03465	0.14424	0.15926	0.38305	0.43379	0.57401	237.0301	232	-0.0217
Zn ¹⁰⁺	30	0.03349	0.13925	0.15304	0.36617	0.41127	0.52997	282.3982	274	-0.0307

^a Radius of the paired 1s inner electrons of twenty-electron atoms from Eq. (10.51).

^b Radius of the paired 2s inner electrons of twenty-electron atoms from Eq. (10.62).

^c Radius of the three sets of paired 2p inner electrons of twenty-electron atoms from Eq. (10.212)).

^d Radius of the paired 3s inner electrons of twenty-electron atoms from Eq. (10.255)).

^e Radius of the three sets of paired 3p inner electrons of twenty-electron atoms from Eq. (10.399).

^f Radius of the paired 4s outer electrons of twenty-electron atoms from Eq. (10.445) for $Z > 20$ and Eq. (10.436) for Ca.

^g Calculated ionization energies of twenty-electron atoms given by the electric energy (Eq. (10.446)).

^h From theoretical calculations, interpolation of isoelectronic and spectral series, and experimental data [2-3].

ⁱ (Experimental-theoretical)/experimental.

The agreement between the experimental and calculated values of

Table 10.20 is well within the experimental capability of the spectroscopic determinations including the values at large Z which relies on X-ray spectroscopy. In this case, the experimental capability is about three to four significant figures which is consistent with the last column. Ionization energies are difficult to determine since the cut-off of the Rydberg series of lines at the ionization energy is often not observed. Thus, the calcium atom isoelectronic series given in Table 10.20 [2-3] relies on theoretical calculations and interpolation of the Ca isoelectronic and Rydberg series as well as direct experimental data to extend the precision beyond the capability of X-ray spectroscopy. But, no assurances can be given that these techniques are correct, and they may not improve the results. The error given in the last column is very reasonable given the quality of the data.

GENERAL EQUATION FOR THE IONIZATION ENERGIES OF ATOMS HAVING AN OUTER S-SHELL

The derivation of the radii and energies of the 1s, 2s, 3s, and 4s electrons is given in the One-Electron Atom, the Two-Electron Atom, the Three-Electron Atoms, the Four-Electron Atoms, the Eleven-Electron Atoms, the Twelve-Electron Atoms, the Nineteen-Electron Atoms, and the Twenty-Electron Atoms sections. Similarly, to Eqs. (10.216) and (10.405), the general equation for the radii of s electrons is given by

$$r_n = \frac{a_0 \left(1 + (C - D) \frac{\sqrt{3}}{2Z} \right)}{\left((Z - (n - 1)) - \left(\frac{A}{8} - \frac{B}{2Z} \right) \frac{\sqrt{3}}{r_m} \right)} \pm a_0 \sqrt{\frac{\left(1 + (C - D) \frac{\sqrt{3}}{2Z} \right)^2}{\left((Z - (n - 1)) - \left(\frac{A}{8} - \frac{B}{2Z} \right) \frac{\sqrt{3}}{r_m} \right)^2} + \frac{20\sqrt{3} \left(\left[\frac{Z - n}{Z - (n - 1)} \right] E r_m \right)}{\left((Z - (n - 1)) - \left(\frac{A}{8} - \frac{B}{2Z} \right) \frac{\sqrt{3}}{r_m} \right)}} \quad (10.447)$$

r_m in units of a_0

where Z is the nuclear charge, n is the number of electrons, r_m is the radius of the proceeding filled shell, the parameter A given in Table 10.21 corresponds to the diamagnetic force, $F_{\text{diamagnetic}}$, (Eq. (10.11)), the parameter B given in Table 10.21 corresponds to the paramagnetic force, $F_{\text{mag } 2}$ (Eq. (10.55)), the parameter C given in Table 10.21 corresponds to the diamagnetic force, $F_{\text{diamagnetic } 3}$, (Eq. (10.221)), the parameter D given in Table 10.21 corresponds to the paramagnetic force, F_{mag} , (Eq. (7.15)), and

the parameter E given in Table 10.21 corresponds to the diamagnetic force, $F_{\text{diamagnetic } 2}$, (Eqs. (10.35), (10.229), and (10.418)). The positive root of Eq. (10.447) must be taken in order that $r_n > 0$. The radii of several n-electron atoms having an outer s shell are given in Tables 1.3, 1.5, 7.1, 10.1, 10.2, 10.10, 10.11, 10.19, and 10.20.

The ionization energy for atoms having an outer s-shell are given by the negative of the electric energy, $E(\text{electric})$, (Eq. (10.102) with the radii, r_n , given by Eq. (10.447)):

$$E(\text{Ionization}) = -\text{Electric Energy} = \frac{(Z - (n - 1))e^2}{8\pi\epsilon_0 r_n} \quad (10.448)$$

except that minor corrections due to the magnetic energy must be included in cases wherein the s electron does not couple to p electrons as given in Eqs. (7.28), (7.47), (10.25), (10.48), (10.66), and (10.68). Since the relativistic corrections were small except for one, two, and three-electron atoms, the nonrelativistic ionization energies for experimentally measured n-electron, s-filling atoms are given in most cases by Eqs. (10.447) and (10.448). The ionization energies of several n-electron atoms having an outer s shell are given in Tables 1.3, 1.5, 7.1, 10.1, 10.2, 10.10, 10.11, 10.19, and 10.20.

Table 10.21. Summary of the parameters of atoms filling the 1s, 2s, 3s, and 4s orbitals.

Atom Type	Electron Configuration	Ground State Term ^a	Orbital Arrangement of s Electrons (s state)	Diamag. Force Factor A ^b	Paramag. Force Factor B ^c	Diamag. Force Factor C ^d	Paramag. Force Factor D ^e	Diamag. Force Factor E ^f
Neutral 1 e Atom <i>H</i>	$1s^1$	$^2S_{1/2}$	$\frac{\uparrow}{1s}$	0	0	0	0	0
Neutral 2 e Atom <i>He</i>	$1s^2$	1S_0	$\frac{\uparrow \downarrow}{1s}$	0	0	0	1	0
Neutral 3 e Atom <i>Li</i>	$2s^1$	$^2S_{1/2}$	$\frac{\uparrow}{2s}$	1	0	0	0	0
Neutral 4 e Atom <i>Be</i>	$2s^2$	1S_0	$\frac{\uparrow \downarrow}{2s}$	1	0	0	1	0
Neutral 11 e Atom <i>Na</i>	$1s^2 2s^2 2p^6 3s^1$	$^2S_{1/2}$	$\frac{\uparrow}{3s}$	1	0	8	0	0
Neutral 12 e Atom <i>Mg</i>	$1s^2 2s^2 2p^6 3s^2$	1S_0	$\frac{\uparrow \downarrow}{3s}$	1	3	12	1	0
Neutral 19 e Atom <i>K</i>	$1s^2 2s^2 2p^6 3s^2 3p^6 4s^1$	$^2S_{1/2}$	$\frac{\uparrow}{4s}$	2	0	12	0	0
Neutral 20 e Atom <i>Ca</i>	$1s^2 2s^2 2p^6 3s^2 3p^6 4s^2$	1S_0	$\frac{\uparrow \downarrow}{4s}$	1	3	24	1	0
1 e Ion	$1s^1$	$^2S_{1/2}$	$\frac{\uparrow}{1s}$	0	0	0	0	0
2 e Ion	$1s^2$	1S_0	$\frac{\uparrow \downarrow}{1s}$	0	0	0	1	0
3 e Ion	$2s^1$	$^2S_{1/2}$	$\frac{\uparrow}{2s}$	1	0	0	0	1
4 e Ion	$2s^2$	1S_0	$\frac{\uparrow \downarrow}{2s}$	1	0	0	1	1
11 e Ion	$1s^2 2s^2 2p^6 3s^1$	$^2S_{1/2}$	$\frac{\uparrow}{3s}$	1	4	8	0	$1 + \frac{\sqrt{2}}{2}$

12 e Ion	$1s^2 2s^2 2p^6 3s^2$	1S_0	$\frac{\uparrow \downarrow}{3s}$	1	6	0	0	$1 + \frac{\sqrt{2}}{2}$
19 e Ion	$1s^2 2s^2 2p^6 3s^2 3p^6 4s^1$	$^2S_{1/2}$	$\frac{\uparrow}{4s}$	3	0	24	0	$2 - \sqrt{2}$
20 e Ion	$1s^2 2s^2 2p^6 3s^2 3p^6 4s^2$	1S_0	$\frac{\uparrow \downarrow}{4s}$	2	0	24	0	$2 - \sqrt{2}$

^a The theoretical ground state terms match those given by NIST [8].

^b Eq. (10.11).

^c Eq. (10.55).

^d Eq. (10.221).

^e Eq. (7.15).

^f Eqs. (10.35), (10.229), and (10.418).

References

1. Purcell, E., Electricity and Magnetism, McGraw-Hill, New York, (1965), pp. 370-389.
2. C. E. Moore, "Ionization Potentials and Ionization Limits Derived from the Analyses of Optical Spectra, Nat. Stand. Ref. Data Ser.-Nat. Bur. Stand. (U.S.), No. 34, 1970.
3. Robert C. Weast, CRC Handbook of Chemistry and Physics, 58 Edition, CRC Press, West Palm Beach, Florida, (1977), p. E-68.
4. A. O. Wistrom, A. V. M. Khachatourian, "Coulomb motor by rotation of spherical conductors via the electrostatic force", Applied Physics Letters, Volume 80, No. 15, (2002), pp. 2800-2802.
5. A. V. M. Khachatourian, A. O. Wistrom, "Journal of Mathematical Physics, "A sum rule for associated Legendre polynomials with spherical triangles", Vol. 44, No. 2, (2003), pp. 849-852.
6. Jackson, J. D., Classical Electrodynamics, Second Edition, John Wiley & Sons, New York, (1975), p. 99.
7. McQuarrie, D. A., Quantum Chemistry, University Science Books, Mill Valley, CA, (1983), p. 215.
8. NIST Atomic Spectra Database, www.physics.nist.gov/cgi-bin/AtData/display.ksh.

From the INTERNATIONAL BUREAU

PCTNOTIFICATION CONCERNING
SUBMISSION OR TRANSMITTAL
OF PRIORITY DOCUMENT

(PCT Administrative Instructions, Section 411)

To:

MELCHER, Jeffrey, S.
Manelli Denison & Selter, PLLC
7th Floor
2000 M Street, N.W.
Washington, DC 20036-3307
ETATS-UNIS D'AMERIQUE

Date of mailing (day/month/year) 29 March 2005 (29.03.2005)	
Applicant's or agent's file reference 62226-PCT-AM2	IMPORTANT NOTIFICATION
International application No. PCT/US05/000073	International filing date (day/month/year) 05 January 2005 (05.01.2005)
International publication date (day/month/year)	Priority date (day/month/year) 05 January 2004 (05.01.2004)
Applicant BLACKLIGHT POWER, INC. et al	

- By means of this Form, which replaces any previously issued notification concerning submission or transmittal of priority documents, the applicant is hereby notified of the date of receipt by the International Bureau of the priority document(s) relating to all earlier application(s) whose priority is claimed. Unless otherwise indicated by the letters "NR", in the right-hand column or by an asterisk appearing next to a date of receipt, the priority document concerned was submitted or transmitted to the International Bureau in compliance with Rule 17.1(a) or (b).
- (If applicable) The letters "NR" appearing in the right-hand column denote a priority document which, on the date of mailing of this Form, had not yet been received by the International Bureau under Rule 17.1(a) or (b). Where, under Rule 17.1(a), the priority document must be submitted by the applicant to the receiving Office or the International Bureau, but the applicant fails to submit the priority document within the applicable time limit under that Rule, the attention of the applicant is directed to Rule 17.1(c) which provides that no designated Office may disregard the priority claim concerned before giving the applicant an opportunity, upon entry into the national phase, to furnish the priority document within a time limit which is reasonable under the circumstances.
- (If applicable) An asterisk (*) appearing next to a date of receipt, in the right-hand column, denotes a priority document submitted or transmitted to the International Bureau but not in compliance with Rule 17.1(a) or (b) (the priority document was received after the time limit prescribed in Rule 17.1(a) or the request to prepare and transmit the priority document was submitted to the receiving Office after the applicable time limit under Rule 17.1(b)). Even though the priority document was not furnished in compliance with Rule 17.1(a) or (b), the International Bureau will nevertheless transmit a copy of the document to the designated Offices, for their consideration. In case such a copy is not accepted by the designated Office as the priority document, Rule 17.1(c) provides that no designated Office may disregard the priority claim concerned before giving the applicant an opportunity, upon entry into the national phase, to furnish the priority document within a time limit which is reasonable under the circumstances.

<u>Priority date</u>	<u>Priority application No.</u>	<u>Country or regional Office or PCT receiving Office</u>	<u>Date of receipt of priority document</u>
05 January 2004 (05.01.2004)	60/534,112	US	09 February 2005 (09.02.2005)
09 February 2004 (09.02.2004)	60/542,278	US	09 February 2005 (09.02.2005)

The International Bureau of WIPO
34, chemin des Colombettes
1211 Geneva 20, Switzerland

Facsimile No. +41 22 740 14 35

Authorized officer

Brasier Jerome

Facsimile No. +41 22 338 89 75
Telephone No. +41 22 338 8394

From the INTERNATIONAL BUREAU

PCTNOTIFICATION CONCERNING
SUBMISSION OR TRANSMITTAL
OF PRIORITY DOCUMENT

(PCT Administrative Instructions, Section 411)

To:

MELCHER, Jeffrey, S.
Manelli Denison & Selter, PLLC
7th Floor
2000 M Street, N.W.
Washington, DC 20036-3307
ETATS-UNIS D'AMERIQUE

Date of mailing (day/month/year) 23 June 2005 (23.06.2005)	
Applicant's or agent's file reference 62226-PCT-AM2	IMPORTANT NOTIFICATION
International application No. PCT/US2005/000073	International filing date (day/month/year) 05 January 2005 (05.01.2005)
International publication date (day/month/year)	Priority date (day/month/year) 05 January 2004 (05.01.2004)
Applicant BLACKLIGHT POWER, INC. et al	

- By means of this Form, which replaces any previously issued notification concerning submission or transmittal of priority documents, the applicant is hereby notified of the date of receipt by the International Bureau of the priority document(s) relating to all earlier application(s) whose priority is claimed. Unless otherwise indicated by the letters "NR", in the right-hand column or by an asterisk appearing next to a date of receipt, the priority document concerned was submitted or transmitted to the International Bureau in compliance with Rule 17.1(a) or (b).
- (If applicable)* The letters "NR" appearing in the right-hand column denote a priority document which, on the date of mailing of this Form, had not yet been received by the International Bureau under Rule 17.1(a) or (b). Where, under Rule 17.1(a), the priority document must be submitted by the applicant to the receiving Office or the International Bureau, but the applicant fails to submit the priority document within the applicable time limit under that Rule, the attention of the applicant is directed to Rule 17.1(c) which provides that no designated Office may disregard the priority claim concerned before giving the applicant an opportunity, upon entry into the national phase, to furnish the priority document within a time limit which is reasonable under the circumstances.
- (If applicable)* An asterisk (*) appearing next to a date of receipt, in the right-hand column, denotes a priority document submitted or transmitted to the International Bureau but not in compliance with Rule 17.1(a) or (b) (the priority document was received after the time limit prescribed in Rule 17.1(a) or the request to prepare and transmit the priority document was submitted to the receiving Office after the applicable time limit under Rule 17.1(b)). Even though the priority document was not furnished in compliance with Rule 17.1(a) or (b), the International Bureau will nevertheless transmit a copy of the document to the designated Offices, for their consideration. In case such a copy is not accepted by the designated Office as the priority document, Rule 17.1(c) provides that no designated Office may disregard the priority claim concerned before giving the applicant an opportunity, upon entry into the national phase, to furnish the priority document within a time limit which is reasonable under the circumstances.

Priority date	Priority application No.	Country or regional Office or PCT receiving Office	Date of receipt of priority document
05 January 2004 (05.01.2004)	60/534,112	US	09 February 2005 (09.02.2005)
09 February 2004 (09.02.2004)	60/542,278	US	09 February 2005 (09.02.2005)
03 January 2005 (03.01.2005)	60/640,213	US	13 June 2005 (13.06.2005)

The International Bureau of WIPO
34, chemin des Colombettes
1211 Geneva 20, Switzerland

Facsimile No. +41 22 338 82 70

Authorized officer

Christelle CROCI (Fax : 338 89 75)

Facsimile No. (41-22) 338.89.75

Telephone No. +41 22 338 9933